JOURNAL OF ATMOSPHERIC AND TERRESTRIAL PHYSICS

EDITORIAL ADVISORY BOARD

H. O. G. ALFVÉN-STOCKHOLM · J. BARTELS-GÖTTINGEN · P. M. S. BLACKETT-MANCHESTER · E. G. BOWEN-SYDNEY · SIR DAVID BRUNT-LONDON · R. BUREAU-BAGNEUX · S. CHAPMAN-ALASKA · J. EGEDAL-COPENHAGEN · H. FICKER-VIENNA V. F. HESS-NEW YORK · E. O. HULBURT-WASHINGTON, D.C. · H. ISRAEL-TÜBINGEN D. H. MENZEL-CAMBRIDGE, MASS. S. K. MITRA-CALCUTTA · M. NICOLET-UCCLE E. H. NORINDER-UPSALA · B. van der POL-GENEVA · J. A. RATCLIFFE-CAMBRIDGE E. REGENER-WEISSENAU (BODENSEE) · O. E. H. RYDBECK-GOTHENBURG · SIR GEORGE SIMPSON-LONDON · H. SOLBERG-OSLO · C. STØRMER-OSLO H. U. SVERDRUP-OSLO · J. VELDKAMP-DE BILT · M. WALDMEIER-ZÜRICH R. v. d. R. WOOLLEY-CANBERRA · J. ZENNECK-ALTHEGNENBERG

EDITOR IN CHIEF

SIR EDWARD APPLETON, F.R.S.
EDINBURGH

VOLUME 5
1954

PERGAMON PRESS LTD · LONDON & NEW YORK

J. Atmosph. Terr. Phys.

VOL.
5
1954

CONTENTS

No. 1

PAGE

RICHARD I. WELLER: The intensity of beta ray ionization of potassium, uranium and thorium 1

JOHN M. KELSO: The determination of the electron density distribution of an ionosphere layer in the presence of an external magnetic field 11

A. P. MITRA: A tentative model of the equilibrium height distribution of nitric oxide in the high atmosphere and the resulting *D*-layer 28

D. M. HUNTEN: A study of sodium in twilight. I. Theory 44

D. M. HUNTEN and G. G. SHEPHERD: A study of sodium in twilight. II. Observations on the distribution 57

Research Notes:

A. OMHOLT: The intensity distribution in the second positive band system of nitrogen in a laboratory light 63

N. C. GERSON: Sources of atmospheric and planetary energy 67

UDO BECKER and J. F. DENISSE: Controls of geomagnetic activity by sunspots . . 70

No. 2

R. NAISMITH: A subsidiary layer in the *E*-region of the ionosphere 73

EDWARD V. ASHBURN: The effect of Rayleigh scattering and ground reflection upon the determination of the height of the night airglow 83

N. J. SKINNER, R. A. BROWN and R. W. WRIGHT: Multiple stratification of the *F*-layer at Ibadan 92

K-indices of geomagnetic activity from the observations at Abinger, Eskdalemuir, and Lerwick, from December, 1953 to February, 1954 101

Erratum: "Semidiurnal currents and electron drifts in the ionosphere" by J. A. FEJER . 103

Research Notes:

A. P. MITRA and R. E. JONES: The enhancement of ionospheric ionization during solar flares 104

W. D. PARKINSON: Atmospheric space charge (followed by comments by J. A. CHALMERS) 106

A. H. DE VOOGT: The use of earth-potential measurements for magnetic- and ionospheric storm-indication 108

Book Reviews 111

Notice: Proceedings of the 3rd Meeting of the Joint Commission on the Ionosphere (1952) 116

No. 3

JOHN M. KELSO: Group height calculations in the presence of the earth's magnetic field 117

MARCEL NICOLET: The aeronomic problem of oxygen dissociation 132

E. V. APPLETON and W. R. PIGGOTT: Ionospheric absorption measurements during a sunspot cycle 141

J. A. RATCLIFFE: The analysis of fading records from spaced fading experiments . . 173

GORDON NEWSTEAD: The determination of the velocity of winds from spaced fading experiments 182

Book Reviews:

Kosmische Strahlung. Edited by W. HEISENBERG (reviewed by P. M. S. BLACKETT) . 186

The Physics of the Stratosphere, by R. M. GOODY (reviewed by A. P. MITRA) . . . 187

Obituary: Sir NELSON JOHNSON by Dr. O. G. SUTTON 188

No. 4

K. BULLOUGH and T. R. KAISER: Radio reflections from aurorae 189

W. R. PIGGOTT: On the interpretation of the apparent ionization distribution in the ionosphere 201

W. H. BENNETT and E. O. HULBERT: Magnetic self-focussed solar ion streams as the cause of aurorae 211

N. C. BARFORD, G. DAVIS, A. J. HERZ, R. M. TENNENT and D. A. TIDMAN: High-altitude free balloon flying 219

S. V. CHANDRASHEKHAR AIYA: Measurement of atmospheric noise interference to broadcasting 230

Research Notes:

A. OMHOLT: Electron density in the *E*-layer during auroral displays deduced from measurements of absolute brightness of the auroral luminosity 243

G. A. M. KING: Electron distribution in the ionosphere 245

K-indices of geomagnetic activity from the observatories at Abinger, Eskdalemuir and Lerwick, from March to June, 1954 247

Book Reviews 250

Nos. 5/6

RITA C. SAGALYN and GERARD A. FAUCHER: Aircraft investigation of the large ion content and conductivity of the atmosphere and relation to meteorological factors . 253
W. J. G. BEYNON and K. DAVIES: Simultaneous ionospheric absorption measurements at widely separated stations 273
N. J. SKINNER and R. W. WRIGHT: F_2-layer regularities at Ibadan 290
F. F. GARDNER: Ionospheric thermal radiation at radio frequencies. II. Further observations 298
C. A. SHAIN and A. P. MITRA: Effects of solar flares on the absorption of 18·3 Mc/s cosmic noise 316
D. R. BATES and A. DALGARNO: Theoretical considerations regarding the dayglow . 329
Research Notes:
PATRICK J. NOLAN: The disappearance of condensation nuclei in a sealed room: Remarks on a paper by SMITH and SCHILLING 345
D. R. BARBER: Note on the seasonal variation of sodium D-line emission in twilight . 347
E. V. APPLETON: The anomalous equatorial belt in the F_2-layer 348
H. A. WHALE: Determination of electron densities in the ionosphere from experimental h', f curves 351
K-indices of geomagnetic activity from the observatories at Abinger, Eskdalemuir and Lerwick, for July and August, 1954 353
Book Reviews:
Millimicrosecond Pulse Techniques, by I. A. D. LEWIS and F. H. WELLS (reviewed by B. COLLINGE) 351
A Textbook of Radar. Edited by E. G. BOWEN (reviewed by R. L. SMITH-ROSE) . . 354
Probability and Information Theory, with Applications to Radar, by P. M. WOODWARD (reviewed by R. L. SMITH-ROSE) 355

AUTHOR INDEX TO VOLUME 5

(B) denotes a book review

AITKEN, A. C. p. 113 (B)
AIYA, S. V. C. p. 230
APPLETON, E. V. pp. 115 (B), 141, 348
ASHBURN, E. V. p. 83
BARBER, D. R. p. 347
BARFORD, N. C. p. 219
BATES, D. R. p. 329
BECKER, UDO p. 70
BENNETT, W. H. p. 211
BEYNON, W. J. G. p. 273
BLACKETT, P. M. S. p. 186 (B)
BROWN, R. A. p. 92
BULLOUGH, K. p. 189
BURGESS, R. E. p. 112
COLLINGE, B. p. 354 (B)
CURRAN, S. C. p. 114 (B)
DALGARNO, A. p. 329
DAVIES, K. p. 273
DAVIS, G. p. 219
DENISSE, J. F. p. 70
FAUCHER, G. A. p. 253
FEJER, J. A. p. 103
GARDNER, F. F. p. 298
GERSON, N. C. p. 67
HERZ, A. J. p. 219
HULBURT, E. O. p. 211
HUNTEN, D. M. pp. 44, 57
JONES, R. E. p. 104
KAISER, T. R. p. 189
KELSO, J. M. pp. 11, 117
KING, G. A. M. p. 245
MITRA, A. P. pp. 28, 104, 187 (B), 316
NAISMITH, R. p. 73
NEWSTEAD, G. p. 182
NICOLET, MARCEL p. 132
NOLAN, P. J. p. 345
OMHOLT, A. pp. 63, 243
PANETH, F. A. p. 115 (B)
PARKINSON, W. D. p. 106
PIGGOTT, W. R. pp. 141, 201
RATCLIFFE, J. A. p. 173
ROSENHEAD, LOUIS p. 112 (B)
RUNCORN, S. K. p. 250 (B)
SAGALYN, RITA C. p. 253
SHAIN, C. A. p. 316
SKINNER, N. J. pp. 92, 290
SMITH-ROSE, R. L. pp. 111 (B), 252 (B), 354 (B), 355 (B)
SUTTON, O. G. pp. 188, 250 (B)
TENNENT, R. M. p. 219
TIDMAN, D. A. p. 219
VOOGT, A. H. DE p. 108
WELLER, R. I. p. 1
WHALE, H. A. p. 351
WRIGHT, R. W. pp. 92, 290

VOL. 5 1954

Journal of Atmospheric and Terrestrial Physics, 1954, Vol. 5, pp. 1 to 10. Pergamon Press Ltd., London

The intensity of beta ray ionization of potassium, uranium, and thorium

RICHARD I. WELLER*

Fordham University, New York

(*Received* 7 *December* 1953)

ABSTRACT

A study of the absolute intensity of beta ray ionization from potassium salts and the ores of uranium and thorium is presented. Ratios of beta to gamma radiation above an infinite body were calculated for these substances. Close to the surface of the earth, beta radiation is calculated to cause much more ionization than gamma radiation. The beta radiation decreases so rapidly that above 100 cm the gamma rays are the principal ionizers from the earth.

INTRODUCTION

The contribution of the beta radiation from the earth to the ionization of the atmosphere has never been directly determined on an absolute basis. This research was undertaken to supply the physical constants necessary for such a determination. In making analyses of the ionization in the lowest regions of the atmosphere, it has been necessary to make assumptions regarding the rate of ion formation and its variation with height (HESS, 1933; CHALMERS, 1946). The principal radioactive substances present in the crust of the earth which can emit beta radiation are potassium and the disintegration products of uranium and thorium.

The number of ion pairs formed per cubic centimetre per second by the gamma rays from m grams of a radioactive substance at a distance r is given by

$$q = K \frac{m}{r^2} e^{-\mu r} \tag{1}$$

where μ is the linear coefficient of absorption and K is a constant known as "Eve's constant" (EVE, 1906). The effects of a continuous distribution of energy from the beta particles of most naturally radioactive elements and the phenomenon of scattering combine in such a manner that beta radiation obeys the exponential absorption law of eq. (1) to a good approximation.

From eq. (1), the ionization produced above an infinite plane body containing uniformly distributed homogeneous radioactive matter, is given by

$$q = 2\pi \cdot \left[\frac{K}{\mu/\rho}\right] \cdot f \tag{2}$$

where ρ represents the density and f, the content of the radioactive matter in grams per gram of the body. It is evident from eq. (2) that the ratio of Eve's constant, K, to the mass absorption coefficient, (μ/ρ), must be known in order to calculate the ionization over the surface of a body such as the earth. When radiation comes from a number of radioactive products in equilibrium, as does the

* Now at the State University Maritime College, Fort Schuyler, New York.

radiation from the ores of uranium and thorium, the mass absorption coefficient does not have a single, fixed value. Although Eve's constant, K, cannot be defined for these substances, Eve's constant divided by the mass absorption coefficient, or $K\rho/\mu$, has a definite physical meaning, and the latter quantity was determined for the uranium and thorium ores.

METHODS

A flat rectangular ionization chamber, 30 cm × 30 cm × 8·0 cm, with aluminium foils of 9·00 mg/sq cm thickness at top and bottom, was connected to a shielded Lindemann-Ryerson electrometer to allow sensitive ionization measurements to be made over extended areas. The ambient background radiation in the laboratory was reduced from approximately 19 I* to 8 I by permitting radon-free air to flow through the chamber before measurements were taken and by surrounding the chamber with iron shielding two inches in thickness. The ionization from the substances measured was at least 40 I above background.

The investigation was carried out with thick layers of the radioactive substances placed immediately beneath the ionization chamber. "Infinite thickness" layers were determined by making a series of measurements on varying thicknesses of fine grained salts and ores. The total ionization measured was due to the combined effects of beta and gamma rays from the salt plus the background radiation. The beta rays were then cut off by an aluminium shield, 888 mg/sq cm in thickness, and the ionization due to gamma rays and the natural background was thus measured. Then, the ionization caused by the beta rays was taken as the difference between the observations with and without the shield. The absorption and scattering of the beta rays by the chamber and by the intervening air, as well as gamma ray absorption, were taken into account in the calculations.

VOL. 5 1954

EXPERIMENTAL PROCEDURE

Potassium

A large area of potassium salt was required to furnish a satisfactorily measurable amount of ionization. Therefore, a long series of measurements was made with thicknesses of the fine granular salt varying from 1·0 mm to 23·7 mm, at a uniform area of 30 cm × 30 cm immediately below the chamber. The variation of measured ionization with salt thickness at a uniform distance between bottom of chamber and top of salt of 5·0 cm is given in Fig. 1. It is evident that the measured ionization increased with thicknesses of the layer of salt until a thickness of 4·0 mm was reached, when the ionization assumed a fixed value and remained constant for greater thicknesses; i.e., "infinite salt thickness" had been attained. SCHWEITZER and STEIN (1950) give a rather extensive bibliography of references which confirm the shape of this curve for a salt in which the radioactive material is uniformly distributed throughout the mass. A mean infinite thickness activity of 43·6 I above background for potassium sulphate was determined from the plateau of Fig. 1.

The same series of measurements was repeated with potassium chloride, giving

* I represents ion pairs per cubic centimetre per second.

a value greater by a factor of 1·171. The ratio of the potassium contents of the two salts is 1·169. This shows a high degree of consistency between the two independent series of measurements and also indicates freedom from radioactive impurities.

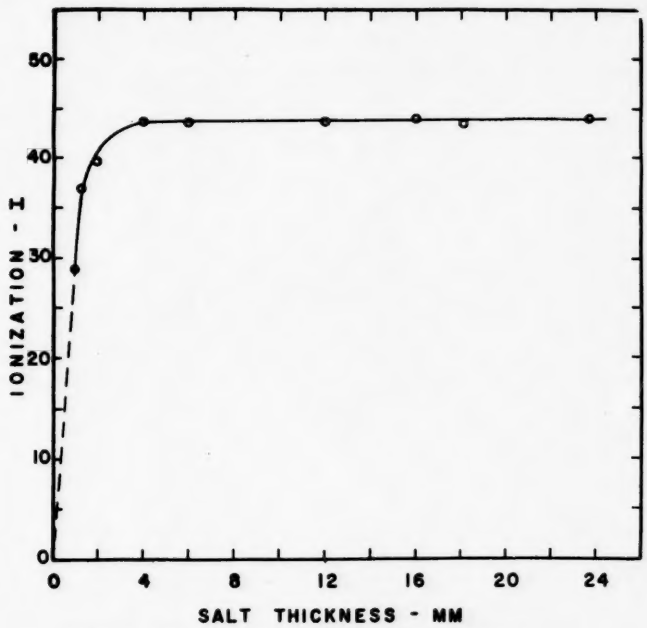

Fig. 1. Variation of ionization with K_2SO_4 thickness

Uranium Ore

The sample of uranium, a native pitchblende ore from Joachimstahl in equilibrium with its decay products, had been analyzed by J. P. MARBLE and E. RONA, and was known to contain 45·7 per cent by weight of uranium and to be free of thorium (HESS, BURNS, and PARKINSON, 1952). Since the uranium ore was much more active than the potassium salts, measurements had to be made of small areas of infinite thickness placed under the centre of the ionization chamber. The area of the source was defined by a sheet of brass in which progressively larger holes were drilled. The brass was held just above the uranium ore.

The curve of ionization plotted against source area, Fig. 2, allowed the mean ratio of ionization to area to be determined. Because of the relatively small areas of radioactive ore exposed compared to the area of the base of the chamber, the curve of ionization against source area is linear; the slope of the line gave an ionization per unit area, $(q/S) = 101\ I$/sq cm. Some of the gamma radiation from the uranium ore is absorbed by the 888 mg/sq cm aluminium sheet. Most of this comes from the entire body of the ore, not only through the hole in the brass sheet. It is therefore independent of the size of this hole. For this reason, the line does not pass through the origin in Fig. 2. The absorption of gamma rays is allowed for by using the slope of the line.

Thorium Ore

The thorium sample was a natural thorite ore from India, containing 9·61 per cent thorium and 0·5 per cent uranium by weight, and was obtained through the

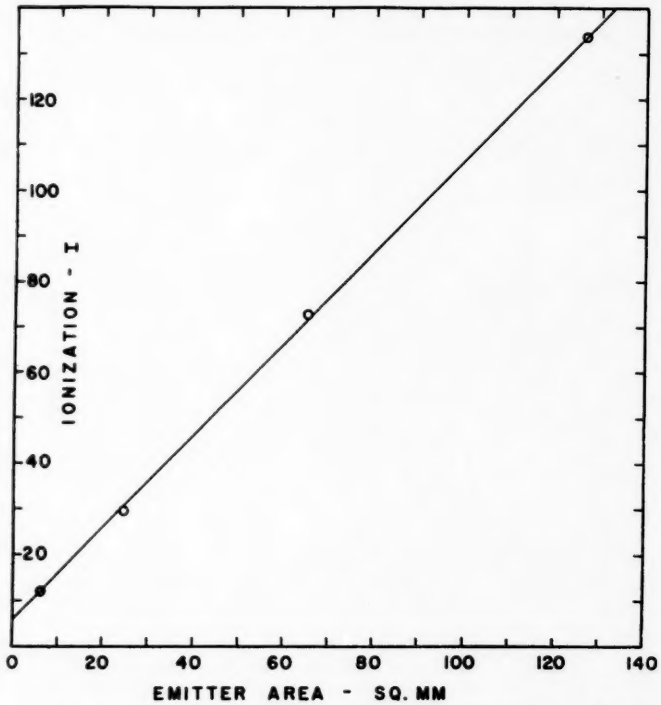

Fig. 2. Variation of ionization with area of uranium emitter

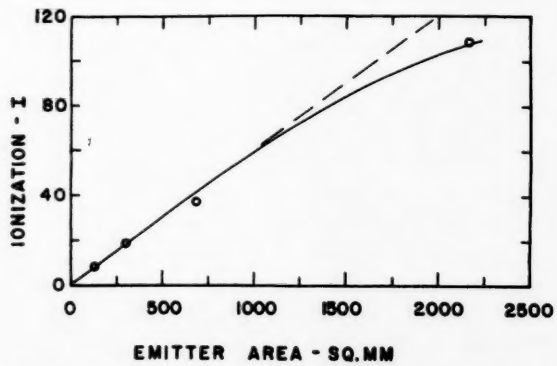

Fig. 3. Variation of ionization with area of thorium emitter

courtesy of L. F. CURTISS of the National Bureau of Standards, Washington, D.C. Using the results reported in the preceding paragraph, a correction was made for the presence of the uranium. Since the thorium was considerably weaker in

VOL. 5 1954

the intensity of its beta radiation than the uranium, larger areas of the thorium ore were required for suitable measurements. Because of these larger areas, the curve of Fig. 3 showing the variation of ionization with area is linear only for the smaller areas. The larger area measurements show the decrease of ionization when the source extends further from the centre of the chamber.

Computations

Geometrical considerations based on eq. (1), show that the measured ionization at a point P from that part of the radioactive material subtending a solid angle dw, is

$$dq_P = K\rho f \int_R^\infty \frac{e^{-\mu(r-R)}}{r^2} e^{-\mu_a R} r^2 \, dr \, dw \tag{3}$$

$$= \frac{K\rho f}{\mu} e^{-\mu_a R} \, dw \tag{4}$$

where μ is the absorption coefficient in the salt, while μ_a denotes the absorption coefficient in air, and R is the distance from the point P to the surface of the salt.

If the source is small and of area S, then

$$dw = S \cos\theta / R^2 \tag{5}$$

and

$$q_P = (K\rho f/\mu)\,(e^{-\mu_a R}/R^2)\, S \cos\theta \tag{6}$$

where θ is the angle between the line joining P to the source and the normal to the surface. If V is the volume of the ionization chamber and e, the charge of an electron, then the measured ionization current is

$$i = e \int_V q_P \, dV \tag{7}$$

the integral being taken over the entire volume of the ionization chamber. So that for a small source

$$i = eS \frac{K\rho f}{\mu} \int_V \frac{e^{-\mu_a R}}{R^2} \cos\theta \, dV \tag{8}$$

or

$$i = (eSK\rho f/\mu) \, . \, F \tag{9}$$

The integral defining F cannot be evaluated in finite terms. However, by a combination of graphical and numerical methods, it can be evaluated for any particular position of the source.

Let the value of F at a point 9 cm below the centre of the chamber be F_0. This was the position used for the uranium ore, so that in this case

$$\frac{K\rho}{\mu} = \frac{i}{eSfF_0} = \frac{qV}{SfF_0} \tag{10}$$

where q is the measured ionization, i.e., the average ionization throughout the chamber. The integral function, F_0, based on the geometry of the apparatus was calculated to be 29·8 cm, and the total volume of the chamber, V, was 7200 cc.

The effects of scattering and absorption of beta radiation were experimentally determined. Together, they introduced a correction factor of 0·995. From the graph of measured ionization plotted against source area for uranium, Fig. 2, (q/S) was 101 I/sq cm, which reduces to 100·5 I/sq cm, after applying the 0·995 correction factor. Therefore, for the uranium ore itself

$$\frac{K\rho}{\mu} = 53{,}200\, I \tag{11}$$

The value of Eve's constant divided by the mass absorption coefficient for the beta radiation from the thorium ore was experimentally determined to be 13,200 I in the same manner as for the uranium ore.

In order to measure the low radiation intensity of potassium, it was necessary to use extended areas of the salts, making the computations somewhat more involved. From eq. (9), for an extended source

$$i = \frac{eK\rho f}{\mu}\int_S F\, dS \tag{12}$$

so that

$$\frac{K\rho}{\mu} = \frac{qV}{f\int_S F\, dS} \tag{13}$$

where q is the observed ionization due to the potassium salt. The quantity F as a function of position was determined in terms of F_0 (the value at the centre) by measuring the ionization due to a "point source" of radiation at various positions. Since F_0 has been calculated, this evaluates $\int F\, dS$, so that all factors on the right side of eq. (13) are known.

The "point source" of radiation consisted of uranium ore shielded by 75·0 mg/sq cm of aluminium. This approximately simulated the hardness of the beta radiation of potassium. A small cylindrical brass holder containing the uranium was symmetrically placed in a large number of locations under the chamber for the observations. The resulting calculations for a test using only one-fourth as many point locations gave close agreement.

The value of $(K\rho/\mu)$ was calculated to be 32·9 I from eq. (13). Since the beta radiation from potassium arises from one nuclear disintegration, a single, constant value of the mass absorption coefficient could be determined, and this was found to be 10·3 sq cm/gm. This value is in good agreement with the results of BRAMLEY and BREWER (1938), who found the mass absorption coefficient for pure potassium chloride to be 10·4, and KUBAN (1928) found a similar figure. In this case, then, Eve's constant may be evaluated as 340 ion pairs/cm-gm-sec. Therefore, 340 ion pairs would be formed in a volume of one cubic centimetre each second by the beta rays from one gram of potassium as a point source at a distance of one centimetre in air at normal temperature and pressure.

VOL. 5 1954

Ratios of Beta to Gamma Radiation

A comparison may be made between the beta and gamma radiation of the three substances measured.

The gamma ray ionization per gram of pure radium, at a distance of one centimetre in air is $4{\cdot}63 \times 10^9 I$ cm²/gm (Hess and Balling, 1945) (this is Eve's constant as originally defined). Now, if the radium is in an equilibrium mixture with its parent uranium, for every gram of uranium there is $3{\cdot}40 \times 10^{-7}$ gm of radium (Lind and Roberts, 1920). Hence, the ionization (due to gamma rays from the products of radium) per gram of uranium from such a mixture is

$$4{\cdot}63 \times 10^9 \times 3{\cdot}4 \times 10^{-7} = 1570\, I \text{ cm}^2/\text{gm} \tag{14}$$

The gamma radiation from all the products of uranium include those from UX_2, the inclusion of which increases this by about 5% (Hess, Burns, and Parkinson, 1952). Hence, Eve's constant for the gamma rays from uranium (in equilibrium with all its decay products) may be taken as $1650\, I$ cm²/gm.

Using the value of 0·0450 sq cm/gm for the mass absorption coefficient for gamma rays (Hess and Roll, 1948), the quantity $(K\rho/\mu)$ for gamma rays is

$$\frac{1650}{0{\cdot}045} = 36{,}700\, I \tag{15}$$

The ratio of this figure to the corresponding figure for beta rays is of some interest, for it represents the ratio of ions formed by gamma rays to those formed by beta rays above a body containing uranium. Its value is

$$\frac{53200}{36700} = 1{\cdot}45 \tag{16}$$

Hess (1947) measured the gamma radiation from the specimen of thorite and found Eve's constant, $K = 742\, I$ per gram thorium, at unit distance, and the mass absorption coefficient $(\mu/\rho) = 9{\cdot}0418$ sq cm/gm. Therefore, $(K\rho/\mu) = 17{,}700\, I$. Thus, the ratio of Eve's constant divided by the mass absorption coefficient for the beta radiation from the thorium ore to the same quantity for the gamma radiation is 0·746. This is the ratio of the ionization due to beta rays to the ionization due to gamma rays immediately above an infinite body containing uniformly distributed thorite.

The value of K for the beta rays of potassium sulphate may be compared with K for the gamma rays of this salt, which was found by Hess and Roll (1948) to be $K = 0{\cdot}260$ ion pairs/cm-gm-sec. Utilizing the value of the mass absorption coefficient, $(\mu/\rho) = 0{\cdot}0513$ sq cm/gm, determined for gamma rays from potassium by Gleditsch and Graf (1947), the following ratio may be written

$$\frac{(K\rho/\mu)_\beta}{(K\rho/\mu)_\gamma} = 6{\cdot}50 \tag{17}$$

This is the ratio of the ionization due to beta rays to the ionization due to gamma rays immediately above an infinite body containing uniformly distributed potassium.

The ratios given above may be useful, because a determination of both beta and gamma radiation from a rock could be used to determine both the amount of potassium and the total amount of uranium and thorium. Thus, if q_β and q_γ are the ionization due to beta and gamma rays, respectively, and if R_K and R_U are the ratios of the ionization due to beta rays to that due to gamma rays for potassium and for uranium-thorium (i.e., $R_K = 6{\cdot}5$ and $R_U \doteqdot 1$), then

$$\text{ionization due to betas from potassium} = \frac{R_K(q_\beta - R_U q_\gamma)}{R_K - R_U} \tag{18}$$

$$\text{ionization due to gammas from potassium} = \frac{q_\beta - R_U q_\gamma}{R_K - R_U} \tag{19}$$

$$\text{ionization due to betas from U and Th} = \frac{R_U(R_K q_\gamma - q_\beta)}{R_K - R_U} \tag{20}$$

$$\text{ionization due to gammas from U and Th} = \frac{R_K q_\gamma - q_\beta}{R_K - R_U} \tag{21}$$

Hence, with these ratios, measurements of total beta and total gamma ray ionization serve to separate the four components.

VARIATION OF IONIZATION WITH HEIGHT

The ionization at a distance h above the surface of the earth is given by

$$q_h = \frac{2\pi f K \rho}{\mu} \cdot \varphi(\mu_a h) \tag{22}$$

which follows from eqs. (2) and (9), if

$$\varphi(\mu_a h) = e^{-\mu_a h} + \mu_a h \cdot Ei(-\mu_a h) \tag{23}$$

where μ_a represents the coefficient of absorption in air. The function $Ei(-\mu_a h)$ denotes the exponential integral

$$Ei(-\mu_a h) = -\int_{\mu_a h}^{\infty} \frac{e^{-x}}{x}\, dx > 0 \tag{24}$$

$$\infty > \mu_a h > 0$$

The values for the function $\varphi(\mu_a h)$ were taken from a table by KING (1912).

Utilizing the beta radiation constants determined in this study and the gamma radiation constants previously quoted, theoretical curves of the decrease of ionization from the earth with increasing height above the earth are presented in Fig. 4 for an intermediate igneous type of rock, assumed to contain $1{\cdot}4 \times 10^{-6}$ gm uranium/gm rock, $4{\cdot}4 \times 10^{-6}$ gm thorium/gm rock, and $1{\cdot}8 \times 10^{-2}$ gm potassium/gm rock.

It is evident that in this case very close to the surface of the earth, most of the earth radiation is caused by beta rays. With increasing height, the beta radiation falls off rapidly and then the gamma radiation predominates. Above approximately 100 cm the contribution of beta radiation to the total ionization becomes negligible.

VOL. 5 1954

Conclusions

The physical constants for beta radiation determined in this investigation, with an estimate of their probable errors, were:

1. For normal potassium (not enriched), Eve's constant, $K = 340 \pm 20$ ion pairs/cm-gm-sec, and Eve's constant divided by the mass absorption coefficient, $(K\rho/\mu) = 33 \pm 2\ I$.

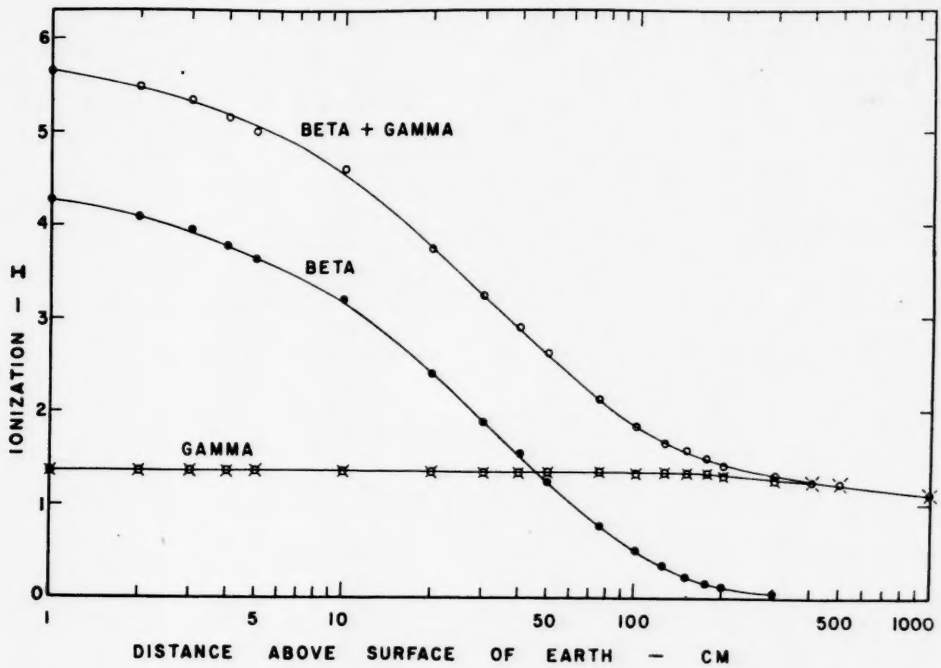

Fig. 4. Variation of ionization with height

2. For naturally occurring uranium ore in equilibrium with its decay products, Eve's constant divided by the mass absorption coefficient,

$$(K\rho/\mu) = 53{,}200 \pm 3{,}200\ I$$

3. For naturally occurring thorium ore in equilibrium with its decay products, Eve's constant divided by the mass absorption coefficient, $(K\rho/\mu) = 13{,}200 \pm 800\ I$.

By utilizing the gamma radiation constants determined by other investigators for the same radioactive substances, the ratios of the ionization due to beta rays to the ionization due to gamma rays above an infinite body containing uniformly distributed radioactive matter were calculated for uranium ore, thorium ore, and potassium to be 1·45, 0·746, and 6·50, respectively.

For an "average rock," up to about 40 cm above the surface of the earth, beta radiation appears to cause more ionization of the atmosphere than gamma radiation from the earth. Above 40 cm, the reverse is true.

Acknowledgments—I take pleasure in expressing my gratitude to Dr. VICTOR F. HESS for his kind guiding interest and ever ready assistance. Also, I am grateful to Dr. W. DUDLEY PARKINSON for his constant friendly advice during the course of this investigation. The research reported in this paper has been sponsored by the Geophysics Research Directorate of the Air Force Cambridge Research Centre, Air Research and Development Command, under Contract No. AF19(122)–409.

REFERENCES

BRAMLEY, A. and BREWER, A. K.	1938	Phys. Rev. **53**, 502
CHALMERS, J. A.	1946	Quart. J. R. Met. Soc. **72**, 312–313, 199
EVE, A. S.	1906	Phil Mag. **12**, 189
GLEDITSCH, E. and GRAF, T.	1947	Phys. Rev. **72**, 640
HESS, V. F.	1933	Gerlands Beitr. z. Geophys. **2**, 95
HESS, V. F.	1947	Norsk geologisk tidsskrift **27**, 1
HESS, V. F. and BALLING, E. M.	1945	Trans. Amer. Geophys. Union **26**, 237
HESS, V. F., BURNS, W. F., and PARKINSON, W. D.	1952	Trans. Amer. Geophys. Union **33**, 657
HESS, V. F. and ROLL, J. D.	1948	Phys. Rev. **73**, 916
KING, L. V.	1912	Phil, Mag. **23**, 242
KUBAN, M.	1928	Sitzber. Akad. Wiss. Wein, Math-naturwiss. Kl. **137** (2a), 5–6, 241
LIND, S. C. and ROBERTS, L. D.	1920	J. Amer. Chem. Soc. **42**, 1170
SCHWEITZER, G. K. and STEIN, B. R.	1950	Nucleonics **7**, 3, 65

VOL.
5
1954

Journal of Atmospheric and Terrestrial Physics, 1954, Vol. 5, pp. 11 to 27. Pergamon Press Ltd., London

The determination of the electron density distribution of an ionosphere layer in the presence of an external magnetic field*

JOHN M. KELSO

Ionosphere Research Laboratory, The Pennsylvania State University
State College, Pennsylvania

(*Received* 30 *November* 1953)

ABSTRACT

An accurate method is given for the determination of the electron density distribution of an ionosphere layer in the presence of an external magnetic field. The shape of the layer is determined in the process of calculation, and is *not* assumed in advance.

Estimates of the thickness and height of the maximum ionization of a layer made by determining the electron density distribution using techniques which neglect the magnetic field are too great by 15 to 20%; i.e., in place of a correct scale height of 8 km, such methods yield a scale height of nearly 10 km. A careful application of the present procedure reduces such overestimation to 2 or 3%.

Methods which assume a particular form of layer, usually parabolic, are subject to great possible errors, depending upon the degree to which the actual layer departs from parabolic form. When the magnetic field is neglected, the errors in thickness found in this way can be too large by a factor of two or three. Even when the magnetic field is considered, such methods can give thicknesses in error by a factor of as much as two. These methods usually give values of the height of maximum ionization which are much better than the values they yield for the thickness. This, however, may depend upon accidental fluctuations in the group path curve.

In the present paper, the electron density distribution is determined by finding the actual heights at which waves of various frequencies are reflected. These true heights are obtained from experimental h'-f curves by obtaining the exact solution, as a convergent series of integrals, of the integral equation giving the group height as a function of frequency. The errors arising in the numerical work are shown by applying the procedure to h'-f curves obtained theoretically from layers of known shape, and such errors are seen to be small compared with those made through use of other procedures.

1. INTRODUCTION

One of the basic problems of ionospheric research is to determine the height variations of the electron density in an ionosphere layer. Because of the simple relation between electron density and reflected frequency, this problem is equivalent to the determination of the height at which various frequencies are reflected. This height is called the "true-height" of reflection, h_T.

Various methods have been devised by BOOKER and SEATON (1939), APPLETON and BEYNON (1940), and others, for the determination of some of the characteristics of an ionosphere layer on the assumption that the layer is of parabolic form, or some other simple form. As originally proposed, these methods do not include the effect of the earth's magnetic field, but they can be modified as indicated by FRIEDMAN (1950) and by SHINN and WHALE (1952) to include this effect.

APPLETON (1930) and DE GROOT (1930) showed that, in the absence of an external magnetic field, the expression for the group height, h', as a function of frequency can be put in the form of ABEL's integral equation (1881). From the solution of this integral equation, given by ABEL a century earlier, the true-height can be determined directly as an integral involving the h'-f curve. This result was discussed and applied by RYDBECK (1939) (1942), PEKERIS (1940), and others, using planimetric integration or other graphical procedures to evaluate the rather large

* The research reported in this paper has been sponsored by the Geophysics Research Division of the Air Force Cambridge Research Centre, Air Research and Development Command, under Contract AF 19 (122)-44.

number of integrals involved. As the method used by these workers required the plotting of many graphs to a new scale before the planimetric integration, it was clear that a more efficient procedure would be desirable. Improvements were made by WHALE (1951), who showed how the integrals could be evaluated rapidly, and without plotting secondary curves, through use of a differential analyzer. KRAUS (1950) provided an efficient method of numerical integration obtained through use of the Gauss-Christoffel quadrature formula (hereafter referred to as the GC formula). This application of the GC formula was extended by KELSO (1952), who obtained an even simpler procedure for the numerical evaluation of the required integral. These last three techniques eliminate the necessity for the numerous intermediate curves, and are applied directly to a single h'-f curve. Using the procedure given by KELSO, it is possible to make a complete determination of the true-height as a function of frequency, from an experimental h'-f curve, in about fifteen minutes using a simple adding machine. Using a sufficient number of points, the errors in the *integration formula* can be made as small as desired (except exactly at a frequency where the h'-f curve has a singularity, which is not a condition which experimental determinations of delay times are capable of reproducing in detail), so that the integration procedure is limited only by the accuracy with which the experimental curve can be read.

All of these procedures based on ABEL'S integral equation, however, are restricted through neglect of the earth's magnetic field. WHALE (1951) attempted to include this field by assuming that the ratio of gyrofrequency to operating frequency is constant, and then transforming the frequency in such a way that ABEL'S integral equation is again obtained. Unfortunately, an error was made in transforming the frequency, so that the method is not correct, although the results appear to be quite reasonable.

In the present paper, we set up the complete integral equation appropriate to the inclusion of the earth's field. The solution of the integral equation is then obtained as a convergent series of integrals. These can be evaluated by use of a differential analyzer, if such a machine is available. Since this equipment is rare in ionospheric laboratories, recourse is made to the use of the GC formula, which is applied three times. With this procedure, it is possible to find the height variation of electron density with an error which is small compared with that made by neglecting the earth's field.

This procedure is applied to three model layers so that the errors can be studied. In the numerical work, we use WHALE'S restriction of a constant ratio of gyrofrequency to operating frequency. This is not required by the mathematical results, but simplifies the work considerably, without introducing very large errors, as noted in the third example, below. In this third example, we analyze a group height curve for a parabolic layer as given by SHINN and WHALE, where they included the variation of the ratio of gyrofrequency to operating frequency. For such a layer with a semi-thickness of 50 km, the electron density curve deduced by the present procedure is displaced by about 1 to 1·5 km above the correct curve given directly by the model. This is to be compared with errors of up to 14 km obtained when the magnetic field is neglected. An experimental curve for the E-layer is also analyzed.

VOL. 5 1954

Although the present method improves the accuracy to a very considerable extent, it is, unfortunately, rather tedious, requiring about as much labour as the methods of planimetric integration, which, however, neglect the magnetic field. For this reason, this technique cannot be recommended for routine use, but rather it is intended for special studies where the layer shape is to be determined with precision. For more routine purposes, an application of the procedures neglecting the magnetic field, or an adaptation of the BOOKER-SEATON or APPLETON-BEYNON technique is indicated.

This work is all carried out under the usual assumptions that the index of refraction is real (zero collisions) and that the electron density increases monotonically with height. These assumptions have been studied in some detail by RYDBECK (1944) and MANNING (1949), respectively. The signal is assumed to be propagated vertically upward in a horizontally stratified ionosphere.

2. CALCULATIONS IN THE ABSENCE OF THE MAGNETIC FIELD

In this section we wish to present the Gauss-Christoffel quadrature formula, and then to show how it may be applied to evaluating the solution of ABEL'S integral equation.

(*A*) *Gauss-Christoffel Quadrature Formula*

Let us suppose that there is some given, non-negative, function $w(x)$, called a weight function, such that over some interval $a \leq x \leq b$, the integral,

$$\int_a^b w(x)\,\mathrm{d}x, \tag{1}$$

exists. Suppose that $p_n(x)$ is a polynomial of degree n from a set of polynomials orthogonal over the interval (a, b) with weight function $w(x)$; and let x_i be the n roots of this polynomial. Then the GC formula can be stated as follows:

If $g(x)$ is an arbitrary polynomial of degree $2n - 1$, then there exist real numbers $\lambda_1, \lambda_2, \cdots, \lambda_n$, such that,

$$\int_a^b g(x)\,w(x)\,\mathrm{d}x = \lambda_1 g(x_1) + \lambda_2 g(x_2) + \cdots + \lambda_n g(x_n). \tag{2}$$

The numbers λ_i are uniquely determined by the weight function $w(x)$, the degree n, and the interval (a, b).

It should be noted that, under the prescribed conditions, the relation in (2) is *exact*, and is *not approximate*. If $g(x)$ is not a polynomial of the specified degree (or of a lower degree) then the right-hand side of (2) is an approximation to the integral on the left, and is *equivalent* to the result obtained by approximating, in a least squares sense, the function $g(x)$ by a polynomial of degree $2n - 1$ and integrating the approximating polynomial exactly. That such approximations can be made, in principle, is shown by WEIERSTRASS'S theorem (1903), which can be stated roughly by saying that, in a closed interval, any continuous function $g(x)$ can be approximated by a polynomial of degree m to within any predetermined limits, provided that the value of m is taken to be sufficiently large. It should be made clear, however, that the GC procedure does *not* require us to determine the approximating

polynomial *explicitly*. In the above sense, we may say that, using our n points in the prescribed way, we get the same accuracy obtained by other numerical integration formulas using, say, almost twice as many $(2n - 1)$ equally spaced points.

The constants λ_i in (2) are given by,

$$\lambda_i = \int_a^b \frac{p_n(x)}{p_n'(x_i)\,(x - x_i)}\, w(x)\, dx, \quad i = 1, 2, \cdots, n, \tag{3}$$

where the prime (′) denotes differentiation with respect to x. The polynomials, $p_n(x) = \sum_{i=0}^{n} a_i x^i$, may be determined by solving the n equations,

$$\sum_{k=0}^{n} a_k \int_a^b x^{j+k} w(x)\, dx = 0, \quad j = 0, 1, 2, \cdots, n - 1 \tag{4}$$

Since there are $n + 1$ coefficients, a_k, we obtain the last n of these in terms of the first, a_0. This coefficient could also be evaluated by requiring the polynomials to be normalized. However, this normalization is not required in the evaluation of λ_i, and we can take $a_0 = 1$.

A detailed proof of the GC formula was given by FRIEDMAN (1950).

(B) Application to the True Height Problem

The GC formula was applied to the solution of ABEL's integral equation by KELSO (1952), with the following result. To find the true-height at some given frequency f_v, i.e., to find $h_T(f_v)$, using experimental values of group height as a function of frequency, $h'(f)$, in the absence of the earth's magnetic field, we evaluate,

$$h_T(f_v) = \frac{1}{n} \sum_{k=1}^{n} h'(f_k), \tag{5}$$

where

$$f_k = f_v \cos \theta_k, \tag{6}$$

and where,

$$\theta_k = \frac{2k - 1}{2n}\, \pi, \quad k = 1, 2, \cdots, n. \tag{7}$$

For $n = 5$ and $n = 10$, the values of $\cos \theta_k$ are:

Table 1

$n = 5$	$n = 10$	
0·9877	0·9969	0·6945
0·8910	0·9724	0·5225
0·7071	0·9239	0·3827
0·4540	0·8526	0·2334
0·1564	0·7604	0·0785

VOL. 5 1954

Thus, to find $h_T(f_v)$, we average the values of $h'(f_k)$ at a set of n frequencies $f_k = f_v \cos \theta_k$, where the $\cos \theta_k$ are given for $n = 5$ and $n = 10$ in Table 1. If extensive use of this procedure is to be made, the process is simplified by tabulating the values of f_k corresponding to a suitable set of frequencies f_v. As an extreme test the author has applied the above results for $n = 10$ to the well-known equation for the h'-f curve for a parabolic layer in the absence of a magnetic field. Since the given function is logarithmic and has a singularity at the critical frequency, it is clearly not of polynomial form, so that the procedure becomes progressively worse as the frequency approaches the critical frequency. Carrying 10 significant figures gives the following results: (a) at $f = 0{\cdot}9f_c$, we get an error of 1 in the ninth significant figure; (b) at $f = 0{\cdot}95f_c$, we get an error of 2 in the sixth significant figure; (c) at $f = f_c$, we get an error of 3·5%.

This whole procedure has been criticized by MANNING (1953), who asserts that it is "a very rough form of integration, in error for second degree polynomials," and that it is futile because of the fact that the data are obtained as empirical values, and, therefore, are not of polynomial form. Since these criticisms have been discussed and refuted in detail by SHINN (1953) and KRAUS (1953), we merely note here that reference to the preceding paragraph and to WEIERSTRASS'S theorem will indicate the unreliability of MANNING'S comments.

3. WHALE'S METHOD FOR INCLUDING THE EARTH'S MAGNETIC FIELD (1951)

Neglecting collisions, the group height of reflection of a signal of frequency f, incident at height $z = 0$ at the bottom of a layer, and reflected at the height z_r, is given by

$$h'(f) = \int_0^{z_r} \mu'(z)\, dz, \tag{8}$$

where μ' is the group index of refraction.

In the absence of an external magnetic field, (8) may be written,

$$h'(f) = \int_0^{z_r} \frac{dz}{\sqrt{1 - f_0^2/f^2}} \tag{9}$$

where $f_0^2 = Ne^2/\pi m$.

In the presence of an external magnetic field, μ' can be obtained from the magneto-ionic equation in the manner indicated by SHINN and WHALE (1952). Assuming constant values of the ratio of the gyrofrequency ($f_H \sim 1{\cdot}5$ mc/s) to the operating frequency, these authors plotted curves of μ' versus the ratio f_0^2/f^2 for the various parametric values of $y = f_H/f$. WHALE'S approach to the inclusion of the magnetic field was to choose one value of y and to treat the resulting μ' curve as correct for some small spread of frequencies. Several such curves were prepared for different ranges of frequency. Such a curve is given in Fig. 1, below, where we use a value of $y = 1/2$, which is appropriate to an E-layer critical frequency of 3 megacycles. This curve differs very slightly from that given by WHALE, since it is computed for a propagation angle of 19° 8′, while WHALE used an angle of 23° 16′. The corresponding μ' curve for $y = 0$ (no magnetic field) is shown dotted in Fig. 1. It should be noted that we use a reciprocal scale for μ'

in this figure, so that accurate estimates of values of the integrals cannot be made by casual inspection.

The following description of the remainder of WHALE'S procedure is a direct quotation from the original paper, with interpolations in brackets by the present author to replace references to specific equations in the original paper.

"The curve for $y = 0$ represents the conditions under which Eq. [9] holds. It is clearly possible to change any of the other curves into a curve of this shape by

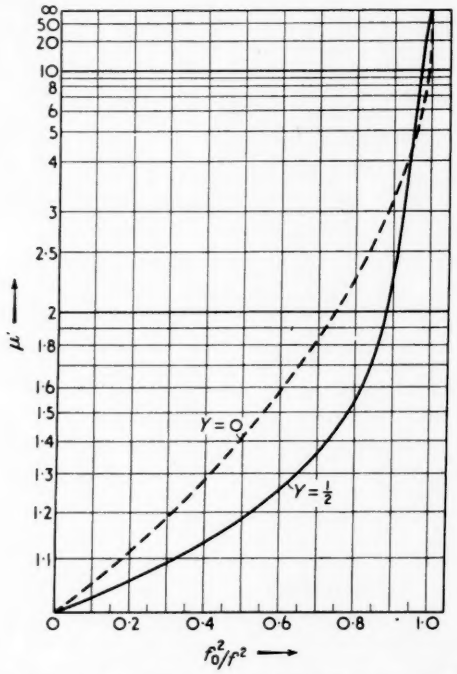

Fig. 1. Group refractive index, μ', for $y = 0$, $y = 1/2$ with propagation angle $\theta p = 19° 8'$.

altering, in a suitable way, the variable plotted along the horizontal axis. This can be done by replacing f by $\zeta(f)$, where $\zeta(f)$ is a complicated function of f. When this has been done, [the expression for μ'] may be written

$$\mu' = \frac{1}{\sqrt{1 - f_0^2(z)/\zeta^2(f)}}."$$

"If it can be assumed that the function ζ retains the same form over a small range of frequencies, say from $y = 1/2$ to $y = 1/3$ (the range which is normally of most interest in investigations of Region E) the integral may be inverted as [when the magnetic field is neglected]."

The difficulty arising here is that to use μ' as given above in ABEL'S integral equation, the variables f_0 and ζ must be essentially independent. However, in making a transformation as described by WHALE, one obtains a quality $\zeta(f_0, f)$, which is a function of both f_0 and f, and not of f alone. Thus, after introducing the

VOL. 5 1954

above expression for μ' into (8), one does not have the simple form of ABEL'S integral equation, so that the inversion of the integral is not possible in the simple manner indicated by WHALE. This, then, appears to invalidate his method.

4. Complete Integral Equation and its Solution

For any given fixed frequency f, there is some curve of μ' versus f_0^2/f^2 as shown in Fig. 1, for an appropriate value of y. At the given frequency, this curve is *exact* within the limitations given in the last paragraph in Section 1, provided that the gyrofrequency remains constant through the region considered. Thus, we can, in principle, obtain μ' for any value of f_0 and f. Let us call this $\mu'(f_0^2, f^2)$, to emphasize that it is a function of both variables. Corresponding to any such value of $\mu'(f_0^2, f^2)$, we can define a new quality $G(f_0^2, f^2)$, as,

$$\mu'(f_0^2, f^2) = \frac{G(f_0^2, f^2)}{\sqrt{1 - f_0^2/f^2}} \tag{10}$$

We write the variables in μ' and G as squares for later convenience. As will be shown below, we do not need to know the actual functional form of $G(f_0^2, f^2)$, but instead will only use sets of values at a small number of discrete points. The values of G will be determined from (10).

Introducing μ' from (10), (8) becomes,

$$h'(f) = \int_0^{z_r} \frac{G(f_0^2, f^2)}{\sqrt{1 - f_0^2(z)/f^2}}\, \mathrm{d}z. \tag{11}$$

Let,

$$\xi(z) = f_0^2(z) \tag{12}$$

$$u(\xi)\, \mathrm{d}\xi = \mathrm{d}z \tag{13}$$

$$F = f^2. \tag{14}$$

Then (11) takes the form,

$$H'(F) = \frac{h'(f)}{f} = \int_0^F \frac{G(\xi, F)\, u(\xi)\, \mathrm{d}\xi}{\sqrt{F - \xi}} \tag{15}$$

This is a form of VOLTERRA'S (1913) integral equation of the first kind with a singular kernel. To obtain a solution, we use a method given by PICARD (1904).

We write,

$$H'(F) = \int_0^F \frac{u(\xi)\, \mathrm{d}\xi}{\sqrt{F - \xi}} + \lambda \int_0^F \frac{[G(\xi, F) - 1]\, u(\xi)\, \mathrm{d}\xi}{\sqrt{F - \xi}} \tag{16}$$

where λ is a parameter. It is clear that as $\lambda \to 1$, (16) reduces to (15), which is the integral equation whose solution is desired. Let,

$$u(\xi) = u_0(\xi) + \lambda u_1(\xi) + \lambda^2 u_2(\xi) + \cdots \tag{17}$$

and substitute this value of $u(\xi)$ into (16). Equating coefficients of like powers of λ on both sides of the equation, we obtain,

$$H'(F) = \int_0^F \frac{u_0(\xi)\,d\xi}{\sqrt{F-\xi}} \tag{18}$$

and

$$\int_0^F \frac{u_n(\xi)\,d\xi}{\sqrt{F-\xi}} = \int_0^F \frac{[G(\xi, F) - 1]u_{n-1}(\xi)\,d\xi}{\sqrt{F-\xi}} \tag{19}$$

The first of these relations has exactly the form of ABEL's integral equation, and can be solved in the well-known manner. Noting from (13) and (17) that we can write,

$$u_0(\xi) = \frac{dz_0}{d\xi}, \cdots, u_n(\xi) = \frac{dz_n}{d\xi}$$

we have the solution of (18) in the form,

$$z_0(f_v) = \frac{2}{\pi}\int_0^{f_v} \frac{h'(f)\,df}{\sqrt{f_r^2 - f^2}}. \tag{20}$$

But this is just the solution which would be obtained by neglecting the effects of the earth's magnetic field. Hence the procedure in Section 2 applies.

Now, multiply both sides of (19) by $dF/\sqrt{(\zeta - F)}$ and integrate from 0 to ζ.

$$\int_0^\zeta \frac{dF}{\sqrt{\zeta - F}}\int_0^F \frac{u_n(\xi)\,d\xi}{\sqrt{F-\xi}} = \int_0^\zeta \frac{dF}{\sqrt{\zeta - F}}\int_0^F \frac{[G(\xi, F) - 1]u_{n-1}(\xi)\,d\xi}{\sqrt{F-\xi}}$$

Applying DIRICHLET's integral formula (VOLTERRA 1913, p. 36) to the left-hand member, we find that,

$$\int_0^\zeta u_n(\xi)\,d\xi \int_\xi^\zeta \frac{dF}{\sqrt{\zeta - F}\sqrt{F-\xi}} = \int_0^\zeta \frac{dF}{\sqrt{\zeta - F}}\int_0^F \frac{[G(\xi, F) - 1]u_{n-1}(\xi)\,d\xi}{\sqrt{F-\xi}} \tag{21}$$

The left-hand member contains the Euler B-integral,

$$\int_\xi^\zeta \frac{dF}{\sqrt{\zeta - F}\sqrt{F-\xi}} = \pi.$$

After differentiation with respect to ζ, (21) becomes,

$$u_n(\zeta) = \frac{-1}{\pi}\frac{d}{d\zeta}\int_0^\zeta \frac{dF}{\sqrt{\zeta - F}}\int_0^F \frac{[G(\xi, F) - 1]u_{n-1}(\xi)\,d\xi}{\sqrt{F-\xi}}$$

Writing,

$$u_n(\zeta) = \frac{dz_n(\zeta)}{d\zeta}, u_{n-1}(\xi) = \frac{dz_{n-1}(\xi)}{d\xi} = z'_{n-1}(\xi)$$

We have, finally,

$$z_n(\zeta) = \frac{-1}{\pi}\int_0^\zeta \frac{dF}{\sqrt{\zeta - F}}\int_0^F \frac{[G(\xi, F) - 1]z'_{n-1}(\xi)}{\sqrt{F-\xi}} \tag{22}$$

VOL. 5 1954

We note that, if we replaced $G(\xi, F) - 1$ by $Q(\xi, F)$, and $z'_{n-1}(\xi)$ by $v(\xi)$ in the second integral, we would have an integral in exactly the form of (15). Thus, this second integral is analogous to a group height as a function of frequency. Hence, if $G(\xi, F)$ is obtained from a curve similar to Fig. 1, for an appropriate value of y, this result will be exact for the given frequency. When the frequency is changed, the value of y should change accordingly. Therefore, the results up to this point are not restricted because of the use of curves such as given by SHINN and WHALE. In application, however, we cannot for practical reasons use a continuous range of y, so that we are restricted by whatever choices are made in the application.

In order to apply the GC formula, we write (22) in the form of two integrals,

$$\phi_{n-1}(F) = \int_0^1 \frac{z'_{n-1}(xF)\,[G(x) - 1]\,dx}{\sqrt{1-x}} \tag{23}$$

$$z_n(f_v) = \frac{-2}{\pi} f_v^2 \int_0^1 \frac{\phi_{n-1}(yf_v)y^2\,dy}{\sqrt{1-y^2}} \tag{24}$$

where

$$\begin{cases} x = \xi/F = f_0^2/f^2, \; F = f^2 \\ y = F/\zeta \\ \zeta = f_v^2 \end{cases} \tag{25}$$

To evaluate (23), we apply the method of Section 2, in order to find a GC formula appropriate to a weight function $1/(1-x)^{1/2}$ over the interval (0, 1). Using five points, and applying direct methods to the evaluation of the constants from (3) and (4),

$$\begin{aligned} \phi_{n-1}(f^2) = {} & 0{\cdot}1338z'_{n-1}(x_1f^2)\,[G(x_1) - 1] + 0{\cdot}2992z'_{n-1}(x_2f^2)\,[G(x_2) - 1] \\ & + 0{\cdot}4382z'_{n-1}(x_3f^2)\,[G(x_3) - 1] + 0{\cdot}5382z'_{n-1}(x_4f^2)\,[G(x_4) - 1] \\ & + 0{\cdot}5905z'_{n-1}(x_5f^2)\,[G(x_5) - 1], \end{aligned} \tag{26}$$

where

$$\begin{cases} x_1 = 0{\cdot}0517 & x_3 = 0{\cdot}5390 & x_5 = 0{\cdot}9779 \\ x_2 = 0{\cdot}2523 & x_4 = 0{\cdot}8125 \end{cases} \tag{27}$$

At this point we must now introduce the numerical values of $G(x_i)$. This requires us for the first time to make a definite choice of the curve of μ' versus f_0^2/f^2, since such a choice was not required previously in the derivation. We choose to define a μ' curve by taking a constant value $y = 1/2$ (reasonably suitable for the E-layer) and a propagation angle of 19° 8′. We then get for $\phi_{n-1}(f^2)$, writing $(f_0^2/f^2)_i = x_i$, and using (10),

$$\begin{aligned} \phi_{n-1}(f^2) = {} & -0{\cdot}00185z'_{n-1}(0{\cdot}0517f^2) - 0{\cdot}02185z'_{n-1}(0{\cdot}2523f^2) \\ & -0{\cdot}07954z'_{n-1}(0{\cdot}5390f^2) - 0{\cdot}1661z'_{n-1}(0{\cdot}8125f^2) \\ & + 0{\cdot}5308z'_{n-1}(0{\cdot}9779f^2) \end{aligned} \tag{28}$$

In the third example below, we use h'-f data from SHINN and WHALE, and for this

purpose, we choose a different μ' curve. In this case, we have a propagation angle of 23° 16′ and use $y = 0{\cdot}32828$ (for a gyrofrequency of 1·149 mc/s and an critical frequency of 3·5 mc/s). Then, instead of (28), we have,

$$\begin{aligned}(28\text{A}) \qquad \phi_{n-1}(f^2) = &-0{\cdot}001401z'_{n-1}(0{\cdot}0517f^2) - 0{\cdot}01670z'_{n-1}(0{\cdot}2523f^2)\\ &-0{\cdot}06208z'_{n-1}(0{\cdot}5390f^2) - 0{\cdot}1362z'_{n-1}(0{\cdot}8125f^2)\\ &+0{\cdot}4204z'_{n-1}(0{\cdot}9779f^2)\end{aligned}$$

Similarly, we evaluate (24), using a GC formula appropriate to the weight function $y^2/(1 - y^2)^{1/2}$ over the interval (0, 1), and, for five points, we obtain,

$$\begin{aligned}(29) \quad z_n(f_v) = &-f_v{}^2[0{\cdot}003685\phi_{n-1}(0{\cdot}1667f_v) + 0{\cdot}02922\phi_{n-1}(0{\cdot}5035f_v)\\ &+ 0{\cdot}08969\phi_{n-1}(0{\cdot}6598f_v) + 0{\cdot}1642\phi_{n-1}(0{\cdot}8696f_v)\\ &+ 0{\cdot}2132\phi_{n-1}(0{\cdot}9851f_v)]\end{aligned}$$

This relation differs from (28) and (28A) in that it does not depend upon the specific choice of the μ' curve. Thus, (29) requires change only if it is desired to increase or decrease the number of points used in the integration.

Then, the procedure for the determination of the true height of reflection is as follows:

(a) Determine the zero-order approximation $z_0(f_v)$ for various values of f_v, using the method given in Section 2, and discussed more fully by KELSO (1952).

(b) Using numerical or graphical differentiation, obtain the derivative,

$$z_0{}'(\zeta) = \frac{\mathrm{d}z_0}{\mathrm{d}\zeta} = \frac{\mathrm{d}z_0}{\mathrm{d}f_v{}^2} = \frac{1}{2f_v}\frac{\mathrm{d}z_0}{\mathrm{d}f_v}.$$

(c) Plotting the result from (b) as a function of f^2, integrate by use of (28), for a sufficient number of f^2 values so that a reasonably well-defined curve of $\phi_0(f^2)$ versus f may be plotted.

(d) Taking the same values of f_v as used in (a), integrate the $\phi_0(f^2)$ versus f curve, using (29). The result is the first correction, $z_1(f_v)$.

(e) Repeat this process using $z_1(f_v)$ in the same manner as $z_0(f_v)$ in order to obtain $z_2(f_v)$, etc.

(f) The true height of reflection at frequency f_v is then given by the sum of all the $z_i(f_v)$, $i = 0, 1, 2, \cdots$

In general, the convergence of this process is assured, according to PICARD. In practice, however, the errors may tend to accumulate, so that the process must be terminated before the next correction step becomes negligibly small. In each of the examples given in the next section, all of the last values of $z_i(f_v)$ were less than 1 kilometre. The rate of convergence is a function of the nearness to the critical frequency, and in the examples in the next section, the convergence was slowest at the critical frequency. Thus, the range of frequencies which must be considered in each repetition of the above process tends to narrow with successive repetitions.

As a differentiation, formula which although crude, seems adequate for most problems of the present type, the author has used the following equation based on

VOL. 5 1954

values at two points equally spaced about the point at which the derivative was desired. Thus,

$$\frac{dy}{dx} = \frac{1}{2\Delta}\{y(x + \Delta) - y(x - \Delta)\}$$

$$\frac{dy}{dx^2} = \frac{1}{2x}\frac{dy}{dx}.$$

5. Applications to Four Examples

We now illustrate the results of applying this procedure to four examples. In the first three cases, we consider theoretical h'-f curves for model layers. In the fourth case, we study an experimental h'-f curve for the E-layer.

The theoretical cases are intended to test the accuracy of the present method, and to compare the results with those obtained by neglecting the magnetic field. In the first two examples, we have used the same restriction ($y = 1/2$) in obtaining the h'-f curves as was applied to the integration formula (28), so that these two examples are tests of the mathematical, but not of the physical, side of the work. The h'-f curve in Example 3 was obtained by using correct values of y for each frequency, so that this does form a test of the physical basis of the procedure.

Example 1. As a first example, we consider a layer whose electron density increases linearly with height, and is such that a frequency of 5 mc/s is reflected at a height of 100 km from the bottom of the layer ($z = 0$). Assuming $y = 1/2$, we integrate the appropriate μ' curve in Fig. 1 in the manner described by Shinn and Whale, using Simpson's rule. For a general linear layer of slope β, where $f_0^2 = \beta z$,

$$h'(f) = 2{\cdot}2906 f^2/\beta \tag{30}$$

In the present case, $\beta = 0{\cdot}25$, so that,

$$h'(f) = 9{\cdot}1642 f^2 \tag{31}$$

Using (5), (6), (31), with $n = 5$ in (5),

$$z_0(f_v) = \frac{1}{n}\sum_{k=1}^{n} h'(f_k) = \frac{9{\cdot}1624}{n} f_v^2 \sum_{k=1}^{n} \cos^2\theta_k$$

$$z_0(f_v) = 4{\cdot}5812 f_v^2$$

Then,

$$\frac{dz_0(f_v)}{df_v^2} = 4{\cdot}5812$$

Introducing this result into (28), we have just 4·5812 times the sum of the coefficients, i.e.

$$\phi_0(f^2) = 4{\cdot}5812\ (0{\cdot}26149) = 1{\cdot}1979$$

Substituting into (29), we have $-1{\cdot}1979 f_v^2$ times the sum of the coefficients, or,

$$z_1(f_v) = -f_v^2(1{\cdot}1979)\ (0{\cdot}5000) = -0{\cdot}59897 f_v^2$$

Repeating this process, we get the true height of reflection, h_T,

$$h_T = f_v^2[4{\cdot}5812 - 0{\cdot}59897 + 0{\cdot}07831 - 0{\cdot}01024 + 0{\cdot}00134] = 4{\cdot}0516 f_v^2$$

The exact value in this case is $h_T = 4f_v^2$, so that we have an error of about 1·3%. When the magnetic field is neglected, we get $h_T = z_0(f_v) = 4{\cdot}5812f_v^2$, which gives an error of about 14·5%. Since all of the steps in this case were carried out exactly the error must be due to the integral formulae used. However, this error cannot arise through use of (29), since only the sum of the coefficients appeared in the result, and this value, 1/2, can be shown to be the correct sum of coefficients for this formula, whatever the number of terms used in the formula. Thus, the only source for this error must arise due to the use of (28). This formula could be improved by using more than five terms, but the improvement would have to come through a greater amount of labour required to apply the formula. This does not seem worth while at the present time.

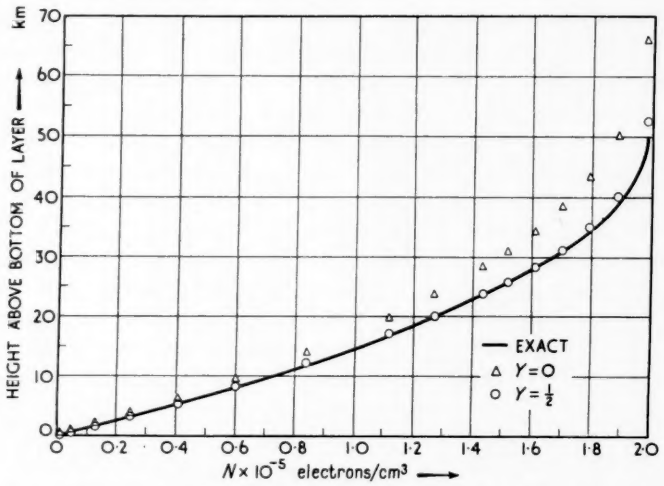

Fig. 2. Electron density for parabolic layer from h'-f curve with $y = 1/2$.

Example 2. The second example to be studied is that of a parabolic layer for which the h'-f curve was obtained by assuming $y = 1/2$, and using a method given by SHINN and WHALE. The layer was assumed to have a half-thickness of 50 km, and a critical frequency of 4·0 mc/s. The true height was obtained by use of terms up to $z_8(f_v)$ for frequencies above 3·7 mc/s, terms up to $z_6(f_v)$ for frequencies above 3·2 mc/s, terms up to $z_4(f_v)$ for frequencies greater than 2·2 mc/s, and terms up to $z_2(f_v)$ for frequencies in excess of 1·0 mc/s. The electron density corresponding to each frequency was obtained by use of the well-known relation $N = 1{\cdot}24 \times 10^4 \times f^2$ (mc/s). The resulting electron densities as a function of height are shown in Fig. 2. The solid curve represents the layer as defined. The circles give the values found by the above procedure, and the triangles show those values obtained by neglecting the external magnetic field, $z_0(f_v)$, found by using 10 points in (5), so that the errors in calculating $z_0(f_v)$ are surely not greater than 0·1 km, except for frequencies above about 3·95 mc/s.

Fig. 2 shows clearly that the procedure described in Section 4 gives a great improvement over the results obtained by neglecting the effects of the external magnetic field.

VOL. 5 1954

Example 3. The preceding example shows the errors in the procedure in Section 4 which arise through the limitations on the numerical integrations. We wish also to consider the errors which appear in the numerical work because of the physical assumption that we can restrict y to a constant value. SHINN and WHALE have computed h'-f curves for a parabolic layer for various values of the gyrofrequency and propagation angle. These computations were carried out on a large digital computer (the EDSAC), and are made by using the proper value of y at each frequency. For present purposes, we use one of their curves for propagation angle of 23° 16′, a gyrofrequency of 1·149 mc/s, a critical frequency of 3·5 mc/s, and a semi-thickness of 50 km. We use $y = f_H/f_c = 0{\cdot}32828$, so that we must use (28A) in place of (28). Determining the true heights as in the previous example,

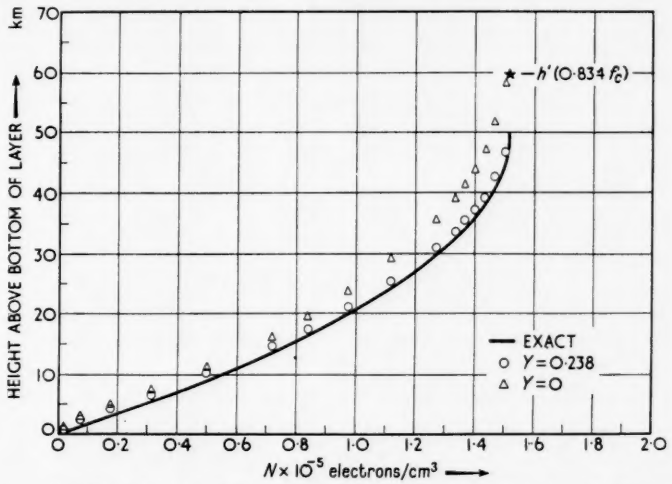

Fig. 3. Electron density determined from h'-f curve for parabolic layer given by SHINN and WHALE, with y varying as frequency changes.

we obtain the electron densities as a function of height as shown in Fig. 3, where the solid curve represents the assumed values, the circles are the results obtained by use of the procedure in Section 4, and the triangles are the values which would be obtained by neglecting the earth's magnetic field. The star represents the height at a frequency of $0{\cdot}834 f_c$, i.e., the height of maximum ionization according to Booker-Seaton method neglecting the magnetic field.

Because SHINN and WHALE did not give values of h' for frequencies sufficiently close to the critical frequency, we were not able to determine the true heights at frequencies above 3·48 mc/s. In practice, the h'-f curve could have been extrapolated a little, so that reasonably good values of h_T at the critical frequency could have been determined. However, this would introduce errors not due to the procedure being tested, so that this extrapolation was not made.

As seen in Fig. 3, the errors made by the present procedure were about 1 to 1·5 km at all heights. Thus the error near the maximum of ionization is of the order of 3 or 4%. This may be compared with the corresponding error of about 16% at $N = 1{\cdot}505 \times 10^4$ when the magnetic field is neglected. The interesting

effect of a nearly constant value of the error is explained by the fact that the errors in the numerical work arising in the use of the procedure of Section 4 decrease with decreasing frequency, while the errors due to the assumption that $y = 0{\cdot}32828$ increase as we go to lower frequencies. Also, the lower part of the curve is in error due to the fact that the h'-f curve was extrapolated for frequencies lower than 1·75 megacycles, which was the lowest frequency used by SHINN and

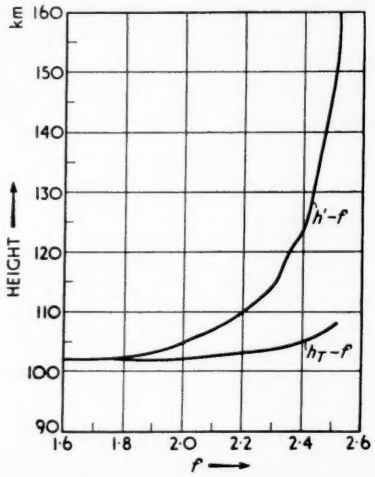

Fig. 4. Experimental h'-f curve taken 20 March 1951, 0750 LMST, with computed h_T-f curve ($y = 1/2$).

WHALE. By coincidence, these effects give a nearly constant error, which amounts to a bodily shift of the layer upwards by one or two kilometres. It is useful to compare Figs. 2 and 3, since the former does not contain errors due to an incorrect value of y.

For comparison, the same h'-f curve was studied using the technique of APPLETON and BEYNON (neglecting the magnetic field) to determine the height of the maximum ionization, h_m, and the semi-thickness, y_m. Since we do not get points lying along a straight line when the points are plotted in the usual manner, the determination is not unique. Four determinations for frequency ranges moving down from the critical frequency give the results in Table 2.

Table 2

	h_m	% Error in h_m	y_m	% Error in y_m
Correct	50		50	
APPLETON and BEYNON method	40.0	20	90	80
	50·0	0	80	60
	53·5	27	76	52
	57·5	35	69	38

SHINN and WHALE recommend that the frequencies near to $0{\cdot}96f_c$ should be used to obtain good values of h_m. This, in fact, corresponds to the $h_m = 50$, $y_m = 80$, above so that their conclusion in this respect is fully upheld in the present case.

VOL. 5 1954

It is obvious that the application of the improved technique of SHINN and WHALE to the present problem would give exactly correct answers. This is true because the h'-f curve studied here is the one on which their method is based, for the given gyrofrequency and propagation angle.

Example 4. As a fourth example, we apply the present procedure to an experimental h'-f record for the E-layer made by C. H. GRACE on 20 March 1951 at 0750 LMST. Fig. 4 shows the experimental values of h'-f and the h_T-f curve computed through use of (28) and (29).

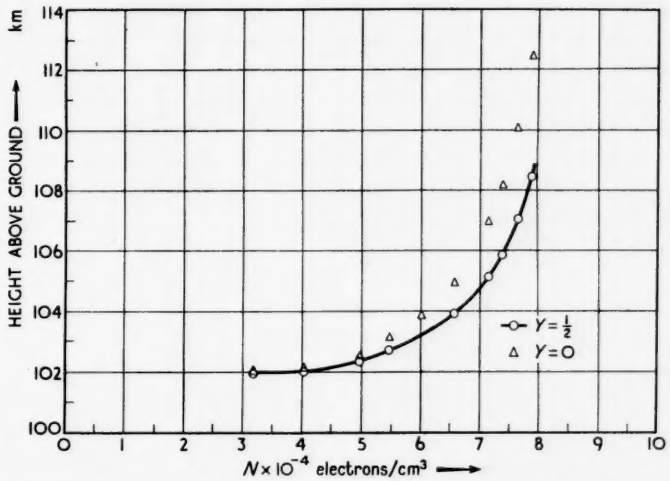

Fig. 5. Electron density determined from experimental h'-f curve taken 20 March 1951, 0750 LMST.

In computing the true heights, it was assumed that h'-f curve had the constant value of 102 km for frequencies below 1·7 mc/s, which was the lowest observed frequency. The electron densities computed with the magnetic field are shown as circles in Fig. 5, where the solid curve is drawn smoothly through these points, and the triangles show the values obtained by neglecting this field.

The same h'-f curve was studied using various of the techniques discussed here. These results are given in Table 3, below.

Table 3

Method	h_m	y_m
N distribution (including magnetic field)	~110	~8
N distribution (neglecting magnetic field)	~114	~12
SHINN and WHALE	110	14
APPLETON and BEYNON (all points $f > 0{\cdot}9\,f_c$)	107	24
APPLETON and BEYNON (points near $f = 0{\cdot}96 f_c$)	96	36

There is every reason to believe that the first answer given here is the most nearly correct solution. The first two results are indicated as approximate, since no answer is obtainable for a frequency exactly equal to the critical frequency. However, these results correspond to a frequency of $0{\cdot}99f_c$, so that the highest value of N shown is very near to the maximum value in the layer.

The result given for the SHINN and WHALE technique is not quite the correct one for this technique. The magnetic field used in the reduction is for a propagation angle of 23° 16′, which is their angle nearest to the angle of 19° 8′ appropriate to the location where the data were taken. Hence, this comparison is slightly unfair to the SHINN and WHALE technique, but any changes would probably be very small compared to the errors made through lack of parabolic form of the layer.

In applying the APPLETON and BEYNON technique (without magnetic field), there was again no unique straight line. Using an average straight line through all the points plotted for frequencies greater than $0{\cdot}9f_c$, we get a reasonable $h_m = 107$. However, if we use the frequencies in the neighbourhood of $0{\cdot}96f_c$ we get the highly improbable answer in the last line.

6. CONCLUSIONS

The examples have shown that it is necessary to include the effects of the earth's magnetic field in calculations of the electron density distribution if accuracy of less than 10 or 15 per cent is desired. A method for carrying out such calculations which reduces the errors considerably has been presented. This method, however, is laborious—requiring as much as 12 hours to reduce a single h'-f curve and cannot reasonably be used except for a comparatively small number of cases. The study of such cases would be valuable in that it would give an opportunity to estimate the accuracy of less exact, but easier, techniques under various conditions.

The advantage of the present electron density distribution method over the parabolic layer methods of APPLETON and BEYNON and of SHINN and WHALE is twofold:

(1) It gives the *distribution* of electron density with height, instead of simply indicating a parabolic fit to the region near to the maximum of the layer; (2) the results are obtained as an integrated effect of the experimental results over the entire range of observed frequencies, whereas the other methods use only a small part of the observed results. Slight ripples in the layer can produce quite large variations in the h'-f curve. The present method takes such variations in its stride, and indicates the corresponding variation in the electron density curve. The parabolic layer techniques, in contrast, suffer considerably in such a case, since the h'-f curve does not at all correspond to that of a parabolic layer. This can lead either to considerable arbitrariness in the result, or to a definitely indicated, but quite incorrect result. The wide variation in the last two lines of Table 3 is indicative of this sort of problem.

The numerical techniques of the procedure presented here are not very good when the h'-f record contains very sharp cusps in the regions of interest. This is because the derivatives of the successive true height corrections undergo a sudden change of sign at the cusp. To deal with such cases, an integration formula

VOL. 5 1954

with a rather large number of points must be used. However, if the mathematical techniques described here were combined with the use of a differential analyzer, this problem should create no difficulty.

The numerical work could be improved by obtaining various formulae (28) with y corresponding to several values of f used in the work. Even choosing two or three values of y for different ranges of f would result in an improvement. However, merely by using the value of y corresponding to the critical frequency, one can reduce the uncertainties and errors in determination of the electron density distribution by very large amounts, as indicated in the discussion in Section 5.

References

Abel, N. H.	1881	Œuvres, Christiania **1**, p. 11
Appleton, E. V.	1930	Proc. Phys. Soc. **42**, 321
Appleton, E. V. and Beynon, W. J. G.	1940	Proc. Phys. Soc. **52**, 518
Booker, H. G. and Seaton, S. L.	1939	Intern. Ass. of Terr. Mag. and Elec., Washington Assembly, September
Friedman, B.	1950	New York Univ., Math. Dept., Res. Group, Research Report EM–17, February
de Groot, W.	1930	Phil. Mag., **10**, 521
Kelso, J. M.	1952	J. Geophys. Res. **57**, 357
Kraus, L.	1950	New York Univ., Math. Dept. Res. Group. Progress Report No. 6
Kraus, L.	1953	J. Geophys. Res. **58**
Manning, L. A.	1949	Proc. I. R. E. **37**, 599
Manning, L. A.	1953	J. Geophys. Res. **58**, 117
Pekeris, C. L.	1940	Terr. Mag. **42**, 205
Picard, E.	1904	Comptes Rendus **139**, 245
Rydbeck, O. E. H.	1939	Tekniska Samfundets Handlingar **3** 135
Rydbeck, O. E. H.	1942	Trans. Chalmers Univ. Technology **3**
Rydbeck, O. E. H.	1944	Trans. Chalmers Univ. Technology **34**
Shinn, D. H.	1953	J. Geophys. Res. **58**, 416
Shinn, D. H. and Whale, H. A.	1952	J. Atmosph. Terr. Phys. **2**, 85
Volterra, V.	1913	Leçons sur les Équations Intégrales, Paris
Weierstrass, K. T. W.	1903	Werke, V. 3, p. 1, Berlin
Whale, H. A.	1951	J. Atmosph. Terr. Phys. **1**, 244

Journal of Atmospheric and Terrestrial Physics, 1954, Vol. 5, pp. 28 to 43. Pergamon Press Ltd., London

A tentative model of the equilibrium height distribution of nitric oxide in the high atmosphere and the resulting *D*-layer*

A. P. MITRA†

Ionosphere Research Laboratory, The Pennsylvania State University, State College, Pennsylvania

(*Received* 2 *September* 1953)

ABSTRACT

An attempt is made to derive a tentative model for the equilibrium distribution of nitric oxide in the height range 50–100 km by considering some of the possible photochemical reactions involving ozone, nitrogen and oxygen (both molecular and atomic) and nitrous oxide. The distribution depends markedly on the types of O and N_2O distributions assumed. In general, under the conditions of photochemical equilibrium, the maximum of NO concentration occurs within 85–95 km with a maximum concentration not exceeding a value of about $2 \times 10^{12}/cm^3$.

The problem of the formation of the *D*-layer by photoionization of NO by L_α is then discussed in some detail. With the NO distributions obtained in this work and the recombination coefficient model given by MITRA and JONES, the process is found to yield adequate ionization for the *D*-layer.

1. INTRODUCTION

Little is known regarding the presence or distribution of NO in the atmosphere. The spectrum of the sun taken during a rocket flight to 55 km showed a broad band lying between λ 2200–2300 Å. This was supposed to be due to NO (DURAND, 1949). If this interpretation is correct, the number of NO molecules above the 55 km level is of the order of $10^{18}/cm^2$. On the other hand, TOUSEY (private conversation) has indicated that the band might well arise from NO existing in the atmosphere of the sun. The only other spectroscopic evidence has been provided by NICOLET (1948) who has drawn attention to the striking coincidences between some of the auroral emissions and members of the β-band system. Even if these evidences are considered sufficiently convincing, the question arises as to actual distribution of NO with height. In the past there has been a tendency for assuming a distribution similar to that of the main atmosphere (BATES and SEATON, 1950). With this assumption it was possible to deduce certain values for NO at ionospheric heights. Such a distribution, however, cannot be accepted without detailed study.

Some idea about the distribution of NO may be obtained from the photochemistry of the relevant portions of the atmosphere. Such calculations for ozone have been found to be useful (CRAIG, 1950; JOHNSTON *et al.*, 1952) and it was thought that similar calculations might throw some light on the problem of NO distribution. The problem can, at best, be studied only tentatively since the photochemical reactions that might appear in the production and annihilation of NO, are as yet inadequately understood. Considerable light has, however, been thrown on the subject in the recent works of BATES and NICOLET (1950), BATES and WITHERSPOON (1952) and BATES (1952).

VOL. 5 1954

* The research reported in this paper has been sponsored by the Geophysics Research Division of the Air Force Cambridge Research Centre, Air Research and Development Command under Contract AF19(122)–44.

† On leave from the Council of Scientific and Industrial Research, Government of India and the Institute of Radiophysics and Electronics, University of Calcutta.

In this work an attempt is made to derive a tentative model for the equilibrium distribution of NO by considering some of the possible photochemical reactions. This distribution has then been used to derive an electron distribution for the *D*-layer, using the recombination coefficient model of MITRA and JONES (1953), the absorption cross section of PRESTON (1940) and WATANABE (private communication) and the solar intensity at L_α given by PIETENPOL *et al.* (1953) of the University of Colorado.

2. DISTRIBUTION OF NO FROM PHOTOCHEMICAL CONSIDERATIONS

2.1 *General Considerations*

There are two possible processes for the production of NO in the upper atmosphere. One is by the three-body recombination with O and the other by photodissociation of N_2O into N and NO (BAMFORD, 1943; GAYDON, 1947; NICOLET, 1952). Thus,

$$N + O + M \rightarrow NO + M(k_1) \tag{1}$$

$$N_2O + h\nu \xrightarrow{\lambda \leq 2400\,\text{A}} NO + N(4_S)\,(J_1) \tag{2}$$

where M in reaction (1) is an unspecified third body. Reaction (2) commences at λ 2400 or slightly above (BAMFORD, 1943; GAYDON, 1947; NICOLET, 1952). In order that sufficient NO molecules be produced from either of the above reactions there should be an appreciable concentration of atomic oxygen, atomic nitrogen and/or of N_2O at the relevant levels.

The presence of atomic oxygen in the lower ionosphere may occur through the photodissociation of O_2 in the strong Schumann-Runge continuum beginning at λ 1759;

$$O_2 + h\nu \rightarrow O(3_P) + O(1_D)$$

and also in the weaker Herzberg continuum beginning at λ 2421:

$$O_2 + h\nu \rightarrow 2O(3_P)$$

While there is some controversy regarding the level of maximum dissociation of O_2 (BATES and NICOLET, 1950; PENNDORF, 1949; RAKSHIT, 1947; MOSES and TA-YOU-WU, 1952; NICOLET and MANGE, 1952), there is little doubt that appreciable quantities of atomic oxygen are present in the region 50–100 km, the region of interest for the present work.

The presence of atomic nitrogen in the atmosphere has been observed in the NI and NII lines in the auroral spectra (PETRIE and SMALL, 1952; MEINEL, 1950; R. BERNARD, 1939, 1941; DUFAY, 1943; GAUZIT, 1942). Some evidence for its presence in regions outside the auroral zone is also available. It is extremely likely that atomic nitrogen does exist in the normal atmosphere, probably as abundantly as in the auroral regions. Theoretically some idea regarding the possible concentrations of N at the relevant levels may be formed by studying the processes of dissociation of N_2. Two such processes have been suggested in recent years. One is the HERZBERG-HERZBERG process (1948), according to which predissociation of N_2 molecules occurs by absorption in the Lyman-Birge-Hopfield band in the wavelength range 1150–1250 Å;

$$N_2 + h\nu \rightarrow N_2(a^1\Pi_g) \rightarrow N + N(J_2) \tag{3}$$

The second process, discussed by BATES (1950) and S. K. MITRA (1951) is represented by:

$$N_2 + h\nu \xrightarrow{\lambda\, 795\,\text{Å}} N_2^+(X') + e$$
$$N_2^+(X') + e \rightarrow N(2_P) + N(2_D) \qquad (4)$$

DEB (1952) has considered the relative importance of the two processes at various heights. The essential feature of his conclusion is that the two processes are operative at quite different levels. The HERZBERG-HERZBERG process is effective in the lower ionospheric regions whereas the dissociative recombination process is only important above about 170 km. DEB's calculations are approximate, and the uncertainties in the parameters involved leave some doubt about the above conclusion, but it should be at least qualitatively correct. Since, in the present work, we are concerned with heights up to about 100 km, we need only consider the HERZBERG-HERZBERG process (see also BATES (1952)).

Regarding N_2O, its presence in the atmosphere was first shown by ADEL (1938, 1939, 1941) from observations on the 7·6 μ portion of the solar spectrum. Further confirmations were presented by other infrared spectroscopists (MIGEOTTE, 1950), and by the mass spectroscopic measurements of SLOBAD and KROGH (1950). The concentration has been found to be 2×10^{19} molecules/cm^2 column. It is believed that N_2O is mainly concentrated near the ground. SLOBAD and KROGH have obtained a fractional volume of 5×10^{-7} near ground against 1×10^{-6} deduced from the total amount in a vertical column. This has originated the suggestion that the nitrous oxide is produced in the soil by some micro-organisms. BATES and WITHERSPOON (1952) have discussed the question in some detail. According to them, while N_2O might originate in the soil, homogeneous gas reactions at low atmospheric levels might also account for the large N_2O concentration near ground. The only reactions which have been found suitable so far are:

$$N_2 + O + M \rightarrow N_2O + M \quad (k_6) \qquad (5)$$
$$O_3 + N_2 \rightarrow N_2O + O_2 \quad (k_5) \qquad (6)$$

where the parent particles O and O_3 may be produced with sufficient rapidity to compensate for the very large destruction rate of N_2O by photodissociation occurring through

$$N_2O + h\nu \xrightarrow{\lambda \leq 2400\,\text{A}} NO + N(4_S) \quad (J_1) \qquad (7)$$
$$N_2O + h\nu \xrightarrow{\lambda \leq 3070\,\text{A}} N_2 + O(3_P \text{ or } 1_D) \quad (J_4) \qquad (8)$$

The equilibrium concentrations of N, N_2O and NO, subject to the reactions (1), (2), (3), (4), (5), (6), (7), (8), and to the following processes of destruction of N and NO:

$$\left.\begin{aligned} N + N + M &\longrightarrow N_2 + M \quad (k_2) \\ N + NO &\longrightarrow N_2 + O \quad (k_3) \\ N + N &\longrightarrow N_2 + h\nu \quad (k_4) \\ NO(X^2\Pi) + h\nu &\xrightarrow{\lambda\lambda\ 2050\text{–}2450} NO(A^2\Sigma^+ \text{ or } C^2\Sigma^+) \\ NO(A^2\Sigma^+ \text{ or } C^2\Sigma^+) &\longrightarrow N + O \quad (J_3) \end{aligned}\right\} \qquad (9)$$

VOL. 5 1954

are given by

$$n^2(\mathrm{N}) = \frac{2J_2 n(\mathrm{N_2}) + J_1 n(\mathrm{N_2O})}{2k_2 n(M) + 2k_4 + \dfrac{k_1 k_3 n(\mathrm{O}) n(M) + \dfrac{J_1 k_3 n(\mathrm{N_2O})}{n(\mathrm{N})}}{k_3(T) n(\mathrm{N}) + J_3}} \tag{10}$$

$$n_1(\mathrm{N_2O}) = \frac{k_6 n(\mathrm{N_2}) n(\mathrm{O}) n(M)}{J_1 + J_4} \tag{11a}$$

$$n_2(\mathrm{N_2O}) = \frac{k_5 n(\mathrm{O_3}) n(\mathrm{N_2})}{J_1 + J_4} \tag{11b}$$

$$n(\mathrm{NO}) = \frac{k_1 n(\mathrm{N}) n(\mathrm{O}) n(M) + J_1 n(\mathrm{N_2O})}{k_3(T) n(\mathrm{N}) + J_3} \tag{12}$$

The coefficients k's and J's are the reaction rates associated with the various reactions and are specified under parenthesis at the end of the corresponding equation. The subscripts 1 and 2 appearing in equations (11a) and (11b) refer to two possible cases of production of N_2O according to (5) and (6) respectively.

2.2 *Physical Characteristics of the Atmosphere in the Height Range of* 50–100 *km and the Values of the Rate Coefficients*

Considerable information regarding the physical characteristics of the upper atmosphere is now available from rocket results (see, for example, NICOLET and MANGE, 1952). Such information on scale height and density distribution of N_2 and O_3 are given in Figs. 2 and 3 (NICOLET and MANGE, 1952; CRAIG, 1950; JOHNSTON *et al.*, 1952). The distribution of atomic oxygen, shown also in Fig. 3, is, however, less certain: it has been obtained for levels above 70 km, by altering

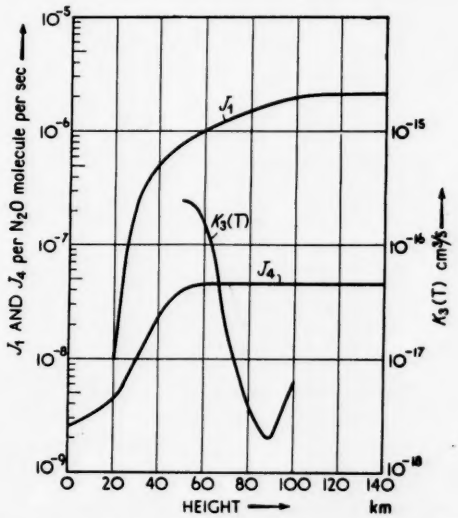

Fig. 1. Height variations of the coefficients J_1, J_4, and K_3.

the MOSES-WU results to provide a qualitative fit with the concepts of NICOLET-MANGE, and for levels below 70 km, from BATES and WITHERSPOON'S paper (1952).

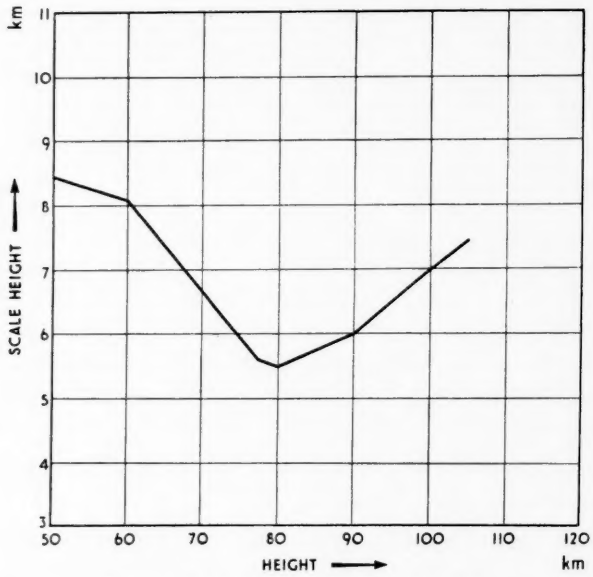

Fig. 2. Height distribution of scale height.

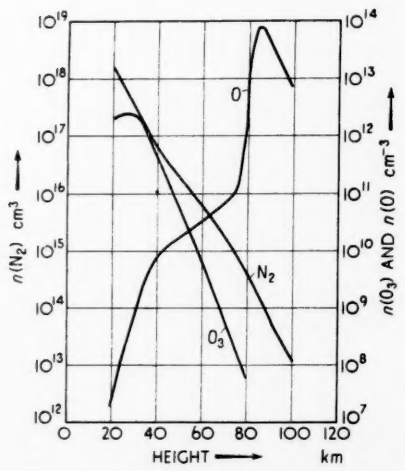

Fig. 3. Distribution of N_2, O_3, and O.

In the present work we are concerned with solar radiation up to a wavelength of 3000 Å. Results obtained from rocket measurements (TOUSEY *et al.*, 1951; FRIEDMAN *et al.*, 1951) in the range 1150–3000 Å are given in Table 1.

Available information about the various rate coefficients are meagre. The

VOL. 5 1954

values for the various k's (shown in Table 2) are taken from literature with some modifications. For the three-body recombination coefficients k_1 and k_2, the value $5 \times 10^{-34}\ T^{\frac{1}{2}}$ cm^6/sec (where T is the absolute temperature) has been assumed following the three-body collision process of atomic oxygen. The coefficient k_3, which is temperature-dependent, is obtained from BATES and shown in Fig. 1.

Table 1. *Solar Energy at Various Wavelengths (from rocket experiments)*

Spectral Region Å	*Ratio R*	*Solar Energy* erg cm^{-2} · sec^{-1}	*Authority*
3000	$\frac{1}{2{\cdot}3}$		TOUSEY *et al.*
2200	$\frac{1}{6{\cdot}8}$		TOUSEY *et al.*
2080	$\frac{1}{15}$		TOUSEY *et al.*
1450–1530	$\frac{1}{200}$		FRIEDMAN *et al.*
1230–1340	$\frac{1}{140}$	0·2	TOUSEY *et al.*
1050–1230	$\frac{1}{8}$	0·4	TOUSEY *et al.*

For k_4 a value of 10^{-21} cm^3/sec has been used, which is a reasonable value for the HERZBERG-HERZBERG dissociation process, where the nitrogen atoms produced are in the normal state. The coefficients k_5 and k_6 have been determined by using the knowledge that the total amount of N_2O in a vertical column near the ground is about 1×10^{-6} of the main atmosphere (11a) and (11b). The values so obtained are: $k_5 = 9 \times 10^{-27}$ cm^3/sec and $k_6 = 5 \times 10^{-39}$ cm^6/sec. In order to determine the coefficients J's, use has been made of the equation:

$$J_r = J_{r\alpha} \exp\left[-\overline{A}_r n(X) H \sec \chi\right] \tag{13}$$

where

$$J_{r\alpha} = g\overline{A} \int_{\lambda_1}^{\lambda_2} Q_{\alpha\lambda}\, \mathrm{d}\lambda \tag{14}$$

In the above equations,

$\overline{A}$ is the average absorption cross section over the relevant wavelength range λ_1 to λ_2

$n(X)$ is the concentration of the active constituent at any height h

χ is the solar zenith angle

$\int_{\lambda_1}^{\lambda_2} Q_{\alpha\lambda}\, d\lambda$ is the total number of photons entering the atmosphere in the waveband λ_1 to λ_2

$H = \dfrac{kT}{mg}$ = scale height

$J_{r\alpha}$ is the value of the coefficient J at the level where the relevant radiation is unattenuated

The subscript r is 1 for equation (2), 2 for equation (3), 3 for equation (9) and 4 for equation (8).

R—ratio of energy observed to energy which would have been emitted by a 6000°K blackbody sun.

Table 2. Rate Coefficients

$J_{1\alpha}$	$J_{2\alpha}$ /molecule/sec	$J_{3\alpha}$	$J_{4\alpha}$	$(k_1$ or $k_2) \times T^{\frac{1}{2}}$ cm$^{6/s}$	k_4 cm$^{3/s}$	k_5 cm$^{3/s}$	k_6 cm$^{6/s}$
$2{\cdot}0 \times 10^{-6}$	$3{\cdot}2 \times 10^{-13}$	1×10^{-7}	$4{\cdot}5 \times 10^{-8}$	5×10^{-34}	10^{-21}	9×10^{-27}	5×10^{-39}

For J_1 and J_4 the values given by BATES and WITHERSPOON have been used (Fig. 1, Table 2). J_2 and J_3 have been calculated using equation (13) and (14) remembering that the relevant effective absorption cross sections are about 10^{-19} cm^2 (WEISSLER *et al.*, 1952; CLARK, 1952) and 7×10^{-24} cm^2 respectively.

VOL. 5 1954

2.3 *Height Distributions of* N_2O, N *and* NO

We are now in a position to compute the height distribution of N_2O, N and NO.

For N_2O, two different distributions have been computed, corresponding to the cases I and II of Section 2.1. These are shown in Fig. 4. In the process involving O_3 (case 1), the concentration of N_2O drops off very rapidly with height, whereas for the process involving three-body recombination of O, N_2, M (case II), the decrease is slower. Further, for the latter process, there is a pronounced maximum around 85 km—the region of O_2–O transition. The distribution of atomic nitrogen was obtained for the above two distributions of N_2O by using a method of successive approximation (Fig. 6). Finally n(NO) was computed (Fig. 7*a*).

It is of interest to note that photodissociation of N_2O provides an appreciable contribution to the production of atomic nitrogen at levels below about 80 km, but at higher levels the contribution from the dissociation of N_2 by the HERZBERG-HERZBERG process is larger (Fig. 5*a* and 5*b*). Other simplifications occur depending on the levels concerned. Thus, between 75–100 km, the region of specific interest for D-region studies,

$$J_1 n(N_2O) < k_1 n(N) n(O) n(M) \quad \text{(Fig. 7b)}$$

$$\frac{J_1 k_3 n(N_2O)}{n(N)} < k_1 k_3 n(O) n(M)$$

$$k_3(T) n(N) < J_3$$

$$2k_4 \ll 2k_2 n(M) < \frac{k_1 n(O) n(M)}{k_3(T) n(N) + J_3}$$

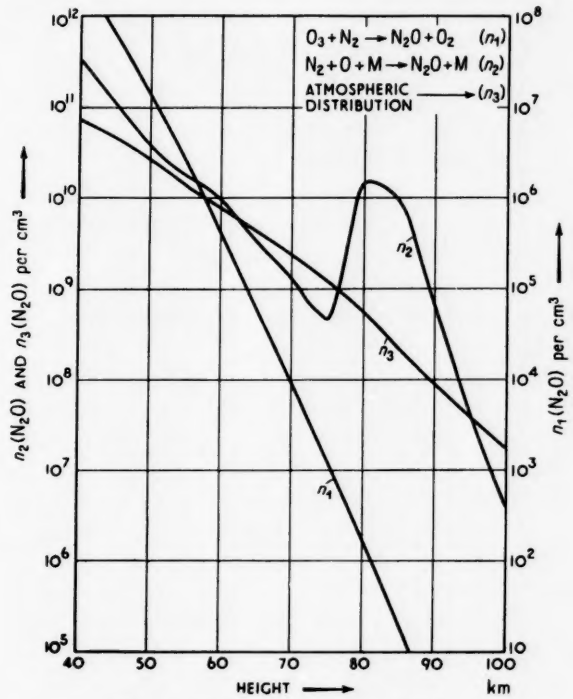
$O_3 + N_2 \rightarrow N_2O + O_2$ (n_1)
$N_2 + O + M \rightarrow N_2O + M$ (n_2)
ATMOSPHERIC DISTRIBUTION $\rightarrow (n_3)$
$n_2(N_2O)$ AND $n_3(N_2O)$ per cm³
$n_1(N_2O)$ per cm³
HEIGHT
km

Fig. 4. Height distributions of N_2O.

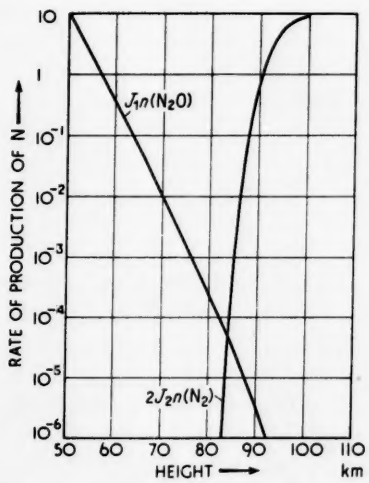

Fig. 5*a*. Relative importance of photodissociation of N_2O and N_2 in yielding atomic nitrogen for case 1.

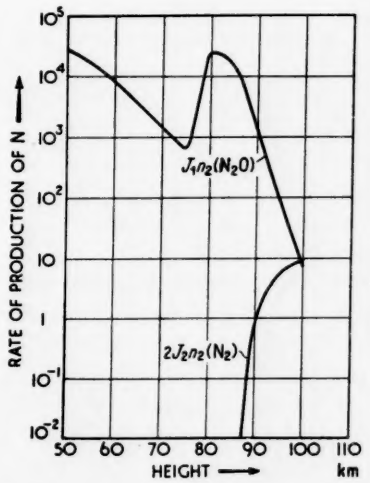

Fig. 5*b*. Relative importance of photodissociation of N_2O and N_2 in yielding atomic nitrogen for case 2.

yielding the simplified equations:

$$n^2(\mathrm{N}) \approx \frac{J_3[2J_2 n(\mathrm{N_2}) + J_1 n(\mathrm{N_2O})]}{k_1 k_3 n(\mathrm{O}) n(M)}$$

$$n(\mathrm{NO}) \approx \frac{k_1 n(\mathrm{N}) n(\mathrm{O}) n(M)}{J_3}$$

and

$$n(\mathrm{NO}) n(\mathrm{N}) \approx \frac{2J_2 n(\mathrm{N_2}) + J_1 n(\mathrm{NO})}{k_3} \tag{15}$$

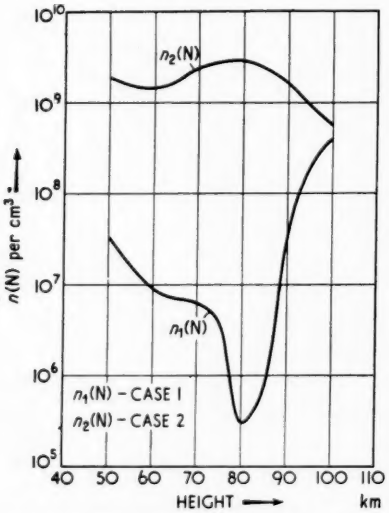

Fig. 6. Distribution of atomic nitrogen.

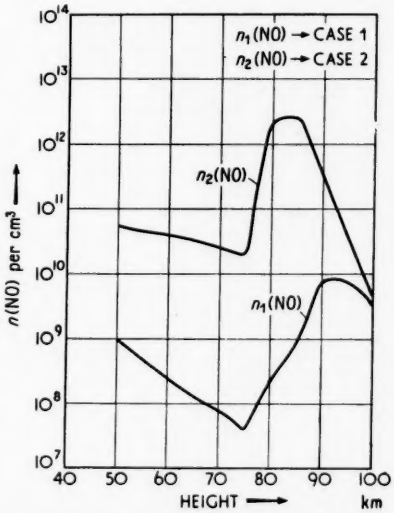

Fig. 7*a*. Distribution of nitric oxide.

For process (7), a further simplification occurs, namely,

$$J_1 n(\mathrm{N_2O}) \gg 2J_2 n(N_2), \text{ so that}$$

$$n_2(\mathrm{NO}) n_2(\mathrm{N}) \simeq \frac{J_1 n(\mathrm{N_2O})}{k_3} \tag{16}$$

It may be seen that the only rate coefficients involved in these calculations are J_1, J_2, k_1 and k_3, and for the product $n(\mathrm{NO})n(\mathrm{N})$, only k_3 and either J_1 or J_2. The uncertainties in the range 75–100 km are, therefore, not nearly as great as one might initially be led to suppose.

In calculating the effect of the solar altitude on the equilibrium concentrations of NO, one has to consider the changes with χ of the concentrations of O, M, $\mathrm{O_3}$ and $\mathrm{N_2}$ and the various J's. Although some seasonal variation of upper atmospheric density has been obtained in meteoric observations (WHIPPLE, 1949), no reliable estimate regarding such variation is available. One need therefore consider only the variations in the J's. Such considerations show that the variation of $n(\mathrm{NO})$

VOL. 5 1954

with solar altitude is given by the factor $\exp\left(\frac{A_2}{2} nH \sec \chi\right)$ for case I of N_2O-formation and by $\exp\left(\frac{A_3}{2} nH \sec \chi\right)$ for case II. Since A_3 is small, of the order of 10^{-23} cm^2, the NO-concentration is effectively independent of solar altitude for the latter case. For the former, however, considerable variation in n(NO) occurs with variation in χ.

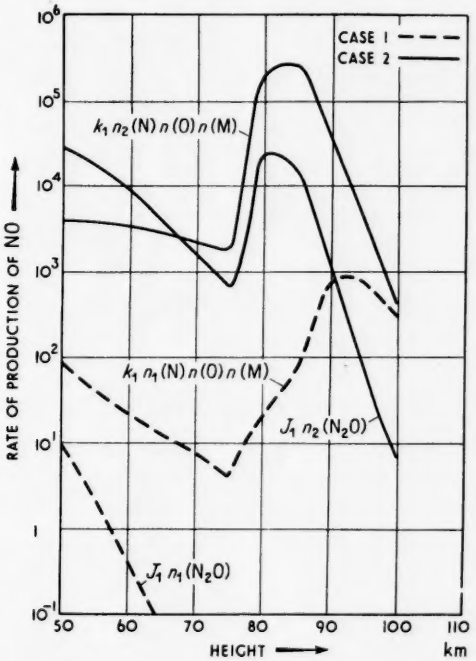

Fig. 7*b*. Relative importance of NO production through three-body recombination process involving N, O, and M and through photodissociation of N_2O.

3. Origin and Structure of the *D*-layer

The atmospheric constituents which are likely to be responsible for the origin of the *D*-layer are O_2, Na (Jouast and Vassy, 1941; Vassy and Vassy, 1941; Bates and Seaton, 1950) and NO (Nicolet, 1948). Of these the first two constituents cannot explain the characteristics of *D*-ionization. Thus, with O_2, calculations using the recent value of $A(O_2)$ for the first ionization potential ($= 5 \times 10^{-18}$ cm^2) (Weissler *et al.*, 1952; Clark, 1952) show that the resulting ionization has a maximum at *E*-region heights and not at *D*-heights. This confirms an earlier conclusion of Lindquist (1952), based on studies of the sunrise effect in equivalent height at 150 kc/s, that the *E*-region is formed by ionization of O_2. With sodium, calculations show an insufficient ionization yield, about 100/cm^3 or less, and no appreciable variation with solar altitude (Fig. 9). The results in Fig. 9 have been obtained for a sodium concentration of 3×10^3/cm^3 at 70 km (Bates

and MASSEY, 1946; BARBIER, 1948) with a height distribution similar to that of the main atmosphere (ELVEY and FARNSWORTH, 1952), absorption coefficients of 10^{19} cm^2 and 7×10^{-24} cm^2 for Na and air respectively, a photon flux of about

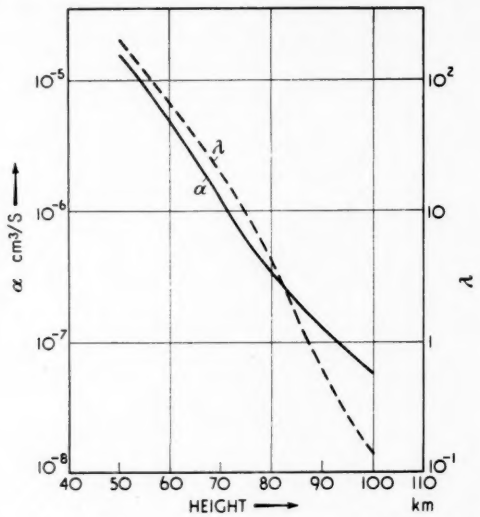

Fig. 8. Distribution of α and λ (from MITRA and JONES).

$1{\cdot}5 \times 10^{14}$ cm^{-2} sec^{-1}, and for the new model on recombination coefficient and negative ion concentration given by MITRA and JONES (1953) (Fig. 8). These results are substantially the same as those of BATES and SEATON (1950) and cast

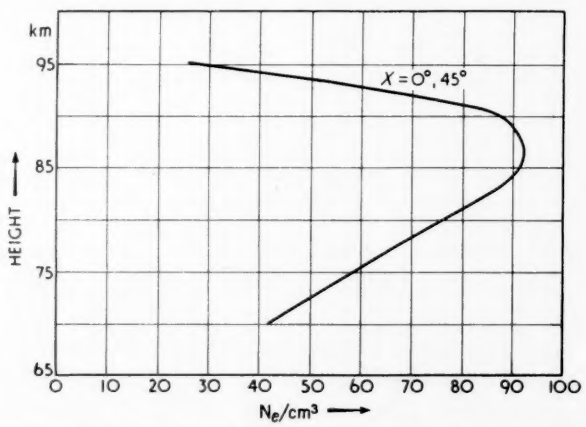

Fig. 9. Distribution of electron density from photoionization of sodium.

doubt on the validity of the theory of "exhaustion" region recently advanced by BRACEWELL (1952) for the *D*-layer and later applied by FRICKER (1953) for the *E*-layer.

The only process left is the photoionization of NO at $\lambda < 1300$, first suggested by NICOLET (1948) and later discussed in some detail by BATES and SEATON, and

VOL. 5 1954

WATANABE, MARMO and INN (1953). The fact that the L_α line (1216 A) is in this wavelength region makes it a very interesting process, both for the normal D-region and for flaretime enhancement of ionization. In view of the NO-distributions derived in section 2 and of the fact that more accurate values of the solar intensity

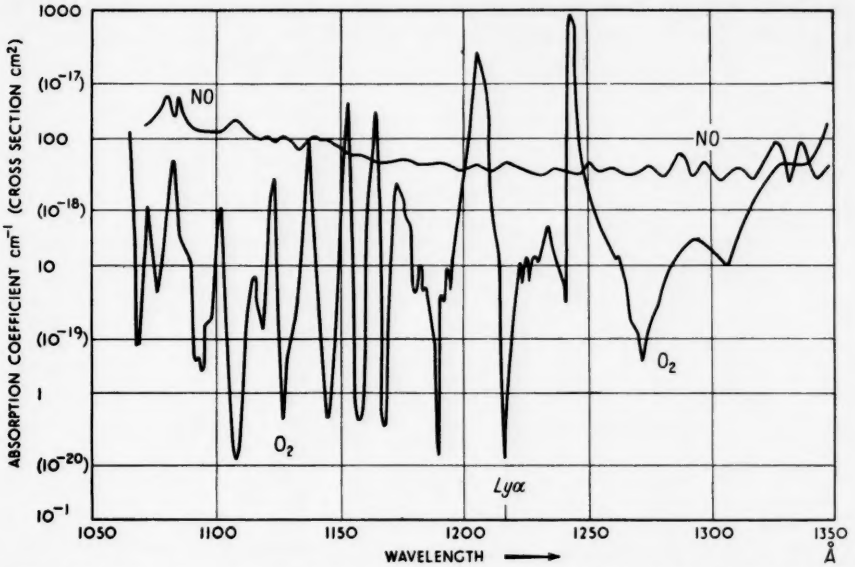

Fig. 10. Absorption cross section of NO and O in the range 1050–1350 (from MARMO *et al.*; and WANTANABE *et al.*).

and of the absorption cross sections of the relevant constituents are now available, it appears worthwhile to reconsider the question. MARMO, ZELIKOFF and TANAKA (1952) have measured the absorption coefficient of NO between $\lambda\lambda$ 1050–1350. Their results are shown in Fig. 10. The same figure also gives the absorption coefficient for O_2 in this particular wavelength range as determined by WATANABE and others (1953). It will be observed that below 1300 Å there are a number of atmospheric windows where the solar radiation may penetrate deep into the atmosphere. One of them includes the L_α region where WATANABE's value for the absorption coefficient of O_2 is $1{\cdot}0 \times 10^{-20}$ cm² against PRESTON's (1940) value of $1{\cdot}04 \times 10^{-20}$ cm². The coefficients of some of the other atmospheric constituents at L_α are given in Table 3.

Table 3. *Absorption Coefficient for Various Constituents at* L_α

Authors	A(O_2) *cm²*	A(N_2) *cm²*	A(O) *cm²*	A(H_2O-*vapour*) *cm²*	A(CO_2) *cm²*	A(*air*) (*dry* CO_2-*free*) *cm²*
PRESTON	$1{\cdot}04 \times 10^{-20}$	$< 1{\cdot}90 \times 10^{-22}$	0	$1{\cdot}44 \times 10^{-17}$	$7{\cdot}4 \times 10^{-20}$	$2{\cdot}3 \times 10^{-21}$
WATANABE *et al.*	$1{\cdot}00 \times 10^{-20}$	$< 3{\cdot}00 \times 10^{-22}$	—	$1{\cdot}44 \times 10^{-17}$	$4{\cdot}3 \times 10^{-20}$	—

The solar spectrum taken at a height of 81 km by means of rockets by the University of Colorado group (PIETENPOL *et al*, 1953) showed that L_α is the only line observed below 1800 Å. The estimated energy of the radiation was 0·03 microwatts/cm². Since there was evidence of increased solar activity at the time at which the data were procured, the normal value is probably lower. It is interesting to note here that FRIEDMAN and CHUBB (private conversation) have obtained a lower intensity in the L_α region in a more recent flight. The solar intensity was

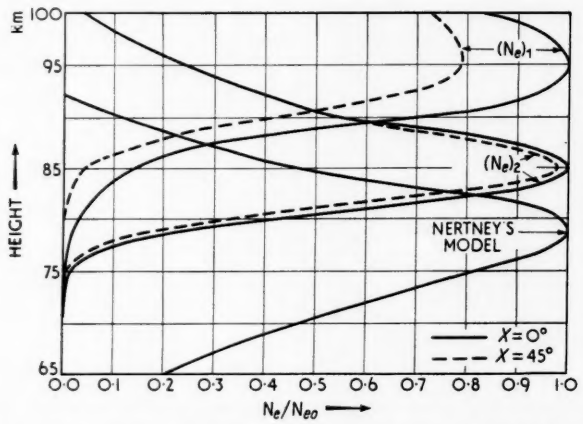

Fig. 11. *D*-electron distribution from photoionization of NO.

measured in the wavelength range 1180–1300 Å, but the equipment was only sensitive near L_α. The estimated observed energy was about 0·01 microwatt/cm²; about 1/3 the value observed in the University of Colorado experiment. According to FREIDMAN and CHUBB this value is reliable within a factor of 2. Thus, a fairly safe estimate of Q_α will be about 1×10^{10} for the Lyman-α region.

In addition to the L_α radiation BATES and SEATON have considered another window between 10 and 11 eV., of width about 20 Å, where appreciable ionization of NO occurs. Although there are a number of atmospheric windows in the vicinity of L_α (Fig. 10), it does not seem likely, however, that any of these will produce ionization comparable to that produced by L_α radiation. This is because solar radiation in this wavelength range is mainly concentrated around L_α.

We are now in a position to calculate the ionization produced by NO. This has been done by using the equation

$$\mathrm{N} = \left[\frac{A(\mathrm{NO})n(\mathrm{NO})Q_\alpha \exp\left(-\sum_k A_k n_k H \sec\chi\right)}{\alpha(1+\lambda)}\right]^{\frac{1}{2}} \tag{17}$$

where α is the effective recombination coefficient and λ, the ratio of the concentration of negative ions to that of electrons (Fig. 8). Such calculations have been made for both the distributions of NO (I and II in Fig. 6). In Fig. 11, these distributions have been plotted as a ratio of N at any level to that at the maximum; $(N_e)_1$ and $(N_e)_2$ correspond respectively to $n_1(N)$ and $n_2(N)$ in Fig. 6.

VOL. 5 1954

The values of N_0 (the maximum electron concentrations) are about $3 \times 10^4/cm^3$ and $2{\cdot}5 \times 10^5/cm^3$ respectively. Thus, in both cases, the ionization produced from NO is sufficiently large. It is, however, necessary to introduce a factor ϕ in equation (17) to take account of the fact that not all the absorbed energy leads to photoionization, nor does every photon act in the ways given by equations (4, 7, 8, 9). In addition there is the complication due to scattering. It is interesting to note that, in order to obtain an electron density of about 10^3 at 85 km, ϕ need

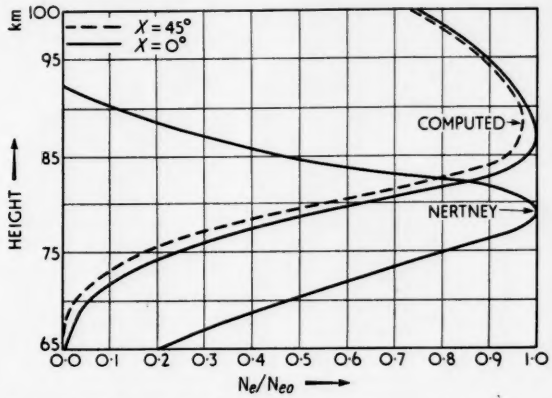

Fig. 12. Electron density distribution for complete mixing.

only be $2{\cdot}6 \times 10^{-3}$ in the second case and $1{\cdot}6 \times 10^{-1}$ in the first case. Thus even if only 16% of the radiation is utilized in the first case or 0·3% in the second case, production of ionization from NO by L_α will be sufficient to explain the observational results on long and short radio waves. These values are sufficiently low to be realized in practice.

4. Discussion

Although, due to the uncertainties in the values of the various parameters involved, neither the absolute values nor the distributions of electron densities given in Fig. 11 can be considered reliable, there is little doubt that photoionization of NO can yield adequate ionization for the *D*-layer. It is of interest to note that smaller values of the coefficients J_1, J_2, k_1, and k_3 would not necessarily reduce the values of n(NO), and considerable alterations in the coefficients would be required to make the ionization yield negligible.

A more serious objection would be the possibility of a departure from photochemical equilibrium. Approximate calculations show that the time required for equilibrium is more than 3 months at 60 km, more than 6 months at 80 km, and more than 2 years at 100 km, indicating that at the levels of interest a departure from photochemical equilibrium will occur. The case of non-equilibrium distribution of NO is complicated, and is not discussed in the present work. It is, however, possible to indicate the effect of a departure from photochemical equilibrium under the condition of complete mixing, with n(NO) following the same distribution as that of the main atmosphere. The ionization produced by these distributions is given in Fig. 12. It is interesting to note that this distribution

approximates more closely to the empirical distribution given by NERTNEY than the distributions in Fig. 11.

Acknowledgment—The author acknowledges with pleasure the help received from Drs. TOUSEY, FRIEDMAN and CHUBB of the Naval Research Laboratory, Washington, D.C., and from Dr. PFISTER and Dr. WATANABE of the Geophysical Research Directorate, Air Force, Cambridge. Thanks are also due to Dr. WAYNICK and the research staff of this laboratory for helpful advice and criticism.

REFERENCES

ADEL, A.	1938	Ap. J. **88**, 186
	1939	**90**, 627
	1941	**93**, 509
BAMFORD, C. H.	1943	Rep. Prog. Phys. **9**, 75
BARBIER, D.	1948	Ann. Geophys. **4**, 193
BATES, D. R.	1950	Phys. Rev. **78**, 492
BATES, D. R.	1952	Ann. Geophys. **8**, 194
BATES, D. R. and MASSEY, H. S. W.	1946	Proc. Roy. Soc. A. **187**, 261
BATES, D. R. and NICOLET, M.	1950	J. Geophys. Res. **55**, 301
BATES, D. R. and SEATON, M. J.	1950	Proc. Phys. Soc. B. **63**, 129
BATES, D. R. and WITHERSPOON, AGNES E.	1952	Mon. Not. Roy. Astron. Soc. **112**, 101
BERNARD, R.	1939	Phys. Rev. **55**, 511
	1941	Ann. d'ap. **4**, 13
BRACEWELL, R. N.	1952	J. Atmosph. Terr. Phys. **2**, 226
CLARK, K. C.	1952	Phys. Rev. **87**, 271
CRAIG, R. A.	1950	Meteorological Monograph, Vol. 1, No. 2, September, published by the American Meteorological Society
DEB, S.	1952	J. Atmosph. Terr. Phys. **2**, 309
DUFAY, J.	1943	Ann. d'ap. **6**, 81
DURAND, E., OBERLY, J. J. and TOUSEY, E.	1949	Astrophys. J. **109**, 1
ELVEY, C. T. and FARNSWORTH, A. H.	1952	Astrophys. J. **96**, 451
FRIEDMAN, H., LICHTMAN, S. W. and BYRAM, E. T.	1951	Phys. Rev. **83**, 1025
FRICKER, S. J.	1953	"Methods of Sharp Ionized Layer Formation," presented at the URSI-IRE meeting, Washington, D.C., April 27–30
GAUZIT, J.	1942	Cahiers de Phys., No. 9, p. 47
GAYDON, A. G.	1947	Dissociation Energies, Chapman and Hall Ltd., London
HERZBERG, G. and HERZBERG, L.	1948	Nature, London **161**, 283
JOHNSON, F. S., PURCELL, J. D., TOUSEY, R. and WATANABE, K.	1952	J. Geophys. Res. **57**, 157
JOUAST, R. and VASSY, E.	1941	C. R. Acad. Sci. **213**, 139
LINDQUIST, R.	1952	J. Geophys. Res. **57**, 439
MARMO, F., ZELIKOFF, M. and TANAKA, Y.	1952	J. Opt. Soc. Amer. **42**, 870
MEINEL, A. B.	1950	Trans. Amer. Geophys. Un. **31**, 9
MIGEOTTE, M. V.	1950	Ap. J. **112**, 136
MITRA, S. K.	1951	Nature **167**, 897

VOL. 5 1954

MITRA, A. P. and JONES, R. E.	1953	Scientific Report No. 44, Ionosphere Research Laboratory, Pennsylvania State College, March 25
MOSES, H. E. and TA-YOU-WU	1952	Phys. Rev. **87**, 628
NERTNEY, R. J.	1953	J. Atmosph. Terr. Phys. **3**, 92
NICOLET, M.	1948	Mixed Commission on the Ionosphere, URSI, Bruxelles, p. 50
NICOLET, M.	1948	The Emission Spectra of the Night Sky and Aurora, Phys. Soc. London, 105
NICOLET, M.	1952	Physics and Medicine of the Upper Atmosphere, University of New Mexico Press, Albuquerque, p. 332
NICOLET, M. and MANGE, P.	1952	Scientific Report No. 35, Ionosphere Research Laboratory, Pennsylvania State College, April 15
PENNDORF, R.	1949	J. Geophys. Res. **54**, 7
PETRIE, W. and SMALL, R.	1952	Astrophys. J. **116**, 433
PIETENPOL, W. B., RENSE, W. A., WATZ, F. C., STACEY, D. S. and JACKSON, J. M.	1953	Phys. Rev. **90**, 156
PRESTON, W. M.	1940	Phys. Rev. **57**, 887
RAKSHIT, H.	1947	Ind. J. Phys. **21**, 57
SLOBAD, R. L. and KROGH, M. K.	1950	J. Amer. Chem. Soc. **72**, 1175
TOUSEY, R., WATANABE, K. and PURCELL, J. D.	1951	Phys. Rev. **83**, 792
VASSY, A. and VASSY, E.	1941	Cahiers de Physique **9**, 28
WATANABE, K., MARMO, F. and INN, E. C. Y.	1953	Phys. Rev. **90**, 155
WEISSLER, G. L., Po LEE and MOHR, E. I.	1952	J. Opt. Soc. Amer. **42**, 84
WHIPPLE, F. L.	1949	The Atmospheres of the Earth and the Planets; edited by G. P. KUIPER, The University of Chicago Press, pp. 149–158

Journal of Atmospheric and Terrestrial Physics, 1954, Vol. 5, pp. 44 to 56. Pergamon Press Ltd., London

A study of sodium in twilight. I. Theory*

D. M. HUNTEN

University of Saskatchewan, Saskatoon

(*Received* 4 *January* 1954)

ABSTRACT

The chemical equilibrium of sodium in the upper atmosphere is shown to lead to a peaked distribution of sodium atoms, the peak coinciding with the transition from O_2 to O. Curves for the intensity of the twilight emission of the *D*-lines are calculated for three model distributions. A study of the ionization of sodium by sunlight suggests that an annual intensity variation similar to the observed one should result, and that any evening-morning intensity difference should be greatest at the equinoxes. Observations are reported in another paper.

INTRODUCTION

Since the sodium emission in twilight was discovered by BERNARD (1938) and CABANNES, DUFAY and GAUZIT (1938), several investigators have studied its distribution in height. Assuming that the intensity of the emission is proportional to the number of sodium atoms illuminated by the sun, the distribution of sodium atoms can be deduced. BERNARD found that the emission disappeared suddenly when the shadow reached 60 km, and thus concluded that the sodium occupied a thin layer. CHAPMAN (1939) suggested that an exponential distribution similar to that of the atmosphere as a whole would lead to a similar result. This was confirmed by ELVEY and FARNSWORTH (1942), who made careful spectrophotometric measurements and found an exponential density distribution from 70 to 115 km paralleling that of the atmosphere.

Apparently unaware of this work and of CHAPMAN'S suggestion, VEGARD and TÖNSBERG (1940; 1941) and later VEGARD and KVIFTE (1945) extended the observations of BERNARD, aiming the spectrograph towards the zenith for one run, and then towards a point near the horizon for another. To make the "disappearance" occur at the same height for both runs, they had to assume that the shadow was cast by a layer ("screening layer") at a height of 44 km. The natural conclusion is that the screening layer is the top of the ozone layer and that the emission is excited by light in the range 2000–3000 Å. Similar results have been found more recently by KVIFTE (1949) and CARIO and STILLE (1950).

On the other hand, BRICARD and KASTLER, studying the characteristics of the emission itself, have concluded that it must be a resonance effect and must therefore be excited by yellow light. Ultraviolet light could only excite the emission by dissociating a sodium compound, and the lines would then be broad and unpolarized. These workers showed them to be narrow (1944) and to have the polarization of around 9% which was expected for resonance excitation (1950). They have also pointed out (1952) that the results of VEGARD and the others are

* The research reported in this paper has been sponsored by the Geophysics Research Directorate of the Air Force Cambridge Research Centre, Air Research and Development Command, under Contract AF 19(122)-152.

VOL. 5 1954

changed when account is taken of the distribution of density with height, the screening height then becoming very small. Since the sodium layer appears brighter near the horizon than at the zenith, the emission will last longer before "disappearing." This error was eliminated by DUFAY (1947), who analyzed data for two evenings by taking the times when the intensity dropped to half its initial value. The result was a screening height of 25 km and a sodium height of 80–90 km. He showed that this screening height was reasonable by calculating the transmission of the atmosphere for a horizontal beam of yellow light, taking into account ozone absorption and extinction by scattering. Such a calculation had already been made by BRICARD and KASTLER (1944).

It was repeated again by BARBIER (1948), who combined the result with several plausible distributions of sodium atoms to give curves of intensity versus the dip angle of the sun. He found that a thin layer did not give a good fit to his observations, and that the best fit was obtained with an exponential distribution of scale height 8 km, sharply cut off at the bottom of altitude 70 km.

This paper examines the chemical equilibrium between sodium and the other constituents of the atmosphere, showing that it may be expected to lead to just such a distribution of free atoms as was found by BARBIER. The bottom should coincide with the transition from molecular to atomic oxygen. The analysis of BARBIER is extended to include the effects of refraction of the incident light by the lower atmosphere and of the diameter of the sun. Intensity curves for comparison with observations are calculated for the sodium distributions suggested by the study of the chemical equilibrium. It is shown that the ionization of sodium by sunlight and the recombination of the ions are probably never in equilibrium. This leads immediately to the prediction of an annual intensity variation very much like the observed one (BRICARD and KASTLER, 1944), and a diurnal variation which is largest at the equinoxes but cannot be larger than 54%.

Observations and their comparison with theory are described in an accompanying paper (HUNTEN and SHEPHERD, 1954) which will be called II.

THE CHEMICAL EQUILIBRIUM OF SODIUM

In accordance with the arguments of CHAPMAN (1939), the important reactions are taken as

$$\mathrm{NaO} + \mathrm{O} \rightarrow \mathrm{Na} + \mathrm{O_2} \qquad \text{(reduction)}$$

$$\left.\begin{aligned} \mathrm{Na} + \mathrm{O_3} &\rightarrow \mathrm{NaO} + \mathrm{O_2} \\ \mathrm{Na} + \mathrm{O} + \mathrm{X} &\rightarrow \mathrm{NaO} + \mathrm{X} \end{aligned}\right\} \text{(oxidation)}$$

The rate coefficients may be estimated by means of the rules given by BATES and NICOLET (1950). This gives

$$\alpha \doteqdot 5 \times 10^{-15}\ \mathrm{cm^3/sec},$$

$$\beta \doteqdot 1{\cdot}5 \times 10^{-11}\ \mathrm{cm^3/sec},$$

$$\gamma \doteqdot 10^{-32}\ \mathrm{cm^6/sec}\ \text{(or less)},$$

for the three reactions. Using these, it can be shown immediately that the three-body oxidation is always negligible compared with the two-body at the altitudes of interest. Therefore, at equilibrium

$$\alpha n(\mathrm{NaO})n(\mathrm{O}) = \beta n(\mathrm{Na})n(\mathrm{O_3})$$

$$\frac{n(\mathrm{Na})}{n(\mathrm{NaO})} = \frac{\alpha}{\beta}\frac{n(\mathrm{O})}{n(\mathrm{O_3})} \doteqdot 3 \times 10^{-4}\frac{n(\mathrm{O})}{n(\mathrm{O_3})}$$

The sodium will be mostly combined where the ratio of the density of oxygen atoms to the density of ozone molecules is less than 3000, and mostly free where it is greater. Since the atomic oxygen density increases with altitude while the ozone density decreases, the sodium is free (and therefore, observable) at the higher altitudes. According to the calculations of BATES and NICOLET (1950), the ratio $n(\mathrm{O})/n(\mathrm{O_3})$ reaches 3000 at about 80 km; this agrees well with the observations reported in II.

If a distribution for the total amount of sodium, free and combined, is assumed, the distribution of free sodium may be found immediately. A plausible assumption is

$$n(\mathrm{Na}) + n(\mathrm{NaO}) = n_0 \exp(-z/7{\cdot}5)$$

where z is the altitude in kilometres and the scale height of 7·5 km is a convenient average for the region from 70 to 100 km. Substituting for $n(\mathrm{NaO})$, one finds

$$n(\mathrm{Na}) = \frac{n_0 \exp(-z/7{\cdot}5)}{1 + \frac{\beta}{\alpha}\frac{n(\mathrm{O_3})}{n(\mathrm{O})}}$$

At the higher altitudes, the second term in the denominator can be ignored, and the distribution is given by the numerator. For the lower altitudes, the distributions of O and $\mathrm{O_3}$ are required. The curves given by BATES and NICOLET can be approximated by $\exp(z/10)$ for O and $\exp(-z/5)$ for $\mathrm{O_3}$; thus

$$n(\mathrm{Na}) \doteqdot k \exp(-z/7{\cdot}5) \exp(z/5) \exp(z/10) = k \exp(z/6)$$

The bottom cuts off with a scale height of −6 km. The altitude of the transition between the two limiting cases has already been found.

Other investigators have found considerably different distributions of O; for example, MOSES and WU (1952) conclude that the density of O increases by many orders of magnitude within a very few kilometres at about 85 km. The density of Na would then behave very similarly, and a sharp cut-off, as suggested by BARBIER, would result.

Because of this uncertainty, three models (A, B and C) of the sodium distribution have been chosen for investigation and comparison with observation. All have an exponential of scale height 7·5 km from altitude z_c up. Model A cuts off sharply at z_c; Model B has another exponential of the same shape for a bottom; and Model C has constant density from z_c down. They are illustrated in Fig. 2. These particular shapes were chosen for their mathematical simplicity as well as their theoretical significance; the final results are so similar for even these three

VOL. 5 1954

widely differing models that details of shape (such as sharp breaks instead of smooth transitions) must be completely unimportant.

Theory of the Intensity Variation

In this section curves of scattered intensity versus solar depression are calculated for comparison with observations. A preferable procedure would be to analyse the observations by a process resembling differentiation to find the sodium distribution. (Such analysis is used to find the cross-section for a photonuclear reaction as a function of energy from experiments with betatron irradiation). Unfortunately, the observations reported in II are not nearly accurate enough for this; they can only serve to distinguish between Models *A*, *B*, and *C*.

The transmission of the atmosphere for horizontal rays of yellow light was calculated (Appendix 1). The extinction due to scattering is easily found; since

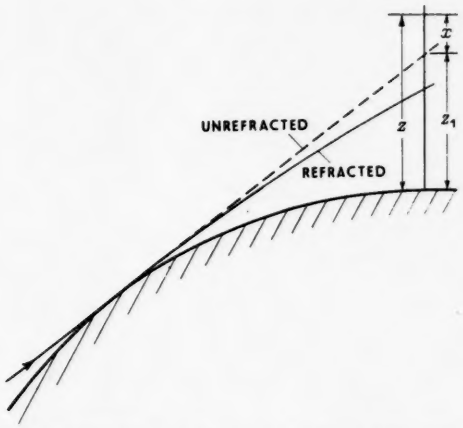

Fig. 1. Geometry of the twilight situation, showing meanings of symbols.

the ozone absorption varies, it was simply scaled from the curve given by Dufay (1947). Two other effects, neglected by previous workers, were included. The first is the "smearing" of the shadow pattern due to the diameter of the sun. The second, considerably more important, is refraction, which lowers the shadow of the earth's surface about 20 km and modifies the intensity distribution of the light. Minor approximations were made in several places to permit analytical treatment of the equations. The resulting transmission function is called $T(x)$ where the x co-ordinate system moves with the shadow and has its origin at the point where the unrefracted shadow of the surface intersects the line of observation (Fig. 1 and 2). Strictly speaking, the refraction varies somewhat with z, as well as with x, but this variation has been neglected.

From Fig. 2 it is seen that the scattered flux will be

$$K(z_1) = \int_{-25}^{\infty} J_0 T(x) \cdot \sigma \cdot n(z) dx \text{ photons/cm}^2\text{/sec/sterad},$$

where J_0 is the flux incident on the atmosphere, σ is the scattering cross-section per unit solid angle of a sodium atom, and $n(z)$ is the density (sodium atoms/cm^3). The lower limit of the integral comes from refraction (20 km) and the radius of the sun (5 km).

Since $z = z_1 + x$,

$$K(z_1) = J_0\sigma \int_{-25}^{\infty} n(z_1 + x) \cdot T(x)\, dx$$

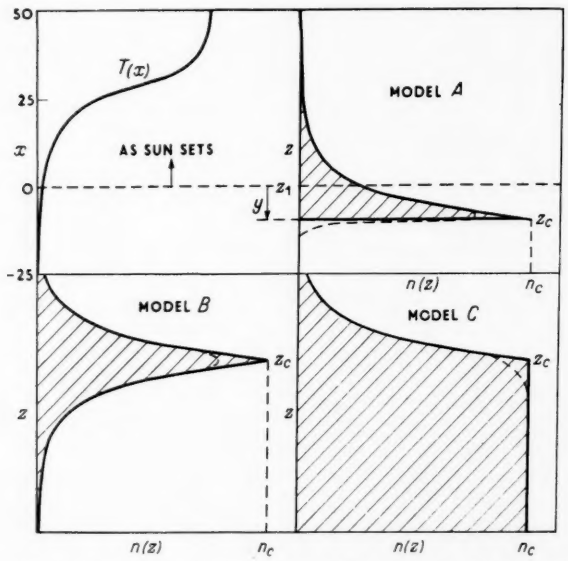

Fig. 2. Schematic representation of the transmission function $T(x)$ and the sodium density $n(z)$ for models A, B, and C.

Suppose first that the sodium atoms are distributed exponentially with a scale height H; then

$$n(z_1 + x) = n_0 \exp\left(-\frac{z_1 + x}{H}\right) = n_0 \exp(-z_1/H) \exp(-x/H) = n(z_1) \exp(-x/H)$$

$$\therefore \quad K(z_1) = J_0\sigma n(z_1) \int_{-25}^{\infty} \exp(-x/H) \cdot T(x)\, dx = J_0\sigma n(z_1) \cdot Z(-25)$$

The integral $Z(-25)$ is a constant (and may be evaluated numerically); the scattered flux thus varies with $n(z_1)$, that is, exponentially. This, however, is contrary to the observations, which show K to be almost constant for z_1 less than 50 km.

A thin layer of sodium will give an intensity curve identical with the function T. The curves for Models A, B, and C may be found in the following way. It is convenient to define $y = z_c - z_1$; then $z = z_c - y + x$. y is the distance of the discontinuity from the unrefracted shadow line.

VOL. 5 1954

Model A. The density is zero for x less than y; above this it is $n_c \exp\left(-\frac{x-y}{H}\right)$; substituting this gives

$$K(z_1) = J_0 \sigma n_c \exp(y/H) \int_y^\infty \exp(-x/H) T(x)\, dx$$
$$= J_0 \sigma n_c \exp(y/H) Z(y)$$
$$= J_0 \sigma n_c A(y)$$

$Z(y)$ is easily evaluated by numerical integration (counting squares) of $T(x) \exp(-x/H)$. This function is shown in Fig. 3, and it is easily seen why it is difficult to

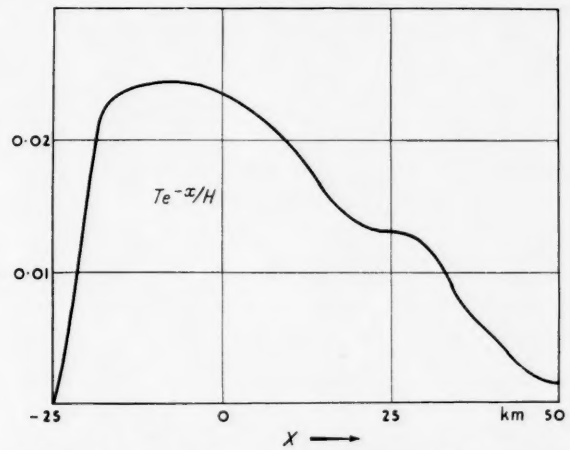

Fig. 3. The function $T(x) \exp(-x/H)$ which shows the relative contributions to the total scattered light from different altitudes for an exponential distribution of sodium atoms.

deduce much about the density distribution from the observations: significant contributions to the scattered light come from a range of about 60 km altitude. The maximum value of $A(y)$ is H (for $T = 1$).

Model B. Below the peak the density is now $n_c \exp\left(\frac{x-y}{H}\right)$, giving

$$K(z_1) = J_0 \sigma n_c \left[\exp(y/H) Z(y) + \exp(-y/H) \int_{-25}^{y} \exp(x/H) T(x)\, dx\right]$$
$$= J_0 \sigma n_c [Z(y) \exp(y/H) + Z'(y) \exp(-y/H)]$$
$$= J_0 \sigma n_c B(y)$$

The new term is evaluated as before and added to that already found for Model A. The maximum value of $B(y)$ is $2H$.

Model C. The density is constant below z_c, giving simply

$$K(z_1) = J_0 \sigma n_c \left[Z(y) \exp(y/H) + \int_{-25}^{y} T(x)\, dx\right]$$
$$= J_0 \sigma n_c C(y)$$

Here there is no maximum value.

The scale height was taken as 7·5 km for all calculations; the results are shown in Table 1. The difference between the three is much less than might appear from the table, since it is the shapes and not the actual magnitudes that are useful. They are much better compared by superposing their high altitude parts, which are essentially identical. Even at low altitudes the deviation is small. With such a fit, z_c for B is 5 km higher, and for C 9 km higher, than for A. The curves are illustrated in II, Fig. 3(b).

Table 1. *Calculated results for atmospheric transmission and for the shape of the brightness-altitude curve with Models A, B, and C*

x or y (km)	$T(x)$	$T\exp(-x/H)$	$A(y)$ (km)	$B(y)$ (km)	$C(y)$ (km)
−25	0	0	0·041	0·041	0·041
−20	0·0011	0·0157	0·077	0·079	0·080
−15	0·0032	0·0237	0·135	0·145	0·149
−10	0·0064	0·0242	0·231	0·254	0·269
−5	0·0126	0·0243	0·390	0·438	0·474
0	0·0236	0·0236	0·633	0·728	0·806
5	0·0420	0·0218	1·00	1·16	1·33
10	0·0750	0·0198	1·56	1·87	2·17
15	0·120	0·0162	2·38	3·00	3·47
20	0·195	0·0136	3·56	4·45	5·43
25	0·36	0·0129	5·11	6·53	8·30
30	0·66	0·0120	6·55	9·21	12·29
35	0·88	0·0076	7·19	11·4	16·86
40	0·955	0·0046	7·50	13·1	21·77
45	0·98	0·0024	7·50	13·9	26·61
50	0·99	0·0013	7·50	14·3	31·54

IONIZATION AND RECOMBINATION OF SODIUM

The photo-ionization of sodium by solar ultraviolet radiation has been examined by BATES (1947), assuming that the sun radiates as a black body of rather over 6000° K. Rocket measurements (TOUSEY, 1953), however, have shown that the intensity just below 2400 Å is about nine times smaller than that of a 6000° black body, or very nearly ten times less than assumed by BATES. The ionization rate i is lowered to 2×10^{-5}/Na atom/sec. BATES concluded that the sodium was mostly ionized, especially at the higher levels, and suggested that the emission might be brighter in the morning than in the evening due to recombination during the night. The most effective recombination process appeared to be charge-transfer between positive and negative ions, and the coefficient α' was taken as 10^{-8} cm^3/sec (the maximum probable value). The calculations of equilibrium have been repeated using the new ionization rate and the densities of sodium found in II. The resulting values of the fraction f of neutral atoms are shown in Table 2, for altitudes of 85 and 110 km and for charge-transfer coefficients of 10^{-8} and 10^{-9}. These values are larger than those found by BATES, of course, but the density of ions is still appreciable.

VOL. 5 1954

These calculations are for equilibrium during the day, but it is unlikely that this equilibrium is ever reached. f increases at night with a time constant $1/k$ (where $k = \alpha' n(-)$), which is seen to be of order 10^5 sec or one day, and decreases during the day with a time constant $1/(i + k)$, which is about half a day. This will have two observable effects: f is larger in the morning than in the evening (diurnal effect); and f is smallest in summer and largest in winter (seasonal effect). A

Table 2. Fraction of the sodium atoms in the neutral state and recombination rate for different altitudes and different charge-transfer coefficients

z	n(Na)	$n(-)$	$\alpha' = 10^{-8}$		$\alpha' = 10^{-9}$	
			f	$k = \alpha' n(-)$	f	k
85	10,000	$= n(\mathrm{Na^+})$	0·69	$4{\cdot}5 \times 10^{-5}$	0·42	$1{\cdot}4 \times 10^{-5}$
110	360	2×10^3	0·50	2×10^{-5}	0·09	2×10^{-6}

seasonal effect of this nature has been observed (Bricard and Kastler, 1944); it occurs in the nightglow (Roach and Pettit, 1952) as well as in the twilight glow, suggesting that the two may be closely related. Assuming that the ionic equilibrium is independent of the chemical equilibrium, the changes are described by the differential equation

$$\frac{\mathrm{d}}{\mathrm{d}t} n(\mathrm{Na}) = -i\, n(\mathrm{Na}) + \alpha' n(-) n(\mathrm{Na^+})$$

$$\frac{\mathrm{d}f}{\mathrm{d}t} = -if + k(1 - f)$$

$$= -k'f + k \qquad \text{where } k' = i + k$$

The solution is

$$f = k/k' + (\text{const}) \exp(-k't)$$

The constant of integration is different for day and night; also, at night $i = 0$ and $k' = k$. Then

$$f = k/k' + D \exp(-k't) \qquad \text{(day)}$$

$$f = 1 - N \exp(-kt) \qquad \text{(night)}$$

The boundary conditions are that $f = f_m$ in the morning and $f = f_e$ in the evening. Let the length of daylight be T and let t be measured from sunrise; then

$$f_m = k/k' + D \qquad = 1 - N \exp(-24k) \qquad \text{(sunrise)}$$

$$f_e = k/k' + D \exp(-k'T) = 1 - N \exp(-kT) \qquad \text{(sunset)}$$

For shortness, T has been expressed in hours rather than seconds, but this should cause no difficulty. These four equations may be solved for f_m and f_e, giving

$$f_m = 1 - M \exp\left[-k(24 - T)\right]$$
$$f_e = 1 - M$$

where

$$M = \frac{i \exp(iT) - \exp(-kT)}{k' \exp(iT) - \exp(-k24)}$$

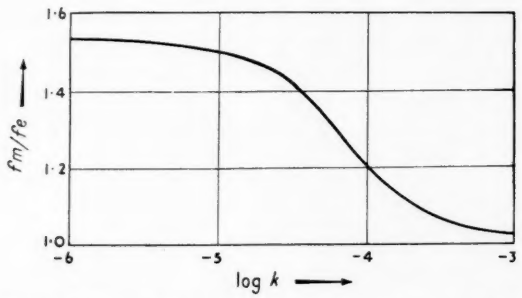

Fig. 4. Morning/evening ratio at the equinoxes. Ionization rate $i = 2 \times 10^{-5}$/Na atom/sec.

VOL. 5 1954

Calculations of f_m and f_e have been made for $T = 4$, 8, 12, 16, and 20 hours, and for k ranging from 5×10^{-5}/sec down, with a view to determining k by observation. It must be noted that absolute values of f cannot be observed; hence, the results presented are the morning/evening ratio for the diurnal effect, and the

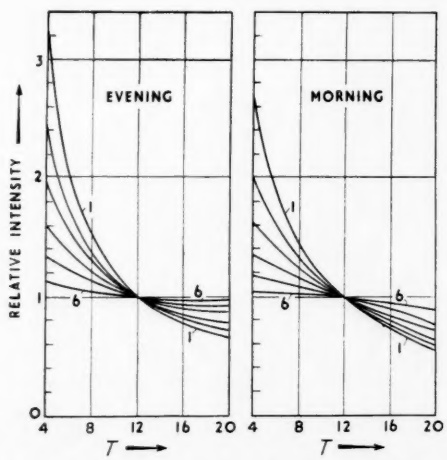

Fig. 5. Relative intensity of the twilight emission as a function of T, the length of the day in hours, for the following values of k: 1, 10^{-6}; 2, 2×10^{-6}; 3, 5×10^{-6}; 4, 10^{-5}; 5, 2×10^{-5}; 6, 5×10^{-5}.

intensity relative to the value at $T = 12$ (equinoxes) for the seasonal effect. For k less than about 10^{-6}/sec the expressions approach a limiting form which makes these ratios independent of k.

The diurnal effect, as would be expected, is largest at the equinoxes and approximately symmetrical about them; since it is not large even then, the ratio f_m/f_e is given only for $T = 12$ hours. From Fig. 4 it may be seen that it is 1·54 for the smallest values of k and approaches unity for the largest. The largest k in Table 2 corresponds to a ratio of about 1·35. There appears to be little chance of finding k from this effect, especially since k is quite likely to vary with altitude. However, an observed morning/evening ratio of about 1·4 would help to confirm the assumptions made in the analysis. It should be noted that T must be calculated for an altitude of 85 km, and that here the equinoxes occur about the middle of February and the end of October for latitude 52°.

Curves for the seasonal effect are shown in Fig. 5. There is evidently a better chance of determining k from these. At latitude 52° the range of T is about 10 to 20 hours; unfortunately, this means that the most widely separated part of the curves is not accessible at Saskatoon. Observations from a station farther north would be desirable.

An alternative explanation of the seasonal effect has been offered by BRICARD and KASTLER (1944): incident sunlight may be weakened by absorption in the wings of water-vapour lines near the D-lines. The seasonal variation would then correlate with humidity instead of with the position of the sun. It might be possible to distinguish between the two causes, since they differ in phase by a month or two.

CONCLUSIONS

Discussion of the chemical equilibrium of sodium in the upper atmosphere has suggested that free sodium atoms should be found at altitudes above about 80 km. Intensity curves for the twilight emission have been derived for three simple model distributions resembling the theoretically expected ones. Comparison with observations should show which model is nearest the truth, and should yield a value of the altitude at which molecular oxygen gives way to atomic. Such a comparison is made in II (HUNTEN and SHEPHERD, 1954).

Ionization of sodium by sunlight and recombination of the ions has been shown to lead to a diurnal and a seasonal intensity variation. The diurnal effect, though never very large, should be largest at the equinoxes; the seasonal effect, also rather small, is similar to what has been observed in both the twilight glow and the nightglow. Comparison with observations should give information about the validity of the assumptions made, and might give information about recombination coefficients. These observations are in progress, and it is hoped that the results will be reported at a later date.

APPENDIX 1. TRANSMISSION OF THE ATMOSPHERE FOR A HORIZONTAL BEAM

1. *Extinction*

The transmission factor of a path of length X of air at normal density is $T = \exp(-\beta X)$ where the extinction coefficient $\beta = 8{\cdot}98 \times 10^{-8}$ cm^{-1} for 5893 A (VAN DE HULST, 1952).

$$X = \frac{1}{n(\mathrm{O})} \int n \, ds = \frac{R}{n(\mathrm{O})} \int n d\theta \text{ since } \theta \text{ is small. (See Fig. A1).}$$

Now $\cos\theta = \dfrac{R+h}{R+z}$. Expanding in series, $1 - \dfrac{\theta^2}{2} \doteq 1 - \dfrac{z-h}{R}$

$$z = \frac{R\theta^2}{2} + h$$

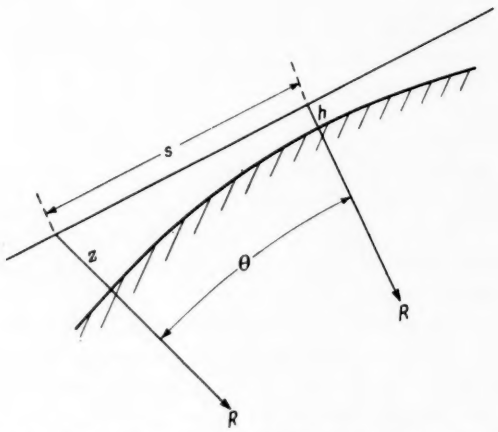

Fig. A1. Co-ordinates for calculating the extinction.

VOL. 5 1954

Taking $n(z) = n(\mathrm{O}) \exp(-z/H)$

$$= n(h) \exp\left(\frac{-R\theta^2}{2H}\right),$$

$$\therefore \qquad X = R\frac{n(h)}{n(\mathrm{O})}\int_{-\infty}^{\infty} \exp\left(-\frac{R\theta^2}{2H}\right) \mathrm{d}\theta = \sqrt{2\pi RH}\,\frac{n(h)}{n(\mathrm{O})}$$

Taking H as 7·12 km (the average value in the region from 0 to 40 km), we find $\sqrt{2\pi RH} = 534$ km and $\beta X = 4{\cdot}79\,\dfrac{n(z)}{n(\mathrm{O})}$.

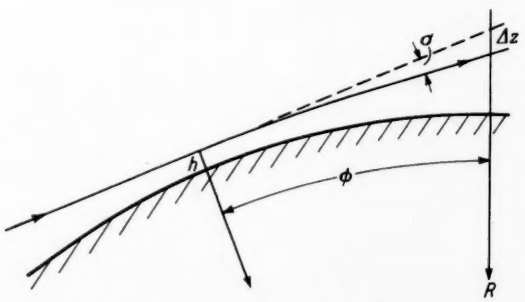

Fig. A2. The calculation of the refraction.

2. *Ozone Absorption*

The amount and distribution of ozone varies through the year and from place to place; the ozone absorption was therefore simply copied from DUFAY's paper by scaling from his curve (DUFAY, 1947).

3. *Refraction*

This requires evaluation of two effects—the bending down of the light rays, and the reduction of the intensity of the light because it is spread over a larger area. It is easily seen from Fig. A2 that

$$\Delta z = R\phi\sigma$$

At the surface, the angle of refraction σ is twice the usual "horizontal refraction," which is 35′; and it varies directly with the density. The angle ϕ changes as the sun sets, but an average value 7°·5 (estimated from the zenith observations in II) was used for simplicity.

Then $\Delta z(h) = 20\,\dfrac{n(h)}{n(\mathrm{O})}$ km.

From Fig. A3,

$$\Delta x = \Delta h - R\phi \cdot \Delta\sigma$$

$$\frac{\Delta x}{\Delta h} = 1 - R\phi\,\frac{\Delta\sigma}{\Delta h}$$

$$\frac{\mathrm{d}x}{\mathrm{d}h} = 1 - R\phi\,\frac{\mathrm{d}\sigma}{\mathrm{d}h}$$

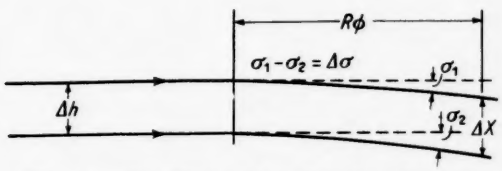

Fig. A3. The dilution of the light by refraction.

If $\sigma = \sigma_0 \exp(-h/H)$, $\dfrac{\mathrm{d}\sigma}{\mathrm{d}h} = -\dfrac{\sigma}{H}$

and $$\frac{\mathrm{d}x}{\mathrm{d}h} = 1 + \frac{R\phi\sigma}{H} = 1 + \frac{\Delta z}{H}$$

The intensity must be divided by this factor.

Since the extinction was calculated for a straight path, it is in error, but by only a small amount.

4. *Diameter of the Sun*

To quite a good approximation, this may be taken into account by "smearing" the pattern already derived over a distance corresponding to 32 minutes of arc, or about 10 km.

5. *Calculations*

Though a constant scale height was assumed to simplify the integrations and differentiations, the actual densities were used for the ratio $\dfrac{n(h)}{n(\mathrm{O})}$. The figures used are those of the Rocket Panel (1952). The transmission as a function of h was calculated as in 1 and 2, and then converted to a function of x as in 3. The result was plotted and smeared (part 4) by eye.

REFERENCES

BARBIER, D.	1948	Ann. Géophys. **4**, 193–210
BATES, D. R.	1947	Terr. Magn. Atmos. Elect. **52**, 71–5
BATES, D. R. and NICOLET, M.	1950	J. Geophys. Res. **55**, 301–27
BERNARD, R.	1938	Z. Phys. **110**, 291–302
BRICARD, J. and KASTLER, A.	1944	Ann. Géophys. **1**, 53–91
BRICARD, J. and KASTLER, A.	1950	Ann. Géophys. **6**, 286–99
BRICARD, J. and KASTLER, A.	1952	Mem. Soc. Roy. Sci. Liège **12**, No. 1–2, 87–96
CABANNES, J., DUFAY, J. and GAUZIT, J.	1938	Astrophys. J. **88**, 164–72
CARIO, G. and STILLE, U.	1950	Abhandl. Braunschw. Wiss. Gesell. **2**, 40–66
CHAPMAN, S.	1939	Astrophys. J. **90**, 309–16
DUFAY, J.	1947	C. R. Acad. Sci. (Paris) **225**, 690–2
ELVEY, C. T. and FARNSWORTH, A. H.	1942	Astrophys. J. **96**, 451–67
HUNTEN, D. M. and SHEPHERD, G. G.	1954	J. Atmosph. Terr. Phys. **5**, 57-62
KVIFTE, G.	1949	Geofys. Publ. **17**, No. 11
MOSES, H. E. and WU, T.-Y.	1952	Phys. Rev. **87**, 628–32
ROACH, F. E. and PETTIT, Helen B.	1952	Mem. Soc. Roy. Sci. Liège **12**, No. 1–2, 13–42
The Rocket Panel	1952	Phys. Rev. **88**, 1027–32
TOUSEY, R.	1953	J. Opt. Soc. Amer. **43**, 245–51
VAN DE HULST, H. C.	1952	The atmospheres of the earth and planets (G. P. KUIPER, ed.). University of Chicago Press 2nd ed. Table 4, p. 55
VEGARD, L. and TÖNSBERG, E.	1940	Geofys. Publ. **13**, No. 1
	1941	Geofys. Publ. **13**, No. 5
VEGARD, L. and KVIFTE, G.	1945	Geofys. Publ. **16**, No. 7

VOL. 5 1954

Journal of Atmospheric and Terrestrial Physics, 1954. Vol. 5, pp. 57 to 62. Pergamon Press Ltd., London

A study of sodium in twilight. II. Observations on the distribution*

D. M. HUNTEN and G. G. SHEPHERD

University of Saskatchewan, Saskatoon

(*Received* 4 *January* 1954)

ABSTRACT

Observations of the *D*-lines in twilight have been made with a recording auroral spectrometer. When properly corrected, the horizon observations agree with the zenith ones, showing that there is no need to assume a "screening layer" high in the atmosphere for the exciting radiation. Comparison of the observed variation of intensity with curves from paper I indicate that the density of atomic sodium is a maximum at 85 $\pm$ 3 km and falls away exponentially above and below this. The upper part has a scale height of 7·5 $\pm$ 2 km to at least 115 km. The shape of the bottom can only be found roughly, but it is similar to that of the top. The peak of the sodium distribution is probably associated with the transition from molecular to atomic oxygen.

INTRODUCTION

In the past fifteen years several investigators have studied the distribution of sodium atoms in the upper atmosphere by observing the twilight emission of the *D*-lines. (References and a historical summary may be found in an accompanying paper (HUNTEN, 1954) which will be called I.) Even with a fast spectrograph, only 8 or 10 exposures can be obtained during a single twilight, and it has therefore been impossible to find more than the general features of the distribution. BARBIER has suggested an exponential of scale height 8 km, sharply cut off at the bottom of altitude 70 km. BLAMONT and KASTLER (1951) have used a much more sensitive photometer, but they were unable to get useful results below 100 km because of interference from the Fraunhofer absorption lines in the scattered sunlight.

We have found that our photoelectric spectrometer (HUNTEN, 1953) which was built for auroral studies is very suitable for observing this phenomenon. The sensitivity is enough to give one spectrum per minute; thus, thirty spectra in the zenith and thirty near the horizon can be obtained in an average twilight. The observations are fitted best by a symmetrical distribution of sodium, falling off exponentially with scale height 7·5 km above and below a peak at 85 $\pm$ 3 km.

Some workers, especially VEGARD and collaborators, have concluded that their zenith and horizon observations could only be brought into accord by assuming that the effective twilight shadow was cast by a "screening layer" at a height of 44 km instead of by the earth's surface. BRICARD and KASTLER have shown that this result was due to the assumption that the sodium occupied a thin layer, and that for an exponential distribution a typical observation of VEGARD's gave a screening height of 25 km. Such a height could be explained by attenuation of the incident sunlight in the lower atmosphere. When our horizon measurements are corrected for the apparent increase of brightness with zenith distance, they agree

* The research reported in this paper has been sponsored by the Geophysics Research Directorate of the Air Force Cambridge Research Centre, Air Research and Development Command, under Contract AF 19(122)-152.

very well with the zenith measurements. This shows conclusively that the suggestion of BRICARD and KASTLER is correct and that there is no need to postulate the existence of a screening layer.

OBSERVATIONAL TECHNIQUE

The spectrometer was set to scan over a spectral range of about 30 Å once a minute. Spectral slit widths of 5 Å and 10 Å were used. The narrower slits suppress the continuous spectrum and permit observations to be extended to lower altitudes; the wider give the greater sensitivity needed for higher altitudes. From May 1953 on, a Polaroid filter was used to cut down the relative intensity of the continuous spectrum; this is possible because the sodium emission is nearly unpolarized. It is of course much more effective in the zenith than near the horizon.

Fig. 1(*a*) shows the appearance of a typical spectrum. The unresolved *D*-lines appear on top of the continuous spectrum which is due to Rayleigh scattering. As shown, the intensity *I* may be measured from a line drawn through the continuous spectrum at the ends; but this must be corrected for the presence of the

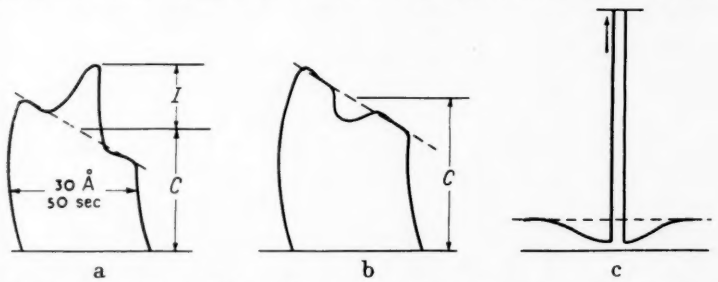

Fig. 1. (*a*) Typical scan showing sodium emission on top of continuous spectrum. (*b*) Scan on scattered sunlight only, showing Fraunhofer *D*-line. (*c*) Schematic drawing showing how (*a*) would appear under very high resolution.

Fraunhofer absorption line. Under the same scanning conditions this appears as in Fig. 1(*b*), the dip being a fraction x of C. (x has varied from 0·06 to 0·14.) The corrected intensity is then $I' = I + xC$, as may be seen from Fig. 1(*c*). Here an absorption and an emission line are shown as they might appear if the resolution were high enough to show their actual widths. The spectrometer slits are much wider than the whole figure, of course. The deflection I in Fig. 1(*a*) is proportional to the difference between the area of the emission line and the area of the absorption line, and the dip in Fig. 1(*b*) is proportional to the area of the absorption line. Therefore, the correction to I must be equal to the dip, that is, to xC. The fact that there are two unresolved lines does not alter this conclusion. When the shadow is below 20 to 30 km (depending on the resolution) the emission line drops right into the absorption and can no longer be measured.

A typical evening's observations consisted of runs at zenith distances of a few degrees and 75°. Zenith observations began at solar dip angles of $4\frac{1}{2}°$ to 6° and ended at $8\frac{1}{2}°$ to 9°. The spectrometer was then lowered to the horizon and observations continued to 12° or 13°. Occasionally the horizon run was omitted or an extra one was made at zenith distance 85°. The order of observations was of course reversed in the morning.

VOL. 5 1954

So that the observations may be compared with the curves derived in I, it is necessary to find the altitude z_1 for each one-minute period. z_1 is the altitude at which the line of sight intersects the line from the sun tangent to the earth's surface. This is not the shadow line because of refraction, but it is used as a reference because its position is easily calculated. Fig. 2 shows the situation. From the law of sines,

$$\frac{R}{\sin \alpha} = \frac{R + z_1}{\sin \zeta}.$$

But $$\alpha = \zeta - \theta,$$

$$\therefore \qquad \sin (\zeta - \theta) = \frac{\sin \zeta}{1 + z_1/R}.$$

Also, $$\sec \phi = \frac{R + z_1}{R} = 1 + z_1/R.$$

θ and ϕ may be found from these two equations for any zenith distance ζ of interest; then $\beta = \theta + \phi$. For the zenith θ is zero and $\beta = \phi$. z_1 need only be

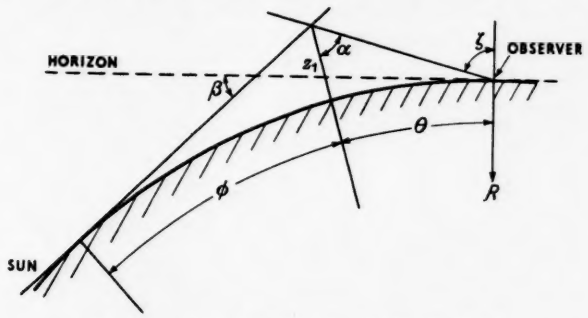

Fig. 2. Angles and distances during twilight.

known to the nearest integer; it is convenient to tabulate the values of β for z_1 even and ranging from 20 to 120 km. β is found from the equation for a spherical triangle, which may be written

$$\sin \beta = \cos l \cos \delta \cos t - \sin l \sin \delta.$$

Here l is the latitude, δ the sun's declination, and t the local time measured from midnight. A nomogram for this equation has been constructed which gives results quickly and with sufficient accuracy.

The apparent brightness of the layer is proportional to $\sec \alpha$ which may be found from the first equation (the VAN RHIJN equation). This factor must be used to correct the horizon observations before they may be compared with the zenith ones; fortunately it varies only slowly with altitude and a constant value 3·3 (for $z_1 = 85$ km) may be used. This is the correction which was omitted by VEGARD and other workers who used the zenith-horizon method.

RESULTS

A typical plot of $\log I'$ against z_1 is shown in Fig. 3*a*. The logarithmic intensity scale is appropriate in view of the nearly exponential variation which is expected.

It has a further advantage in that it permits theoretical curves to be fitted simply by moving them about, with no change in shape caused by a varying scale factor. It will be seen that the corrected horizon data agree very well with the zenith data; no screening layer need be postulated. The horizon points do not appear to be lowered appreciably by atmospheric extinction.

To learn something about the distribution of sodium it is necessary to try to fit the observations with the calculated curves from I. These were found for three model distributions, A, B, and C. All have an exponential of scale height 7·5 km from altitude z_c up. Model A cuts off sharply at z_c; Model B has another exponential of the same shape for a bottom; and Model C has constant density from z_c down. The three curves are shown with the observations in Fig. 3*b*. A and B are so similar that it is not easy to distinguish between them, but B seems to fit somewhat better; C disagrees definitely. One would hesitate to choose between A and B on the basis of Fig. 3 alone, but all our other observations favour B in a similar manner. It therefore seems safe to conclude that the shape of the sodium distribution is close to that of Model B.

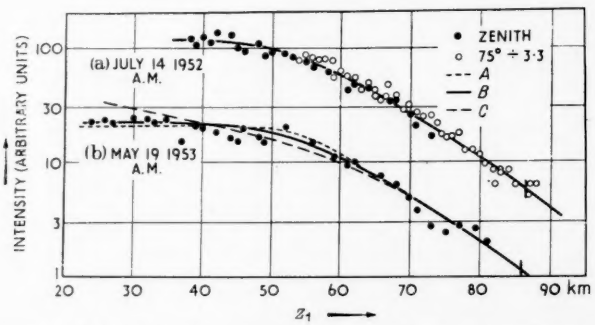

Fig. 3. (*a*) Observations of July 14, 1952, A.M. The corrected horizon intensities agree very well with the zenith ones. A Model B curve is shown. (*b*) Observations of May 19, 1953, A.M. Curves from Models A, B, and C are shown; the B seems to fit best and C seems to be excluded.

The altitude z_c of the peak is that value of z_1 which corresponds to the point $y = 0$ on the theoretical curve (See I). This point may be marked on the curve as in Fig. 3, where $z_c = 87$ and 86 km for a and b. The results obtained to date are collected in Table 1. The average value of z_c is 84·7 $\pm$ 0·7 km, where the probable error has been calculated as if the errors were statistical. Some allowance should be made for possible systematic error, however; for example, curve A gives a z_c about 5 km less than curve B. A final result of $z_c = 85 \pm 3$ km appears reasonable.

The density n_c of sodium atoms at z_c may be found if the brightness of the emission at the plateau is known. We have not yet measured this, but BRICARD and KASTLER (1944) have found it to be 8×10^8 quanta/cm^2 column/sec/unit solid angle. In I it was shown that for Model B this is equal to $2J_0\sigma Hn_c$, where J_0 is the flux of solar radiation incident on the atmosphere, σ is the scattering cross-section per unit solid angle of a sodium atom, and H is the scale height for the sodium. BATES and MASSEY (1946) have shown that $4\pi J_0\sigma$ is about 1 quantum/atom/sec, with a large uncertainty in J_0 because the depth of the

VOL. 5 1954

Fraunhofer D-lines is not at all accurately known. Then n_c is of order of magnitude 10^4 Na atoms/cc.

Discussion and Conclusions

The present results may be compared with those of Barbier (1948) (see also the introduction), who was able to fit his observations using essentially a Model A distribution with $z_c = 70$ km. Undoubtedly Model B would have fitted just as well, and would have had $z_c = 75$ km. This result would be expected to be lower than ours, since no account was taken of refraction in its derivation. It thus appears that Barbier's result is not in disagreement with our more accurate one.

Table 1. *Results found for the altitude z_c of the peak of a Model B sodium distribution*

Date	z_c (km)	*Date*	z_c (km)
July 14/52 a.m.	86	May 25/53 p.m.	79
July 28/52 a.m.	91	May 26/53 a.m.	85
April 18/53 p.m.	84	June 5/53 p.m.	87
April 19/53 p.m.	84	June 6/53 a.m.	88
May 19/53 a.m.	86	June 6/53 p.m.	85
May 19/53 p.m.	86	Aug. 20/53 a.m.	80
May 20/53 a.m.	86	Aug. 20/53 p.m.	91
May 20/53 p.m.	76	Aug. 28/53 p.m.	87
May 21/53 a.m.	80	Average	$84{\cdot}7 \pm 0{\cdot}7$

It is difficult to say how accurate our scale height of 7·5 km for the top half of the distribution is, or how high it extends. This particular figure was chosen as an approximate average for the region 50 to 70 km where it was thought the sodium would be found, and was retained for simplicity. From 85 to 100 km 7·0 km would be more appropriate, but is probably indistinguishable by observation. We feel that our observations indicate a scale height of $7{\cdot}5 \pm 2$ km up to about 100 km. For higher altitudes we must turn to the results of others.

Those of Elvey and Farnsworth (1942), when plotted by our method, extend from $z_1 = 70$ to 106 km and may be fitted by this part of our theoretical curve. Although they scatter over an intensity range of 3 to 1, they indicate that the distribution extends with no very large change to 115 km. Elvey and Farnsworth measured the contribution from the nightglow and subtracted it from their observations; this was apparently not done by Blamont and Kastler (1951) who used an ingenious and very sensitive photoelectric photometer. Such a background from the nightglow may account for the very large scale height of 85 km which they found for the region 130 to 200 km.

As for the shape of the bottom of the distribution, it is obvious that anything resembling Model B will be just as good, since it is almost impossible to distinguish between shapes as different as Models A and B.

We conclude that the sodium is distributed exponentially with scale height $7{\cdot}5 \pm 2$ km from 85 ± 3 to 100 and probably to 115 km; below 85 km it drops off

quite rapidly; and that the density at 85 km is roughly 10^4 atoms/cc. It was shown in I that the peak is probably associated with the transition from molecular to atomic oxygen; specifically, that it should be at the altitude where the ratio (number of oxygen atoms/cc)/(number of ozone molecules/cc) reaches 3000. The atomic oxygen density itself would be of order of magnitude 10^{11} atoms/cc.

REFERENCES

BARBIER, D.	1948	Ann. Géophys. **4**, 193–210
BATES, D. R. and MASSEY, H. S. W.	1946	Proc. Roy. Soc. A **187**, 261–96
BLAMONT, J. E. and KASTLER, A.	1951	Ann. Géophys. **7**, 73–89
BRICARD, J. and KASTLER, A.	1944	Ann. Géophys. **1**, 53–91
ELVEY, C. T. and FARNSWORTH, A. H.	1942	Astrophys. J. **96**, 451–67
HUNTEN, D. M.	1953	Canad. J. Phys. **31**, 681–90
	1954	J. Atmosph. Terr. Phys. **5**, 44–56

VOL.
5
1954

RESEARCH NOTES

The intensity distribution in the second positive band system of nitrogen in a laboratory light source and in the aurorae

(*Received* 26 *January* 1954)

ABSTRACT

The intensity distribution in the second positive band system of N_2 emitted from an ordinary discharge lamp is measured, and the relative transition probabilities are derived. VEGARD's intensity measurements of these bands in high latitude aurorae are discussed, the most likely relative population of the upper vibrational levels ($N_2C^3\Pi_u$) being found to be $g(0) = 1{\cdot}0$, $g(1) = 0{\cdot}6$ and $g(2) = 0{\cdot}35$. It can be shown that the excitation mechanisms $N_2(^1\Sigma_g^+) + e \rightarrow N_2(C^3\Pi_u) + e$ or $N_2^+(X^2\Sigma_g^+) + e \rightarrow N_2(C^3\Pi_u) + h\nu$ cannot alone be responsible for this population.

1. INTRODUCTION

As pointed out by BATES (1949), the intensity distribution within a band system may give us valuable information about the excitation mechanism responsible for the emission. The total intensity of a band is approximately proportional to

$$(1) \qquad I(v'v'') = \frac{g(v')\, h\nu(v'v'')^4\, p(v'v'')}{\sum_{v''} p(v'v'')\, \nu(v'v'')^3} \qquad \sum_{v''} p(v'v'') = 1$$

where $g(v')$ is the population of the upper vibrational levels, $\nu(v'v'')$ is the frequency of the band, and $p(v'v'')$ is the Franck-Condon factor (which is determined by the vibrational wave functions).

If we know the complete set of the p's for the v'-progressions in which we are interested we can easily find the relative $g(v')$'s from the band intensities.

BATES has calculated theoretically the p's for the first and second positive systems of N_2 and the first negative system of N_2^+, and compared the values with data derived experimentally. The agreement is rather poor, probably because of the inaccuracy of the laboratory measurements.

2. INTENSITY MEASUREMENTS OF THE SECOND POSITIVE SYSTEM OF N_2

Results of some new measurements of the second positive system of $N_2(C^3\Pi_u \rightarrow B^3\Pi_g)$ are given in this paper and the p's are derived from them by means of the formula

$$(2) \qquad p(v'v'') = \frac{I(v'v'')/\nu(v'v'')^4}{\sum_{v''} I(v'v'')/\nu(v'v'')^4}$$

In earlier measurements the intensities seems to have been determined as the "peak" intensity, i.e. the intensity corresponding to the maximum density (TAWDE, 1934). This is an unreliable method. The intensity given by eq. (1) is the total intensity of the band. As the resolving power, the dispersion and lens errors of the spectrograph will take part in the formation of the band profile, the actual distribution of the band energy on the plate will vary from band to band, and the peak intensities will not correspond to relative values of the total band intensities.

In the new measurements a Hilger Littrow type quartz spectrograph with very broad slit has been used, so that each band has a continuous intensity distribution on the plate. The total intensity was found by integration over the whole band. As a standard, a calibrated tungsten band lamp from *Kipp & Zonen*, Delft, was adopted. Spectra from this lamp were taken on each plate.

The nitrogen light source was a Hilger discharge lamp with a quartz window. A lamp was selected which had very few impurities, and this proved very good. Kodak B 10 plates were used. These have no great variation in sensitivity from 2900 to 4200 Å. The necessary correction for plate sensitivity is therefore small, and so are the errors. The γ-value of the plate, however, varies rather greatly with wavelength and the H-D curve had to be drawn for each band.

The results of the intensity measurements are given in Table 1, and the derived p's in Table 2. The intensities of the bands with $v' \geqslant 3$ were too weak to be determined accurately and are therefore excluded.

Table 1. *Intensity distribution in the second positive system of* N_2 ($C^3\Pi_u \rightarrow B^3\Pi_g$) *with Hilger discharge lamp as source*

v' \ v''	0	1	2	3	4	5
0	46	30	9·8	2·18		
1	26	0·8	10·1	7·1	2·78	
2	3·6	10·1	0·3	1·1	1·88	1·37

Table 2. *p's for* N_2 $C^3\Pi_u \rightarrow B^3\Pi_g$. *Derived from Table* 1.

v' \ v''	0	1	2	3	4	5	6
0	0·44	0·36	0·150	0·044	(0·01)		
1	0·38	0·02	0·24	0·21	0·108	(0·03)	
2	0·126	0·43	0·02	0·072	0·157	0·148	(0·04)

Table 3. *p's for* N_2 $C^3\Pi_u \rightarrow B^3\Pi_g$. *Theoretical values* (BATES, 1949)

v' \ v''	0	1	2	3
0	0·48	0·32	0·14	$0·04_5$
1	0·39	$0·03_8$	0·22	0·19
2	0·12	0·37	$0·00_9$	$0·09_4$

The agreement between the values in Tables 2 and 3 seems satisfactory. The errors in the experimental results are estimated to be less than 5–8%, except for the (1–1) and (2–2) bands, which are more uncertain. The values in brackets are estimated from the measurements of TAWDE.

VOL. 5 1954

3. Calculations of $g(v')$ from Intensity Measurements in High Latitude Aurorae

L. Vegard (1932, 1933) has published intensities of auroral lines and bands, including the second positive system of N_2. The agreement with the laboratory measurements is rather poor. There are several possible reasons for this. The intensities are probably "peak" intensities, and seem to have been determined chiefly in order to confirm the identification. The spectrograms are taken without step filter or any other intensity reduction device, so that all intensities on a spectrogram cannot have a density suitable for accurate measurement. The spectrographs have rather high light power, which means great lens errors and deviations from the expected band profiles.

Whatever the actual reason may be we can conclude, however, that *the error in any intensity ratio will be greater the greater the wavelength difference, and the greater the density difference.* We should therefore suppose only the intensity ratios within any one sequence to be approximately correct, and put most trust in the intensity ratios which are closest to unity.

All the intensities for the second positive system given by Vegard and his collaborators seem to be based upon the values from Tromsö published in 1933. These are mean values of several spectrograms, including those described in 1932.

From eq. (1) we get:

$$\frac{g(v_1')}{g(v_2')} = \frac{I(v_1'v_x'')\,\nu(v_2'v_y'')^4\,p(v_2'v_y'')\sum_{v''} p(v_1'v'')\,\nu(v_1'v'')^3}{I(v_2'v_y'')\,\nu(v_1'v_x'')^4\,p(v_1'v_x'')\sum_{v''} p(v_2'v'')\,\nu(v_2'v'')^3} \tag{3}$$

We can thus determine the relative values of $g(v')$ from each sequence. The intensity ratios derived from Vegard's values are given in Table 4, column 3. The intensity of the first member in each sequence is put equal to 1·00. The g's, given in column 4, are then determined by eq. (3) and data from Table 2.

Table 4. High latitude aurorae (Tromsö)

v'—v''	λ	I_{rel}	$g(v')$	v'—v''	λ	I_{rel}	$g(v')$
0–3	4059	1·00	1·00	0–1	3577	1·00	1·00
1–4	3998	1·07	0·44	1–2	3537	0·50	0·77
2–5	3943	1·72	0·23	2–3	3500	0·22	1·22
0–2	3805	1·00	1·00				
1–3	3755	0·85	0·61	1–0	3159	1·00	(0·60)
2–4	3710	0·50	0·51	2–1	3136	0·61	0·35

The intensity differences in the (0–0) sequence are too great to give reliable results and this sequence is therefore ignored. The intensity of the (2–3) band clearly cannot be trusted. The $g(1)$ from the (1–0) band is put equal to 0·60, and the $g(2)$ from the (2–1) band is then found to be 0·35.

According to these considerations the data in Table 4 give $g(0) = 1{\cdot}0$, $g(1) = 0{\cdot}6$ and $g(2) = 0{\cdot}35$ *as the most probable values of the population of the vibrational levels of the upper electronic state of the second positive system of nitrogen in high latitude aurorae (Tromsö).*

4. Discussion

These values differ appreciably from those estimated by Bates (1949, 1·0, 0·9, 0·8). Even the new estimates of the population require, however, according to Bates, a temperature of about 4000°K if the excitation mechanism should be electron impact with N_2 molecules in the ground state $X^1\Sigma_g^+$.

It can also be shown that the process $N_2^+(X^2\Sigma_g^+) + e \rightarrow N_2(C^3\Pi_u) + h\nu$ require about the same temperature. The p's for this process are also calculated by Bates (1949), and the relative population of the $N_2(C^3\Pi_u)$ states from this process can easily be calculated: $g(v'') = \sum_{v'} g(v')\, p(v'v'')$. With the ground state of N_2^+ in thermal equilibrium at 1000°K we get $g(0) = 1{\cdot}00$, $g(1) = 0{\cdot}22$ and $g(2) = 0{\cdot}05$. For very high temperatures the p's given by Bates (for v' and $v'' \leq 2$ only) are not sufficient to calculate the g's. It is, however, easily shown that the temperature required to give the values found in high latitude aurorae must be about 4000–6000°K.

The temperature measured by Vegard, Tönsberg and Kvifte (1951, 1952) from the rotational structure of the first negative system of N_2^+ is about 220°. The author, who was Professor Vegard's assistant during this work, judges the errors in this value to be less than 10–20%. One seems therefore forced to admit that other excitation mechanisms may be at least partly responsible for the emission of the second positive system of the N_2 molecule in the aurorae.

Acknowledgments

In conclusion I wish to express my thanks to Professor G. Kvifte for his interest in, and encouragement of this work. My thanks are also due to the Physical Institute of Oslo University and to the Central Institute of Industrial Research for the use of laboratories and equipment, and to the Norwegian Research Council for Science and the Humanities for financial support.

Appendix

After having received this paper, the Editor kindly drew the attention of the author to a paper by Petrie and Small (1952). In this paper is published a series of intensity measurements of the second positive group of nitrogen in high latitude aurorae (Saskatoon, Canada). The general trend of these intensities is in better agreement with laboratory measurements, but also these intensities at shorter wavelength are too small compared with laboratory data.

Treating the values given by Petrie and Small in the same manner as those given by Vegard, we get, however, the same mean values of the $g(v)$'s.

The Auroral Observatory, Tromsö. A. Omholt

References

Bates, D. R.	1949	Proc. Roy. Soc. A. **196,** 217
Petrie and Small	1952	J. Geophys. Res. **57,** 51
Tawde, N. R.	1934	Proc. Phys. Soc. **46,** 324
Vegard, L.	1932	Geofys. Publ. **9,** No. 11
	1933	Geofys. Publ. **10,** No. 4
Vegard, L., Tönsberg, E. and Kvifte, G.	1951	Geofys. Publ. **18,** No. 4
Vegard, L., and Tönsberg, E.	1952	Geofys. Publ. **18,** No. 8

VOL. 5 1954

Sources of atmospheric and planetary energy

(*Received* 30 *December* 1953)

ABSTRACT

The radiation incident upon the earth by the sun, the moon, meteors, cosmic rays, the aurora and various contributions to night skylight have been determined and tabulated for comparative purposes. It is certain that most sources of energy, other than solar, are about equal to 10^{17}–10^{19} ergs/sec.

It is interesting to determine the energy received by the earth or expended in the atmosphere from various cosmic and terrestrial sources. These are listed in Table 1. With the exception

Table 1. *Energy available from various solar and terrestrial sources*

Source	*Energy (erg/sec)*	*Ratio:* $\frac{\textit{source indicated}}{\textit{normal sun}}$
Normal sun	$1{\cdot}76 \times 10^{24}$	1·00
Full moon	$3{\cdot}09 \times 10^{19}$	$1{\cdot}76 \times 10^{-5}$
Lightning	$1{\cdot}60 \times 10^{19}$	$9{\cdot}09 \times 10^{-6}$
Skylight	$2{\cdot}61 \times 10^{17}$	$1{\cdot}48 \times 10^{-7}$
Bright aurora	$2{\cdot}53 \times 10^{17}$	$1{\cdot}44 \times 10^{-7}$
Cosmic rays	$1{\cdot}63 \times 10^{17}$	$9{\cdot}26 \times 10^{-8}$
Meteors	$1{\cdot}44 \times 10^{17}$	$8{\cdot}18 \times 10^{-8}$
Night (or background) airglow	$1{\cdot}12 \times 10^{17}$	$6{\cdot}37 \times 10^{-8}$

of the sun's radiation, all remaining energy sources (except that of long wave radiation, exchange of latent heat, etc.) are in the range 10^{17}–10^{19} ergs/sec. A discussion of the values is given below:

1. SOLAR. The outstanding source of terrestrial energy is, of course, the sun, in comparison with which all other sources are insignificant. Not all incident solar energy is retained by the planet. Since the planetary albedo (S. Fritz, 1949) is about 35·5 per cent, only 64·5 per cent is retained by the earth, distributed between the surface and the atmosphere as shown in Table 2. Although the results in this tabulation were derived for the

Table 2. *Disposition of solar energy* (*Northern Hemisphere*)

	Percent	*Percent*
Incoming radiation received at top of atmosphere		100
Radiation reflected and scattered to space	35·5	
Radiation absorbed by the atmosphere	14·5	
Radiation absorbed by the earth's surface	50·0	

Northern Hemisphere (J. LONDON, 1951), they probably apply fairly closely to the planet as a whole. The albedo in the Southern Hemisphere may be somewhat greater because of the greater water surface (SVERDRUP, 1943; BRUNT, 1939) but this increase may be offset by a decreased total cloudiness (HEWSON, 1943; NEIBURGER, 1949; ALDRICH, 1919). The radiation retained by the atmosphere is absorbed principally by three constitutions (DOBSON, 1942; CRAIG, 1950; HUELPER, 1943): (a) water vapour (10·5 per cent); (b) ozone (2·5 per cent); and (c) liquid water mainly in clouds (1·5 per cent). This radiation is generally in the infrared region of the spectrum although some of the incident ultraviolet radiation is also absorbed. The total energy absorbed at the surface of the earth includes direct insolation as well as that transmitted through partially opaque forms (clouds, etc.) and that scattered downwards by molecules and dust.

As the net energy balance of the planet is zero, the retained energy is eventually returned to space in the form of long wave radiation. However, prior to the escape of this radiation to space an elaborate energy exchange between the atmosphere and the earth's surface occurs.

The value of the solar constant has been studied for a number of years and is generally considered to be 1·98 gm calories/cm^2 min (NICOLET, 1951). However, recent rocket measurements indicate that the value may be 2·04 gm calories/cm^2 min (GAST, 1953). Employing the former value, the energy received on a disk tangent to the subsolar point and located outside the atmosphere is $1{\cdot}76 \times 10^{24}$ ergs/sec when the radius of the disk equals the radius of the earth. If the planet is considered, the disk radius equals that of solid earth plus atmosphere; the energy deposited in this case is $2{\cdot}35 \times 10^{24}$ ergs/sec.

2. LUNAR. As the solar energy absorbed by the moon is much less than one per cent, the energy directed earthwards (either by radiation or reflection) by the lunar surface is essentially the solar energy received by the moon. The total energy received by a disk (whose radius equals that of the moon) tangent to the moon at the subsolar point is $1{\cdot}12 \times 10^{23}$ ergs/sec, from which the energy intercepted by the solid earth is $3{\cdot}09 \times 10^{19}$ ergs/sec, and by the earth and its atmosphere, $4{\cdot}15 \times 10^{19}$ ergs/sec. It should be noted that on this basis the ratio of (lunar/solar) energy is $1{\cdot}76 \times 10^{-5}$.

On a luminous basis the results are somewhat different. The sun's brightness is considered equivalent to 150,000 candles/cm^2 and that of a full moon 0·37 candles/cm^2; thus the brightness ratio (moon/sun) is $2{\cdot}47 \times 10^{-6}$. It might be mentioned that the moon's albedo is only 7 per cent, and that its brightness at half-moon is only one ninth that of the full moon.

3. LIGHTNING. It has been estimated (ISREAL, 1942) that an average lightning stroke requires $1{\cdot}60 \times 10^{17}$ ergs and that 100 lightning strokes/sec occur over the earth's surface daily (WILSON, 1929). On this basis the energy dissipated in electric discharges over the globe is at least $1{\cdot}60 \times 10^{19}$ ergs/sec.

4. METEORS. The total meteoric mass impinging upon the terrestrial atmosphere is about $1{\cdot}16 \times 10^4$ gm/sec. As the average speed of a meteor may be taken as $5{\cdot}0 \times 10^6$ cm/sec, the kinetic energy dissipated by meteors (WHIPPLE, 1952) in the terrestrial atmosphere is $1{\cdot}44 \times 10^{17}$ ergs/sec. This energy is distributed as heat: light: ionization (HERLOFSON, 1948) in the proportion $10^4 : 10^2 : 1$.

5. NIGHT AIRGLOW. The night airglow may be considered to consist of background residual emission which exists constantly in the atmosphere. During twilight periods, the airglow emissions are strongly augmented, and during daylight very much enhanced over the background airglow because of the absorption of sunlight. This background (or residual) airglow remains at night, where it is defined as the night airglow. In determining the energy of the night airglow, the following were considered to be average values for the specified transitions/cm^2 column (RAYLEIGH, 1930; CERANIAJEV *et al.*, 1936; J. CABANNES

VOL. 5 1954

et al., 1938; ROACH, 1950a; BATES *et al.*, 1950; ROACH *et al.*, 1950b; HULBURT, 1951): 5577 Å—2×10^8; (b) 6300 Å—1×10^7; (c) sodium *D*-lines—5×10^7; (d) OH bands (from 4600 Å—11,600 Å)—6×10^9. Using these values the average energy of the background or night airglow is $1{\cdot}12 \times 10^{17}$ ergs/sec over the entire hemisphere (sunlit and dark) if the mean emission altitude is about 100 km.

It may be of interest to note that the total intensity of the night skylight is of the same order of magnitude as that of the night airglow. Table 3 indicates several estimates of the

Table 3. *Sources contributing to the intensity of the night skylight*

	CABANNES (1951)	MITRA (1952)	BARBIER (1947)	*New estimate*
Airglow: Resolved bands	25	40	20	25
Skylight: Continuous background	75	60	80	75
Unresolved stars	20	30	12	25
Extra galactic light	—	—	—	5
Zodiacal light	15	15	15	15
Galactic light	10	5	—	5
Unknown origin	30	—	53†	25
Scattered light	—	10*	—	—

* Light scattered by the atmosphere but arising from other sources; e.g., the resolved bands, galactic and zodiacal light.
† Band wings.

sources contributing to the night skylight intensity (CABANNES, 1951; MITRA, 1952; BARBIER, 1947). The last column is an estimate of the best probable values. The latter were determined after consideration of the work of MEINEL (1953) and OLIVER and CHAMBERLAIN (1953) in resolving part of the continuum attributed to the night skylight. On the basis of the new estimates, the energy received from the skylight on both the dark and light hemispheres of the earth is $2{\cdot}61 \times 10^{17}$ ergs.

6. AURORA. The visual intensity of a bright aurora has been considered to be 100 times as intense as that of the night skylight in the green region ($\lambda = 5577$ Å). (The aurora has no strong OH radiations.) It was assumed that the aurora is emitted simultaneously in the Northern and Southern auroral zones, in the daylight as well as in the darkened hemisphere. The auroral zone is defined as the zone 10° wide located at an average distance of 23° from the geomagnetic poles. On some occasions very bright aurorae having a luminous intensity equal to that of the full moon have been reported. If this brightness occurs everywhere throughout both auroral zones (which is doubtful) the energy may be greater than that listed above by a factor of about one hundred.

7. COSMIC RAYS. To determine the energy introduced by cosmic rays, it is assumed that they arrive with about 20×10^9 eV/cm^2 sec everywhere over the surface of the earth. The total energy thus admitted is $1{\cdot}63 \times 10^{17}$ ergs/sec.

Geophysics Research Directorate
Air Force Cambridge Research Centre
Air Research and Development Command

N. C. GERSON

References

Aldrich, L. B.	1919	Smithsonian Misc Collection **69**, No. 10
Barbier, D.	1947	Ann. Astrophys. **10**, 141
Bates, D. R. and Nicolet, M.	1950	J. Geophys. Res. **55**, 235
Brunt, D.	1939	Physical and Dynamical Meteorology, Cambridge University Press
Cabannes, J.	1951	L'Astronomie **65**, 457
Cabannes, J., Dufay, G., and Gauzit, J.	1938	Astrophys. J. **88**, 164
Ceraniajev, V. I., Khvostikov I. A., and Panschin, A. B.	1936	J. de Physics **7**, 149
Craig, R.	1950	The Observation and Photochemistry of Atmospheric Ozone, Met. Monographs **1**, No. 3
Dobson, G. M. B.	1942	Quart. J. Roy. Met. Soc. **68**, 202
Fritz, S.	1949	J. Met. **6**, 277
Gast, R.	1953	A.F. Cambridge Research Centre, Private Communication
Herlofson, N.	1948	Rept. Prog. Phys. **11**, 444
Hewson, E. W.	1943	Quart. J. Roy. Met. Soc. **69**, 47
Huelper, O.	1943	Met. Zeit. **60**, 37
Hulburt, E. O.	1951	Compendium of Meteorology, American Met. Soc., Boston
Isreal, H.	1942	Die Electrischenschein der Gewittes
London, J.	1951	Report 131.06, New York University, College of Engineering, New York
Meinel, A. B.	1953	Astrophys. J. **118**, 200
Mitra, S. K.	1952	The Upper Atmosphere, The Asiatic Soc., Calcutta
Neiburger, M.	1949	J. Met. **6**, 98
Nicolet, M.	1951	Ann. Astrophys. **14**, 249
Oliver, N. J. and Chamberlain, J.	1953	Astrophys. J. **118**, 197
Rayleigh, Lord	1930	Proc. Roy. Soc. **A129**, 458
Roach, F. E. and Barbier, D.	1950a	Trans. Amer. Geophys. Union **31**, 7
Roach, F. E., Pettit, H., and Williams, D. R.	1950b	J. Geophys. Res. **55**, 183
Sverdrup, H. V.	1943	Oceanography for Meteorologists, Prentice-Hall, New York
Wilson, C. T. R.	1929	J. Franklin Inst. **208**, 1
Whipple, F.	1952	Bull. Amer. Met. Soc. **33**, 13

VOL. 5 1954

Controls of geomagnetic activity by sunspots

(*Received* 13 *December* 1953)

ABSTRACT

Radio and geometric properties of sunspots are shown to provide a useful basis for forecasting magnetic activity.

Controls of geomagnetic activity by sunspots were recently demonstrated in two independent ways.

(*a*) It was first pointed out (Denisse, 1951, 1952, 1953) that an average *increase* of geomagnetic activity follows the central meridian passage (C.M.P.) of sunspots that are sources of strong radio noise (*R* spots). On the contrary C.M.P. of sunspots that do not show any noticeable radio emission (*Q* spots) are followed by a regular *decrease* of magnetic activity.

(*b*) It was also shown (BECKER, 1953) that a similar *decrease* of magnetic activity occurs when two spots, or groups of spots, of comparable degrees of evolution, are symmetrically located on the disc with respect to the solar equator.

In all cases, the induced variation of magnetic activity is a maximum during the period of two or three days following the C.M.P. of the corresponding spot.

About one third of the *R* and *Q* spots selected in (*a*), belong to one of the symmetrical pairs considered in (*b*). In such occasions it is found, as expected, that both effects are

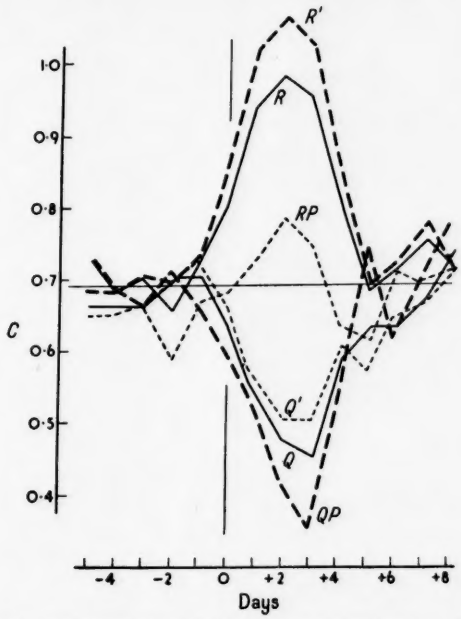

Fig. 1. Mean value of the magnetic figure *C* for 5 days preceding (—) and 8 days following (+) the C.M.P. of different kinds of sunspots selected as explained in the text.

added for *Q* spots and opposed for *R* spots. An interesting point is that, when both effects are combined together, the probabilities of finding either a quiet day or a disturbed day, according to the situation, are large enough to be profitably used for short term forecasting of magnetic and probably ionospheric activity.

Fig. 1 summarizes the results obtained for the three years period 1948–49–50. The mean value of the international magnetic figure *C* is plotted according to the superposed epochs method for days following and preceding the C.M.P. of each selected spot.

Controls by *R* and *Q* spots described in (*a*) are illustrated by curves (*R*) and (*Q*) which correspond, respectively, to 114 *R* spots of types *D*, *E*, *F*, and *G* (following the BRUNNER classification) and to 107 *Q* spots of types *E*, *F*, *G*, and *H*.

Curve (*R'*) is related to the 82 *R* spots that do not belong to symmetrical pairs. The subsequent increase of magnetic activity is very large at days +1, +2, and +3, and can be compared with the weak maximum, barely significant, shown by the (*RP*) curve derived from the 32 *R* spots that are part of symmetrical pairs.

Curve (*QP*) is related to the C.M.P. of 39 quiet symmetrical pairs; it shows a very pronounced decrease of magnetic activity occurring mainly at days +2 and +3. The decrease seen on the (*Q'*) curve, plotted with the 68 quiet spots left, is much less marked but quite regular.

Table 1 gives a numerical account of the preceding results. It indicates the percentage of the time when the magnetic figure C is included between given limits, during days $+2$ and $+3$ after C.M.P. of Q' and QP spots and during days $+1$, $+2$, and $+3$ after C.M.P. of R' spots. $Cm = 0{\cdot}7$ is the mean value of C during the three years.

Table 1

Spots \ C	$C < 0{\cdot}5$	$C < 0{\cdot}7$	$C \geqslant 1{\cdot}0$
QP	72	87	2
Q'	50	75	5
R'	19	27	55
All days	35	57	25

Number of cases (in %) where the magnetic figure C takes values included in the limits indicated on the first line:

for days $+2$ and $+3$ after C.M.P. of a QP spot,
for days $+2$ and $+3$ after C.M.P. of a Q' spot,
for days $+1$, $+2$, and $+3$, after C.M.P. of an R' spot,
for days taken at random.

VOL. 5 1954

Particularly worthy of notice is the very regular decrease of magnetic activity following the passages of Q' and specially QP spots; probabilities of finding a quiet day ($C < 0{\cdot}7$) or even a very quiet day ($C < 0{\cdot}5$) are very large; on the other hand, the perturbed days ($C \geqslant 1{\cdot}0$) are practically absent during those periods.

The increase of magnetic activity related to R' spots is less regular, but far more frequent than for days taken at random. It corresponds either to magnetic storms showing well defined sudden commencements, or to periods of moderate activity ($0{\cdot}8 < C < 1{\cdot}8$) with no 27 days recurrence tendency.

Obviously, the efficiency of forecast founded on such effects varies strongly according to the phase of the solar cycle. For periods similar to the one considered here it seems possible, each year, to forecast on an average, about 80 perturbed days and 75 days particularly quiet.

Udo Becker,
Fraunhofer Institut, Freiburg i. Br. Schauinsland

Jean Francois Denisse,
Observatoire de Meudon, Meudon (S & O)

References

Denisse, J. F., Steinberg, J. L., et Zisler, S. 1951 Compt. Rend. **232**, 2290
Denisse, J. F. 1952 Ann. de Geophys. **8**, 55
Denisse, J. F. 1953 Compt. Rend. **236** 1856
Becker, U. 1953 Z. Astr. **32**, 195

Journal of Atmospheric and Terrestrial Physics, 1954, Vol. 5, pp. 73 to 82. Pergamon Press Ltd., London

A subsidiary layer in the *E* region of the ionosphere

R. NAISMITH

Radio Research Station, Slough

(*Received* 21 *January* 1954)

ABSTRACT

Reasons and methods of identification are given for the recognition of an independent layer at 90–100 km height. It is suggested that the ionisation in this layer results from the impact of meteors on the atmosphere and that it may therefore be called the meteoric *E*-layer. The distinctive properties may be used to extend the use of the ionosphere for intermediate distance radio communication.

1. INTRODUCTION

A considerable amount of evidence has accumulated in recent years to indicate that the ionisation observed in region-*E* of the ionosphere by radio methods is due to a variety of causes. APPLETON and NAISMITH (1935) presented evidence which indicated the separate existence in this region of ionisation due to solar ultra-violet light and that due to other causes. The region in which the former occurs is now known as the normal *E*-layer and in the latter as the sporadic *E*-layer.

In a later communication (APPLETON and NAISMITH, 1947) the same authors suggested a further sub-division of the sporadic *E* phenomenon by recognising the separate existence of short bursts of ionisation which were identified in the same communication with the incidence of sporadic meteors. The term "meteoric layer" has already been suggested (HEY and STEWART, 1947) as a name for the ionisation formed in this manner but, since it is physically situated within the region-*E* it would appear preferable to qualify the title to indicate this and the term "meteoric *E*-layer" seems to be appropriate. This would leave the term "sporadic *E*-layer" to denote ionisation in region-*E* other than that due to ultra-violet light or sporadic meteors. We could then denote the highest frequencies on which these three types of region-*E* echoes occur at vertical incidence, namely, ultra-violet, meteor and sporadic by the symbols *fE*, *fEm* and *fEs* respectively. In the following paper evidence is given to show that these phenomena can be separated and hence that this suggestion is practicable.

2. THE METEORIC *E* LAYER AT VERTICAL INCIDENCE

(*a*) *Identification*

The three types of region-*E* echoes described above may be observed at vertical incidence with the normal type of ionospheric recorder. Examples of them are shown in Photograph 1. The variation of the echo pattern over the frequency range 2·6 to 5 Mc/s is shown at (A). The variation of the *Em* and *Es* echoes with time on a single frequency of 4·2 Mc/s is shown at (B). The same observation is repeated on the higher frequency of 4·6 Mc/s which demonstrates how the greater separation existing between the *Em* echo and the extraordinary component of the *Es* echoes enables the former to be clearly identified. It also shows the existence of appreciable reflections at these lower levels. The three records were taken immediately following one another.

The case for the separate identification of the meteoric *E*-layer rests to a large

extent on the feasibility of separating the echoes denoted *fEm* and *fEs* above. When the records are less clear than those reproduced in Photograph 1 there are general features which still enable this identification to be made. The intermittent character of the *Em* echoes is probably the best guide. Another is the low reflection coefficient which makes it rarely possible to see a second reflection. There have been no observations of *Em* ionisation obscuring reflections from or above the normal *E*-region. Over the range of frequencies on which *Em* echoes are observed the height of reflection is extraordinarily uniform and no group retardation effects are ever observed (see Photograph 1).

Sources of ionisation not immediately overhead may also produce *Em* echoes. When these are observed their "height" will appear to be greater than the true height, the amount depending upon the amount of deviation present.

The above identification of the meteoric *E*-layer is based on the appearance of the echoes obtained from it on the normal type of ionospheric recorder. As indicated in (*g*) below the layer was also identified when special equipment was used. WATSON (1941) records that "the average heights at which meteors appear and disappear are well known from scientific visual observations. For ordinary meteors the heights of appearance are consistently near 95 km." This may be compared with the heights of 90–97 km observed in the course of Loran measurements described in Section 3 below.

(*b*) *Limitations in recording*

The conclusions reached in this paper are based almost entirely on measurements made in Great Britain but they are believed to be generally applicable. In parts of the world where the background noise level is particularly high greater power would be necessary to establish the existence of the meteoric *E*-layer. Also, in polar regions there is a substantial amount of ionisation in the sporadic region-*E* which is associated with some form of particle ionisation so that once again it would be more difficult to separate completely the ionisation due to sporadic meteors. It therefore appears that measurements made in Great Britain are particularly suitable for the establishment of the separate existence of a meteoric *E*-layer.

The highest frequency (*fEs* or *fEm*) on which echoes of the sporadic type are observed from the lower part of region-*E* will depend upon the amount of interference present, the degree of absorption, the power of the transmitter and the sensitivity of the receiver. For this reason comparisons of measurements using different equipments are seldom satisfactory and it is impossible to compare measurements from different parts of the world. Even on the same recorder the varying sensitivity with frequency will cause the observed values of *fEs* and *fEm* to appear more often on some frequencies than on others. A change of aerial, too, may cause a variation in the response on certain frequenoies.

(*c*) *Measurements to be discussed*

The measurements discussed below were made during the routine hourly observations on the ionosphere at the Radio Research Station, Slough. They are, therefore, not a continuous observation but should be regarded as a sample observation made during a period of five minutes centred on each hour.

VOL. 5 1954

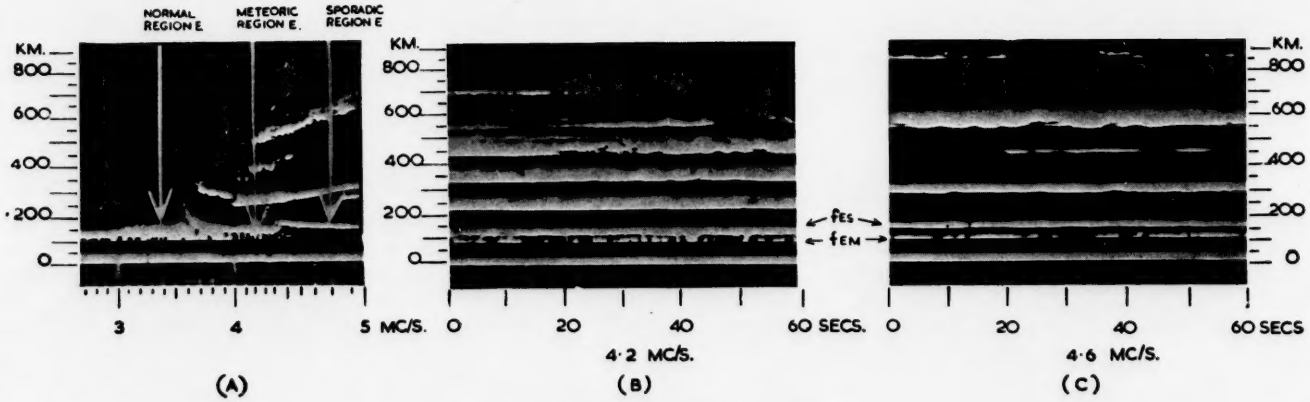

PHOTOGRAPH 1. METEOR TYPE ECHO

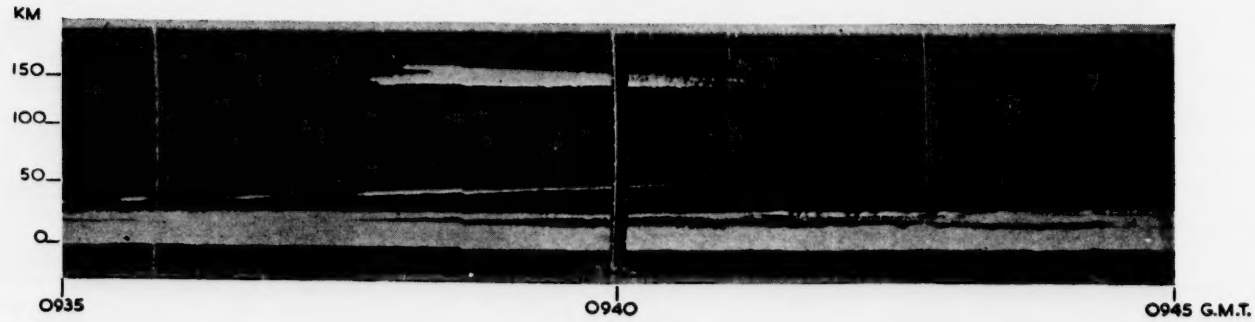

PHOTOGRAPH 2.

VOL.
5
1954

Although "trailing echoes" from heights near 100 km have been observed at Slough for many years (APPLETON *et al.*, 1939) instrumental difficulties have prevented their separation from other forms of *Es* with certainty. About three years ago special adjustments were made to the Slough recorder to enable reliable records of these weak echoes to be obtained and there are, in consequence, over 25,000 hourly measurements now available. This is considered to be an adequate sample to illustrate the features described below.

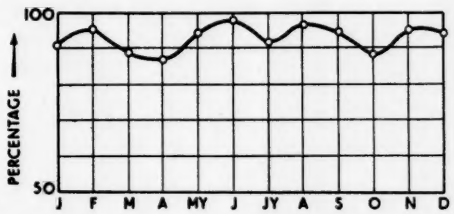

Fig. 1. Seasonal variation in the percentage of time *fEs* was recorded.

It has been shown in the introduction that until the separate existence of the meteoric *E*-layer is accepted it is necessary to regard it as part of the sporadic *E*-region. A close examination of the records obtained since the alteration to the recorder shows that meteoric *E*-reflections are observed on higher frequencies than the remainder of the sporadic *E*-reflections for 70% of the occasions when any sporadic *E*-echoes are present in summer and for 95% of the occasions in winter. (Using the symbols with the meaning attached to them in the introduction, *fEm* is greater than *fEs* for 70% of the occasions in summer and for 95% in winter.)

This is a sufficiently great predominance of the meteoric *E*-phenomenon to enable the already published values of *fEs* to be interpreted as predominantly a measure of meteoric *E* and to use them as such to discover the main features of the variations in meteoric *E*. The data presented in Figs. 1 to 4 is based on the total of all sporadic *E*-echoes observed during three years. It is probable that part of the summer maximum shown in Fig. 2 is due to some form or re-distribution of *Es* ionisation. There is, for example, an increase in sporadic *E*-ionisation in the southern hemisphere also in local summer.

(*d*) *Seasonal variations*

The percentage of all hours in the month during which *Es* echoes were recorded on any frequency is plotted in Fig. 1. It is probable that the phenomenon actually occurs more often than is shown on this graph since excessive interference and absorption would decrease the percentage. It will be noted that there is no marked seasonal variation in this quantity.

The same observations are plotted in Fig. 2 to show the mean frequency of *fEs* for each month. This frequency, of course, depends on the peak power radiated which, in this case, is about 1 kW. The marked enhancement of *fEs* during the summer months is well known and occurs at the same season in the southern hemisphere. It is during this period that it is most difficult to read the value of *fEm*.

(e) Diurnal variations

The diurnal variations are now considered. The number of observations shows a marked night-time dip starting at 1800 U.T. and reaching a minimum just before 2200 U.T. from whence it rises steadily to a maximum value of 96% at 0400 U.T. The curve is plotted in Fig. 3.

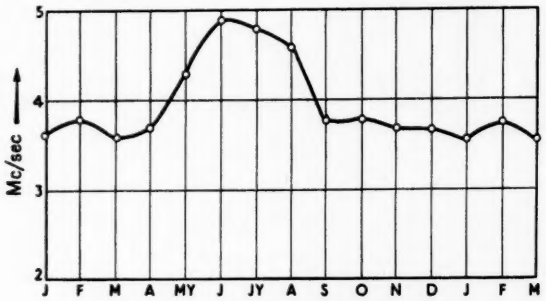

Fig. 2. Seasonal variation in *fEs*.

The marked diurnal variation of *fEs* averaged over the year and shown in Fig. 4(*c*) reaches the maximum value of roughly 5 Mc/s at noon and drops to 3 Mc/s at midnight. This diurnal variation appears to be quite definite and the times of maximum and minimum do not change markedly with season. The same minimum

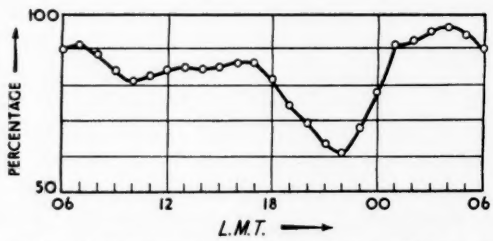

Fig. 3. Diurnal variation in percentage of time *fEs* was recorded.

value of 3 Mc/s is recorded at midnight in June and December, Fig. 4(*a*) and (*b*) but the maximum around 1200 L.M.T. in June is twice the midnight value and is considerably higher than the corresponding December maximum. In this connection it must be recalled that this layer is embedded in a part of the ionosphere which is also subject to solar influence during daylight. Thus the resultant ionisation depends both on the incidence of the phenomenon and on the response of the atmosphere.

(f) Daily variations

The number of hours each day during which *fEs* was recorded in the months of January 1949 and February and March 1950 is plotted in Fig. 5. The values of *fEs* averaged over the day for the same months are plotted in Fig. 6. The five international magnetic disturbed days occurring in each month and the dates of central meridian passage of sunspots are marked on both Figs. 5 and 6. There is no indication of any direct association with either quantity.

VOL. 5 1954

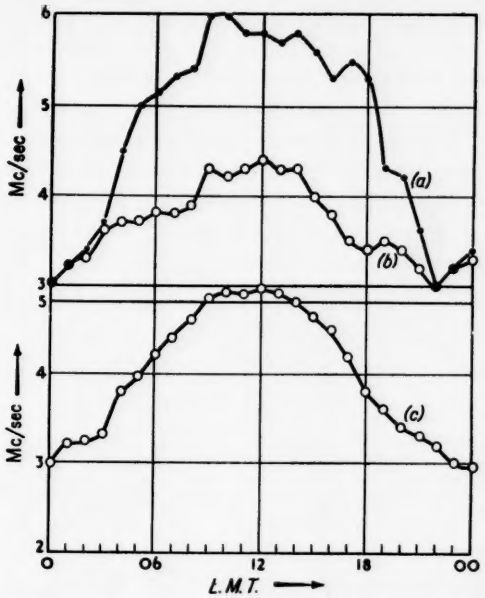

Fig. 4. Diurnal variation of *fEs* (*a*) in June (*b*) in December, and (*c*) averaged over year.

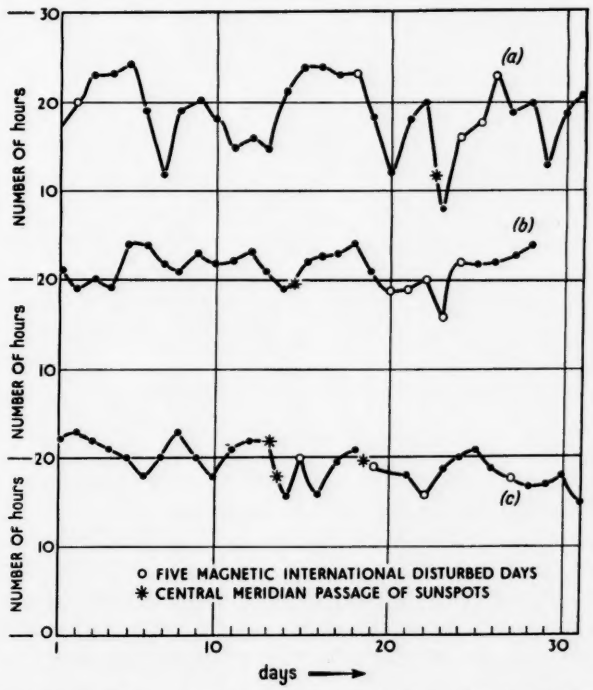

Fig. 5. The number of hours *fEs* was recorded each day (*a*) in January 1949, (*b*) in February 1950, and (*c*) in March 1950.

Lastly, the effect of solar flares is considered. Since this effect will be most pronounced around noon and will not occur at all during the hours of darkness only the five hours centred on noon have been considered. This gives a total of 2730 hours of observation from January 1949 to June 1950, the period of the analysis. Only solar flares which started or were in progress at the time of the ionospheric measurement have been considered. This gave a total of 146 for the period giving

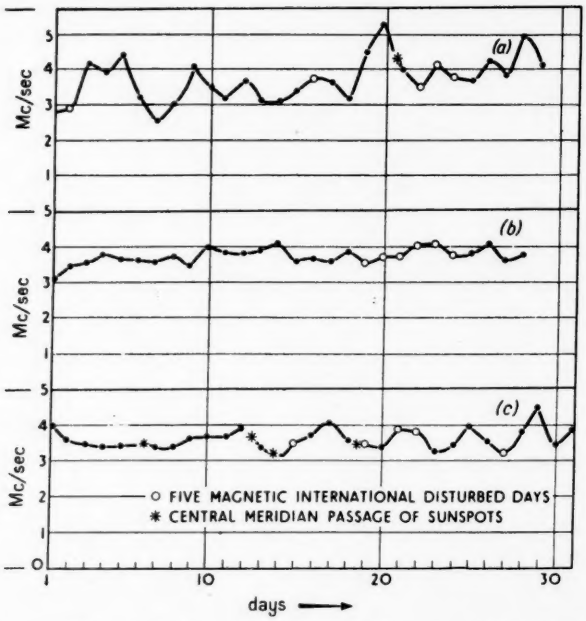

Fig. 6. The value of *fEs* averaged over the day (*a*) in January 1949, (*b*) in February 1950, and (*c*) in March 1950.

a coincidence with the radio observation of under 5%. The analysis shows that out of the above 146 occasions there was no apparent effect on 127 occasions. Marked absorption or S.I.D. fade-outs were observed to coincide on 10 occasions and there were sudden substantial increases in *fEs* values on 7 occasions. Solar flare phenomena are therefore unlikely to account for any appreciable reduction in the number of echoes recorded and do not affect the daily variations.

(*g*) *Observations using high-power transmitters*

The peak power used in the above observations was slightly less than 1 kW and the minimum recorded echo was about 1 μV/m.

Using higher power (2·3 kW) and a tuned aerial with maximum power radiated upwards APPLETON and PIDDINGTON (1938) recorded the same type of echo on a frequency of 8·8 Mc/s and succeeded in measuring the equivalent reflection coefficient. This appears to lie most frequently within the range 0·0005–0·005. MOHANTY (1938) continued the investigation and recorded the same type of echo on a frequency of 16 Mc/s. The short bursts of ionisation referred to in the introduction (APPLETON and NAISMITH, 1947) were also recorded at vertical

VOL. 5 1954

incidence. The power on this occasion was about 100 kW and the frequency was 27 Mc/s. One of the longer duration echoes recorded on this frequency is shown in the second photograph. The typical "arrow head" appearance of the meteor echo is apparent and in this case the ionisation lasted for $3\frac{1}{2}$ minutes. Several other echoes of only a few seconds duration are also visible. (The lower traces on the record are due to reflections from aircraft.) Observations have also been recorded on 73 Mc/s of meteor echoes at vertical incidence by HEY and STEWART (1947). The number of echoes observed per hour was naturally small on this very high frequency.

It must be stressed that because the ionisation in the meteoric clouds is at times very high and the reflection coefficient very low the ionisation bursts may only be observed at vertical incidence on the higher frequencies referred to above when high power is available.

From observations on frequencies between 1·6 and 4 Mc/s, DIEMINGER (1952) reported a close connection between the absorption of short radio waves and the height of echoes received from a region extending downwards from the *E*-layer to about 70 km. He has also observed solar control to be operative in this region. Although this part of his observation has little relation to the subject of this paper, his further observation that the daytime echoes merge at sunset to form a region at 95 km with meteoric dust as the source of its ionisation could refer to the *Em* layer discussed in this article.

3. Oblique Incidence Observation

Studies of the results obtained in the use of the long range navigation system known as "Loran" show (NAISMITH and BRAMLEY, 1951) that, for transmission on 2 Mc/s, a fairly well-defined region of reflection lies between 90 and 97 km and this is identified with the meteoric *E*-layer. There is, as yet, little evidence on the higher frequencies to show the nature of oblique transmission by this layer but it is one of the objects of this communication to indicate the possibility of using this layer for intermediate distance radio communication when high power is available.

In particular it is necessary to study the manner in which the signal strength varies with the radio frequency used, with the power of the transmitter and with the distance apart of the transmitter and receiver.

4. Discussion

The evidence which has been obtained at vertical incidence indicates the existence of a fairly well-defined layer of ionisation possessing certain characteristics which may have important practical applications. Some of the characteristics already mentioned may be summarised thus:

(*a*) *Vertical incidence*

1. Echoes from this layer have an apparently intermittent character and exhibit definite characteristics when recorded by the normal routine ionospheric recorder (e.g. Photograph 1).

2. The rate of occurrence remains fairly uniform from 0800–1800 U.T. but there is also a marked diurnal variation having a minimum around 2200 U.T.

3. Echoes from this layer may be recorded for over 85% of the time and this percentage shows very little seasonal variation.

4. There is a marked diurnal variation in the mean value of fEm. The minimum is at midnight and the maximum at noon. The actual values reached at midnight are identical in June and December but the noon values are much greater in June.

5. Except for the summer months of May—August the average value is remarkably uniform throughout the year. This indicates that the effect of the major meteor streams on the total ionisation produced in the region is subordinate to the more general effect of the sporadic meteors.

6. Magnetic disturbances and sunspots have no apparent influence on the average value or on the number of hours during which the echoes are recorded.

7. Solar flares produce no marked reduction in the number of echoes recorded.

8. When higher power is used individual echoes from this region have been detected at vertical incidence on frequencies at least up to 73 Mc/s.

9. The echoes appear to diminish both in amplitude and rate of occurrence as the frequency is increased.

(*b*) *The meteoric E-layer at oblique incidence*

1. The most probable heights of reflection lie within the fairly narrow range of 90–100 km. The higher value is associated with the shorter distance and the lower with maximum obliquity (APPLETON *et al.*, 1939).

2. When viewed obliquely the intermittent character of the individual bursts of ionisation disappear and the layer appears to be more homogeneous. Indeed, it appears to be as permanent as any of the other ionospheric layers so far identified.

3. The short period variations in equivalent height are sufficiently small to enable the echoes from this layer to be used for the Loran type of radio navigation aid.

4. The amount of incident energy returned from the meteoric E-layer at vertical incidence is sufficiently low to cause only slight interference with the more normal reflections from the higher parts of the ionosphere. The equivalent reflection coefficient most frequently observed at vertical incidence lies between 0·0005 and 0·005 (APPLETON and PIDDINGTON, 1938).

5. On frequencies above the maximum possible for transmission by region-F it is frequently possible to obtain transmission by the meteoric E-layer when high power is available. One example may be the reception in the London area of the television signals from Kirk o' Shotts on a frequency of 56·75 Mc/s and over a distance of 500 km. There is, of course, the alternative explanation of transmission by bending in the troposphere but this is unsatisfactory as a complete explanation for the following reasons.

(i) The signals have been received under a wide variety of tropospheric conditions.

(ii) Stronger signals have been heard from Kirk o' Shotts when the nearer television transmissions from Holme Moss were weak. The latter give more frequently the stronger signal.

6. ISTED (1953) has reported the reception of a slowly varying signal on a frequency of 53 Mc/s over a distance of 330 miles.

VOL. 5 1954

5. The Use of the Meteoric *E*-Layer

The comparatively high degree of consistency in the heights of reflection makes this the most satisfactory layer in the ionosphere for any purpose requiring this condition to be fulfilled (e.g. radio navigation aids).

The reflecting properties of the layer may be used on frequencies above the maximum possible by way of region-*F*. This will be increasingly important round sunspot minimum periods.

When sufficient power is available it should be possible to effect transmission over paths requiring more than one reflection from the layer.

The signals would be comparatively unaffected by atmospherics from great distances.

The interruptions due to magnetic disturbances are largely eliminated.

The effect of chromospheric eruptions is negligible.

In the last three cases therefore it would be possible to operate over a greater percentage of time on a given frequency by way of the meteoric *E*-layer than by way of any of the other layers normally affected by one or all three conditions.

It would be very difficult to jam this type of transmission.

No alteration is required at the receiving site to make use of it.

6. Conclusion

There appears to be a *prima facie* case for the separation of the ionisation produced within the sporadic region-*E* by the impact of meteors from that due to other causes. Reasons and methods of identification have been given for the recognition of the layer of the ionosphere in which the former is produced as the meteoric *E*-layer.

The characteristics of this layer have been established from vertical incidence measurements and a limited amount of confirmation has been secured at oblique incidence up to distances of 1200 km on a single frequency.

The work requires extension both in range and in frequency to confirm the deductions which follow from the vertical incidence measurements.

The use of the meteoric *E*-layer for transmissions on frequencies above the M.U.F. for region F_2 will be of particular value in years of sunspot minimum.

7. Acknowledgments

The work described above was carried out as part of the programme of the Radio Research Board. This paper is published by permission of the Director of Radio Research of the Department of Scientific and Industrial Research.

The author also desires to acknowledge the assistance rendered by Mr. W. M. Curtis, who maintained an exceptionally high standard of measurement throughout the whole six-year period.

References

Appleton, E. V., and Naismith, R. 1935 Some further measurements of upper-atmospheric ionisation. Proc. Roy. Soc. A **150**, 685.

Appleton, E. V., and Naismith, R. 1947 The radio detection of meteor trails and allied phenomena. Proc. Phys. Soc. **59**, 461

APPLETON, E. V., NAISMITH, R., and INGRAM, L. J.	1939	The critical frequency method of measuring upper atmospheric ionisation. Proc. Phys. Soc. **51**, 81
APPLETON, E. V., and PIDDINGTON, J. H.	1938	The reflection coefficients of ionospheric regions. Proc. Roy. Soc. A **164**, 467
DIEMINGER, W.	1952	Uber die Ursache der exzessiven absorption in der Ionosphäre an Wintertagen. J. Atmosph. Terr. Phys. **2**, 340
HEY, J. S., and STEWART, G. S.	1947	Radar observations of meteors. Proc. Phys. Soc. **59**, 858
ISTED, G. A.	1953	Multiple bursts of signal in long distance very-high-frequency propagation. Nature Lond. **171**, 617
MOHANTY	1938	Cambridge Ph.D. Thesis
NAISMITH, R., and BRAMLEY, E. N.	1951	Time-delay measurements on radio transmissions. Wireless Engineer **28**, 271
WATSON, F. G.	1941	"Between the Planets." The Blakistone Co. p. 93

VOL.
5
1954

Journal of Atmospheric and Terrestrial Physics, 1954, Vol. 5, pp. 83 to 91. Pergamon Press Ltd., London

The effect of Rayleigh scattering and ground reflection upon the determination of the height of the night airglow

EDWARD V. ASHBURN

Michelson Laboratory, U.S. Naval Ordnance Test Station, Inyokern, China Lake, California

(*Received* 3 *March* 1954)

ABSTRACT

CHANDRASEKHAR'S theory of radiative transfer was used to calculate the effect of atmospheric scattering and ground reflection upon the determination of the height of the night airglow for values of the extinction coefficient, τ, 0·01, 0·05, 0·10, 0·15, 0·25, and 1·00. It was found that atmospheric scattering is a significant factor for $\tau > 0{\cdot}01$, and for an albedo of 0·80 (snow cover) the albedo correction term is significant for $\tau > 0{\cdot}05$. For usual albedos ($\tau \leq 0{\cdot}25$) the albedo correction term is only significant for $\tau > 0{\cdot}15$

INTRODUCTION

The altitudes of the emission layers responsible for the night airglow have been determined by two independent methods. One method requires an interpretation of the ratio of the light intensity at zenith distance θ to the intensity at zenith distance 0^0. The other method involves a study of the photochemical reactions in the atmosphere as a function of the concentrations of atmospheric particles. The two methods have yielded results that are not in harmony.

In a review of the subject BATES and DALGARNO (1953) summarize the published determinations of the altitudes of the luminous layers in the earth's atmosphere and state that a precise knowledge of these altitudes is of utmost importance in connection with the theory of the excitation processes, and indeed with upper atmospheric physics in general.

In their study of the excitation processes BATES and DALGARNO (1953) concluded that the case against the altitudes derived from the photometric data is strong, and for the λ 5893 line appears to be apodictic. It is difficult to see how the excitation processes discussed by these authors account for the definite periodic and aperiodic variations in the intensity of the airglow but their conclusions cannot be dismissed lightly. It therefore appears to be profitable to re-examine the published interpretations of the photometric data and attempt to definitely establish the heights of the luminous layers. This paper will present a determination of the corrections that should be applied to the photometric data due to Rayleigh scattering in the atmosphere and to reflection of the airglow by the ground. The corrections and errors due to other factors will not be discussed.

THE DETERMINATION OF THE LIGHT OF THE NIGHT SKY DUE TO RAYLEIGH SCATTERING AND GROUND REFLECTION

The equations of radiative transfer in an atmosphere which scatters light according to Rayleigh's law were derived and solved by CHANDRASEKHAR (1950). The specific problem that CHANDRASEKHAR solved for the first time may be expressed as follows: A parallel beam of natural light of net flux πF per unit area normal to itself is incident in a specific direction on a plane-parallel atmosphere of optical thickness τ. It is required to find the angular distribution of the light below the surface at τ.

The equations given by CHANDRASEKHAR (1950) express the light intensities (and the Stokes parameters giving the polarization of the light) as functions of τ; λ, the albedo of the ground at the surface τ; μ_0 the cosine of the angle of incidence of the parallel light; μ, the cosine of the zenith distance of observation; and ϕ, the azimuth angle. SEKERA (1952) and SEKERA and ASHBURN (1953) have published tables of the numerical values of the light intensities for $\tau = 0{\cdot}01$, $0{\cdot}02$, $0{\cdot}05$, $0{\cdot}10$, $0{\cdot}15$, $0{\cdot}25$, and $1{\cdot}00$ and for reasonable intervals of the other parameters. The publication of these tables, which involved extensive use of IBM computors, makes it possible to readily adapt CHANDRASEKHAR'S work on radiative transfer to the problem of the night sky.

The specific problem that is considered in this paper may be expressed as follows: A parallel beam of natural light of net flux F per unit area normal to itself is incident from the zenith on a plane-parallel atmosphere of optical thickness τ. At all other zenith distances the incident parallel light has a net flux of

$$\left[1 - \left(\frac{R}{R+h}\right)^2 \sin^2\theta\right]^{-1/2} F$$

where R = radius of the earth

h = height of the airglow emission layer

θ = zenith distance.

The term in the brackets is the relative thickness of the airglow emission layer on a curved earth (Van Rhijn formula). What is the angular distribution of the intensity of the scattered light transmitted below the surface at τ?

To apply the results given in references (3) and (4) to the problem of the night airglow it was necessary to evaluate the integrals

$$\int_0^{\pi/2}\int_0^{2\pi} (I_l + I_r) \sin\theta \, d\theta \, d\phi \tag{1}$$

and

$$\int_0^{\pi/2}\int_0^{2\pi} (I_l^* + I_r^*) \sin\theta \, d\theta \, d\phi \tag{2}$$

for a reasonable number of zenith distances of observation. I_l and I_r are the intensities of the light whose planes of polarization are parallel and normal respectively to the vertical plane containing the sun. I_l^* and I_r^* are the comparable values for the intensities due to the reflection from the ground.

In references (3) and (4), I_l, I_r, I_l^* and I_r^* are given for $\phi = 0^0$ and 180^0 azimuth. The equations relating the intensities at an azimuth, ϕ, from the sun's azimuth, ϕ_0, are:

$$I_l(\mu, \phi) = I_l \cos^2 \tfrac{1}{2}(\phi_0 - \phi) + I_{la} \sin^2 \tfrac{1}{2}(\phi_0 - \phi) + \mu^2 Z \sin^2(\phi_0 - \phi) \tag{3}$$

$$I_r(\mu, \phi) = I_r - Z \sin^2(\phi_0 - \phi) \tag{4}$$

where μ is the cosine of the zenith distance; and

$$Z = \frac{3\mu_0(1 - \mu_0^2)}{16(\mu - \mu_0)} X^{(2)}(\mu_0) Y^{(2)}(\mu) - Y^{(2)}(\mu_0) X^{(2)}(\mu)$$

VOL.
5
1954

where μ_0 is the cosine of the zenith distance of the incident light and the X and Y functions are given in references (3) and (4). I_i^* and I_r^* are independent of azimuth.

When equations (3) and (4) are substituted into equation (1) it is obvious that

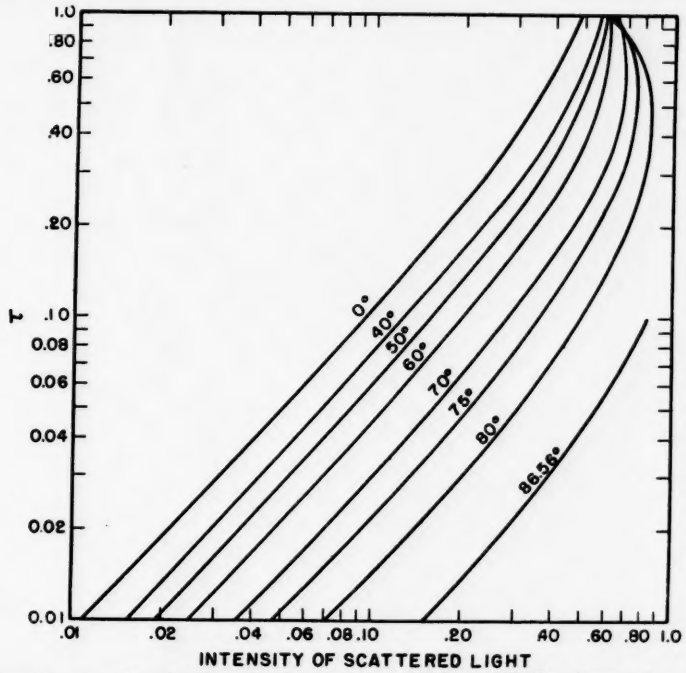

Fig. 1. Intensity of scattered light. Airglow layer at 100 km. Albedo of ground = 0·0.

the integration with respect to ϕ is readily obtainable. The integration with respect to θ must be done by approximate methods from the values of I_i and I_r given in the published tables (references (3) and (4)). The results obtained from these integrations are given in Table 1. The figures in Table 1 are in terms of incident flux F at the zenith.

The evaluation of the integral in equation (2) for different values of the albedo and μ is relatively simple since

$$I_r^* = \frac{\lambda}{4(1-\lambda\bar{s})}\,\mu_0\,[\gamma_i(\mu_0)+\gamma_r(\mu_0)]\,[1-\gamma_r(\mu)]$$

$$I_i^* = \frac{\lambda}{4(1-\lambda\bar{s})}\,\mu_0[\gamma_i(\mu_0)+\gamma_r(\mu_0)]\,[1-\gamma_i(\mu)]$$

where s and the gamma functions are given in references (3) and (4). If the integral in equation (1) is evaluated for one λ and one μ for any given τ then the integral can be quickly evaluated for other values of λ and μ. The results are given in Table 1.

Figs. 1 and 2 illustrate graphically a portion of Table 1. The curves connecting

the computed points for a given zenith distance lie on a comparatively simple curve so it appears that interpolation for values of the scattering term for τ's intermediate between those given in Table 1 can be done with relative confidence.

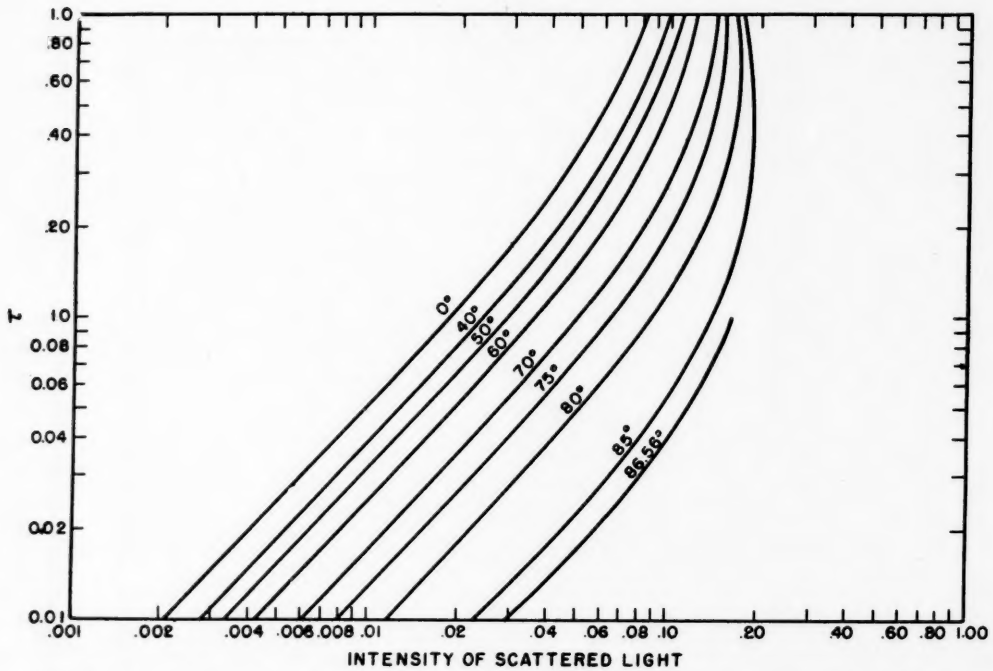

Fig. 2. Correction to intensity of scattered light for reflection of light by the ground. Airglow layer at 100 km. Albedo of ground = 0·25.

THE USE OF TABLE 1

The results given in Table 1 can be applied easily to the reduction of photometric measurements of the light of the night sky to determine the heights of the airglow layer. As an illustration of the use of the tabular values the ratio of I/I_0 were computed for $I_\theta = 75°$ and for a height of the emitting layer of 100 km. The equations used were

$$\text{Van Rhijn: } I_{75}/I_0 = \frac{e^{\tau(1-m)}}{\sqrt{1-\left(\frac{R}{R+h}\right)^2 \sin^2\theta}}$$

where m is air mass relative to zenith air mass = 1.

$$\text{Albedo} = 0\text{: } \frac{I_{75}}{I_0} = \frac{e^{-\tau m} + \text{scattering term for } \theta = 75°}{e^{-\tau}\sqrt{1-\left(\frac{R}{R+h}\right)^2 \sin^2\theta} + \text{scattering term for } \theta = 0^0}$$

VOL. 5 1954

Table 1. *Intensity of scattered light*

$\tau = 0{\cdot}01$

Ground Albedo = 0·0

Height of emitted light	*Zenith distance*							
	0°	40°	50°	60°	70°	75°	80°	86·58°
∞	0·00495	0·00655	0·00785	0·0100	0·0143	0·0189	0·0278	0·0770
300 km	0·00889	0·0122	0·0151	0·0197	0·0286	0·0375	0·0552	0·156
200	0·00956	0·0133	0·0164	0·0214	0·0310	0·0409	0·0604	0·170
100	0·01070	0·0152	0·0187	0·0244	0·0355	0·0472	0·0697	0·194
Ground Albedo = 0·25								
∞	0·00124	0·00162	0·00194	0·00248	0·00355	0·00472	0·00697	0·0191
300 km	0·00190	0·00252	0·00303	0·00385	0·00551	0·00727	0·0107	0·0324
200	0·00198	0·00261	0·00315	0·00401	0·00574	0·00755	0·0112	0·0306
100	0·00210	0·00280	0·00335	0·00426	0·00605	0·00795	0·0117	0·0294
Ground Albedo = 0·50								
∞	0·00248	0·00324	0·00388	0·00496	0·00710	0·00944	0·0138	0·0382
300 km	0·00380	0·00504	0·00606	0·00770	0·0110	0·0145	0·0214	0·0588
200	0·00396	0·00522	0·00630	0·00802	0·0115	0·0151	0·0224	0·0612
100	0·00420	0·00560	0·00670	0·00852	0·0121	0·0159	0·0234	0·0648
Ground Albedo = 0·80								
∞	0·00398	0·00521	0·00624	0·00797	0·0114	0·0152	0·0224	0·0614
300 km	0·00613	0·00810	0·00973	0·0124	0·0177	0·0234	0·0344	0·0945
200	0·00638	0·00839	0·0101	0·0129	0·0185	0·0243	0·0361	0·0983
100	0·00675	0·00901	0·0108	0·0137	0·0195	0·0256	0·0376	0·1040
$\tau = 0{\cdot}05$								
Ground Albedo = 0·0								
∞	0·0243	0·0310	0·0362	0·0460	0·0680	0·0875	0·129	0·283
300 km	0·0425	0·0574	0·0720	0·0950	0·134	0·173	0·245	0·543
200	0·0453	0·0615	0·0755	0·0995	0·142	0·187	0·267	0·595
100	0·0499	0·0675	0·0845	0·109	0·160	0·209	0·305	0·665
Ground Albedo = 0·25								
∞	0·00575	0·00740	0·00885	0·0122	0·0158	0·0208	0·0299	0·0688
300 km	0·00903	0·0118	0·0139	0·0176	0·0250	0·0322	0·0458	0·1058
200	0·00929	0·0122	0·0144	0·0182	0·0182	0·0333	0·0475	0·1090
100	0·00985	0·0128	0·0152	0·0192	0·0272	0·0353	0·0500	0·1152
Ground Albedo = 0·50								
∞	0·0116	0·0150	0·0179	0·0227	0·0320	0·0421	0·0605	0·139
300 km	0·0183	0·0239	0·0282	0·0352	0·0507	0·0652	0·0928	0·214
200	0·0188	0·0247	0·0292	0·0369	0·0523	0·0675	0·0962	0·221
100	0·0200	0·0259	0·0308	0·0389	0·0551	0·0715	0·1013	0·233
Ground Albedo = 0·80								
∞	0·0189	0·0243	0·0391	0·0368	0·0519	0·0684	0·0981	0·226
300 km	0·0297	0·0388	0·0457	0·0578	0·0822	0·106	0·150	0·348
200	0·0305	0·0402	0·0474	0·0598	0·0847	0·109	0·156	0·358
100	0·0324	0·0420	0·0500	0·0630	0·0892	0·116	0·164	0·379

Table 1 (*continued*)

$\tau = 0{\cdot}10$

Ground Albedo = 0·0

Height of emitted light	*Zenith distance*							
	0°	40°	50°	60°	70°	75°	80°	86·58°
∞	0·0487	0·0601	0·0697	0·0896	0·126	0·156	0·218	0·391
300 km	0·0820	0·110	0·135	0·173	0·239	0·308	0·422	0·790
200	0·0857	0·115	0·141	0·181	0·255	0·327	0·443	0·837
100	0·0941	0·125	0·154	0·200	0·282	0·358	0·496	0·934
Ground Albedo = 0·25								
∞	0·0110	0·0142	0·0170	0·0215	0·0300	0·0381	0·0523	0·0983
300 km	0·0168	0·0217	0·0264	0·0327	0·0446	0·0568	0·0800	0·148
200	0·0175	0·0227	0·0275	0·0342	0·0472	0·0598	0·0838	0·154
100	0·0184	0·0239	0·0290	0·0360	0·0496	0·0630	0·0877	0·162
Ground Albedo = 0·50								
∞	0·0227	0·0291	0·0347	0·0438	0·0613	0·0770	0·107	0·200
300 km	0·0355	0·0444	0·0540	0·0668	0·0911	0·116	0·164	0·308
200	0·0357	0·0463	0·0562	0·0710	0·0965	0·122	0·171	0·319
100	0·0376	0·0488	0·0596	0·0728	0·101	0·129	0·179	0·335
Ground Albedo = 0·80								
∞	0·0374	0·0479	0·0571	0·0722	0·101	0·128	0·176	0·330
300 km	0·0584	0·0731	0·0889	0·110	0·150	0·191	0·269	0·500
200	0·0587	0·0763	0·0926	0·117	0·159	0·202	0·282	0·518
100	0·0620	0·0803	0·0977	0·121	0·167	0·212	0·295	0·548
$\tau = 0{\cdot}15$								
Ground Albedo = 0·0								
∞	0·0697	0·0882	0·103	0·127	0·176	0·214	0·284	—
300 km	0·118	0·157	0·190	0·243	0·322	0·410	0·538	—
200	0·124	0·164	0·198	0·252	0·344	0·427	0·555	—
100	0·137	0·178	0·216	0·278	0·376	0·465	0·620	—
Ground Albedo = 0·25								
∞	0·0157	0·0201	0·0240	0·0303	0·0415	0·0520	0·0680	0·0910
300 km	0·0243	0·0306	0·0363	0·0448	0·0600	0·0763	0·103	0·150
200	0·0248	0·0319	0·0378	0·0467	0·0632	0·0800	0·106	0·158
100	0·0261	0·0335	0·0396	0·0490	0·0675	0·0845	0·113	0·163
Ground Albedo = 0·50								
∞	0·0324	0·0415	0·0495	0·0625	0·0856	0·107	0·140	0·188
300 km	0·0501	0·0631	0·0749	0·0924	0·124	0·157	0·212	0·309
200	0·0512	0·0658	0·0780	0·0963	0·130	0·165	0·219	0·326
100	0·0538	0·0691	0·0817	0·101	0·139	0·174	0·233	0·336
Ground Albedo = 0·80								
∞	0·0539	0·0690	0·0823	0·104	0·142	0·178	0·233	0·312
300 km	0·0834	0·105	0·125	0·154	0·206	0·262	0·353	0·515
200	0·0851	0·109	0·130	0·160	0·217	0·274	0·364	0·542
100	0·0895	0·115	0·136	0·168	0·232	0·290	0·388	0·559

VOL. 5 1954

Table 1 (*continued*)

$\tau = 0{\cdot}25$

Ground Albedo = 0·0

Height of emitted light	*Zenith distance*							
	0°	40°	50°	60°	70°	75°	80°	85°
∞	0·110	0·136	0·157	0·192	0·250	0·294	0·354	—
300 km	0·182	0·240	0·283	0·349	0·455	0·536	0·645	—
200	0·192	0·250	0·296	0·366	0·485	0·572	0·693	—
100	0·206	0·277	0·327	0·402	0·527	0·623	0·763	—
	Ground Albedo = 0·25							
∞	0·0242	0·0303	0·0354	0·0434	0·0576	0·0693	0·0872	0·113
300 km	0·0358	0·0449	0·0524	0·0643	0·0854	0·103	0·130	0·168
200	0·0372	0·0467	0·0546	0·0670	0·0888	0·107	0·134	0·174
100	0·0390	0·0490	0·0572	0·0701	0·0930	0·112	0·141	0·182
	Ground Albedo = 0·50							
∞	0·0508	0·0637	0·0743	0·0911	0·121	0·146	0·183	0·237
300 km	0·0752	0·0943	0·110	0·135	0·179	0·216	0·272	0·352
200	0·0781	0·0981	0·115	0·141	0·187	0·224	0·283	0·366
100	0·0819	0·103	0·120	0·147	0·195	0·235	0·296	0·384
	Ground Albedo = 0·80							
∞	0·0865	0·108	0·127	0·155	0·206	0·248	0·312	0·404
300 km	0·128	0·160	0·187	0·230	0·305	0·368	0·462	0·598
200	0·133	0·167	0·195	0·239	0·317	0·382	0·481	0·622
100	0·139	0·175	0·204	0·250	0·332	0·400	0·504	0·652
	$\tau = 1{\cdot}00$							
	Ground Albedo = 0·0							
∞	0·291	0·325	0·342	0·362	0·367	0·355	0·334	—
300 km	0·445	0·506	0·528	0·550	0·567	0·556	0·529	—
200	0·460	0·529	0·551	0·574	0·589	0·576	0·548	—
100	0·483	0·560	0·586	0·614	0·627	0·611	0·572	—
	Ground Albedo = 0·25							
∞	0·0525	0·0618	0·0685	0·0768	0·0890	0·0950	0·103	0·110
300 km	0·0772	0·0908	0·100	0·113	0·131	0·140	0·151	0·161
200	0·0795	0·0935	0·104	0·116	0·135	0·144	0·156	0·166
100	0·0831	0·0978	0·108	0·122	0·141	0·150	0·162	0·173
	Ground Albedo = 0·50							
∞	0·120	0·141	0·157	0·176	0·204	0·218	0·235	0·251
300 km	0·177	0·208	0·230	0·258	0·299	0·309	0·346	0·368
200	0·183	0·214	0·237	0·265	0·308	0·330	0·356	0·379
100	0·190	0·224	0·247	0·278	0·323	0·345	0·372	0·396
	Ground Albedo = 0·80							
∞	0·225	0·265	0·294	0·329	0·382	0·407	0·440	0·470
300 km	0·331	0·389	0·430	0·483	0·560	0·598	0·647	0·690
200	0·341	0·400	0·444	0·597	0·576	0·617	0·667	0·709
100	0·356	0·419	0·467	0·520	0·604	0·645	0·695	0·741

Albedo = 0·80:

$$\frac{I_{75}}{I_0} = \frac{e^{\tau m} + \text{scattering term for } \theta = 75^\circ + \text{albedo term}}{e^{-\tau}\sqrt{1 - \left(\frac{R}{R+h}\right)^2 \sin^2\theta} + \text{scattering term for } \theta = 0^\circ + \text{albedo term.}}$$

The results are as follows:

Table 2. I_{750}/I_0

Method	τ					
	0·01	0·05	0·10	0·15	0·25	1·00
Van Rhijn	3·144	2·809	2·439	2·118	1·598	0·193
Van Rhijn plus correction for $\tau = 0$	3·158	2·877	2·568	2·294	1·896	0·801
Van Rhijn plus correction for $\lambda = 0{\cdot}80$	3·162	2·899	2·618	2·372	2·018	1·099

VOL. 5 1954

It is obvious from this table that for $\tau > 0{\cdot}01$ that the scattering correction term is significant and that its relative size increases with increasing τ until at $\tau = 1{\cdot}00$ the scattering correction is larger than the Van Rhijn term. For an albedo of 0·80 (snow cover) the albedo correction term becomes significant for $\tau > 0{\cdot}05$. For more usual albedos ($\leq 0{\cdot}25$) the albedo correction term is only significant for $\tau > 0{\cdot}15$. The relative importance of the scattering and albedo correction terms increases with increasing zenith distance.

An inspection of the Van Rhijn formula shows that I_θ/I_0 for a given θ and τ increases with decreasing height of the airglow layer. Therefore a neglect or underestimation of the scattering and albedo corrections would lead to an estimate of the height from the photometric data that would be too low. It is thus obvious that the application of these corrections alone would lead to an even greater difference in the estimated height of the luminous layer by the photometric and excitation methods than now exist.

Accuracy of Table 1 when used to Determine Height of Airglow Layer

The values of I_l, I_r, I_l^* and I_r^* given in references (3) and (4) are accurate to at least four decimal places. The numerical integrations performed for the preparation of Table 1 are accurate to within approximately 1%. It is doubtful if greater accuracy is justified. Chandrasekhar's equations of radiative transfer are rigorous for the idealized state of a Rayleigh plane parallel atmosphere. The radiative transfer in the actual atmosphere differs from that due to Rayleigh scattering. This difference is associated with some large particle scattering and

absorption lines and bands. In addition, CHANDRASEKHAR (1950) states "While there is no formal difficulty in carrying out this reduction for any given law of reflection of the ground, in view of the practical difficulties of specifying, in given cases, the reflecting properties of the ground accurately, it should suffice, for most purposes, to idealize the 'ground' as a surface which reflects according to Lambert's law with some albedo λ."

It is the opinion of the writer that at present there is no justification to attempt to improve the figures given in Table 1 until other possible sources of large errors in the Van Rhijn formula are investigated (for example, the separation of the airglow from the extraterrestrial light). It appears that no reasonable modification of the results given in Table 1 would produce the effect of reducing the estimated height to the extent required by BATES and DALGARNO (1953).

REFERENCES

[1] BATES, D. R., and DALGARNO, A. (1953) The altitudes of the luminous layers in the earth's atmosphere. J. Atmosph. Terr. Phys. **4**, 112–123

[2] CHANDRASEKHAR, S. (1950) Radiative Transfer. Oxford, The Clarendon Press

[3] SEKERA, Z. (1952) Tables Relating to Rayleigh Scattering of Light in the Atmosphere, Univ. of Calif. at Los Angeles, Dept. of Meteorology, Sci. Report No. 3.

[4] SEKERA, Z., and ASHBURN, E. V. (1953) Tables Relating to Rayleigh Scattering in the Atmosphere, U.S. Naval Ordnance Test Station, Inyokern, Nav. Ord. Rept. 2061

Journal of Atmospheric and Terrestrial Physics, 1954, Vol. 5, pp. 92 to 100. Pergamon Press Ltd., London

Multiple stratification of the *F*-layer at Ibadan

N. J. Skinner, R. A. Brown, and R. W. Wright

Physics Dept., University College, Ibadan

(*Received* 4 *March* 1954)

ABSTRACT

The ridges observed in the F_2-layer at Ibadan, Nigeria, have been recorded. There is a maximum occurrence of ridges around 1000 hours and 1500 hours. The morning ridges are more pronounced. A pronounced seasonal variation is found and most ridges occur when the midday minimum of f_0F_2 occurs early in the day. A lunar variation is found in the rate of ridge formation at 0900 hours. Ridges in F_1 are also discussed but it is concluded that there is little relation with those in F_2 and that the F_1 ridges are connected with the E_2-layer. The observed facts can be explained by means of oscillatory vertical ionic drifts such as those suggested by Martyn (1947). Possible phases consistent with the phenomena are considered.

1. Introduction

Routine ionospheric measurements have been made since December, 1951, at Ibadan, Nigeria, lat. 7°26′ N, long. 3°54′ E, where the magnetic dip is about 5° S. The equipment used is an automatic $h'f$ recorder of the type developed by the Radio Research Station, Slough, England.

Since Ibadan is an equatorial station, the midday minimum of the critical frequency of the F_2-layer is a normal occurrence throughout the year. This minimum is often preceded and followed by the formation of ridges or very thick structures in the F-region. Osborne (1951) has observed similar perturbations in the F_2 region at about corresponding times at Singapore. McNish (1950) and Ratcliffe (1951) have also observed these occurrences in $h'f$ records from Huancayo, particularly at sunspot minima. Delobeau (1952) has reported a similar effect in records taken at Dakar.

This paper describes the results of a detailed investigation of the phenomena associated with the midday minimum in f_0F_2 at Ibadan, during the period December, 1951 to January, 1953. An attempt is then made to relate these results to the various explanations which may be put forward.

2. Ridge and Thick Layer Formation

Superficial examination of Ibadan $h'f$ records is quite sufficient to illustrate the presence of ridges in the F_2-layer around 0900 hours to 1000 hours. When an actual ridge is not present at these hours then there is usually a thick layer, and accordingly the $h'f$ curve is no longer of the shape associated with a simple Chapman layer. We have used Osborne's (1951) definition of a thick layer, i.e. the $h'f$ curve has a slope of 150 km per Mc/sec at frequencies appreciably lower than those affected by severe group retardation near the critical frequency. Each hourly record has been examined and the presence of a ridge or thick layer denoted by R. The percentage probability of the presence of R at each hour of the day has been calculated for each month. Fig. 1 shows the variation for each month, and Fig. 2 the annual mean variation of the percentage occurrence of R throughout the day.

VOL. 5 1954

It will be seen that the percentage occurrence of R has maxima at sunrise, 1000 hours and 1500 hours. The first peak is intimately connected with sunrise effects with which we are not concerned at present. The 1000 hour peak and the 1500 hour peak differ in one major factor. At 1500 hours there are a great many more thick layer occurrences than ridges, whereas at 1000 hours there are more ridges than thick layers.

It is apparent that throughout the year there was a 70% chance of this phenomenon occurring at 1000 hours and in fact it is extremely rare (about once a

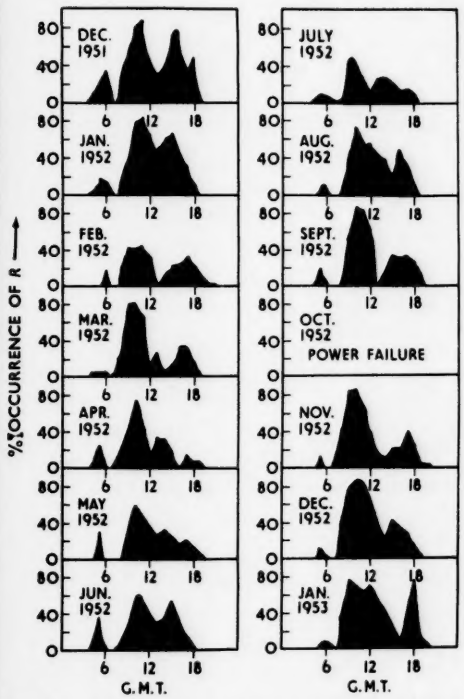

Fig. 1. Average percentage occurrence of "ridges" and "thick layers" throughout the day for each individual month.

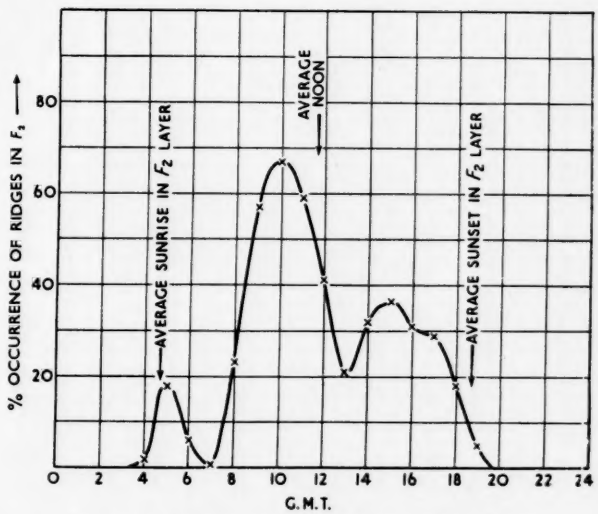

Fig. 2. Average percentage of "ridges" and "thick layers" throughout the day (annual mean).

month) that a morning goes by without a ridge being observed on one of the hourly records between 0800 hours and 1200 hours. Every month shows a peak in one of the hours 0900–1100.

The effect is thus a normal one at this stage of the sunspot cycle although conflicting evidence exists as to whether ridges are observable at all times in the cycle. It is interesting to note that whereas RATCLIFFE (1951) found no ridges for a year near sunspot maximum at Huancayo, both DELOBEAU (1952) (at Dakar) and OSBORNE (1951) (at Singapore) observed many ridges in 1949 near sunspot maximum.

The seasonal variations of the probability of occurrence of R is shown in Fig. 3. Curve I illustrates the average probability of R occurrence during the hours

0900, 1000, and 1100 in each month. The variation of the cosine of the zenithal angle (χ) of the sun is plotted on the same graph (Curve IV) and in general it is seen that when R is a maximum, cos χ is minimum and *vice versa*. This is in agreement with OSBORNE'S (1951) observations but DELOBEAU (1952) finds that the occurrence of ridges at Dakar follows cos χ closely.

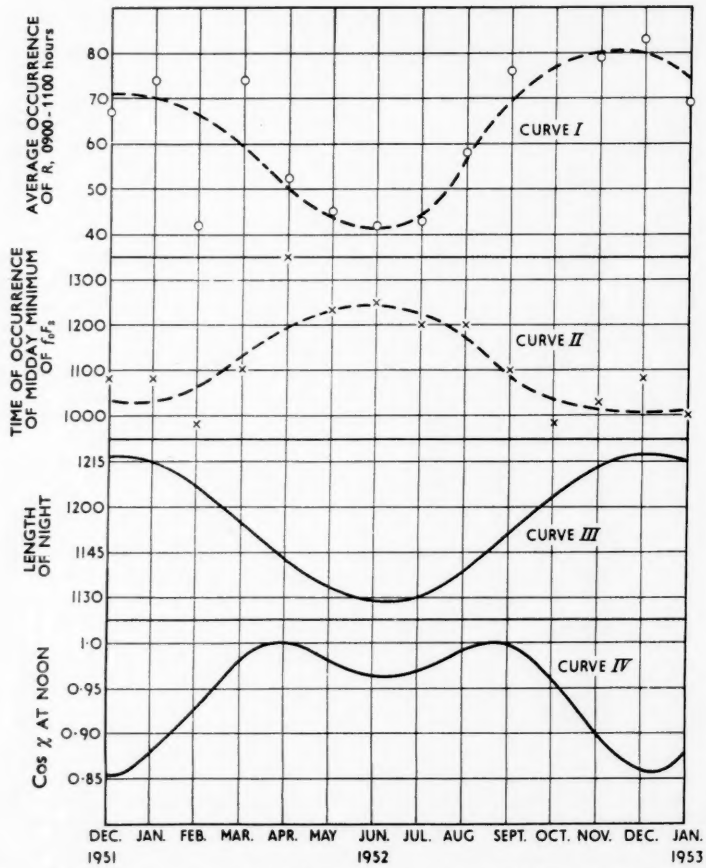

Fig. 3. Curve I shows seasonal variation of average probability of R occurrence during hours 0900–1100. Curve II shows seasonal variation of time of midday minimum of f_0F_2. Curve III shows seasonal variation of length of night. Curve IV shows seasonal variation of cos χ.

Curve II shows the time of occurrence of the midday minimum of f_0F_2 throughout the year. It will be observed that this curve is in antiphase with Curve I. Curve III of Fig. 3 shows the average length of night throughout the period and it is seen that its shape is very similar to that of Curve I.

3. THE MOON AND RIDGE FORMATION

It has been claimed that the occurrence of ridges in the F_2-region is dependent on the phase of the moon (MCNISH, 1950). We find that the frequency of occurrence

VOL. 5 1954

at Ibadan is considerable at all phases of the moon but that a lunar semi-diurnal variation is clearly detectable during the morning hours 0900–1100. Fig. 4 shows percentage occurrence of R against age of moon for various times of day, the figures being based on 14 lunar periods. It would be extremely dubious to draw any conclusions from the afternoon curves but it seems clear that the phase of the moon controls the time of commencement of the phenomena in the morning.

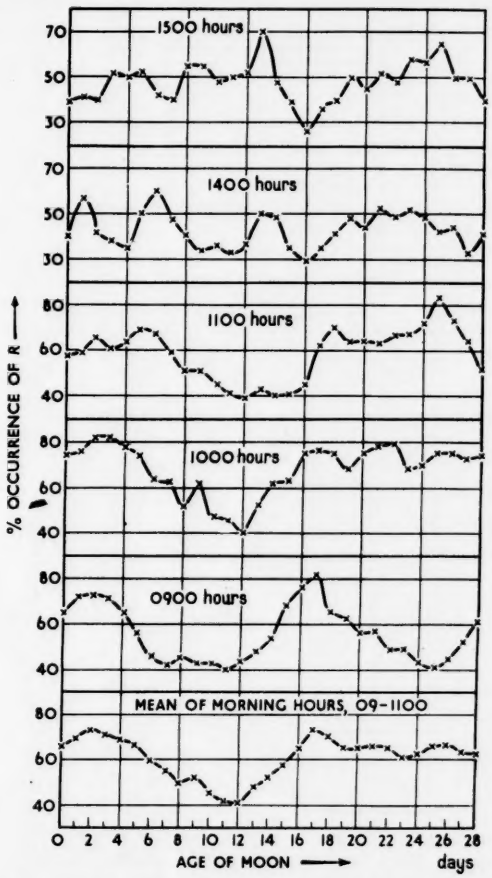

Fig. 4. Variation of percentage occurrence of R with age of moon for various times of day.

Fig. 4 shows that maximum ridge occurrences at 0900 hours come at the second and seventeenth days of the age of the moon. It is significant that at these times the lunar perturbation causes f_0F_2 at noon at Ibadan to be minimum. McNish and Gautier (1949) have obtained the same phase for the noon f_0F_2 lunar tide at Huancayo.

4. Ridges in the F_1-Layer

Ridges have also been observed in the F_1-layer at Ibadan which do not seem to have been described previously. These have been studied to determine whether

there is any similarity with the F_2 structures. The examination is rendered more difficult than that for F_2 ridges for two reasons: (1) F_1 often does not possess a clearly defined maximum of ionization, (2) an E_2-layer frequently forms in the early morning and rises to form a ridge in the F_1-layer. This ridge appears to break away from the F_1-layer towards the E-layer in the late afternoon and it is

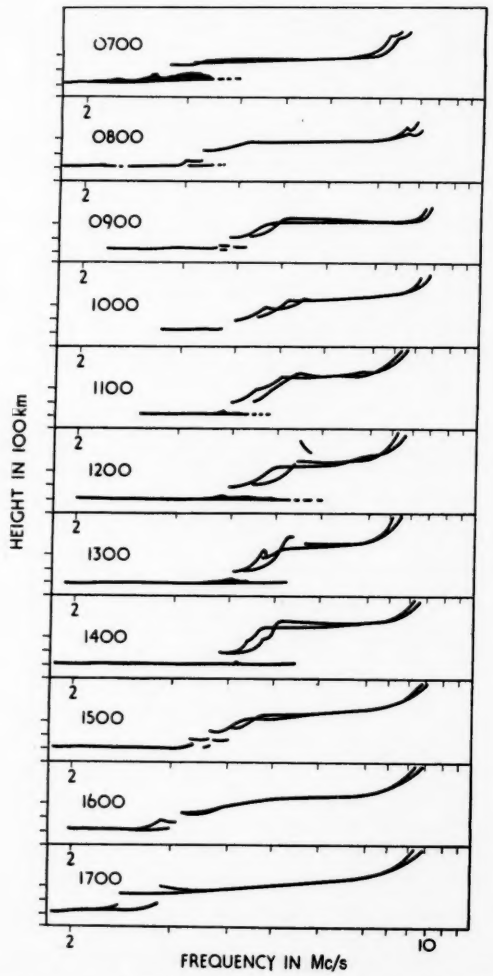

Fig. 5. Typical sequence of records illustrating F_1 layer ridges observed on 13 December 1952.

then difficult to decide whether or not the ridges observed are examples of the E_2-layer. Fig. 5 shows a typical sequence of records illustrating the growth and decay of a ridge in the F_1-layer on 13th December, 1952. In Fig. 6 Curve I is the percentage presence of ridges of any nature in F_1 and E, and Curve II is the percentage probability omitting those which would normally be called E_2-layers.

In order to determine whether there is any connection between these ridges

VOL. 5 1954

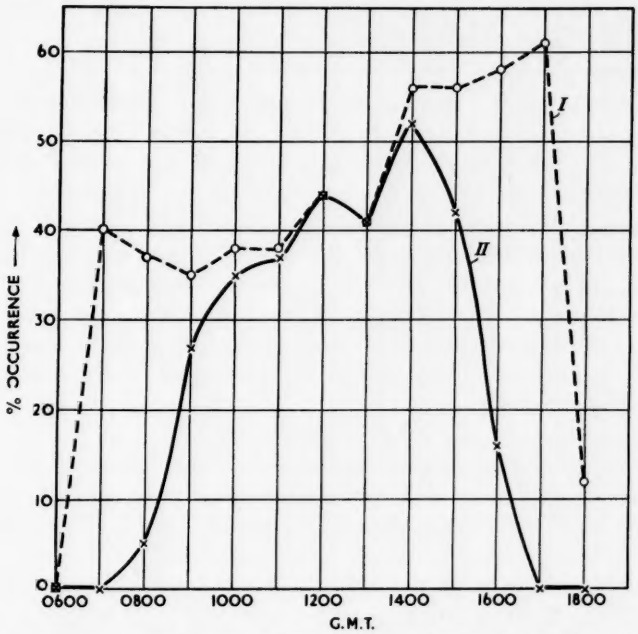

Fig. 6. Percentage occurrences of ridges in the F_1 layer. I. All ridges observed. II. Omitting those ridges which are obviously E_2.

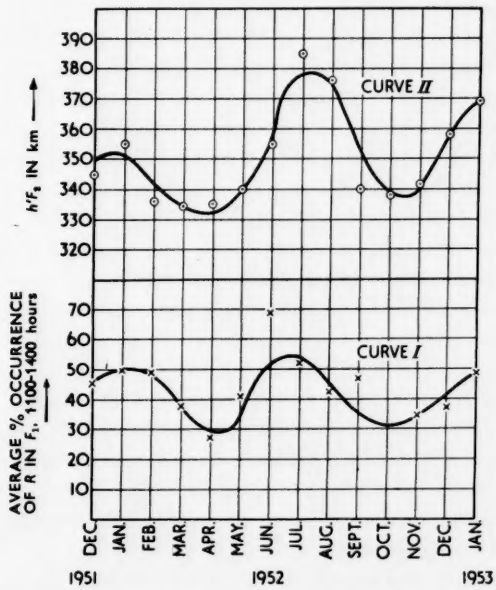

Fig. 7. Curve I, seasonal variation of a ridge occurring in F_1 layer during hours 1100–1400. Curve II, seasonal variation of $h'F_2$ at noon.

and those of F_2, we have plotted in Fig. 7, Curve I the seasonal variation of the average probability of a ridge occurring in the hours 1100 to 1400. The variation of Curve I is very different from that of the occurrence of ridges in F_2 (Fig. 3, Curve I). We feel that the two kinds of ridges are due to different causes. It also seems unnecessary to assume two types of ridges in F_1; all the ridges appear to be generated near the E_2-layer, being low near the E-layer in the morning, rising into the F_1-layer around noon. The fact that the variation of the midday occurrences is similar to the seasonal variation of the noon values of $h'F_2$, Fig. 7, Curve II, may be relevant since $h'F_1$ varies little with season, and therefore the greater $h'F_2$ at noon, the greater the separation and speed of separation of F_1 and F_2. However, the ridges in F_1 are least when cos χ is greatest and the fact that the F_1 ridge curve is more symmetrical than the cos χ curve is probably due to the influence of the magnetic latitude of Ibadan, as APPLETON (1950) has pointed out for the seasonal variation of $h'F_2$.

5. DISCUSSION

No satisfactory theory has as yet been suggested to explain the presence of ridges in equatorial regions. Ridges are not stationary occurrences and any explanation of their origin must be linked up with a dynamic process involving fairly rapid vertical ionic drift.

A mechanism whereby vertical ion drift could take place has been suggested by MARTYN (1947) who examined the perturbation of an ionized region by atmospheric tides in the presence of a magnetic field. A current system is produced in the ionosphere by the "dynamo" action of horizontal tidal air currents flowing across the vertical component of the earth's magnetic field. The associated electric field when crossed with the magnetic field gives rise to vertical movement of ions with a solar and lunar control. MARTYN (1947) examined the effect of the vertical ionic drift velocity upon the shape of a Chapman layer under the restricted conditions of no ion production or recombination He found that considerable distortion of the layer could take place under these conditions and that h_m, the height of maximum ionization, could be increased or decreased depending on the variations of drift velocity with height. If the foregoing restrictions are removed ions will tend to be formed at the original height of maximum ionization causing further distortion to the layer shape. This mechanism could account for the various types of distributions of electron density with height assumed by RATCLIFFE (1948) in his analysis of equatorial $h'f$ curves and also could account for the presence of ridges.

This is obviously an over-simplified picture since modern theory regards the F_1- and F_2-regions as manifestations of a single "Chapman" region, the greater electron density in F_2 being due to the lower value of α in that region.

The main experimental facts that must be accounted for at Ibadan are:

(1) There is a maximum ridge occurrence at 1000 hours and a minimum occurrence at 1300 hours, followed by a less clearly defined secondary maximum in ridge occurrences at 1600 hours.

(2) There are more morning ridges in winter than in summer.

(3) There is a correlation between the maxima in the lunar tide of morning ridge occurrence and the minima in the lunar tide of noon f_0F_2.

VOL. 5 1954

(4) There is a midday minimum in f_0F_2 which occurs at about 1100 hours in winter and 1300 hours in summer.

(5) The separate maximum of F_1 is less pronounced in winter than in summer.

(6) The semi-thickness (y_m) of the F_2-layer has its maximum before noon in winter and after noon in summer.

We now proceed to suggest possible phases of vertical drift velocities which could explain these results.

If the velocity gradient of the drift is large and α, the coefficient of recombination, is small then N_m will have a 90° phase lag behind the ionic velocity in the F_2-layer. The midday minimum in N_m can thus be explained by assuming a downward drift velocity with a maximum three hours before the time of the midday minimum, i.e. at Ibadan, ionic velocities $\downarrow$ 0800 hours in winter and $\downarrow$ 1000 hours in summer (using MARTYN'S notation). The pre-noon maximum is considered due to the rapid increase in solar radiation in the morning, the downward drift gradually taking control and reducing the ionization to a minimum at midday. It will be seen then that the midday minimum of ridges occurs at the time of zero vertical velocity. This is consistent with experimental fact 3, that the lunar tide of f_0F_2 noon values has a minimum when the 0900 hours ridge occurrence is a maximum, and suggests that ridges occur around the time of maximum ionic velocity. The fact that the morning ridge maximum occurs at 1000 hours throughout the year and not at 0800 hours in winter may be explained as follows. In winter, at 0800 hours, the F_1- and F_2-layers are but little separated, in fact, maximum bifurcation does not occur until 1000 hours throughout the year. If the drift in the F_1-layer is $\uparrow$ 0800 hours all the year round (i.e. approximately that suggested by MARTYN, 1948) then in winter there will be exact phase opposition between F_1 and F_2 drift which could easily lead to ridge formation. In summer the rate of change of phase with height would be less and lead to fewer ridges, as is observed. Such an arrangement of phases would appear to explain all the day-time phenomena at Ibadan, and, if the velocity is of the same phase in the E- and F_1-layers, we might suggest that the E_2 phenomena is a result of this drift velocity.

Alternatively, if we assume that F_1 and F_2 would form separate layers without the assistance of tidal motion, due entirely to a decrease of α with height, then a straight-forward drift velocity decreasing with height would give rise to distorted layers and ridges. The phases would still be $\downarrow$ 0800 hours in winter and $\downarrow$ 1000 hours in summer in the F_2, whilst to provide the seasonal variation the F_1 drift would be $\downarrow$ 0800 hours.

MARTYN (1948) has deduced that the equatorial phase of the drift velocities will be $\downarrow$ 1200 hours in the F_2 and $\uparrow$ 0900 hours in the F_1 by a consideration of world wide distributions of ionization. He does not, however, appear to consider the midday minimum of N_m to be a first order phenomena. The phases of the drifts suggested in our first model are not at great variance with these, though MARTYN considers, on experimental evidence, that there is a phase lag of π between maximum downward drift and minimum N_m. The assumption of a phase change of velocity with height could, however, imply a considerable change of phase in the perturbation of F_2 between day and night, and caution must be exercised in

attempting to fix a phase relevant to the day-time from the night-time observations alone.

It should be mentioned that MCNISH and GAUTIER (1949) have propounded an alternative mechanism whereby vertical drift of ions could occur. It is doubtful whether it would be of sufficient magnitude to explain both the ridges and the midday minimum of N_m, but it may be a contributory factor.

It is realized that the above discussion is of a very tentative and qualitative nature. Any discussion of the phases of drifts must eventually be related to a world wide system and we have here considered one station only, so that the phases suggested are not necessarily unique interpretations of the results. It is clear that more experimental evidence from equatorial regions is required before a fully adequate theory can be developed. In this, the existence and prevalence of ridges should form an important pointer towards determining phases. We would, however, suggest that the name "lunar ridge" which has been applied to the F_2 ridges is a misnomer, since their occurrence is governed in only a very slight way by the moon.

Acknowledgments—The authors are extremely grateful for the co-operation of the D.S.I.R. Radio Research Station at Slough, England, in particular to Dr. R. L. SMITH-ROSE and Mr. A. F. WILKINS, both for the loan of the equipment and much advice. We are very indebted to Mr. W. R. PIGGOTT for many discussions relevant to this paper.

VOL. 5 1954

REFERENCES

APPLETON, Sir E. V.	1950	J. Atmosph. Terr. Phys. **1,** 106
DELOBEAU, F.	1952	C.R. Acad. Sci. (Paris) **235,** 1673
MARTYN, D. F.	1947	Proc. Roy. Soc. A. **189,** 241
	1948	Proc. Roy. Soc. A. **194,** 445
MCNISH, A. G.	1950	Proc. Conf. Ionospheric Physics, Pennsylvania State College, p. 10, CC
MCNISH, A. G., and GAUTIER, T. N.	1949	J. Geophys. Res. **54,** 181
OSBORNE, B. W.	1951	J. Atmosph. Terr. Phys. **2,** 66
RATCLIFFE, J. A.	1951	J. Geophys. Res. **56,** 487
	1951	J. Geophys. Res. **56,** 463

Journal of Atmospheric and Terrestrial Physics, 1954, Vol. 5, pp. 101 to 103. Pergamon Press Ltd., London

Indices of geomagnetic activity

of the Observatories ABINGER (*Ab*), ESKDALEMUIR (*Es*) and LERWICK (*Le*)

December to February 1954

The figures given on pages 101 to 103 represent the K-indices for three-hour intervals, beginning with 00.03 hrs for the first and ending with 21–24 hrs for the eighth figure.

December 1953

Day	*Ab* Range for $K = 9 : 500\gamma$		*Sum*	*Es* Range for $K = 9 : 750\gamma$		*Sum*	*Le* Range for $K = 9 : 1000\gamma$		*Sum*	*Day*
	K-Indices			*K-Indices*			*K-Indices*			
1	0011	1111	6	0010	0001	2	0100	1001	3	1
2	1021	1111	8	1021	0111	7	1011	1111	7	2
3	2111	1123	12	1101	1122	9	1111	1112	9	3
4	4122	1233	18	4111	0132	13	4111	0122	12	4
5	3211	1210	11	2111	0210	8	2111	1110	8	5
6	1011	3222	12	1001	3212	10	1011	2222	11	6
7	3122	1113	14	3111	0003	9	3211	0002	9	7
8	1111	2233	14	0010	1223	9	1111	1123	11	8
9	4011	1241	14	4000	0242	12	3000	1242	12	9
10	1012	1313	12	1002	1202	8	1011	1102	7	10
11	2334	5444	29	2323	4444	26	2223	4454	26	11
12	4332	3443	26	4222	2443	23	3231	2434	22	12
13	3212	2253	20	1121	2152	15	4211	1142	16	13
14	1121	1232	13	1111	1232	12	0111	1232	11	14
15	1112	2133	14	0102	1133	11	1111	1133	12	15
16	2112	1212	12	2112	1112	11	1111	1112	9	16
17	2212	2324	18	2111	1213	12	2111	1213	12	17
18	3012	2222	14	2000	2222	10	2011	2222	12	18
19	1021	2332	14	1010	1222	9	1010	1232	10	19
20	1111	2322	13	1110	2222	11	1110	2231	11	20
21	2112	2114	14	2010	1104	9	2110	0003	7	21
22	2231	2342	19	2222	2232	17	2121	2242	16	22
23	1011	2232	12	1000	2131	8	0011	2132	10	23
24	2132	1122	14	2222	0012	11	2111	1012	9	24
25	2121	1313	14	2021	1213	12	2121	1213	13	25
26	1002	2123	11	1001	2113	9	1011	2123	11	26
27	1122	2235	18	1112	2234	16	1111	2124	13	27
28	3222	3232	19	3111	2222	14	3211	2121	13	28
29	3112	3324	19	2002	2323	14	3101	2213	13	29
30	1121	1211	10	1111	1211	9	1111	1111	8	30
31	0022	2111	9	0122	1001	7	1022	0001	6	31

January 1954

Day	*Ab* Range for $K = 9 : 500\gamma$		Sum	*Es* Range for $K = 9 : 750\gamma$		Sum	*Le* Range for $K = 9 : 1000\gamma$		Sum	Day
	K-Indices			*K-Indices*			*K-Indices*			
1	2212	1022	12	2210	1012	9	2210	0011	7	1
2	3233	5533	27	3233	4423	24	3222	4422	21	2
3	3112	2102	12	2112	2101	10	2111	1101	8	3
4	0011	1110	5	0000	0001	1	0010	0000	1	4
5	1002	1234	13	1000	1234	11	1100	1134	11	5
6	2321	2211	14	1221	2211	12	1211	1211	10	6
7	1222	2331	16	0210	2331	12	0111	1332	12	8
8	3222	1223	17	3122	0223	15	3121	1113	13	8
9	3111	2113	13	3102	2112	12	3101	1112	10	9
10	0102	1122	9	0100	1121	6	0110	1122	8	10
11	1122	1313	14	0122	1223	13	1121	1213	12	11
12	2213	2432	19	2112	1332	15	1112	1332	14	12
13	3232	2123	18	3222	0113	14	3221	1114	15	13
14	1011	1233	12	0000	1223	8	1100	1123	9	14
15	2132	3224	19	2122	2224	17	1121	1124	13	15
16	3211	2141	15	2111	1131	11	2111	1131	11	16
17	0111	1332	12	1102	2332	14	0111	1222	10	17
18	2122	3235	20	2211	3135	18	1111	2225	15	18
19	3233	2454	26	3132	2454	24	4223	2455	27	19
20	4233	3342	24	4232	2332	21	3322	2332	20	20
21	4333	3333	25	4332	2233	22	4321	2233	20	21
22	3332	3232	21	3332	2232	20	3222	2231	17	22
23	3333	2332	22	3333	2222	20	3322	1221	16	23
24	2111	1120	9	2112	1210	10	2111	1111	9	24
25	1111	1321	11	1111	1321	11	1111	1321	11	25
26	2211	1211	11	2111	1211	10	2100	1111	7	26
27	2111	1221	11	2000	2221	9	2001	1221	9	27
28	2121	2111	11	2011	1000	5	2011	1000	5	28
29	1111	1211	9	1100	1211	7	1100	0210	5	29
30	1022	1223	13	1002	1122	9	1011	1213	10	30
31	1212	1323	15	1201	0323	12	1211	1323	14	31

February 1954

1	2333	3434	25	2333	3334	24	1332	3444	24	1
2	4223	4324	24	4323	3324	24	3322	3214	20	2
3	4233	3224	23	3233	3224	22	4323	2223	21	3
4	3332	1222	18	3222	1222	16	3321	1222	16	4
5	2112	2333	17	2102	1233	14	1111	1233	13	5
6	2221	1101	10	1110	1000	4	1111	1001	6	6
7	1122	1233	15	1000	2022	7	1010	0032	7	7
8	2222	3232	18	2101	2031	10	2101	1032	10	8
9	2122	3321	16	1012	2320	11	1011	2221	10	9
10	1231	3233	18	1221	3233	17	1220	2233	15	10
11	4322	2234	22	4212	1234	19	4311	1235	20	11
12	2122	2223	16	2010	1123	10	2010	1113	9	12

VOL. 5 1954

February 1954 (*cont.*)

Day	*Ab* Range for $K = 9 : 500\gamma$		Sum	*Es* Range for $K = 9 : 750\gamma$		Sum	*Le* Range for $K = 9 : 1000\gamma$		Sum	Day
	K-Indices			*K-Indices*			*K-Indices*			
13	2212	2123	15	2112	2113	13	2112	2113	13	13
14	1123	3343	20	0012	2333	14	0011	2233	12	14
15	1425	4544	29	1324	4443	25	1333	4543	26	15
16	3422	3454	27	3321	3444	24	5321	2345	25	16
17	4223	4443	26	4223	4443	26	4322	3443	25	17
18	2224	3452	24	2223	3352	22	1113	2352	18	18
19	1143	3333	21	1232	2233	18	1132	2233	17	19
20	2123	2222	16	2022	2222	14	2011	2232	13	20
21	2223	3555	27	1112	3545	22	1222	3575	27	21
22	5433	4355	32	5433	3344	29	6532	3354	31	22
23	4333	3444	28	4322	3444	26	5432	3445	30	23
24	3223	3334	23	3023	3334	21	3012	3343	19	24
25	2223	1333	19	2112	1333	16	1111	1233	13	25
26	2235	3454	28	2235	4454	29	2234	4455	29	26
27	3343	3524	27	3233	3524	25	4233	3525	27	27
28	4222	4333	23	3122	3333	20	4122	3333	21	28

OL.
5
954

ERRATUM

Semidiurnal currents and electron drifts in the ionosphere

J. A. Fejer

Correspondence with Dr. D. F. Martyn, F.R.S., and reading of his recent paper (1953), drew the attention of the author to the fact that the horizontal drift velocity of patches of ionisation is not equal to the horizontal drift velocity of electrons in a "smooth" ionosphere although the vertical drift velocity of layers of ionisation is equal to the vertical drift velocity of electrons, which in this case is associated with an equal drift velocity of positive ions.

The vertical electron drift velocities calculated in § 8 of the author's paper therefore still represent the vertical movement of ionospheric layers, but the horizontal electron drift velocities calculated in § 9 can not be interpreted as horizontal movements of patches of ionisation, to which all "wind" measurements must refer.

The formulae (28*a*) (28*b*) of § 9 could be converted into formulae for the velocity components of the drift of neutral ionisation by substituting $(\tau_{0e} + \tau_{0i})/2$, $(\tau_{1e} + \tau_{1i})/2$, $(\tau_{2e} + \tau_{2i})/2$ for τ_{0e}, τ_{1e}, τ_{2e} respectively, although, as Dr. Martyn points out in his paper, this drift also does not represent the velocity of patches of ionisation in the ionosphere. The calculation of the latter is apparently a more complex problem.

Reference

Martyn, D. F. 1953 Phil. Trans. Roy. Soc. A, **246**, 306.

RESEARCH NOTES

The enhancement of ionospheric ionization during solar flares*

(*Received* 20 *January* 1954)

The various ionospheric disturbances accompanying solar flares arise from the sudden enhancement of electron concentration in Region *D*. Considering that under ionization equilibrium conditions,

$$N = \sqrt{\frac{q}{\alpha(1+\lambda)}}$$

where N is the electron concentration, q is the rate of electron production, α the effective recombination coefficient, and λ the ratio of negative ion to electron concentrations, one

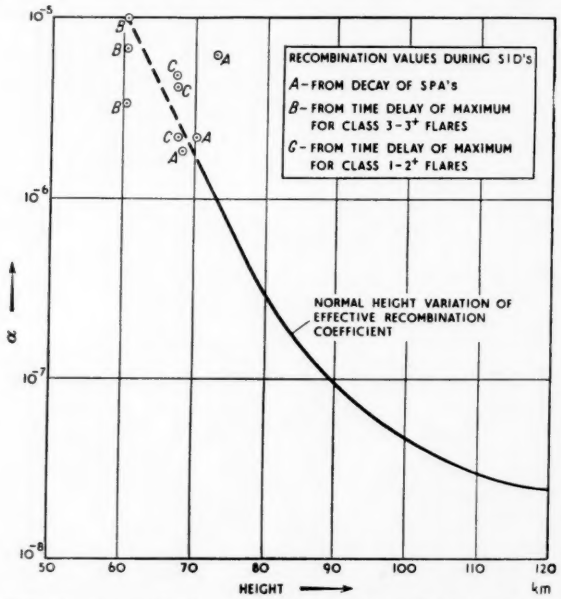

Fig. 1. Effective recombination coefficient during sudden ionospheric disturbances.

may attribute the observed enhancement in N during a flare to either an increase in q or a decrease in λ. The former is the more direct process and can occur either through an enhancement of the normal solar ionizing radiation or of some normally less effective radiation. The alternative, a decrease in λ, has been suggested in recent years by BATES and others (BATES and SEATON, 1950; BATES and MASSEY, 1951) as being brought about by an increased photodetachment due to the enhanced $L\alpha$ radiation during a flare. The hypothesis was believed to be confirmed by the very rapid recovery, reported by BRACEWELL and STRAKER (1949), after a sudden phase anomaly (SPA), the apparent rapid recombination being attributed to loss of electrons by attachment.

* The research reported in this note has been sponsored by the Geophysics Research Division of the Air Force Cambridge Research Center, Air Research and Development Command, under Contract AF19(122)-44.

VOL. 5 1954

In a recent study of the recombination coefficient in the lower ionosphere (MITRA and JONES, 1953), we have attempted to determine if the recovery of the ionosphere after a sudden ionospheric disturbance (SID) does really indicate an effective recombination coefficient greater than that at normal times. The results of the study based on the decay of SPA's at 16 kc/s and of the sudden enhancement of atmospherics (SEA) have yielded values much smaller than 3×10^{-5} cm^3/s as reported by BATES and SEATON. Measurements of the time delay between the time of maximum of a flare and the times of maxima of SPA and SEA also suggest smaller values. In fact, these results strongly indicate that, for any height, the value of the recombination coefficient remains unaltered during an SID and the apparent change is explained by the decrease in height. This is shown in Fig. 1. The full line gives the height distribution of recombination coefficient obtained from various ionospheric measurements. The circled points represent the values during SID's. The heights have been computed from a normal height level of 75 km for reflection of 16 kc/s radio waves. It will be seen that the values during SID's are not appreciably larger than what would be expected for these heights at normal times. This would indicate that λ is not changed appreciably and, hence, any enhancement of electron concentration must be interpreted as an enhancement in q.

Table 1. *Ionization enhancement for a typical class* 2 *solar flare*

	Source	*Approximate Height (km)*	τ_n *(minutes)*	τ_f *(minutes)*	N_f/N_n
1.	SPA (16 kc/s)	68	22	8	2·8
2.	Absorption (150 kc/s)	Entire region	70	23	3·0
3.	SEA (27 kc/s)	69	21	7	3·0

A second objection to the above hypothesis is that, in order to produce an appreciable change in λ, the relevant ultraviolet wavelength must be enhanced by a very large amount. Thus, in the example given by BATES and MASSEY, a change of the photo-detachment coefficient of only about 1×10^{-1}/s is obtained for an enhancement of $L\alpha$ radiation by a factor of 10^5; assuming a normal photon flux of about 2×10^{10}/cm^2/s and a photodetachment cross-section of 5×10^{-17} cm^2. On the other hand, the hypothesis of direct enhancement of q requires only an increase in the $L\alpha$ radiation by a factor of about 10 for a typical flare.

In view of above it seems reasonable to assume that the only way the fadeout enhancement of ionization may occur is from increase or generation of ionization through direct photoionization. There need not be any difficulty on this point if, as was originally suggested by NICOLET (1945), the relevant process is the ionization of NO by enhanced $L\alpha$ radiation. In this case the ionization enhancement is an *overall increase in the entire D-region*. There is some evidence that such enhancement does actually occur. At any level, h, the enhanced flare ionization, N_f, may be computed from the relation

$$\frac{N_f(h)}{N_n(h)} = \frac{\tau_n(h)}{\tau_f(h)}$$

where τ is the relaxation time for the level and the subscripts n and f refer to the normal and flare times, respectively.

Let us consider the experimental results on SPA's at 16 kc/s, the SEA results at 27 kc/s and the absorption results at 150 kc/s. The SPA and SEA results refer to heights around 70 km and the absorption results to the entire region affected by the enhancement. For a typical class 2 flare the ratio $N_f/N_n \simeq 3$ in all these cases (Table 1) which strongly indicates a uniform enhancement of the electron concentration in the entire D-region.

A. P. Mitra and R. E. Jones

Ionosphere Research Laboratory,
The Pennsylvania State University, State College, Pennsylvania.

References

D. R. Bates and M. J. Seaton	1950	Proc. Roy. Soc. B. **63,** 129
D. R. Bates and H. S. W. Massey	1951	J. Atmosph. Terr. Phys. **2,** 1
R. N. Bracewell and T. W. Straker	1949	Mon. Not. Roy. Astr. Soc. **109,** 28
A. P. Mitra and R. E. Jones	1953	Scientific Report No. 44, Pennsylvania State University
M. Nicolet	1945	Mém. Roy. Mét. Inst. Bel. **19,** 1

Atmospheric space charge

(*Received* 3 *March* 1954)

VOL. 5 1954

In a recent research note Chalmers (1953) states that the total charge on the lower side of the ionosphere is zero, the positive charge above areas of fine weather being balanced by the negative charge over areas of thunderstorms. To prove this, Chalmers considers a closed surface S_1 above the cloud level (enclosing the solid earth) on which the conductivity λ_1 is constant. He then applies Gauss' theorem to the volume between S_1 and a surface S_2 at still higher altitude within the ionosphere. The total space charge between S_1 and S_2 is given by

$$4\pi Q = \int_{s_1} F.\, ds + \int_{s_2} F.\, dS$$

Chalmers apparently neglects F on the surface S_2, on the grounds that it is within the ionosphere, a conductor. This may be legitimate in calculating Q, i.e. under purely electrostatic conditions, but we cannot then equate $-dQ/dt$ to

$$\left(\frac{1}{4\pi}\right) \lambda_1 \int_{s_1} F.\, ds$$

but must put

$$-dQ/dt = \left(\frac{1}{4\pi}\right) \left(\lambda_1 \int_{s_1} F.\, dS + \int_{s_2} \lambda F.\, dS\right)$$

for λ at S_2 is many times greater than λ_1.

The concept of the ionosphere as the positive plate of a condenser of which the ground is the negative plate and the lower atmosphere the dielectric, is worth considering carefully. We do know that there is a negative charge on those areas of the surface of the earth which are enjoying fair weather. We also know that, in general, the electric field is vertical. If there were a perfect conductor at some finite height and no space charge in the atmosphere, then all the lines of force originating from the negative charge on the ground would terminate on positive charges on the under surface of this conductor. This can take place

only if the conductivity is uniform. A gradient of conductivity requires the existence of a space charge. For steady conditions, the current density must be uniform so that

$$i = F.\lambda = F_0.\lambda_0$$

where the subscript "0" refers to ground level. The amount of positive charge in a column of height h and unit crossection is

$$\int_0^h q \, . \, dz$$

where q is the positive space charge density. This is given by Poisson's equation

$$4\pi q = -\frac{d^2V}{dz^2} = -\frac{dF}{dz}$$

Integrating to a height h

$$4\pi \int_0^h q \, . \, dz = F_0 - F(h)$$

$$= F_0 - \frac{F_0\lambda_0}{\lambda(h)}$$

The surface charge on the ground σ is given by

$$4\pi\sigma = F_0$$

Hence in a column of height h, the space charge is equal and opposite to a fraction x of the surface charge. This fraction is

$$x = \frac{F_0 - F_0\lambda_0/\lambda(h)}{F_0}$$

$$= 1 - [\lambda_0/\lambda(h)]$$

Values of x can be assigned for each height from values of the conductivity. The following table is based on values of total conductivity given by CALLAHAN *et al.* (1951).

h	$\lambda(h)$	x
0 ft	3×10^{-4} (assumed)	0
5,000	4·2	0·28
10,000	7·3	0·59
15,000	11·7	0·74
20,000	19·0	0·84
25,000	27·7	0·89
30,000	38·5	0·92

Thus it is not necessary to evoke the ionosphere or even the stratosphere; 90% of the lines of force emanating from the earth's negative charge end in the lowest 10 km of the atmosphere. In other words the troposphere is a sufficiently good conductor to shield the earth almost completely from the ionosphere.

It is true that, in the absence of disturbing factors, the current density as measured at one place varies with the supply current. The catch, however, is in the condition "absence of disturbing factors." One would imagine that stations well away from centres of industry such as Watheroo and Tucson would be free of disturbing factors. However during the years 1931 to 1939 the annual mean current density at Tucson showed a steady increase

by a factor of 1·3 followed by a decrease of the same magnitude from 1939 to 1947. No such change was recorded at Watheroo. If each station reflects worldwide thunderstorm condition, they should vary together.

W. D. PARKINSON

Physics Department, Fordham University,
New York 58, *N.Y.*

REFERENCES

CHALMERS, J. A. 1953 J. Atmosph. Terr. Phys. **3**, 345
CALLAHAN, Rita C., CORONITI, S. C., PARZIALE, A. J., and PATTEN, R. 1951 J. Geophys. Res. **56**, 545

* * * * * * * * * *

At the author's request the above communication was sent to Dr. J. Alan Chalmers, who comments on it as follows:

It all depends upon where one takes the surface S_2 referred to by PARKINSON. His term $\int_{S_2} \lambda F \, ds$ gives the vertical current through the surface S_2; now since there is an upward current through S_1 above storms and a downward current above fine weather, there must somewhere be a transverse, horizontal current. If we take S_2 to be above the level where most of this horizontal current occurs, then $\int_{S_2} \lambda F \, ds$ is small.

Actually, the result in the earlier note can be obtained slightly differently. Let us apply Gauss' theorem to the volume inside the surface S_1, including the earth, then we get $\int_{S_1} F \, ds = -4\pi Q$, without any S_2 (the negative sign arising from the sign convention used in atmospheric electricity), and, by the same argument as in the earlier note, if the surface S_1 is one of constant conductivity, Q decreases to zero and remains zero thereafter. Q is here the total charge below the surface S_1; but this must equal the total charge above the surface S_1 up to the ionosphere, as can be seen by realizing that lines of force cannot penetrate the ionosphere, or by applying Gauss' theorem to the whole volume enclosed by a surface S_2 drawn within the ionosphere at a level where there can be no field; this seems completely to obviate PARKINSON's criticism and to prove that the charge between S_2 and S_1 becomes and remains zero.

J. ALAN CHALMERS

Physics Department, Durham Colleges,
Durham University

The use of earth-potential measurements for magnetic- and ionospheric storm-indication

(*Received* 22 *March* 1954)

It is a well-known fact, that the measurement of the earth-potential differences between points, separated by distances of several kilometres and more, give indications of more or less abrupt changes in the earth magnetic field.

Using the underground telephone cables in the Netherlands these potentials in an East-West and North-South direction were measured and registered. However, in starting these

VOL. 5 1954

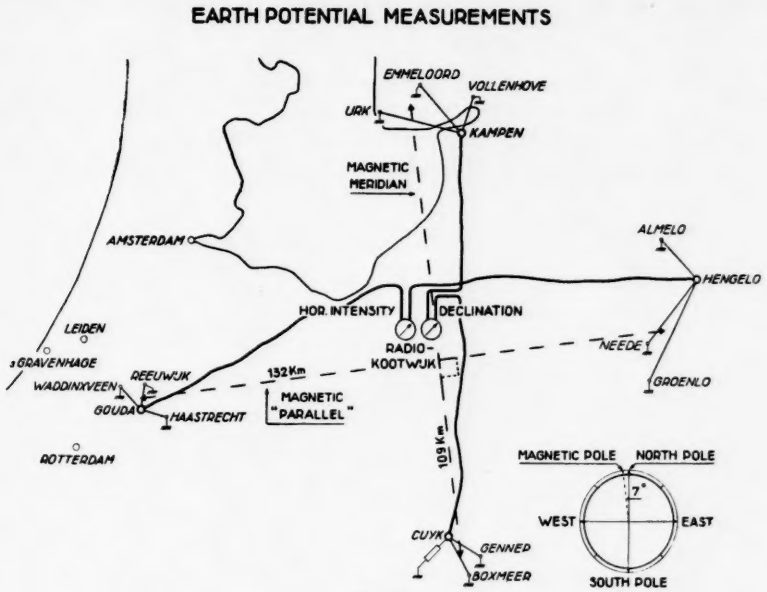
EARTH POTENTIAL MEASUREMENTS
EMMELOORD
VOLLENHOVE
URK
KAMPEN
MAGNETIC MERIDIAN
AMSTERDAM
ALMELO
HENGELO
HOR. INTENSITY
DECLINATION
LEIDEN
RADIO-KOOTWIJK
NEEDE
's GRAVENHAGE
REEUWIJK
132 Km
GROENLO
WADDINXVEEN
MAGNETIC "PARALLEL"
GOUDA
HAASTRECHT
109 Km
ROTTERDAM
MAGNETIC POLE
NORTH POLE
7°
WEST
EAST
CUYK
GENNEP
BOXMEER
SOUTH POLE

Fig. 1

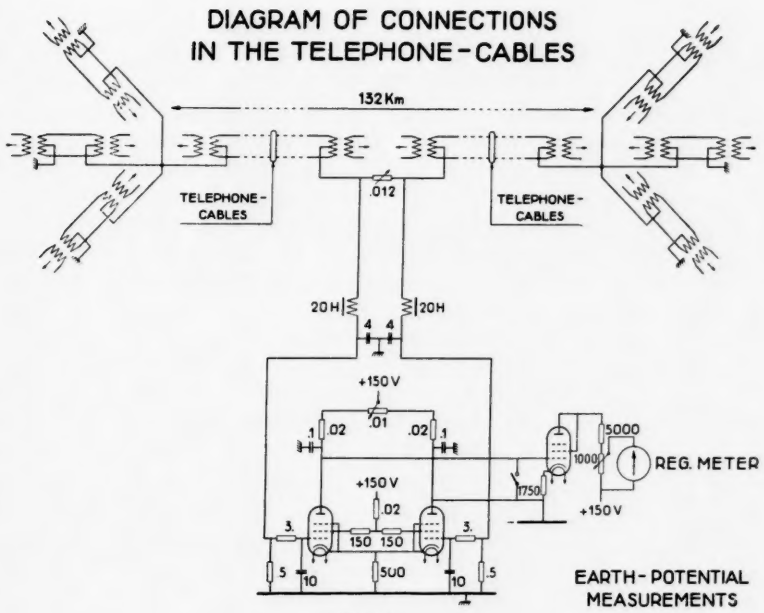
DIAGRAM OF CONNECTIONS
IN THE TELEPHONE-CABLES
132 Km
TELEPHONE-CABLES
.012
TELEPHONE-CABLES
20 H
20 H
4
4
+150 V
.01
.1
.02
.02
.1
5000
1000
REG. METER
1750
+150 V
+150 V
.02
3.
3.
150
150
5
10
500
10
.5
EARTH-POTENTIAL MEASUREMENTS

Fig. 2

measurements the results were very poor in consequence of the heavy electric railway traffic disturbing the diagrams.

An important improvement, resulting finally in a practically perfect agreement of the registrograms with the magnetograms of the magnetic station of the Royal Netherlands Meteorological Institute (K.N.M.I.) in the Bilt, was arrived at, by using the connections indicated in the diagram of Fig. 1. The main feature of this diagram is that at the end of the circuit not *one* earthing-point is chosen, but *several* earthing-points and that these

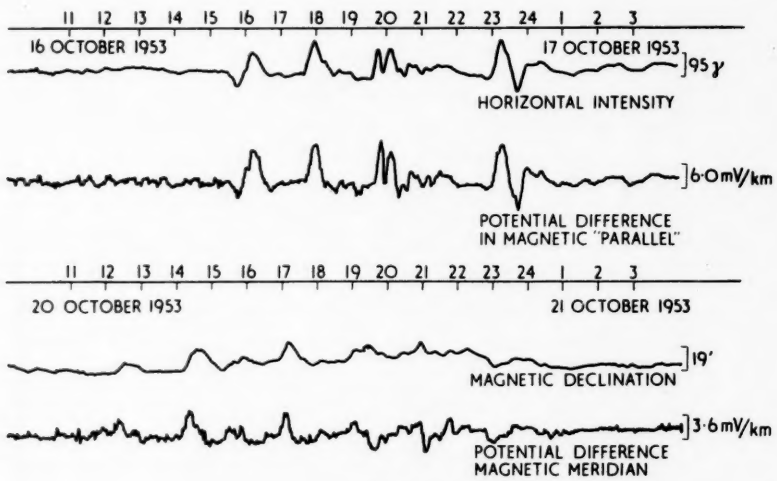
11 12 13 14 15 16 17 18 19 20 21 22 23 24 1 2 3
16 OCTOBER 1953
17 OCTOBER 1953
95 γ
HORIZONTAL INTENSITY
6·0 mV/km
POTENTIAL DIFFERENCE
IN MAGNETIC "PARALLEL"
11 12 13 14 15 16 17 18 19 20 21 22 23 24 1 2 3
20 OCTOBER 1953
21 OCTOBER 1953
19'
MAGNETIC DECLINATION
3·6 mV/km
POTENTIAL DIFFERENCE
MAGNETIC MERIDIAN

Fig. 3

points are situated 5–10 KM in various directions from the end-point of the toll-cable circuit.

The circuit in the cable is the so-called "mid-point" of the telephone circuit, often indicated as the "superposed"-connection formerly used for telegraph purposes. The diagrams of Figs. 1 and 2 need no further explanation; the east-west-direction is chosen as close as possible to the magnetic parallel; the north-south-direction to the magnetic meridian. The registering-meter of the first direction gives the horizontal intensity H of the earth-magnetic field, the second the declination. The slow changes in H, i.e. the diurnal change, is not followed by the potential-diagram; however, the changes, like "crochets", sudden-commencements and storms are clearly indicated (see Fig. 3.). The scientific staff of the K.N.M.I. are studying the phenomenon further.

The registering-meters are placed in the control-room of the radio-station of P.T.T. in Radio-Kootwijk, thus enabling the operating staff to note instantaneously the magnetic conditions with all its consequent effects on the radio-traffic.

A. H. De Voogt

Netherlands P T T
The Hague

VOL. 5 1954

Book reviews

Communication Theory. Edited by WILLIS JACKSON. Pp. xii + 532. Butterworths Scientific Publications, London 1953. 65s.

The publication of this book constitutes a very satisfactory conclusion of a symposium on "Applications of Communication Theory," which was held at the Institution of Electrical Engineers, London in September 1952. There were about two hundred and seventy participants in this symposium and these included ninety visitors from sixteen countries overseas. A useful and interesting account of the proceedings at the meetings, which extended over five days, was published in *Nature* for 20th December 1952, Vol. 170, p. 1051. The volume now available comprises the complete text of the thirty-eight papers presented at the various sessions together with the discussions, some of which are most illuminating and considerably enhance the value of the individual contributions.

Engineers and scientists who are actively engaged in the development or practice of electrical communication have long been aware of the need to use every practicable device and technique which would economise the means employed to convey the desired information or intelligence from one point to another. The radio engineer has become all too conscious of the limitations of the frequency spectrum in accommodating the vast range of requirements of modern communication, broadcasting and television services. The radar operator encounters an analogous problem in his attempt to extract the utmost information from a somewhat different type of signal, which is not always easily distinguishable from the random noise background which is inherent in any communication system.

While the theory of the transmission of information has been explored by some investigators for about a quarter of a century it is only in the past five years or so that the subject has become one of major interest in research laboratories in many parts of the world. Unlike many preceding publications the present volume has a distinct practical bias which arises from the fact that the objective of the symposium held in London in 1952 was to examine and assess the practical value of the recent theoretical work to the problems of electrical communication.

After an opening address by Prof. WILLIS JACKSON, the organizer of the symposium and editor of the volume under review, a summary of communication theory is given by Dr. D. GABOR. The remainder of the book is divided into seven sections which together contain thirty-six papers, of which sixteen were contributed by workers in this country and the sources of the remainder were equally divided between the United States of America and Europe.

Nine papers in the section on "Transmission Systems and Coding" discuss the relative merits of various types of modulation used in communication technique. This is followed by a section dealing with various aspects of the problem of selecting the desired signals to be received in the presence of a background of disturbing noise. Next the subject of "Characteristics of Transmission Channels" is dealt with, including the study of the capacity of a transmission channel and its dependence upon the propagation time of the channel. The following three papers show the usefulness of Information Theory in its application to television problems. This is a subject of great topical interest in view of the advances being made towards higher definition and the use of colour, and the need to economise as far as possible the bandwidths used for television transmission. Later portions of the book are devoted to "A Theory of Hearing," the "Transmission and Analysis of Speech" and to "Associated Studies," including generators of information, human and other kinds, and the influence of informational theory on the structure of language.

The book is rounded off by the concluding discussion in which several of the authors participated, and which completes a very satisfactory and handy presentation of the proceedings of an important and timely symposium. Both the editor and the publishers are to be congratulated on taking the trouble to place on record what will undoubtedly form a basis for further progress in the art and practice of communication as a necessary accompaniment of modern civilisation.

R. L. SMITH-ROSE

TERMAN, F. E. and PETTIT, J. M.; **Electronic Measurements.** xii + 707 pp., 449 figures. McGraw-Hill, 1952. 72s. 6d.

This volume in the McGraw-Hill "Electrical and Electronic Engineering Series" is the successor to Prof. TERMAN'S "Measurements in Radio Engineering," which was published in 1935. Although it is regarded as the second edition of the latter, the revision and expansion of the material has been so radical that the book is effectively new. The change of title reflects the broadening of the scope and the realignment of outlook occasioned by the present-day ready availability of a great range of commercial electronic measuring equipment.

As the authors point out in the preface no set experiments suitable for use in university courses are described since the emphasis has been on the fundamental principles of measurement and of their synthesis into more elaborate techniques for specific purposes or circumstances.

The first two chapters are concerned with voltage, current and power. Particular attention is devoted to the valve voltmeter whose versatility merits the detailed discussion of circuital variations and of frequency and waveform effects.

Bridges, null networks and resonant circuits are next considered in relation to the measurement of circuit elements and this is logically followed by an exposition of those properties of transmission lines, waveguides and cavities which enable measurements to be made at the highest frequencies, with systems having distributed constants.

Consecutive chapters deal with frequency and with waveform, phase and time-interval measurements and discuss the determination of the parameters of modulated waves.

A short chapter on valves serves as an introduction to amplifier and receiver measurements in which transient response, non-linear distortion and noise are adequately treated. Antennas and waves are considered in the two following chapters and brief reference is made to the determination of the properties of the ionosphere and the ground. The last four chapters are concerned with the design considerations of the laboratory equipment required in the types of measurement already described, viz. oscillators, waveform generators, reactance and resistance standards, and attenuators and signal generators.

The presentation of the material is comprehensive and yet critical. Over a thousand footnote references to original papers in American and British journals are given; there are numerous illustrations and these are well designed and expressively annotated.

Although there are minor blemishes of detail, these hardly detract from the undoubted usefulness and achievement of the volume both for reference and as a text book for students of radiophysics and radio engineering.

R. E. BURGESS

LYTTLETON, R. A.: **The Stability of Rotating Liquid Masses.** Cambridge University Press, 1953, 147 pages. 35s.

In this book Dr. LYTTLETON is concerned with the "fission" theory of the origin of binary stars —a theory which will always be associated with the name of JEANS. According to this theory the origin of such double stars is due to the break-up of a single mass by rotation. There are in any case a number of well-known difficulties in the astro-physics of this theory, but the author is not here concerned with them—the present volume is restricted to investigating whether the fission process *as proposed by its advocates* is consistent with the principles of classical dynamics. The problem of the evolution of rotating liquid masses has exercised the minds of many world-famous mathematicians, and LYTTLETON has performed a very valuable service in producing such an excellent connected account of this classical problem of mathematical astronomy.

The book is effectively a critical review of numerous papers, many of an exploratory nature, which have appeared on this subject. The account is largely self-contained and includes excellent sections on those branches of pure mathematics—ellipsoidal harmonic analysis, Lamé functions, etc.—a knowledge of which is essential to appreciate the argument. But the most valuable aspect of the book is that it places on record in connected form the author's own

VOL. 5 1954

contributions to this problem—his elegant proofs of results obtained more laboriously by others; his careful investigation of stability, the point where JEANS fell into error; and his version of the cosmogonical implications of the correct solution of the mathematical problem. In spite of the difficulty of the subject the author has produced a very lucid readable account, a state of affairs to which the Cambridge University Press has made a notable contribution by maintaining its very high standards of printing and display.

The following is a sketch of the main contents of the book, though it does not follow the order of the chapters. The author investigates the possible forms which may be assumed by a steadily rotating mass of gravitating incompressible fluid of constant density, and demonstrates very elegantly the existence of an infinite linear series of Maclaurin spheroids and an infinite linear series of Jacobi ellipsoids; he shows how the shape in any particular case is connected with the angular momentum of the rotating body—a gradual increase of angular momentum implying an evolution along the sequence of forms.

He then investigates which of the forms are dynamically stable when subjected to a general infinitesimal disturbance of the free surface not accompanied by any over-all change of volume. A general disturbance will contain all surface harmonics, and if any of the amplitudes shows an initial tendency to increase without limit, the basic form on which it is superposed is said to be unstable.

It is here that great care has to be exercised in discussing stability questions for rotating systems, since unlike statical systems there are now two different criteria—that of secular stability and that of ordinary stability—which may not by any means always be simultaneously satisfied. An important chapter of the work is devoted to making absolutely clear, perhaps for the first time, the various distinctions between these, and the complete investigation of stability relevant to the problem in hand is duly carried out later in the book.

In considering the cosmogonical implications of the study, LYTTLETON shows that JEANS' explanation of the origin of binary stars, even granting all JEANS' assumptions (now known to be largely unacceptable astrophysically), based on the famous fission theory, is not tenable. Fission of a uniform mass can almost certainly occur, but the masses of the two main portions must be far from equal, probably at least in the ratio 7 or 8 to 1, and more important still, the outcome of such fission must be to endow the components with relative velocity sufficient for complete escape from each other and not to set them in close orbital motion.

The main contribution of the book to astronomical theory lies in the fact that it would seem to dispose completely of the fission hypothesis and thereby remove what has been one of the major obstructions to progress with the greater problem of stellar evolution.

LOUIS ROSENHEAD

BROOKS, C. E. P., and CARRUTHERS, N.; **Handbook of Statistical Methods in Meteorology** viii + 412 pages. H.M. Stationery Office, London. 1953. £1 5s. net.

This book is described in the Preface as intended to serve both as a textbook and as a book of reference. It is, however, best regarded as a handbook. As a textbook it is incomplete in omitting (except for asterisked sections) the proofs of many of the results cited and used. Naturally only by such omission could the ground be covered in some 400 pages.

The book falls into three parts. The statistical standpoint is eclectic, being neither ultra-conservative in the old style nor quite contemporary in the new. The nine chapters of Part I are occupied with such topics, namely observations, variates, distributions and parameters, as find place in the standard texts. The distinctive feature is that the examples and exercises (with answers provided at the end) are drawn almost entirely from meteorological data. Any reader (such as the present reviewer) who is not a meteorologist will be struck by the richness of statistical material in this field. Part I ends with a chapter on analysis of variance, well illustrated, in the two-way classification, by a hypothetical example of readings of four barometers by five observers. Interaction is treated in a starred section.

Part II treats of multivariate distribution and correlation. To the reviewer the special and

most interesting feature is Chapter 11, on vector distributions, the illustrations being drawn largely from statistics of wind speed and direction, clearly a field congenial to the authors. The treatment of correlation is along the usual lines. Part II concludes with chapters on smoothing and interpolation, and on curve-fitting. If there is an antithesis here, perhaps its meaning is that interpolation and smoothing are primarily computational, while curve-fitting, carried out as it frequently is by least squares, is statistical. Even so, some of the methods of curve-fitting are based more on practical convenience than on theory. One of these (p. 298) is BROSTER's method of fitting a polynomial. Divided differences of the data are taken until at some stage, say third differences, they show no trend. They are assumed to be constant but for random error; their mean a_3, by NEWTON's formula, then provides the highest term a_3x^3 in the polynomial. Its contribution is numerically removed from the data, which are then similarly treated for terms of lower degree. This seems to work well enough, but clearly has little basis in statistical theory, since divided differences are correlated in a rather subtle manner. With respect to polynomial fitting, the reviewer does not know the form or nature of the tables mentioned as compiled by Schumann; his own experience is that for evenly spaced data the Fisher-Yates tables of orthogonal polynomials are adequate. The linear case of orthogonal polynomial fitting is exactly the same as that here ascribed (p. 281) to MARVIN. Perhaps a cautionary point might have been made in this chapter, namely that if a nonlinear transformation, such as the taking of logarithms, is applied to data then the weights are altered.

Part III deals with time-series, persistence, periodicity, harmonic analysis and periodograms. The harmonic analysis follows the usual lines, though with a minimum of theory, and sets out variants of the usual schemes for 12 and 24 time units. The discussion of periodograms is more interesting, especially the comparison (p. 372) of computing times taken on a test series by different periodograms. The short methods of ALTER, of CARRUTHERS and of BROOKS, seem to come out very well. The book concludes with formulae, tables and a bibliography, largely meteorological but with some purely statistical textbooks and articles as well.

The general impression is of a compilation of great value to researchers in meteorology, but not only to them; it should be supplemented, however, by some textbook on statistics proper.

A. C. AITKEN

VOL. 5 1954

BRUINING, H.; **Physics and Applications of Secondary Electron Emission.** Pergamon Press Ltd. London, and McGraw-Hill Co., New York. xii + 178 pp. 130 figures. 25s. net or **$5.**

The subject of secondary emission has been something of a Cinderella in physics, and this is perhaps the more remarkable when it is realized how extremely important practically all associated phenomena are in the fields of radio, radar and television, to mention the outstanding examples. In his chapters on applications Dr. BRUINING makes it very obvious that there are now many further applications of secondary emission and more to be expected. These chapters, and particularly the last of the ten which form this volume, prove most interesting, and indeed stimulating as they point clearly to the possibilities of fresh approaches in such recent developments as storage tubes for television, computing machines and memory devices in general.

The literature on secondary emission is extremely extensive and it appears in a great variety of sources. If Dr. BRUINING had done no more than to indicate the nature of this literature and to give us references to the relevant sources it would have been a great service. This he has done in thorough fashion, and much more besides. The general treatments of the subject are almost as markedly limited as the more detailed are numerous. The author himself is in fact the writer of the only other treatment of the subject in book form. His first book (in German) published in 1942 was a very necessary source book for many, and in this new volume they will find an answer to almost all of their needs in the expanding field.

The subject has not proved particularly fascinating to the academic researchers, but this may well prove to be a serious error of judgment on their part. Perhaps as a result of this, one feels that the treatment of theory so far made is rather sketchy and general, although clearly

the obstacles in the way of detailed theory are many. It is to be hoped that the strong growth of interest which is apparent at present will be stimulated by the appearance of this book. It covers practically everything of importance, and should serve as an admirable guide to workers in all branches of electronics and students of the associated phenomena.

There is one branch not discussed here—the emission produced by positive ions and atoms. It is of course not entirely pertinent to the main treatment, but already there is so much information in this compact volume that one is inclined to regret its separation from the rest.

The treatment is admirably clear and free of any noticeable blemishes or errors. It is right up-to-date in discussion. It is produced in a very acceptable fashion with an unusually large number of figures and plates (130) which make for a quicker and clearer understanding. The book can be most highly recommended to all as a volume that will serve a very useful part in their work and study. It should indeed be of great value to beginner and expert alike.

S. C. CURRAN

SUTTON, O. G.: **Mathematics in Action.** G. Bell & Sons, Ltd., London, 226 pages, 16s. net.

This is a lively account of the parts which mathematics can play in scientific progress. Its author, who has quite evidently enjoyed writing it, is a distinguished applied mathematician who has, since 1928, been associated with a number of fields of Government science, especially radar and meteorology. Till recently he was the Dean of the Royal Military College of Science and a Professor of Mathematical Physics; he is now Director of the Meteorological Office. Dr. SUTTON sees the task of the applied mathematician modestly, for it is that of using the tools provided by the pure mathematician to clarify and extend the observations of the physicist. Much of his book, therefore, is concerned with the tools of his trade, with the techniques by which he constructs imaginary worlds as an aid to the exploration of the real one. His chapters on examples deal, respectively, with ballistics, waves, flight, statistics and the weather, in the course of which he pays special tribute to the work of the Rev. FRANCIS BASHFORTH on ballistics, F. W. LANCHESTER on the theory of the finite aerofoil and of L. F. RICHARDSON on weather forecasting by numerical processes.

It should, however, be stressed that in spite of the author's easy style, and Mr. A. J. LAURIE'S engaging picture-diagrams, the book cannot be termed a popular one. A knowledge of the Calculus is assumed on the part of the reader; but, with that, the author takes us up to the frontiers of knowledge in fields as fascinating as they are important. Perhaps a special recommendation of this volume might be proffered to the nuclear physicist—for it tells him about other worlds than his.

E. V. A.

LYTTLETON, R. A: **The Comets and their Origin.** Cambridge University Press, 1953. 25s. net.

In this book the author gives an account of his new theory of the origin of the comets; the main part is rather technical, but since the author is of the opinion that the features of comets are not too well known even to astronomers, he begins by describing the dynamical and physical properties of comets as established by observational astronomy. These first two chapters of the book, which are enlivened by a great number of carefully chosen photographs of comets, can replace some of the earlier books on comets which appealed to a large circle of readers owing to the interest these unusual celestial objects arouse. The two subsequent chapters distinguish this book from all those previously written; here a new explanation for the origin and formation of comets and their tails is given which can claim to be a scientific theory, open to quantitative examination. The principal idea is briefly that the sun, during passages through galactic dust clouds, by its gravitational action causes the aggregation of dust particles; these clusters

will revolve round the sun and, under favourable conditions, become visible to us as comets.

It will be for astronomers to test how far this new theory can explain all the strange observations made on comets throughout the centuries. It has the advantage of not introducing like most of the earlier comet theories new and unfounded hypotheses as for instance ejection of the cometary material from the sun or the planets, or pulverization of an asteroid. For the existence of dust clouds, on which the author's theory is based, there is ample evidence, and his views are also in full agreement with other recent cosmological theories which were developed without reference to the problem of comets.

One point may be of special interest to readers of this journal. Since SCHIAPARELLI's work we know that at least some periodic meteor swarms are genetically related to comets, and this assumption has sometimes been extended by astronomers to meteorites because it seemed simplest to consider meteors and meteorites as essentially the same celestial bodies, differing only in size. It is to the credit of geologists to have insisted that objects like meteorites can only have their origin in a celestial body akin to our earth, and not in a comet. Dr. LYTTLETON's inference that comets must be composed of small particles confirms this view. It is of course possible, and even likely, that some meteorites are so small that they are completely consumed during their flight through the terrestrial atmosphere and it may not be feasible, by watching the luminous effect in the sky, to distinguish them from meteors. But a meteor, of cometary origin, can never have the size, and even less the structure, of the meteorite specimens of our museums. If we make use of CHAMBERLIN's distinction between the "two solar families", planets and comets (and their relatives), then the meteors—at least those connected with comets—belong to the second family, but meteorites to the first.

F. A. PANETH

VOL.
5
1954

NOTICE

The Secretary-General of the International Scientific Radio Union (U.R.S.I.), announces the publication of the Proceedings of the Third Meeting of the Joint Commission on the Ionosphere (Canberra, 1952).

This book is available at the General Secretariat of the U.R.S.I., 42 Rue des Minimes, Brussels (Belgium), at the following price: 200 Belgian francs, or £1 9s., or $4.0 (U.S.A.), postage included.

Journal of Atmospheric and Terrestrial Physics, 1954, Vol. 5, pp. 117 to 131. Pergamon Press Ltd., London

Group height calculations in the presence of the earth's magnetic field*

JOHN M. KELSO**

Ionosphere Research Laboratory, The Pennsylvania State University,
State College, Pennsylvania

(*Received* 16 *March* 1954)

ABSTRACT

A method is given for the computation of an h'-f curve for an ionosphere of arbitrary shape. The effects of the earth's magnetic field may be included. The method is based on integral formulae involving the derivative of height with electron density, dz/dN, and misbehaviour of this derivative curve leads to inaccuracies in the results. The two integral formulae used are obtained as special cases of the Gauss-Christoffel quadrature formula.

The procedure is applied to: (1) a linear layer; (2) a parabolic layer; (3) a cosine layer; and (4) an arc-cosine layer. The first three cases are studied with and without the earth's magnetic field, and the results of the first two are compared with exact calculations by other workers. The cosine layer results are compared with those for a Chapman layer. The arc-cosine layer shows a maximum in the h'-f curve which does not correspond to any prominent feature of the electron density curve, showing a need for care in the study of h'-f curves.

A different method is given for the calculation of an h'-f curve in the case of penetration of a layer of arbitrary shape.

1. INTRODUCTION

In the course of a theoretical study of ionosphere layer production or of ionospheric irregularities, a worker frequently obtains a theoretical curve of electron density as a function of height. It would be desirable to have also a theoretical curve of group height as a function of frequency (an h'-f curve) for this layer, so that experimental h'-f records could be examined to determine whether the predicted result actually occurs in practice. Although such h'-f curves can always be computed by direct numerical integration, this is usually quite tedious, especially when the effects of the earth's magnetic field are included.

In the present work, we exhibit a method for carrying out such calculations rapidly and with considerable accuracy. This method is based on integration formulae which were obtained as special cases of the Gauss-Christoffel quadrature formula. These formulae were originally obtained by KELSO (1952) and (1954), for use in the solution of the integral equation for the electron density distribution. When the earth's magnetic field is neglected, the present procedure is exact in principle if the derivative of height with electron density, dz/dN, is a polynomial (of not more than the ninth degree for the five-point integral used in most of this work, of not more than degree $2n - 1$ if an integral formula with n points is used). If dz/dN is not such a polynomial, then the degree of the approximation depends upon how closely some polynomial of degree $2n - 1$ could approximate the derivative curve. It should be noted carefully that it is *not* necessary to determine the approximating polynomial explicitly; the integration formula automatically accounts for the approximation. When the earth's magnetic field is included, the limits on the accuracy of the procedure are not so easily stated,

* The research reported in this paper has been sponsored by the Geophysics Research Division of the Air Force Cambridge Research Center, Air Research and Development Command under Contract AF19(122)-44.

** Now with the Glenn L. Martin Company, Baltimore, Md.

but a comparison with exact results for linear and parabolic layers shows that the method is still quite good.

In illustration of the procedure, it is applied to four different layers: (a) Linear layer; (b) Parabolic layer; (c) Cosine layer; and (d) Arc-cosine layer. All four of these cases are studied without the earth's magnetic field, and the first three are also treated with the field included. In cases (a) and (b) we compare our results with and without the earth's magnetic field. In case (c) we compare our result with the exact result for the cosine layer without the magnetic field, and with similar results for a Chapman layer, and a parabolic layer. Case (d) is one for which exact results are not available. These layers were chosen so as to include a number of different forms of behaviour, and to illustrate various points to be discussed in detail below.

This method is limited to the consideration of horizontally stratified media where the index of refraction may be considered to be real, and where ray theory can be applied. In addition, we note that the fact that the curve of dz/dN is implicitly approximated by a polynomial leads to difficulties when this derivative curve has discontinuities, cusps, infinities, or otherwise misbehaves. The most common form of such misbehaviour is an infinity, which occurs, in particular, whenever the electron density, N, has a maximum value at some height, z. Thus, the integration formulae given here are valid only when studying a layer below the first maximum. However, in Section 7, we consider a different procedure which can be used, in some cases, to eliminate some of the worst effects of this difficulty.

VOL. 5 1954

2. THE INTEGRATION FORMULAE

Neglecting collisions, the group height of reflection, $h'(f)$, for a signal of frequency f, incident at the height $z = 0$ at the bottom of a layer, and reflected at the height z_r, is given by,

$$h'(f) = \int_0^{z_r} \mu'(z)\, dz, \tag{1}$$

where $\mu'(z)$ is the group index of refraction, and where the value of $h'(f)$ is measured above the height $z = 0$.

In the absence of an external magnetic field, (1) may be written,

$$h'(f) = \int_0^{z_r} \frac{dz}{\sqrt{1 - f_0^2/f^2}}, \tag{2}$$

where $f_0^2 = Ne^2/\pi m$.

In the presence of an external magnetic field, μ', can be obtained from the Appleton-Hartree equation in the manner indicated by SHINN and WHALE (1952). Following the procedure in KELSO (1954), we define a quantity $G(f_0^2/f^2)$ by,

$$\mu' = \frac{G(f_0^2/f^2)}{\sqrt{1 - f_0^2/f^2}}. \tag{3}$$

When the magnetic field is neglected, $G(f_0^2, f^2) \equiv 1$.

Introducing this expression into (1), we obtain,

$$h'(f) = \int_0^{z_r} \frac{G(f_0^2/f^2)\, dz}{\sqrt{1 - f_0^2/f^2}}. \tag{4}$$

The group index of refraction, μ', and, in consequence, G, depends only upon the ratios f_0^2/f^2, and $y = f_H/f$ (where f_H = the gyrofrequency), and upon the propagation angle θ_p. Since the integration in (4) is taken at constant frequency, this integral will be *exact* if the quantity $G(f_0^2, f^2)$ is calculated for a value of y corresponding to the (constant) frequency being used, and to the proper value of θ_p.

We are now in a position to develop two integration formulae. The first, which we call Formula A, is used throughout most of this work, and requires five points for an integration. Since it is difficult to extend this formula to use more than five points, we give at the end of this section, a second formula, Formula B, which is easily extended to use any desired number of points.

To develop Formula A, we let,

$$\begin{aligned} \xi(z) &= f_0^2(z) \\ u(\xi) &= dz/d\xi \\ F &= f^2 \end{aligned} \tag{5}$$

Then (4) becomes,

$$h'(f) = f \int_0^F \frac{G(\xi/F)\, u(\xi)\, d\xi}{\sqrt{F - \xi}} \tag{6}$$

We note that,

$$u(\xi) = dz/d\xi = dz/d(f_0^2) = dz/dN \text{ times a constant.} \tag{7}$$

Writing,

$$x = \xi/F = f_0^2/f^2, \tag{8}$$

then (6) may be written,

$$h'(f) = f^2 \int_0^1 \frac{dz}{d(f_0^2)}\, G(x)\, \frac{dx}{\sqrt{1 - x}} \tag{9}$$

This equation has the same general form as Equation (23) in the paper by KELSO (1954), and for which the following integral formula was obtained through use of the Gauss-Christoffel quadrature formula,

$$h'(f) = f^2 \sum_{i=1}^{5} \lambda_i \frac{dz}{d(f_0^2)}(x_i) G(x_i)^* \tag{10}$$

where

$$\begin{aligned} \lambda_1 &= 0{\cdot}13378 & x_1 &= 0{\cdot}05169 \\ \lambda_2 &= 0{\cdot}29920 & x_2 &= 0{\cdot}25226 \\ \lambda_3 &= 0{\cdot}43824 & x_3 &= 0{\cdot}53905 \\ \lambda_4 &= 0{\cdot}53817 & x_4 &= 0{\cdot}81252 \\ \lambda_5 &= 0{\cdot}59046 & x_5 &= 0{\cdot}97788 \end{aligned} \tag{11}$$

Before we can use the expression in (10), it is necessary to determine the values of $G(x_i)$ under suitable conditions. For present purposes we use a propagation angle of $\theta_p = 23°16'$ (i.e., a dip angle of 66°44') and seven values of y which correspond to a gyrofrequency of 1·149 megacycles, and operating frequencies of 3·5, 3·25, 3·0, 2·5, 2·0, 1·5, and 1·0 megacycles per second. The corresponding values

* It should be noted that x_i appears in this equation to emphasize functional dependence, and is not to be interpreted as a factor.

of y are given in Table 1, and it is emphasized that any set of frequencies and gyrofrequency which lead to these values of y can be used as well as the set above.

In Table 1, we also list the products,

$$\varepsilon_i = \lambda_i G(x_i) \tag{12}$$

for the seven values of y. Then (10) may be written,

$$h'(f) = f^2 \sum_{i=1}^{5} \varepsilon_i \frac{dz}{d(f_0^2)}(x_i) \quad : \quad \text{Formula A} \tag{13}$$

This is the first of the two integral formulae to be considered here. Other magnetic field conditions may be introduced by computing a different set of ε_i.

Table 1. *Coefficients in Formula A*

y	ε_i				
	$i = 1$	$i = 2$	$i = 3$	$i = 4$	$i = 5$
0·32828	0·13238	0·28250	0·37616	0·40198	1·0109
0·35354	0·13231	0·28174	0·37379	0·40049	1·0356
0·38300	0·13224	0·28091	0·37123	0·39932	1·0611
0·45960	0·13207	0·27901	0·36561	0·39849	1·1111
0·76600	0·13160	0·27396	0·35239	0·41155	1·2015
1·14900	0·13128	0·27068	0·34594	0·43782	1·2354

VOL. 5 1954

We wish now to return to (4) in order to develop the second integral formula. Formula B. Let,

$$t = f_0/f$$
$$u(t) = dz/dt = f\, dz/df_0 \tag{14}$$

Then (4) becomes,

$$h'(f) = \int_0^1 \frac{G(t^2)\, u(t)}{\sqrt{1 - t^2}}\, dt \tag{15}$$

If we assume that,

$$u(-t) = u(t), \tag{16}$$

then,

$$h'(f) = \tfrac{1}{2} \int_{-1}^{+1} \frac{G(t^2)\, u(t)}{\sqrt{1 - t^2}}\, dt \tag{17}$$

KELSO (1952) applied the Gauss-Christoffel quadrature formula to the evaluation of a similar integral, and obtained the result, which is written in our present notation as,

$$h'(f) = \frac{2n}{\pi} \sum_{k=1}^{n} G(t_k^2) u(t_k) \quad : \quad \text{Formula B} \tag{18}$$

where

$$t_k = \cos \theta_k$$
$$\theta_k = \frac{2k - 1}{2n}\, \pi, \; k = 1, 2, \ldots, n. \tag{19}$$

To make Formula B suitable for calculations including the earth's magnetic field, it would be necessary to prepare a table similar to Table 1, but with $\frac{\pi}{n} G(t_k^2)$ replacing the ε_i, and calculated for appropriate values of t_k as indicated in (19).

Both of the integral formulae A and B, being based on the Gauss-Christoffel quadrature formula, have the property that the integration is exact, in principal, provided that the integrands (which are $u(x_i)G(x_i)$ and $u(t_k)G(t_k^2)$, respectively) are polynomials of degree not more than $2m - 1$, where m points are used in the integration. If the integrands are not polynomials of appropriate degree, then the results are approximations, as stated in the introduction. In the case of Formula A, we use five points, so that the degree of the integrand must be not more than 9, to give exact results. In the case of Formula B, we use n points in the formula, but $2n$ points over the doubled interval $(-1, 1)$. Thus, the results here are equivalent to integrating an approximating polynomial of degree $4n - 2$. (To fit the criterion of $2m - 1$, this would be a degree of $4n - 1$, but (16) requires the polynomials to be even, and the greatest even polynomial of degree not more than $4n - 1$ is of degree $4n - 2$). Thus, using $n = 10$ as in Section 4, we have the equivalent of an approximating polynomial of degree 38, over the double interval.

3. Application to a Linear Layer

We consider a layer whose electron density increases linearly with height, so that,

$$Ne^2/\pi m = f_0^2 = \alpha z, \tag{20}$$

for a constant value of α.

Then,

$$dz/d(f_0^2) = 1/\alpha.$$

Since the derivative, $dz/d(f_0^2)$, is a constant, the integral Formula A, becomes,

$$h'(f) = \frac{f^2}{\alpha} \sum_{i=1}^{5} \varepsilon_i. \tag{21}$$

(a) *No magnetic field*

When the magnetic field is neglected ($y = 0$), the $G(x_i) \equiv 1$, so that $\lambda_i = \varepsilon_i$. From (11), the sum of the λ_i is seen to be equal to 1·99985. Kelso (1954) showed that the exact value of this sum is 2, and that the difference between the two results arises because of numerical errors in computing the values in (11).

Then,

$$h'(f) = 2f^2/\alpha,$$

which is the value from (21) using the correct $\sum\lambda_i$, and which can also be found by direct integration for this problem. Thus, the present procedure gives results which are exact to within the limitations of the numerical work upon which the Formula A was based.

(b) *With the magnetic field*

Finding the $\sum\varepsilon_i$ from Table 1, we get the values shown in Table 2 for various y. The third column of this table is taken from Fig. 3 of the paper by Shinn (1953).

This last column is not very exact, since it was obtained by interpolation from SHINN's system of curves (the curves are exact, but the interpolation was done by inspection).

Table 2. $\Sigma\varepsilon_i$ *to be introduced into Equation* (21)

y	$\Sigma\varepsilon_i$ (*from Table* 1)	$\Sigma\varepsilon_i$ (*from* SHINN)
0·32828	2·204	2·22
0·35354	2·224	2·23
0·38300	2·245	2·25
0·45960	2·286	2·27
0·57450	2·328	2·30
0·76600	2·371	2·33
1·14900	2·421	2·42

The agreement here appears to be about as good as can be expected, considering the errors in interpolation.

4. APPLICATION TO A PARABOLIC LAYER

Let us now consider the parabolic layer defined by,

$$z = y_m[1 - \sqrt{1 - f_0^2/f^2}], \tag{22}$$

where y_m is the semi-thickness of the layer, and f_c is its critical frequency. Differentiating,

$$f^2 = dz/d(f_0^2) = \frac{y_m R}{2\sqrt{(1/R^2) - x}} \tag{23}$$

where $R = f/f_c$.

(a) *No magnetic field*

As before, we use the integral Formula A, with $\varepsilon_i = \lambda_i$, where λ_i and x_i are taken from (11). As an example of the calculations which follow, we consider in detail the case $R = 0{\cdot}9$. Then we have,

x_i	λ_i	$f^2\, dz/d(f_0^2)$	$\lambda_1 f^2\, dz/d(f_0^2)$
0·05169	0·13378	$0{\cdot}41375y_m$	$0{\cdot}05535y_m$
0·25226	0·29920	$0{\cdot}45403y_m$	$0{\cdot}13585y_m$
0·53905	0·43824	$0{\cdot}53958y_m$	$0{\cdot}23646y_m$
0·81252	0·53817	$0{\cdot}69268y_m$	$0{\cdot}37278y_m$
0·97788	0·59046	$0{\cdot}88819y_m$	$0{\cdot}52444y_m$
			$h' = \text{sum} = 1{\cdot}32488y_m$

VOL. 5 1954

In Table 3 we show values of h' for various $R = f/f_c$. The exact values in the third column are obtained through use of the well-known expression for h' in a parabolic layer,

$$h' = \tfrac{1}{2} y_m R \ln \frac{1 + R}{1 - R}. \tag{24}$$

Table 3. Group heights for a parabolic layer in the absence of a magnetic field

$R = f/f_c$	h' (*Formula A*)	h' (*exact*)	% *error*
0·2	$0{\cdot}040546 y_m$	$0{\cdot}040544 y_m$	0·006
0·4	$0{\cdot}16945 y_m$	$0{\cdot}16946 y_m$	0·006
0·6	$0{\cdot}41586 y_m$	$0{\cdot}41589 y_m$	0·006
0·8	$0{\cdot}87886 y_m$	$0{\cdot}87888 y_m$	0·002
0·9	$1{\cdot}3249 y_m$	$1{\cdot}3250 y_m$	0·008
0·95	$1{\cdot}7391 y_m$	$1{\cdot}7402 y_m$	0·06
0·99	$2{\cdot}5524 y_m$	$2{\cdot}6202 y_m$	2·6

Inspection of the derivative in (23) shows that it has an infinity at $R = 1$ and $x = 1$. Thus, we would expect the results in Table 3 to behave as they do, becoming less exact as we near the critical frequency. The error can be decreased by using an integral formula using more points in the integration, i.e., by using a higher degree for the implicit approximating polynomial. We do that in the present case by applying Formula B with 10 points. This is *equivalent* to integrating an approximating even polynomial of degree 38. For $R = 0{\cdot}99$, we get $h' = 2{\cdot}6178 y_m$. Thus, we have about 0·1% error. The increase in precision was obtained at the expense of about twice as much computational labour in achieving the result.

(b) *With the earth's magnetic field*

Exact results for this problem were given by SHINN and WHALE, using direct numerical integration of a transformed integral.

Calculations for the parabolic layer in the presence of the earth's magnetic field are carried out in the same manner as in (a), except that appropriate values of ε_i from Table 1 are used in place of λ_i.

Since the values of y used in Table 1 were chosen without regard to the frequencies used by SHINN and WHALE, exact comparisons with their results are not possible. However, we show three sets of points for which the value of y is sufficiently close to give a good comparison with the exact results of SHINN and WHALE. This comparison is given in Table 4, where the fifth column is the value of y actually used with Formula A, and the sixth column shows the correct value of y appropriate to the operating frequency.

Table 4. Group height for a parabolic layer in the presence of the earth's magnetic field

$R = f/f_c$	h' (*Formula A*)	h' (SHINN *and* WHALE)	*Error* %	y (*used*)	y (*correct*)
28/32 = 0·875	$1{\cdot}1467y_m$	$1{\cdot}4108y_m$	0·4	0·38300	0·37512
30/32 = 0·937	$1{\cdot}9865y_m$	$1{\cdot}9868y_m$	0·9	0·35354	0·35020
31·75/32 = 0·992	$3{\cdot}5223y_m$	$3{\cdot}9623y_m$	11·1	0·32828	0·33084

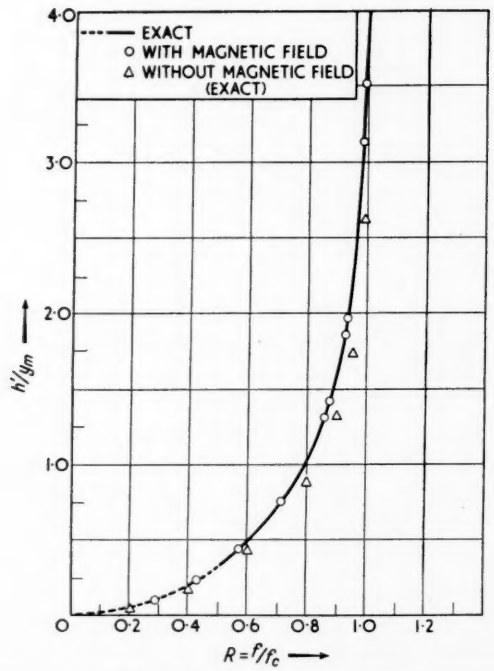

Fig. 1. Group heights for parabolic layer including the earth's magnetic field, compared with exact results for this layer with and without the magnetic field.

These results are quite good except when we are very near to the critical frequency.

By adding seven values of h' corresponding to the values of y in Table 1, we obtain enough points to make a good test. These are shown as circles on Fig. 1, with the exact values from SHINN and WHALE being given by the solid curve. The dotted portion of the curve indicates the region over which the results of SHINN and WHALE must be extrapolated. The triangles show the exact results which would be obtained if the magnetic field were not present.

Other methods for treating the parabolic layer in the presence of the earth's magnetic field were given by MARIANI (1953) and ARGENCE and MAYOT (1953).

VOL. 5 1954

5. Application to a Cosine Layer

We now wish to consider a layer which has two special properties of interest. The first property is that the cosine layer is a much better approximation to a Chapman layer than the usual parabolic layer is. The second property is that this layer not only has the infinity in dz/dN at the maximum of the layer (which is of importance at or near the critical frequency), but it also has an infinity in this derivative at $N = 0$, independently of frequency. Some of the results for this layer were discussed by Friedman (1950).

We define the layer by the expression,

$$f_0^2 = \frac{f_c^2}{2}\left[1 + \cos \pi(y_m - z)/y_m\right], \tag{25}$$

where f_c is the critical frequency, and y_m is the semi-thickness of the layer. The form of this curve is given in Fig. 2, along with the corresponding curves for a

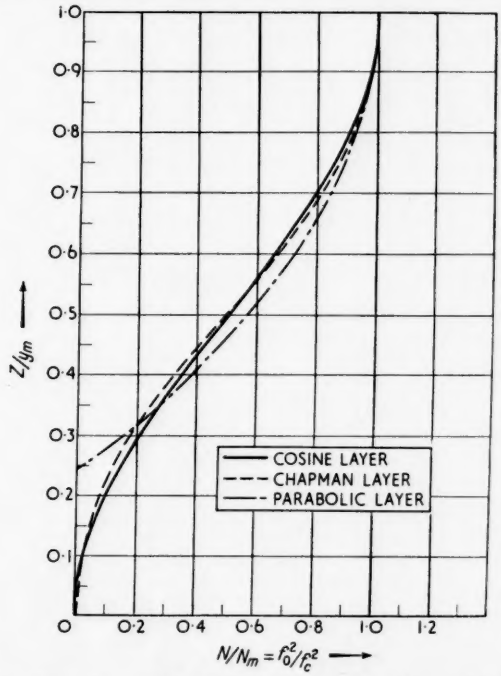

Fig. 2. Electron density distributions as functions of height for the cosine, Chapman, and parabolic layers.

Chapman layer and the usual parabolic approximation to a Chapman layer. The height z is measured above the level where $f_0^2 = 0$ in (25), and the three layers are taken with their maxima in coincidence.

Without the magnetic field, the h' for this layer is given exactly by,

$$h' = \frac{2y_m R}{\pi} K(R), \tag{26}$$

where $K(R)$ is a complete elliptic integral of the first kind, and where $R = f/f_c$.

Differentiating (25),

$$f^2\, dz/d(f_0^2) = \frac{2y_m R^2}{\pi} \frac{1}{\sqrt{1-(2R^2x-1)^2}}. \tag{27}$$

When $x = 0$, this expression is infinite, independently of f.

We use the derivative in (26) with Formula A, to obtain h' for this cosine layer with and without the magnetic field. The results are plotted in Figs. 3 and 4. In Fig. 3, the correct h' for the cosine layer in the absence of a magnetic field, as obtained from (27), is shown as a solid curve. The results from Formula A are given as circles when the magnetic field is included and as triangles when it is neglected. The error in this case is seen to be greater at all frequencies than it

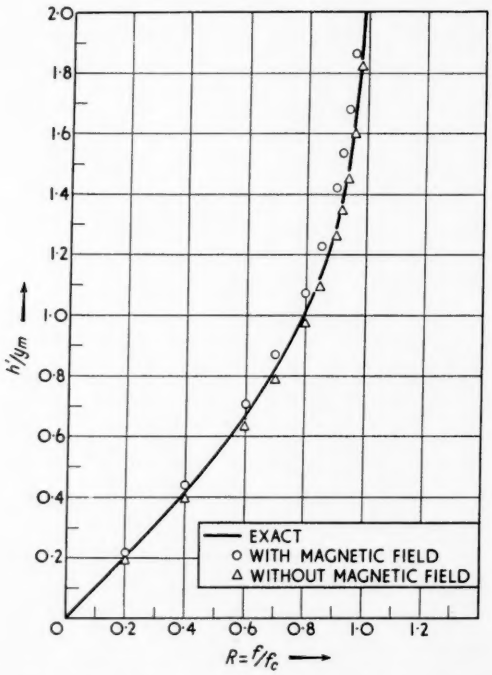

Fig. 3. Group heights for a cosine layer calculated by the present method, with and without magnetic field, compared with exact results excluding the magnetic field.

was in the case of the parabolic layer. This is because of the lower infinity in the derivative curve. As we go to higher frequencies, the error due to the lower infinity decreases, but we find that we are approaching the infinity at the layer maximum.

In Fig. 4, we again give the results for the cosine layer in the absence of a magnetic field (using the results of (26)). This curve is shown solid. The exact results for a Chapman layer in the absence of a field are given as a dotted curve plotted from results given by JAEGER (1947). Corresponding results for a parabolic layer are given in the dashed curve. The circles on this Fig. show "corrected" values for the cosine layer in the presence of the earth's magnetic field. These

VOL. 5 1954

corrected values were obtained by finding the ratio at a given frequency by which the results from Formula A would have to be increased to give the exact results, both in the absence of a magnetic field. Then we apply a proportional correction to the results from Formula A including the magnetic field. This should yield

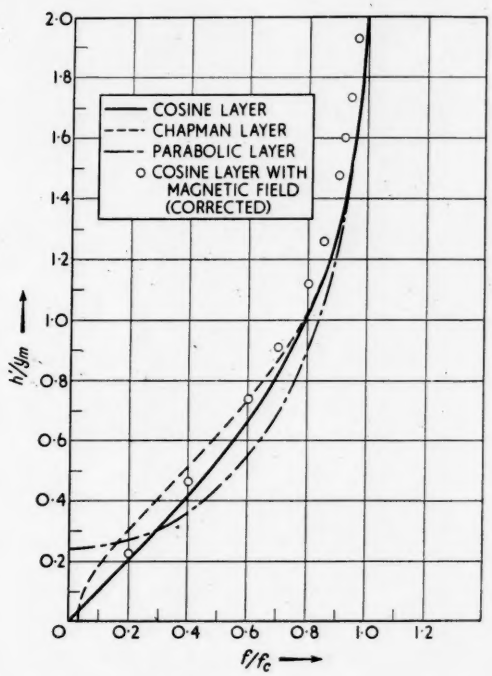

Fig. 4. Exact group heights for the cosine, Chapman, and parabolic layers, neglecting the magnetic field, compared with corrected group heights for the cosine layer in the presence of the magnetic field.

values for h' which are extremely near to the correct results. Fig. 4 clearly shows the superiority of the cosine layer over the parabolic layer as an approximation to a Chapman layer. The advantage of the parabolic layer lies in the fact that its equation is more easily applied to various problems.

6. Application to the Arc-cosine Layer

The cases studied above have all been considered many times. by many authors. Even the cosine layer, which has not been used as often as the linear and parabolic layers, is nearly of the shape of the well-known Chapman layer. In the present section, we wish to study a layer which has a quite different form. This layer shape, while different from those usually considered, does not seem to be totally unrealistic, and some useful information can be obtained by studying this layer.

We define this arc-cosine layer in two parts. The first part, for $0 \leq f_0 \leq f_1$ (where f_1 represents some fixed frequency), represents one complete cycle of the

layer variation. The second part amounts to a repetition of the first cycle, and extends from $f_1 \leq f_0 \leq \sqrt{2}f_1$. Thus,

$$z = y_m[1 + \cos \pi(xR_1^2)], \qquad 0 \leq f_0 \leq f_1 \tag{28}$$

$$z = 2y_m + y_m[1 + \cos \pi(xR_1^2 - 1)], \qquad f_1 \leq f_0 \leq \sqrt{2}f_1. \tag{29}$$

where

$$x = f_0^2/f^2 \tag{30}$$

$$R_1 = f/f_1$$

These relations define the layer whose reflection height, h_T, is given as a function of $R_1 = f/f_1$ in Fig. 5. Differentiating (28) and (29), we obtain

$$f^2\, dz/d(f_0^2) = \pi y_m R_1^2 \sin(\pi x R_1^2), \qquad 0 \leq f_0 \leq f_1, \tag{31}$$

$$f^2\, dz/d(f_0^2) = \pi y_m R_1^2 \sin \pi(xR_1^2 - 1), \qquad f_1 \leq f_0 \leq \sqrt{2}f_1. \tag{32}$$

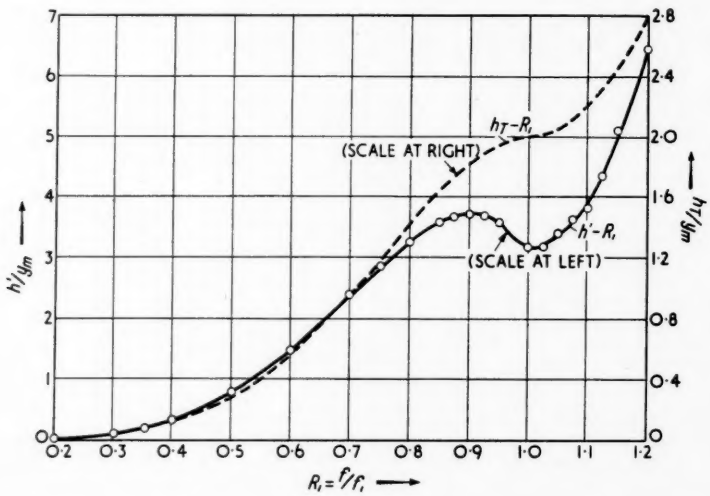

Fig. 5. Exact group and true heights of reflection for the arc-cosine layer, with computed group heights given as circles. Earth's magnetic field neglected.

Neglecting the earth's magnetic field, and using the derivatives in (31) and (32), we find h' for this layer. The result is shown as a function of $R_1 = f/f_1$ in Fig. 5. The computed points are shown as circles, and a smooth curve is drawn through the points. Over the lower region, $0 \leq f_0 \leq f_1$, the points lie very well on such a smooth curve. For the upper region, there is a greater scatter, for reasons to be discussed below.

The h' curve for this layer is very interesting. We note first that the minimum of the h' curve coincides very nearly with the point, at $R_1 = f/f_1 = 1$, where the h_T curve changes its curvature from concave downwards to concave upwards. The maximum of the h' curve at about $R_1 = 0{\cdot}9$, however, does not show any correlation with any obvious special feature of the h_T curves. Although such behaviour could have been predicted by a careful consideration of the layer shape.

VOL. 5 1954

it does serve to emphasize the need for great caution in assuming that marked physical changes in the layer are the reason for anomalous behaviour of h'-f records. On the basis of the present h'-f curve alone, one might be tempted to suppose that there was some kind of "ledge" or "ripple" in the layer, and that the maximum of the h'-f curve occurred because of this "ledge." This is, of course, not the case.

The singularities appearing at the critical frequency for the parabolic layer and cosine layer, and also at zero frequency for the cosine layer, give illustrations of one type of misbehaviour of the derivative dz/dN which leads to errors when the present integral formulae are applied. The derivative for the arc-cosine layer exhibits another type of misbehaviour. For $f \leq f_1$, this derivative curve is simply a sine curve, which is easily approximated by polynomials. However, for $f \geqslant f_1$, the derivative curve undergoes an abrupt change at $f_0 = f_1$. That is, the derivative curve has the form of the absolute value of the sine of an angle over an interval from zero to something greater than π. When $xR_1^2 = 1$, i.e., at $f_0 = f_1$, we are at the zero point of the curve corresponding to an angle of π. As we pass through this point the slope of the derivative curve changes abruptly from $-\pi y_m R_1^2$ to $+\pi y_m R_1^2$. A polynomial cannot fit this region of the derivative curve very well. As we increase f, and thus R_1, the fit of the implicit ninth-degree polynomial changes somewhat erratically, so that the results become subject to an error, which is not uniform with f. Therefore, the points for $f \geqslant f_1$ are subject to a scatter. This scatter does not prevent the results from being sufficiently accurate for most purposes to which h'-f curves are put.

7. Layer Penetration

It is not possible to obtain useful information concerning the group path for frequencies above the critical frequency using the present method, at least without profound modifications. In such a case, the derivative curve has an infinity inside the range of integration. This infinity arises because dz/dN is infinite where the layer has a maximum. When applying either Formula A or Formula B, the resultant h'-f curve will have in it infinities which appear each time one of the points x_i, or t_k, coincides with the infinity of dz/dN. Since these infinities are physically unreal, the h'-f curve for $f > f_c$ is more or less meaningless.

If we have two layers to consider, such as an E-layer and an F-layer, we can treat the problem in three stages. We can first consider the group path of the signal in the two layers independently. This can be done for frequencies less than the layer critical frequency by the present method. Thus we have separate h'-f curves for the E-layer and the F-layer. For frequencies up to the E-layer critical frequency, no signal reaches the F-layer, so that the E-layer h'-f represents the correct curve for the combined layer up to this frequency, and the corresponding portion of the F-layer h'-f curve can be omitted. For higher frequencies, the signal penetrates to the F-layer and the F-layer h'-f curve must be used. However, to these values of h' we must add the group path in passing through the E-layer. This last part of the group path is for the case that cannot be studied by the present method. Thus, we are interested in a procedure for finding the group path for a signal which penetrates a layer.

For this penetration case, direct integration of the integrals for h' given in (2) and (4) would, in general, be easier than in a case where the signal is reflected in the layer, since the denominators of the integrands will not vanish. However, this can still involve a great amount of computational labour if the integration cannot be carried out explicitly. In the present section, we offer another method which can be of use in some cases. We consider only the case where the magnetic field is neglected, but the extension of this material to include the magnetic field is obvious.

Consider the integral (2) for the group height, with the upper limit replaced by z_1, which represents a fixed height up to which we wish to integrate. Since the signal is assumed to penetrate the entire slab through which we integrate, the ratio f_0/f is always less than unity. Hence, we can expand the denominator in an infinite series, obtaining,

$$h' = z_1 + \tfrac{1}{2}\int_0^{z_1} (f_0^2/f^2)\, dz + \tfrac{3}{8}\int_0^{z_1} (f_0^2/f^2)^2\, dz + \ldots \tag{33}$$

The layer can be defined in terms of a function,

$$N/N_m = f_0^2/f_c^2 = F(z), \tag{34}$$

where N_m is the maximum value of the electron density, and f_c is the critical frequency.

Now,

$$f_0^2/f_c^2 = (f_0^2/f^2)\,(f^2/f_c^2)$$

Thus,

$$f_0^2/f^2 = (1/R^2)F(z) \tag{35}$$

where $R = f/f_c$. Then, (33) becomes,

$$h' = z_1 + \frac{(1/2)}{R^2}\int_0^{z_1} F(z)\, dz + \frac{(3/8)}{R^4}\int_0^{z_1} F^2(z)\, dz + \tag{36}$$

$$+ \ldots + \frac{(1/2)\,(1/2+1)\,(1/2+2)\ldots(1/2+n)}{R^{2n}\, n!}\int_0^{z_1} F^n(z)\, dz + \ldots$$

The sequence of integrals involved here is independent of the frequency, which appears only in the R. In the more straightforward way of finding the h'-f curve, one would have to deal with a single integral, but one which changed with frequency. This variation with frequency is no difficulty if the integration is carried out exactly, but can be troublesome in numerical work. Thus the present material is especially suitable for layers where $F^n(z)$ can be integrated conveniently, but where $1/\sqrt{1 - F(z)/R^2}$ cannot.

As an example of this method, we consider complete penetration through a cosine layer, whose equation is given by (25). The exact solution can be obtained here, and is given by,

$$h' = \frac{4y_m}{\pi} K(1/R) \tag{37}$$

where $K(1/R)$ is a complete elliptic integral of the first kind.

VOL. 5 1954

The integrals in (36) are also easily computed in this case. In Table 5, we give a comparison of the results of applying (36) and the exact results for several values of $R = f/f_c$. The second column gives the exact results, while the remaining columns give the sum of (6) up to three terms, five terms, ten terms, and twenty terms.

Table 5. Group heights for penetration through a cosine layer

$R = f/f_c$	*exact* h'	*Sum of* (36) *after n terms*			
		$n = 3$	$n = 5$	$n = 10$	$n = 20$
1·1	2·95663	2·6053	2·7853	2·9329	2·9537
1·2	2·63224	2·4829	2·6140	2·6303	2·6321
1·5	2·30418	2·2778	2·3036	2·3041	—
2·0	2·14636	2·14258	2·14633	—	—
2·5	2·08805	2·0872	2·08811	—	—
5·0	2·02050	2·02045	2·02046	—	—
10·0	2·00503	2·00506	—	—	—

The dashes in the table indicate that the values did not change appreciably as succeeding terms were added. The labour involved in computing the values in this table (and for 8 other values of R) is less than would be required if (2) were evaluated for the same number of frequencies by direct numerical or graphical integration. The convergence of the series is seen to be quite slow when R is very nearly equal to unity. However, for fairly large values of R, the convergence is quite rapid. The number of significant figures carried here is considerably larger than needed for most group height problems. Thus, even the worst case in Table 5 gives the result to within an error of 3 in the third place with 10 terms. A similarly accurate result is obtained with only 5 terms for $R = 1{\cdot}2$, and not more than 3 terms for the remaining cases. Since this is less than the usual experimental errors in this type of work, the present method is seen to be suitable for many problems.

References

Argence, E., and Mayot, M.	1953	J. Geophys. Res. **58**, 147
Friedman, B.	1950	New York University, Mathematics Dept., Research Group, Res. Rep. EM-17
Jaeger, J. C.	1947	Proc. Phys. Soc. **59**, 87
Kelso, J. M.	1952	J. Geophys. Res. **57**, 357
	1954	J. Atmosph. Terr. Phys. **5**, 11
Mariani, F.	1953	An. Geofis. **6**, 21
Shinn, D. H.	1953	J. Atmosph. Terr. Phys. **4**, 240
Shinn, D. H., and Whale, H. A.	1952	J. Atmosph. Terr. Phys. **2**, 85

Journal of Atmospheric and Terrestrial Physics, 1954, Vol. 5, pp. 132 to 140. Pergamon Press Ltd., London

The aeronomic problem of oxygen dissociation

MARCEL NICOLET

Ionosphere Research Laboratory, The Pennsylvania State University, State College, Pennsylvania

(*Received* 23 *March*, 1954)

ABSTRACT

The vertical distribution of molecular oxygen above 100 km, obtained from recent rocket data, cannot be explained by photo-chemical equilibrium.

An aeronomic study of departures from photo-equilibrium conditions in the lower thermosphere shows that atmospheric mixing or diffusion must be operative. It is concluded that the process of diffusion contributes increasingly to molecular oxygen concentrations at greater heights. By considering a diffusive equilibrium, it is found that new information can be obtained for various aeronomic processes.

1. INTRODUCTION

It has been shown by NICOLET and MANGE (1952, 1954) that the problem of oxygen dissociation above 100 km does not depend on photo-equilibrium conditions, but on atmospheric processes such as molecular diffusion and mixing.

Using incomplete observational data they have discussed the conditions for departure from photochemical equilibrium. Recently, NICOLET (1954a) has considered the atmospheric motions which are necessary to maintain mixing effects in a vertical distribution of molecular oxygen.

Consistent rocket data on the total content of molecular oxygen have been obtained very recently by BYRAM, CHUBB, and FRIEDMAN (1954). They are particularly useful in checking the atmospheric behaviour as far as the dissociation of oxygen is concerned. Thus, this question is considered in this paper.

2. VERTICAL DISTRIBUTIONS

Above 110 km, the atmospheric behaviour is well represented by the equation

$$p/p_0 = (H/H_0)^{-1/\beta} \tag{1}$$

in which p denotes the pressure, H the scale height, and β the constant gradient of the scale height.

According to HAVENS, KOLL, and LAGOW (1952), we can adopt, at 120 km, $p_0 = 3{\cdot}5 \times 10^{-5}$ mm of Hg, $H_0 = 10$ km and $\beta = 0{\cdot}2$.

In the aeronomic problem (NICOLET and BOSSY, 1949), the atmospheric concentration will be given by the equation

$$n/n_0 = (H/H_0)^{-(1+\beta)/\beta} \tag{2}$$

in which n denotes the concentration of the principal constituent.

When we consider a minor constituent such as O_2 in an atmosphere consisting of atomic oxygen and molecular nitrogen, it is possible to consider *a priori* a vertical distribution of this molecule according to various laws. Therefore, we can write the following equation

$$n(O_2)/n_0(O_2) = (H/H_0)^{-\chi(1+\beta)/\beta} \tag{3}$$

VOL. 5 1954

in which X is a parameter determining a certain distribution. It is evident that $X = 1$ means a vertical distribution of O_2 following the atmospheric distribution. When $X = 1{\cdot}28$, molecular oxygen is distributed with height according to a diffusive equilibrium, for it is easy to show that

$$X = [\beta + m(O_2)/m(M)]/1 + \beta \tag{4}$$

is satisfied under this condition.

When $X = 2{\cdot}92$, equation (3) describes molecular oxygen which is in photochemical equilibrium at altitudes where the optical depth is negligible. In other words, the photochemical equilibrium equation is

$$n(O_2) = k_1 n(M) n^2(O)/J_2 \tag{5}$$

in which $k_1 n(M)$ is the recombination coefficient depending on three-body collisions with the atmospheric particle M, and J_2 is the photodissociation rate coefficient which is constant. Since $k_1 \propto T^{1/2} \propto H^{1/2}$ and $n(M)n^2(O) \propto H^{17{\cdot}5}$, the exponent leads to 2·92 for the value of X.

Any intermediate value between $X = 1$ and $X = 1{\cdot}28$ in equation (3) represents a vertical distribution of O_2 between mixing and diffusive equilibrium, and any value between $X = 1{\cdot}28$ and $X = 3$ a distribution corresponding to unstable conditions between diffusive equilibrium and photo-equilibrium.

3. Calculated Concentrations

Rocket data published by Byram, Chubb, and Friedman (1954) give the total number of molecules versus height, namely values of the order 6×10^{-3} atmo-cm (N.T.P.) at 108 km, 3×10^{-3} at 112 km and 10^{-3} at 118 km. These values indicate a slow decrease with height of the concentration above 110 km.

According to equation (3), the concentration will be given by

$$n(O_2) = \frac{X(1 + \beta) - \beta}{H} \int_z^\infty n(O_2)\, dz \tag{6}$$

if the observations are represented by

$$\int_z^\infty n(O_2)\, dz = \frac{n(O_2)H}{X(1 + \beta) - \beta} \tag{7}$$

Adopting $3{\cdot}5 \times 10^{-3}$ atmo-cm at 110 km, the observational data are accounted for by a value of $X = 1{\cdot}28$. Fig. 1 shows the vertical distribution versus height of the total number of O_2 molecules compared with the total number of atmospheric molecules if there is no dissociation.* With such a distribution the rocket data are followed with a precision of $\pm 15\%$. In other words the observational points are inside of the two dashed curves corresponding to $(3{\cdot}5 \pm 0{\cdot}5)\ 10^{-3}$ atmo-cm at 110 km.

Therefore, the vertical distribution of O_2 is obtained from (6) using $X = 1{\cdot}28$.

* These data do not agree exactly with those published by the Rocket Panel (1952). However, following Naval Research Laboratory data closely, there is only a difference in height of between 1 and 2 km.

4. DEPARTURE FROM PHOTO-EQUILIBRIUM CONDITIONS

Considering that $n(O_2) < n(O)$ and that the differential equation representing photochemical conditions for oxygen is

$$\frac{dn(O_2)}{dt} = n(O_2)J_2 - k_1 n(M)n^2(O) \tag{8}$$

we may write the approximate solution as follows

$$n(O_2) = n_{t=0}(O_2)e^{-J_2 t} + \frac{k_1 n(M)n^2(O)}{J_2}[1 - e^{-J_2 t}] \tag{9}$$

From observational results $n_{t=0}(O_2)$ must be, at least, the concentrations obtained by diffusive equilibrium. They are greater than the photochemical values. Therefore, the times which it is important to consider are given by the exponential factor $J_2 t$. Since $J_2 = 1{\cdot}56 \times 10^{-6}$ sec^{-1} at zero optical depth (NICOLET and MANGE, 1954), the decrease of $n(O_2)$ as a function of time is very slow. As may be seen from Fig. 2, 5 days (of 12 hours duration) are required to reduce the concentration to 70% of its initial value. Furthermore, 35 days are needed to reach 10% of the diffusive equilibrium value. On the other hand, it also requires 35 days to reach the photochemical value (90%) and we are dealing with aeronomic conditions corresponding to departures from photoequilibrium conditions.

Using the numerical values indicated in Section 2 and $k_1 = 5 \times 10^{-34} T^{1/2}$ (BATES and NICOLET, 1950), equation (3) with $X = 3$ provides the photochemical values of $n(O_2)$. At 108 km, the concentration is $1{\cdot}5 \times 10^{11}$ cm^{-3} while the value adopted from rocket data is of the order of $1{\cdot}5 \times 10^{11}$ cm^{-3} at 110 km. Therefore, we may choose 110 km as a sufficiently good approximation for an initial level to compare all the possible vertical distributions of O_2.

The results are given in Fig. 3 in which the full curves show vertical distributions of O_2 according to mixing, diffusion and photochemical equilibrium. Dotted curves represent intermediate states between diffusion and photo-equilibrium conditions. Since the photochemical values are negligible (10^4 times less at 170 km) compared with the observational values, it is important to determine the magnitude of diffusive transport effects.

5. UPWARD DIFFUSION OF MOLECULAR OXYGEN

If the loss of oxygen molecules by photodissociation is not more than 10% per day, the increase of concentration by diffusive transport is very large.

Considering that the velocity of diffusion of a minor constituent is given by the following equation (CHAPMAN and COWLING, 1939)

$$w(O_2) = -\frac{D}{H}\left[\frac{1}{n(O_2)}\frac{\partial n(O_2)}{\partial z} - \frac{1}{H}\left(\beta + \frac{m(O_2)}{m(M)}\right)\right] \tag{10}$$

in which D is the ordinary diffusion coefficient, we can calculate the velocities of diffusion using various values of X.

VOL. 5 1954

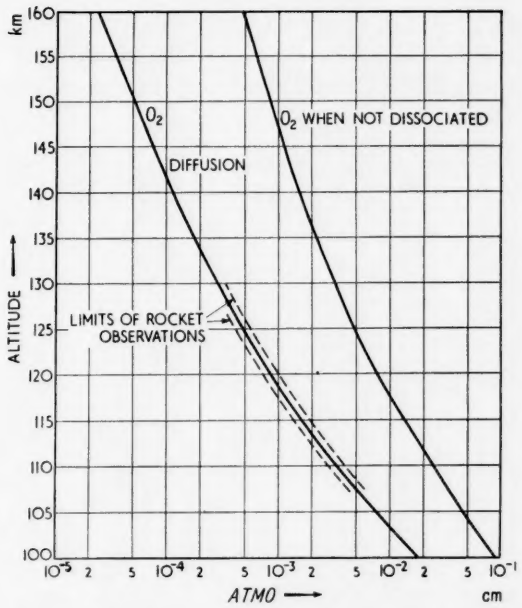

Fig. 1. Total number of O_2 molecules versus height. One atmo-cm equals $2{\cdot}7 \times 10^{19}$ molecules. The vertical distribution of undissociated O_2 molecules corresponds to the atmospheric distribution in a mixed atmosphere; the diffusive equilibrium distribution is based on an absolute value at 110 km given by rocket observations.

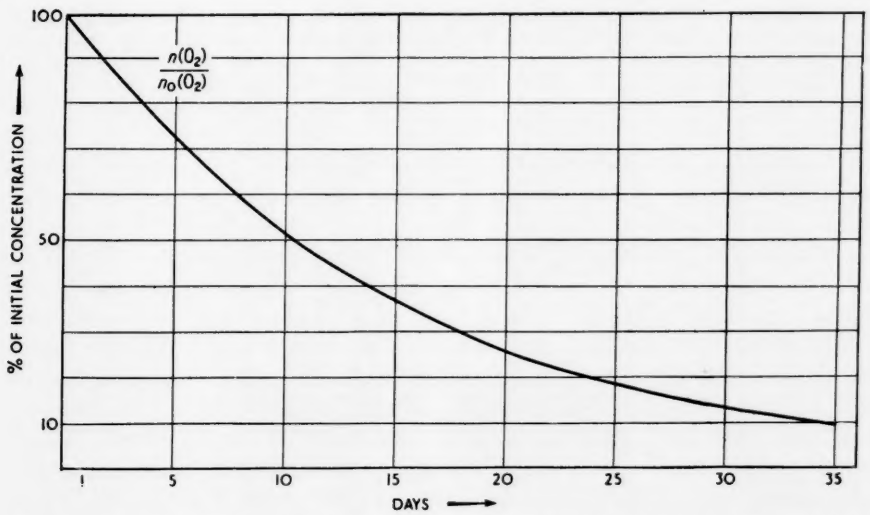

Fig. 2. Variation of O_2 concentration that is larger than a photo-chemical equilibrium value when solar photodissociation is acting. The number of days (12 hours duration) corresponds to a dissociation effect associated with a 4500°K radiation temperature.

Starting with $X = 3$ (photochemical equilibrium) we see in Fig. 3 that the upward transport velocities increase with height. At 160 km, for example, the O_2 concentration has increased more than 10 times in less than 3 hours.

In other words, when the time required to reach photoequilibrium is several days, the time to reach diffusive equilibrium is only a matter of hours or a few

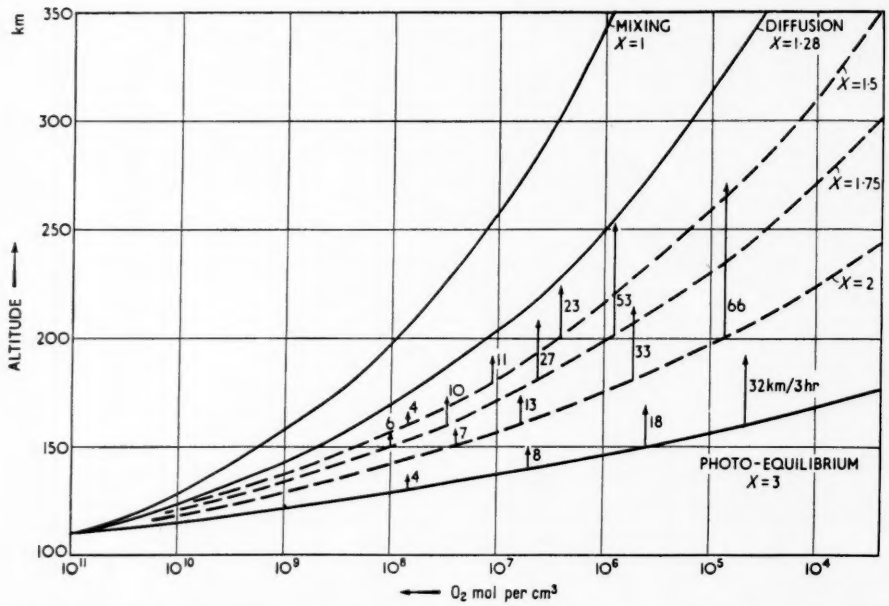

Fig. 3. Vertical distribution of molecular oxygen from 110 km to 350 km following mixing, diffusive and photochemical equilibriums. The effect of vertical velocities due to the diffusion process is shown by arrows indicating an upward motion of O_2 molecules during an average time of 3 hours.

days. Since it is not the purpose of this paper to attempt to discuss the entire problem of diffusion of O_2, the numerical values will not be considered further. However, it can be pointed out that the molecular oxygen concentration must decrease with height following a diffusive equilibrium if atmospheric mixing is not involved. In other words, the values obtained from a diffusive equilibrium correspond to minimum values. Since mixing due to atmospheric motions (vertical winds) must exist, it is possible that the vertical distribution of O_2 follows that of the atmosphere. It appears that this would not lead to a regular distribution. However, in their analysis of other rocket data, more difficult to interpret, NICOLET and MANGE (1954) have found that there is a possibility of strong mixing. In any case, the actual concentration of O_2 will be given by an intermediate distribution between mixing (maximum value) and diffusion (minimum value). At 200 km, for example, the concentration of O_2 is 10^7 cm^{-3}, but can reach 10^8 cm^{-3}. This problem will be discussed in a forthcoming paper.

VOL. 5 1954

6. The Transition Region below 110 km

The percentage dissociation of O_2 can be obtained if an atmospheric model based on pressures obtained from rocket data is assumed. In this paper, the value of the pressure at 120 km published by Havens, Koll, and LaGow (1952) is used with a linearly varying scale height of gradient $\beta = 0{\cdot}2$. Above 110 km this model, which does not differ appreciably from the Rocket Panel (1952) model, leads to correct values for the concentrations. However, when the percentage dissociation of O_2 is computed, the result is very sensitive to the assumed model.

If we compare the number of molecules per cm^3 (see Table 1) obtained from the Rocket Panel Model and from our model for an atmosphere without dissociation, it is evident that the differences can be neglected.

Table 1. *Concentrations of molecules in an undissociated atmosphere*

Altitude (km)	*Rocket Panel*	*Nicolet*
100	$1{\cdot}80 \times 10^{13}$	$1{\cdot}70 \times 10^{13}$
110	$4{\cdot}32 \times 10^{12}$	$3{\cdot}92 \times 10^{12}$
115	$2{\cdot}18 \times 10^{12}$	$1{\cdot}94 \times 10^{12}$
120	$1{\cdot}18 \times 10^{12}$	$1{\cdot}03 \times 10^{12}$
125	$6{\cdot}67 \times 10^{11}$	$5{\cdot}74 \times 10^{11}$
130	$3{\cdot}97 \times 10^{11}$	$3{\cdot}39 \times 10^{11}$

However, when the percentage of dissociation is computed from the formula

$$\% = [1 - n(O_2)/0{\cdot}2n(M)]100 \qquad (11)$$

it is found that the value obtained is very sensitive to small variations in $n(O_2)$ and $n(M)$. For this reason, it is very difficult to determine the aeronomic conditions below 110 km where the percentage of dissociation is less than 70 or 80%, while it is easy to follow the dissociation above 120 km. In diffusive equilibrium we have the results shown in Table 2. These results are of the same order as the observational results obtained by Byram, Chubb, and Friedman (1954) between 120 and 130 km.

Table 2. *Percentage of oxygen dissociation above* 120 *km in diffusive equilibrium*

Altitude (km)	*Percentage*	*Altitude*	*Percentage*
120	85	145	90·5
125	86	150	91·5
130	87·5	155	92·0
135	89	160	92·5
140	89·5	170	93·5

This procedure cannot be used below 110 km. In this region, $n(O_2)$ becomes of the same order as $n(O)$, while solution (9) of equation (8) is only valid when $n(O) > n(O_2)$. Furthermore, the photochemical equilibrium value of $n(O_2)$ is not very different from its diffusive equilibrium value so that it is difficult to follow theoretically the vertical distribution of O_2 and O at lower heights. Finally, the photo-equilibrium value is dependent on the increasing optical depth in terms

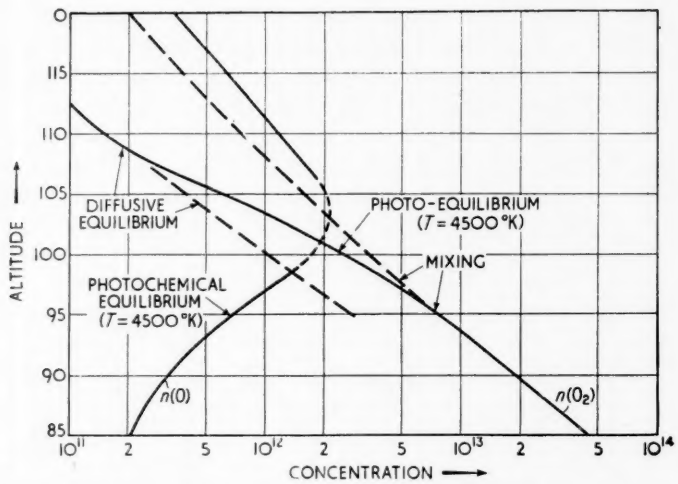

Fig. 4. Vertical distribution of molecular and atomic oxygen in the transition region when the photochemical equlibrium depends on a 4500°K radiation temperature.

of the total number of O_2 molecules. Using the equation of photochemical equilibrium (equation (8) in which $dn(O_2)/dt = 0$)

$$n(O_2)J_2 = k_1 n(M)n^2(O)$$

and the numerical values of J_2 given by NICOLET and MANGE (1954), it is easy to see that the transition region must be between 95 and 105 km.* In Fig. 4, the curve of $n(O)$ below 108 km represents an equilibrium distribution showing that the maximum of the concentration of atomic oxygen is of the order of 2×10^{12} cm^{-3}.

However, considering a specific level, such as 97 km, where $n(O) < n(O_2)$, it is easy to see that the time, τ_{Rec}, of recombination defined by

$$\tau_{Rec}(O) = 1/k_1 n(M)n(O)$$

is still longer than one month. For this reason, all the indicated concentrations below 100 km are minimum values. Atmospheric motions may act during one month to enhance the atomic oxygen concentration increasingly in the downward

(*) The parameter of temperature is 4500°K.

VOL. 5 1954

direction. If a concentration of 2×10^{12} atoms is reached at 97 km, the time of recombination is still one month. This result means that the percentage of dissociation of O_2 equals 20%.

As an example, let us consider a concentration of oxygen atoms of the order of 2×10^{12} cm^{-3} between 85 and 95 km, namely a percentage of dissociation from 2% to 13%. The time of recombination increases from 85 km to 95 km, by steps of 2·5 km, from 4 to 6, 9, 14, and 20 days. These results demonstrate that concentrations of atomic oxygen do exist which are larger than those given by photochemical equilibrium.

Therefore, even if the entire process in the transition region depends primarily on the photochemical action, the exact vertical distribution of atomic oxygen, nevertheless, is subject to atmospheric motions.

7. Conclusions

Since molecular oxygen has a vertical distribution above 110 km which is completely different from a photo-equilibrium distribution, many aeronomic processes must be studied in another form.

The presence of O_2^+ bands which was found by Nicolet (1948) in the auroral spectrum and recognized afterwards in their spectra by Vegard (1950), Petrie and Small (1952) and Gartlein and Sherman (1952) are not limited in altitude by the O_2 content but by the process of excitation.

An excitation process of the oxygen green line in the airglow (Nicolet, 1954b) can be identified with a dissociative recombination process $O_2^+ + e \rightarrow O + O$ following a charge transfer process like $O^+ + O_2 \rightarrow O_2^+ + O$. If such a mechanism may be operative in the aurora (Seaton, 1954), it is not limited only to the lower regions, and consequently may depend on the variation of the electron concentration.

It was formerly postulated that the rapid decrease of O_2 with altitude was an objection against the origin of the *E*-layer by ionization of O_2. In fact, the problem of the formation of the *E*-layer depends on the number of solar photons emitted in the ultraviolet region 1030–910A and in the x-ray region. According to recent rocket measurements (Byram, Chubb, and Friedman, 1953), the number of x-ray photons appears to be larger than the number of ultraviolet photons and, therefore, the origin of the *E*-layer should be due to x-rays. Nevertheless, the presence of O_2 at high altitudes must have an important effect in Region *F*, in that it can explain the charge transfer needed by Bates and Massey's (1947) hypothesis for the recombination.

Acknowledgments—The author is indebted to Dr. H. Friedman and his collaborators at the Naval Research Laboratory in Washington, D.C., for their comments on published rocket data and particularly for their generosity in supplying details of their observational results in advance of publication.

The research reported in this paper has been sponsored by the Geophysics Research Division of the Air Force Cambridge Research Center, Air Research and Development Command, under Contract AF19(122)-44.

REFERENCES

BATES, D. R., and MASSEY, H. S. W.	1947	Proc. Roy. Soc. A **192,** 1
BATES, D. R., and NICOLET, M.	1950	J. Geophys. Res. **55,** 301
BYRAM, E. T., CHUBB, T. A., and FRIEDMAN, H.	1953	Phys. Rev. **93,** 1066
BYRAM, E. T., CHUBB, T. A., and FRIEDMAN, H.	1954	J. Opt. Soc. Amer. in print
CHAPMAN, S., and COWLING, T. G.	1939	The Mathematical Theory of Non-Uniform Gases, Cambridge Univ. Press
GARTLEIN, C. W., and SHERMAN, D. F.	1952	Mém. Soc. Roy. Liège **12,** 187
HAVENS, R. J., KOLL, R. T., and LAGOW, H. E.	1952	J. Geophys. Res. **57,** 59
NICOLET, M.	1948	Report Gassiot Comm., Phys. Soc. London, p. 105
NICOLET, M.	1954a	Rocket exploration of the Upper Atmosphere, Ed: R. L. F. BOYD and M. J. SEATON. Pergamon Press, London, p. 359 or 363
NICOLET, M.	1954b	Phys. Rev. **93,** 633
NICOLET, M., and BOSSY, L.	1949	Ann. Geophys. **5,** 275
NICOLET, M., and MANGE, P.	1952	Ionosphere Res. Lab., Penna. State Univ. Scientific Report No. 35
NICOLET, M., and MANGE, P.	1954	J. Geophys. Res. **59,** 1
PETRIE, W., and SMALL, R.	1952	J. Geophys. Res. **57,** 51
Rocket Panel	1952	Phys. Rev. **88,** 1027
SEATON, M. J.	1954	J. Atmosph. Terr. Phys. **4,** 295.
VEGARD, L.	1950	Ann. Geophys. **6,** 157

VOL.
5
1954

Journal of Atmospheric and Terrestrial Physics, 1954, Vol. 5, pp. 141 to 172. Pergamon Press Ltd., London

Ionospheric absorption measurements during a sunspot cycle

Sir EDWARD APPLETON,* F.R.S., and W. R. PIGGOTT,† B.Sc.

(*Received* 14 *April* 1954)

CONTENTS

		PAGE
1.	Introductory	142
2.	Some Relevant Theoretical Considerations	
	(a) Non-deviative absorption	144
	(b) Deviative absorption	145
3.	The Absorption of Waves Travelling through an Ionized Layer	145
4.	The Experimental Programme	147
5.	Some Experimental Results	148
	(a) The Geophysical Time Series of Noon Absorption Measurements on 4 Mc/s	148
	(b) The Variation of Absorption with Frequency	150
	(c) The Relation between Absorption and Solar Zenith Distance	152
	(d) Further Studies of the Diurnal Variation of Absorption	159
	(e) Absorption Variations during Sudden Ionospheric Disturbances	161
	(f) Further Investigations of the Winter Anomaly	164
6.	Discussion of the Experimental Results	166
7.	Acknowledgments	171
8.	References	171

ABSTRACT

The results of a comprehensive series of observations on the absorption of radio waves during the process of ionospheric reflection are described. Such observations have included experimental studies of the dependence of atmospheric absorption $|\log \rho|$ (ρ being the effective ionospheric reflection coefficient), on the radio wave frequency f, on solar zenith distance χ and on solar activity as expressed by the sunspot number R. For the last-mentioned purpose the time-series of comparable observations has extended over a period of nearly two sunspot cycles. It is found that the variation of $|\log \rho|$ with f is adequately explained by the magneto-ionic theory of ionospheric dispersion and absorption, provided that $\nu^2 \ll (f + f_L)^2$, where ν is the electron collision frequency and f_L is the gyro-frequency corresponding to the vertical component of the geomagnetic field. On the other hand, the dependence of $|\log \rho|$ on $\cos \chi$, examined either diurnally or seasonally, is found to be irreconcilable with simple theory if ν is so restricted and the absorbing layer is formed in an isothermal atmosphere of uniform composition in which the electron recombination coefficient is independent of pressure. Such a simple theory predicts that $|\log \rho|$ should be proportional to $(\cos \chi)^n$ where n is 1·5, whereas some hundred diurnal examinations of this relationship yield an average value for n of the order of 0·75. Possible explanations of this discrepancy are that the electron recombination coefficient falls off to some extent with increasing height and that the temperature of the absorbing stratum is not uniform, but increases upwards. It seems, however, clear that the removal of electrons from the absorbing layer cannot take place by way of a process described by an attachment law.

Seasonal studies of the dependence of $|\log \rho|$ on $\cos \chi$ have confirmed the existence of a winter anomaly, which has been evident during the months of November to February ever since the series of observations was started in 1935. This winter anomaly is characterized by the occurrence of excessive absorption on certain groups of days during the months mentioned, a phenomenon which is not paralleled during the rest of the year. A statistical study shows that the occurrence of these days of high absorption is directly correlated with the occurrence of sporadic reflecting strata below the level of the E Layer.

A series of noon measurements of absorption, of eighteen years' duration, has demonstrated a general direct correlation of $|\log \rho|$ with sunspot number R. Sunspot-cycle control is, however, more evident in summer than in winter.

* The University, Edinburgh.

† Radio Research Station, Slough.

Sir Edward Appleton, F.R.S., and W. R. Piggott, B.Sc.

Various lines of evidence emerging from the experimental results show that the absorbing stratum must be located below the *E* Layer, and the general conclusion reached is that it lies within the *D* Region. Arguments are also advanced for concluding that the *D* Layer cannot be the seat of the currents responsible for the quiet-day solar magnetic variations S_q; while other considerations indicate that the layer of temporarily enhanced ionization caused by solar flares can, likewise, not be identified with the S_q current layer, as has previously been widely supposed. It does, however, seem most probable that sudden ionospheric disturbances associated with solar flares are due to augmentations of ionization in the normal absorbing layer, the ionization density being increased there by a factor of from 5 to 10.

1. Introductory

The present communication deals with the results of an extensive series of observations on the absorption of radio waves in the ionosphere. This series of observations was begun, as far back as 1935, by way of a sequence of daily noon measurements of the ionospheric reflection coefficient, at vertical incidence, on a frequency of 4 Mc/s. While this sequence has been continued up to date it has also been supplemented by similar studies on other radio-frequencies and at other times of the day. Our object in this work has been to identify the ionospheric stratum mainly responsible for the absorption of radio waves as well as to reveal its diurnal, seasonal and sunspot-cycle characteristics. The experiments have shown that this absorbing stratum is to be identified with the atmospheric range of levels usually designated as the *D* Region, and our work has therefore developed into an investigation of geophysical events in that stratum. It may be added that we do not at present know of any other radio method of obtaining wholly comparable information, though upper-atmospheric rocket sounding may well be expected to yield information about the *D* Layer which even our radio absorption experiments fail to disclose.

VOL. 5 1954

A very full account of the experimental techniques we have used to determine the absorption of waves in the ionosphere has appeared recently elsewhere (Piggott, 1953a) and we shall, therefore, not discuss the details of the procedure in this paper. Using these techniques, the data presented here have been analyzed in such a manner as to minimize errors due to spatial attenuation, scattering and fading phenomena, or polarization and dispersion changes.

In this paper we have, therefore, restricted our discussion to the interpretation of our measurements of absorption in terms of ionospheric and magneto-ionic theories and to the relations between the ionospheric structures suggested by the data and other geophysical phenomena.

2. Some Relevant Theoretical Considerations

In the normal method of ionospheric exploration by pulse sounding the intensity of the returned echo is determined by three types of attenuation. In the first place there is the usual spatial attenuation; secondly there is the "frictional" attenuation due to the communication of wave energy to the gaseous medium by way of electronic vibrations and collisions; while, thirdly, there are possible scattering effects caused by the diversion of wave energy from the main stream by ionospheric irregularities.

In the usual method of measuring the ionospheric reflection coefficient ρ by comparing the amplitudes of successive echoes in a sequence of multiple reflections between the ionosphere and the ground, we automatically allow for the normal

spatial attenuation. The magnitude of the ionospheric reflection coefficient is then determined by "frictional" attenuation and by scattering. Since, however, we consider the scattering by electronic clouds to be very much the minor of these two processes, we shall, for the time being, neglect it as a first approximation.

We picture, then, the ionospheric attenuation with which we are concerned as taking place along the radio wave path and as expressible in terms of the usual type of absorption coefficient κ where

$$E = E_0 e^{-\kappa s} \tag{1}$$

Here E is the emergent electric intensity of a plane wave, of incident electric intensity E_0, after passing through a uniform stratum of thickness s and of absorption coefficient κ.

In the case of the ionosphere, however, κ is, in general, a function of both position and direction of propagation relative to the earth's magnetic field, so that (1) becomes

$$I = I_0 e^{-\int \kappa \, ds} \tag{2}$$

where the integration of κ is taken over the whole path traversed by the waves. If we deal with the case of vertical incidence, I_0 refers to the strength of the incident wave on the ionosphere and I to the emergent wave. We can then call I/I_0 the apparent reflection coefficient (ρ) though it should be noted that, although ρ is formally analogous to the reflection coefficient of a sharp boundary, the physical processes envisaged are not the same in the two cases. In the ionospheric case, for example, the actual attenuation often takes place in parts of the ionosphere which do not bend the wave tracks appreciably. The quantity is however a convenient parameter to use in the reduction of experimental observations.

It will readily be seen that

$$\rho = \frac{I}{I_0} = e^{-\int \kappa \, ds} \tag{3}$$

or

$$\int \kappa \, ds = -\log \rho \text{ (nepers)} = -8{\cdot}7 \log \rho \text{ decibels} \tag{4}$$

The measurements of absorption considered below are expressed in terms of the quantity $\int \kappa \, ds$, the units used being nepers. It is convenient to use the expression "the absorption" to denote the quantities $\int \kappa \, ds$ or $-\log \rho$, qualifying this expression where necessary to indicate the limits between which κ is integrated.

The general magneto-ionic theory of the absorption of radio waves, passing through a gaseous medium containing free electrons in the presence of an imposed magnetic field has been extensively developed by Appleton (1932 and 1937), Booker (1935), and Farmer and Ratcliffe (1935), and need not be given here. It is sufficient for our present purpose to take over the basic formulae relating κ to the other relevant physical quantities.

Let us consider first, for simplicity, the case of no imposed magnetic field. We have a medium containing N electrons per cc, each of charge e and mass m, through which waves of angular frequency ω are travelling. If, further, the collisional

frequency of the electrons with gas molecules is ν and c is the velocity of light in free space, we have

$$\kappa = \frac{2\pi e^2}{mc\mu}\left(\frac{N\nu}{\nu^2 + \omega^2}\right) \tag{5}$$

where μ is the refractive index of the medium. The variation of the refractive index with radio wave frequency may be expressed in the form

$$\mu^2 = 1 - \frac{{\omega_0}^2}{\nu^2 + \omega^2} \tag{6}$$

where

$${\omega_0}^2 = \left(\frac{4\pi e^2}{m}\right) N$$

When $\mu \to 1$, the variation of the absorption coefficient κ with frequency is independent of μ and is given by $\kappa \propto 1/(\nu^2 + \omega^2)$. When, however, $\mu \to 0$ the variation of μ with frequency is dominant and κ depends mainly on the variation of $1/\mu$ with frequency. The physical differences implicit in these characteristics justify the division of absorption phenomena into two classes: (a) Non-deviative absorption which takes place at those heights for which $\mu \fallingdotseq 1$, and (b) deviative absorption which takes place whenever μ is sufficiently small for the variation of μ with frequency to affect κ significantly.

VOL. 5 1954

(a) *Non-deviative absorption*

Apart from the zone near the magnetic equator, the absorption coefficient κ for non-deviative attenuation of high radio frequencies is given with sufficient accuracy by the quasi-longitudinal approximation of the magneto-ionic theory.

$$\kappa = \frac{2\pi e^2}{mc}\left(\frac{N\nu}{\nu^2 + (\omega \pm |\,\omega_L\,|)^2}\right) \tag{7}$$

where ω_L is the angular frequency corresponding to the longitudinal component of the earth's magnetic field. The positive sign in (7) refers to the ordinary component of the wave and the negative to the extraordinary component. It will be noticed that, in (7), the introduction of a magnetic field has altered ω in (7) to a new value $(\omega \pm |\,\omega_L\,|)$ which we shall call the effective angular frequency.

Equation (7) ceases to be valid when $\omega \fallingdotseq |\,\omega_L\,|$, the effective angular frequency, ω_E, then being slightly increased relative to the quantity $(\omega \pm |\,\omega_L\,|)$. It is, however, convenient to use (7) as an exact expression since it is seldom desirable to measure absorption on frequencies for which it is seriously inaccurate. In such cases, moreover, an effective angular frequency calculated from the general magneto-ionic equation may be used in place of $(\omega \pm |\,\omega_L\,|)$. (In South-East England $\omega_L = 8{\cdot}10^6$ radians/sec at vertical incidence and (7) is reasonably accurate for working frequencies, $\omega/2\pi$, above 2 Mc/s.)

We may note that the variation of κ with ω_E is critically dependent on the relative magnitudes of ν^2 and ω^2. As we shall see, our experimental evidence shows that almost all the non-deviative absorption occurs at heights for which

$$\nu^2 \ll {\omega_E}^2$$

In this case equation (7) may be simplified to the form

$$\kappa = \frac{2\pi e^2}{mc}\left(\frac{Nv}{(\omega \pm |\omega_L|)^2}\right) \tag{8}$$

a formula we shall have much occasion to use later.

(b) *Deviative absorption*

When the refractive index is small compared with unity, it is convenient to express our basic equation for κ in the absence of a magnetic field in the form

$$\kappa = \frac{\nu}{2c}\left(\frac{1}{\mu} - \mu\right) \tag{9}$$

We then find that the total absorption for a trajectory is

$$\int \kappa \,.\, \mathrm{d}s = \frac{\bar{\nu}}{2c}(P' - P) \tag{10}$$

where P' is the group path and P the phase path, and $\bar{\nu}$ is an average value of ν dependent on the variation of ν and μ with height. When a magnetic field is present, P' is no longer given by $\int \frac{\mathrm{d}s}{\mu}$, but the total absorption may still be expressed with adequate accuracy in the form

$$\int \kappa \,.\, \mathrm{d}s = \frac{\nu_e}{2c} M (P' - P) \tag{11}$$

where ν_e is a modified collisional frequency and M is a factor, of order unity, depending on the magneto-ionic component involved and a function of the actual and gyro frequencies.

Thus for the ordinary wave $M \fallingdotseq 1$ and for the extraordinary wave $M \fallingdotseq \left(\frac{\omega}{\omega - |\omega_L|}\right)$.

Now, in practice, P' usually varies much more rapidly with frequency than does P so that the variation of P' with frequency can be used to determine whether deviative absorption is likely to be important or not.

While deviative absorption is usually small at vertical incidence compared with non-deviative absorption during daytime, except for frequencies near critical penetration values, it is at night the dominant source of attenuation and prevents the night time total absorption from falling below about 0·3 nepers. Studies of the non-deviative absorption at night are, therefore, most easily made using oblique incidence propagation for which the relative roles of the two types of absorption are reversed as compared with the case of vertical incidence.

3. The Absorption of Waves Travelling through an Ionized Layer

In order to develop the above theoretical formulae into a form suitable for comparison with experimental results it is necessary to examine the case of waves

travelling completely through an absorbing layer on their way to and from the level of reflection. When we began our work in 1935 it was not known whether the E or the D Layer was the main stratum responsible for the non-deviative absorption of waves reflected by the F Layer. It was therefore necessary to estimate theoretically the absorption of a layer at any level allowing for the fact that ν (which, *inter alia*, is proportional to the atmospheric pressure) varies with height.

We take two extreme cases of ionization distribution which might be expected as a result of a photo-ionization process such as has been discussed by Chapman, assuming, in case (a), that the recombination coefficient α is independent of pressure; and, in case (b), that α is proportional to pressure. Case (a) gives us the classical Chapman distribution of N with height.

The total absorption for waves which have travelled through a Chapman layer, and have been reflected without deviative losses from a higher layer, has been given by Appleton (1937) as follows—

$$\int \kappa \,.\, \mathrm{d}s = \frac{4\pi e^2 N_0 H}{mc} \left(\frac{\exp}{\nu_0(\omega \pm |\,\omega_L\,|)} \right)^{\frac{1}{2}} X \tag{12}$$

where

$$X = \int_0^\infty \frac{t^{\frac{1}{2}}}{1+t^2} \exp(-at) \,.\, \mathrm{d}t \tag{13}$$

and

$$a = \frac{(\omega \pm |\,\omega_L\,|)}{2\nu_0} \sec \chi \tag{14}$$

Here N_0 is the number of electrons per cc, of charge e and mass m, at the level of maximum electron production when χ, the solar zenith distance, is equal to zero; ν_0 is the electron collision frequency at the same level, H is the scale height of the atmosphere and exp. is the exponential logarithm base. Formulae (12), (13) and (14) enable us to predict the variation of $\int \kappa \,\mathrm{d}s$ with $\cos \chi$, or with ω, both relations which can be examined experimentally.

In the corresponding case where the recombination coefficient varies directly with pressure it is easy to show that

$$\int \kappa \,.\, \mathrm{d}s = \frac{4\pi e^2 N_0 H}{mc} \frac{\sqrt{\exp}}{(\omega \pm |\,\omega_L\,|)} Y \tag{15}$$

where

$$Y = \int_0^\infty \frac{\exp(-at)}{1+t^2} \,.\, \mathrm{d}t \tag{16}$$

and where

$$a = \frac{(\omega \pm |\,\omega_L\,|)}{2\nu_0} \sec \chi \tag{17}$$

We now consider special examples of the two cases, when a layer is situated at a level of sufficiently low pressure for ν_0 to be small compared with $(\omega \pm |\,\omega_L\,|)$, that is $a \gg 1$. In the case where α is independent of pressure (12) becomes

$$\int \kappa \,.\, \mathrm{d}s = \frac{4\pi e^2 N_0 H \nu_0}{mc} \sqrt{2\pi \exp} \frac{\cos \frac{3}{2}\chi}{(\omega \pm |\,\omega_L\,|)^2} \tag{18}$$

VOL. 5 1954

while, in the case where α is proportional to pressure we have, from (15),

$$\int \kappa \, . \, ds = \frac{4\pi e^2 N_0 H \nu_0}{mc} \sqrt{4} \exp \frac{\cos \chi}{(\omega \pm |\omega_L|)^2} \tag{19}$$

It will be noted that the dependence of $\int \kappa \, . \, ds$ on $\cos \chi$ is different in the two cases.

When the value of a is not subject to such restriction, recourse must be had to integration by quadrature of the quantity X, with results given graphically by APPLETON (1937). For a corresponding evaluation of Y we are indebted to Dr. G. F. C. SEARLE, who has pointed out to us that

$$Y = \left\{\frac{\pi}{2} - Si(a)\right\} \cos a - \{Ci(a)\} \sin a \tag{20}$$

A graph relating Y to a, similar to that given in the Bakerian Lecture (1937) for the relation between X and a, is shown in Fig. 1; it is also due to Dr. SEARLE.

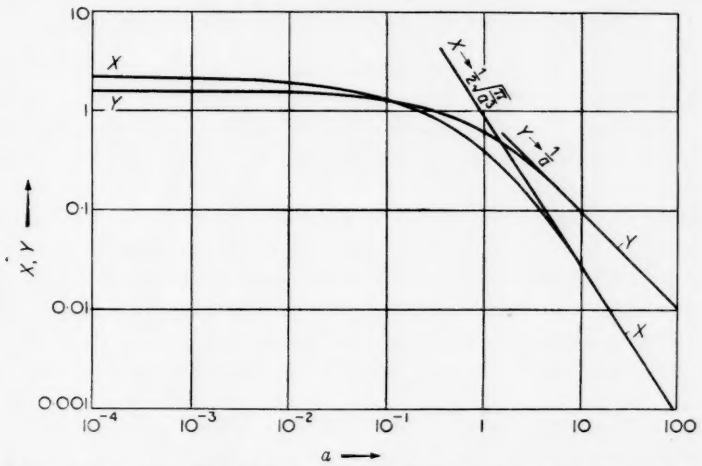

Fig. 1. Graphs showing, logarithmically, the values of X and Y as a function of a, as defined in equations (13), (14), (16) and (17).

We may note that, in both cases, if an appreciable part of the ionization is found at heights for which $\nu^2 \fallingdotseq (\omega \pm |\omega_L|)^2$ the variation of total absorption with frequency will no longer be proportional to $(\omega \pm |\omega_L|)^2$; and, in general, there will also be changes in the variation of absorption with $\cos \chi$ from the relations (18) and (19) indicated above. The frequency-dependence criterion is clearly crucial and provides a firm foundation for statements concerning the relative magnitudes of ν^2 and $(\omega \pm |\omega_L|)^2$.

4. THE EXPERIMENTAL PROGRAMME

The adopted method of measuring ρ and hence the apparent absorption $|\log \rho|$ was based on that described by APPLETON (1932), in which the amplitudes of multiple echoes were compared.

As previously mentioned the work was begun by the determination of a geophysical time-series of $|\log \rho|$ measurements at noon on 4 Mc/s. These results

immediately disclosed a seasonal variation, $|\log \rho|$ being greater in summer than in winter. It was, however, at once realized that there was no numerical agreement with either (18) or (19) so far as the variation with cos χ is concerned; for in South-East England,* where the measurements were made, the ratio of the summer and winter noon values of cos $\frac{3}{4}\chi$ is 6·4, and of cos χ 3·4, whereas the experimental ratio of the summer and winter values of $|\log \rho|$ was 2·6.

Further measurements of the $|\log \rho|$ dependence on cos χ were therefore made using the diurnal variation of χ. Meanwhile BEST and RATCLIFFE (1938) had found good proportionality between $|\log \rho|$ and cos $\frac{3}{4}\chi$ in diurnal studies of absorption on a group of carefully selected days.

The other possible relationships for experimental test may again be seen from (7). There is the comparison of the values of $|\log \rho|$ for both ordinary and extraordinary waves of the same frequency. This had been measured by FARMER and RATCLIFFE (1935) who found agreement with the theoretical ratio $\left(\frac{\omega - |\omega_L|}{\omega + |\omega_L|}\right)^2$. But also there is the general dependence of $|\log \rho|$ on angular frequency $(\omega + |\omega_L|)$. This has been examined by WHITE and BROWN (1936) whose curves relating $|\log \rho|$ with frequency do not fall off as rapidly as the $1/(\omega \pm |\omega_L|)^2$ relation would suggest. These two sets of experimental results of previous authors are therefore not consistent and it was considered desirable to examine the matter further.

To elucidate the seasonal anomaly suspected from the earliest measurements it was also decided to make a series of constant-cos χ measurements on two frequencies, one of which was always 2 Mc/s. The value chosen was cos $\chi = 0{\cdot}25$ which occurs at noon in winter but in the early morning and late evening in summer.

Finally a study has been made of the temporary increase of $|\log \rho|$ during fade-outs caused by solar flares.

5. SOME EXPERIMENTAL RESULTS

(a) *The geophysical time-series of noon absorption measurements on 4 Mc/s*

As has been explained above, our whole enquiry began with these measurements and it was due to anomalies which they disclosed that further work was undertaken. All the results obtained to date are exhibited in Fig. 2 which is a graph of the monthly means for the period 1935–1952 inclusive. The seasonal effect is at once apparent in that summer values are, in general, higher than winter values. A marked sunspot-cycle control is also evident though it may be noted that this control is much more evident in summer than in winter.

To eliminate the effect of seasonal control, and so disclose the sunspot-cycle control more transparently, we could, of course, have used the usual device of plotting a curve of 12-month running means as a function of time. We have, however, instead used another method of eliminating the seasonal variation which has certain advantages when a detailed comparison with sunspot activity is desired.

We have found that for any particular month there is a linear relation between

* The measurements were made 1935–36 in London, 1936–39 in Cambridge and 1939 to date in Slough.

VOL. 5 1954

$|\log \rho|$ and R the sunspot number. We have therefore used all the 4 Mc/s data for the period and found, by the method of least squares, the best straight line relating $|\log \rho|$ to R for each month. In this way we write, generally,

$$|\log \rho| = a_n(1 + b_n R) \tag{21}$$

and find the twelve pairs of parameters (a_1, b_1; a_2, b_2; etc.) for the 12 months of

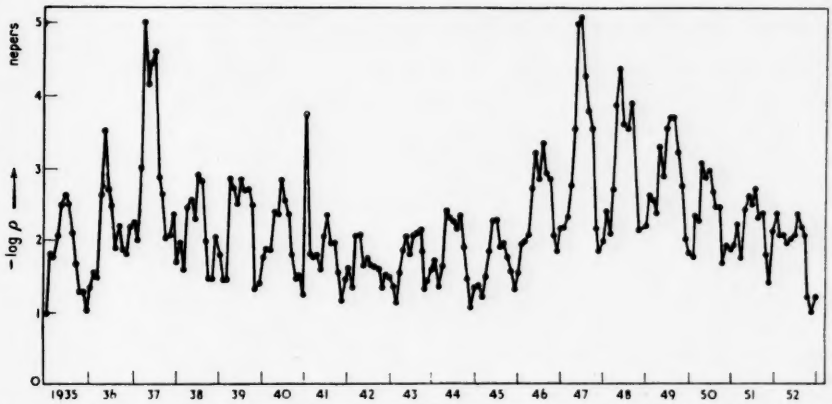

Fig. 2. Graph illustrating the sunspot-cycle variation of noon ionospheric absorption, in nepers, on 4 Mc/s.

the year. These are set out in Table 1. Here it will be seen that the coefficient b_n varies during the course of the year and, in itself, illustrates the greater response of $|\log \rho|$ to sunspot activity in summer than in winter. The parameter a_n which represents, theoretically, the value of $|\log \rho|$ for zero sunspot number, is also greater in summer than in winter.

Table 1. $|\log \rho| = a(1 + bR)$.

Showing parameters for relating $|\log \rho|$, on 4 Mc/s, to sunspot number R, for the months of the year (1935–1952). The values of r give the appropriate correlation coefficients.

	Jan.	*Feb.*	*Mar.*	*Apr.*	*May*	*June*	*July*	*Aug.*	*Sept.*	*Oct.*	*Nov.*	*Dec.*
a	1·2	1·3	1·4	1·4	1·5	1·4	1·5	1·5	1·4	1·1	1·0	1·0
$10^3.b$	9·2	7·0	7·5	11·3	10·9	13·2	11·1	8·5	8·8	8·9	8·3	9·6
r	0·7	0·7	0·7	0·75	0·9	0·85	0·85	0·9	0·9	0·8	0·75	0·6

It is not superfluous to mention here that corresponding determinations of a_n and b_n in the case of the E Layer ionization (as represented by $(fE)^2$), also for Slough, do not exhibit entirely similar characteristics. These values, obtained in the same way, are given in Table 2. Here it will be seen that the response of $(fE)^2$ to increase of R, as indicated by the values of b_n, is practically uniform throughout the year. We therefore submit that the information in Tables 1

and 2 alone indicates that the stratum responsible for absorption has different sunspot cycle characteristics from those exhibited by the E Layer.

Table 2. $(fE)^2 = a(1 + bR)$

Showing parameters for relating $(fE)^2$ to sunspot number R for the months of the year (1934–1953). The values of r give the appropriate correlation coefficients.

	Jan.	*Feb.*	*Mar.*	*Apr.*	*May*	*June*	*July*	*Aug.*	*Sept.*	*Oct.*	*Nov.*	*Dec.*
a	5·9	7·1	8·0	9·1	10·0	10·1	10·1	9·6	8·6	7·5	6·2	5·3
$10^3.b$	4·2	3·9	4·7	4·0	3·4	3·6	3·4	3·4	3·6	3·6	4·4	5·0
r	0·96	0·93	0·92	0·89	0·95	0·93	0·90	0·96	0·98	0·93	0·95	0·91

To exhibit the variation of $|\log \rho|$ throughout the sunspot cycle in a manner in which the seasonal effect is removed and which still does not eradicate the detailed variations, we may proceed as follows. Let us define a new quantity, R_D, by way of the equation

$$R_D = \frac{|\log \rho| - a_n}{a_n b_n} \tag{22}$$

Here R_D may be regarded as an effective sunspot number for D Layer absorption. Taking the value of $|\log \rho|$ for any month, and using the appropriate monthly pair of parameters, a_n and b_n, we can find R_D for that month. The values so obtained, together with the monthly values of sunspot number R, are exhibited in Fig. 3. The general over-all relationship between R and R_D is evident, though it is noted that there is not a marked correlation in detail. A word may here be interpolated concerning the physical significance of the quantity R_D. It expresses the increase of $|\log \rho|$ above the value for zero sunspot number for any given month automatically compensated for the varying susceptibility of $|\log \rho|$ to increase of solar activity during the different months of the year.

(b) *The variation of absorption with frequency*

The variation of absorption with frequency provides one of our main tools for identifying the position and characteristics of the absorbing layer. Using equations (18) or (19) for the ordinary wave, which is always the stronger of the two components and is therefore measured, we have

$$|\log \rho| = \frac{A}{(f + f_L)^2} \tag{23}$$

where A is a constant for any set of conditions and f and f_L are, respectively, $\omega/2\pi$ and $\omega_L/2\pi$, or

$$\frac{1}{\sqrt{|\log \rho|}} = \frac{1}{\sqrt{A}}(f + f_L) \tag{24}$$

VOL. 5 1954

In Fig. 4 is shown an experimental plot of $(|\log \rho|)^{-\frac{1}{2}}$ as a function of f for noon on 11th July, 1950. It will be seen that there is good agreement with the theoretical relation (23) and that the experimental value for the intercept f_L is 1·2 Mc/s as compared with the theoretical value of 1·16 Mc/s. Now the experimental points

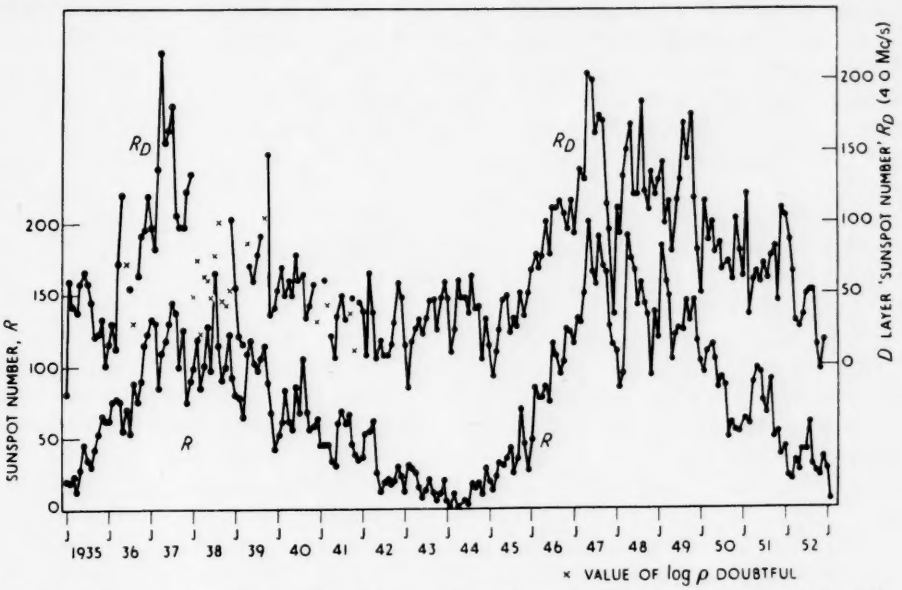
SUNSPOT NUMBER, R
D LAYER 'SUNSPOT NUMBER' R_D (4 0 Mc/s)
R_D
R
1935 36 37 38 39 40 41 42 43 44 45 46 47 48 49 50 51 52
× VALUE OF log ρ DOUBTFUL

Fig. 3. Curves showing the variation of the monthly values of R_D and R for the years 1935–1952. R_D is the effective sunspot number for D Layer absorption on 4 Mc/s at noon: R is the sunspot number.

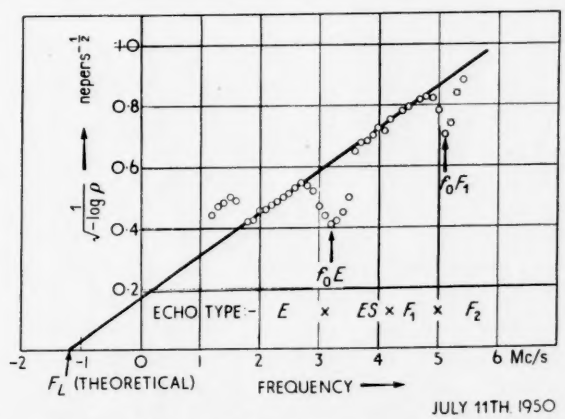

Fig. 4. Plot illustrating the variation of absorption with radio wave frequency; $(|\log \rho|)^{-\frac{1}{2}}$ is shown as a function of frequency f.

in Fig. 4 refer to reflections from the lower level of the E Layer, from the abnormal E clouds which are situated round the level of maximum ionization in the normal E Layer and also from the F Layer; and yet the absorption in all cases, apart

from all frequencies near critical values, is reconcilable in terms of the absorption of a single layer. Thus the absorption due to ionization near the height of maximum density of the *E* Layer and between this layer and the *F* Layer must have been negligible compared with that present below the level of reflection in the *E* Layer. The accuracy with which the points fit the theoretical variation with frequency also shows that a negligible amount of absorption was present at heights for which ν^2 is comparable with $(\omega + |\omega_L|)^2$. Thus we have two boundaries between which the main absorbing zone must be situated. Numerous similar experiments confirm these results and show that the non-deviative absorption above the lower reflecting edge of the *E* Layer (near 100 km) is seldom more than 10% of that found at lower heights.

Examining the noon data in detail we find that about 80% of days on which accurate multifrequency measurements have been made are consistent with our example illustrated in Fig. 4, the remainder showing irregular variations which are mainly due to abnormal deviative absorption and/or scattering losses.

When the operating frequency falls below about 0·6 of the critical frequency of the *E* Layer, the exact fraction varying somewhat throughout the year, the total absorption is often *less* than would be expected from that observed at higher frequencies, the difference usually increasing rapidly with further decrease in frequency. The frequency at which the discrepancy first appears is often well defined. (It can, for example, clearly be seen at 1·7 Mc/s on Fig. 4.) We interpret this result as implying that the true height of reflection is now actually falling rapidly and is, in fact, within the main absorbing region. Since, however, the *apparent* height seldom decreases appreciably under these circumstances, we may conclude that the rate of change of ionization with height has decreased by a considerable factor. The detailed examination of this particular phenomenon must await the development of a convenient technique for applying the magneto-ionic theory to the trajectories.

We now turn to the discrepancy, mentioned earlier, between the results of previous workers on the subject of the variation of absorption with frequency. It may be recalled that White and Brown (1936) found only a small dependence of absorption on frequency whereas Farmer and Ratcliffe (1935), and now ourselves, have found variations agreeing with theoretical predictions for non-deviative absorption. Now White and Brown used only frequencies exceeding about 3 Mc/s and therefore their values of absorption refer to the frequency band where non-deviative absorption is small and deviative absorption comparatively large. It is easy to show that, under such conditions, only a minor dependence of absorption on frequency would be expected. In our own work we have sought to concentrate our measurements on non-deviative absorption and have always used the normal height-frequency (h', f) curves to indicate, for avoidance, frequencies associated with group-retardation and thus with deviative absorption.

(c) *The relation between absorption and solar zenith distance*

A substantial part of our experimental enquiry has related to the dependence of $|\log \rho|$ on the solar zenith distance χ. Guided by the formulae (18) and (19) we note the convenience of finding the relation between $|\log \rho|$ and $\cos \chi$ rather

VOL. 5 1954

than between $|\log \rho|$ and χ. Also we have always used, for the lower range of values, the term which CHAPMAN has shown must replace $\cos \chi$ in ionospheric layer formation theory, namely $1/\mathrm{Ch}(R, \chi)$, where $\mathrm{Ch}(R, \chi)$ is the appropriate Chapman function for the atmospheric level under consideration. As will be readily seen, we can study the relation between $|\log \rho|$ and $\cos \chi$ $\left(\text{or } \frac{1}{\mathrm{Ch}(R, \chi)}\right)$ from either diurnal or seasonal data. The diurnal data have the advantage that sunspot activity can be considered constant over one day.

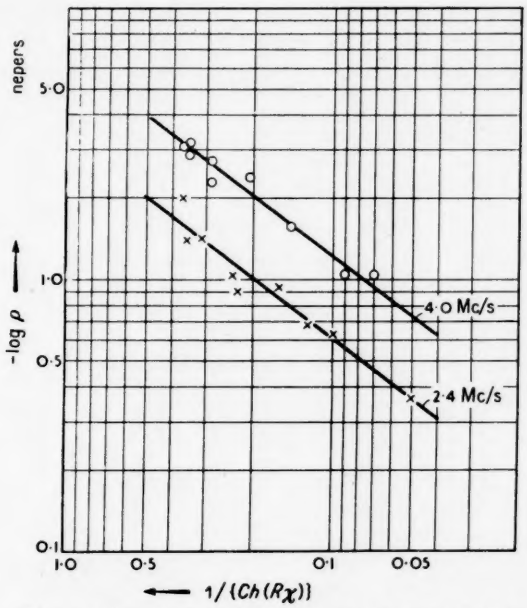

Fig. 5. Logarithmic plots of $|\log \rho|$ and $1/\mathrm{Ch}(R, \chi)$ for the two fixed frequencies of 4·0 Mc/s (F Layer echoes) and 2·4 Mc/s (E Layer echoes). (November 12th, 1948.)

As has been mentioned, BEST and RATCLIFFE (1938) found in their diurnal studies that $|\log \rho|$ varied as $(\cos \chi)^{\frac{3}{4}}$ and so got agreement with the relation (18) for absorption in a simple layer for which $\nu^2 \ll (\omega + |\omega_L|)^2$. TAYLOR (1948), however, using the results of several years' measurements of the field strength of continuous wave signals on two frequencies, found quite different results in that $|\log \rho|$ varied as $(\cos \chi)^n$ where n varied from 0·7 to 1·0. We have therefore given some consideration to this discrepancy.

We have found it instructive to examine the diurnal variation of absorption on several fixed frequencies, used in sequential order throughout the day. For example, if we select two frequencies which are reflected from the E Layer and F Layer respectively, and which are unlikely to be affected by deviative absorption, we find that plots of $\log |\log \rho|$ with $\log (\cos \chi)$ are linear and parallel, in conformity with our view that the same absorbing stratum is operative in the two cases. This is illustrated in Fig. 5 where the two graphs refer to the frequencies of

4·0 Mc/s (*F* Layer echoes) and 2·4 Mc/s (*E* Layer echoes).

The difference in the magnitudes of the absorption generally can be explained in terms of the law relating absorption to effective frequency. The value of the exponent n in the expression $(\cos \chi)^n$ is 0·8, supporting therefore the observations of Taylor (1948).

If, however, we choose a frequency which, while reflected from the *F* Layer, is also within about 20% of the noon critical frequency of the densest layer below the *F* Layer, we have noted that higher values of n than 0·8 are obtained, the relation between $\log (|\log \rho|)$ and $\log (\cos \chi)$ being, nevertheless, fairly linear. This state of affairs is illustrated in Fig. 6 which illustrates logarithmic plots of $|\log \rho|$ with $\cos \chi$ for the fixed frequencies of 1·6, 4·0 and 4·8 Mc/s on Dec. 17th, 1948. It may be noted that this was a day of strong and persisting E_2 Layer reflections.

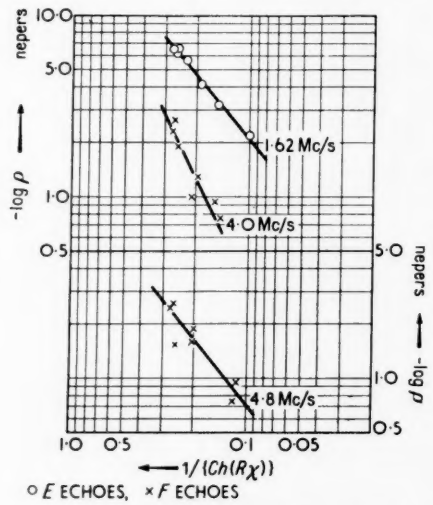

Fig. 6. Logarithmic plots of $|\log \rho|$ and $1/\mathrm{Ch}(R, \chi)$ for the fixed frequencies of 1·6, 4·0 and 4·8 Mc/s on December 17th, 1948. The curve for 4·0 Mc/s indicated a high value of n due to the effect of deviative absorption.

An examination of the slopes of the three graphs in Fig. 6 shows that the value of the exponent was 1·1, 2·0 and 1·1 for the frequencies 1·6, 4·0 and 4·8 Mc/s respectively. We regard the anomalous value of 2·0 for n as due to the fact that the frequency of 4·0 Mc/s was not far from the noon critical frequency of the E_2 Layer, in which case some deviative absorption was operative. The selection criteria used by Best and Ratcliffe (1938) may well have resulted in their observations being influenced in this way. The difference between the values of n obtained by Taylor (1948) for high and low radio frequencies in certain months also appears to us to derive from the same phenomenon of the intrusion of deviative absorption.

Summarizing the main features of several hundred day runs we can make the following general statements—

(i) A change from *F* reflections to totally reflecting *E* sporadic reflection

VOL. 5 1954

does not alter the nature of the diurnal variation when conditions are such as to exclude the influence of deviative absorption.

(ii) When the change from F reflections to E reflections occurs early in the morning, so that the operating frequency is not for any length of time near the critical frequencies of the E or E_2 Layers, we get the most consistent agreement between the straight lines illustrating the two types of reflection.

(iii) The values of the exponent n for curves relating to E and F reflection are found to be equal within 10% provided deviative absorption is not present. Occasionally when there is abnormally dense ionization between the E and F Layers we have found that the value of n for the F Layer echoes is up to 20% greater than that for the E Layer echoes.

(iv) When constant frequency observations are made on a frequency which appears at some stage to be reflected *within* the absorption region itself, the diurnal variation, expressed logarithmically, may usually be represented by two parallel straight lines, the absorption changing abruptly from one level to another. Occasionally such a change is associated with a brief period of high absorption similar to that experienced, say, when the observing frequency lies in the neighbourhood of a critical penetration frequency.

We now turn to the results of our examination of the day-to-day and seasonal variation of the value of the exponent n in the expression $(\cos \chi)^n$. Taking the winter results first, we have divided the full range over which the absorption varies into 5 equal parts and calculated the mean and maximum values of n for each group. The result is that both mean and maximum values of n are found to increase uniformly with absorption magnitude, the lowest values of absorption being associated with values of n as low as those experienced in summer. The range of variation of the mean value of n is from 0·75 to 1·05, though maximum values as high as 1·35 are found associated with the occasions of highest absorption. Individual values range from 0·5 to 1·3, but values between 0·8 and 1·1 predominate. The appropriate value of n for summer conditions is most conveniently determined using the results of our noon measurements and of a parallel set of observations made throughout the year when $\chi = 75°$ (i.e. $\cos \chi = 0{\cdot}25$). For each day we have compared the logarithm of the ratio of the absorptions with the logarithm of the ratio of the appropriate Chapman functions leading to a direct determination of n. The distribution of n values so obtained for sunspot minimum conditions is illustrated in Fig. 7, where the mean value is seen to be 0·7, very few observations lying outside the range $n = 0{\cdot}4$ to $n = 1{\cdot}0$. In a period of sunspot maximum the corresponding analysis gives a mean value of $n = 0{\cdot}75$, very few values lying outside the range 0·6 to 0·95. The slight difference between the two sets of results may well be due entirely to the intrusion of deviative absorption effects in sunspot minimum years. We consider that there is no evidence for a significant change in the value of n with varying solar activity.

We now examine the seasonal variation of absorption and its relation with χ for constant frequency, using both our long sequence of measurements at noon on 4 Mc/s and the special set of observations made when χ was maintained constant, i.e. at $\cos \chi = 0{\cdot}25$. For this purpose we have been able, since 1942, to

supplement our measurements on 4·0 Mc/s, described above, by measurements on 4 or 5 other frequencies, thus eliminating effects due to deviative absorption when the working frequency approaches the critical frequency of either the E or F_1 Layers. Thus we can eliminate the possibility that the anomalies in the seasonal variation are due to deviative absorption in these layers.

Even after only one year of observations it became quite clear that noon $|\log \rho|$ did not vary according to $(\cos \chi)^{\frac{3}{2}}$, for a constant frequency, and all our work since has confirmed this conclusion. The ratio of summer to winter $|\log \rho|$ has been found to vary during the sunspot cycle, but has always remained between 2 and 3. In attempting to find how absorption is dependent on $\cos \chi$ using seasonal, as distinct from diurnal, data, we encounter the difficulty of the effect of month to

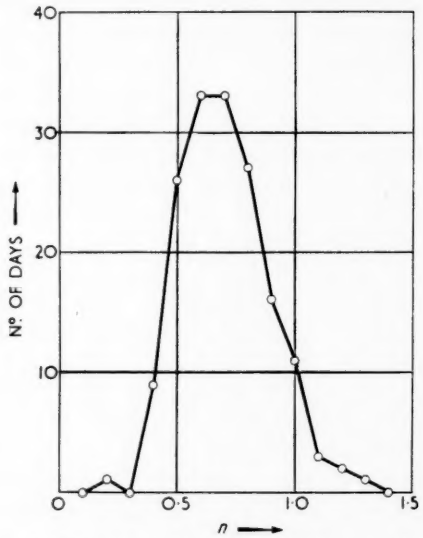

Fig. 7. Curve showing the distribution of n values appropriate to the relation

$$\frac{(|\log \rho|)_\chi}{(|\log \rho|)_{75°}} = \left(\frac{\mathrm{Ch}(R, 75°)}{\mathrm{Ch}(R, \chi)}\right)^n$$

where χ relates to noon on each day. The results relate to 162 days during a period of sunspot minimum 1943–1944.

month changes in solar activity. It is, however, possible to eliminate the effect of this in two ways. One method is to average the absorption for each particular month over one or more complete solar cycles, the assumption being that sunspot activity does not depend on terrestrial season. The second method, which we count to be preferable, is to use data such as are given in Table 1 for reducing our monthly absorption values all to the same value of sunspot number R. Taking the monthly figures for the parameters a_n and b_n in Table 1 we have calculated the noon value of $|\log \rho|$ on 4 Mc/s for the selected sunspot number of $R = 100$ and $R = 200$. In Fig. 8 are plotted the logarithms of the values of $|\log \rho|$ so derived with the logarithms of the appropriate monthly noon values of $1/\mathrm{Ch}(R, \chi)$. The values to the left of the diagram obviously relate to the summer months; those on the right refer to winter. It will be noticed that the values of $\log(|\log \rho|)$

VOL. 5 1954

for summer and the equinoxes fit reasonably well on straight lines, but that the values for November to February lie well above such lines. We think this diagram exposes what we have called the winter anomaly in a very direct fashion.

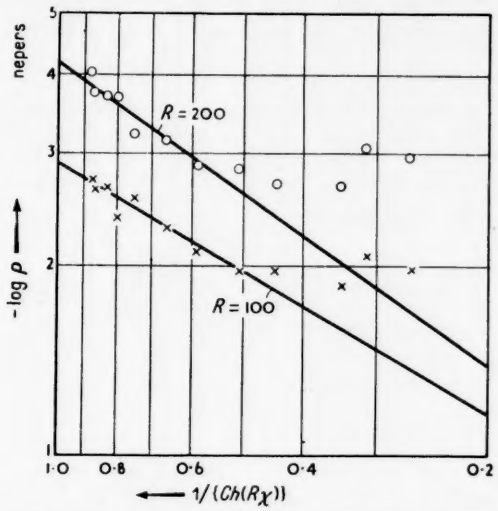

Fig. 8. Logarithmic plots of $|\log \rho|$ and $1/\mathrm{Ch}(R, \chi)$ for monthly noon values of absorption, corrected to refer to constant sunspot numbers of $R = 100$ and $R = 200$. The upper curve refers to the higher sunspot activity.

The same point can however be illustrated, possibly even more effectively, using our measurements of absorption made under constant-χ conditions. These results are shown for the years 1942–49 in Fig. 9.

Here it will be seen that, over the summer months, $|\log \rho|$ is fairly constant

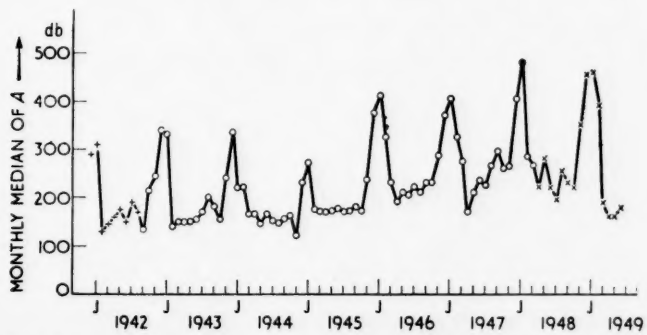

Fig. 9. Showing the variation of absorption for conditions of constant solar zenith distance ($\cos \chi = 0{\cdot}25$) at Slough. The values of A are the measured values in decibels reduced to an equivalent frequency of 1 Mc/s, using equation (25).

for the constant value of χ, but that, during winter, notably higher values are obtained. It is clear, from an examination of the run of sunspot numbers over the period, that the higher winter values are not to be ascribed to enhanced sunspot

activity during those particular periods; and we must conclude that the phenomenon arises from a real physical difference between the operation of the absorbing layer in winter and in summer.

A further word is necessary on the day-to-day variability of these measurements. In summer we find that such variability can be ascribed to—

(i) the sampling error in the actual experiments;

and (ii) changes in sunspot-activity, e.g. 27-day recurrence tendencies.

For example if we examine the day-to-day fluctuations relative to a 9-day running

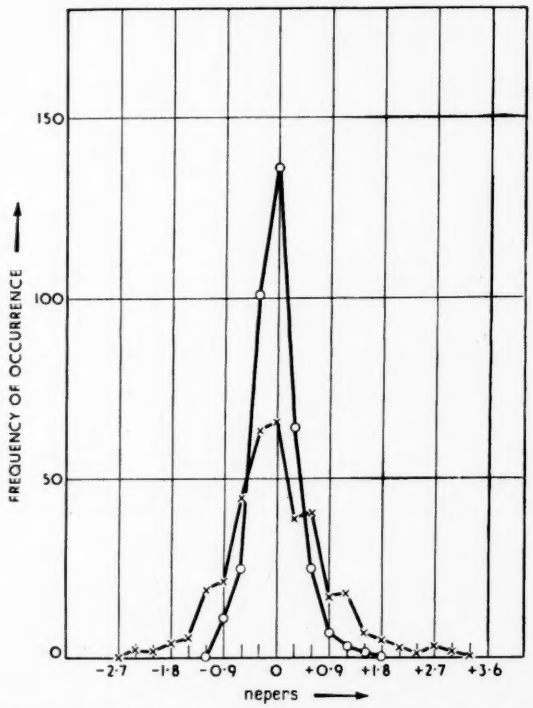

Fig. 10. Showing the variation of noon absorption on 2 Mc/s relative to 9-day running means. The two curves relate to summer and winter days during a period of sunspot minimum, 1942–1945.

mean, thus eliminating the influence of (ii), the standard deviation found does not differ substantially from that found from a study of the statistics of fading.

In winter, however, the variability of $|\log \rho|$ is greater than in summer, although considerable conservation is to be noted in the data, days of high absorption tending to occur in groups. Such winter variability, as has been shown by Dieminger (1952), is not to be ascribed to solar activity and appears inherent in the absorbing mechanism itself. To illustrate the difference in the variability of absorption in summer and winter we show, in Fig. 10, the variation of the absorption measured at noon on 2 Mc/s relative to 9-day running means for both summer and winter. The standard deviation is seen to be, in winter, about twice the summer value. If, on the other hand, we consider the daily deviations from

VOL. 5 1954

monthly means the difference between winter and summer variability is even greater. Our investigations in the latter connection lead us to conclude that the high *average* value of absorption in winter is largely due to the occurrence of rather variable, excessive absorption on certain groups of days.

(d) *Further studies of the diurnal variation of absorption*

We now examine the changes of absorption during the day in more detail considering, in particular, the effect of the finite rates of electron production and

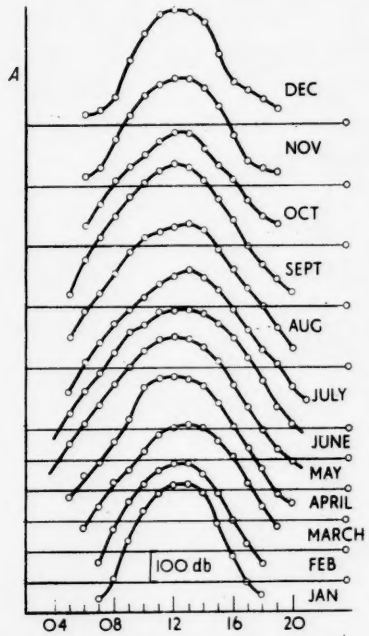

Fig. 11. Showing curves of mean diurnal variation of absorption A for each month 1945–1948.

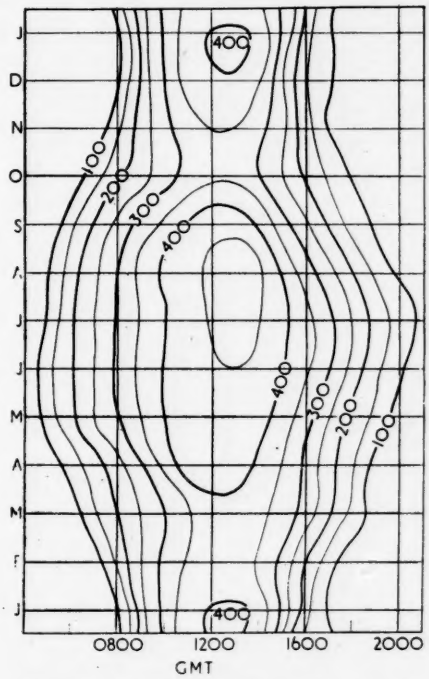

Fig. 12. Showing contours of constant absorption A for the year as a whole, during daylight period, 1945–1948.

disappearance. It is convenient to minimize the effects of deviative losses by representing the absorption by the non-deviative absorption index A, deduced from the equation

$$8{\cdot}7 \mid \log \rho \mid = \frac{A}{(f + f_L)^2} \tag{25}$$

using measurements on a number of frequencies. A is expressed in decibels, while f and f_L are expressed, numerically, in Mc/s.

In Figs. 11 and 12 we exhibit the results of all diurnal measurements of this kind made between 1945 and 1948. In Fig. 11 are shown the diurnal variations for each month separately, while in Fig. 12 the contours of constant absorption for the year as a whole are shown for the daylight period. It will be noticed in

both curves that the maximum absorption, as expressed by A, occurs definitely after local noon, the average delay being about 20 minutes. Now it has been shown (Appleton, 1953) that the ionization maximum in any layer lags behind the maximum of electron production, which latter is determined by cos χ, by a time of approximately $\frac{1}{2\alpha N}$ seconds, where α is the recombination coefficient and N is the ionization density at noon. We find in this way a value of αN for the absorbing layer of $(3{\cdot}6 \pm 1{\cdot}6) \,.\, 10^{-4}$ sec^{-1}.

Similar information may be obtained in another way. Following the method given by Appleton (1937), let us consider two times, before and after noon, at which the value of cos χ is the same. We then have for the two cases

$$\frac{dN_1}{dt} = q_0 \cos \chi - \alpha N_1^2 \tag{26}$$

and

$$\frac{dN_2}{dt} = q_0 \cos \chi - \alpha N_2^2 \tag{27}$$

or

$$\alpha = \frac{\frac{dN_1}{dt} - \frac{dN_2}{dt}}{N_2^2 - N_1^2} \tag{28}$$

Now since N_1 and N_2 are not very different, the diurnal curve being fairly symmetrical, and since $\frac{dN_1}{dt}$ and $\frac{dN_2}{dt}$ are numerically about the same, though their signs are different, we have

$$\alpha = \frac{\left|\frac{dN}{dt}\right|}{N \,.\, \Delta N} \tag{29}$$

where $\Delta N = (N_2 - N_1)$. From (29) we therefore have

$$\alpha N = \frac{\left|\frac{dN}{dt}\right|}{\Delta N} \tag{30}$$

Now absorption, other things being equal, is proportional to N and we have, therefore,

$$\alpha N = \frac{\frac{d}{dt}(|\log \rho|)}{\Delta(|\log \rho|)} \tag{31}$$

Applying equation (31) to our results we find that the median value of N for the five hours centred on noon is $3{\cdot}7.10^{-4}$ sec^{-1}, the median for all hours of the day being $4{\cdot}1.10^{-4}$ sec^{-1}. We should expect residual deviative losses to become more important towards sunrise and this may well explain the apparent increase of αN towards these times. By carefully selecting a day on which such losses are negligible we have found that the diurnal variation of αN is very roughly proportional

VOL. 5 1954

to N for most of the day. However it is clear that the value of αN for the absorbing stratum is of the order 4.10^{-4} sec^{-1}, and this is entirely different from the value of αN, calculated by similar methods for the case of the E Layer, which is 12.10^{-4} sec^{-1}.

We now turn to the variation of non-deviative absorption with time after sunset. The residual absorption at vertical incidence is very small after sunset and is difficult to estimate accurately owing to the influence of deviative losses. At oblique incidence, however, the non-deviative absorption is increased by the secant of the angle of incidence at the absorbing layer and thus comes into greater prominence. Thus we can investigate the law of variation of non-deviative absorption with time by using the results of oblique incidence measurements, using preferably a comparatively low frequency so as to bring into emphasis the non-deviative losses. The results of a typical experiment of this type are shown in Fig. 13 in which we plot $1/|\log \rho|$ as a function of time for night-time propagation of 1·0 Mc/s over a 700 km path from Burghead to Slough. We conclude from the

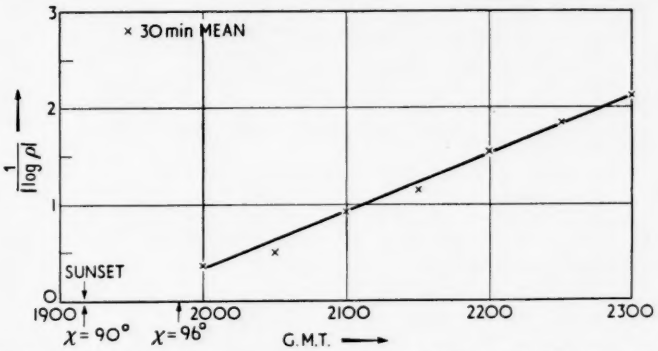

Fig. 13. Showing a plot of the reciprocal of $|\log \rho|$ on 1·0 Mc/s with time for oblique-incidence transmission over a 700 km path during evening conditions, 28th April, 1943.

linear relationship obtained that the observed variation of absorption in the late evening is consistent with the recombination hypothesis. From the curve we find that αN about 2030 h. is $0{\cdot}6.10^{-4}$ sec^{-1} and that this falls to $0{\cdot}24.10^{-4}$ sec^{-1} by 2245 h. Such values are reasonably consistent with the noon values, assuming that α is approximately the same at both periods.

(e) *Absorption variations during sudden ionospheric disturbances*

We have made observations of the variation of total absorption during a number of fadeouts. Such observations are less difficult than might have been expected since the fading fluctuations are usually abnormally small during the periods when the absorption is changing rapidly. We find that large fadeouts, occurring in the middle of the day and lasting for half an hour or more, are usually remarkably similar, the total absorption increasing by a factor of between 5 and 10 and the rate of disappearance of the excess absorption being consistent with a recombination law. Measurements of the variation of absorption with frequency, which are admittedly very rough, are consistent with those found for normal absorption, the value of $|\log \rho|$ being proportional to $(\omega + |\omega_L|)^{-2}$.

We first consider the rate of decay of the excess ionization during a fade-out. Let N_x be the excess ionization density and N_0 the undisturbed value maintained by the normal solar radiation. We then have as our continuity equation

$$\frac{dN}{dt} = q - \alpha N^2 \tag{32}$$

where N is equal to $(N_0 + N_x)$. Substituting for N we therefore find

$$\frac{dN_0}{dt} + \frac{dN_x}{dt} = q - \alpha N_0^2 - \alpha N_x^2 - 2\alpha N_0 N_x \tag{33}$$

In the undisturbed condition we have, however,

$$\frac{dN_0}{dt} = q - \alpha N_0^2 \tag{34}$$

and thus if $N_x \gg N_0$ we have

$$\frac{dN_x}{dt} = -\alpha N_x^2 \tag{35}$$

Turning now to the effect of the excess ionization in producing excess absorption $\Delta \mid \log \rho \mid$ we can write, since $\Delta \mid \log \rho \mid$ is proportional to N_x.

$$\frac{1}{\Delta \mid \log \rho \mid} - \frac{1}{\Delta \mid \log \rho_0 \mid} = \alpha C t \tag{36}$$

where C is a constant involving the electron collisional frequency and $\Delta \mid \log \rho_0 \mid$ is the excess absorption at time $t = 0$. As will be seen from (33) above, a more complicated expression is necessary when $\Delta \mid \log \rho \mid$ falls to a value comparable with the normal absorption. Plotting $\frac{1}{\Delta \mid \log \rho \mid}$ with time t, as in Fig. 14, we note an excellent agreement with the approximate equation (36). This being so we are encouraged to find the variation of αN_x with time, since from (35) we have

$$-\alpha N_x = \frac{\frac{dN_x}{dt}}{N_x} = \frac{\frac{d(\Delta \mid \log \rho \mid)}{dt}}{\Delta \mid \log \rho \mid} \tag{37}$$

Some typical values are summarized in the subjoined table.

t (secs.)	120	270	500	750
$\Delta \mid \log \rho \mid$ nepers	8·5	6·0	4·3	3·2
αN_x(sec^{-1})	24.10^{-4}	22.10^{-4}	11.10^{-4}	8.10^{-4}

We note that the values of αN_x are proportional to $\Delta \mid \log \rho \mid$ and hence to N and that the maximum value of αN_x is 6·5 times that given above for the normal layer, the corresponding ratio of absorption being 6·7.

VOL. 5 1954

We have also found that we can test the variation of absorption with frequency during a sudden ionospheric disturbance by using results obtained with (h', f) recorders. This avoids the difficulty of eliminating fading errors on several frequencies in the very short times before the absorption changes significantly.

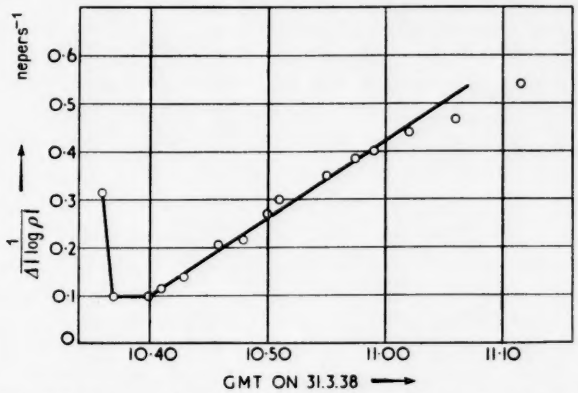

Fig. 14. Illustrating fall of excess absorption with time during a sudden ionospheric disturbance, $(\Delta \mid \log \rho \mid)^{-1}$ being plotted with t.

We assume, as is usually true, that the sensitivity of the recorder varies slowly with frequency and that the lowest frequency on which echoes are observed, $f_{\min}$, is determined by the absorption present. If the absorption varies with the inverse square of the effective frequency, $(f + f_L)^2$, and we put $f = f_{\min}$ the absorption variation with time is proportional to $(f_{\min} + f_L)^2$. Hence plotting $(f_{\min.} + f_L)^{-2}$

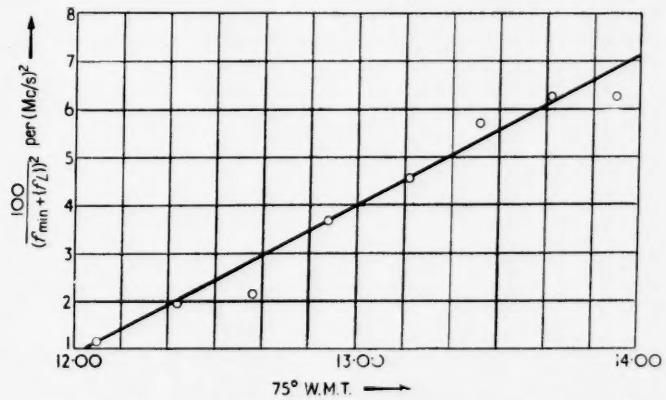

Fig. 15. Illustrating the fall of absorption with time during a major sudden ionospheric disturbance, $(f_{\min} + \mid f_L \mid)^{-2}$ being plotted with time t.

against time we might expect to obtain a straight line representing the recombination of the S.I.D. ionization.

We have applied this method to the exceptionally great fadeout of July 31st, 1937, described by BERKNER and WELLS (1937); and in Fig. 15 is shown a plot of $(f_{\min} + f_L)^{-2}$ with time t. It will be seen that the relationship is sensibly linear,

as suggested above. Moreover, comparing the fade-out values of $f_{\min}$ with the normal values it is possible to show that the maximum additional absorption probably exceeded 12 times the normal value. Using this figure we can make a rough estimate of the value of αN_x for the period when echoes were first again observed after the onset of the fadeout and find that it lies between 10.10^{-4} and 30.10^{-4} sec^{-1}. This is not inconsistent with our own values obtained by direct measurement or with similar estimates made by ELLISON (1953).

Additional evidence relating to the amount of excess absorption during a fade-out can also be derived from observations of the diminution of galactic noise. We use in this connection the observations of HEY, PARSONS and PHILLIPS (1947). On August 1st, 1947, for example, these observers found that a solar flare, seen shortly after 1500 h., caused the amplitude of the galactic noise to drop to 0·67 of its previous value. This extra attenuation corresponded to a value, for $|\log \rho|$, of 0·4 neper on the frequency of 25 Mc/s which was used at the time. We can show, using the frequency relation (23), that such an attenuation would correspond to an absorption of 10 nepers on a frequency of 4 Mc/s and of 27 nepers on 2 Mc/s, values about six times normal.

(*f*) *Further investigations of the winter anomaly*

We now turn to a consideration of further results which bear on the nature of the winter anomaly in absorption, since this anomaly has been evident in every year since we started the absorption investigations in 1935. We may first note that days of anomalous absorption occur mainly in the months of November to February inclusive; and, as mentioned above, such days are not to be associated with individual events in the variation of solar activity. DIEMINGER (1952) has, however,

VOL. 5 1954

Table 3.

Showing the association of high absorption and the occurrence of echoes from low heights.

		Occurrence or absence of high absorption	
		+	−
Occurrence or absence of echoes from low heights	+	110	41
	−	19	507

Observed

		Occurrence or absence of high absorption	
		+	−
Occurrence or absence of echoes from low heights	+	28	123
	−	101	581

Expected by chance

pointed out that days of high absorption are often associated with weak reflections from low heights of the order of 75 to 95 km. We have also noticed the same phenomenon and have attempted to study the general incidence of such echoes from low heights throughout the year. Very often, when atmospheric noise and artificial interference are unusually weak, we have been able to detect weak reflections from low heights in any month of the year, the average rate of daily occurrence being 0·5 per month in summer. In the four winter months, however,

this rate of occurrence is greatly exceeded; and we have found that the occurrence of these echoes and the occurrence of high absorption are closely associated. This correlation may be demonstrated in the two following ways. In Fig. 16 are shown plots of the monthly values of the daily rate of the occurrence of low echoes and of the monthly values of the daily rate of the occurrence of high absorption. It will be seen that the two curves, which relate to seven years of observations, are very similar, the two sets of abnormal events occurring in the same months. The same relationship may be tested further by a consideration of events on individual days. In Table 3 are given the results of an investigation of the occurrence, or absence, of the association on 682 winter days. Comparing

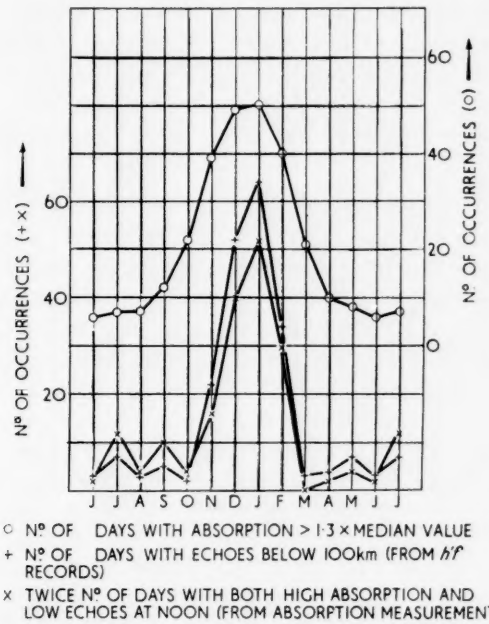
Nº OF OCCURRENCES (+ ×)
Nº OF OCCURRENCES (○)
60
40
20
0
J J A S O N D J F M A M J J
○ Nº OF DAYS WITH ABSORPTION > 1·3 × MEDIAN VALUE
+ Nº OF DAYS WITH ECHOES BELOW 100km (FROM h'f RECORDS)
× TWICE Nº OF DAYS WITH BOTH HIGH ABSORPTION AND LOW ECHOES AT NOON (FROM ABSORPTION MEASUREMENTS)

Fig. 16. Showing monthly numbers of the occurrence of days of high absorption and of days when echoes from low heights were experienced over the years 1943–1951. (Note that the numbers of the occurrences of days of high absorption with low echoes have been multiplied by 2.)

the observed and random numbers of occurrences, we find that days when both high absorption and echoes from low heights occurred are four times as frequent as would be expected by chance.

We have also sought to find if days of high absorption and periods of magnetic activity are connected, but have found no correlation. However we have noticed that sequences of days of high absorption often cease with the onset of a magnetic storm. Selecting the five magnetically quiet days for the winter months we find that these are associated with high absorption 1·2 times as frequently as would be expected by chance. Neither of these observations is really very significant but perhaps together they suggest that there is a tendency for high absorption to occur under conditions of magnetic calm.

A more detailed examination of the variation of absorption with frequency, and with solar zenith distance, on days of high absorption, shows that, on many such days, quite normal relationships exist between $|\log \rho|$ and f, and between $|\log \rho|$ and $\cos \chi$, apart, of course, from the high general level of the absorption. On other days, however, we have noted the frequent occurrence of a sudden break in the $(|\log \rho|)^{-\frac{1}{2}}/f$ curves at a frequency lying between 2·0 and 2·4 Mc/s. A corresponding effect can also be noted in the plots of $\log(|\log \rho|)$ with $\log\left(\frac{1}{\mathrm{Ch}(R, \chi)}\right)$. In both cases we interpret the results as showing that the range of frequencies below 2·0 to 2·4 Mc/s, have been subjected to a weaker absorption mechanism than have the higher frequencies. Since such effects are to be noted particularly on the days of the occurrence of low echoes, we are inclined to consider this low relative absorption on the low frequencies as being due to the fact that they are reflected at a level within the D Layer itself. In such an event their attenuation would be less than that of the higher frequencies, which have to traverse the whole of the D Layer before they experience reflection at the E Layer.

6. Discussion of the Experimental Results

As will have been seen, the foregoing sections have dealt with the results of our experimental study of the dependence of absorption on the three variables, radio wave frequency f, solar zenith distance χ and sunspot number R. We now examine the bearing of these results (which are, in fact, only typical of a much greater body of experimental data) on more general geophysical matters, taking first the question of the physical location of the absorbing stratum in the atmosphere. There are, in this case, three lines of evidence which lead us to locate it *below* the normal E Layer of the ionosphere. First the diurnal variation of absorption for two different frequencies (Fig. 5) one of which is reflected by the E Layer and the other for the F Layer, give substantially the same exponent n in the expression $(\cos \chi)^n$. Second, if a diurnal study is made of absorption on a frequency which becomes equal to the critical value for the E Layer during the course of the day. the logarithmic plot of $|\log \rho|$ with $\cos \chi$ can be represented by the same straight line, apart, of course, from the period where the operating frequency is in the neighbourhood of fE. Moreover, the same result is obtained if an F Layer echo is temporarily replaced by an echo from a totally reflecting sporadic E stratum. Thirdly, the variation of absorption with frequency illustrated in Fig. 4 can only be explained on the assumption that the frequencies reflected from all levels are absorbed by the same magneto-ionic medium. All three lines of evidence thus point to the identification of the absorbing layer with what is generally known as the D Region.

On the question of actual heights in the atmosphere, we can say at once that the lower boundary of the absorbing stratum cannot be situated lower than the height of reflection of very long waves. We thus have a lower limit of about 70 km by day, and about 90 km by night. However the observed relationship between $|\log \rho|$ and f for frequencies exceeding about 2 Mc/s indicates conclusively that the main ionization in the D Layer must be situated at a level for which

VOL. 5 1954

$\nu^2 \ll (\omega + |\omega_L|)^2$, which indicates that ν must be less than $2{\cdot}10^7$ per sec. Now Briggs (1951) has shown, from sporadic E Layer studies, that ν is $1{\cdot}6.10^4$ per sec. at 117 km, which would suggest that the absorbing ionization round noon must lie above 75 km. Shaw (1951) from a study of ionospheric cross-modulation, has found that ν has the much higher value of $1{\cdot}8.10^6$ per sec. at a level of 90 km. Using his value we can show that most of the absorbing ionization would lie above 80 km.

It is next necessary to enquire whether the absorbing stratum is merely the lower part of the E Layer or whether it has an independent existence. In this connection we may first note the marked variability of absorption in winter as compared with summer, which is not paralleled in the case of E Layer ionization. We can, therefore, at least say that the E Layer is not the effective absorbing mechanism in winter. Considering the relation between $|\log \rho|$ and $(fE)^2$ in more detail, we note, first, that the change of $|\log \rho|$ with $\cos \chi$, during, say, the course of a single day, is due in part to change in ionization and in part to changes in electron collision frequency, the layer being situated at a lower level when $\cos \chi$ increases. Now from Table 2 we can show that $(fE)^2$ is proportional to $(\cos \chi)^n$ where n is approximately 0·5, for $R = 100$; whereas from Table 1 we find, for the same sunspot number, that $|\log \rho|$ is proportional to $(\cos \chi)^n$ where n is 0·75. The former value of n agrees with the theoretical value for a simple layer with a constant recombination coefficient. The latter result could only be reconciled with the former if ν^2 is comparable with $(\omega + |\omega_L|)^2$, which we know not to be the case. It does not therefore seem possible to ascribe the absorption to a layer in which the recombination coefficient is independent of the height.

A consideration of events in the course of a solar cycle also indicates a difference in the behaviour of the absorbing layer and the E Layer. From Table 2 we note that the mean value of b_n for E Layer ionization, as represented by $(fE)^2$, is 0·004. whereas, from Table 1, we see that the corresponding value for $|\log \rho|$ is 0·0096. a value more than twice as great. Finally, comparing the values of αN for the absorbing layer and for the E Layer near noon we have—

$$\alpha_D N_D \fallingdotseq 3{\cdot}7.10^{-4}\ \text{sec}^{-1}; \qquad \alpha_E N_E \fallingdotseq 12.10^{-4}\ \text{sec}^{-1}.$$

Representing N_E by $(fE)^2$ and N_D by $(fD)^2$, where fD represents the hypothetical critical frequency of the absorbing stratum for the level where $N\nu$ is a maximum. we have

$$\frac{\alpha_D}{\alpha_E} = 0{\cdot}3 \left(\frac{fE}{fD}\right)^2 \tag{38}$$

Now in summer, during the period of maximum solar activity, our (h', f) measurements indicate that fE is of the order of 4 Mc/s while fD certainly cannot greatly exceed 1·0 Mc/s, the lowest heights of reflection observed in routine recording being about 100 km at frequencies of the order of 1·4 Mc/s, thus α_D/α_E must certainly be greater than 2·4 and may well be greater than 5. We conclude, then, that the rate of recombination in the absorbing stratum is definitely different from that in the maximum of the E Layer.

We now consider the bearing of our results on the characteristics of the D

Layer, recognized now as a separate entity. The relatively regular control of absorption by the sun's zenith distance in both summer and winter would suggest that the ionization is produced by solar photons. This conclusion is confirmed by measurements of the ionospheric reflection coefficient during eclipses, when a return towards night-time conditions is obtained during the period when the sun's disc is obscured (Appleton, 1927; Smith-Rose, 1946; Piggott, 1953b).

An important matter here is the identification of the process by which the electrons disappear in the absorbing layer. Here we are assisted both by the studies of the variation of $|\log \rho|$ with $\cos \chi$ and by the measurements of $|\log \rho|$ during fade-outs. It is found that both diurnal measurements and also the seasonal measurements over the greater part of the year, yield a value of about 0·75 for the exponent n in the expression $(\cos \chi)^n$. The fact that this quantity is less than unity is significant for the following reasons. During, say, a diurnal variation of $\cos \chi$, the absorption varies because both N and ν vary. In the case of the standard Chapman model investigated in Section (3) above, N varies as $(\cos \chi)^{\frac{1}{2}}$ while ν varies as $\cos \chi$. This explains the origin of the value of 1·5 for n in the expression $(\cos \chi)^n$. In the case of the second model dealt with in Section (3) in which α varies as the pressure, we can regard the value of 1·0 for n as being wholly due to the variation of ν, for in such a layer N itself would not vary with $\cos \chi$. Such considerations show us at once that an attachment law of electron disappearance, for which N would vary as $\cos \chi$ must correspondingly yield a value of 2·0 for n. Clearly such a state of affairs would be impossible to reconcile with the observed value, and rules out at once such a law of electron decay. Further evidence pointing the same way is obtained in S.I.D. studies (Section 5 (e)) where a recombination law has been found to hold.

VOL. 5 1954

The problem of explaining why n is less than unity remains. We could, of course, assume that N itself varies as $(\cos \chi)^{\frac{1}{2}}$ as is required in a Chapman layer, which would require that ν should vary as $(\cos \chi)^{0·25}$, to give $(N\nu)$ varying as $(\cos \chi)^{0·75}$. Such a small variation of ν is, however, hardly likely. If, however, the atmospheric temperature increased with height, as is most probable at the levels in question, the variation in ν would be less than that required by a direct proportionality with $\cos \chi$. We must, however, remember that the value of α in the D Layer has been shown to be greater than its value in the E Layer, which indicates some falling off of its value with height in the levels we are considering. This suggests that possibly it might be most appropriate to write $\alpha = \alpha_0 + \alpha_1 e^{-z}$ in which case we must also assume that ν itself varies as $(\cos \chi)^a$ where a is substantially less than unity. The positive gradient of atmospheric temperature suggested above is therefore also required to fit the experimental results obtained. Nicolet (1951) has published an interesting evaluation of the influence of vertical temperature gradients in the atmosphere on the ionization density and absorption of a layer which leads to essentially the same conclusion.

Detailed calculations, too elaborate to set out here, do in fact show that it is possible to obtain the observed values of n and αN with plausible assumptions of the variation of ν with the scale height of the atmosphere.

As to the actual magnitude of α at the level of maximum $N\nu$, it is only possible to make the most approximate assignment. It is true that $(\alpha N)_D$ has been shown

to be 4.10^{-4} sec^{-1}, but we can only roughly estimate N_D as being of the order of 10^3 to 10^4 electrons per cc in summer in sunspot maximum years. If this were the case the corresponding value of α_D would lie between 4.10^{-7} and 4.10^{-8}/cc/sec which may be compared with a current estimate of $1{\cdot}0.10^{-8}$/cc/sec for α_E, recently given by PIGGOTT (1953b).

We now turn to a consideration of the anomalous behaviour of ionospheric absorption in winter. Actually this anomaly may be characterized in two ways. First we have noted that enhanced general absorption (as expressed, say, by A values) is found in winter on a relatively high proportion of days; while, second, it is found that, in winter, the value of the exponent n in the expression $(\cos \chi)^n$ is higher than during the rest of the year. Now it is a remarkable fact that if we select, for each of the winter months which exhibit the anomaly, the 20% least absorbed days instead of all days, the two anomalies mentioned above largely disappear. This suggests that for some winter days the same absorption mechanism is operative as in summer; and that the high absorption experienced on the other winter days is due to some factor which always increases the basic absorption already there. To account for this additional absorption in winter there would appear to be only two possibilities—either an additional ionizing source is present or some agency is operative which causes a redistribution of ionization within the levels of ν which brings about an increased integrated value of $N\nu$ within the absorbing stratum.

Since the days of high absorption in winter still exhibit a normal type of diurnal variation as exhibited in $\log (|\log \rho|)/\log (\cos \chi)$ curves, we consider it unlikely that the excess absorption is caused by particle radiation, though we do not yet feel that such a possibility can be entirely ruled out. A comparison of the Slough absorption measurements with similar observations made at Singapore and in the Falkland Islands shows that, as perhaps might have been expected, no anomalous behaviour is to be noted at any time of the year at Singapore, while, at the Falkland Isles, the high absorption anomaly is to be found during the local winter months of May to August. The phenomenon is evidently connected with conditions of low $\cos \chi$ and definitely not to changes in the intensity of solar radiation. It does not, however, appear profitable to pursue this discussion further until a more general picture of the world morphology of the phenomenon is available.

Finally we consider the light which our absorption measurements throw on two important matters of geophysical interest, namely the location of the atmospheric strata (i) in which the S_q magnetic currents flow and (ii) in which the abnormal ionization is produced by solar flares. We start by recalling that MCNISH (1939) has demonstrated that, during a typical fade-out associated with a solar flare, the quiet-day solar diurnal variation of the geomagnetic field, S_q, increases by as much as 60%; and this result has been interpreted by him and others as indicating that the S_q currents must flow in the D Layer. MARTYN (1947) in particular has sought to develop a comprehensive theory of both solar and lunar magnetic diurnal variations and their dependence on solar activity, based on the assumption that the major current contributions to these effects came from the D Layer, the E Layer playing only a minor role in the same connection. It should, however, be pointed out that because S_q is augmented during

a fade-out it does not necessarily follow that the S_q current layer and the temporary fade-out layer are identical. All that McNISH's result really demonstrates is that the temporary currents in the fade-out layer are in the same phase as those which operate normally in the S_q current layer.

Our own absorption measurements during fade-out periods are material in the above connection, since we have found that the extra absorption experienced during such periods—which must be electronic in origin—can be as much as 5 to 10 times the normal value (APPLETON and PIGGOTT (1949)). It is natural to assume, as a first hypothesis, that this means that the electron density of the normal absorbing layer has been increased by the same factor. But if the S_q current layer is also to be associated with the absorbing D Layer, as suggested by McNISH and others, we are led to a quite different conclusion, namely, that the ionization is increased only by 60% during a fade-out. This is a difficulty we have previously mentioned (1949).

Let us deal with the problem in its most general terms. We are evidently concerned with three strata of geophysical interest (a) the S_q current layer. (b) the normal absorbing layer and (c) the abnormal (fade-out) absorbing layer. Now it is possible to prove, in the following way, that (a), (b) and (c) cannot all be the same stratum. During the sunspot cycle, from sunspot minimum to sunspot maximum, S_q is increased by 60% while during a fade-out it is increased by about the same amount. On the other hand, $|\log \rho|$ increases correspondingly in the course of the sunspot cycle by a factor of 2 to 3; whereas, when a fade-out occurs, it is increased by a factor of 5 to 10. This argument we believe completely proves that (a), (b) and (c) cannot all be the same layer.

Now our absorption studies have led us to conclude that the ratio of the values of αN during the fade-out and under normal conditions is approximately equal to the ratio of the corresponding absorptions. This is only likely to be the case if a substantial part of the additional ionization caused by the solar flare is situated at the level of the normal absorbing layer. This would suggest that (b) and (c) are identical. In addition, the different factors whereby the magnitudes of $|\log \rho|$ and of S_q vary during a solar cycle indicate that the S_q currents cannot flow in the normal absorbing layer—that is, the locations of (a) and (b) are not identical. Summarizing the results of the above considerations, we can therefore say that (a), (b) and (c) cannot be the same; that (a) cannot be (b); that (a) cannot be (c), though we think it highly probable that (b) and (c) are identical.

The above conclusions concerning the separate identity of the S_q current layer and the fade-out layer may be supported in another way. In the observations published by McNISH for the three fadeouts of 8th April, 25th August and 6th November, 1936, it is possible to compare the dependence, on cos χ, of (i) S_q and (ii) the augmentation of S_q associated with the fade-out. Now S_q for the magnetic stations cited is proportional to $(\cos \chi)^n$ where n lies between 0·5 and 1·5. On the other hand, for the additional magnetic forces during fade-outs, we find a variation proportional to $(\cos \chi)^n$ where n lies here between 1·0 and 2·5. These two results, we believe, are sufficiently different for us to conclude that the fade-out currents and the solar diurnal currents do not flow at the same levels in the ionosphere.

VOL. 5 1954

It is, however, possible to proceed much further by accepting our evidence that both the fade-out layer and the normal absorbing layer are located at about the same level, namely that of the *D* Layer. As stated above, increasing the conductivity of the *D* Layer nine times produces a magnetic contribution of only 60% of that produced by the S_q Layer. We may therefore conclude that, under normal quiet conditions, the *D* Layer contributes to the magnetic variations only about 7% of the contribution of the S_q Layer itself. If we made the further assumption that the atmospheric tidal motions at the level of the *D* Layer are equal in magnitude to those at the S_q Layer level, we arrive at the result that the total direct-current conductivity of the *D* Layer must be only 7% of that of the S_q Layer. However, it is probable that atmospheric tidal motions are reduced with decreasing height, so this figure cannot be relied on. We do, however, believe that the above argument shows that the *D* Layer does not contribute substantially to the diurnal magnetic variations as has previously been supposed. This is in agreement with the views of COWLING and BORGER (1948) who have shown that any stratum situated below the *E* Layer must have insufficient conductivity to be the seat of the currents which cause the solar diurnal magnetic variation. It is interesting to note that the most recent theoretical work on this subject (HIRONO, 1950, 1951; and BAKER and MARTYN, 1953), in which completely revised estimates have been made of upper-atmospheric conductivity, leads to the conclusion that the S_q current flows at *E* Layer levels.

Acknowledgments—The work described above was carried out as part of the programme of the Radio Research Board of the Department of Scientific and Industrial Research and is published by permission of the Director of Radio Research.

REFERENCES

APPLETON, E. V.	1928	A study of signal fading. J. Inst. Elect. Eng. **66,** 872
	1937	Regularities and irregularities in the ionosphere—I. Proc. Roy. Soc. A **162,** 451
	1953	A note on the "sluggishness" of the ionosphere. J. Atmosph. Terr. Phys. **3,** 282
APPLETON, E. V., and PIGGOTT, W. R.	1949	Ionospheric absorption measurements throughout a sunspot cycle. General Assembly Proceedings, International Scientific Radio Union **VII,** 320
BAKER, W. G., and MARTYN, D. F.	1953	Conductivity of the ionosphere. Proceedings of the Third Meeting of the Mixed Commission on the Ionosphere, Brussels, p. 9
BERKNER, L. V., and WELLS, H. W.	1937	Further studies of radio fade-outs. Terr. Mag. **42,** 301
BEST, J. E., and RATCLIFFE, J. A.	1938	The diurnal variation of the ionospheric absorption of wireless waves. Proc. Phys. Soc. **50,** 233
BOOKER, H. G.	1935	The application of the magneto-ionic theory to the ionosphere. Proc. Roy. Soc. A. **150,** 267
BRIGGS, B. H.	1951	The determination of the collisional frequency of electrons in the ionosphere from observations of the reflection coefficient of the abnormal *E* layer. J. Atmosph. Terr. Phys. **1,** 345
COWLING, T. G., and BORGER, R.	1948	Electrical conductivity of the ionospheric *D* layer. Nature **161,** 515

Dieminger, W.	1952	On the causes of excessive absorption in the ionosphere on winter days. J. Atmosph. Terr. Phys. **2,** 340
Ellison, M. A.	1953	The Hα radiation from solar flares in relation to sudden enhancements of atmospherics on frequencies near 27 kc/s. J. Atmosph. Terr. Phys. **4,** 226
Farmer, F. T., and Ratcliffe, J. A.	1935	Measurements of the absorption of wireless waves in the ionosphere. Proc. Roy. Soc. A. **151,** 370
Hey, J. S., Parsons, S. J., and Phillips, J. W.	1947	Solar and terrestrial radio disturbances. Nature **160,** 371
Hirono, M.	1950	On the influence of the Hall current on the electrical conductivity of the ionosphere. J. Geomag. Geo-elect **2,** 1
	1951	*Ibid* **2,** 113
Lange-Hesse, G.	1953	27-Day variations in the absorption of the *D* region of the ionosphere over Singapore and Slough. J. Atmosph. Terr. Phys. **3,** 153
Martyn, D. F.	1947	Location of the currents causing the solar and lunar diurnal magnetic variations. Nature **160,** 535
McNish, A. G.	1939	Physics of the earth—VIII. Terrestrial Magnetism and Electricity; New York and London, p. 381
Nicolet, M.	1951	Effects of the atmospheric scale height gradient on the variation of ionization and short wave absorption. J. Atmosph. Terr. Phys. **1,** 141
Piggott, W. R.	1953a	The reflection and absorption of radio waves in the ionosphere. Proc. Inst. Elect. Eng., Part III **100,** 61
	1953b	Ionospheric measurements at Ibadan, Nigeria, during the eclipse of the sun, February 25th, 1952. Report of the Proceedings of the Third Meeting of the Mixed Commission on the Ionosphere, Brussels, p. 42
Shaw, I. J.	1951	Some further investigations of ionospheric cross-modulation. Proc. Phys. Soc. B. **64,** 1
Smith-Rose, R. L.	1946	The influence of the eclipse of the sun on the ionosphere. J. Brit. Inst. Radio Engrs. **6,** 82
Taylor, E. W.	1948	Absorption of radio waves reflected at vertical incidence as a function of the sun's zenith angle. Jour. Res. Bur. of Stand. **41,** 575
White, F. W. G., and Brown, L. W.	1936	Some measurements of the reflection coefficient of the ionosphere for wireless waves. Proc. Roy. Soc. A. **153,** 639

VOL. 5 1954

Journal of Atmospheric and Terrestrial Physics, 1954, Vol. 5, pp. 173 to 181. Pergamon Press Ltd., London

The analysis of fading records from spaced receivers

J. A. RATCLIFFE
The Cavendish Laboratory, Cambridge

(*Received* 3 *May* 1954)

ABSTRACT

The paper is concerned with the fading of a single radio pulse reflected at vertical incidence from the ionosphere to three receivers on the ground. Records of this fading, made when the three receivers are at the corners of a right-angled triangle, and distant about one wavelength from each other, have often been used in the measurement of ionospheric "winds." It is shown that a "wind" constant both in direction and magnitude could produce a markedly variable record. Two actual records, each lasting one hour, are analysed. One is shown to correspond to an occasion when the "wind" was constant. The other record can not be explained on such a simple assumption. The need for a more detailed method of analysis is stressed.

1. INTRODUCTION

In one method for investigating movements in the ionosphere records are made, at three nearby points, of the variations in the amplitude of a reflected radio wave from a pulsed sender (MITRA, 1949; PHILLIPS, 1952), or of the transmitted wave from a radio star (HEWISH, 1952; MAXWELL and LITTLE, 1952). If the receiving points are close enough the records are similar in general form, but the maxima and minima occur at slightly different times on the different records. It frequently happens that the mean of the time differences is significantly different from zero, so that, on the whole, one record is displaced in time relative to another. By considering these mean time-delays for three recording points situated at the corners of a right-angled triangle it has been possible to draw interesting conclusions about the mean velocity of the amplitude-pattern over the ground and, by implication, about the mean velocity of the irregularities of electron-density in the ionosphere (PHILLIPS, 1952; SALZBERG and GREENSTONE, 1951; CHAPMAN, 1953; MILLMAN, 1952; BRIGGS and SPENCER, 1954). It is often said, with proper reservations, that these measurements give information about the "winds" in the ionosphere, and for the sake of having a convenient nomenclature we shall call them winds here.

All those who have used this method of investigation have noticed that the time-delays between any two records are very variable and many have wondered whether this implies a corresponding variability in the magnitude or direction of the ionospheric wind. Numerous questions have then arisen. If the wind varies rapidly over a wide range can the mean wind have any physical significance? Can the magnitude of the variable component be deduced from the records so that theories, for example of ionospheric turbulence, can be tested? Or is there perhaps some fundamental error in the method, so that the irregularity arises from some unexplained diffraction effect as the radio wave travels down from the ionosphere?

It is the purpose of this paper to point out that a considerable variability of the time-delays between pairs of records is just what would be expected even if the wind were constant. It is further suggested that the "variable" part of the information which is discarded when a mean is taken might be used to give information about any rapid variations which might occur in the wind vector.

A variable record lasting one hour is analysed and is shown to behave as if the ionospheric wind were constant for that time. A second record is analysed and is shown not to fit the simple explanation, and it is suggested that, when a fuller analysis is available, it may be possible to determine the variability of the wind on this occasion.

In a companion paper Dr. GORDON NEWSTEAD has carried the present analysis considerably further and has laid the foundation for the more detailed analysis required.

2. THE NATURE OF THE RECORDS

The nature of the records, and the methods of obtaining them, are fully described in the literature. Here it is sufficient to explain one type of record, introduced by

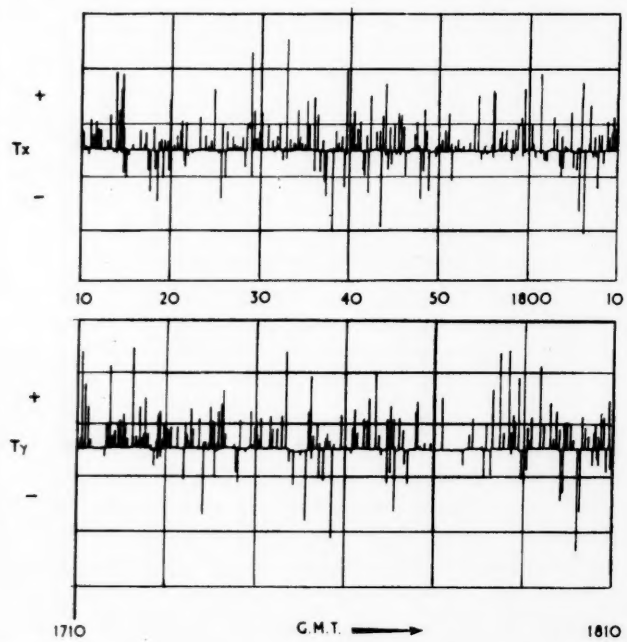

Fig. 1. Record of the "Phillips" type made in Cambridge between 1710 and 1810 GMT on June 13 1951. The frequency was 2 Mc/sec. For description see text.

PHILLIPS, which we shall call a "Phillips record." An example, made in Cambridge between 1710 and 1810 local time (GMT) on June 13 1951 is shown in Fig. 1. It represents the results of an experiment in which the pulses emitted on a radio frequency of 2 Mc/s were received, after reflection from the E layer at three points situated as shown at O, A and B in Fig. 2. The e.m.f.s received at points O and A were applied to a special apparatus so constructed that, every time the received wave passed through a maximum of intensity at both the points, a line was drawn on the record, of length proportional to the time interval T_τ between the occurrence of the maximum at O and that at A. The line was drawn upwards if the maximum at O preceded that at A and downwards if the order was reversed. This record is

VOL. 5 1954

shown at X in Fig. 1. A similar record relating to the receiving points O and B is shown at Y.

It is at once obvious that there is considerable variability in these records. It will now be shown that this variability is to be expected and that it does not necessarily indicate a variable wind.

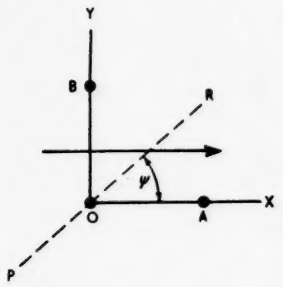

Fig. 2. Schematic diagram of three receiving points.

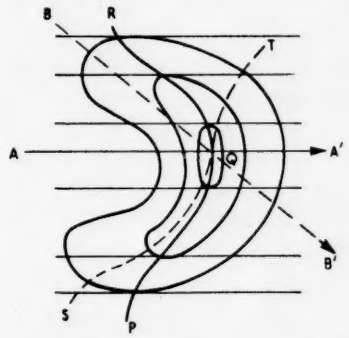

Fig. 3. PQR represents a "line of maximum amplitude" when the signal contours shown move in the direction AA'. SQT is the corresponding line for movement in the direction BB'.

3. A Simple Reason for Considerable Variability in the Records

(a) *The "lines of maximum amplitude"*

The wave reflected from an irregular ionosphere produces, over the ground, an irregular distribution of amplitude, which can be represented, at one instant, by contours of constant amplitude as in Fig. 3. Consider what would be observed if this amplitude distribution moved, without change of form, parallel to a line AA'. Let lines be drawn parallel to AA' so as to touch successive contour lines at PQR. Then maxima of amplitude are observed simultaneously at all points on this line as the amplitude distribution moves past. We will call a line constructed in this way a "line of maximum amplitude." Near any one part of the pattern the "lines of maximum amplitude" are approximately straight lines, but at different parts of the pattern these lines have different orientations.

It should be noticed that the positions of the "lines of maximum amplitude" depend jointly on the nature of the amplitude pattern and the direction of movement. A movement in the direction BB' for example would give rise to a "line of maximum amplitude" SQT.

(b) *The Phillips record for a simple case*

Let O, A, and B (Fig. 2.) represent three observing points at the corners of a right-angled triangle and let $OA = OB = a$. Let us investigate the nature of the Phillips record for the simple case where the amplitude pattern moves with velocity V in the direction OX without change of form. Suppose POR is a "line of maximum amplitude," then the corresponding maximum is observed in succession as it is

swept past the points B, O, and A and the time intervals between the observations at B and O (T_y) and those at O and A (T_x) are given by

$$T_y = \frac{a}{V} \cot \psi$$

$$T_x = \frac{a}{V}$$

In different parts of the amplitude pattern the "lines of maximum amplitude" have different orientations ψ, so that the times T_y have different values, they may be either positive or negative, according as $\psi < \pi/2$ or $\psi > \pi/2$. In the simple case here considered T_x is always the same.

If the magnitudes and signs of T_x and T_y were plotted on a Phillips plot it would look like that of Fig. 4. At first glance a record of this type might be taken to

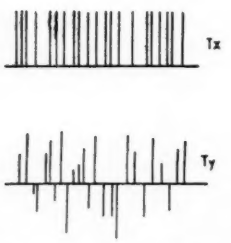

Fig. 4. The form of the "Phillips" type of record for the situation depicted in Fig. 2.

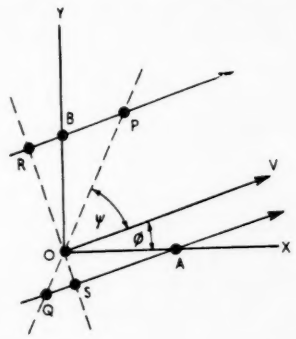

Fig. 5. To illustrate the general case.

indicate that the pattern moved with a velocity which had a constant X-component, but that the Y-component was varying markedly, so that the direction of the velocity was varying violently. The derivation given above shows, however, that this conclusion does not necessarily follow, and, indeed, a record like that of Fig. 4 could equally well correspond to a constant velocity in the X-direction, and all the variability in the values of T_y might be produced by the fact that the amplitude pattern had different shapes at different places.

(c) *The Phillips record for more complicated cases*

If the direction of movement of the amplitude pattern is inclined both to the X- and the Y-axes then there will be considerable variation both in T_x and T_y as "lines of maximum amplitude" having different inclinations ψ are swept past. This variation will not necessarily be evidence for a changing velocity, it could be produced by the random orientation of the pattern even if the velocity were constant. The details are examined in the next Section.

4. Detailed Calculation of a Simple Case

Let the receivers be situated at O, A, B, (Fig. 5.) where O is the origin of a set of rectangular coordinates, A is the point (a, o) and B is the point (o, a). Let an

VOL. 5 1954

unchanging amplitude pattern move with velocity V in a direction making an angle ϕ with OX and let a portion of a "line of maximum amplitude" be represented by QOP, making an angle ψ with V. Let OP pass O at a time T, A at a time $T + T_x$ and B at a time $T + T_y$. Then T_x and T_y can be calculated as follows:

$$T_x = \frac{QS + SA}{V} = \frac{a}{V}(\sin\phi \cot\psi + \cos\phi)$$

$$= \frac{a}{V}\cos\phi\,(1 + \tan\phi \cot\psi) \tag{1}$$

$$T_y = \frac{-(RP - RB)}{V} = -\frac{a}{V}(\cos\phi \cot\psi - \sin\phi)$$

$$= \frac{a}{V}\sin\phi\,(1 - \cot\phi \cot\psi) \tag{2}$$

Now make the following assumptions

V is constant (constant wind speed)

ϕ is constant (constant wind direction)

ψ takes all values equally at random (random orientation of the "lines of maximum")

Then, if a bar over a magnitude represents the mean over a long sample of record

$$\overline{T_x} = \frac{a}{V}\cos\phi \tag{3}$$

$$\overline{T_y} = \frac{a}{V}\sin\phi \tag{4}$$

$$(\overline{T_x})^2 + (\overline{T_y})^2 = \frac{a^2}{V^2} \tag{5}$$

$$\overline{T_y}/\overline{T_x} = \tan\phi \tag{6}$$

These results show that the magnitude (V) and direction (ϕ) of the constant wind can be deduced from the mean time-delays ($\overline{T_x}$ and $\overline{T_y}$) read from the record.

We next investigate the way in which the individual readings for $\overline{T_x}$ and $\overline{T_y}$ are distributed. Differentiation of equations (1) and (2) with respect to ψ gives:

$$\Delta T_x = \frac{a}{V}\sin\phi\,(1 + \cot^2\psi)\,\Delta\psi \tag{7}$$

$$\Delta T_y = -\frac{a}{V}\cos\phi\,(1 + \cot^2\psi)\,\Delta\psi \tag{8}$$

Now if the directions of the "lines of maximum" vary randomly so that successive equal ranges $\Delta\psi$ of the angle ψ are occupied for equal times then successive ranges ΔT_x, as given by eq. (7), are occupied for equal times. Hence the time for which

unit range of T_x is occupied is proportional to $1/\Delta T_x$. If we now write $P(T_x)\,\Delta T_x$ to indicate the probability of finding T_x between T_x and $T_x + \Delta T_x$, we then have

$$P(T_x) \propto 1/\Delta T_x \propto \frac{1}{1 + \cot^2 \psi}$$

Now from eqs. (1), (3) and (4)

$$\cot \psi = \frac{T_x - \frac{a}{V}\cos\phi}{\frac{a}{V}\sin\phi}$$

$$= \frac{T_x - \overline{T}_x}{\overline{T}_y}$$

so that

$$P(T_x) \propto \frac{1}{1 + \left(\frac{T_x - \overline{T}_x}{\overline{T}_y}\right)^2} \tag{9}$$

A similar calculation shows that

$$P(T_y) \propto \frac{1}{1 + \left(\frac{T_y - \overline{T}_y}{\overline{T}_x}\right)^2} \tag{10}$$

The probability distribution functions of expressions (9) and (10) tell us the variability to be expected in the Phillips records when the wind is constant in magnitude and direction but the "lines of maximum amplitude" are randomly distributed so as to have all directions equally frequently. The shape of the curve relating $P(T_x)$ to $(T_x - \overline{T}_x)$ is shown in Fig. 6. Its scale depends on the magnitude

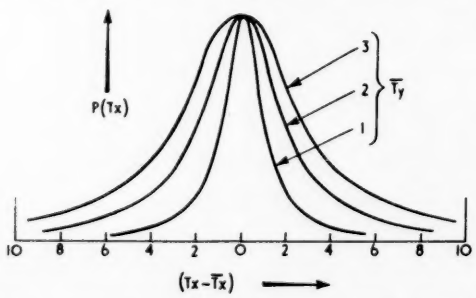

Fig. 6. Plots of equation (9) for different values of $\overline{T}_y$.

of T_y. If, as in the simple example of Section 3(b), $\overline{T}_y = 0$ then the distribution function $P(T_x)$ is infinitely narrow, in agreement with our previous conclusion as represented in the schematic Phillips plot of Fig. 4.

5. Analyses of Actual Records

The record of Fig. 1 was analysed by counting the number of occasions when the recorded "spike" had its end between any two neighbouring calibration lines. For the present purpose the absolute calibration of the equipment is of no importance,

VOL. 5 1954

it is sufficient to know that the sensitivity was the same on the two records (X and Y). The distance between calibration marks on the record was taken as a unit and the following mean values were deduced

$$\overline{T_x} = 2 \qquad \overline{T_y} = 2$$

Hence $\tan \phi = 1$ and $\phi = 45°$

and $$\frac{a}{V} = 2\sqrt{2}$$

Next the number of occasions when $T_x - \overline{T_x}$ lay within the ranges ..... -4 to -2, -2 to 0, 0 to $+2$, $+2$ to $+4$ ..... were determined and were plotted against the value of T_x at the middle of the range as in Fig. 7. The observed values of T_y were also plotted. Since $\overline{T_y}$ and $\overline{T_x}$ both have the same value, 2, the theoretical

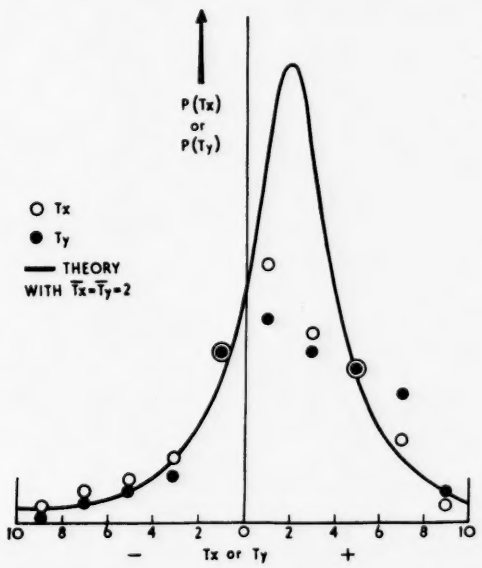

Fig. 7. Values of $P(T_x)$ and $P(T_y)$ obtained from the record of Fig. 1 and compared with theory (equations 9 and 10).

curves for $P(T_x)$ and $P(T_y)$ as given by eqs. (9) and (10) are the same. They are represented by the line of Fig. 7, in which the vertical scale has been adjusted so that it gives the best fit with the observed points.

It appears from Fig. 7 that the record of Fig. 1 agrees about as well as could be expected with a simple theory in which the wind is supposed to be constant, and the amplitude pattern is randomly distributed. The variability in the records is just what would have been expected, even with a constant wind.

Another record, made between 1100 and 1200 local time on 18.7.51, with a

frequency of 2.4 Mc/s gave results which could not be explained on the simple hypothesis used above. On this occasion

$$\overline{T_x} = -1.8 \qquad \overline{T_y} = +3.7$$

and the observed values of T_x and T_y were distributed as shown in Fig. 8 (a) and (b). The continuous lines represent the theoretical distribution functions of equations (9) and (10), plotted with an arbitrary vertical scale, and it does not seem that any adjustment of the scale would be likely to make the curve fit the experimental points.

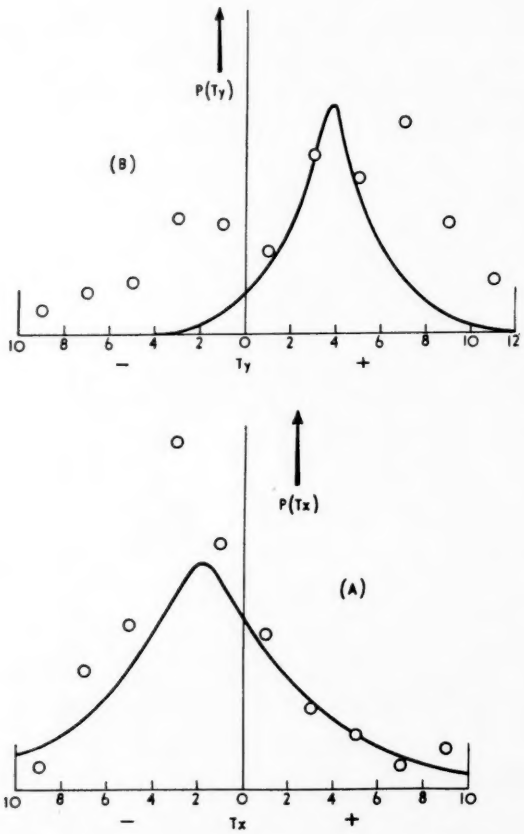

Fig. 8. Values of $P(T_x)$ and $P(T_y)$ obtained from a record made in Cambridge between 1100 and 1200 GMT on 18.7.51 with a frequency of 2.4 Mc/s reflected from the E layer. There is little agreement with the curves which were plotted from equations (9) and (10).

6. CONCLUSIONS

The results exhibited in Fig. 1 and Fig. 7 could be explained in terms of a constant wind and an isotropically random amplitude pattern. It is possible, but not likely, that they could also be explained in terms of a variable wind. For the present it is assumed that, on this occasion, the wind was constant.

VOL. 5 1954

The results exhibited in Fig. 8 could not be explained in this way. The explanation will presumably require the assumption of a variable wind, or a non-isotropic amplitude pattern, or both.

It is important to develop methods of analyses which would be applicable to these more complicated situations.

References

Briggs, B. H., and Spencer, M.	1954	Reports on Prog. in Phys: Vol. XVII
Chapman, J. H.	1953	Canad. J. Phys. **31,** 120
Hewish, A.	1952	Proc. Roy. Soc. A. **214,** 494
Maxwell, A., and Little, C. G.	1952	Nature **169,** 746
Millman, G. H.	1952	Ann. Geophys. **8,** 365
Mitra, S. N.	1949	Proc. Instn. Elect. Engrs. **96** (Pt. III), 441
Phillips, G. J.	1952	J. Atmosph. Terr. Phys. **2,** 141
Salzberg, C. D., and Greenstone, R.	1951	J. Geophys. Res. **56,** 521

OL.
954

Journal of Atmospheric and Terrestria lPhysics, 1954, Vol. 5, pp. 182 to 185. Pergamon Press Ltd., London

The determination of the velocity of winds from spaced fading experiments

GORDON NEWSTEAD
The Cavendish Laboratory, Cambridge

(*Received* 3 *May* 1954)

ABSTRACT

The statistical variations of radio fading records made at three points are discussed. It is shown what information can be obtained about the statistical variations of the wind-like movements responsible for the fading.

1. INTRODUCTION

MITRA'S (1949) method of measuring winds in the ionosphere involves the making of fading records at three spaced receivers and the measurement of time delays between correlated parts of these records. BRIGGS, PHILLIPS, and SHINN (1950) have considered the analysis of these records on the assumption that over a selected length of the record the mean wind velocity is constant, but that the diffraction pattern over the ground changes in form as it moves. PHILLIPS has developed an apparatus which measures directly the time delays between the two pairs of receivers and from an inspection of the records produced by this method the question immediately presents itself as to what part of the variations is due to a slow fluctuation of the mean wind velocity. RATCLIFFE (1954), in a companion paper, has given an elementary analysis of this problem, and has shown that on a simple plausible model, some of the Phillips records which at first sight seem to suggest a variable wind, are in fact consistent with a constant wind. He has drawn attention to the need for a more detailed analysis of records of this type.

In the present paper it is shown how the statistical variations in the Phillips record are related to the statistical variations in the magnitude and direction of the wind and in the shape of the amplitude pattern of the wave over the ground. It is shown that there is not enough information in the records to provide information about the statistics of all three of the quantities concerned, but if some assumption is made about the nature of the amplitude pattern, then the statistics of the wind variation can be deduced.

2. STATEMENT OF THE PROBLEM

In the figure let OX, OY be rectangular coordinate axes and let the wind have a speed V in a direction making an angle ϕ with OX. Let O, A, and B be the three stations with $OA = a = OB$. Assume that a line of maximum signal moving over the ground can be represented by a straight line QOP making an angle ψ with the direction of the wind. Let T_x, T_y be the times for the line of maximum signal to travel from O to A and B respectively and assume that V, ϕ, and ψ remain constant while this line passes over A and B Then it follows immediately that

$$\left.\begin{aligned} T_x &= \frac{a}{V}\frac{\sin(\phi+\psi)}{\sin\psi} = \frac{a}{v}\sin\theta = T_0\sin\theta \\ T_y &= \frac{a}{V}\frac{\cos(\phi+\psi)}{\sin\psi} = \frac{a}{v}\cos\theta = T_0\cos\theta \end{aligned}\right\} \qquad (1)$$

where

$$\left\{\begin{aligned} \theta &= \phi+\psi \\ v &= V\sin\psi \\ a/v &= T_0 \end{aligned}\right.$$

VOL. 5 1954

The problem is now to find from the statistics of T_x and T_y, which can be measured from the Phillips record, the statistics of V, ϕ, and ψ. It will be shown that, in general, this cannot be done, but that it is possible to find the statistics of the quantities T_0 and θ which define an equivalent wind whose velocity is V and whose direction is θ. The statistics of two of the quantities V, θ, and ψ can then be deduced if the statistics of the third are assumed known.

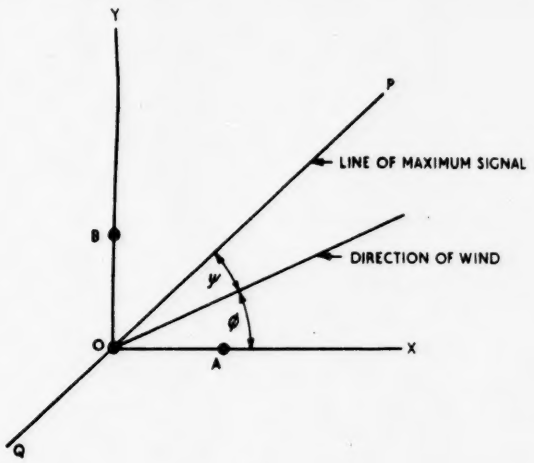

Fig. 1.

We assume that the experimental records are used to provide information about the probability $P_{x,y}(T_x, T_y)\, dT_x\, dT_y$ that T_x has a value in the range of width dT_x centred on T_x, and that simultaneously T_y has a value in the range of width dT_y centred on T_y.

It is required to find some or all of the probability density functions $P_{T_0}(T_0)$, $P_\theta(\theta)$, $P_V(V)$, $P_\phi(\phi)$, and $P_\psi(\psi)$ which refer to the variables indicated by the subscripts. First we will show how $P_\theta(\theta)$ and $P_{T_0}(T_0)$ can be found.

3. Determination of $P_\theta(\theta)$ and $P_{T_0}(T_0)$

From equation (1) we have

$$T_0 = \sqrt{T_x^2 + T_y^2} \tag{2}$$

and by definition

$$P_{x,y}(T_x, T_y)\, dT_x\, dT_y$$

is the probability that T_x will have a value in an interval of width dT_x centred on T_x and simultaneously T_y will have a value in an interval of width dT_y centred on T_y. Hence

$$P_{x,y}(\sqrt{T_0^2 - T_y^2}, T_y) \frac{dT_x}{dT_0}\, dT_y\, dT_0$$

is the probability that T_y will have a value in the interval of width dT_y centred on T_y and simultaneously T_x will have the value $\sqrt{T_0^2 - T_y^2}$ in an interval of width

dT_x centred on $\sqrt{T_0^2 - T_y^2}$. It is also the probability that T_0 has a value in an interval of width dT_0 centred on T_0 and simultaneously by T_y has a value in an interval of width dT_y centred on T_y. Hence integrating over all possible values of T_y, i.e. from $-T_0$ to T_0, we obtain

$$P_{T_0}(T_0)\,dT_0 = \int_{-T_0}^{+T_0} \left\{ P_{x,y}(\sqrt{T_0^2 - T^2},\, T_y) \frac{dT_x}{dT_0}\, dT_0 \right\} dT_y$$

Substituting the value of $\dfrac{dT_x}{dT_0}$ obtained from (2), in terms of T_0 and T_y and cancelling dT_0 we obtain

$$P_{T_0}(T_0) = T_0 \int_{-T_0}^{+T_0} \frac{P_{x,y}(\sqrt{T_0^2 - T_y^2},\, T_y)}{\sqrt{T_0^2 - T_y^2}}\, dT_y \tag{3}$$

By a similar argument it may also be shown that

$$P_\theta(\theta) = \sec^2\theta \int_{-\infty}^{+\infty} T_y\, P_{x,y}(T_y \tan\theta,\, T_y)\, dT_y \tag{4}$$

4. Expression of P_V and P_ϕ in terms of P_θ, P_{T_0} and P_ψ

In order to make further progress let us assume that P_ψ is known, P_V and P_ϕ can then be deduced as follows. From equation (1) we obtain

$$V = a/(T_0 \sin\psi) \tag{5}$$

If we let $P_V'(V, \psi)\,dV$ be the probability that V lies in an interval of width dV centred on V for a given value of ψ then

$$P_V'(V, \psi) = P_{T_0}\, dT_0/dV$$

Using equation (5) we find that

$$dT_0/dV = -a/(V^2 \sin\psi)$$

and so

$$P_V'(V, \psi) = -\{a/V^2 \sin\psi\}\, P_{T_0}(a/V \sin\psi)$$

Now values of ψ occur with probability of $P_\psi(\psi)\,d\psi$ and hence

$$\begin{aligned} P_V(V) &= \int_{-\pi}^{\pi} P'_V(V, \psi)\, P_\psi(\psi)\, d\psi \\ &= -\frac{a}{V^2} \int_{-\pi}^{\pi} \frac{1}{\sin\psi}\, P_{T_0}\left(\frac{a}{V \sin\psi}\right) P_\psi(\psi)\, d\psi \end{aligned} \tag{6}$$

By a similar argument it can be shown that

$$P_\phi(\phi) = \int_{-\pi}^{\pi} P_\theta(\theta + \psi)\, P_\psi(\psi)\, d\psi \tag{7}$$

Equations (6) and (7) taken in conjunction with (3) and (4) complete the formal deduction of P_ϕ and P_V in terms of $P_{x,y}$ and P_ψ.

VOL. 5 1954

Conclusion

It has been shown that, if some assumption is made about the statistics, represented by P_ψ, of the distribution of the lines of maximum signal over the ground, then it is possible, in principle, to deduce the statistics of the wind variation, as represented by P_V, and P_ϕ, from values of $P_{x,y}$ read from a Phillips record. Further progress depends either on the making of reasonable assumptions about P_ψ, or on the results of experiments designed to determine this function.

Possible reasonable assumptions for the form of the function P_ψ include

(1) P_ψ constant for all values of ψ.

(2) P_ψ has a maximum at right angles to the wind; thus $P_\psi \propto \cos^{2n} \psi$ might be a reasonable assumption.

(3) P_ψ has a maximum in some particular preferred direction; $P_\psi \propto \cos^{2n} (\psi - \psi_0)$ might then be a reasonable assumption.

References

Briggs, B. H., Phillips, G. J., and Shinn, D. H.	1950	Proc. Phys. Soc. B **63**, 106
Mitra, S. N.	1949	Proc. Instn. Elect. Engrs. **96** (Pt. III), 441
Ratcliffe, J. A.	1954	J. Atmosph. Terr. Phys. **5**, 173

Book reviews

Vorträge über Kosmische Strahlung: 2nd edition, edited by W. HEISENBERG. Springer-Verlag, Berlin, 1953. 260 pages, 257 figures, DM. 78.—.

The first edition of this book was published in Germany in 1943 and an American edition appeared in 1946. In his introduction to the first edition the editor Professor HEISENBERG explains how the book originated in a series of colloquia in Berlin on various aspects of cosmic rays during 1941–42. Some of the articles were reviews of the general state of knowledge in a given branch of the subject and some were original contributions. The American edition of the book was of considerable value to cosmic ray research workers starting work again after the War. The second German edition, published just ten years after the first, is a much larger book and all the articles are new. However, the pattern remains similar, in that some of the articles are surveys of the state of knowledge of the different fields, whereas others are more in the nature of original contributions. The articles are again based on a series of colloquia held during recent years in Göttingen. Some two dozen authors are responsible for some forty articles, of varying length and importance, covering in a rather haphazard fashion the main fields of modern cosmic ray research. In general there is little or no indication of a planned style or level of exposition, and the amount of space devoted to any particular subject seems to have depended more on the inclination of the various authors rather than on a particular estimate of its present-day importance for the cosmic ray research worker. Thus, for instance, in a book of 600 pages, 60 are devoted to the μ-meson, 50 to the electronic component and 9 to the heavy mesons. This would not be a bad balance if the book were intended mainly to give advanced students the background to modern work: however, clearly it is not so intended. The book, in fact, tends to fall between the two stools of not being either a balanced textbook for the advanced student or, on the other hand, of not giving in all cases a really up-to-date, comprehensive and authoritative survey of the fields which are the growing points of the subject to-day. The bibliography is the most complete known to me and is very valuable.

VOL. 5 1954

In spite of these minor criticisms of the book as a whole, it does contain a number of articles of great interest to specialist workers. Moreover, it contains a valuable set of appendices giving derivations of standard relativistic relations, numerical data and energy-range relations, etc.

An entirely new section devoted to the "Origin of Cosmic Rays" is edited by BIERMANN, who has himself made important contributions to this subject. This most interesting article is, I think, the first general review of this fascinating field of—I was going to write "research," but perhaps it would be more accurate to write "speculation." However, the article could have so well been much more comprehensive. The 18 pages of Dr. BIERMANN's survey of origin theories are far too little. He has clearly read everything of importance, but only mentions much of it in passing. A few topics such as FERMI's theory of the origin of the rays and the relation between interstellar magnetic fields and the turbulence of interstellar gas are given in detail. One misses, however, an assessment by so eminent an astrophysicist as Dr. BIERMANN of the observational evidence for Galactic magnetic fields and for their structure, as deduced from the polarization of the light from stars. I would like also to have seen much more about the outstanding problem of the experimental isotropy of the cosmic rays and of the types of hypotheses about the distribution of sources and of scattering by magnetic irregularities. Then the acceleration of particles by stars with oscillating magnetic fields is hardly mentioned. Those aspects covered in detail by Dr. BIERMANN are excellently done. My criticism is only that the detailed coverage is somewhat perfunctory.

Other articles of special interest are those of HEISENBERG on multiple meson production and those of MOLIÈRE on extensive showers.

HEISENBERG's introduction to the first edition, reprinted in the second, is of some historic interest as it reminds us of some facts about the use of academic scientists in the German war effort. When the first German edition of 1943 became available after the War, British physicists were definitely surprised that the colloquia in Berlin on cosmic rays on which the book was based should have taken place at all. At that time in England there were few British cosmic ray physicists who had not left their laboratories and were engaged on urgent defence problems.

We had not realized how little German civilian life must have been disturbed during the first years of war. By the time the volume went to the publishers in June, 1943, things, of course, had changed, and HEISENBERG records this in his opening sentences: "Die Forschungen über kosmische Strahlung werden von der Ungunst der Zeiten besonders stark betroffen. Denn einerseits müssen sie in den meisten physikalischen Laboratorien naturgemäss hinter anderen Problemen zurückstehen. . . ."

P. M. S. BLACKETT

GOODY, R. M.; **The Physics of the Stratosphere.** (Cambridge monographs on Physics. General Editors: N. FEATHER, F.R.S., and D. SHOENBERG, Ph.D., F.R.S.). Cambridge University Press, London. (American Branch: New York. Agents for Canada, India, and Pakistan; Macmillan) pp. 187, 1953. 21s. net.

Research on the vast regions of the atmosphere lying above the lowest few kilometres of weather-forming layers is a fairly recent venture, and great progress has been made on this subject using both direct and indirect methods. The direct methods include use of sounding balloons, smoke shells, sound explosions, radio wave exploration, and, more recently, high altitude rockets, such as the V2, the Viking and the Aerobee. The indirect methods include study of meteors, solar and atmospheric spectroscopy, noctilucent clouds, meteors, barometric oscillations and the terrestrial magnetic variations. Some of these methods are of use only within definite height ranges; others have more extensive applications. A large amount of literature is now available on the application of these different methods and although much more has yet to be done it is possible now to make a coherent picture of the high atmosphere. There is however a dearth of books adequately dealing with the topic. A pioneering book in this line is "The Upper Atmosphere" by S. K. MITRA which deals with the whole atmosphere from the ground to the exosphere. For those who are specifically interested in the atmosphere between 15 to 75 km, the present book offers excellent reading material.

The title is perhaps misleading to some of the physicists to whom the stratosphere is a fairly narrow region beginning with the troposphere and ending at about 30 km. The present book considers the stratosphere to extend up to about 75 km where the second minimum in temperature is reached. This therefore includes the "mesosphere" as defined by CHAPMAN and the "Chemosphere" as defined by GERSON and KAPLAN.

The first chapter, which introduces the subject and defines the atmospheric nomenclature used, also describes the various tools of research in this subject, such as balloons, aircraft, and rockets. Chapter II gives a very able description of the various methods of measurement of atmospheric temperature. The data for the lower stratospheric regions up to about 20 km as obtained by balloon-borne radio sondes are described. For the higher levels, temperature is obtained from the propagation of sound, from meteors, from rockets, and less directly from noctilucent clouds, from solar and atmospheric spectroscopy, from collision frequency and sometimes from certain ionospheric parameters. Chapter III describes the density distributions of various atmospheric constituents including such minor constituents as water vapour, carbon dioxide, the rare gases, and some of the nitrogen compounds. The existence of atmospheric sodium is mentioned, but no details are given. The ozone layer which causes the first temperature maximum above the ground is discussed in Chapter IV. Chapter V describes the various measurements on stratospheric winds, a subject of considerable importance to synoptic meteorology. The last chapter describes the intensities of the solar radiation at various wavelengths, the line and band absorption of the radiation by various atmospheric constituents, and the resulting temperature distribution of the atmosphere.

The book is well arranged and the material is excellent. Doubtful results have been left out. In doing so, however, some interesting aspects of the atmosphere have not been given proper emphasis. There may be appreciable dissociation of molecular oxygen and of water vapour at the top of the "stratosphere" as defined in this book. Between 30–80 km, which has sometimes been described as the "Chemosphere," various reactions occur, involving molecular and atomic

oxygen, ozone, and the various nitrogen oxides. The photochemistry of these constituents forms a fascinating study; such chemical reactions have only been considered in passing in this book (Chapter IV).

Little mention has been made of the ionospheric region *D* which extends down to 70 km and perhaps even to lower heights, specially during the times of sudden ionospheric disturbances.

Excepting these few details of perhaps restricted interest, the book has covered the various aspects of the atmosphere between 15 to 75 km in a satisfactorily comprehensive way, and will be of use to those who are interested in the upper regions of the atmosphere.

A. P. MITRA

Obituary

SIR NELSON JOHNSON, K.C.B., D.Sc., A.R.C.S.

On 23rd March meteorologists everywhere were shocked to hear of the death, in tragic circumstances, of Sir NELSON JOHNSON, late Director of the Meteorological Office. His friends had known for some time that he was a sick man, but had hoped that medical science, even if it could not bring about a complete recovery, would at least slow down the progress of the disease enough to ensure a happy retirement, but this was not to be.

NELSON KING JOHNSON was born in 1892 and began his career as an astronomer, working with Sir NORMAN LOCKYER. Throughout his life he retained a deep interest in astronomy. During World War I he became a pilot in the R.F.C., and there is a legend, better founded than most, that an accident in which he was involved, being largely caused by the current lack of knowledge of meteorology as it affected aviation, first turned his thoughts towards the science of the atmosphere. However, the scientific work for which he is best remembered deals with conditions in the lowest layers of the atmosphere. When in 1921 he was appointed to the post of Head of the Meteorology Section at the Chemical Warfare Station at Porton, he found an almost unexplored field before him. He gathered around him a band of young men who were infected by his enthusiasm, and some of the most notable work ever done in meteorology was the result of his leadership. When he left this post in 1928 he had founded the science of micrometeorology, and his *Geophysical Memoirs* on the temperature field near the ground will always be regarded as classical.

JOHNSON climbed rapidly after this, becoming Director of Experiments at Porton, then Chief Superintendent of the Chemical Defence Research Department and finally Director of the Meteorological Office in 1938, a post which he took up with enthusiasm and high hopes. But war was declared in the following year and JOHNSON had to turn all his energies to the vast task of expansion and reorganisation. His sense of duty was so strong that undoubtedly he overworked and damaged his health, but in 1945 he could look with pride on a meteorological service that was second to none in the world. It was characteristic of the man that in 1943, when our fortunes were at a low ebb, he founded the Meteorological Research Committee and simultaneously gave the Meteorological Office, for the first time, a strong and well-directed research side. After the war he turned his attention to international matters, and it was largely through his skill, tact and unfailing courtesy that the World Meteorological Organization was well founded. For this alone his name deserves to be honoured.

JOHNSON was quiet in manner, modest to a fault and invariably courteous to all with whom he dealt. His interests were primarily those of the scholar, but he did not spare himself in promoting the well-being of all who served under him. He was regarded with affection by his staff and only those who worked closely with him know how much of his time and energy he gave to his job. Our deepest sympathies go to Lady JOHNSON and their two children.

O. G. S.

VOL. 5 1954

Journal of Atmospheric and Terrestrial Physics, 1954 ,Vol. 5, pp. 189 to 200. Pergamon Press Ltd., London

Radio reflections from aurorae

K. BULLOUGH and T. R. KAISER
Jodrell Bank Experimental Station, University of Manchester

(*Received* 17 *April* 1954)

ABSTRACT

The paper offers an interpretation of auroral echoes observed at Jodrell Bank on two occasions in 1953. It is concluded that in each case the echoes are due to direct, non-specular reflection from an auroral arc extending more than 1000 km along a parallel of geomagnetic latitude. The reflection apparently occurs in a region of the arc of limited vertical extent at a height of about 125 km. The observed line of sight velocities of intense reflecting centres are interpreted as true motions along the arc with velocities of the order of 1–2 km sec^{-1}.

1. INTRODUCTION

Extensive observations of aurorae by metre wave radio echo techniques have been made in recent years at Jodrell Bank (lat. 53°13′53″ N, long. 2°18′11″ W, LOVELL *et al.*, 1947; ASPINALL and HAWKINS, 1950) as well as in Canada (FORSYTH, 1953; CURRIE *et al.*, 1953; MCKINLEY and MILLMAN, 1953), Norway (HARANG and LANDMARK, 1954), and Sweden (HELLGREN and MEOS, 1952).

In the previous work at Jodrell Bank the aerial systems were either fixed, or, if steerable, were pointed in one or more fixed directions during the observations. The equipment with which the present results were obtained is designed both for meteor and auroral observations and differs from the previous techniques in the aerial system which rotates about a vertical axis and has a fairly narrow, low elevation, pencil beam. It has operated almost continuously since March 1953. During the period March–December 1953, auroral echoes have been obtained on three occasions, March 9, May 15–16, and October 15. The May and October echoes occurred during daylight, hence no simultaneous visual observations could be made, however they conform in direction, range, and general character with previous ones obtained when seeing conditions permitted direct visual correlation.

While the observational material is thus not very extensive, the interpretation seems sufficiently unambiguous to resolve (at least for these particular aurorae) some disputed questions. These include the doubt raised by HARANG and LANDMARK (1954) as to whether the echoes are, in fact, due to direct reflection from aurorae, as well as the question raised by various workers as to whether or not the reflection is specular (from auroral surfaces or rays). The analysis leads, in addition, to some detailed conclusions concerning the geometry and structure of the particular aurorae.

The discussion is limited to the aurorae of 1953 Oct. 15 and May 15–16 since on March 9 the equipment was not functioning during the hours 0115–0415 and strong auroral echoes were observed during only one aerial rotation (at 0443 hr.).

2. THE EQUIPMENT

The equipment parameters are: Wavelength 4·1 m, peak transmitter power 10 kW, pulse length 40 μs, pulse repetition frequency 150 sec^{-1}, receiver sensitivity 2×10^{-14} watt. Pulses are transmitted in pairs separated by 333 μs, corresponding

to a range displacement of 50 km. The aerial system consists of an array of two, six element, Yagi aerials mounted at a height of 20 ft. above ground on a motor driven turntable which has a period of rotation of approximately 6 min. The aerial beam (Fig. 1) has an azimuthal width of 20° between half power points and its maximum gain of about 90 (compared to a hypothetical isotropic radiator) occurs at elevation +10°. Comparison between the sporadic meteor rate observed on this and other equipments suggests that the actual echo power sensitivity may be an order of magnitude less than the value calculated from the above figures.

The echoes are displayed in rectangular range-time co-ordinates by means of an intensity modulated cathode ray tube photographed on a continuously moving film.

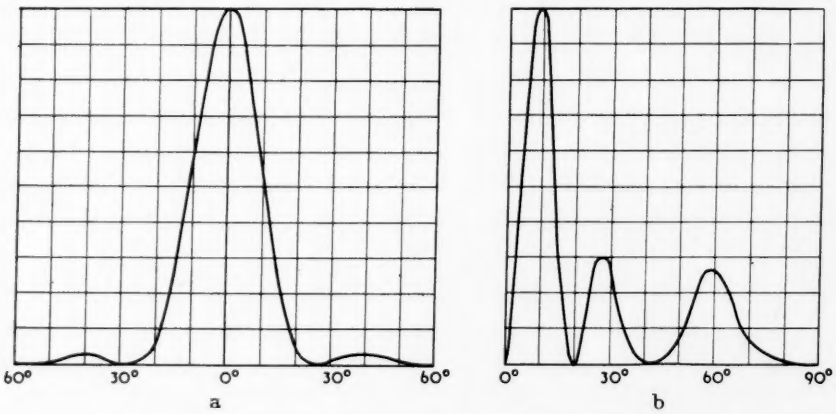

Fig. 1. Aerial power polar diagrams. (a) Horizontal, (b) Vertical.

3. The Aurora of October 15, 1953

Echoes were first observed at 1300 hr. (U.T.) on a somewhat more sensitive apparatus and increased considerably in intensity shortly before 1800 hr. The rotating aerial equipment was brought into operation at 1751·2 hr. and strong echoes were obtained during three revolutions of the aerial beam; the observations were then interrupted and shortly afterwards echoes ceased completely. The records obtained are shown in Fig. 2. A simultaneous record obtained on another equipment (Aspinall and Hawkins, 1950) which has a narrow pencil aerial beam directed at elevation 8°, azimuth 68° W of N is shown in Fig. 3; in this direction the echoes increased abruptly in amplitude at 1752·5 hr. and remained high until about 1815 hr. when they disappeared.

Interpretation of the echo structure

The echoes are mainly diffuse (i.e. extended in range) with, however, some discrete structure visible in the NE direction at ranges of about 500 and 700 km in Figs. 2a and 2b respectively. The gap which appears at range 530 km in the NE in Fig. 2b is due to receiver saturation effects. The detailed form of the echoes shows marked changes between the three records (which are separated by time intervals of 6 min.). The mean echo range during the complete aerial revolutions corresponding to Figs.

VOL. 5 1954

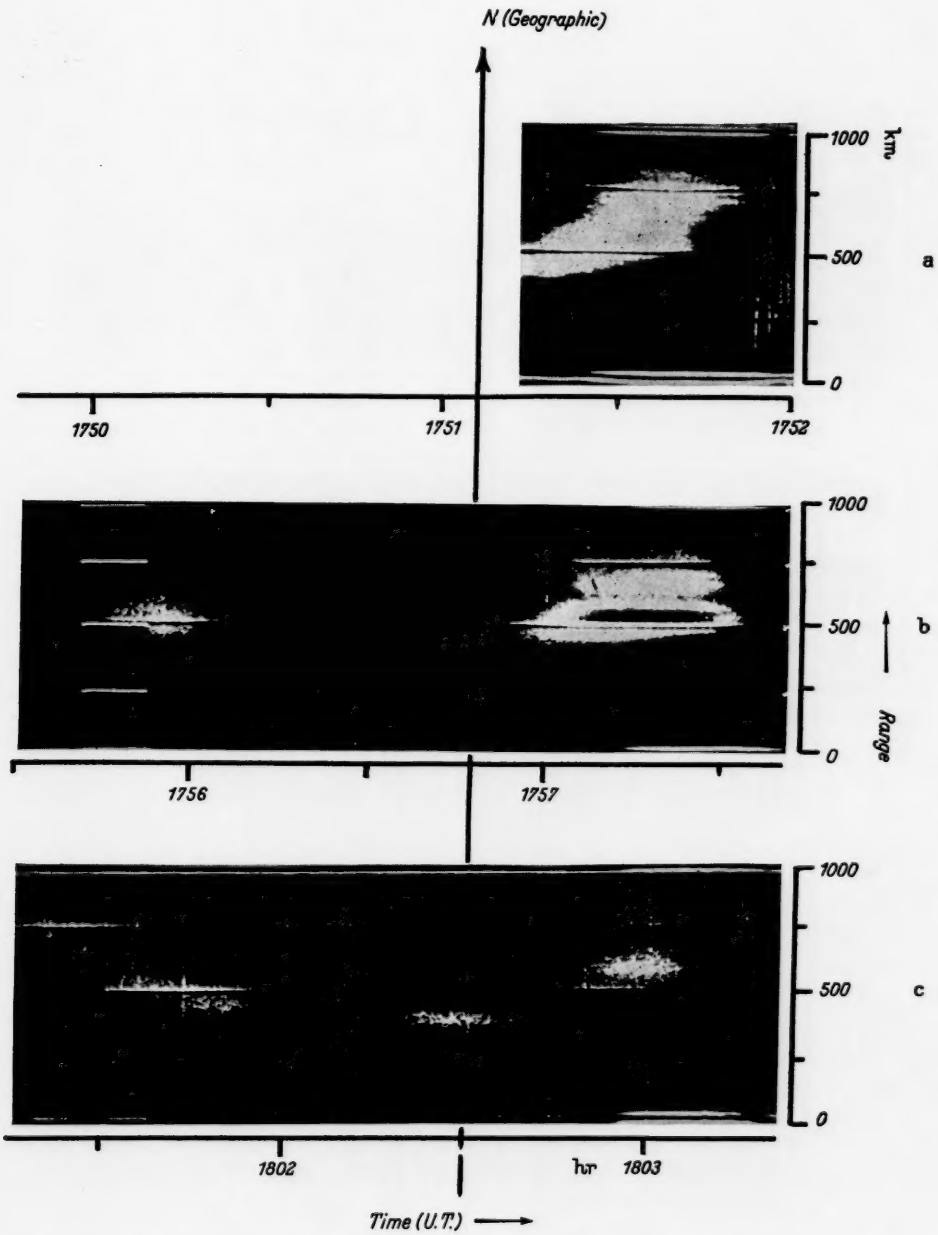

Fig. 2. Auroral echoes, Oct. 15, 1953, displayed in range-time coordinates. (a), (b) and (c) correspond to three successive aerial rotations.

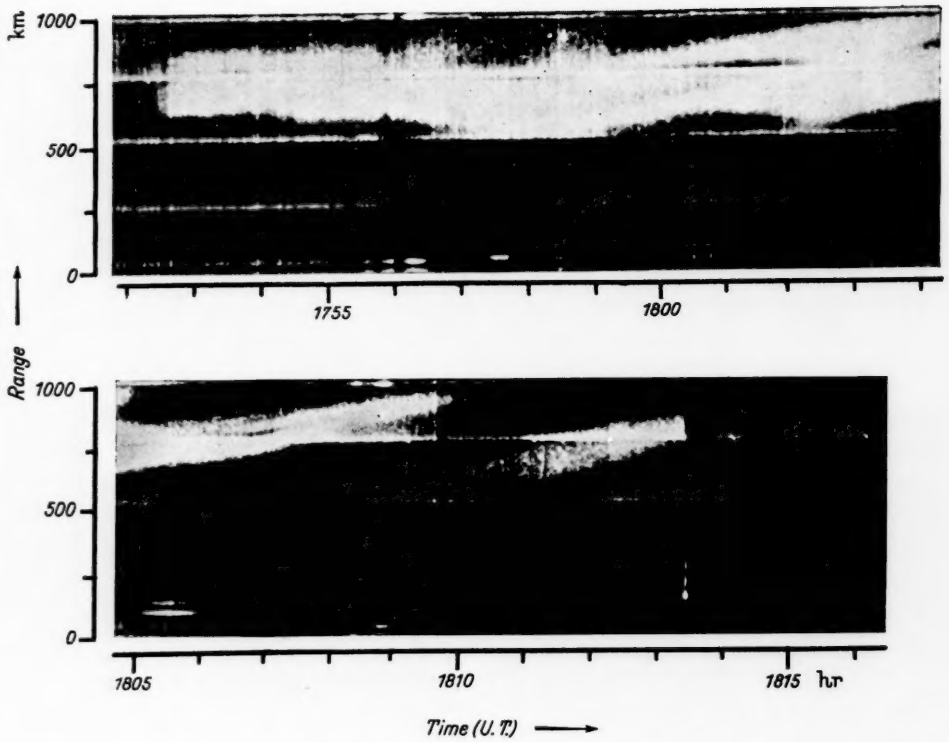

Fig. 3. Auroral echoes, Oct. 15, 1953, observed with the narrow aerial beam directed towards N.W.

VOL.
5
1954

2b and 2c appears to lie along an arc which is symmetrical about a direction 16° W of N and there is a marked spread in range which is a minimum at the centre of the arc (minimum range).

The simplest interpretation of these results is that the reflection occurs along a line of geomagnetic latitude about 3° to the north of Jodrell Bank (geomagnetic latitude 56°). In Fig. 4 this line is shown dashed in range-azimuth co-ordinates

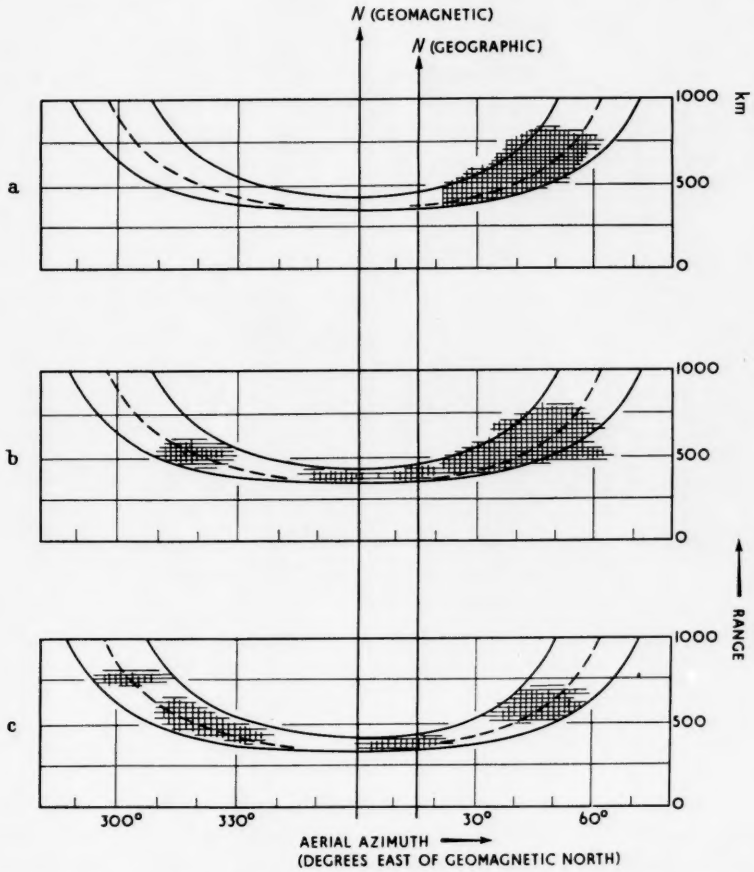

Fig. 4. The echoes of Fig. 2 (hatched) are superimposed on theoretical echo contours (full lines) corresponding to a low elevation reflecting arc along a parallel of geomagnetic latitude (broken line).

(assuming the height of the reflecting region to be of the order of, or less than, 100 km), with the actual echo forms superimposed. The full lines give the theoretical echo range limits taking account of the finite aerial beam width and pulse separation. The best fit was obtained by taking the magnetic meridian to be $16° \pm 2°$ W of N, which is in close agreement with the value 18°26′ given by CHAPMAN (1953) for the location of Jodrell Bank.

The position of this assumed reflecting arc is shown in Fig. 5, projected on to a

plane which is tangent to the earth at Jodrell Bank; the limits of the arc correspond to the observed range limits of the echoes.

Since reflections are obtained along the whole length of this arc, we conclude that the auroral formation behaves as a rough reflector along this line, i.e. that it exhibits a rough surface or, more likely, consists of an aggregate of reflecting centres, a number of which lie within the aerial beam at any instant. It is clear

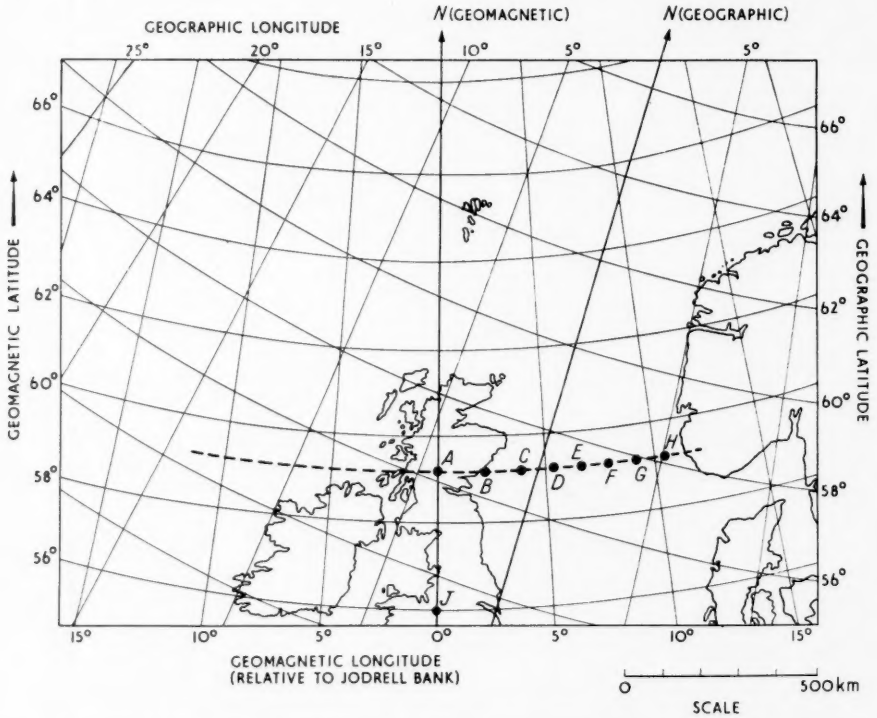

Fig. 5. Location of the assumed reflecting arc (broken line) projected on to a plane tangent to the earth at Jodrell Bank (J). The limits of the arc correspond to the observed maximum echo ranges.

from Fig. 4 that the spread in range is due almost entirely to the finite beam width and pulse spacing. The minimum range spread (observed in the direction of the magnetic meridian) is only of the order of the latter (50 km) hence we conclude that the thickness of the reflecting region normal to the arc is not more than 10–20 km.

Non-specular reflection

The hypothesis that the reflection is specular and derives from those parts of the aurora where the vector from the observer intersects normally the direction of the terrestrial magnetic field has been advanced by various authors (Lovell *et al.*, 1947; Aspinall and Hawkins, 1950; Hellgren and Meos, 1952; Booker *et al.*, 1954; Chapman, 1952), while the opposing view is held by the Canadian workers (Currie *et al.*, 1953).

VOL. 5 1954

It should be noted that the conclusions drawn above concerning the "roughness" of the reflecting structure are not inconsistent with the idea of specular reflection; for instance the reflecting arc could consist of auroral rays following the direction of the terrestrial magnetic field and distributed along the assumed parallel of latitude. However, the following additional arguments appear to rule out specular reflection in the present case.

The theory of CHAPMAN (1952) appertaining to this type of specular reflection has been evaluated numerically by CAIN (1953) for the location of Jodrell Bank. Table 1 gives the heights and elevations of the specular reflection points derived from CAIN's figures for the points A, B—H along the assumed reflecting arc (see Fig. 5). Thus on the specular reflection hypothesis the reflecting arc lies below 80 km over more than half of its length, while its extremes fall below the horizon. According to HARANG (1951): "On the basis of many thousands of height determinations we must conclude that the possible occurrence of aurorae below 80 km must be exceedingly rare."

Since the reflection is non-specular, the most logical hypothesis would appear to be that it occurs in the most intensely ionized part of an aurora, probably in a fairly restricted height range near the lower boundary.

Table 1. *Theoretical heights and elevations, assuming specular reflection*

Position on arc (Fig. 5)	A	B	C	D	E	F	G	H
Elevation (deg.)	13·5	12	10	8	6	4	2	0
Height (km)	94	93	89	83	76	67	57	44

Further discussion of the echo geometry

Other possible interpretations of the echoes which remain to be eliminated are: (i) Since the echoes are recorded with a repetitive 1000 km timebase, it is possible that the true ranges are an integral multiple of 1000 km in excess of the apparent range given in Fig. 2. (ii) That the echoes are due to long range scattering from an irregular terrain, combined with skip reflection from an ionized region at a height of the order of 100 km as suggested by HARANG and LANDMARK (1954).

The first possibility is unlikely on the following grounds: The reflecting region would appear convex towards the observer when plotted in the co-ordinates of Fig. 5 and its height would have to be in excess of 200 km in order that it should be visible above the horizon.

The second hypothesis would require the distance of the actual reflecting region to be about one half of the observed echo ranges. In this case, assuming a height of about 100 km, the part of the region at range 280 km (corresponding to an echo range of about double this figure) will coincide with the first zero in elevation of the aerial beam whereas in fact the echoes are most intense at a range of 500–600 km. Also, we would expect that long range scattering from land or sea would give rise to a considerable spread in range in addition to that due to the finite aerial beam width, however, as has been shown above, this latter accounts satisfactorily for the observed range spread.

The height of the reflecting region

Adopting the hypothesis that we are dealing with a reflecting arc of constant and fairly well defined height which is situated along a parallel of geomagnetic latitude, we can evaluate theoretical echo contours for various heights. Up to 100 km or so these are substantially independent of height and are as given in Fig. 4. Figs. 6(a) and (b) show the contours for 150 km and 200 km respectively, with the echoes of Fig. 2(c) sketched for comparison. The divergence between the theory and observation is marked at 200 km and is apparent even at 150 km, suggesting that the echoes originate below this level.

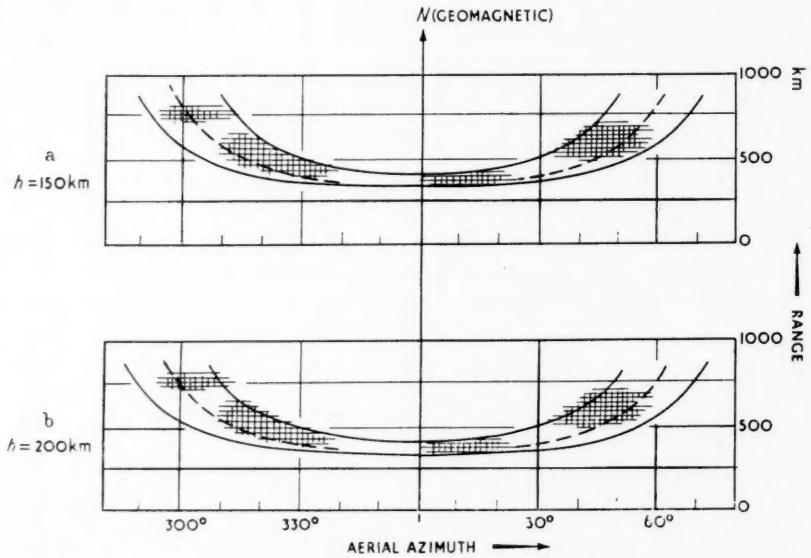

Fig. 6. Theoretical echo contours for a reflecting arc along a parallel of geomagnetic latitude at various heights, h, above the earth. The echoes of Fig. 2(c) are shown hatched, for comparison.

It may be argued that the true height may be above 150 km but that the actual auroral geometry differs from that assumed to an extent sufficient to give this apparent result. However, further evidence is obtained from a consideration of the variation of echo amplitude with range. If the reflections were uniform along the arc we would expect this to depend upon the variation of the elevation angle of the reflecting region (and hence of the effective aerial gain), the varying angle of incidence to the arc, and on the spatial attenuation. Fig. 7 gives the predicted echo amplitude as a function of range derived from the polar diagram of Fig. 1(b) combined with an assumed inverse square amplitude-range law. The detailed echo structure changed considerably in the aerial rotation period (6 min.), however superposition of Figs. 2(b) and 2(c) shows that echoes were observed at all ranges from the minimum (360 km) to a maximum of about 800 km. This implies a height below 125 km otherwise (see Fig. 7) there should be a gap corresponding to the first zero in elevation of the polar diagram. On the other hand the fact that

VOL. 5 1954

the most intense echoes occur in the range interval 500–600 km suggests that the height is not much below 125 km, it would certainly appear to be above 100 km.

Motion of reflecting centres

Changes with time in the echo structure were observed both on the rotating and fixed beam equipments (Figs. 2 and 3 respectively). In this latter case they manifest themselves in part as a displacement with time of the range of relatively intense

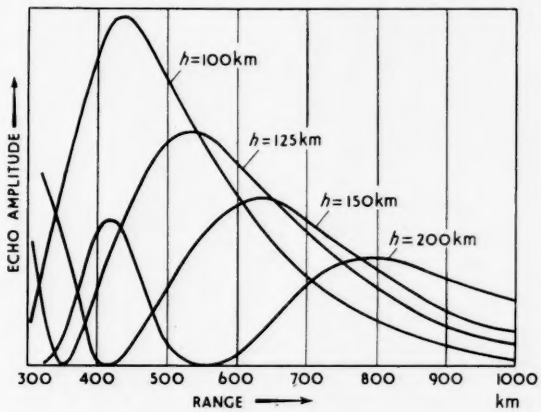

Fig. 7. Predicted variation of echo amplitude with range for various heights, h, of the reflecting region.

echoing regions corresponding to a receding line of sight velocity of about 1·3 km. sec^{-1}. The discrete echoes observed with the rotating beam equipment (which must be due to particularly localized centres of ionization) also exhibit range displacements; they occur in the NE at about 700 km (Fig. 2a) 500 and 700 km (Fig. 2b) and have approaching line of sight velocities of about 1·4, 0·8 and 0·8 km sec^{-1} respectively. These movements may be interpreted as motion of intense reflecting regions along the arc (due presumably to the motion of the ionizing agent rather than the mass motion of the ionized regions), in which case the motion is towards the west (the fixed beam is directed 68° W of N) with a true velocity of between 1 and 2 km sec^{-1}. It is interesting to note that Fig. 3 indicates the presence of several intense centres spaced by several hundred km which appear to follow one another along the arc.

4. The Aurora of May 15–16, 1953

Although the observations on this occasion cover a much longer period of time than those reported above, it is not possible to make such a detailed analysis since the speed of the recording film was several times slower and echoes were partly obscured by local electrical interference during most of the period of observation.

On May 15 diffuse echoes were received during three aerial rotations at, respectively, 2032 hr U.T. (ranges 500–700 km, signal amplitude of the order of twice noise), 2050 hr (ranges 500–600 km, 1·5 × noise echo) and 2113 hr when the signal

was just detectable. In every case the echoes appeared when the aerial beam was directed towards NE.

The sequence of diffuse echoes on May 16 commenced with a relatively intense echo in the NE (6 × noise) at 1513 hr which disappeared until 1542 hr when it was observed again in the NE, at about 1·5 × noise. Subsequently it was present almost continually until 1839 hr, the signal amplitude fluctuating between zero and about eight times the receiver noise level. From 1650 until 1839 hr echoes

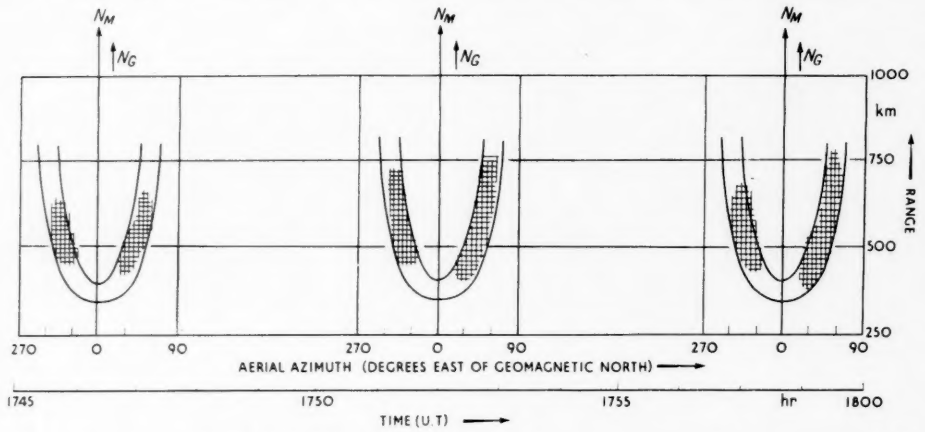

Fig. 9. The echoes of Fig. 8 (hatched) are superimposed on the theoretical echo contours (full lines) corresponding to a low elevation reflecting arc along a parallel of geomagnetic latitude. N_M — Geomagnetic North, N_G — Geographic North.

were visible in both the NE and NW but with relatively small amplitude in the latter direction. The echoes in the NE and NW formed together a horseshoe shape with the maximum echo amplitude occurring usually at a range of about 500 km. At no time were echoes visible at the base of the horseshoe, hence the range corresponding to this point was difficult to determine accurately; however, it appeared to vary between 320 and 380 km. A record showing echoes in both the NE and NW is shown in Fig. 8.

Interpretation of the echo structure

The echoes of Fig. 8 are sketched in Fig. 9 together with the theoretical echo limits for a low elevation reflecting arc along the same parallel of geomagnetic latitude as was assumed for the Oct. 15 aurora. Because of this close similarity with the Oct. 15 observations, the conclusion reached above that the echoes are due to direct, non-specular reflection applies here also.

The complete absence, during three hours' observation, of echoes at the estimated minimum range of the arc (350 km) is almost certainly due to the part of the arc corresponding to this range falling in the first zero in elevation of the aerial beam. Hence, referring to Fig. 7, the height of the region must be close to 125 km. This is supported by the maximum of echo intensity at about 500 km.

There is no discrete echo structure apparent, nor were echoes obtained with the fixed beam equipment referred to above, hence no line of sight velocities were

VOL. 5 1954

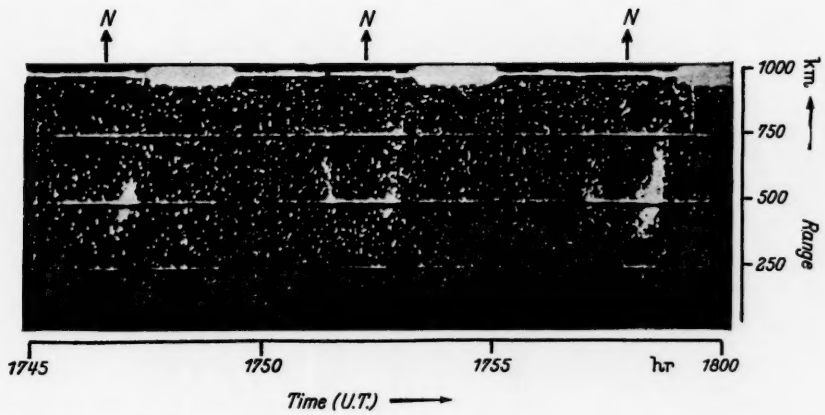

Fig. 8. Auroral echoes, May 16, 1953, observed during three successive aerial rotations.

VOL.
5
1954

obtained. However, the echo structure exhibited considerable change with time, which is quite likely due in part to motion along the arc of relatively intense reflecting regions.

5. Correlation of the Auroral Echoes with Other Phenomena

According to Paton and McInnes (1954), aurorae were visible during March–Dec. 1953 (the period covered in the present discussion) in, and south of, geomagnetic latitude 58° on the nights given in Table 2. The dates are grouped according to 27 day recurrence sequences and the southwards penetration is indicated by the geomagnetic latitudes in brackets.

Table 2. *Visual auroral observations, March–Dec.* 1953

D. March 8–9 (55); April 2–3 (58) and 3–4 (57)
E. May 16–17 (56); Sept. 1–2 (56), 2–3 (58), and 3–4 (56)
F. June 29–30 (58); Sept. 18–19 (58); Oct. 16–17 (57) and 17–18 (57); Nov. 12–13 (56).

It is clear from Table 2 that the radio observations coincide with the presence of aurorae in low geomagnetic latitudes on the same nights for the March 9 and May 16 echoes and on the following night for the Oct. 15 results. Drs. Paton and McInnes have kindly sent us detailed information of the visual observations on and near these dates, from which it appears that there was extensive obscuring cloud on the night 15–16 Oct. No radio echoes were observed on or near the other dates in Table 2, although the apparatus was operating on all occasions with the exception of the hours 1530–1700 on Nov. 12.

On all three occasions there was considerable magnetic activity. The K-indices recorded at Abinger, Eskdalemuir, and Lerwick for the appropriate periods are given in Table 3*.

The aurora of Oct. 15 is probably also associated with a Class I solar flare which was observed at the Royal Observatory, Edinburgh, on Oct. 14, 1025–1050 hr.

Table 3. *Indices of geomagnetic activity at Abinger (Ab), Eskdalemuir (Es) and Lerwick (Le)*

		Ab	Es	Le
March 9	0000–0300 hr	5	6	8
	0300–0600	2	2	4
May 15	1800–2100	6	6	8
May 16	1500–1800	5	5	6
	1800–2100	6	5	7
Oct. 15	1500–1800	6	7	7
	1800–2100	5	6	7

* J. Atmosph. Terr. Phys. 1953, **3**, 350; 1953, **4**, 86; 1954, **4**, 346.

6. Summary and Discussion

Auroral echoes were observed in March, May, and October of 1953 on a 4m radio echo equipment with a narrow beam aerial rotating continuously in a horizontal plane. The dates of the radio observations correlate closely with occasions on which aurorae were visible in, and south of, geomagnetic latitude 58°. The more extensive results on the latter two occasions admit of an extremely simple interpretation in terms of direct reflection from an ionized region which closely follows a parallel of geomagnetic latitude (in both cases about 3° to the north of Jodrell Bank). An outstanding feature is the tremendous extent of the arc from which echoes were obtained (exceeding 1000 km in both cases). It should be noted that the extreme limits are very likely set by geometrical factors (decreasing elevation and increasing range of the reflecting region) and hence may not represent the actual limits of the auroral activity.

The diffuse character of the echoes (their extension in range) can be accounted for by the finite width of the aerial beam, hence it is concluded that the horizontal thickness of the reflecting region is not more than 10–20 km. The echo geometry is inconsistent with the hypothesis of specular reflection from structures following the direction of the terrestrial magnetic field, and the suggested explanation is that the reflection occurs in a narrow height range (perhaps of the order of the atmospheric scale height) at about 125 km for the May 16 aurora and slightly less on Oct. 15.

VOL. 5 1954

Intense reflecting regions in the aurora of Oct. 15 exhibited line of sight movements of the order of 1 km sec^{-1}. This is consistent with a true velocity of 1–2 km sec^{-1} in the direction E to W along the arc. A comparison of this figure with the normal *E*-region wind velocities (50–100m sec^{-1}) and with the velocity of sound ($\sim$300m sec^{-1}) suggests that the motion is of the ionizing agent rather than a mass movement of the ionized gas. The regions responsible for the discrete echoes in the NE must have been less than a few tens of km in extent, hence, if the above hypothesis is true, the ionization must decay to a value below the limit of detection in a few tens of seconds after removal of the ionizing agent. A simple calculation* suggests that the actual decay time may be of the order of 1 sec or less.

Aspinall and Hawkins (1950), using a fixed aerial beam directed 68° W of N, obtained on various occasions line of sight velocities ranging between $-1{\cdot}5$ and $+3{\cdot}5$ km sec^{-1}. Hence, if we assume that the auroral geometry on these occasions was similar to that deduced above, we find that the motion may be in either direction (E–W or W–E) along the arc. Maxwell and Dagg (1953) have observed the scintillation of radio stars viewed through the auroral zone at times of bright visual aurorae and on two occasions in 1953 (March 8–9 and April 16–17) deduced drift velocities in the irregular region responsible for the scintillations in excess of 1 km sec^{-1} in the directions towards SE (March 8–9) and due west (April 16–17). The first date (March 8–9) coincides with the radio observations but on April 16–17

* The electron density will decay through recombination to the critical value n_c appropriate to the wavelength concerned in a time which is less than $\tau = (\alpha n_c)^{-1}$ where α $cm^3 sec^{-1}$ is the recombination coefficient. Taking $\alpha \simeq 10^{-8}$ (the *E*-region value), $n_c \simeq 7 \times 10^7$ cm^{-3} (for a wavelength of 4·1 m) we get $\tau \simeq 1$ sec.

no radio echoes were obtained on the rotating beam equipment which was, however, out of action for considerable periods.

MAXWELL (1953) finds the scale of the auroral irregularities causing the radio star scintillations to be a few km and it is tempting to suggest that the reflecting region consists of blobs of ionization of this order of size. We do not wish to enter into a detailed discussion of the mechanism of reflection, except to say that we support the conclusion of FORSYTH (1953) and SEATON (1954) that the electron density in the individual reflecting elements is above the critical value appropriate to the wavelength employed ($6{\cdot}7 \times 10^7 \mathrm{cm}^{-3}$ for a wavelength of 4·1 m).

The above interpretation may be compared with the characteristics of visual auroral formations as summarized by HARANG (1951). The distribution of the echoing region along a parallel of geomagnetic latitude suggests one of the various arc forms and it is interesting to note that HARANG describes an arc of 800 km length, extending from the sunlit to the dark region of the atmosphere. The height of the lower border of such arcs increases from about 100–110 km in the dark region to 120–130 km in the sunlit atmosphere. This latter figure is in excellent agreement with the height deduced above, indicating that the radio reflections occurred near the lower boundary. The changes in the structure of the echoes and the rapid movements of intense reflecting regions on Oct. 15 would be consistent with one of the fluctuating arc forms (pulsating and flashing). It should be noted that the radio observations, particularly on Oct. 15, suggest that the arc lies within at least a few degrees of the magnetic meridian whereas visual observations (HARANG, 1951; JENSEN and CURRIE, 1953) indicate a considerable spread in the orientation measured from the magnetic meridian to the westward extension of the arc, with a mean between 97° and 100°.

Acknowledgments—This work was supported by a grant from the Department of Scientific and Industrial Research. We wish to thank Drs. J. PATON and B. MCINNES of the Royal Observatory, Edinburgh, for providing details of visual auroral observations and also the Royal Observatory, Edinburgh, for the solar flare data. We are indebted to Mr. T. DAVIDSON who assisted with the October observations and to other colleagues at Jodrell Bank, including Dr A. MAXWELL, for helpful discussions. One of us (T. R. K.) is indebted to Messrs. I.C.I. Ltd. for a Research Fellowship.

REFERENCES

ASPINALL, A., and HAWKINS, G. S.	1950	J. Brit. Astron. Assoc. **60,** 130
BOOKER, H. G., GARTLEIN, C. W., and NICHOLS, B.	1953	School of Electrical Engineering, Cornell University Research Report EE 169
CAIN, J.	1953	J. Geophys. Res. **58,** 377
CHAPMAN, S.	1952	J. Atmosph. Terr. Phys. **3,** 1
CURRIE, B. W., FORSYTH, P. A., and VAWTER, F. E.	1953	J. Geophys. Res. **58,** 179
FORSYTH, P. A.	1953	J. Geophys. Res. **58,** 53
HARANG, L.	1951	"The Aurorae," The International Astrophysics Series (Chapman and Hall, London)
HARANG, L., and LANDMARK, B.	1954	J. Atmosph. Terr. Phys. **4,** 322
HELLGREN, G., and MEOS, J.	1952	Tellus **4,** 249
JENSEN, R. E., and CURRIE, B. W.	1953	J. Geophys. Res. **58,** 201

Lovell, A. C. B., Clegg, J. A., and Ellyett, C. D.	1947	Nature (London) **160,** 372
Maxwell, A.	1953	Ph.D. Thesis, University of Manchester
Maxwell, A., and Dagg, M.	1954	Phil. Mag. **45,** 551
McKinley, D. W. R., and Millman, P.	1953	Canad. J. Phys. **31,** 171
Paton, J., and McInnes, B.	1954	Observatory **74,** 46
Seaton, M. J.	1954	J. Atmosph. Terr. Phys. **4,** 285

VOL.
5
1954

Journal of Atmospheric and Terrestrial Physics, 1954, Vol. 5, pp. 201 to 210. Pergamon Press Ltd., London

On the interpretation of the apparent ionization distribution in the ionosphere

W. R. PIGGOTT

(Official communication from D.S.I.R. Radio Research Station, Slough)

(*Received* 28 *May* 1954)

ABSTRACT

Methods of deducing the highest and lowest ionization distributions which are consistent with a given $h'f$ pattern are indicated and the sources of error when using rapid methods of analysis are briefly discussed. Some examples are given.

1. INTRODUCTION

It has been known for many years (APPLETON, 1930; DE GROOT, 1930) that it is often impossible to deduce a unique function for the variation of height of reflection with frequency from the observed variation of the apparent height with frequency ($h'f$ pattern). It is, therefore, interesting to find the limits of the zone of heights in which must lie all distributions capable of giving the $h'f$ pattern and to discuss the factors which determine the width of this zone. Furthermore, popular methods of analysis (BOOKER and SEATON, 1940; APPLETON and BEYNON, 1940 and 1947; MANNING 1947; KELSO, 1952) often produce results which differ appreciably. Some of these differences are due to the approximations inherent in the methods and some due to the existence of the zone of equivalent distributions. It is convenient to call the zone which includes both deviations "the zone of possible error." The purpose of this paper is to summarize the main limitations and the more insidious experimental difficulties encountered when it is desired to analyse numerous ionization distributions with height.

The discussion given below neglects effects due to the earth's magnetic field. These may be introduced by noting that the main effect of the field is to alter the apparent thickness of the ionization distributions without greatly changing the heights at which they are maximum. This will increase the gaps between successive layers. An adequate appreciation of the magnitude of the differences between the apparent distributions with and without the magnetic field has been given by SHINN and WHALE (1952).

2. LIMITING IONIZATION DISTRIBUTIONS

When the height to density function of the ionization distribution is single-valued the actual height of reflection, h_v, of any frequency, f_v, may be deduced from the apparent height pattern:

$$h' = \phi(f) \tag{1}$$

using

$$h_v = \phi(0) + \frac{2}{\pi}\int_0^{f_v} \frac{\phi(f)\,df}{\sqrt{f_v^2 - f^2}} \tag{2}$$

If the ionization distribution has a maximum with a critical frequency, f_0, h_v is indeterminate for $f_v \geqslant f_0$. We wish to find the upper and lower limits of $h_v, f \geqslant f_0$.

It is not difficult to see that these are both unique and may be found with the aid of equation (2).

The upper limit is obtained by minimizing the group retardation in the upper layer at $f = f_0$ and maximizing the group retardation below this layer. For the upper layer

$$h_v = h(f_0) \quad \text{for} \quad f_v \leqslant f_0 \tag{3}$$

Maximum group retardation below the point of reflection is obtained by replacing the actual distribution above the maximum of the lower layer by a slab of constant density having a critical frequency equal to f_0. The thickness of this slab may be easily deduced by noting that

$$h_v \geqslant h(f_0) \quad \text{for all} \quad f_v > f_0 \tag{4}$$

If we now subtract the group retardation due to the slab and the lower layer distribution we obtained the reduced $h'f$ pattern:

$$\left.\begin{aligned} h' &= \phi_1(f), \quad f \geqslant f_0 \\ h' &= h(f_0), \quad f \leqslant f_0 \end{aligned}\right\} \tag{5}$$

which may be solved uniquely using equation (2).

The lowest distribution consistent with the observed $h'f$ pattern is obtained by maximizing the ionization density at the lower heights so that it increases continuously from the maximum of the lower layer. Such distributions are consistent with equation (2) and hence if equation (2) is applied to the original $h'f$ pattern, $h' = \phi(f)$, the lowest limit distribution, will be obtained.

The fundamental difference between the two ionization distributions is the existence of an empty gap between the top of the slab ionization and the bottom of the upper reflecting layer. If this gap were absent both curves would be identical and the solution unique. The width of the zone of equivalence at a frequency, f, above f_0 is proportional to this gap and to a function of f/f_0. It is obvious that this width is critically dependent on the shape of $h' = \phi(f)$ when $f \fallingdotseq f_0$. Since this part of the trace is often complicated or missing in practical records it is often necessary to neglect the slab entirely. This increases the possible error appreciably.

3. Methods of Determining the Height of Reflection

Methods of determining the height of reflection from an $h'f$ pattern fall into two groups:

(a) Techniques based on the integral equation (equation (2)), the restriction being ignored.

(b) Techniques based on matching the $h'f$ patterns observed with those calculated from simplified models.

It is convenient to call group (a) "integral methods" and group (b) "model methods." In most practical cases, integral methods give distributions near the lower boundary of the indeterminate zone and model methods solutions near the upper boundary but considerable departures are possible when the technique used is inadequate.

VOL. 5 1954

In general, it is difficult to delineate small changes in shape by integral methods and approximate techniques are adequate only when the height does not change rapidly between sampling points. Model techniques can define shape very accurately but are very sensitive to small errors in measuring frequency or frequency ratios. Care must also be taken that the actual ionization distribution may be represented with reasonable accuracy by the type of model used. In both cases the analysis is greatly simplified if the original $h'f$ pattern is expressed using linear h' and logarithmic frequency scales.

(a) *Integral methods*

RYDBECK (1940) and MANNING (1947) have shown that equation (2) can be evaluated neatly by putting $f = f_v \sin\theta$ and solving the Schlömilch integral, equation (6), graphically:

$$h_v = \phi(0) + \frac{2}{\pi}\int_0^{\pi/2} \phi(f_v \sin\theta)\,.\,d\theta \tag{6}$$

In practice $\phi(f)$ is replotted, for each f_v, in the form $\phi(f_v \sin\theta) : \theta$ and the areas under the curves found. This procedure may be considerably shortened, at the expense of some loss in accuracy, by using one of the classical methods of deducing the area under a curve from the magnitudes at a limited number of ordinates.

Thus we may apply SIMPSON's rule to the original $h'f$ curve by observing the apparent heights on the frequencies fk,

$$f_k = f_v \sin\left(\frac{k\pi}{2n}\right) \quad \text{for } k = 0, 1 \ldots n \tag{7}$$

giving

$$h_v = \frac{1}{n}\left\{\sum_{k=0}^{k=n-1} h'_k + \frac{h'_n - h'_0}{2}\right\} \tag{8}$$

It is usually more convenient to determine the average from the ordinates at the middle of each sampling area, i.e. using

$$f = f_v \sin\left(\frac{2k-1}{2n}\cdot\frac{\pi}{2}\right) \quad \text{for } k = 1, 2 \ldots n \tag{9}$$

and

$$h_v = \frac{1}{n}\sum_{1}^{n} h'_k \tag{10}$$

This enables the height h_v to be determined even when h'_n, equation (8), is infinite, i.e. at a critical frequency.

Equations (9) and (10) are identical with those obtained by KELSO (1952) who applied orthogonal functions to solve equation (2) by successive approximations. It is clear that his method is equivalent to a sampling process for finding the area under the curve of equation (6). This work has provoked interesting discussions about the optimum method of sampling (MANNING, 1953; SHINN, 1953; KELSO, 1954) and about sampling techniques which introduce the effects of the earth's magnetic field (KELSO, 1954). These are, however, really more applicable to accurate analyses of small samples of observations than to our problems.

Sampling methods cannot give an accurate solution when the width of the sampling band is large and h' varies considerably over the band. In particular, systematic errors may be expected whenever a sampling frequency is near f_0 where $\phi(f_0) \to \infty$. As f_v increases from $f_v = f_0$, each of the sampling frequencies, f_k, becomes equal to f_0 in sequence. The value of h'_k increases from values appropriate to the lower layer to infinity, when $f_k = f_0$, and then falls to values

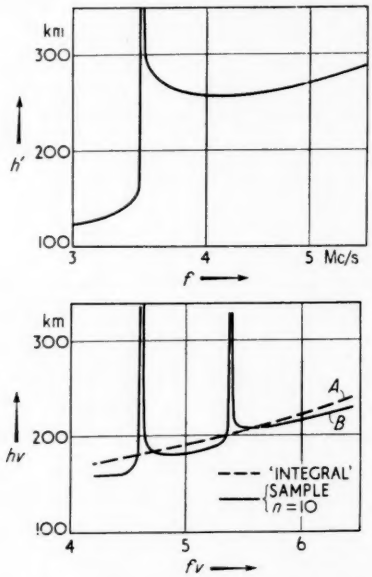

Fig. 1. Typical $h'.f$ pattern between E and F. Sampling distortion when $n = 10$.

appropriate for the upper layer. Thus h_v increases to infinity and then decreases to a level about $\frac{1}{n}(h'_{k+1} - h'_{k-1})$ above its original value. This gives a large error at $f_k = f_0$ superposed on a step-like variation, Fig. 1. The analytical procedure makes the algebraical sum of the areas between the apparent and true $h_v : f$ curve zero but as the infinities can seldom be plotted accurately, the deduced most probable curve will normally lie rather low. A reasonably smooth, but displaced, curve can be obtained by ignoring the group retardation near $f = f_0$.

When using scales or sliders to deduce ionization distributions for a large number of records it is usually advantageous to include the boundaries of the zones which are being represented by each ordinate. These are delineated, of course, by the additional ordinates obtained by replacing 'n' by '$2n$' in equation 7 or 9. The probable importance of the sampling error (Fig. 1) is then immediately obvious.

(b) *Model methods*

Model methods can be used to deduce either the ionization distribution for important parts of the reflecting strata or to represent ionization below the point of reflection. Since the variation of density near the maximum of a layer is often

VOL. 5 1954

parabolic the parabolic models developed by BOOKER and SEATON (1940) and APPLETON and BEYNON (1940 and 1947) are used widely to deduce the position of the maximum density in the ionized layers. Slabs of constant density are frequently valuable for representing the large group retardation sometimes present near the minimum frequency reflected in the upper layer and for upper limit calculation. Linear ionization gradients are also useful for application to $h'f$ patterns obtained at low latitudes. RATCLIFFE (1951a, b) has exploited model methods for finding the shape and ionization content of the F_2 layer.

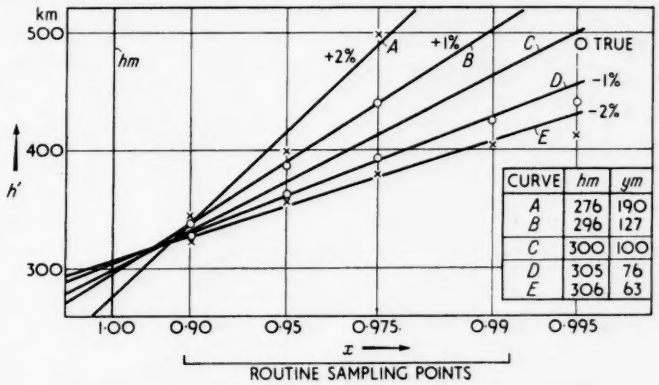

Fig. 2. Errors in h_m and y_m due to incorrect critical frequency. APPLETON–BEYNON analysis.

It is important to note that the deduction of layer shape and ionization content by model techniques is remarkably sensitive to very small errors in frequency measurement. We will illustrate this using a typical example analysed by the APPLETON-BEYNON technique, Fig. 2, but it should be noted that analogous errors may occur whenever the frequency variation along a record differs from its assumed law. The curve matching procedure, in which theoretical and observed $h'f$ curves are compared directly with the aid of suitable transparencies, shares the errors almost equally between h_m and y_m and is less sensitive to small errors in the frequency variation than the example given.

None of the models in common use provide exact determinations of upper or lower boundary curves but, provided they are used discreetly, they frequently enable approximate solutions to be obtained quickly. Thus if the distribution in the upper layer is approximately parabolic, standard parabolic methods can give a solution which is remarkably close to the true upper limit curve. The position of the lower limit curve can also be estimated by calculating one value of h_v near f_0F_2 from equation (2) and then moving the parabola of best fit down in height till it goes through this point. When the model matches a limited part of the distribution only these techniques can introduce large errors of either sign and the procedure in section 2 must be employed.

4. SOME EXAMPLES OF IONIZATION DISTRIBUTIONS

We now illustrate these general remarks by examining a few ionization distributions using both model and integral methods.

(a) *A simple maximum height model*

We assume an E and an F layer having parabolic distributions of density with height over those heights at which the ionization can be detected and no ionization at any other height. Using the typical values of the critical frequencies f_0E, f_0F, heights of maximum density h_mE, h_mF and apparent semithicknesses y_mE, y_mF given in Table 1 below, we deduce the $h'f$ pattern and then use parabolic and integral methods to deduce the apparent position of the ionization. These give the results shown in Fig. 3 and summarized in Table 1.

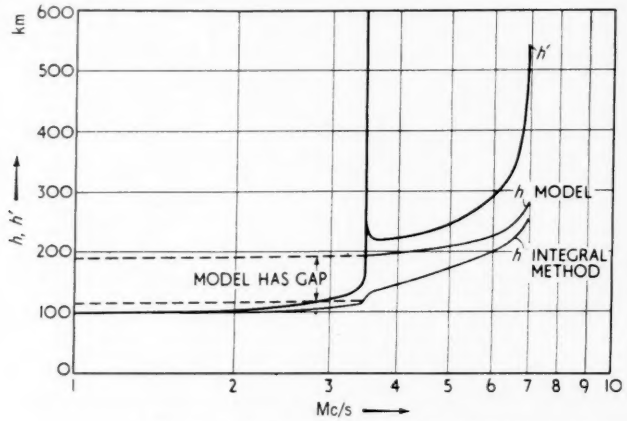

Fig. 3. A simple maximum height model.

Table 1

	f_0E	h_mE	y_mE	f_0F	h_mF	y_mF
	Mc/s	*km*	*km*	*Mc/s*	*km*	*km*
Model	3·5	120	20	7·0	280	100
Parabolic analysis	3·5	120	20	7·0	282	100
Integral analysis	3·5	120	20	7·0	255	100
Difference between curves: Just above f_0E c 70 km; Just below f_0F c 27 km						

Thus with $f_0F = 2f_0E$ and a gap of 73 km between h_mE and the bottom of F we have a possible error of 27 km in deducing h_m near f_0F.

Applying these models to find the maximum usable frequency (M.U.F.) for 4000 km we find that the possible range of error in M.U.F. is 8%, the parabola giving factors which could be too low, the integral method, factors which could be too high. While a complete analysis of the M.U.F. factors allowing for the ionization in the lower part of the layer would decrease this range, such analyses are impractical for our present purposes, all simple and rapid methods of M.U.F.

VOL. 5 1954

computation implying some simplification of the actual ionization distribution and thus introducing errors up to the limits indicated.

Although the values of h_mE and h_mF are representative, it is impossible that this distribution could occur in practice and hence the actual range of error physically likely is appreciably smaller.

If $\Delta\, hEF$ is the size of the gap and we are using a sampling technique with k of n frequencies reflected from the E layer the range in h_mF, $\Delta\, h_mF$, is

$$\Delta\, h_mF \doteqdot \frac{k}{n}(\Delta\, hEF) \tag{11}$$

In many practical cases we may estimate $\Delta\, hEF$ from the apparent constants of the parabolae of best fit giving:

$$h_mF \doteqdot \frac{k}{n}(h_mF - y_mF - h_mE) \tag{12}$$

with an accuracy of about

$$\pm \frac{1}{k} \cdot \Delta\, h_mF$$

This rule must be used with caution when the F layer appears to be abnormally thick.

(b) *Model "a" with a constant density slab between E and F*

Apart from a very small error due to $\frac{dN}{dh}$ being finite at the bottom of F this is a maximum height distribution. It is also a minimum height distribution, i.e. the zone of error should be zero. This is found to be true when exact methods are used but the large group retardation near $f = f_0$ introduces serious errors in the approximation solutions. Thus a parabolic solution neglecting ionization below F region, is 14 km high and a smooth curve through ten-point KELSO or SIMPSON rule approximation may be 20 km low. The group retardation found near f_0E considerably exceeds that observed in practice. This suggests that the layers overlap to a much greater extent than in this model.

(c) *A three-layer model*

An $h'f$ pattern closely similar to those found in temperate latitudes can be built up using a semiparabolic E layer with $f_0E = 3{\cdot}5$ Mc/s, $h_mE = 120$ km and $y_mE = 20$ km together with an F_1 layer represented by the lower part of the parabola with $f_0F_1 = 4{\cdot}9$ Mc/s, $h_mF_1 = 200$ km, $y_mF_1 = 100$ km cut off at $f = 4{\cdot}87$ Mc/s, $h = 188$ km and $f = 3{\cdot}5$ Mc/s, $h = 130$ km. The F_2 layer is the upper part of the parabola $f_0F_2 = 7{\cdot}0$ Mc/s, $h_mF_2 = 260$ km, $y_mF_2 = 100$ km truncated at $h = 188$ km. This is an upper limit model with an EF gap of 10 km and no ionization between E and F (Fig. 4). The group retardation just above f_0E is slightly less than is found in practice—as would be expected—and this makes $h'F_1$ rather low. Otherwise this pattern is fairly representative of those found in temperate latitudes.

The variation of h' with frequency above 6 Mc/s is indistinguishable from that

for model "a" for which h_mF_2 was 280 km. Thus the F_1 region has caused the apparent value of h_mF_2 to be increased by about 20 km. Using BOOKER-SEATON methods the corresponding value is 288 km. The lower limit curve lies between about 5 km below the model near f_0F_2 and 10 km below it just above f_0E. The zone of possible error using popular techniques greatly exceeds the zone of equivalent distributions.

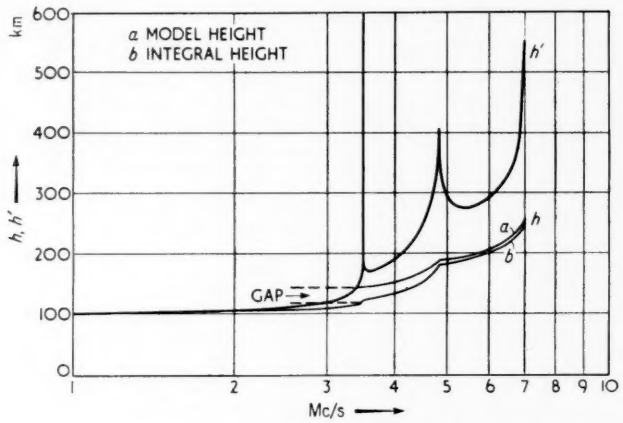

Fig. 4. An E, F_1, F_2 model.

It is interesting to note that the minimum apparent height of F_1, $h'F_1$, is very sensitive to the presence of ionization between E and F. If the layers are joined by a slab of constant density with $f_0 = f_0E$—thus making the height curve determinate—the apparent values of $h'F_1$ increase by 20 km, h_mF_1 by 10 km, and h_mF_2 by 5 km. The $h'f$ curve is now quite typical. For these conditions there is no zone of equivalent distributions but the errors due to the use of approximate methods are practically unaltered.

The apparent value of h_mF_1 is about 8 km above the model value if the true critical frequency is used, y_mF_1 being almost correct. Using the apparent value which is 1% low decreases y_mF_1 by 15% and increases h_mF_1 by about 5%. Increasing the overlap so that the apparent value of f_0F_1 is 2% low introduces prohibitive errors in both determinations. The shape of the F_1–F_2 discontinuity cannot be determined using sampling techniques with $n = 10$ and is difficult using MANNING's method.

Similar phenomena will also occur when dense Es forms low in the E layer.

(d) *An almost linear F model*

It is instructive to examine a minimum height model in which the major part of the F layer is not parabolic. We assume a semi-parabolic E layer, as in model "a", with an F layer having a linear ionization gradient from h_mE until it is tangential to a small parabolic nose at $f_v = 6{\cdot}8$ Mc/s, $h_v = 278$ km. The nose is the top of the parabola, $f_0F = 7{\cdot}0$ Mc/s, $h_mF = 300$ km, $y_mF = 100$ km. The integral method and its approximations all give the model exactly, as would be expected. An APPLETON-BEYNON analysis gives $h_mF = 400$ km, $y_mF = 85$ km. The range

VOL. 5 1954

Δh_m is 100 km, a fairly typical value for linear distributions. The $h'f$ curve, Fig. 5, shows remarkably little group retardation near f_0E and the surprisingly high value of 170 km for $h'F$. The general form of the F curve is similar to an equatorial "thick" layer trace suggesting that these layers are not necessarily high. The probable error in deducing h_m by parabolic methods may be as high as 30% in this case. It is remarkable that a linear layer, having a slope different to the slope—at corresponding frequencies—of a parabola fitted to the nose of a layer, may alter the apparent value of h_m to a comparable extent as the F_1 group retardation for storm conditions which greatly modifies the appearance of the $h'f$ pattern!

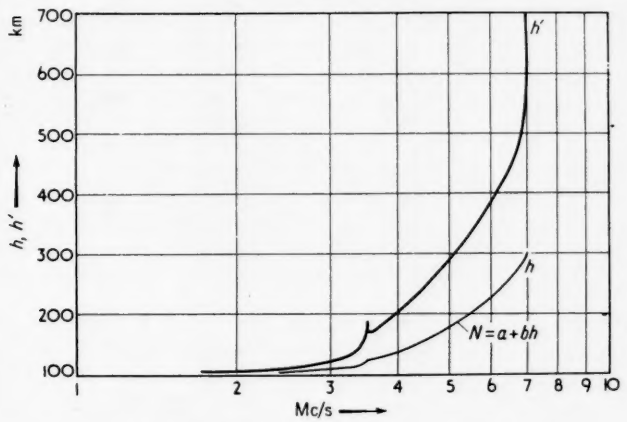

Fig. 5. An almost linear F model ($N = a + bh$).

(e) *Sporadic E*

Totally reflecting sporadic E greatly increases the zone of indeterminancy for the F structure, the upper boundary curve being dependent on the minimum apparent height of the F reflection. Thus the maximum width is approximately equal to the minimum distance between the E and F traces. The lower boundary curve is greatly distorted and physically improbable. The analysis is formally similar to that of model "a" above and probable parameters can be estimated from this model substituting the actual EF minimum separation for the 73 km gap and changing all other height intervals proportionately.

Acknowledgments—The work described above was carried out as part of the programme of the Radio Research Board. This paper is published by permission of the Director of Radio Research of the Department of Scientific and Industrial Research.

References

Appleton, E. V.	1930	Some notes on wireless methods of investigating the electrical structure of the upper atmosphere. Proc. Phys. Soc. **42**, 321
Appleton, E. V., and Beynon, W. J. G.	1940	The application of ionospheric data to radio communication problems. Part I. Proc. Phys. Soc. **52**, 518
	1947	ibid. Part II. Proc. Phys. Soc. **59**, 58

BOOKER, H. G., and SEATON, S. L.	1940	The relation between the actual and virtual ionospheric height. Phys. Rev. **57,** 87
DE GROOT, W.	1930	Some remarks on the analogy of certain cases of propagation of E.M. waves and the motion of a particle in a potential field. Phil. Mag. **10,** 521
KELSO, J. M.	1952	A procedure for determining the vertical distribution of the electron density in the ionosphere. J. Geophys. Res. **57,** 357
	1954	The determination of the electron density distribution of an ionospheric layer in the presence of an external magnetic field. J. Atmosph. Terr. Phys. **5,** 11
MANNING, L. A.	1947	The determination of ionospheric electron distribution. Proc. Inst. Radio Engrs. **35,** 1203
	1953	Discussion of the KELSO paper: A procedure for determining the vertical distribution of the electron density in the ionosphere. J. Geophys. Res. **58,** 117
RATCLIFFE, J. A.	1951a	A quick method for analysing ionospheric records. J. Geophys. Res. **56,** 463
	1951b	Some regularities in the F_2 region of the ionosphere. J. Geophys. Res. **56,** 487
RYDBECK, O.	1940	The propagation of E.M. waves in an ionized medium and the calculation of the true heights of the ionized layers of the atmosphere. Phil. Mag. **30,** 282
SHINN, D. H.	1953	Further remarks on KELSO's paper. J. Geophys. Res. **58,** 416
SHINN, D. H., and WHALE, H. A.	1952	Group velocities and group heights from the magneto-ionic theory. J. Atmosph. Terr. Phys. **2,** 85

VOL. 5 1954

Journal of Atmospheric and Terrestrial Physics, 1954, Vol. 5, pp. 211 to 218. Pergamon Press Ltd., London

Magnetic self-focussed solar ion streams as the cause of aurorae

W. H. BENNETT and E. O. HULBURT
Naval Research Laboratory, Washington, D.C., U.S.A.

(*Received* 7 *June* 1954)

ABSTRACT

The theory of magnetic self-focussed solar ion streams assumes that a jet of equal numbers of fast moving positive ions and negative electrons emerges from the sun. As the jet proceeds through the corona the fast electrons are scattered out more rapidly than the ions and are replaced continually by slow electrons. The excess of fast ions over fast electrons results in an electric current whose magnetic field repels the remaining fast electrons from the stream but exerts little magnetic force on the slow electrons. The excess positive charge electrically repels the slow positive ions, but exerts little magnetic force on them. Thus the stream continues to repel fast electrons and slow ions while retaining fast ions and slow electrons. At all times all parts of the stream and surrounding gas are closely (but not exactly) electrically neutral. For a proton stream which carries sufficient energy for an aurora the density of space ionization between the sun and the earth is calculated to be at least about 10^{-4} electron ion pairs cm^{-3} to support magnetic self-focussing. The speed of the auroral ions is estimated to be about 10^{10} cm/sec. The auroral display is supposed to be due both to energy transferred to the atmosphere from the ions on their way in and to atmospheric oxygen and nitrogen particles blown outward, and made luminous, as a result of the energy and charge of the ions dissipated in the upper atmosphere.

Recently a new solar particle theory of the aurora was outlined (BENNETT and HULBURT, 1954) which owed its existence to two things, the one being recent experiments which gave for the first time direct evidence that high speed ions were present in the upper atmosphere in the region of aurorae, and the other being the introduction of a new idea into the theory, the idea of magnetic self-focussing of ion streams, which removed a number of the difficulties which have beset the older particles theories. It is the purpose here to discuss further details of the theory.

The new experimental evidence was that of MEINEL (1951) and of VAN ALLEN *et al.* (1954). With spectrographs of great light gathering power MEINEL discovered that the H_α line of hydrogen was present for 20 to 30 minutes in the pale greenish quiet arc which often occurs at the beginning of an auroral display. He observed a broadening but no Doppler shift in H_α when observing toward the magnetic horizon, but when observing toward the magnetic zenith he observed a Doppler shift indicating that protons of speeds of at least $3{\cdot}3 \times 10^8$ cm/sec, and probably much greater, were entering the earth's upper atmosphere. By means of cosmic ray equipment on high altitude rockets MEREDITH, VAN ALLEN, and GOTTLIEB discovered ionic particles having a penetrating power greater than that of 18 Mev protons, and less than 100 Mev protons at north magnetic latitudes 64° and 74°, which are near the zone of maximum auroral frequency, and did not observe such ionic particles at north magnetic latitudes 89° and 56° which are remote from the auroral zone. BOWEN (1954) reported observations of solar flares with 1 to 7 metre waves which he interpreted as indicating that ions were leaving the sun at velocities one-fifth to one-tenth of the velocity of light.

In the present theory it is assumed that the sun emits a conical jet of an electrically neutral mixture of electrons and positive ions, that the solar atmosphere is completely ionized and electrically neutral, and that the space between the sun

and the earth is filled with an ionized, electrically neutral gas. As the jet rises through the sun's atmosphere the electrons are scattered out of the jet more rapidly than the ions are, due to collisions with the charged particles of the solar atmosphere. To calculate the filtering action of the solar atmosphere on the jet we use the scattering formulae of THOMAS (1928) for the deceleration of a charged particle of speed v and mass m in a completely ionized, electrically neutral gas of particles of mass m' and particle density n cm^{-3}. All particles are singly charged with the electronic charge e. v is assumed to be considerably greater than the speeds of the gas particles.

Substituting THOMAS' Eqs. (2·1) and (5·3) into (4·31) leads to

$$dv/dt = 4\pi e^4 An \{\log (2B/\log B) - \gamma - 1\}/mv^2, \tag{1}$$

where $A = (m + m')/mm'$,

$B = 3v^6/4\pi e^6 A^3 n$,

and $\gamma = 0{\cdot}5772$ is EULER's constant.

Approximately, within 2 per cent error, (1) may be written

$$dv/dt = (4\pi e^4 An/mv^2) \log (2B/\log B). \tag{2}$$

The distance ds which the particle moves in time dt is $ds = vdt$ or

$$ds = vdv/(dv/dt). \tag{3}$$

Let s be the range, i.e. the distance which the particle moves when decelerated from a speed v to 0. Let m and M be the mass of an electron and a proton, respectively. The range s_e of an electron in a mixture of equal densities n of slow electrons and protons is

$$s_e = \int_0^v \frac{m^2 v^3 dv/4\pi e^4 n}{2 \log (2B_1/\log B_1) + \log (2B_2/\log B_2)}, \tag{4}$$

and the range s_p of a proton in a similar mixture is

$$s_p = \int_0^v \frac{Mv^3 dv/4\pi e^4 n}{(1/m) \log (2B_2/\log B_2) + (2/M) \log (2B_3/\log B_3)}. \tag{5}$$

where $B_1 = 3m^3 v^6/32\pi e^6 n$,

$B_2 = 3m^3 v^6/4\pi e^6 n$,

$B_3 = 3M^3 v^6/32\pi e^6 n$. (6)

Values of s_e and s_p were obtained from (4) and (5) by numerical integration and are given in cm in Tables 1a and 1b, respectively.* Since the distance from the sun to the earth is $1{\cdot}49 \times 10^{13}$ cm it follows from Tables 1a and 1b that the average particle density of a proton electron gas between the sun and the earth must be less than about 10^2 and 10^{10} for solar protons of speeds 10^8 and 10^{10} cm/sec,

* We are indebted to Dr. T. C. DOYLE and Mr. J. H. HANCOCK of the Mathematics Department for these integrations.

VOL. 5 1954

respectively, to reach the earth, and less than about 10^{-2} and 10^{6} for solar electrons of speeds 10^{8} and 10^{10} to reach the earth.

In Table 2 are given average values (HAGEN, 1951) of the particle density N in the solar atmosphere at an altitude h km above the photosphere and the total number $\overline{N}$ of particles in a 1 cm² column above h. If the solar atmosphere (the corona) is composed mainly of protons and an equal number of electrons, it is

Table 1a. Range s_e of electrons of speed v in electron-proton gas of density n

n	1	10^{6}	10^{12}	10^{18}
v				
10^{8} cm/sec	$2{\cdot}4 \times 10^{11}$	$3{\cdot}4 \times 10^{5}$	$6{\cdot}0 \times 10^{-1}$	$2{\cdot}2 \times 10^{-6}$ cm
10^{9}	$1{\cdot}8 \times 10^{15}$	$2{\cdot}4 \times 10^{9}$	$3{\cdot}4 \times 10^{3}$	$6{\cdot}0 \times 10^{-3}$
10^{10}	$1{\cdot}4 \times 10^{19}$	$1{\cdot}8 \times 10^{13}$	$2{\cdot}4 \times 10^{7}$	$3{\cdot}4 \times 10^{1}$

Table 1b. Range s_p of protons of speed v in electron-proton gas of density n

n	1	10^{6}	10^{12}	10^{18}
v				
10^{8} cm/sec	$1{\cdot}3 \times 10^{15}$	$1{\cdot}8 \times 10^{9}$	$3{\cdot}0 \times 10^{3}$	$9{\cdot}0 \times 10^{-3}$ cm
10^{9}	$9{\cdot}6 \times 10^{18}$	$1{\cdot}3 \times 10^{13}$	$1{\cdot}8 \times 10^{7}$	$3{\cdot}0 \times 10^{1}$
10^{10}	$7{\cdot}9 \times 10^{22}$	$9{\cdot}6 \times 10^{16}$	$1{\cdot}3 \times 10^{11}$	$1{\cdot}8 \times 10^{5}$

seen that electrons of speeds up to 10^{10} cm/sec emerging from the photosphere will be stopped in the corona, and that photospheric protons must have velocities greater than 5×10^{9} cm/sec in order to get through the solar atmosphere. These conclusions will be modified if the density in the initial front of the jet is so great as to make a range calculation inapplicable, or if there are other complications as

Table 2. Average values of N and $\overline{N}$ in the solar atmosphere

Altitude h above photosphere	N	$\overline{N}$
0 km	10^{12}	$1{\cdot}2 \times 10^{20}$
2000	10^{11}	$2{\cdot}8 \times 10^{18}$
7000	10^{10}	$6{\cdot}3 \times 10^{17}$
15000	10^{9}	$2{\cdot}8 \times 10^{17}$
100000	10^{8}	$2{\cdot}4 \times 10^{16}$
400000	10^{7}	10^{16}
1000000	10^{6}	10^{15}

chromospheric magnetic fields or wide deviations of solar atmospheric densities from average values.

The features of magnetically self-focussing ion streams have been studied in the laboratory (WARE, 1951; COUSINS and WARE, 1951) and the theory has been worked out in some detail (BENNETT, 1934); we describe here only the essential physics of the mechanism. As has just been explained the solar atmosphere scatters out the electrons from the jet more rapidly than the ions, producing an excess of positive ions in the jet. Two actions then set in. The first action arises from the fact that the fast moving positive ions of the jet constitute an electric current which has a magnetic field, the magnetic lines of force being circles around the axis of the current. Fast moving positive ions are constrained by the magnetic field to swing in and move in oscillatory paths along the axis; fast moving negative ions and electrons are magnetically repelled and thrown away from the current axis. Thus the positive stream keeps its positive charges together by its own magnetic attraction; it is said to be "magnetically self-focussed." The second action is electrostatic. The excess positive charge of the current attracts electrons from the ionized gas through which the jet is moving; this counteracts the tendency of the positive ions to disperse each other by electrostatic repulsion. The two processes go on simultaneously and continually, and the fast stream of positive ions progresses in a straight line through space without expanding. At all times all parts of the stream and of the surrounding gas are closely (but not exactly) electrostatically neutral, and the stream progresses as an electric current in a straight line until it comes into the influence of the magnetic field of the earth.

VOL. 5 1954

It has been shown (BENNETT, 1934) that the condition for magnetic self-focussing is that the total electric current i in the stream of fast particles must be greater than

$$i = c^2 m v_t^2 / ev, \tag{6}$$

where v is the velocity of the particles along the axis of the stream and v_t is the root mean square velocity transverse to the axis. m and e (e.s.u.) are the respective mass and charge of the particle and c is the velocity of light. (6) merely expresses the condition that the magnetic field of the current i is sufficiently great to divert into the stream particles of velocity v which diverge in a cone of half angle α. Neglecting the effect of temperature

$$v_t = \sqrt{2} v \tan \alpha,$$

and

$$i = 2c^2 (m/e) v \tan^2 \alpha. \tag{7}$$

In Table 3 are given values of α calculated from (7) for various values of i for protons. The Table brings out the fact that the cone angle of a jet which becomes magnetically focussed is small and increases with the current in the jet and decreases with the proton speed.

In order for a magnetically self-focussed positive ion stream to propagate itself through space it must be able to acquire slow electrons from the interplanetary gas in approximately the same density as the density of the fast protons in the stream. The density is estimated by assuming that a portion of the energy

of the stream appears as auroral light. The typical brightness of a quiet auroral arc during August 1949, was observed to be about 3×10^{-6} lambert, equivalent to an emission of order 1 erg cm^{-2} sec^{-1}; auroral rays and bright patches of a display were much more intense than the quiet arc. During an active display of August 3, 4, the illumination on a horizontal surface was $1{\cdot}7 \times 10^{-3}$ foot candles, equivalent to about 10^{-1} erg cm^{-2} sec^{-1}; much higher values occasionally occurred

Table 3. *Half angle* α *of cone, minutes of arc*

	$i = 10$ *amp*	1000 *amp*	100000 *amp*
v			
10^8 cm/sec	24	237	2076
10^9	7·5	75	738
10^{10}	2·4	24	237

in other displays (CURRIE, 1950). For the purpose of calculation we assume that an auroral display emits an energy of illumination of 1 erg cm^{-2} sec^{-1} over a circular area 100 km in diameter, and that the energy is supplied by 1 per cent of the kinetic energy of the proton stream. Then the number of protons cm^{-3} and the total current in the stream is given in Table 4 for various proton speeds. The particle densities of column 2, Table 4, are those necessary in the space between the sun and the earth

Table 4. *Density and current of proton stream*

velocity $cm\ sec^{-1}$	*protons per* cm^3	*current amperes*
10^8	120	150000
10^9	0·12	1500
10^{10}	0.00012	15

in order that the stream progress with magnetic self-focussing. The densities are perhaps an over-estimate because the diameter of the proton stream is probably greater in space than it is at the earth because of the focussing action of the earth's magnetic field. It is hardly necessary to point out that although most of the present calculations are based on protons, mainly because these were observed, the theory is not limited to protons but would apply as well to other types of ions if these were observed.

If the space between the earth and the sun were a perfect vacuum the solar jet could not progress as a magnetically self-focussed stream. It would immediately disperse because of the electrostatic repulsive forces of its like charged ions, or if the ions picked up neutralizing electrons from the solar atmosphere the stream would progress as an electrostatically neutral ionized cloud in the manner contemplated in the magnetic storm theory of CHAPMAN and FERRARO (1941). If on the other hand the particle densities of space were those of Table 4, or greater, the neutral ionized cloud theory is untenable because magnetic self-focussing sets in.

The system comprised of the sun, the earth, and the intervening space is a stable electrical system. The loss of positive charge from the sun in the fast auroral ion stream is compensated by a slow drift of positive space ionization to the sun and by a slow drift of negative ionization from the sun to space, so that the sun as a whole remains electrically neutral. Likewise the earth, although it receives a positive charge from the stream, remains electrically neutral because of the charge compensation it receives from the space ionization. In the present state of development of the theory and observation it is difficult to estimate the diameter of the solar ion stream in space. Nor is the relation clearly known between the diameter of the stream and the geographical extent of the aurora and the duration of the display.

Although the speed with which the solar protons approach the earth can not be determined with certainty from available experimental evidence, a speed of 10^9 or 10^{10} cm/sec seems indicated. The maximum value which MEINEL (1951) determined from the Doppler spread of H_α in the quiet arc was $3{\cdot}3 \times 10^8$ cm/sec, but he pointed out that the speed outside the earth's atmosphere must be much greater, and that the value $3{\cdot}3 \times 10^8$ was merely the value to which the protons had been slowed down in the atmosphere before they picked up electrons and got into the excited state necessary for the emission of H_α. The quiet greenish white auroral arc, which often is the precursor of auroral displays of rays and of moving and coloured forms, appears at altitudes of about 80 to 140 km. If it is assumed that the lower boundary of the arc at 80 km marks the end of the range of the incoming protons one encounters a difficulty. The vertical thickness of the air above 80 km is 10 cm at NTP (HAVENS *et al.*, 1953), and to penetrate this thickness a proton speed of $2{\cdot}2 \times 10^9$ cm/sec is required. However, the calculations of STÖRMER (1917) have shown that a proton must approach the earth with a speed of 10^{10} cm/sec in order to reach the zone of maximum auroral frequency at magnetic latitude 65° to 70°; with such speeds the proton range in air is 25 metres, and the protons would plunge down to an altitude of about 40 km before being stopped. This difficulty is of long standing; several suggestions may be made towards its explanation. In the first place the lower boundary of the quiet arc may not be related directly to the range of the incoming protons, but may be controlled by atmospheric processes of light emission and densities of excited atoms. This seems reasonable, for the lower boundary always appears to be at about 80 km at all latitudes and longitudes where its height has been measured. Secondly, one may point out that the STÖRMER calculation refers to a single charged particle, and that an electric current has greater magnetic stiffness than the particles of which it is composed; however, the exact calculation of the bending of a current of particles by the earth's magnetic field is difficult and has not been done. Thirdly one may suppose that some of the incoming auroral particles are not protons but are heavier ions. These, because of their greater magnetic stiffness, might enter lower magnetic latitudes without plunging too deeply into the atmosphere. But this idea can not be examined critically because the ranges of high speed ions in air are not completely known; and experimental search by means of rockets for such ions in low latitude auroral displays might yield valuable results.

Fourthly, the earth is a rotating magnet, and due to the effect of unipolar

VOL. 5 1954

induction. from the point of view of an observer at rest outside of the earth there is an electric field directed from each pole of the earth to the equator. This field will cause positive ions shot from the sun to reach lower latitudes than those given by a STÖRMER calculation. The magnitude of the effect depends upon the mass and velocity of the ion, and a rough estimate indicates that the effect may be appreciable. Complete calculations should be made but these may be difficult. Finally, one may invent equatorial ring currents, as was done by STÖRMER, which modify the terrestrial magnetic field and permit auroral particles to enter lower latitudes; this seems speculative.

It is known that magnetic storms may be associated with visible solar flares, and it seems fairly certain that a radiation from the flare travels to the earth and causes the magnetic storm. From a list of 55 cases of intense solar flares the average time interval from the appearance of the flare to the beginning of the magnetic storm was about 22 ± 4 hours for the very great storms and 30 ± 15 hours for all storms (NEWTON and JACKSON, 1951). 20 and 30 hours correspond to speeds of 2×10^8 and $1{\cdot}3 \times 10^8$ cm/sec, respectively, of the radiation. The temporal relations between magnetic storms and aurorae are confused. HULBURT (1929) and DAVIES (1931) concluded that auroral displays occurred about a day after the commencement of world-wide magnetic storms. This would put them about two days after a solar flare, which would indicate a speed of about 10^8 cm/sec for the flare radiation to travel to the earth. Such a low velocity is probably inadmissible, and one may conclude that the *observed visible* inceptions of flare and aurora are indirectly related. VEGARD (1916) compared auroral observations at Bossekop, Norway, with simultaneous magnetic records from the same locality and found that the hourly interval of strongest aurorae usually coincided with an interval of high magnetic activity, but he also found cases where strong aurorae appeared fairly near the zenith without marked magnetic effect.

No detailed explanation has yet been worked out of the manner in which the energy of the incoming solar protons is converted into aurora light. Protons of speeds even as great as 10^{10} cm/sec follow the lines of the earth's magnetic field in rather tight spirals, the radii of the spiral being about 20 and 30 km at altitudes 100 and 1000 km, respectively. It is possible that some of the energy of the protons on their way in through the atmosphere is transferred to the atmospheric gases causing oxygen and nitrogen emissions. It is also possible that when the protons are finally stopped in the upper atmosphere, due to their charges and absorbed energy, oxygen and nitrogen particles are ejected outward to great heights and, upon becoming luminous, give rise to the rays and moving clouds of an aurora display. But the details of the luminous processes are complicated and more experiments are needed before they are understood. For example, BRANSCOMB, SHALEK, and BONNER (1954) concluded from their experiments with 100 kv protons and hydrogen atoms projected into air at a few mm pressure that it was quite likely that more than one mechanism was responsible for auroral excitation of nitrogen bands and that the balance between the mechanisms varied with time and location. A theoretical study of excitation processes of permitted and forbidden atomic lines in aurorae is being undertaken by SEATON (1954) which should lead to valuable conclusions about this part of auroral theory.

References

Bennett, W. H.	1934	Phys. Rev. **45,** 890
Bennett, W. H., and Hulburt, E. O.	1954	Phys. Rev., July 15
Branscomb, L. M., Shalek, R. J., and Bonner, T. W.	1954	Trans. Amer. Geophys. Un. **35,** 107
Bowen, E. G.	1954	J. Geophys. Res. **59,** 163
Chapman S., and Ferraro, V. C. A.	1941	Terr. Mag. **46,** 1
Cousins, S. W., and Ware, A. A.	1951	Proc. Phys. Soc. **64,** 159
Currie, B. W.	1950	Trans. Amer. Geophys. Un. **31,** 539
Davies, F. T.	1931	Terr. Mag. **36,** 199
Hagen, A. J.	1951	Astrophys. J. **113,** 547
Havens, R. J., Knoll, R. T., and LaGow, H. E.	1953	J. Geophys. Res. **27,** 59
Hulburt, E. O.	1929	Phys. Rev. **34,** 344
Meinel, A. B.	1951a	Astrophys. J. **113,** 50
	1951b	Mem. Soc. Roy. Sci. Liège **12,** 203
Newton, H. W., and Jackson, W.	1951	Relations entre les phènoménes solaires et terrestres, 7th Rapport, 107
Seaton, M. J.	1954	J. Atmosph. Terr. Phys. **4,** 294
Störmer, C.	1917	Terr. Mag. **22,** 23
Thomas, L. H.	1928	Proc. Roy. Soc. **A 121,** 464
Van Allen, J. A., Meredith, L. M., and Gottlieb, M. B.	1954	J. Geophys. Res. In press
Vegard, L.	1916a	Vid. Akad. Skr. I. No. 13
	1916b	Ann. Physik. **50,** 853
Ware, A. A.	1951	Phil. Trans. Roy. Soc. **243,** 197

VOL.
5
1954

Journal of Atmospheric and Terrestrial Physics, 1954, Vol. 5, pp. 219 to 229. Pergamon Press Ltd., London

High-altitude free balloon flying

N. C. Barford, G. Davis[1], A. J. Herz[2], R. M. Tennent[3], and D. A. Tidman[2]

Imperial College of Science and Technology, London

(*Received* 12 *June* 1954)

ABSTRACT

An account is given of experience gained in the high altitude flying of extensible balloons, and a theory is derived, based on the elementary gas laws, which agrees well with this. Both theory and practice show that it is very difficult to decide how much free lift to give to closed extensible balloons at launching in order to achieve level flight at a predetermined height. This difficulty may be overcome by using a valve which opens the balloon when it reaches the desired altitude, and the reliability of the balloon then becomes the chief consideration.

Laboratory experiments were also carried out to provide quantitative information about the properties of various balloon fabrics.

Introduction

In the study of the cosmic radiation it has become increasingly important to expose nuclear-research emulsion and other apparatus at very high altitudes in the atmosphere.

As nuclear-research emulsions are continuously recording, an ideal flight is one in which the balloon rises rapidly to the ceiling altitude and remains there floating for several hours. A release mechanism is used to jettison the equipment after a suitable time. Prolonged flights of this type have been obtained in the United States, Great Britain, and Sweden by the use of very large open-necked constant-volume plastic balloons. Flights lasting six to eight hours at altitudes around 90,000 feet are common with this technique. However, the ceiling altitudes depend upon the size of the balloons, and to obtain level flights at over 100,000 feet the balloons used would have to be extremely large and expensive. In addition, because of their great size, it is very difficult to launch these balloons unless the ground wind is very light.

Because of this difficulty in launching open-necked plastic balloons, and because of their great expense, it was decided to concentrate on the cheaper closed extensible ones. These are made either of natural rubber (latex) or of artificial rubber (neoprene), and they are similar to those used for meteorological purposes, but larger. They are comparatively robust and can be launched in winds up to fifteen knots. Their unextended (flaccid) diameter is about twelve feet; they expand to 25–50 feet diameter before bursting.

The balloons used were made from three different materials, supplied by three different companies, as follows:

1. Latex	2 kg and 4·25 kg	Guide Bridge Rubber Co. ("Beritex")
	2·4 kg	Dewey & Almy Chemical Co. ("Darex")
2. Neoprene	2·4 kg	Dewey & Almy ("Darex")
3. Neoprene	4·5 kg	Molded Latex Products Inc., U.S.A. ("Kaysam")

[1] Now at the Technion, Haifa.
[2] Now at the University of Sydney.
[3] Now at the University of Leeds.

Neoprene (Darex) requires to be heated before the balloon is inflated, neoprene (Kaysam) is postplasticized and does not have to be heated.

Theory

(i) *General*

Applying the gas laws it is easily shown that the relations between the pressure altitude and the other variables involved are

$$p = \left(\frac{p_g T_i L}{T_g V} + \rho_H p_\sigma\right) \Big/ \left(\frac{\rho_A T_i}{T} - \rho_H\right) \tag{1}$$

$$p = \frac{p_g T_i L_g}{T_g V(\rho_A - \rho_H)} - p_\sigma \tag{2}$$

where p = pressure altitude (g cm^{-2})

p_g = pressure at ground level (g cm^{-2})

p_σ = excess pressure caused by tension in balloon (g cm^{-2})

T_i = absolute temperature of gas in balloon at altitude p

T_g = absolute temperature of gas in balloon at ground level

T = absolute temperature of the air at altitude p

V = volume of balloon at altitude p (cm^3)

L = lift of the gas in the balloon at altitude p (gram weight)

L_g = lift of the gas in the balloon at ground level (gram weight)

ρ_H = density of balloon gas at p_g, T_g

ρ_A = density of air at p_g, T_g

At ground level, the temperature of the gas is assumed to be equal to that of the surrounding air, and $p_\sigma = 0$.

Some of the constants in relations (1) and (2) have to be determined experimentally, others have to be estimated from the scanty data available. The most recent measurements of the temperature of the upper atmosphere are those of the Rocket Panel (1952). For an altitude of 100,000 feet a.s.l. (10·5 g cm^{-2}), the temperature is about 230°K. The experiments described below show that the temperature inside the balloon is about 40° above ambient, due to the solar radiation. Accordingly, we have taken the following values for the constants:

$T = 230$°K $\qquad p_g = 1000$ g cm^{-2}

$T_i = 270$°K $\qquad \rho_A = 1{\cdot}22 \times 10^{-3}$ g cm^{-3}

$T_g = 288$°K $\qquad \rho_H = 8{\cdot}5 \times 10^{-5}$ g cm^{-3}

The balloon is assumed to be filled with hydrogen. With these values we obtain, from (1) and (2),

$$p = 6{\cdot}96 \times 10^5 \frac{L}{V} + 0{\cdot}063 p_\sigma \tag{3}$$

$$p = 8{\cdot}33 \times 10^5 \frac{L_g}{V} - p_\sigma \tag{4}$$

VOL. 5 1954

Relation (3) is very insensitive to variations in T_i and the term containing p_a can usually be neglected. The opposite is true of relation (4) and this has important practical consequences.

Suppose we require the balloon to float at pressure p_f with a total load W. Equation (3) gives the volume of the balloon at ceiling. Provided this is safely less than the bursting value, equation (4) can now be used to determine L_g, the lift at ground level. However, because of the uncertainties in T_i and p_a it is difficult to be sure that the calculated value of L_g will give the required floating altitude.

Thus, a normal 2400 g neoprene balloon with a greatest "safe" volume of $4{\cdot}3 \times 10^8$ cm^3 and carrying an external load of 2000 g would have, from equation (3), a maximum altitude at pressure $p_f = 7{\cdot}1$ g cm^{-2}. If we take $p_a = 0{\cdot}3$ g cm^{-2}, equation (4) then indicates a ground lift of 3830 g. (Since this is less than the total load of 4400 g, a subsidiary balloon would be required to raise the assembly to somewhere near the ceiling altitude when it could be released.) But if T_i were 280°K instead of 270°K the balloon would rise to an altitude given by $p_f = 3{\cdot}7$ g cm^{-2} where it would have a volume of $8{\cdot}3 \times 10^8$ cm^3—well above the safe value.

We have made several flights using two closed balloons, one of which was to carry the load at constant level after the other had burst. Only one flight (No. 4, see Fig. 4 below) was moderately successful, but this was most likely due to chance.

The probability of getting a level flight with closed balloons can be increased by using clusters of small balloons. It is intended that these should burst one after the other, thus decreasing the lift in small steps until it is nearly equal to the load (Clarke and Korff, 1941; Clark, 1952; Taylor, 1953). This technique, however, appears to be unreliable and it does not give predictable results.

Flights made at night differ from daytime ones because T_i equals T. Owing to the effect of the tension of the balloon fabric, the lift decreases continuously as the balloon rises, and L is related to L_g by the relation

$$L = \frac{L_g}{\rho_A - \rho_H}\left(\frac{p\rho_A}{p + p_a} - \rho_H\right) \tag{5}$$

The balloon will float when the lift equals the load, and for that case we may write approximately

$$W = L_g p/(p + p_a) \tag{6}$$

Thus, in principle, a sustained night flight could be achieved with a single closed balloon if the ground lift were suitably chosen. It is found, however, that the rate of ascent would be very small. A successful flight with a variant of this method has been made by Professor von Friesen (Lund, Sweden).

(ii) *The performance of balloons fitted with gas-release valves*

In view of the difficulties of closed-balloon techniques, the possibilities of balloons fitted with gas-release valves were explored. If a balloon is fitted with a valve which permits gas to escape when its size exceeds a predetermined safe value, the balloon will always attain equilibrium at the altitude corresponding to the safety

volume. Such a balloon behaves like an open-necked balloon at altitude, but at ground level it has the advantages of a closed balloon.

The floating altitude of a valved balloon is determined by its size and the external load. Since, as we shall see later, p_σ is less than 1 g cm^{-2}, the effect of surface tension in determining the altitude can be neglected in practice and equation (3) may be replaced by

$$p = 6{\cdot}96 \times 10^5 \, L/V \tag{7}$$

The greatest possible altitude is, of course, obtained when there is no external load and L is equal to the weight of the balloon. For a given type and thickness of fabric and a given "safe" extension ratio, the pressure at this altitude is inversely proportional to the unstretched diameter of the balloon.

The maximum altitude is approached in practice by using more and more balloons for lifting a given external load, although it is always better to use a few large balloons than many small ones of the same fabric if they are available.

The valve orifice must be large enough to permit the gas to flow at a rate that will stop the balloon from expanding once the safety volume has been reached. It can be shown that the area of the orifice, A, must satisfy the relation

$$A \geq \frac{u}{(2gp)^{\frac{1}{2}}} \left(\frac{\rho_H}{\rho_A - \rho_H} L_g V \right)^{\frac{1}{2}} \frac{\rho_A T_g}{p_g T} \frac{p}{(p + p_\sigma)} \tag{8}$$

where u is the rate of ascent at the moment at which the valve opens (cm sec^{-1}), and g is introduced because the pressures are measured in g cm^{-2} and not dynes cm^{-2}. If we assume that $p_\sigma = 0{\cdot}2$ g cm^{-2}, $u = 750$ cm sec^{-1}, $L_g = 6000$ g, then relation (7) gives $A \geq 25$ cm^2. Our valve, when fully open, has an area of 40 cm^2, and it has proved satisfactory in use.

A further danger lies in the possibility of overshoot due to the inertia of the balloon assembly. This causes the balloon to lose too much gas, and it will therefore float at an altitude lower than p_f. We have made an approximate calculation of this effect, and it shows that the floating altitude is reduced to p_f', where

$$p_f' = p_f \frac{p_\sigma}{p_\sigma - 0{\cdot}9\Delta p} \tag{9}$$

and where Δp is the overshoot in terms of pressure.

It is clear that an overshoot comparable to the balloon-tension pressure would be serious. A calculation shows that with a typical single-balloon assembly it would be about 0·016 g cm^{-2} and approximately independent of altitude. At a height of 100,000 feet this corresponds to an overshoot of 85 feet and a loss of altitude of 1800 feet. Overshoot will not, therefore, impair the performance of valved balloons seriously.

Laboratory Experiments

(i) *Balloon materials*

We have frequently mentioned the excess pressure, p_σ, caused by the tension in the balloon fabric. This section is devoted to the experiments which were performed in the laboratory in order to determine the magnitude of this quantity and its variation with temperature and extension.

VOL. 5 1954

A sheet of the material to be investigated was clamped between two plates of brass, the upper one having a circular hole, about 30 cm in diameter. The material was inflated by air entering through a tube soldered into the lower plate, and expanded in the form of a bubble through the hole in the upper plate. The excess pressure inside the bubble and its radius of curvature were measured. The tension, σ, was then calculated for each value of the linear extension ratio, λ. The σ, λ relations for our three materials are shown in Fig. 1 for temperature of $+18°C$ and $-18°C$. It can be seen that the tension is sensitive to temperature. For

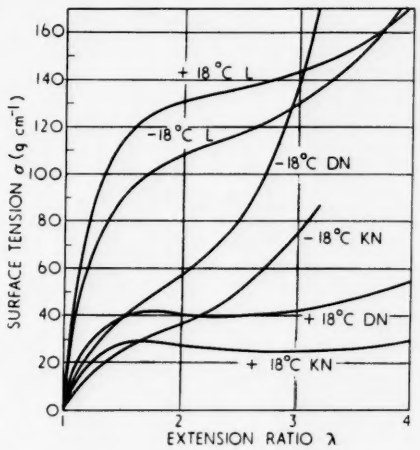

Fig. 1. Performance of Darex Latex (L), Darex Neoprene (DN), and Kaysam Neoprene (KN).

extension ratios greater than those shown (i.e. $\lambda > 4$) it rapidly increases with decreasing temperature. In our flights we have usually chosen the safety volume to correspond to $\lambda = 2{\cdot}5$; the values of p_σ for a 2400-gm balloon at this volume are given in Table 1. The radius of curvature, R, was chosen to be equal approximately to that of a complete balloon at high altitude.

Table 1. *Values of* p_σ *for balloon fabrics at* $\lambda = 2{\cdot}5$ *and* $R = 470$ *cm* ($g\ cm^{-2}$)

	$+18°C$	$-18°C$
Latex	0·58	0·50
Darex neoprene	0·17	0·34
Kaysam neoprene	0·11	0·21

The results obtained in the stratosphere chamber (see below) indicate that the mean temperature of the balloon fabric at about 100,000 feet is approximately $-18°C$, while at 120,000 feet it is about $0°C$. For calculations the value $p_\sigma = 0{\cdot}2$ g cm^{-2} has been chosen as representing a lower limit to the tension pressure.

(ii) *Release mechanisms*

Initially balloons were released by cutting through the cord with a hot wire which was switched across a battery by a pre-set clock. However, the purely mechanical clockwork release, described by Leide and von Friesen (1953), has the advantage that it could suffer from no difficulties due to the freezing of batteries and tests showed it to be quite reliable when cleaned and lubricated carefully. The movements we used were taken from Smith "Victory" alarm clocks and were treated as follows:

(a) Wash in CCl_4, then degrease in CCl_4 vapour bath.

(b) Immerse the whole movement in a 3% solution of silicone oil D.C.200/100c.s. in CCl_4 to achieve slight uniform oiling.

(c) Lubricate each bearing individually with a 20% solution of D.C.200/100c.s. in CCl_4.

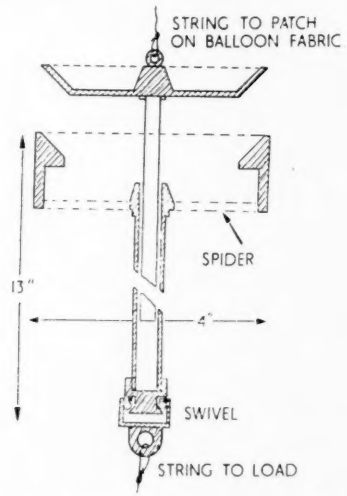

Fig. 2. The gas-release valve for balloons.

(iii) *Balloon valves*

The valve is designed to have an effective open area well in excess of the required 25 cm^2 (see above). Its external diameter is 4 inches, and it is cemented into the neck of the Darex or Kaysam balloons instead of the normal filling tube. A diagram of the valve is shown in Fig. 2. It is made from dural and requires a force of about 340 g wt. to open it. The stem is made long to allow the balloon to oscillate without straining it too much.

The valve is controlled by a string stretched across the diameter of the balloon, attached on the top to a patch of cotton material, about 8 inches in diameter, cemented to the inside of the balloon. The cement we used was "Boscoprene 2400/1" (manufactured by the B.B. Chemical Co.).

A similar valve suitable for flights to altitudes around 90,000 feet a.s.l. has recently been described by Hopper and Wilson (1953).

VOL. 5 1954

(iv) *The stratosphere-chamber tests*

A balloon, when floating at high altitude during daytime is subjected to radiation intensities of about 20, 50, and 60 watts per square foot in the ultra-violet, visible, and infra-red regions respectively. Apart from heating the fabrics and the gas inside the balloon, there is reason to believe that the solar radiation affects the properties of the fabric. Accordingly, we carried out stratosphere-chamber tests which were directed towards finding the temperature of the gas and the performance of the fabrics under conditions closely approximating those of the upper atmosphere.

The chamber was kindly placed at our disposal by the directors of Messrs. Vickers-Armstrongs Limited. It could be evacuated to a pressure of 70 g cm^{-2}, and the temperature in it could be reduced to −60°C. The equipment to be tested was placed into the chamber at −60°C and remained there during evacuation. It was not possible to reproduce the conditions of a balloon flight where the temperature and pressure decrease simultaneously.

To simulate the conditions of a daytime flight, two large ultra-violet discharge tubes and twelve infra-red lamps were disposed at distances such that the total radiation was equivalent to that due to the sun in the upper atmosphere.

In all, twenty-four specimens of fabric were tested, four at a time, in the chamber. Each was inflated in the manner already described and its extension ratio determined from the height of the bubble.

Table 2 shows the mean linear extension ratios at which various specimens burst.

Table 2

Material	*Bursting extension*	
	With radiation	*Without radiation*
Darex latex	4·7	5·6
Darex neoprene	4·2	4·3
Kaysam neoprene	5·6	—

These values are in reasonable agreement with those found for sounding balloons (W.M.O., 1953; Scrase, 1949) and are well in excess of the safety value chosen in our balloon flights. It would, therefore, be expected that balloons intended to float at this "safe" extension would not burst, yet in practice they often do so. This may be caused by local imperfections in the fabric (which would make the probability of premature bursting proportional to the surface area of the balloon), or by fatigue effects due to continued stretching.

Another possible cause of failure is the change from turbulent to streamline flow of the air relative to the balloon. It has been noted that this occurs with sounding balloons (W.M.O., 1953) and with our balloons and rates of ascent (750–1250 ft min) would occur around 70,000 to 100,000 ft. This might well result in excessive stresses being imposed on the balloons.

In the presence of radiation, all the latex specimens developed slow leaks, but

neoprene specimens did not leak noticeably before they burst. In the one experiment without radiation, the latex had a greatly improved performance; no leaks developed, and the bursting extension was higher than in the presence of radiation (see Table 2).

At the lowest temperatures, the tension of the neoprene reached about ten times the room-temperature value. The tension of the natural latex showed no significant change.

During all the tests with radiation, the temperature of the gas inside the bubbles was measured. Fig. 3 shows the results, plotted as function of the chamber pressure. It can be seen that at low pressures the temperature rises as the pressure drops, reaching $-25°C$ at 70 g cm^{-2}. As the ambient temperature was

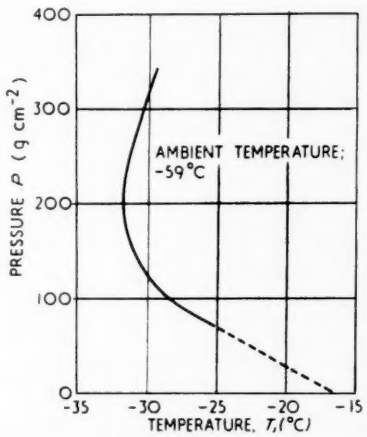

Fig. 3. Internal balloon temperature vs. stratosphere chamber pressure.

$-59°C$ throughout, the difference must be attributed to the radiation. Unfortunately, the chamber pressure could not be reduced below 70 g cm^{-2}, but extrapolation of the curve in Fig. 3 suggests that the gas temperature at zero pressure would be about 40° above ambient. If this is correct, then it is reasonable to assume that the temperature of the balloon fabric will be about 20° above ambient.

Balloon Flights

In all twenty-one balloon flights were launched by the Imperial College group, from February 1951 until May 1953, mostly from the meteorological station at Larkhill, but also from the stations at Fazackerly and Hemsby. Upper wind forecasting was sufficiently good and radar tracking accurate enough to enable us to recover the apparatus from all except one flight, often on the same day as the flight. Because of the distances involved, it was found useful to attach two radar reflectors (type Umbrawind Mk. 3) to the balloon assembly instead of the usual one.

The altitudes of the balloons were given by the radar readings; they were translated into pressure measurements by means of tables (Montgomery, 1949).

VOL. 5 1954

For the first ten flights pressures were also transmitted to the launching station by means of a radio-sonde. Since these agreed excellently with those obtained from the radar readings, the use of the radio-sonde was discontinued in order to save weight.

For the first nine flights two closed balloons were sent up, attached to each other, with an electrical switch designed to cut away whichever balloon burst first. The results are given in Fig. 4. Flight 2 is not recorded as a squall tore both balloons away from the rest of the equipment at 3000 feet.

FLIGHT No.	1	2	3	4	5	6	7	8	9
LATEX (KG)	4·25	2·0	2·0	2·0				4·25	
DAREX NEOPRENE (KG)				3·3	2·4	2·4	2·4		3·0

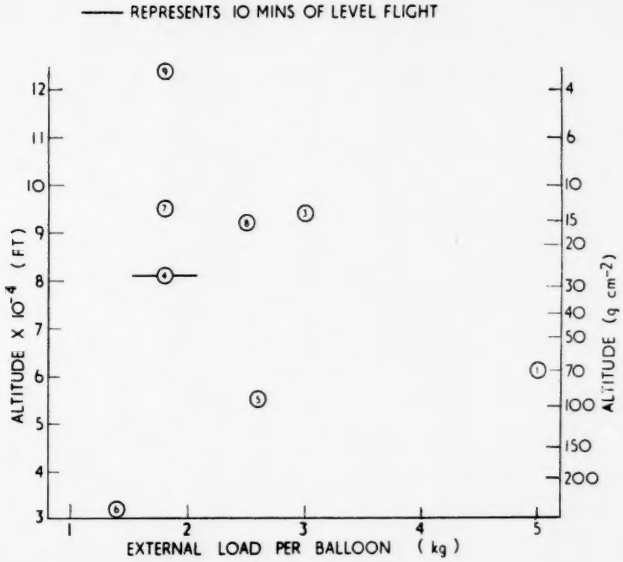

Fig. 4. Flights with closed balloons.

For flight 4 one latex and one neoprene balloon were used and for the remainder two of the same type. The material and weight of the balloons are given in the accompanying table. The numbered circle gives the maximum altitude reached and the horizontal line the altitude and duration of level flight.

In several cases the two balloons burst simultaneously or within a few minutes of each other. Only in flight 4, when two different balloons were used, did the technique succeed in giving level flight. In flight 7 the first balloon burst at 86,000 feet and the second 20 minutes later when it had been floating at 95,000 feet for a few minutes. Flight 9 is notable because the balloons rose to 124,000 feet, possibly an altitude record for balloon flights in this country.

The remaining flights were all made using balloons fitted with valves. The results are summarized in Fig. 5. Flight 15 is not given as the balloon was lost by the radar at 10,000 feet.

It can be seen that in those cases where level flight was achieved, the overshoot

was small and the floating altitude close to the theoretical value, which was calculated from the external load and the length of the valve string, using equation (7). In flight 19 one balloon burst at 62,000 feet. The predicted floating altitude for the remaining balloon was then 89,000 feet which is very close to that observed.

In all the flights, except in two cases when valved balloons were used, the flights terminated through a balloon bursting or developing a leak.

In the first fifteen flights, electrical release mechanisms were used but, because of doubts about their reliability, they were later replaced by mechanical ones of the von Friesen type.

FLIGHT No.	10	11	12	13	14	15	16	17	18	19	20	21
DAREX NEOPRENE (KG)	2·6	2·4	2·7	2·6	2·4	2·4	2·6	2·2	3·2	2·2		
KAYSAM NEOPRENE (KG)											4·6	4·5
'SAFE' EXTENSION RATIO λ	2·0	2·5	2·25	2·5	2·5	2·5	2·5	2·5	2·5	2·5	2·7	2·7

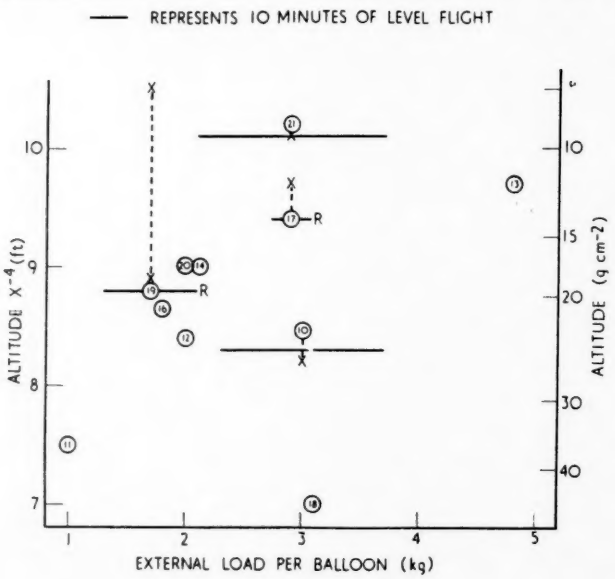

Fig. 5. Flights with valved balloons.

One balloon was used for each flight except numbers 11 and 19 when three and two of the same type were used respectively. The material and weight of the balloons and the allowed extension ratio are given in the accompanying table. The numbered circle gives the maximum altitude reached. Where level flight was achieved, its altitude and duration are given by a horizontal line and the predicted floating altitude by a cross. Flights terminated by a release mechanism are marked *R*.

Discussion and Conclusions

The work described here has confirmed that it is possible to obtain level flights at predetermined altitudes with extensible balloons. The theoretical relations which we have derived agree very well with the experimental results, and we are satisfied that they describe the experimental situation with sufficient accuracy.

VOL. 5 1954

We have shown that a single large extensible balloon can take a payload of about 3000 g to 90,000–100,000 feet for a level flight, and it follows that it should be possible to take similar loads to altitudes around 120,000 feet with clusters of two or three valved balloons. The maximum altitude accessible to the large plastic constant-volume "Skyhook" balloons is only about 105,000 feet.

An additional advantage of the extensible balloons is that they can be launched easily, and that the whole of the equipment can be loaded onto a small truck. It is thus possible to launch these balloons from practically any accessible site.

Against those advantages must be placed the fact that the materials available for the balloons are not wholly reliable. By day, in the presence of radiation, latex appears to crack and develop small leaks so that sustained level flights with latex balloons are improbable, although a high ceiling may be obtained. Neoprene does not leak in this way. However, the measurements indicate that latex retains its elasticity at low temperatures to a greater degree than neoprene so that the former may be the better material for night flights.

For both types of material the balloons often burst prematurely. Whether this is due to thin spots occurring during the making of the balloon, or to a weakening of the materials when stretched for long periods in the presence of radiation, or to excessive strains encountered while the balloon is ascending at high altitude, we cannot yet say.

Acknowledgments—We are most grateful to the Meteorological Office for their constant help and co-operation during the flights. The radar tracking was done by Meteorological Office staff, often during their off-duty periods, and we take this opportunity to thank them. In particular, we should like to thank the officers in charge of the meteorological stations we used: Mr. C. E. Britton, Mr. A. Lee, and Mr. H. E. Butler.

We should like to thank the Directors of Vickers-Armstrongs Limited for allowing us to use their stratosphere chamber, and Major P. L. Teed, Mr. A. D. Grant, and the whole of the stratosphere-chamber crew for their help and co-operation.

We are indebted to Mr. R. G. Pritchard and Mr. B. W. Hanchett of the Hackbridge and Hewittic Electric Company Limited for designing and operating the ultra-violet lamps used in the stratosphere chamber.

Finally, we should like to thank Sir George Thomson and Dr. E. P. George for the support they gave to the work.

References

Clark, M. A.	1952	Phys. Rev. **87**, 87
Clarke, E. T., and Korff, S. A.	1941	J. Franklin Inst. **232**, 339
Hopper, V. D., and Wilson, A. R. W.	1953	J. Sci. Instrum. **30**, 211
Leide, G., and von Friesen, S.	1953	Ark. f. Fys. **6**, 395
Montgomery, D. J. X.	1949	Cosmic Ray Physics (Princeton University Press)
Rocket Panel	1952	Phys. Rev. **88**, 1027
Scrase, F. J.	1949	Met. Mag. **78**, 284
Taylor, H. J.	1952	Proc. Ind. Acad. Sci. **36**, 41
W.M.O. Publication No. 8	1953	(formerly O.M.I. Publication No. 78), 102

Journal of Atmospheric and Terrestrial Physics, 1954, Vol. 5, pp. 230 to 242 Pergamon Press Ltd., London

Measurement of atmospheric noise interference to broadcasting

S. V. Chandrashekhar Aiya

College of Engineering, Poona

(*Received* 24 *May* 1954)

ABSTRACT

The paper gives a general survey of the problem of atmospheric noise measurement and establishes, by a subjective method, a criterion for assessing the annoyance value of the noise to broadcast reception. There follows the development of an objective method of measurement and a comparison is made between these measurements and the subjective observations, etc.

Ten impulses per minute are estimated to have an annoyance value to the listener of broadcast programmes. Noise is classified into three types: (*a*) type A noise giving the impression of continuous noise, (*b*) type B noise coming as distinct impulses, and (*c*) type C noise, a special form of type B noise arising from local thunderstorms. The importance of bringing statistical considerations into the field of assessment of atmospheric noise interference is discussed and a procedure for the collection of data and its assessment for obtaining monthly values for a specific service, broadcasting, is described.

Introduction

Broadcasting, both standard and secondary, has to be planned in countries like India to serve large areas with very limited resources. The magnitude of atmospheric noise is high and it becomes necessary to develop as good a method as possible for the assessment of atmospheric noise interference to broadcasting. With this idea in view, extensive preliminary investigations were carried out for long periods spread over several years by listening to noise only and to noise in the presence of programmes over the whole frequency spectrum of interest to broadcasting, viz. 150 Kc/s to 22·0 Mc/s. These investigations were of a qualitative character. Broadcast receivers, communication receivers with and without AVC, receivers fitted with meters etc. were used. As a result of such investigations, certain conclusions were reached and it was felt that a fresh approach to the problem was necessary.

The paper gives a general survey of the problem of atmospheric noise measurement, and establishes, by a subjective method, a criterion for assessing the annoyance value of the noise to broadcast reception. The development of an objective method of measurement is described and a comparison is made between measurements by this method and the subjective observations, etc.

2. Statistical Nature of Atmospheric Noise

The nature of atmospherics and their associated fields have been extensively investigated by Appleton, Chapman, Watson-Watt, Schonland, and their collaborators and by Lutkin, Allbright, McEachron, Norinder, and others. The results of these classical investigations have been summarized (Bruce and Golde: Thomas and Burgess). Briefly, the conclusions are as follows. An atmospheric, received on a receiving aerial, may be due to a single elementary disturbance or an aggregate of elementary disturbances. The time duration of impulses due to atmospherics varies from impulse to impulse in some statistical manner. For multiple flashes, the median value of the duration of an impulse is

VOL. 5 1954

about 0·25 sec. The number of flashes lasting more than one second is negligible and the number lasting less than 0·1 sec is less than 30 per cent of the total number. The magnitude of an impulse varies from impulse to impulse. The number of impulses received per minute may vary from minute to minute. These facts indicate very clearly that atmospheric noise is a statistical phenomenon. Therefore, any satisfactory system of measurement must involve (a) the development of measuring technique, (b) a procedure for the collection of data, and (c) a method for the assessment of data. All the three aspects are equally important and related to each other and to the purpose for which the assessment is made.

It may be that the behaviour of these impulses as heard through the loudspeaker of a receiver shows departures from the results of investigations on the nature of atmospherics for a variety of reasons such as the effect of receiver circuits, the actual aural sensation due to the sound produced, etc. It is necessary, therefore, to obtain experimental results on the time duration etc. of an atmospheric impulse, as actually heard by the ear, and compare them with the results of experiments on the nature of atmospherics. Such experiments cannot be very refined or satisfactory, but so long as they represent the most realistic and realizable approach to the question they must be undertaken. If the results of such experiments are statistically assessed, slight inaccuracies of the measurements by individual observers disappear in the final computation. Subjective acoustical experiments of the type referred become necessary for assessments involving the annoyance of noise to listening with the ear.

OL.
5
954

3. Practical Considerations

Noise data are required for the communication services and measurements of noise interference in engineering terms are desirable. The method of measurement, the equipment and its calibration must follow a standardized character so that similar measurements can be carried out by others elsewhere without any ambiguity on the extent to which the set up and calibration are identical. For service purposes, it is not desirable to present data in the form of a set of curves or elaborate tables. It would be most useful to give monthly or seasonal averages for specific periods of the day. These considerations must also be given their due weightage in the design of experiments, assessment of data, etc.

Experimental investigations cannot possibly be carried out at a very large number of places. If the data collected at a few places leads to a suitable theoretical picture, it becomes possible to estimate noise levels. Therefore, the data obtained must be quantitatively explained on the basis of known thunderstorm activity and the laws of propagation. This may require the reduction of the actual source to an equivalent idealized source and other assumptions. So long as they are not inconsistent with known facts, they should be considered justifiable. It is always the discrepancy between theory and experiment that ultimately leads to a correct understanding of the problem.

Noise measurements must always be related to standards necessary for satisfactory service. This involves continuous measurements of noise and field strengths of desired signals, and listening. These are tedious experiments but, unless they are undertaken, satisfactory standards evolved under natural conditions become

impossible and the actual noise measurement unrelated to satisfactory signal standards reduces itself to work of academic interest.

All the facts discussed so far do not become equally important in the study of atmospheric noise at all places. In regions far removed from the equator, atmospheric noise mostly exhibits itself in a form similar to continuous noise most of the time and problems of investigation become comparatively simpler. The complexities of the problem increase enormously in countries like India and, even in India, the problem does not present a uniform set of difficulties all over the land. In fact, it is fair to state that the suitability or otherwise of a complete system for the assessment of atmospheric noise interference can only be tested in tropical countries like India. Most of the methods for the measurement of atmospheric noise, however, have been developed on the basis of experiments in northern latitudes and used at other latitudes also.

4. Existing Methods

Several methods have been used to measure atmospheric noise during the last thirty years. (Espenschield : Thomas : Thorn, Newby, and Loveless : Beer, Bray, and Lowry : Beer, Swindlehurst, and Bray : Aggers, Foster, and Young : Friiś : Gerson : Reiche : Yabsley.) They are generally classified into two broad types:—

(*a*) Subjective Methods

(*b*) Objective Methods

Extensive measurements have been taken by a subjective method described by Thomas. It really measures the minimum field intensity required for a predetermined degree of intelligibility for C.W. transmission. The actual noise intensity has to be indirectly evaluated. This can be attempted for continuous type of noise approximately. If such attempts are made when impulses are being received at an audible rate, the indirect result obtained for actual noise has really no significance and cannot be considered even approximately correct. The measurement has no real subjective significance for fading signals. Even for steady signals, the method is not as subjective as it is considered to be. During a certain period, say one hour, one measurement is taken. Such a step assumes that, *during this whole hour*, the duration and value of all the impulses and the number of impulses per minute are all constant. Such an assumption has no support from the experimental results, which clearly show that atmospheric noise is a statistical phenomenon. In fact, the subjective method is subjective only for the few moments of observation even for steady signals! When a high degree of accuracy is not necessary for the assessment of noise, the results obtained by the method may be useful at high latitudes where atmospheric noise appears in a manner similar to continuous noise.

There are, of course, other handicaps. The measurement is dependent on the subjective observation of the experimenter. It is not possible to take the large number of observations that statistical considerations demand.

In the objective methods, the time constants of the measuring system are adjusted to give readings which correspond as closely as possible to the annoyance

VOL. 5 1954

value of noise. The performance of some of these noise meters has been investigated. (BURRILL : DINGER and PAINE.) The criteria adopted for relating the time constants of the measuring system to the annoyance value, the method of calibration, and the carrying out of subsidiary experiments to relate these noise measurements to standards of satisfactory signals are important and the necessary attention to all these factors has not been given. The measuring system should come after the detector of the receiver to take account of the detector action on the wave form and to evaluate the audio output with which one is primarily concerned.

Apart from the general considerations mentioned, it appears that, in noise measurements, the necessary importance has not so far been attached to the fact that the duration, magnitude, and number per minute of the atmospheric noise impulses vary in a statistical manner. This fact requires the development of criteria not only for the measurement but also for the collection and assessment of data. On this hangs the real importance of noise measurements.

5. PRELIMINARY SUBJECTIVE INVESTIGATIONS

For a rational assessment of impulsive noise which shows statistical variations, it is necessary to consider the magnitude and duration of the impulses and the number of impulses per minute. Information on these aspects is available from the results of the study of lightning discharges. But, as stated earlier, the nature of the impulses may be changed by the receiver and the impulse as actually heard by the ear may be different from the impulse as recorded electrically. It is necessary, therefore, to carry out subjective experiments, see if they are consistent with the results of experiments on lightning discharges, and then to utilize the data for evolving criteria, etc.

Atmospheric noise was listened to for long periods spread over many years. It was found that the number of impulses received can vary from one or two per minute to such a number that one gets the impression of continuous noise. The magnitude of the impulse was not constant so long as impulses could be distinguished from each other. Nothing can be gained by listening when the number of impulses becomes too large to allow individual impulses to be distinguished by ear. The duration of the impulse varied from impulse to impulse. All these facts are well known but do require a restatement for the formulation of criteria. It is necessary to point out that the ear is not able to make out whether the impulse is due to a single elementary disturbance or an aggregate of elementary disturbances; but it can only feel the duration of the impulses.

6. DURATION OF IMPULSES

To investigate the statistical variation of the duration of the impulses as heard, the following experiment was carried out. A number of persons were trained to use precision stop watches which had separate arrangements for starting and stopping them. By using these stop watches it was possible to say whether an impulse *as heard* lasted less than 0·1 sec, or whether it lasted between 0·1 and 0·2 sec, and so on, i.e. it was possible to sort the impulses and state in which group they could be classified. A receiver, adjusted to the conditions under which noise

was to be measured, was tuned to receive noise which could be heard as distinct impulses. Different observers heard and recorded the duration of the impulses, i.e. when they heard an impulse and found by their stop watch measurement that it lasted between say 0·2 and 0·3 sec, it was allotted to an appropriate group. Thousands of observations were taken in this way and all the results were collated. A cumulative curve was drawn to obtain the median value of the duration of an impulse. This is shown in Fig. 1.

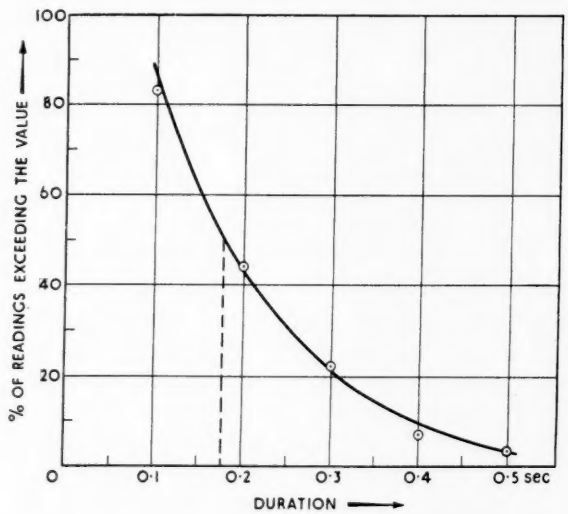

Fig. 1.

It is clear from the figure that the median value of the duration of an impulse is 0·18 sec. 97 per cent of the impulses as heard through the loudspeaker lasted less than 0·5 sec. The duration of the effect on the ear was more than 0·1 sec for 83 per cent of the impulses.

The ear has a tendency of not responding as well as instruments to extremely sharp impulses. Further, when there is a long drawn out impulse, its effect on the ear may not last as long as when electrically recorded. Taking these two facts into account, there is nothing inconsistent with the results of experiments on the lightning discharges, and their associated fields in conclusion of these listening experiments. It is useful to point out that the wide variety of impulses like those due to local sources, near sources, etc., cannot be obtained even in Poona at any time. Opportunities are afforded only during some periods of the monsoon season.

Utilizing the results of these experiments, it will be assumed for the rest of the paper that (*a*) the median value of the duration of an impulse as heard is 0·2 sec, (*b*) over 80 per cent of the impulses as heard last more than 0·1 sec, and (*c*) the number of impulses lasting more than 0·5 sec is negligible. The minimum number of impulses that has an annoyance value depends on the duration of the impulses, and the results of subjective experiments on this question can be examined on the basis of these results.

VOL. 5 1954

7. Assessment of Annoyance

The number of impulses per minute that has an annoyance value was investigated as follows. When a large number of impulses due to atmospherics was being received, a receiver was tuned to different stations coming through with varying strengths and a number of listeners made to listen to the programme. A few could notice the presence of five impulses per minute. There were a few who could only notice the presence of fifteen or more impulses per minute, but the majority could notice the presence of ten impulses per minute. In these investigations the programme tuned was speech, as the effect of noise is most pronounced on speech. These results can be understood. An average Indian speaks 90 to 100 words per minute. This is a little higher than the value for some Europeans but it is better to take the higher value. Allowing for the time interval between words, the average time per word can be taken as 0·5 sec. An atmospheric impulse lasting 0·2 sec (median value) coming at any part of the word is adequate to destroy its clarity. Ten such impulses per minute would affect 10 per cent of the words and this appears to be large enough to be noticed. In actual practice, the audio frequency wave form of noise is superposed on the wave form of speech and is equivalent to distortion. Further, ten impulses lasting 0·2 sec each means the superposition of the noise wave form for 2 secs in a total period of 60 secs, i.e. 3 per cent of the time.

This criterion of ten impulses per minute, as the minimum number of impulses per minute for causing annoyance, is evolved by taking into account the statistical variation of the duration of impulses and is the criterion which includes the duration and number per minute aspects of impulsive noise. It becomes unnecessary when the number of impulses per minute becomes very large and this happens, among other cases, for noise due to distant sources only. However, such particular cases cannot justify the elimination of the criterion for the general case. The criterion becomes extremely important in assessing impulsive noise, especially in countries like India. Occasions arise when only a few impulses of large magnitude are received. In such cases, it becomes absolutely necessary to have a basis for deciding when to take them into account and when to ignore them.

Impulses of the highest magnitude will obviously cause the maximum of annoyance. Therefore, when there are a large number of impulses per minute, it is necessary to measure the magnitudes of the ten highest impulses. Experimental results indicate that arithmetical averaging of these ten highest impulses is adequate in the large majority of cases. Hence, the arithmetically averaged value of the ten highest impulses should be stated as the quasi-peak value.

8. Classification of Noise

Several attempts have been made to classify atmospheric noise. A fresh attempt to classify noise on the basis of listening experiments becomes necessary if a type is to indicate by its classification exactly what it means. When atmospheric noise is heard through the loudspeaker of a receiver, it may be possible to distinguish the individual impulses from each other and so long as this is possible, the type of noise received will be called type B noise. When this type of noise is due to extremely local thunderstorms, the quasi-peak value becomes very large and shows

considerable variations from impulse to impulse. This special form of type B noise will be called type C noise. Type B noise appears to be due to a large number of thunderstorms spread over a wide area while type C, the special form, may be due to very few thunderstorms, even one.

As the number of impulses per minute goes on increasing, the ear finds it more and more difficult to distinguish each separate impulse and the resolving power of the average ear is crossed when the number of impulses per minute exceeds fifty. When the impulses come at this rate or higher, the ear gets the impression of a continuous noise which may appear similar to fluctuation noise. This type of noise will be called type A noise. But, it must be remembered that this type of noise is also due to impulses, and hence must be measured by the same standards as the other two types of noise.

When only type A noise is present, it should be measured and stated. Superposed on type A noise, there may appear type B or type C noise. In such cases, the latter are always of higher magnitude than type A noise. Therefore, when the number of impulses due to type B or type C noise exceeds ten per minute, it is only necessary to state the value of type B or type C noise. When the number of impulses is less than five per minute, only type A noise may be stated. When the number of impulses is five or more than five, but less than ten per minute, it is desirable to state both type A and either type B or type C noises.

VOL. 5 1954

9. Objective Measurements of Noise

The investigations of Steudel (1933) justify the construction of noise meters of the rapid charge slow recovery type for atmospheric noise measurements. In the objective methods of measurement, attempts have been made to evaluate the charge and discharge time constants which result in relating the actual measurement to the annoyance value of noise. There can always be differences of opinion on the most suitable values. In fact, it may be stated that no one set of time constants can possibly relate the measurement to the annoyance value for all types of impulses received. This statement does not require further elaboration when it is realized that we are dealing with a statistical phenomenon. What is required is to find out whether the time constants chosen do actually relate the measurement to the annoyance value in the majority of cases, and state clearly the limitations of the meter performance. It is, however, desirable to have only one set of time constants for all types of noise. Further, it is desirable to carry out subsidiary experiments to evolve standards for satisfactory service on the basis of the noise measurements. If this data can be provided, it becomes possible to compare the results of experiments on noise by objective methods employing different time constants. Absence of such information makes comparisons difficult.

10. The Objective Method of Measurement Adopted

Since statistical considerations require the recording of a large number of observations, it was decided to adopt the objective method of measurement. The time constants chosen for the noise meter were as follows:—

Charging time constant = 10 milliseconds
Discharging time constant = 500 milliseconds.

The C.I.S.P.R. has recommended a charge time constant of one millisecond and a discharge time constant of 160 milliseconds. The United States Joint Co-Ordination Committee which went into this question has recommended a charge time constant of 10 milliseconds and a discharge time constant of 600 milliseconds. It is said that these large time constants result in indications more in conformity with the annoyance value of noise. Other advantages claimed are that such meters are easier to construct and that the response of the meter becomes unimportant.

11. Subjective Tests of Noise Meter Performance

The time constants chosen for the noise meter were based on trial and error experiments carried out to see if the meter satisfied the following requirements:—(*a*) whether what was read on the meter corresponded to what was heard and (*b*) whether the meter failed to record kicks when the ear got the impression of continuity. It was found that the time constants chosen gave the closest possible realization of the above requirements and were thus most suitable. The values chosen are about the values recommended by the American Joint Co-Ordination Committee, the only difference lies in the discharge time constant which is 100 milliseconds lower. This may be due to the resolving power consideration indicated as (*b*) above.

Over a million observations have been taken with these time constants by different students who listened to the noise. From these, the following statements may be made: (*a*) For very sharp impulses, i.e. for impulses lasting about 0·1 sec or less, the meter readings are higher than the effect on the ear; (*b*) For the majority of impulses for the greater part of the time, there is satisfactory correlation between the effect on the ear and the meter reading; and (*c*) there is no data for impulses lasting a very long time, i.e. over 0·4 sec. This is because the number of such impulses have been few and, if they did appear in type A noise, nothing can be made out. Examining these conclusions on the meter performance with the results of experiments on the duration of impulses, it appears that these time constants are adequate for about 70 per cent of the impulses. It is possible that a large proportion of the long duration impulses are present in type A noise. Making an allowance for this from the results of experiments on lightning discharges, it will be reasonable to say that *the meter does relate satisfactorily the reading to the annoyance value for fifty per cent of the impulses.* The question of improving the time constants is constantly kept in view while measurements are being taken and is also being theoretically examined. If it is found in the course of the next few years that better time constants can be evolved, they will be used and the results obtained with the now used time constants converted to correspond to the new time constants by carrying out subsidiary experiments. Although there is at present no indication towards such an eventuality, the statement is being made to emphasize the fact that the question of time constants is a complex one.

12. Equipment and its Installation

For engineering evaluations, it is useful to work with equipment which conforms to the usual types. The receiver should be of the usual commercial type, like a communication receiver. Its bandwidth characteristics should be adjusted to

6 Kc/s at 6 db down. This is more in conformity with those met with in commercially mass produced receivers than the higher bandwidths recommended. The second channel selectivity must be 80 db down. The A.F. output from the detector should be fed to the noise meter.

It is not possible to have the same installation and equipment for measurements over the whole frequency spectrum. The polar diagram of the aerial must be such that it can at least pick up equally well from all the directions from which noise is expected on considerations of the distribution of thunderstorm activity. The ratio of the radiation to loss resistance of the aerial must be considered. This naturally leads to the question of the earth system. The aerial to be used must be such that its effective height and electrical constants can be determined at site with reasonable accuracy. At very high frequencies, the problem of eliminating other noises which become comparable with atmospheric noise presents special problems of its own. Taking these several factors into account, it is found useful to have separate installations for each of the following bands:—

(*a*) 100 to 400 Kc/s

(*b*) 500 to 1500 Kc/s

(*c*) 2·5 to 20·0 Mc/s

(*d*) 20 to 30 Mc/s.

VOL. 5 1954

The use of automatic recording has been found unsuitable. There are frequent changes of noise intensity which require changes of range, if accuracy is to be maintained. Otherwise, observations may get recorded when the receiver or amplifier is made to operate under overload conditions, leading to incorrect readings. Further, the trouble due to interference is most serious. Over certain ranges of frequencies, it is difficult to find dead spots at any time. Even in other cases, it becomes impossible on some days to take continuous measurements. Since statistical considerations require the taking of a large number of observations and this has to be done manually, observations can only be recorded at one frequency in the band at a time or, at best, at two frequencies. This naturally leads to either the prolongation of the experiments or the use of more equipment, but there is no other way out.

13. Calibration

Atmospheric noise is a form of interference. The noise source should be considered a form of radiator and its field strength should be measured in microvolts per metre. The noise meter thus becomes a noise field strength meter. A standard signal generator should be used for calibration purposes. Since measurements are made on the audio frequency side, the question of a suitable audio frequency and a suitable percentage modulation arises. 30 per cent modulation by a 400 c/s note is usually used for receiver testing, etc. The same should also be used in this case. All the results can be given on this basis. In addition, it is useful to provide conversion data for converting these results to what would be obtained with 15 per cent and 50 per cent modulation. While carrying out the calibrations, it is necessary to feed the output of the signal generator through the equivalent impedance of the aerial at the point at which the aerial is connected. For maintaining

calibration accuracy, the power to the receiver must be supplied through a constant voltage transformer and the calibration periodically checked.

For theoretical purposes, it is necessary to appreciate the significance of this calibration. The noise field strength is due to the noise source operating as a radiator at a particular frequency within the limits of the defined band width of the receiver. This radiator is considered as equivalent to a radiator at the same frequency carrying a 30 per cent modulation by a 400 c/s note.

14. Recording and Analysis of Observations

In all statistical phenomena, great importance is attached to the collection and assessment of data having regard to the purpose for which the assessment is made and it is an accepted fact that the fewer the observations, the less reliable is the result. It is unfortunate that noise measurements have been carried out without taking these important facts into account. After taking into account the statistical requirements, experimental difficulties, and the practical necessity, a system has been evolved and it is as follows:

Observations are taken continuously for ten minute periods, three times an hour. All impulses are generally recorded, but when the number of impulses exceeds twenty per minute about twenty of the highest during the minute are recorded. The general practice is to record about 600 impulses per hour. The continuous background noise, here called type A noise, is recorded by reading the meter twice in each ten minute interval. This is done very carefully when the number of impulses per minute, due to type B noise, is less than ten. Higher values will be recorded for type A noise, in the noise meter described in this paper, when a large number of impulses due to type B or type C noise is also present. But this is of no significance, as the type A noise which appears as a background is never stated when the number of impulses due to type B or type C noise exceeds ten per minute.

Type A noise which is read twice in each ten minute interval gives six readings for the hour. They are arithmetically averaged to give the average for the hour. A similar procedure is adopted for averaging type B or type C noise. The 300 highest values recorded during the 30 minutes in any hour of observation are arithmetically averaged to obtain the average value of the ten highest peaks per minute. This is stated as the quasi-peak value of type B or type C noise for the hour.

The hourly values so obtained are tabulated for the whole month. The twenty four hours of the day are divided into four divisions:—06·00 to 12·00, 12·00 to 18·00, 18·00 to 24·00 and 00·00 to 06·00. This division has been made having regard to broadcasting as a utility service and the use of the Indian Standard Time is found convenient in India. Separate tables of hourly values for the whole month are prepared for the four divisions. The monthly table of one division is examined at a time. During some months, the number of impulses per minute due to type B or type C noise is less than five throughout. In such cases, analysis of only type A noise is resorted to and observations of type B or type C noise, if any, are ignored. During some months, the number of impulses due to type B or type C noise always exceeds the rate of ten per minute. In such cases, type A noise is ignored. During

a few other months, however, the number of impulses per minute due to type B noise varies and has values below ten also. For such months, the median value of the number of impulses per minute is computed for the whole month. If this is less than five, type B noise is ignored. If it is more than five and less than ten, values of both type A and type B noises are computed and given. If it is more than ten, only type B noise is computed.

The following procedure is adopted in all cases for obtaining the magnitude of noise in one division of the day for the whole month. The hourly averaged readings for the month are sorted into groups and a graph is drawn—percentage of readings exceeding a value against the value. From this graph, the median value for the month and the value that is exceeded during only 10 per cent of the hours of observation, the higher decile value, are both obtained. In giving noise figures for the month, it should be adequate to state the median value of the hourly averages for each of the four divisions of the day but, if a higher figure is desired, it is best to state the higher decile value also for each division of the day.

Sometimes, when the hourly values are sorted into groups, it is found that they fall into more than one set. In such cases, the median value, etc., are obtained for each set separately as each may have a different source of origin. Monthly values are obtained by weighting the value of each set in proportion to the frequency of its occurrence. Under no circumstances are the results of type A, type B, and type C noises mixed up. (Experiments have been carried out in which atmospheric noise as such is measured, i.e. all the different types of noise as classified here are mixed up. The results of such experiments are of no real value for evolving standards of satisfactory signals for a particular type of service. The theoretical interpretation of the results becomes impossible. The diurnal variation obtained loses its significance. A discussion of these is outside the scope of this paper.)

Before proceeding to compute the results, the following general principles are observed. To compute the hourly average, there must be at least two ten minute periods of continuous observations, the two ten minute periods to lie in the two halves of the hour. For any six hour division of the day, there must be at least three hourly averages and these hours must be alternate. For computing monthly averages, there must be readings for at least ten days of the month and the days must be spread over the whole month. In actual practice, observations should be obtained far in excess of these minima.

15. Conclusion

Atmospheric noise is an impulsive noise and is a statistical phenomenon. The assessment of its interference must be approached from this standpoint. When annoyance to listening is to be considered, it is necessary to approach the question on the basis of experiments carried out on actual listening. This leads to a classification of noise as type A, type B, and type C and this classification has significance for evolving standards of satisfactory service. A minimum number of ten impulses per minute is considered to have an annoyance value, and this takes account of the duration and number of impulses of atmospheric noise. The statistical variation of the magnitudes of impulses is taken into account in the method of recording and assessing the data. The latter also takes account of the purpose for which the

VOL. 5 1954

assessment is made. In the particular case, it is for a continuous broadcast service. The time constants of the measuring system are satisfactory for at least fifty per cent of the impulses. The objective method has been adopted as it is more suitable when a large number of observations have to be taken to meet statistical requirements.

In all noise measurements, it is desirable to provide the following information:—(*a*) details of the aerial, (*b*) bandwidth characteristics of the receiver, (*c*) detailed particulars of the receiver and the measuring system, (*d*) method of calibration, (*e*) criteria of the number of impulses per minute and, if possible, suitable data for converting the results to other criteria, (*f*) the details of the way the observations have been recorded and assessed, and (*g*) standards of satisfactory signals in relation to the noise level as measured. Absence of details on the several points mentioned make comparisons of results of different workers very difficult. An attempt, however unsatisfactory it be, must be made to interpret the results theoretically.

Measurements of atmospheric noise interference to broadcasting in the different bands mentioned by the method described in the paper and a discussion of the results obtained will be presented in future papers. The proper evaluation of standards of satisfactory service in relation to the assessment of noise interference by the method described here will be reported in due course. It may be necessary, however, to state here that the problem is extremely complicated when considered in relation to fading signals, but is certainly capable of solution.

This paper is confined exclusively to discussing the problem of the assessment of atmospheric noise interference to broadcasting. The utility of the results of such measurements to other services is outside the scope of this paper.

16. Acknowledgment

The author's thanks are due to Messrs. S. K. Pramanik, L. A. Ramdas, and K. N. Rao for permission to use the library of the India Meteorological Department, and to Mr. S. P. Venkiteswaran for the loan of stop watches, and to his students, Messrs. K. R. Phadke, R. D. Joshi, C. G. Khot, M. N. Gadre, and S. Padmanabhan, for the invaluable co-operation given to him in carrying out the tedious listening experiments.

References

Aggers, C. V., Foster, D. E., and Young, C. S.	1940	Electr. Engr. **59,** 178
Beer, H. G., Bray, W. J., and Lowry, W. R. H.	1937	Post Office Radio Report No. 330
Beer, H. G., Swindlehurst, R. J. K., and Bray, W. J.		ibid
Bruce, C. E. R., and Golde, R. H.	1941	J. Instn. Elect. Engrs. **88(2),** 487
Burrill, C. M.	1941	Proc. Inst. Radio. Engrs. **29,** 433
	1942	ibid **30,** 473
Dinger, H. E., and Paine, H. G.	1947	ibid **35,** 75
Espenschield, L.	1931	ibid **19,** 1951
Friis, H. T.	1926	Bell. Syst. Tech. J. **5,** 282
Gerson, N. C.	1950	Proc. Inst. Radio. Engrs. **38,** 905
Reiche, H.	1949	Electronics **22,** 110
Thomas, H. A., and Burgess, R. E.	1947	Rad. Res. Sp. Report. No. 15

Thomas, H. A.	1950	J. Inst. Elect. Engrs. **97(3)**, 329
Thorn, D. A., Newby, D. P., and Loveless, E. R.	1942	Post Office Radio Report No. 791
Steudel, U.	1933	Hochfrequenztech u. Electroakust. **41**, 116
Yabsley, D. E.	1950	Austral. J. Sci. Res. **3**, 409

VOL.
5
1954

RESEARCH NOTES

Electron density in the *E*-layer during auroral displays deduced from measurements of absolute brightness of the auroral luminosity

(*Received* 8 *June* 1954)

In a recent paper SEATON (1954) has made some interesting estimates of the electron densities in the auroral region during an auroral display, based on the absolute intensity of the negative nitrogen bands (N_2^+, $B^2\Sigma_u^+ - X^2\Sigma_g^+$).

Assuming the process

$$N_2(X^1\Sigma_g^+) + X \rightarrow N_2^+(B^2\Sigma_u^+) + e + X \qquad (1)$$

to be the only important one both for the ionization and for the excitation of the negative nitrogen bands, the electron density can be calculated from the formula:

$$n(e) = \left[\frac{\eta(\text{N.G.})}{\alpha^{\text{rec}}}\right]^{\frac{1}{2}} \qquad (2)$$

Here are $n(e)$ the electron density in electrons per cm^3, α^{rec} the coefficient of recombination in cm^3 sec^{-1} for the *E*-layer and η(N.G) the total photon emission per cm^3 per sec of the negative bands in the aurorae.

There is, however, a lack of knowledge about the absolute brightness of the aurorae. SEATON made assumptions about this based on visual observations. In this paper values are given which have been measured during preliminary experiments with photoelectric equipment.

The auroral form was by a lens focused on a small circular opening on the front of a 1P-22 photomultiplier. Interference filters transmitting respectively $\lambda = 5577$ Å and $\lambda = 4278$ Å were placed before the lens. The current was measured by a galvanometer. The sensitivity of the apparatus was measured by means of a standard lamp, the emission of which was known in ergs solid angle^{-1} sec^{-1}Å^{-1}. To ensure even illumination of the photocathode this lamp was, with the same optical system, focused 5 cm before the circular opening on the front of the photomultiplier. The emission of the aurorae in erg per cm^2 column per sec per solid angle could thus be calculated by taking into account the geometry of the system, the transmission profiles of the filters, and the atmospheric extinction coefficient.

Measurements was made during three nights with bright auroral displays. In the table, column 2, is given some typical values of the auroral emission in erg per cm^2 column per sec for the negative band 4278 Å (0–1). The absolute intensity of the green line 5577 Å was found to be about 2·5 times that of the 4278-band, a factor which showed only small variations in spectra from various ordinary, bright aurorae.

In column 3 of the table is given the number of photons emitted per cm^2 column per sec., in column 4 the estimated length of the light emitting column in radial direction, and in column 5 the number of photons, η (4278), emitted per cm^3 per sec in the aurorae.

Using Eq. (2), the electron density can be calculated and is given in column 6. α^{rec} is

taken to be 10^{-8} cm^3 sec^{-1}. η(N.G.), the total photon emission per cm^3 per sec in the negative band system, is given by

$$\eta(\text{N.G.}) = \eta(4278)\,\frac{\sum_{v'v''} I(v', v'')/h\nu(v', v'')}{I(0, 1)/h\nu(0, 1)} \qquad (3)$$

$I(v', v'')$ and $\nu(v', v'')$ are the relative intensity and the frequency of the $(v'\text{-}v'')$-band in the 1 . negative band system of nitrogen. Using the values published by BATES (1949, Tables 6 and 20), we find η(N.G.) = η(4278) . 6·5.

Auroral forms	*Intensity* erg cm^{-2} sec^{-1}	*Photon emission* cm^{-2} sec^{-1}	*Estimated length of column* km	*Photon emission* cm^{-3} sec^{-1}	*Electron density n(e)* electrons/cm^3
Faint arc	$2 . 10^{-2}$	$0{\cdot}4 . 10^{10}$	10	$0{\cdot}4 . 10^{4}$	$1{\cdot}6 . 10^{6}$
Weak, pulsating surfaces	$1 . 10^{-2}$	$0{\cdot}2 . 10^{10}$	10	$0{\cdot}2 . 10^{4}$	$1{\cdot}1 . 10^{6}$
Medium rays	$3\text{–}6 . 10^{-2}$	$0{\cdot}6\text{–}1{\cdot}2 . 10^{10}$	1	$6\text{–}12 . 10^{4}$	$6\text{–}9 . 10^{6}$
Medium arcs	$8\text{–}16 . 10^{-2}$	$1{\cdot}5\text{–}3{\cdot}2 . 10^{10}$	10	$1{\cdot}5\text{–}3{\cdot}2 . 10^{4}$	$3{\cdot}1\text{–}4{\cdot}5 . 10^{6}$
Strong rays	$16 . 10^{-2}$	$3{\cdot}2 . 10^{10}$	1	$32 . 10^{4}$	$14 . 10^{6}$
Strong arcs	$33 . 10^{-2}$	$6{\cdot}7 . 10^{10}$	10	$6{\cdot}7 . 10^{4}$	$6{\cdot}6 . 10^{6}$
Lower border of strong drapery	$45 . 10^{-2}$	$9 . 10^{10}$	5	$18 . 10^{4}$	$11 . 10^{6}$
Very bright display in rapid movement	$75 . 10^{-2}$	$15 . 10^{10}$	10	$15 . 10^{4}$	$10 . 10^{6}$
Strongest aurorae measured, band in rapid movement	$100 . 10^{-2}$	$20 . 10^{10}$	10	$20 . 10^{4}$	$12 . 10^{6}$

From the table, column 6, it is evident that the electron density $n(e)$ for a medium to strong display seldom exceeds a value of 10^7 electrons per cm^3, if we assume that the process given by Eq. (1) is the only important one both for the ionization and for the excitation of the negative nitrogen bands.

The errors involved in the quantitative measurements of the energy emission in the auroral spectrum given here are comparatively large, and may even be as large as $\pm 50\%$. As seen from Eq. (2) this gives errors in $n(e)$ of $\pm 30\%$. Some more uncertainty in $n(e)$ is, however, introduced by the possible errors in the estimated length of the light emitting column in the aurorae.

An electron density of 10^6 electrons per cm^3 gives a critical frequency of 9 Mc/sec on vertical incidence, a value which is often observed during faint auroral displays overhead. Quantitative measurements on the correlation between the *E*-layer electron density and the auroral luminescence will be continued.

The Auroral Observatory, Tromsö. A. OMHOLT.

REFERENCES

BATES, D. R. 1949 Proc. Roy. Soc. A **196,** 217
SEATON, M. J. 1954 J. Atmosph. Terr. Phys. **4,** 285

VOL. 5 1954

Electron distribution in the ionosphere

(*Received* 1 *June* 1954)

The true height, h, at which is found an electron density, N, is related to the virtual height, h', at frequency f by

$$h'(f) = \int_0^{N=kf^2} \mu'(f, N)\, d\, h(N)$$

where μ' is the group refractive index.

Let $\phi(N)$ be any single valued function, and let $\bar{\mu}'$ be the mean value of μ' over the interval considered.

Approximately,

$$\begin{aligned}\Delta h'(f) &= \bar{\mu}'(f, N)\,.\,\Delta h(N)\\ &= \bar{\mu}'(f, N)\,.\,\Delta\phi(N)\,.\,\frac{\Delta h(N)}{\Delta\phi(N)}\\ &= \int_{\Delta\phi(N)} \mu' d\phi(N)\,.\,\frac{\Delta h(N)}{\Delta\phi(N)}\\ &= a \times D\end{aligned}$$

in a convenient symbolism.

Over consecutive intervals 1, 2, 3, etc.

$$h'_i = \sum_j a_{ij}\,.\,D_j$$

$$\therefore \qquad D_i = \sum_j b_{ij}\,.\,h'_j$$

where

$$b_{ij} = \frac{A_{ij}}{|a|}$$

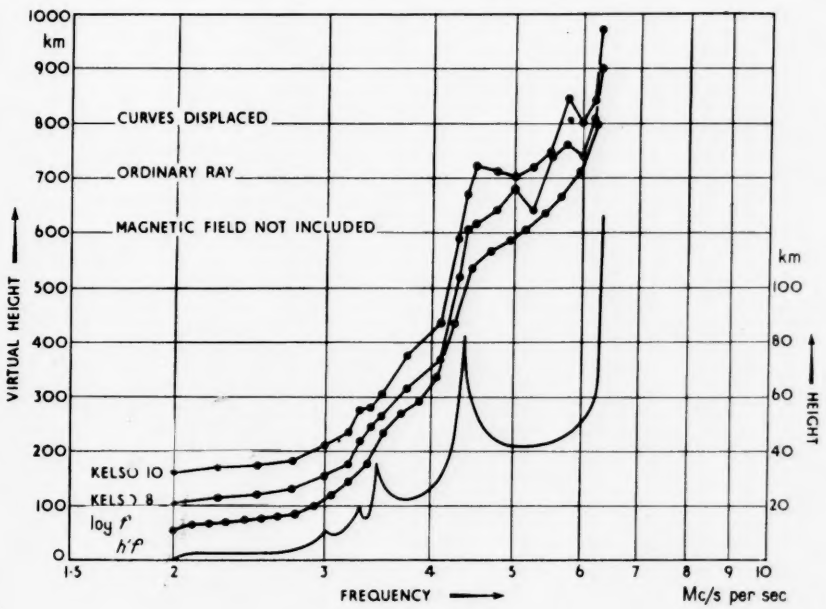

One can obtain, thus, the gradients $\frac{\Delta h(N)}{\Delta \phi(N)}$ and, from them, h. Different forms of $\phi(N)$ lead to different approximate methods of analysing h', f records. KELSO's method (1952) is such that the a's are equal.

To form an idea of the errors in reduction, sample records have been analyzed. The diagram shows the Christchurch record of 1952, Nov. 13d. 14h. reduced by KELSO's method using both 8 and 10 ordinates and also by a method which uses 25 ordinates at equal intervals of $\log f$. The last method is the best of the three, both because of the greater number of ordinates and because of the improved spacing.

This type of analysis can be used to include the effect of the earth's magnetic field. Thus, KELSO's method can be extended by altering the relative spacing of the ordinates. Half a dozen scales, each covering part of the frequency range, will then give an analysis which includes the magnetic field. There is no need for the tedious process set out in KELSO (1954).

This work is part of the programme of the Geophysical Observatory of the New Zealand Department of Scientific and Industrial Research. The help given by the Director, Mr. J. W. BEAGLEY, and by members of the staff is gratefully acknowledged.

Geophysical Observatory,
Christchurch,
New Zealand.

G. A. M. KING.

REFERENCES

KELSO, J. M. 1952 J. Geophys. Res. **57**, 357
1954 J. Atmosph. Terr. Phys. **5**, 11

VOL. 5 1954

Journal of Atmospheric and Terrestrial Physics, 1954, Vol. 5, pp. 247 to 249. Pergamon Press Ltd., London

Indices of geomagnetic activity

of the Observatories ABINGER (*Ab*), ESKDALEMUIR (*Es*), and LERWICK (*Le*)

March to June 1954

The figures given on pages 247 to 249 represent the *K*-indices for three-hour intervals, beginning with 00–03 hrs for the first and ending with 21–24 hrs for the eighth figure.

March 1954

Day	*Ab* Range for $K = 9 : 500\gamma$			*Es* Range for $K = 9 : 750\gamma$			*Le* Range for $K = 9 : 1000\gamma$			*Day*
	K-Indices		*Sum*	*K-Indices*		*Sum*	*K-Indices*		*Sum*	
1	2222	2124	17	2111	2024	13	2221	2114	15	1
2	4312	2243	21	4322	2033	19	4332	2133	21	2
3	3221	2322	17	3210	2212	13	3220	1223	15	3
4	2231	2233	18	1121	2233	15	1121	1223	13	4
5	3223	3324	22	3222	3224	20	3322	2213	18	5
6	3222	2233	19	3202	2223	16	3211	2233	17	6
7	2323	3344	24	2312	3343	21	3322	3343	23	7
8	2212	2233	17	2212	2223	16	2211	2224	16	8
9	3223	3552	25	3122	3542	22	3222	2543	23	9
10	2122	3243	19	1112	3233	16	0111	2133	12	10
11	3333	3444	27	2332	3444	25	2322	3343	22	11
12	3232	3343	23	3231	3333	21	3131	2233	18	12
13	2222	3454	24	2101	3353	18	2211	2453	20	13
14	3332	3554	28	3323	3544	27	4332	3554	29	14
15	4443	4344	30	4443	3244	28	5332	3234	25	15
16	2333	4343	25	2323	3342	22	2323	3343	23	16
17	3222	3543	24	2112	3443	20	3212	2444	22	17
18	4323	3342	24	4323	3341	23	5333	2342	25	18
19	3212	3334	21	3111	3243	18	3111	3233	17	19
20	3233	3443	25	3233	3433	24	3322	3335	24	20
21	3123	2343	21	3022	2343	19	4212	1243	19	21
22	3223	2255	24	3112	1254	19	3211	1255	20	22
23	4333	3366	31	4333	3365	30	5433	3266	32	23
24	4334	2444	28	4334	2445	29	4433	1444	27	24
25	4333	3342	25	4332	2242	22	4332	2242	22	25
26	2233	4443	25	2223	3343	22	2222	3333	20	26
27	3223	1122	16	3222	1121	14	3321	1022	14	27
28	3121	2233	17	3011	1222	12	3111	1232	14	28
29	2122	2223	16	1011	2223	12	2011	1223	12	29
30	4222	4335	25	4211	3335	22	4311	3335	23	30
31	2222	2344	21	2222	2234	19	3221	2234	19	31

April 1954

Day	*Ab* Range for $K = 9 : 500\gamma$		Sum	*Es* Range for $K = 9 : 750\gamma$		Sum	*Le* Range for $K = 9 : 1000\gamma$		Sum	Day
	K-Indices			*K-Indices*			*K-Indices*			
1	1122	2324	17	1011	1323	12	1111	1214	12	1
2	2113	3334	20	2002	3334	17	2012	3334	18	2
3	3222	3235	22	2222	2234	19	3212	2234	19	3
4	3332	2144	22	3332	2134	21	3322	1144	20	4
5	2332	1112	15	1232	0002	10	2221	1112	12	5
6	3222	3223	19	3212	3223	18	3112	2223	16	6
7	2222	2242	18	2112	2242	16	3121	2242	17	7
8	1123	3244	20	0002	2244	14	1111	1134	13	8
9	3222	3323	20	3212	3322	18	3221	2322	17	9
10	2223	3432	21	2222	2332	18	2221	2332	17	10
11	3122	2456	25	3111	1457	23	3111	1359	24	11
12	6543	4334	32	6642	4334	32	8842	3345	37	12
13	3122	3333	20	3113	3333	20	4312	3333	22	13
14	2322	2221	16	2222	2211	14	3322	3211	17	14
15	3223	3444	25	3213	3344	23	3223	3343	23	15
16	2123	3232	18	2022	3232	16	2121	2232	15	16
17	2222	2333	19	1211	2323	15	1111	2222	12	17
18	3223	3333	22	3223	3243	22	3223	3233	21	18
19	2223	2332	19	2213	2332	18	2122	2331	16	19
20	3223	3442	23	3222	3442	22	3321	3442	22	20
21	3333	4322	23	3233	3312	20	2232	3322	19	21
22	3232	3211	17	2221	3101	12	3321	2101	13	22
23	3333	3344	26	3322	3343	23	3222	3353	23	23
24	3222	2344	22	2212	1333	17	3311	1334	19	24
25	3211	1232	15	3221	1232	16	3110	1232	13	25
26	3321	3334	22	3321	3334	22	3321	2245	22	26
27	4232	1232	19	4332	1242	21	5432	1242	23	27
28	3122	2223	17	3111	2122	13	2111	2112	11	28
29	3222	2222	17	3112	3122	15	3121	3221	15	29
30	1233	2222	17	1222	2222	15	1223	3222	17	30

May 1954

1	3211	2112	13	3011	2202	11	3111	1101	9	1
2	2322	2222	17	2321	1221	14	2321	1111	12	3
3	2212	2223	16	2200	2213	12	1211	1212	11	3
4	2222	3434	22	2222	3334	21	2122	2334	19	4
5	3233	2321	19	2222	3222	17	2222	2211	14	5
6	3322	1221	16	2220	0010	7	3222	0111	12	6
7	1112	2322	14	0000	2322	9	0101	1211	7	7
8	2222	3443	22	2111	3443	19	2111	2343	17	8
9	3323	2333	22	3322	2233	20	4322	2223	20	9
10	1122	2242	16	1122	1232	14	1111	1232	12	10
11	3233	2332	21	3223	2332	20	4322	2232	20	11
12	2212	3232	17	2002	3232	14	3111	2232	15	12
13	3222	3332	20	2122	3332	18	2111	3222	14	13
14	3223	2222	18	3112	1221	13	3212	1121	13	14
15	2222	4323	20	2221	4323	19	2211	3322	16	15
16	3222	1121	14	2212	1220	12	3211	1121	12	16

VOL. 5 1954

May 1954 (*contd.*)

Day	*Ab* Range for $K = 9 : 500\gamma$		*Sum*	*Es* Range for $K = 9 : 750\gamma$		*Sum*	*Le* Range for $K = 9 : 1000\gamma$		*Sum*	*Day*
	K-Indices			*K-Indices*			*K-Indices*			
17	0122	2222	13	0001	1112	6	0100	1011	4	17
18	3323	3233	22	3313	3233	21	3312	2233	19	18
19	4222	2333	21	3212	2233	18	3112	2233	17	19
20	2222	3344	22	2211	2343	18	3211	2233	17	20
21	3322	3432	22	3222	4432	22	4211	3332	19	21
22	2221	1123	14	2110	1123	11	2110	1123	11	22
23	2121	1222	13	2120	1122	11	3221	1111	12	23
24	1212	2232	15	2112	2232	15	1112	2222	13	24
25	2212	2121	13	2111	2120	10	2211	1111	10	25
26	2222	3322	18	1121	3321	14	1111	2211	10	26
27	2321	1210	12	2211	1210	10	2311	0111	10	27
28	0113	2222	13	0113	2222	13	1012	2121	10	28
29	3232	3332	21	3232	3222	19	3231	2221	16	29
30	2222	2212	15	1012	2202	10	1112	1101	8	30
31	2122	3332	18	1112	3332	16	1112	2221	12	31

June 1954

1	2211	2212	13	2202	2211	12	2101	2211	10	1
2	1223	2202	14	1213	2212	14	1212	2111	11	2
3	1122	2221	13	0122	2121	11	1121	2111	10	3
4	2232	1231	16	2222	1221	14	2221	1221	13	4
5	1112	2222	13	0000	1222	7	1000	1212	7	5
6	2112	3322	16	1101	2221	10	1110	2112	9	6
7	2222	4332	20	1101	4232	14	2110	3222	13	7
8	1122	2222	14	1021	2111	9	1111	1101	7	8
9	2212	2323	17	3112	2213	15	2111	1212	11	9
10	3243	2332	22	3232	2332	20	3331	1221	16	10
11	1112	2211	11	1002	2211	9	1102	2110	8	11
12	0013	2442	16	0002	2442	14	0011	1332	11	12
13	2212	2432	18	1102	2432	15	1111	1321	11	13
14	2222	4331	19	1012	3331	14	0111	3220	10	14
15	2221	1122	13	1111	1112	9	1111	1112	9	15
16	2212	1111	11	1102	1111	8	1111	1100	6	16
17	1012	2223	13	1001	2112	8	1011	2113	10	17
18	1111	2343	16	0111	1343	14	1110	1243	13	18
19	0213	3222	15	0112	2222	12	0111	1121	8	19
20	2122	2222	15	2112	2222	14	2111	2112	11	20
21	1112	3224	16	0002	3224	13	1011	1123	10	21
22	3322	2323	20	3211	2322	16	3310	2221	14	22
23	2212	2332	17	1101	1332	12	1111	1221	10	23
24	1213	2222	15	1101	2222	11	1111	1111	8	24
25	1123	4321	17	0012	4311	12	0111	3210	9	25
26	1122	3332	17	1112	2232	14	0111	2222	11	26
27	2222	3333	20	1122	3333	18	1111	2222	12	27
28	3332	2331	20	3232	2231	18	4322	2221	18	28
29	1221	2112	12	1121	1202	10	1121	1112	10	29
30	2122	2324	18	1011	2224	13	1111	1213	11	30

Book reviews

Advances in Geophysics. Ed. by H. E. LANDSBERG, Vol. 1, 1952, Academic Press Inc., New York, 362 pp. $7.80.

THE present development in geophysics is greatly assisted by the publication of review articles. The field included by the term geophysics is very considerable, covering branches of the science of the Earth in which the techniques and methods of approach range from those of the geologist to those of the mathematician. Any research worker in geophysics may quite suddenly find his special field has need of a well established, but totally strange, discipline. The geomagnetician has had in the past few years to acquire an understanding of the approach of the geologist, in his need to unravel the history of the geomagnetic field through the magnetisation of igneous and sedimentary rocks. Similarly in future the vulcanologists may find the pursuit of their ancient science requires the use of the knowledge of temperature distribution in the deeper parts of the earth's mantle, which is being developed from the study of geomagnetism and from the theoretical studies of the properties of solids which the physicist has developed in the last twenty years.

The book under review is a valuable attempt to meet this need. It contains eight review articles all of which have excellent bibliographies. It is perhaps biased on the practical side: the imagination is not stimulated by being confronted with any of the great unsolved problems of the physics of the Earth. Perhaps the nearest approach is Dr. BOLIN's discussion of the lack of any real understanding of the physical mechanism which drives the general circulation of the atmosphere. But within this limit the book is full of interesting material.

The first article by J. C. BELLAMY describes the techniques of recording and exhibiting geophysical data. There must be many cases of data being obtained in the field in a form unsuitable for future use. Then follows an article by ARNOLD COURT on "Some new Statistical techniques in Geophysics." The reader is introduced to a circular distribution though it is not clear for what geophysical applications this provides an appropriate discussion of precision. Of much wider relevance to the problems of geophysical research, in which one very often wishes to discuss the precision of mean directions in space, is a recent paper by Sir RONALD FISHER in the Proceedings of the Royal Society on dispersion on a sphere. WHIPPLE'S article on the exploration of the upper atmosphere by meteoritic techniques is of great interest. D. W. PRITCHARD writes fully on estuarine hydrography. G. P. WOOLLARD surveys carefully "The Earth's Gravitational field and its Exploitation," both on the geodetic and geological sides.

The last article is by J. R. BALSLEY on "Aeromagnetic Surveying." It is probably the best article in the book as it contains some examples of the remarkably detailed and beautiful isomagnetic charts, which the application of this technique has provided. It is also probably the most useful article as no comparably detailed account of the design and use of the airborne magnetometer has been published before.

As will be seen the book should contain something of interest in all branches of geophysics and as such is much to be welcomed.

S. K. RUNCORN

JOHN C. JOHNSON: **Physical Meteorology.** pp. 393 + xii. London, Chapman & Hall. 60s.

The subject matter of this book—more often referred to in this country as "atmospheric physics"—is a study of atmospheric phenomena and processes not specifically related to the movements and circulations which cause weather. The book may be regarded as following (but in no slavish sense) the path pioneered by HUMPHREYS' *Physics of the Air*, but in the present volume the impact of modern techniques, such as radar, on methods of exploring the atmosphere is made evident in many ways.

VOL. 5 1954

As might be expected, the book pays much attention to radiation, both visible and invisible. The first three chapters deal with atmospheric refraction (including the anomalous propagation of high-frequency radio waves), scattering (with a good account of polarization of the daylight sky), and the theory of visibility. Radiation, both solar and terrestrial, is considered in two chapters, the second of which includes a short account of the heat budget of the Earth. The treatment of short-wave radiation and the solar constant is good, but the real difficulties of the water-vapour absorption spectrum are not properly explored. There is room in meteorological literature for a full account of this very complicated problem and here, if anywhere, the student might expect to find it. Still less complete is the account of the heat balance, but here one may sympathize with the author who clearly could not find room for anything like a proper treatment of convection in a book which sets out to cover a very wide field at graduate, but hardly post-graduate, level. In passing, it is worth while pointing out that the expression for the heat flux in a solid in terms of the conductivity and the temperature gradient is not, as stated here, NEWTON's law of cooling. NEWTON's law of cooling, that the rate of loss of heat from a body is proportional to its temperature above the ambient, is a boundary condition which integrates the effects of conduction, convection and radiation at a surface.

Chapter 6 deals with the well-explored field of meteorological optics; rainbows, fog bows, glories, haloes, sun pillars, and all the varied phenomena of the heavens are dealt with in a succinct but admirably clear fashion. Here the theories are, for the most part, well established, but the same can hardly be said of the microphysics of clouds and the mechanism of precipitation, discussed in the next two chapters. The author gives a good summary of the main developments in this field and has been bold enough to attempt an assessment of artificial precipitation. Not all, or perhaps even a majority of, meteorologists will agree with his statement that "the results, to date, indicate that man under extremely favourable conditions has under his control the factors necessary to start precipitation" or that "there is evidence that cloud seeding . . . will cause rain to fall on the ground in measurable amounts." For most of us the verdict is still "not proven," and doubts are growing stronger, not weaker.

The three final chapters deal with atmospheric electricity, the ionosphere, and the ozonosphere, and finally, the structure of the "upper atmosphere" (from about 25 to 100 km) as revealed by acoustical measurements, meteors, and by direct exploration by large rockets. The last is a particularly interesting chapter which shows the author's gift for condensation at its best.

It will be seen from the above that the field covered by this book is very wide, so that really deep treatment cannot be expected. It is primarily a book for the student (each chapter concludes with examples for solution) rather than for the research worker, but there will be few meteorologists who will not be glad to have this volume on their shelves. In any case, those who may wish to pursue a particular topic deeper will find their task made easier by the excellent references given at the end of each chapter. In short, by uniting in one volume work carried out in many fields—meteorology, astronomy, radio, aerodynamics—the author has performed a most useful work.

The book is well printed and illustrated and is furnished with a good index.

O. G. SUTTON

Advances in Electronics. Edited by L. MARTON. Vol. V, pp. xi + 420. New York: Academic Press, Inc. London: Academic Books, Ltd., 1953. $9.50.

This book is the fifth in a series which have been published at intervals since 1949, and which comprise critical and integrated reviews of specific topics in the field of physical electronics and in selected branches of engineering electronics. The present volume contains eight contributions, the authors of which, with one exception, are associated with various establishments and research organizations in the United States of America.

The first essay is by R. CLARK JONES and is entitled "Performance of Detectors for Visible and Infra-red Radiation." It deals with the various types of detector used for such radiation, including thermal and photoemissive detectors, photoconductive cells, photographic negatives, radio antennae, and the human eye. An extensive and quantitative assessment of the performance of all these detectors is presented, special attention being given to the various types of "noise" which limit the "detectivity" or ratio of "responsivity" to noise.

Next follows a somewhat shorter survey of "Beta-Ray Spectrometers," by R. W. HAYWARD, which describes briefly some of the instruments recently developed for improving the experimental study of electron spectra. The review is confined to two classes of instruments: prismatic spectrometers in which the source, central ray of the electron beam, and detector lie in a plane perpendicular to the magnetic field; and lens spectrometers in which the source, central ray, and detector are axially symmetrical to the magnetic field.

The branch of solid-state physics that is concerned with the phenomena associated with light emission from solids is reviewed by F. E. WILLIAMS under the title, "Solid-State Luminescence"; and this is followed by an article on "Thorium Oxide and Electronics," by W. E. DANFORTH, describing certain practical applications of thorium-oxide cathodes, and referring to the need for more decisive experiments to supplement theoretical developments, which are in a fragmentary state. The great increase in research and application in the field of electronics has resulted in a demand for accelerated production technique applied to high vacuum pumping equipment. "A Review of Modern Vacuum Pumps in Electronics Manufacturing," by H. C. WEINGARTNER and S. W. KENNEDY, surveys current vacuum practice in the electronics industry.

In previous volumes in this series there have been four papers on various aspects of the magnetron. In the work now under review, the only contributor from a British establishment, R. Q. TWISS, presents an analytical treatment of the pre-oscillation state in cylindrical and linear magnetrons in a paper entitled, "On the Steady-State Theory of the Magnetron." It is pointed out that the experimental evidence so far available is too scanty and inconsistent to be very useful in verifying the theory.

The last two papers in this book are of considerable topical interest. C. J. HIRSCH in "A Review of Recent Work in Color Television," describes the status of colour television in the U.S.A. in June 1953, and deals in an excellent manner with the compatible system developed by the National Television System Committee. With an appendix on Colorimetry, a Glossary of terms, and a test specification of the system, this contribution will be found invaluable by those now concerned with development and exploitation in this field. In a concluding contribution, entitled "Junction Transistor Applications," J. S. SCHAFFNER presents a treatment of junction transistor circuits and their application to linear amplifiers, and, to a lesser extent, oscillators. The author emphasizes the difficulty of making a useful review in this field where developments are taking place very rapidly, due mostly to commercial pressure.

Each of the articles referred to above is well illustrated and accompanied by a comprehensive list of references to the subject under discussion. The book concludes with a new feature—a cumulative author and subject index of all the articles presented in the first five volumes of this series. This index considerably enhances the usefulness of these surveys of progress, and the subject index shows at a glance the wide field covered by the term "electronics." The choice of subjects dealt with so far would, however, appear to be consistent with the following definition put forward in 1952 by the International Electrotechnical Commission: "*Electronics*—That branch of science and technology which deals with the study of the phenomena of conduction of electricity in a vacuum, in a gas and in semiconductors, and with the utilization of devices based on these phenomena." The present series of books is serving an admirable purpose in enabling students, scientists, and engineers to keep themselves informed on the many and diverse lines of progress so intensively being pursued in this subject.

R. L. SMITH-ROSE

VOL. 5 1954

Journal of Atmospheric and Terrestrial Physics, 1954, Vol. 5, pp. 253 to 272. Pergamon Press Ltd., London

Aircraft investigation of the large ion content and conductivity of the atmosphere and their relation to meteorological factors

RITA CALLAHAN SAGALYN and GERARD A. FAUCHER
Air Force Cambridge Research Center, Air Research and Development Command

(*Received* 18 *May* 1954)

ABSTRACT

Recent simultaneous measurements of electrical conductivity, large-ion concentrations, temperature and humidity in the altitude range 700 to 15,000 feet by means of aircraft are described. The results of forty flights show that over continental areas in fair weather there exists a layer adjacent to the ground varying in depth from 1000 to 10,000 feet in which the vertical distributions of charged nuclei and electrical conductivity are controlled primarily by atmospheric turbulence. At the upper boundary of this layer there is observed a sharp decrease in temperature gradient and in a transition region approximately 800 feet in depth, the conductivity is found to increase by a factor of 1·5 to 6·0; the large ion content to decrease by a factor of 1·5 to 100. Above this transition region the large ion content is reduced to very low values and the electrical conductivity increases with altitude in the same manner as determined from earlier experiments. Analysis shows that the surface layer can be identified with the friction layer familiar to meteorologists. Application of the small ion equilibrium equation shows that the destruction of small ions by collisions with nuclei is the most important factor removing small ions throughout this region. The columnar resistance of the surface layer is shown to make a significant contribution to the total resistance of the atmosphere. Observed correlations between horizontal variations in the measured electrical and meteorological variables are described and interpreted.

1. INTRODUCTION

The observations described in this paper are a continuation and extension of an investigation of the electrical properties of air in the troposphere described in a previous paper (CALLAHAN *et al.*, 1951). It was shown there that above the first few kilometres the electrical conductivity of the air is a result of the existence of equilibrium between the production of small ions by cosmic radiation and their destruction by recombination. The conductivity in the lowest part of the atmosphere was found to be less than would be expected from cosmic ray activity data which indicated that destruction of small ions by combination of small ions with charged and uncharged nuclei becomes an important factor in determining equilibrium. It was, therefore, decided to investigate the concentration of charged nuclei (large ions) and to determine the factors controlling their distribution in the atmosphere. Electrical conductivity, temperature, humidity, and pressure were also recorded.

Previously, information about the large ion content of the atmosphere could only be inferred from the results of a limited number of balloon flights on which condensation nuclei were measured. These measurements were carried out principally by WIGAND (1919). LANDSBERG (1938) has summarized the data available on the vertical distribution of nuclei in the atmosphere. The results show a rapid decrease in concentration with altitude in the first few kilometres; the concentration at 10,000 feet being only a few per cent of the surface value.

Knowledge of the large ion content of the atmosphere is not only necessary for the investigation of the processes involved in ion equilibrium but is also important

to the understanding of the effect of atmospheric turbulence on the electrical properties of the lower atmosphere.

2. METHOD OF OBSERVATION

The results of over forty flights are described in this paper. Most of the measurements were carried out on a fixed flight path, 25 miles long, located southeast of Concord, New Hampshire. Several measurements were also carried out on selected flight paths near San Antonio, Texas, and in the mountainous regions of Southern California. In New Hampshire and Texas, locations for the measurements were chosen where the elevation of the surface above sea level was relatively constant (height of the surface above sea level varied not more than 200 feet) and over which there was believed to be no large source of industrial pollution. All flights in a given area were made over the same fixed flight path.

The aircraft was flown along the chosen flight path making one pass at specified altitudes between 800 and 15,000 feet above ground. The altitude intervals were 1000 to 2000 feet unless the records showed that any of the measured parameters were changing rapidly with altitude in which case the altitude intervals were reduced. The measurements were carried out through all seasons of the year and throughout the day. The discussion of results is limited to those obtained in fair weather, which we define as days on which there was no unbroken cloud layer to inhibit the development of the daily turbulent cycle.

VOL.
5
1954

The type of continuous record which is obtained during level flight is shown in Figs. 12 and 13. The parameters are positive conductivity λ_+, concentration of positive large ions N_+, temperature T, relative humidity $R.H.$, and pressure P. The horizontal scale is time, in minutes, the aircraft speed is approximately 160 miles per hour. The recorded values are relatively steady except for short periods at certain altitudes when the recorded values of conductivity, large ion concentration, and humidity show a rapid deviation from the steady value. The significance of these fluctuations will be discussed later. In evaluating the records the mean value of a parameter at a given level is taken from the steady part of the record, the short period fluctuations are included in Table 1 under "Limits of Variation."

3. APPARATUS

(a) Instruments were installed in a B-17 aircraft to measure and record simultaneously electrical conductivity, temperature, pressure, relative humidity, air speed, large ion concentration, and the air flow through the large ion apparatus. In order to continuously measure these parameters in flight with only one operator, it was found essential to use automatic recording and a central control system.

A general view of the arrangement of the instruments on the aircraft is shown in Fig. 1. All power lines, timing circuits, etc., pass through the main control panel. Four chart recorders, electrometer amplifiers, battery boxes and the control panel, located near the rear of the fuselage, are positioned so that the operator can control and check the operation of all instruments. A four-switch Haydon Timer is used to synchronize all records by placing a timer signal on each record at ten-minute intervals. The airflow through each ion counter is shut off

by means of remotely controlled valves in order to obtain absolute zero and to check for insulation leakage. It has been found necessary to shock-mount all electrometers, recorders, conductivity, and large ion chambers.

(b) *The electrical conductivity* of the atmosphere was measured with a cylindrical condenser system, based on principles first outlined by GERDIEN (1905). A description of the apparatus used in these experiments is given in CALLAHAN (1951). In the experiments under discussion the cylindrical condenser and the electrometer preamplifier are located in the nose of the aircraft while the electrometer amplifier, recorder, and batteries supplying a constant d.c. potential to the conductivity chamber were located in the waist compartments. Using the results

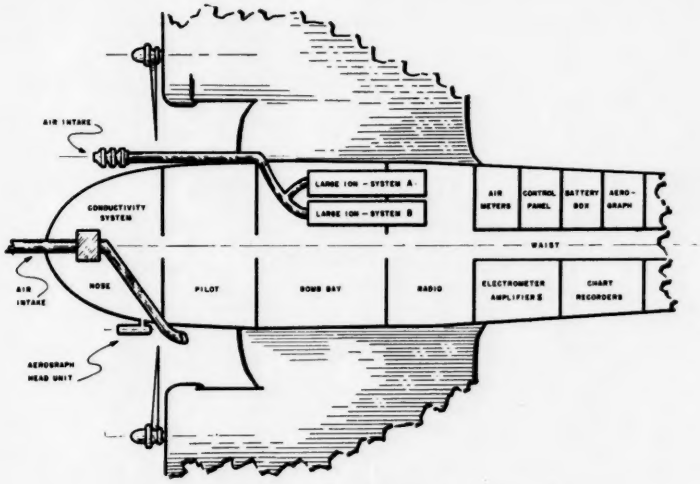

Fig. 1. Arrangement of apparatus on aircraft.

of our earlier experiments in which it was found that above a few hundred feet $\lambda_+/\lambda_- = 1 \pm 0{\cdot}1$, the electrical conductivity produced by ions of only one sign is measured.

(c) *The meteorological parameters*: temperature, pressure, relative humidity as well as the air speed of the aircraft are measured and recorded with an Aerograph System developed at the Air Force Cambridge Research Center (GUSTAFSON, 1954). It consists essentially of a temperature and humidity transmitter mounted on the nose of the aircraft, a pressure and air speed transmitter, and a 5-channel graphic recorder for continuously recording these variables, which is mounted in the waist. The fifth channel is used for an automatic time signal. The temperature and relative humidity sensing elements are, respectively, a thermistor bead and a carbon coated strip.

(d) A schematic diagram of the apparatus used for measuring *large ion concentrations* is shown in Fig. 2. The air sample enters the system through a louvred intake designed to reduce the airflow to approximately 4 litres per second while maintaining laminar flow. This intake is located near the nose of the aircraft approximately 6 feet in front of the propellers. The air sample is then passed into

the ion counting instruments located in the bomb bay through a brass tube 2 in. in diameter. In the bomb bay the airstream is first passed into a Y pipe section which divides the air flow in half and then passes through two identical systems in parallel. In each system the airstream is first passed through an electrostatic filter which removes all ions with mobility greater than 0·7 cm²/sec-volt. The air sample next passes through the "large ion counter," then into an output tube and is finally exhausted into the radio compartment. The velocity of air through the instrument is measured with a Hastings Precision Thermal Anemometer Probe mounted in the output tube. The output of this instrument is recorded on a two-channel Brown Electronik Recorder. The special advantage of the Hastings Air

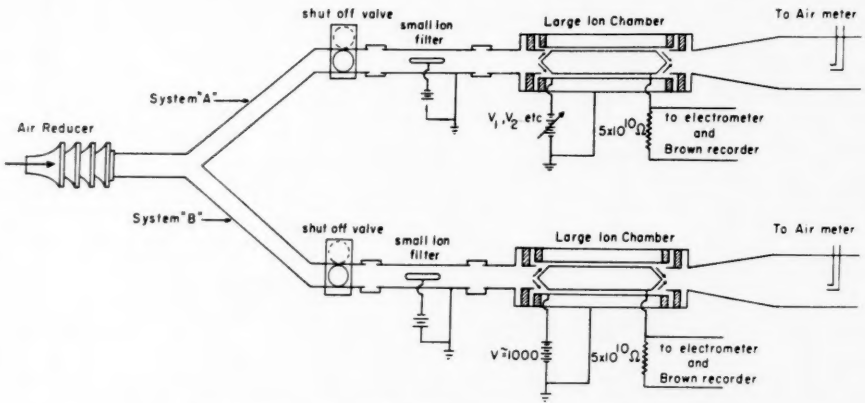

Fig. 2. Schematic diagram of large ion apparatus.

Meter for air flow measurements in the free atmosphere is that the correction which must be applied for density variations with altitude can be easily determined.

The large ion counter used in these experiments is essentially the same as the one designed by G. R. WAIT and O. W. TORRESON (1934) for surface measurements with special modifications for aircraft use. It consists of three concentric insulated cylinders approximately one metre long. The air stream passes between the central and intermediate cylinders 1·27 cm apart, made of highly polished stainless steel. A d.c. voltage is applied across the intermediate and outer (grounded) cylinders. The central cylinder is connected to ground through a resistance of the order of 10^{10} ohms. The voltage developed across this resistance, determined by the rate at which charged particles in the air stream are drawn to the central cylinder under the influence of the applied electric field, is measured with a vibrating reed electrometer and recorded on a Brown Recorder. By suitably adjusting the air flow and applied potential all charged particles in the air stream of either sign with mobility greater than $2{\cdot}0 \times 10^{-4}$ cm²/sec-volt can be measured with this instrument.

If the atmospheric ions were distributed in such a way that there were no ions with mobility less than the limiting mobility of this instrument the measurement of large ion concentrations would be relatively simple. With the airflow and

VOL. 5 1954

applied potential adjusted to obtain "saturation" for the instrument, the large ion content may be obtained from the relation

$$i = WNe \tag{1}$$

where i is the electrometer current, W the airflow through the system, e the charge per ion and N the concentration of large ions of one sign. However, in agreement with results reported by ISRAEL (1933), SIKSNA (1952) and others, preliminary laboratory experiments showed the existence of atmospheric ions with mobility lower than the limiting value for this instrument. For this reason the theory developed by H. ISRAEL (1931) is applied to determine the concentration of atmospheric ions from the current-voltage characteristic of the large ion chamber. ISRAEL'S analysis shows that if the concentration of atmospheric ions remains constant during the period of measurement which in our experiments is approximately 20 minutes, then the concentration of charged particles of one sign in the mobility range k_g to ∞ is given by the equation:

$$\int_{k_g}^{\infty} dn = Z - V\,dZ/dV \tag{2}$$

With $Z = i/We$ plotted vs. V the applied potential (2) is the equation of a straight line which is tangent to the Z vs. V curve at the point $k_g \alpha 1/V$ and which intercepts the ordinate at the point $\int_{k_g}^{\infty} dn$. dn is the ion concentration in the mobility range k to $k + dk$. The limiting mobility k_g is obtained from the relation, $k_g = W/4\pi CV$, where W is the airflow, V the maximum applied potential and C is the capacitance of the chamber.

In the free atmosphere the concentration of large ions is seldom constant, although the fluctuations at constant altitude were often found to be less than at the surface. If the ion spectrum does not vary significantly during the period of measurement, errors introduced in the current-voltage characteristic due to varying ion content can be eliminated with the experimental arrangement described above. The voltage on one of the two large ion chambers in parallel is varied in arbitrary steps while on the second, the "reference system," a constant potential is maintained. A characteristic independent of the absolute number of ions is obtained by plotting Z/Z_0 vs. V; $Z_0 = i_0/W_0 e$ is obtained from the reference system. The analysis is essentially unchanged by this modification. Thus, the total ion concentration in the mobility range 2×10^{-4} to 0·7 cm²/sec-volt, which we will refer to as the large ion concentration, is equal to the value of the ordinate at the point where the tangent intercepts the ordinate times the average value of Z_0. (All ions in the mobility region 0·7 cm²/sec-volt to ∞ are removed with the electrostatic filter.) A more detailed analysis of the current-voltage characteristic to obtain the size distribution of atmospheric ions in the range covered by the instrument will be given in a paper to be published shortly.

The maximum experimental error in the measurement of electrical conductivity is ± 6 per cent; relative humidity ± 7 per cent; temperature ± 1°C. The experimental error in the large ion measurement due to the accuracy with which circuit parameters can be determined is ± 7 per cent. To this must be added an error which is a function of the magnitude of the large ion concentration; the error in

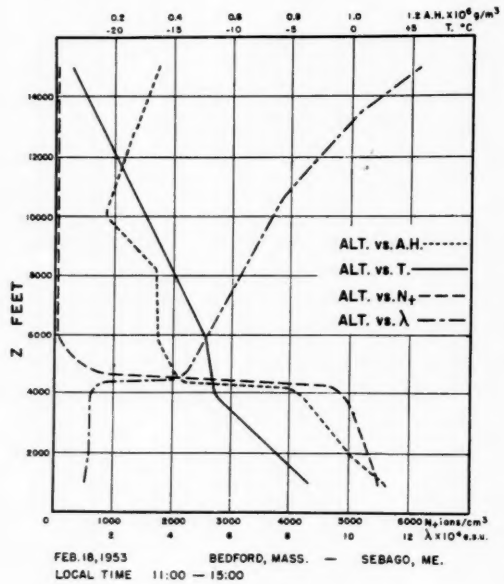

Fig. 3.

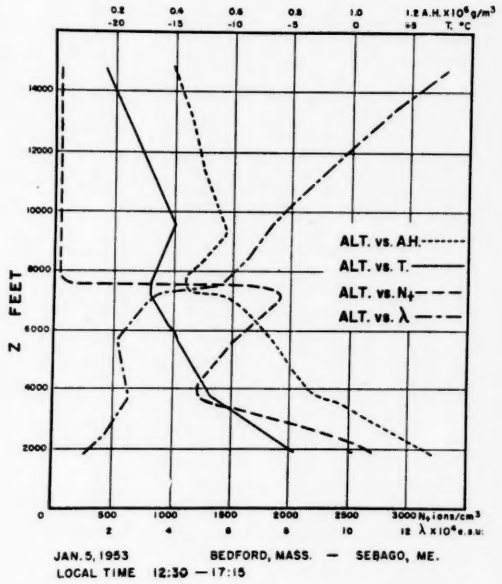

Fig. 4.

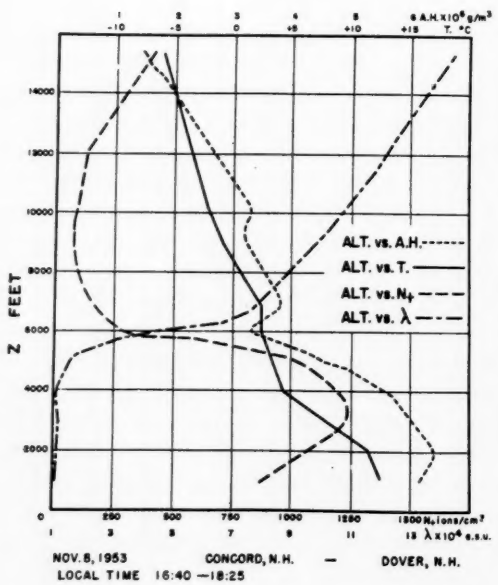

Fig. 5.

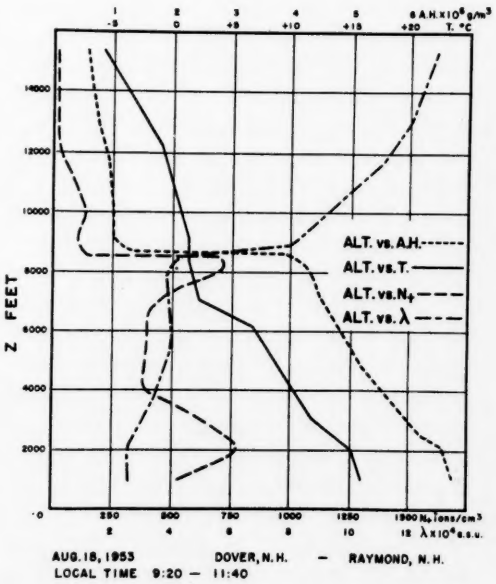

Fig. 6.

Figs. 3, 4, 5, 6. Variation of absolute humidity ($A.H.$), temperature (T), positive large ion concentration (N_+) and total electrical conductivity (λ) with altitude above sea level (Z).

VOL. 5 1954

the ratio Z/Z_0 is only a few per cent for concentrations above 1000 per cc and approaches 10 per cent for concentrations of the order of 200 per cc.

4. Observations—Variation with Height

(a) *General description*

In Figs. 3, 4, 5, and 6 are shown the variation with altitude of electrical conductivity, positive large ion content, temperature, and humidity observed on four flights. The most striking characteristics of the vertical distribution of the measured parameters which have been observed on all fair weather flights are shown on these curves. The results show that in fair weather over continental areas the troposphere is divided into two layers with distinct electrical characteristics. The lower layer is characterized by high large ion content, high humidity and low electrical conductivity. At constant altitude in this layer the small ion content deduced from conductivity measurements is approximately inversely proportional to the large ion content. The conductivity, large ion, temperature and humidity records show that the horizontal variations of these parameters tend to decrease with altitude, except in the vicinity of the top of the layer where large fluctuations are usually observed. Hereafter, this lower region will be referred to as the exchange (austauch) layer. The depth of the exchange layer has been found to vary from 1000 to 10,000 feet in the course of this investigation.

At the top of the exchange layer a change to a more stable temperature lapse rate is observed, which sometimes consists of an inversion and which is always less than adiabatic. In a transition region varying in depth from a few hundred to a few thousand feet there is observed a sharp change in the large ion concentration, electrical conductivity, and humidity. During the course of these experiments the total conductivity has been found to increase in this region by factors ranging from 1·5 to 6 and the positive large ion content has been found to decrease by a factor of 1·5 to 100. Horizontal variations of the electrical properties and humidity reach a maximum in this region. Passing upward through this region a noticeable decrease in mechanical turbulence is also observed throughout the daylight hours. This is noted by a pronounced decrease in the random tossing of the aircraft and also by a sharp decrease in the instantaneous fluctuations about the mean in the aerograph air speed records. Above this transition region, the large ion content is reduced to very low values often close to zero, and the electrical conductivity increases rapidly with altitude in the same manner as determined from earlier experiments.

To illustrate the general nature of the distribution described above, the results of conductivity and large ion measurements obtained on nine flights chosen at random between December 1952 and August 1953 over a fixed flight path in New Hampshire are summarized in Figs. 7 and 8. As shown on the figures, H, the depth of the exchange layer, varies between 3200 and 9500 feet. In Fig. 7, the ratio of the height h at which constant altitude measurements were obtained to the height H of the exchange layer is plotted as a function of the ratio λ_m/λ_c. λ_m is the measured value of conductivity at height h and λ_c is the computed conductivity value assuming equilibrium exists between the production of small ions by cosmic radiation and their destruction by volume recombination. Using the results of

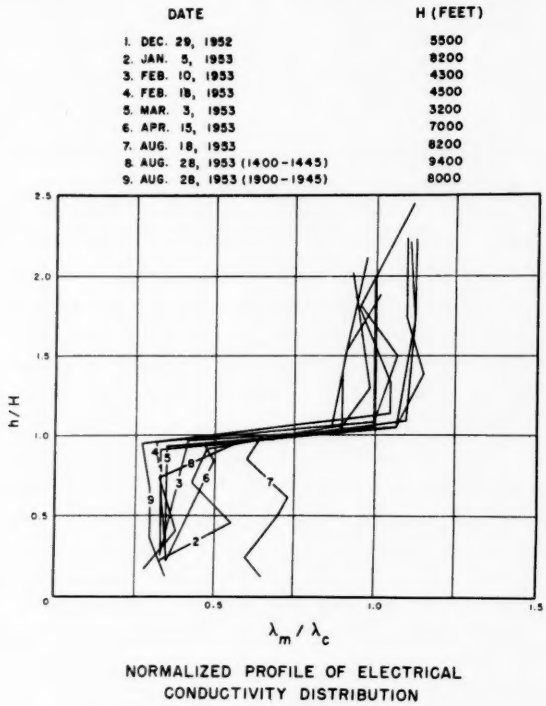

Fig. 7. Aircraft altitude (h)/height of exchange layer (H) vs. conductivity measured (λ_m)/conductivity computed from cosmic ray data (λ_c).

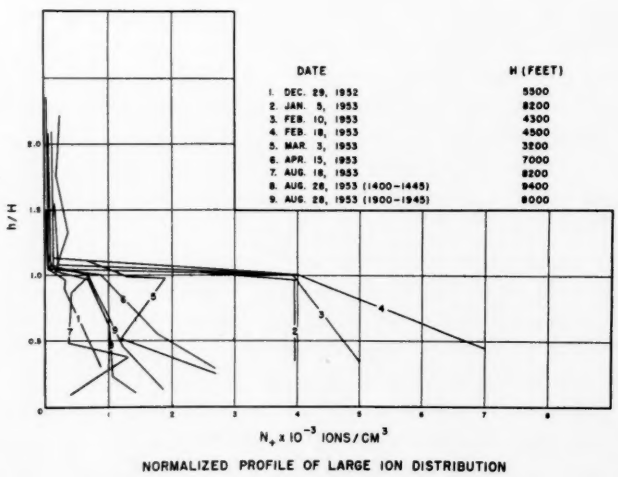

Fig. 8. Aircraft altitude (h)/height of the exchange layer (H) vs. positive large ion concentration (N_+).

VOL. 5 1954

THOMSON's theory for the volume recombination coefficient, the polar conductivity of air is given by the expression:

$$\lambda_c = \frac{ek_0 M^{1/4}}{C^{1/2}} \left(\frac{I_0}{\epsilon}\right)^{1/2} \left(\frac{P_0}{P}\right)^{1/2} \left(\frac{T}{T_0}\right)^{5/4} \tag{3}$$

where e is the charge per ion, k_0 and I_0 are mobility and ionization intensity at N.T.P., i.e., at $T_0 = 273°$ absolute and $P_0 = 760$ mm Hg. M is the average molecular weight of ions in air, C is a constant with the value $1{\cdot}73 \times 10^{-5}$ cm^3 sec^{-1}, ϵ is a probability function which is a function of temperature and pressure. The exact expression for λ_c was used in the present computation because the approximation used in CALLAHAN *et al.* (1951) does not hold with sufficient accuracy below 5000 feet. This manner of representing the results is necessary to illustrate the general features of the distribution because of the large variations in the height of the mass exchange layer from day to day. Above the exchange layer the ratio λ_m/λ_c should approach unity if the simple type of equilibrium assumed in the derivation of equation (3) exists. The results show a maximum deviation of 10 per cent from this value which may be due to statistical fluctuations in cosmic ray intensity or to small variations in the value of the constants used in the computation of λ_c. Large fluctuations in this ratio are to be expected in the exchange layer because of large variations in nuclei content and rate of production of ions from day to day. The results given in Fig. 7 show a maximum fluctuation about the mean of approximately 80 per cent. In Fig. 8, h/H is plotted as a function of N_+, the concentration of positive large ions. The layer-like nature of the conductivity and large ion distributions in the troposphere is clearly indicated by these figures. The application of these simultaneous large and small ion measurements to a study of ion equilibrium in the exchange layer will be discussed in a later paper.

(b) *Variability of profile in exchange layer*

Figs. 3 to 6 were chosen to illustrate the general features of the vertical distribution of the electrical parameters in the lower troposphere and to show the variability in the height of the exchange layer, in the magnitude of the measured parameters and the complexity of the profile often observed in the exchange layer. In general, the observed profiles can be explained in terms of the vertical temperature distribution and horizontal winds; for example, significant changes in the distribution of charged nuclei are always accompanied by changes in the temperature lapse rate.

Since in the exchange layer, it has been found that variations in conductivity are largely brought about by changes in nuclei content, it is considered sufficient to describe only the charged nuclei distributions in further detail. In this region, the profiles of charged nuclei can be roughly divided into five types which are illustrated in Figs. 3 to 8.

(1) Approximately 55 per cent of the results show a decrease with altitude to the top of the exchange layer. See Fig. 3 and curves 1, 3, 4, 6, 8, 9 of Fig. 8. This is usually accompanied by a small increase of λ, a continuous decrease in absolute humidity with altitude and an approximately constant temperature gradient from 1000 feet to the top of the layer.

(2) A nearly uniform distribution with altitude has been observed throughout the exchange layer on about 5 per cent of the flights. See curve 2 of Fig. 8. This type of distribution is accompanied by high winds, intense turbulence and an adiabatic temperature lapse rate. The conductivity and absolute humidity distributions are similar to type 1. Both types 1 and 2 were usually developed by early afternoon and thus are characteristic of a fully developed turbulent layer.

(3) On approximately 10 per cent of the flights there was observed first a decrease, then an increase with altitude to the top of the exchange layer. See Fig. 4 and curves 5 and 7 of Fig. 8. As shown in Fig. 4 the conductivity distribution is roughly the inverse of the large ion distribution. When this type of distribution was observed a cloud deck often developed later in the day in the region of increase of large ion content with height.

(4) Several of the late afternoon and evening flights, approximately 10 per cent of the total, show first an increase with altitude, then a decrease to the top of the exchange layer (see Fig. 5). The temperature gradient is observed to be more stable at lower levels than at intermediate levels. The results suggest that although the source of nuclei has been cut off, enough residual turbulence remains to transport vertically nuclei that have been previously introduced into the atmosphere.

(5) The morning flights, consisting of about 20 per cent of the total, generally show the most complicated nuclei distributions. Then the magnitude of the nuclei content up to the level to which turbulence has penetrated is significantly higher than the concentration at higher altitudes in the exchange layer. See Fig. 6. (This example is further complicated by an increase of nuclei at the top of the exchange layer, characteristic of type 3.) Periodic measurements carried out throughout the day show that when vertical mixing penetrates to the top of the exchange layer, usually by early afternoon, this develops into a distribution of types 1, 2, or 3.

VOL. 5 1954

(c) *Limits of variation*

The limits of the variation in the electrical parameters, conductivity and positive large ion content as a function of height above sea level observed during the period of this investigation are shown in Table 1. Along the flight path the elevation of the surface above sea level was approximately 250 feet. The limits of variation in total nuclei content can be obtained by using the experimentally determined value 2·5 for the ratio of uncharged to charged nuclei (LANDSBERG, 1938, p. 210) and in agreement with the results of the present experiments assuming the positive large ion content equal to the negative. The extreme variability of these parameters in the altitude range 3000 to 9000 feet is partly due to the fact that these levels were sometimes in the exchange layer and sometimes above it. The variation indicated at 2000 feet is representative of the variation at a given level when the results are restricted to data obtained in the exchange layer. The limits of variation above 10,000 feet were 0–500 ions/cc except for three days in August when nuclei penetrated the boundary of the exchange layer. Changes in air mass accounted for some of the largest variations in nuclei content observed on successive days. Arithmetic means of electrical conductivity and positive

Table 1

Altitude above sea level (feet)	*Total conductivity (sec^{-1}) e.s.u.* $\times 10^4$			N_+ *(no./cm³)*		
	Limits of variation	*Mean*		*Limits of variation*	*Mean*	
		In exchange layer	*Above exchange layer*		*In exchange layer*	*Above exchange layer*
1,000	0·62– 3·10	1·71	—	496–14,000	2519	—
2,000	0·30– 5·70	1·95	—	131– 7,000	1577	—
3,000	0·32– 6·00	2·45	—	0– 5,700	1250	—
4,000	0·40– 6·38	2·80	4·27	63– 4,887	1139	352
5,000	1·32– 6·70	3·52	5·39	0– 4,120	770	247
6,000	0·80– 7·21	4·45	5·88	0– 3,280	744	156
7,000	1·50– 8·59	4·48	7·14	0– 1,920	480	133
8,000	1·65– 9·52	4·79	7·22	0– 2,320	701	335
9,000	3·75–10·28	5·37	8·57	0– 1,650	353	195
10,000	4·26–11·10	—	8·90	0– 1,200	—	230
12,000	6·92–14·58	—	12·05	0– 875	—	118
15,000	7·38–19·75	—	15·16	0– 2,450	—	275

large ion content for all observations are also given in Table 1. At altitudes which were sometimes in the exchange layer and sometimes above it, means were computed for these two cases. The average values must be viewed with caution, since the vertical distribution obtained from these values does not give an accurate picture of the profile on individual days.

(d) *Variation with area*

The general character of the vertical distribution described above is found to be essentially unchanged with area even over mountainous regions. Experiments carried out in the summer months in the mountainous regions of Southern California over peaks up to 14,000 feet above sea level show that the exchange layer

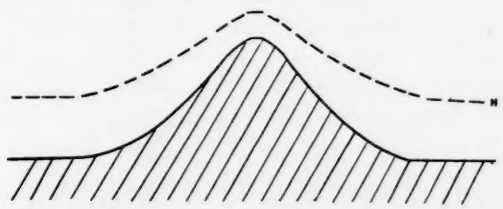

Fig. 9. Variation in height of exchange layer over mountain.

exists over mountains but is reduced in height as indicated in Fig. 9, where the dashed line indicates the top of the exchange layer. The layer in this region was found to vary from a few hundred to 5000 feet in depth. Thus, the records show, for example, the electrical conductivity 1000 feet above a peak 7000 feet above

sea level was four times lower than the conductivity 8000 feet above sea level over a valley a few miles away. These results lead us to believe that the large differences between the conductivity values reported by PLUVINAGE and STAHL (1953) at Central Station, Greenland, altitude 2·99 km during July and August 1951, and the results of our earlier measurements at the same altitude in the free atmosphere are due to the fact that the exchange layer extended above Central Station during the period of measurements. During the winter months when convection is greatly reduced, undoubtedly the exchange layer does not penetrate the top of many high mountains; then this important difference between surface and free air measurements will be reduced or entirely eliminated.

These experiments have been carried out through all months of the year. The most significant seasonal trends are an increase in the average height of the exchange layer in the summer months; in New England the average height in January and February was approximately 4500 feet, while in August it extended to approximately 8000 feet. There was also observed a higher nuclei content on the average above the exchange layer in the summer months. Two flights in August show that large ions penetrated the boundary region in the middle of the day as turbulence reached a maximum even though the temperature gradient remained very stable in the vicinity of the boundary.

VOL. 5 1954

5. DISCUSSION OF RESULTS OF SECTION 4

(a) *Identification with friction layer*

The simultaneous measurements of temperature and humidity distributions as well as the information obtained on atmospheric turbulence, described in the last section, show that in general the exchange layer is to be identified with the layer found in many meteorgraph records which meteorologists refer to variously as the austauch, friction, turbulent and boundary layer. The layer is characterized by a nearly adiabatic temperature lapse rate with a sharp decrease in lapse rate at the top, uniform specific humidity and in many cases obviously produced by frictional turbulence. It is the layer in which the horizontal wind velocity differs from the wind velocity in the general circulation because of the frictional influence of the surface of the earth. There were, however, a few occasions when the boundary of the exchange layer defined as the altitude at which very rapid changes in the electrical properties were observed did not coincide with the boundary friction layer familiar to meteorologists. For example, upon the arrival of a new air mass the height of the exchange layer was found to be lower than the friction layer and very unstable. After several hours of turbulent mixing, this height became equal to the height of the friction layer.

Application of thermodynamic principles to the observed temperature distribution shows how the upper boundary of the exchange layer acts as a barrier to the vertical transport of nuclei, water vapour, etc. Upward moving elements of air are cooled at the adiabatic lapse rate (approximately 1 degree C for every 100 metres of ascent) so that as soon as an air sample passes through the top of the exchange layer its temperature is less than its surroundings. The density of the upward moving element will then be greater than that of its surroundings and

thus it will sink back to a lower level unless a very strong mechanical force pushes it upward. The same analysis applies for a downward moving element.

(b) *Role of atmospheric turbulence*

The principal factors controlling the mean state of turbulence in the atmosphere and thus the vertical distribution of nuclei and all physical properties produced at the surface are known from past investigations (*Compendium of Meteorology* 1951). The most important of these are gradient wind velocity, roughness of the surface, vertical temperature distribution, and latitude. Results showing the dependence of the profile of the electrical properties on temperature lapse rate and wind velocity were indicated in the last section.

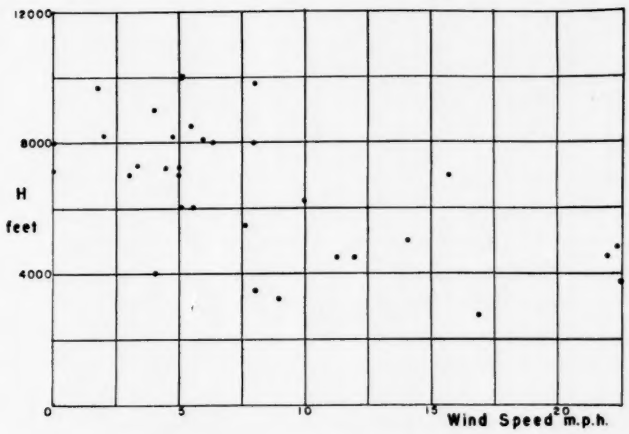

Fig. 10. Height of exchange layer vs. surface wind speed.

The theoretical investigations of the effect of turbulence on mean motions in the atmosphere by ROSSBY and MONTGOMERY (1935) give a definite upper limit to the layer of frictional influence which can be written in the form:

$$H = C \frac{W_a}{f \ln \frac{z_a + z_0}{z_0}} \tag{4}$$

where C is a constant, W_a is the total wind velocity at anemometer height z_a, the Coriolis Parameter $f = 2\omega \sin L$, where ω is the angular velocity of the earth and L the latitude, z_0 is a length characteristic of the roughness of the ground. Thus, over a region with constant roughness parameter z_0, the height should be proportional to the wind velocity at anemometer level. All data on the height of the exchange layer over the New England flight path has been plotted as a function of wind velocity for the same period obtained from local surface stations to determine whether surface wind measurements can be used to predict the height of the exchange layer for individual days. As shown in Fig. 10, however, a linear

relation is not found. This disagreement is probably largely due to the simplifying assumptions made in the development of the theory where an adiabatic temperature lapse rate and gradient wind direction and velocity constant with elevation were assumed. Because it was realized that extraneous influences such as large temperature inversions or marked instability at the surface might cause wide scatter of individual results, ROSSBY and his collaborators used averages of large numbers of observations for the original check of the theory.

These results indicate that interested surface stations could not obtain a reliable estimate for the height of the exchange layer from the Rossby theory. However, comparison of the present results with simultaneous balloon sonde data shows that H can be accurately obtained from temperature and humidity balloon sonde records.

(c) *Small ion equilibrium*

The small ion equilibrium equation can be written in the form:

$$q = \alpha n^2 + \beta n N \tag{5}$$

where q is the rate of production of small ions, α is the volume recombination coefficient, n is the concentration of small ions of one sign which is related to the polar conductivity by the expression $\lambda = nek$; k and e are the mobility and charge respectively of the small ion, N is the concentration of charged nuclei (large ions) of one sign, the coefficient $\beta = \eta_{10} + \eta_{20} N_0/N_+$ and is thus a function of the combination coefficients for collisions between small ions and nuclei and of the ratio of uncharged to charged nuclei. The present observations show that throughout the exchange layer in fair weather βnN is 10 to 30 times greater than αn^2 which means that destruction of small ions by collisions with nuclei is the most important factor removing small ions. Thus, through their control of the vertical distribution of atmospheric nuclei, meteorological factors have a dominant influence on the electrical conductivity of the atmosphere in this region. Furthermore, experiments now in progress, which are being carried out periodically throughout the day show a systematic daily variation of electrical conductivity and nuclei concentration limited to the exchange layer, due to the action of the daily cycle of turbulence.

Above the exchange layer the influence of nuclei on the electrical conductivity terminates abruptly and in agreement with earlier measurements to higher altitudes in the troposphere, the variation of conductivity with height is found to be determined by the simple equilibrium relation $q = \alpha n^2$ (see Fig. 7). Also above the exchange layer no systematic daily variation in the electrical parameters has been found. This is to be expected, since the diurnal variation in cosmic radiation is negligible.

(d) *Columnar resistance over continents*

It is of interest to consider the effect of these results on our understanding of the columnar resistance of the atmosphere over continents. The resistance R of a vertical column of the atmosphere 1 cm^2 in cross section extending from the earth's

VOL. 5 1954

surface to the height h is equal to $\int_0^h r\,dh$; the atmospheric resistivity $r = 1/(\lambda_+ + \lambda_-)$.

The results of the balloon Explorer II indicated that the total columnar resistance from the earth to the upper conducting layers was of the order of 10^{21} ohms. The present results give values of R varying from 9×10^{20} to $2{\cdot}5 \times 10^{21}$ ohms. R was computed from conductivity values; measured values were used to 15,000 feet and values computed from equation (3) assuming cosmic radiation the only source of ionization were used at higher altitudes.

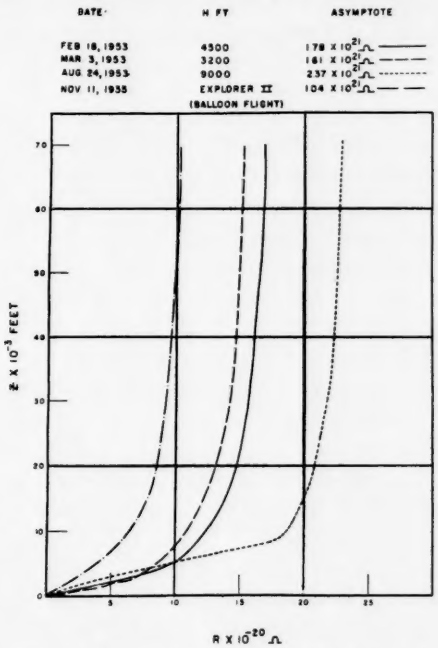

Fig. 11. Resistance (R) of air column 1 cm² in cross section as a function of altitude above sea level (Z).

Computations of the resistance of a vertical column one cm² in cross section from the surface to the top of the exchange layer have been found to vary considerably from day to day and with time of day and amount to from 40 to 73 per cent of the total resistance; the average value was found equal to approximately 60 per cent of the total. These results were obtained in a relatively unpolluted area. The contribution of the resistance of the exchange layer to the total in industrial areas must be greater on the average. Variations in the resistivity of the exchange layer brought about by meteorological factors will therefore have a significant influence on the total columnar resistance of the atmosphere even though it is generally restricted to the lowest three kilometres.

As would be expected from the previous discussion, the altitude variation of R computed from conductivity values is subject to considerable variation. The results obtained on three flights chosen arbitrarily are given in Fig. 11; the altitude variation of R obtained from the Explorer II results is given for comparison.

The results given in Section 4 qualitatively agree with the atmospheric model suggested by G. R. WAIT (1942) and later employed by H. ISRAEL to explain atmospheric electric measurements at the ground. WAIT assumed that the columnar resistance could be considered as divided into two parts; R_1, a lower component varying with local time and R_u, a component constant in time. However, the assumptions made in determining the height to which local influences penetrate leads to misconceptions about the electrical characteristics of the atmospheric friction layer. For example, the present experiments show that the height of the layer often varies in a systematic manner through the day and is also found to vary many thousands of feet from day to day in a given season. Furthermore, the assumption that the atmospheric resistivity is constant throughout the exchange layer is not valid in general.

6. VARIATIONS IN THE HORIZONTAL

Above the exchange layer in fair weather in a given air mass horizontal variations in electrical conductivity, large ion concentration and relative humidity were usually found to be small, amounting to not more than 10 per cent of the mean value at constant altitude. In the exchange layer, in addition to the small, gradual variations observed at higher altitudes, large rapid fluctuations were often observed which sometimes amounted to more than a 100 per cent change in the mean value at a given level. These fluctuations usually consisted of an abrupt deviation from the mean value which continued over distances from a few hundred feet to several miles and then a rapid return to the original value. These localized variations tend to decrease with altitude in the first few thousand feet, then increase within a few thousand feet of the top of the exchange layer, reaching a maximum in the transition region. Over 95 per cent of the results show that in the relative humidity range (10 to 80 per cent) a definite relation exists between variations in the electrical parameters and relative humidity; that is, an increase in large ion concentration is accompanied by an increase in humidity and decrease in electrical conductivity, and vice versa. Examples of this relation are shown in Figs. 12 and 13, where portions of records are reproduced. Large ion content, conductivity, temperature, pressure and humidity are plotted as a function of time; one minute corresponding to approximately $2\frac{3}{4}$ miles.

Several flights were analyzed in considerable detail to determine whether this observed relation between the electrical parameters and relative humidity was the result of a common cause or due to a functional relation between them. The analysis strongly supports the former explanation, that is, that the observed relation is due to turbulent and convective transport of parcels of air in non-uniform regions of the atmosphere where water vapour and nuclei are subject to the same laws of vertical transport.

The following discussion is given in support of this explanation. (1) The temperature measurements obtained simultaneously show that when the prevailing temperature lapse rate departs appreciably from the adiabatic the variations in large ion content, conductivity and humidity are accompanied by a change in temperature (Figs. 12 and 13). Whether the temperature is greater or less than the mean temperature of the layer depends on whether the parcel has been

VOL. 5 1954

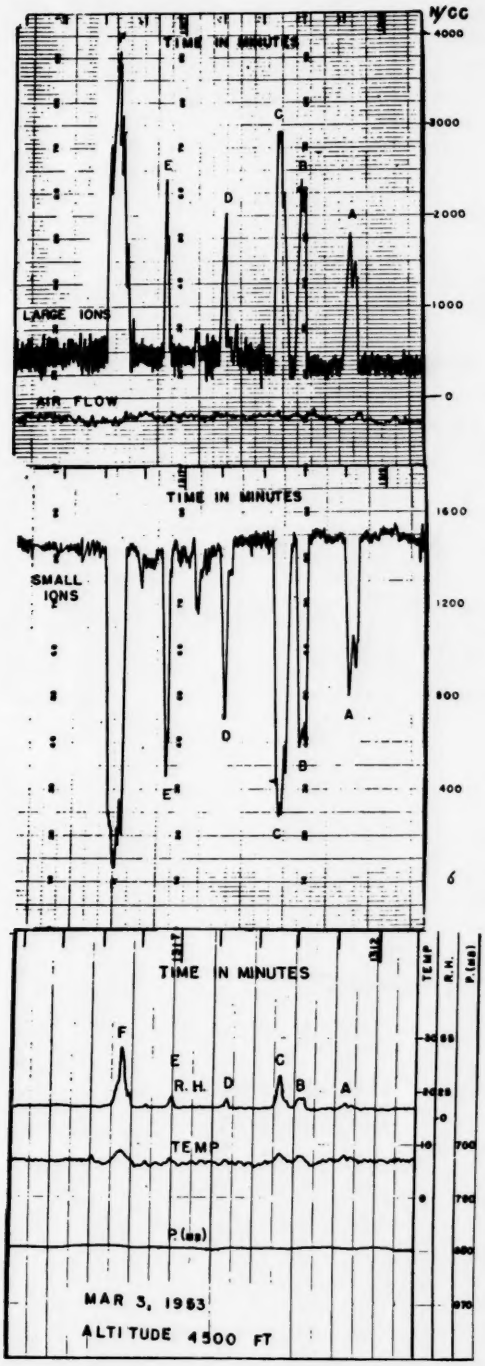

Fig. 12. Horizontal variation of large ion content, electrical conductivity, relative humidity, and temperature.

transported from a higher or lower level. The prevailing lapse rate is always equal to or less than adiabatic. (2) At all altitudes large ion vs. humidity curves show that an increase in large ion content corresponds to an increase in humidity, and vice

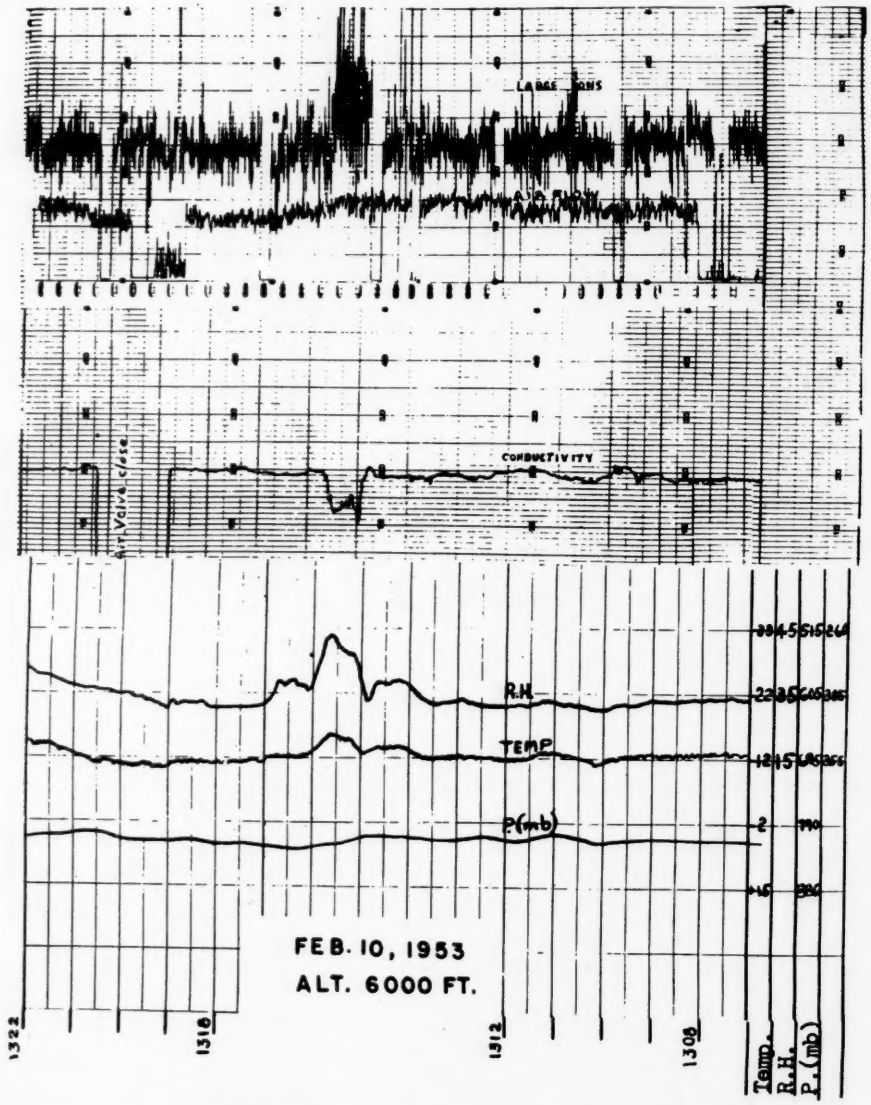

Fig. 13. Horizontal variation of large ion content, electrical conductivity, relative humidity, and temperature.

versa; however, there was found no correlation between the absolute values of large ion content and humidity at a given altitude from day to day. In general, the results obtained above the exchange layer showed less dependence on humidity

VOL. 5 1954

than those obtained in it. (3) The ratio of large ion concentration just before to the concentration just after a variation was plotted as a function of the ratio of the relative humidities observed at the same times to determine whether an exact relation existed between these variables independent of their absolute values at a given altitude. No correlation was observed between the resulting ratios from day to day. For example, for four days analyzed in this manner a humidity ratio of 1·2 corresponded to large ion ratios of 1·25 to 7·0 at 6000 feet. (4) For the localized fluctuations a good correlation was obtained upon comparing relative changes in large ion content at level A with the ratio of the mean value at level A to the mean value at level B obtained from the vertical distribution curves. The magnitude of the relative humidity was used as reference to determine from what level (altitude B) a parcel of air had been transported, neglecting diffusion, etc.

Since these experiments were carried out down to 700 feet above the surface, the same interpretation should be applicable to results obtained at the surface away from intense sources of nuclei. However, if a statistical analysis of the surface data is made, these relations may be obscured by air mass changes with time.

Summary

The present investigation has shown that there exists a layer adjacent to the surface of the earth which we refer to as the "Exchange" Layer:

1. The height of this layer varies between 1000 and 10,000 feet, with an average value of approximately 6000 feet. It varies with season, reaching a maximum in the summer months.

2. At all altitudes in the exchange layer, the limits of variation of charged nuclei were greater than an order of magnitude for the days investigated.

3. The vertical distributions of large ions can be roughly divided into five types which can be explained in terms of atmospheric turbulence, i.e., temperature gradient, horizontal winds, etc.

4. Throughout this layer the small ion content, and therefore, the electrical conductivity is determined primarily by the magnitude of the nuclei concentration.

5. Horizontal variations of large ion content, conductivity, and humidity reach a maximum in the transition region at the top of the exchange layer.

6. At the top of the layer, a change to a more stable temperature lapse rate is observed.

7. A sharp change in the magnitude of the absolute humidity, nuclei content and conductivity is observed at the top of the layer.

8. A reliable estimate of the height of the layer can be obtained from temperature and humidity balloon sonde records. The Rossby Theory does not hold with sufficient accuracy for individual days.

9. In general, the profiles of absolute humidity and charged nuclei are similar.

10. The exchange layer exists over mountains, though reduced in height.

11. The exchange layer was found to contribute 40 to 73 per cent to the total columnar resistance of the atmosphere.

12. The exchange layer can be identified with the atmospheric friction layer.

13. Immediately above the transition region the concentration of charged nuclei of one sign averages approximately 200 ions/cc.

14. Above the exchange layer the electrical conductivity is determined primarily by the intensity of cosmic radiation, in agreement with earlier experiments.

General

15. In the cases examined, the ratio N_+/N_- was found equal to unity on the average with a maximum departure of $\pm 0{\cdot}17$, in the altitude range 1000 to 15,000 feet.

16. Over 95 per cent of the results show that at constant altitude an increase in large ion concentration is accompanied by an increase in humidity and by a decrease in conductivity. Analysis indicates that this relation is due to the turbulent and convective transport of parcels of air in regions of the atmosphere where water vapour and nuclei are subject to the same laws of vertical transport.

The authors wish to acknowledge the work of ROLAND MATSON and MARIA MAHONEY, who assisted in carrying out the experiments and in the analysis of the data. We also thank the personnel of the 6520th Flight Test Squadron, Hanscom Air Force Base, Bedford, Massachusetts, who flew and maintained the aircraft.

REFERENCES

CALLAHAN, RITA C., *et al.*	1951	J. Geophys. Res. **56,** 545–551
GERDIEN, H.	1905	Terr. Mag. **10,** 65–79
GUSTAFSON, P.	1954	Instrumentation for Geophys. Res. No. **3,** Air Force Cambridge Research Center
ISRAEL, H.	1931	Gerlands Beitrage für Physik **31,** 173–216
ISRAEL, H., and SCHULZ, L.	1933	Terr. Mag. **38,** 285–302
LANDSBERG, H.	1938a	Atmospheric Condensation Nuclei Monograph, Penn. State College (Feb.)
	1938b	Beitr. Geophys. (Supp) 3, 155–252
PLUVINAGE, P., and STAHL, P.	1953	Annales de Geophysique **9,** 34–44
ROSSBY, C. G., and MONTGOMERY, R. B.	1935	M.I.T. and Woods Hole Oceanog. Inst., Papers in Phys. Oceanog. and Meteorology **3,** No. 3
SIKSNA, R.	1952	Arkiv för Geofysik **1,** No. 18, 483–518
TORRESON, O. W., and WAIT, G. R.	1934	Terr. Mag. **39,** 47–64
WAIT, G. R.	1942	Terr. Mag. **47,** 243–249
MALONE, T. F., Editor	1951	Compendium of Meteorology, 483–509, Waverly Press Inc., Baltimore, Md.
WIGAND, A.	1919	Ann. der Physik. **59,** 689–742

VOL. 5 1954

Journal of Atmospheric and Terrestrial Physics, 1954, Vol. 5, pp. 273 to 289. Pergamon Press Ltd., London

Simultaneous ionospheric absorption measurements at widely separated stations

W. J. G. Beynon and K. Davies
Department of Physics, University College of Swansea

(*Received* 26 *April* 1954)

ABSTRACT

Simultaneous normal incidence 2 Mc/s ionospheric absorption measurements made daily at noon at Slough and Swansea (230 km apart) have been compared. The same measuring technique has been employed at the two stations. The correlation between the two sets of measurements is generally high. The average correlation coefficients between daily observations are 0·85 and 0·81 for the winter and summer months respectively. Some measurements in which variations in the received signal intensity from c.w. senders at distances of 366 km and 666 km have been compared with normal incidence amplitude measurements on the equivalent frequency are also described. These, and the Slough-Swansea observations, give some indication of the progressive decrease with increasing distance in the degree of correlation between simultaneous ionospheric absorption measurements at different stations. The use of simple field strength recording as a quantitative measure of ionospheric absorption is briefly considered.

Introduction

In a recent publication Rawer (1951) has compared ionospheric absorption measurements made at two stations, Freiburg and Slough. These stations are some 400 km apart and the observations concerned referred to noon measurements over a period of 26 months. It was noted that, in general, the correlation coefficient for the two sets of data was positive but only of the order of 0·5. On individual days the differences between the values measured at the two sites was sometimes quite appreciable. It was suggested that part of these differences might represent real differences in ionospheric absorption at the time of the experiments but this conclusion was somewhat uncertain since the method of measurement was not the same at the two stations, and, as Rawer states, the consequences of this need further investigation.

In the present paper we describe experiments of a similar character carried out at Swansea during 1951 in which absorption measurements have been compared with those made daily at the Radio Research Station, Slough. In this case the distance between the two observing sites is smaller than that in the work mentioned above and furthermore the comparison has the advantage that the same method of measurement was used at the two stations.

In addition, we describe some experiments in which the intensities of signals from two short wave broadcasting stations have been compared with vertical incidence amplitude measurements. In this way we have obtained some supplementary information on the spatial variation of ionospheric absorption and on the application of such data to simple oblique incidence problems.

2. Experimental Technique

In these experiments the usual pulse sender and receiver have been used with signals incident normally on the ionosphere. The effective reflection coefficient has been calculated from a comparison of the mean amplitudes of the successive echo reflections. If these mean amplitudes be represented by A_1, $A_2 \ldots A_n$ and if ρ and ρ_g

represent the reflection coefficients of the ionosphere and ground respectively then we have

$$\rho\rho_g = \frac{2A_2}{A_1} = \left(\frac{3A_3}{A_1}\right)^{\frac{1}{2}} = \ldots \left(\frac{nA_n}{A_1}\right)^{\frac{1}{n-1}} \tag{1}$$

For the wavelengths concerned in our experiments we assume $\rho_g = 1$.

The actual measuring procedure was identical with that which has been employed for many years at the Radio Research Station, Slough, and which has been described in detail by PIGGOTT (1953). The echo signals reflected by the ionosphere are viewed on a cathode ray tube and an accurately calibrated attenuator is continually adjusted (approximately once every 10 seconds) so as to maintain a preselected echo amplitude. For calculating the absorption the average of many such amplitude measurements is used, so that errors due to short period amplitude fluctuations are reduced. Further discussion of the inaccuracies of the technique is given below.

2.1. *Absorption measurements and signal fading*

In experiments of this kind some care is necessary in applying formula (1) since it is strictly only applicable to the reflection of signals between a perfectly smooth ionosphere and ground. Irregularities in one or both of these reflectors, in particular variable irregularities in the ionosphere, impose some limitations on its practical application. The observed fluctuations in the amplitude of a single echo signal reflected from the ionosphere may result from a number of causes such as direct changes in electron density and/or height of the reflecting layer, or may arise indirectly from such changes by giving rise to variations in the state of polarization of the reflected signal. RATCLIFFE (1948) and others have suggested that the net signal received is not that due to a single mirror-like reflection but rather consists of a number of separate signals reflected from an appreciable area of the ionosphere. Interference between these signals gives rise to the observed variability in the amplitude of the observed echo signal. In attempting ionospheric absorption measurements by measuring the amplitudes of signals reflected by the ionosphere some means has to be adopted whereby the amplitude changes characteristic of true changes in ionospheric absorption may be singled out from changes due to other causes. In practice the amplitude of a single echo from the ionosphere sometimes varies by factors of the order of 10 in an interval of a few seconds, and, without special arrangements whereby the various possible causes of echo fading are successively identified and eliminated, it would appear impossible to determine those variations in ionospheric absorption of period comparable with that due to these other causes. In these experiments it is assumed that by averaging values over a period which is long compared with the period of the fading due to other causes, such as polarization changes, a mean amplitude is obtained which can be taken as a measure of the average ionospheric absorption over the period concerned. The question then arises as to what constitutes a reliable sample of amplitude measurements and in deciding this point we have, in practice, to be guided by the facts that in too small a sample the variations due to extraneous factors may predominate over those due to ionospheric absorption and that in obtaining a very large sample of amplitude measurements

VOL. 5 1954

appreciable changes in the ionospheric absorption may occur during the period of observation. Some guidance in this matter was obtained from a series of preliminary experiments which are described in the next section.

2.2. *Sampling of amplitude measurements*

During October 1950 some experiments were made on a frequency of 2·0 Mc/s in which 200 measurements of the amplitude of an *E* echo were taken, at intervals of 10 seconds, within the period 1200–1300 G.M.T. The immediate post-noon period was chosen for these tests since on the average one could expect the ionospheric absorption to remain sensibly constant over this period. An examination of the monthly mean diurnal variation curve of ionospheric absorption shows this to be a reasonable assumption. We further assume that the mean of the 200 measurements is the correct value to be used for calculating the absorption. To estimate the

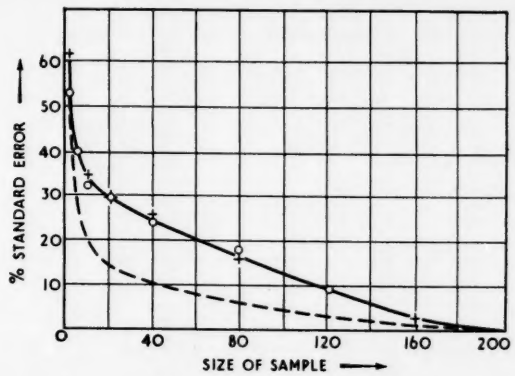

Fig. 1. Sampling of amplitude measurements. Variation in percentage standard error with size of sample. Observations taken at 10 sec intervals. Dotted curve shows variation expected for random values.
o o Observer A + + Observer B

reliability of any group of consecutive amplitude measurements we considered the means of every possible sample of 2, 5, 10, 20, 40, 80, 120, and 160 consecutive values selected from the total 200 amplitude measurements. For each sample we determined the deviation of the mean of the sample from the grand mean. In this way a series of running averages of amplitude measurements was obtained for each group in turn and the standard error (i.e., the root mean square deviation) of these averages, expressed as a percentage of the mean of the whole set of 200 measurements, was then determined. The mean values of the standard errors, for the samples of different sizes, for all days of observation were then computed. The variation of the percentage standard error with the size of sample is shown in Fig. 1. The curve of Fig. 1 enables one to estimate the average standard error to be expected for a group of consecutive amplitude measurements at 10 second intervals. Thus the average standard error for a sample of say 20 successive measurements taken at intervals of 10 seconds near noon is likely to be about 30%. A similar series of tests with a different observer was made in March 1952. The results of this test are also included in Fig. 1. The remarkable agreement between the two sets of results indicates that the mean curve has real significance.

We also examined the consequences of selecting amplitude measurements spread uniformly over the whole period of the observations rather than taking groups of successive 10 second observations. By selecting values in this way, we make some allowance for variations in ionospheric absorption which may have occurred over the whole period concerned. In this analysis the same sets of 200 measurements have been studied. Each set was first divided into 2 groups each of 100 consecutive measurements and 100 samples of 2 measurements selected by taking the first of each group, then the second member of each group, and so on. The percentage standard error for this set of 100 samples of two observations was then calculated. This procedure was repeated for samples of 10, 20, 40, 80, and 120 measurements selected in a similar manner so as to be uniformly spread over the whole observation period. This was carried out for all days of observation and the data combined to give the average values of the percentage standard error for the samples of different

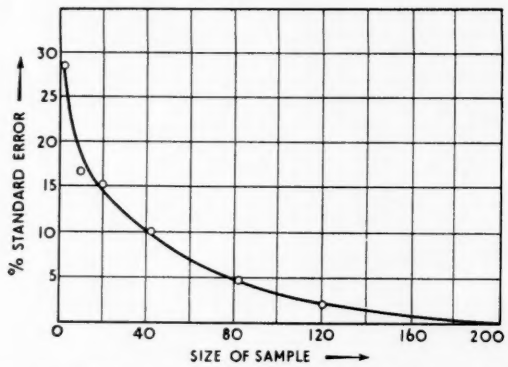

Fig. 2. Sampling of amplitude measurements. Variation in percentage standard error with size of sample. Observations uniformly distributed over whole observing period.

size. The mean values so obtained are plotted in Fig. 2. This curve enables one to estimate the error to be expected when a sample of measurements spread uniformly over the whole period of the observations is made smaller and smaller. For example, if near noon a sample of 20 measurements uniformly spread over a period of about 35 minutes (the actual time required for the 200 measurements) is taken, then a standard error of about 15% may be expected.

A comparison of Figs. 1 and 2 indicates, as one might expect, that on the average it is preferable to spread a given number of amplitude measurements over a long period rather than concentrate them into a short period. Thus for 40 measurements taken over a period of about 8 minutes the standard error to be expected is about 25%, whereas for the same number of measurements taken over a period of about 35 minutes the standard error is about 10%.

If the amplitude measurements were completely independent and distributed in a random manner about the mean, the standard error σ_n of the mean of a sample of n measurements would vary approximately inversely as the square root of the size of the sample,

i.e., $$\sigma_n = \sigma_1/\sqrt{n} \qquad (2)$$

VOL. 5 1954

where σ_1 is the standard error of the individual values. For comparison with the observed variations the mean curve obtained from an identical analysis, but using sets of 200 values taken from tables of figures in random order, is also plotted in Fig. 1. The difference between the experimental curve and that for random values is clear and serves to emphasize the degree of conservation (cf. CHAPMAN and BARTELS, 1940) which exists in sequences of amplitude measurements.

3. *Absorption measurements at Swansea and Slough*

We now consider the results of a series of vertical incidence absorption measurements made daily near noon at Swansea over the period September 1950–August 1951. The measuring technique employed at Swansea is very similar to that employed at the Radio Research Station, Slough, and hence we can justifiably compare the results obtained daily near noon at the two stations. The Slough values are taken from the published Bulletin of ionospheric data.

Slough is situated some 230 km in a direction almost due east of Swansea and ionospheric absorption measurements are made there each day near noon on a number of selected frequencies, viz., 2·0, 2·4, 2·8, 3·2 and 4·0 Mc/s. For the present investigation it was decided to restrict the comparison to the lowest frequency since it was felt that measurements on this frequency might be expected to be least liable to disturbance by such factors as local variations in critical frequency of the normal region *E*.

The daily noon values of the ionospheric absorption $-\log_e \rho$ for the two stations for the 12 month period are shown in Fig. 3. (It should be noted that for convenient presentation we have omitted days on which simultaneous observations were not made and plotted the remaining days in sequence.) Fig. 3 shows that in general there is quite close correlation between the two curves. The absolute values of the ionospheric absorption are sometimes different but the relative day-to-day changes follow one another closely. The curves suggest an appreciable difference in the estimates of the absolute magnitude of the ionospheric absorption throughout the month of September 1950, but this is almost certainly due to an inaccurate calibration of the equipment at Swansea, this being the first month of measurements at that site. A study of Fig. 3 shows that the differences between the two sets of values are generally smaller in the summer than in the winter months. It is probable that part of this seasonal difference is due to the anomalously high and variable absorption which occurs on many winter days.

The monthly mean values, the standard deviations and correlation coefficients are given in Table 1. Although individual monthly values for the absolute magnitude of the ionospheric absorption differ by as much as 0·7 neper (omitting September 1950 for reasons already mentioned) the average values over the whole period agree to within 0·2 neper. Both sets of values indicate a much greater day-to-day variability in absorption during the winter compared with that during the summer months. The average standard deviation of the Swansea measurements is a little smaller than that for Slough and this is almost certainly due to the fact that the absorption values for Swansea involve a mean of 120 amplitude measurements whereas 50 values are taken at Slough. The correlation coefficients are in general quite high, the average for the year being 0·74.

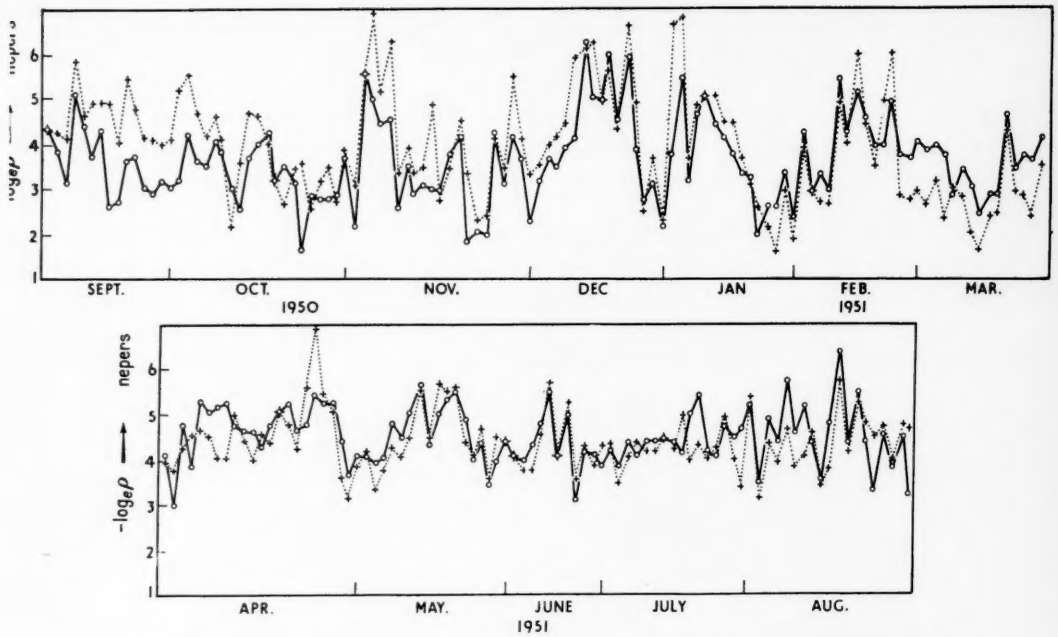

Fig. 3. Daily noon values of 2 Mc/s ionospheric absorption at Swansea o——o and at Slough + - - - +.

Table 1. *2 Mc/s vertical incidence absorption measurements at Swansea and Slough*

Month	*Mean value of absorption (nepers)*		*Standard deviation*		*Correlation coefficient*
	Swansea	*Slough*	*Swansea*	*Slough*	
September (1950)	3·57	4·53	0·77	0·54	0·60
October	3·33	3·82	0·62	0·85	0·53
November	3·41	4·10	1·03	1·21	0·82
December	4·25	4·70	1·21	1·20	0·89
January (1951)	3·65	4·04	0·98	1·62	0·85
February	4·14	3·96	0·72	1·15	0·88
March	3·53	2·83	0·59	0·63	0·67
April	4·70	4·55	0·61	0·78	0·59
May	4·55	4·51	0·60	0·71	0·84
June	4·28	4·32	0·60	0·63	0·89
July	4·44	4·22	0·38	0·42	0·70
August	4·56	4·44	0·83	0·64	0·60
Mean values	4·03	4·17	0·74	0·87	0·74

VOL. 5 1954

3.1. *Comparison with the results of* Rawer

As stated in the introduction Rawer (1951) has published the results of a similar kind of analysis in which absorption values for Freiburg were compared with the published Slough values. Freiburg is approximately 400 km south-east of Slough. In the case of the 2 Mc/s measurements Rawer found a correlation coefficient of 0·5 (median monthly value) over a period of 26 months. For several of the 26 months considered, an insignificant or even negative correlation between the Slough and Freiburg measurements was noted. From this and other comparisons of absorption data from the two stations Rawer concluded that the results were to some extent inconclusive in that they did not establish whether the differences were really due to true differences in ionospheric absorption or to other factors such as differences in measuring techniques. In the present work, although the average correlation coefficient is appreciably larger than that found by Rawer, and all months show a very significant positive correlation, it must be remembered that the distance between the stations concerned is also considerably less and furthermore that the measuring techniques are in the present case substantially the same.

A study of Fig. 3 shows that on some days the measured values at Swansea and Slough differed by 1 or 2 nepers. We have given special attention to such cases and find that some of these differences are probably quite significant in that storm conditions with marked spatial and temporal variability prevailed at the time of the observations, but there remain a number of instances in which no obvious explanation for such large differences can be offered.

4. Oblique Incidence Continuous Wave Signals and Vertical Incidence Ionospheric Absorption

We now consider some experiments in which a comparison has been made between the day-to-day changes in the intensity of signals received from short wave broadcast senders and in the vertical incidence ionospheric absorption on the "equivalent" frequency. The experiments yield additional information on the problem of defining the useful range of vertical incidence absorption measurements made at a single station.

In this work recordings were taken daily of the received field-strength from two short wave broadcasting stations, viz.,

(a) The B.B.C. station GWL radiating on a frequency of 7·21 Mc/s and located at Skelton, some 366 km approximately north of Swansea.

(b) The French station Allouis, frequency 6·3 Mc/s located 666 km approximately south-east of Swansea.

The signals were received on standard communication-type receivers each having a pen recording milliammeter inserted in the detector stage. Recordings were made daily for a period of one hour or more and the mean amplitude over the period was estimated from the ink record.

In each case simultaneous vertical incidence pulse amplitude measurements were made on the appropriate "equivalent" frequency. (If f is the signal frequency

incident at angle i on the reflecting layer then $f \cos i$ is termed the "vertical incidence equivalent frequency.")

We shall discuss the two sets of recordings separately.

4.1. *Signals from Skelton*

In this case the equivalent vertical incidence frequency was in the neighbourhood of 6 Mc/s—the exact value depending principally on the equivalent height of reflection of the layer at the time of the observations. In practice, the equivalent vertical incidence frequency varied from near 5·9 Mc/s in winter to about 6·2 Mc/s in summer. Measurements of the c.w. relative signal strength (S) and of the amplitude of the first order pulse reflection from region F_2 (F) were made near noon on as many days as possible over the period October 1950 to January 1952 with the exception of September 1951. Monthly mean values of S and F are shown in Fig. 4. It will be seen that S and F are closely correlated. A study of the day-to-

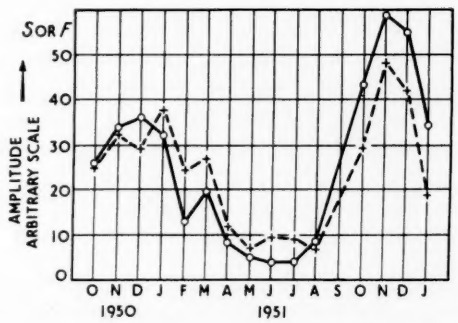

Fig. 4. Monthly mean values of signal amplitude (S) from c.w. sender (Skelton 7·21 Mc/s) o——o and of first order F_2 reflections (F) on the equivalent frequency + - - - +.

day correspondence between S and F shows that, with the exception of May and June 1951, the correlation is generally high. For the winter months November to January (1950–51 and 1951–52) the average correlation coefficient between daily values is 0·76. For the summer months May to July the corresponding average coefficient is 0·43. Although we have no conclusive evidence, the vertical incidence pulse observations indicate that during May and June 1951 local patches of sporadic E were almost certainly responsible for the reduced correlation between S and F during these two months.

4.2. *Signals from Allouis*

In this case the frequency of transmission (6·2 Mc/s) and the distance of transmission (666 km) were such that, at the time of the observations, simultaneous reflections from both regions E and F were probable. Thus for region E reflections the equivalent vertical incidence frequency is near 2·0 Mc/s, and for region F_2 near 4·0 Mc/s. Here again the precise values of these equivalent frequencies varied a little from day to day but calculations indicate that the values would only vary slightly from these figures (2·0 and 4·0 Mc/s) and it was decided to make all the vertical incidence pulse measurements on these two frequencies. The signal

VOL. 5 1954

intensity from Allouis (S) and the vertical incidence pulse amplitude measurements on 2 Mc/s and 4 Mc/s (first order reflections E and F) were made daily between 0915 and 1045 G.M.T. on as many days as possible between February and December 1951, with the exception of September 1951. Monthly mean values of S, F, and E are plotted in Fig. 5. No value for E is shown for December 1951, since during that month fE was less than 2·0 Mc/s. It will be seen that there is clear correlation between S and both F and E. The general correspondence between the three curves in Fig. 5 shows that in these experiments the controlling absorbing layer must, in all three cases, have been located below region E, i.e., the major absorption occurred in the D-layer. Accepting this fact, it is then readily shown that the

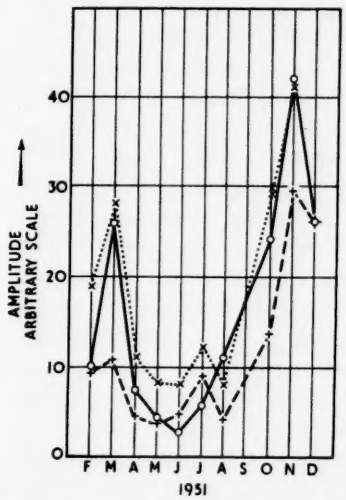

Fig. 5. Monthly mean values of signal amplitude (S) from c.w. sender (Allouis 6·2 Mc/s) and of first order E and F reflections on the equivalent frequencies: S o——o; F + – – – +; E x·····x.

D-layer absorption of the F reflection must have been less than one half that of the E reflection. This conclusion, that most of the signal consisted in the first F-region reflection, is borne out by the fact that in December 1951, due to the reduction of the vertical incidence E-region critical frequency below 2·0 Mc/s, the E signal must have been completely absent, yet there was no significant change in the signal intensity or in the degree of correlation. A study of the day-to-day correlation between S and E and S and F shows that, in general, it was not as close as was found in the case of the Skelton signals. The average correlation coefficients for three winter months November, December and February were 0·55 between S and E and 0·65 between S and F. These compare with an average of 0·76 found for the correlation coefficient between S and F during the winter months in the case of the signals from Skelton. In the case of the Allouis signals we again find a decreased correlation during the summer months. The average coefficient for the three months May, June and July is 0·33 between S and E and 0·30 between S and F. In the case of the Allouis experiments throughout the summer period the critical frequency of region F_2 was always well above the equivalent frequency,

and the diminished correlation in summer is again to be attributed to the incidence of sporadic E ionization.

5. Discussion of Results

5.1. *Absolute magnitudes of absorption values at Swansea and Slough*

As stated in Section 3, the daily estimates of the noon ionospheric absorption at Slough and Swansea are based on groups of 50 and 120 amplitude measurements respectively. From Fig. 1 we estimate that for samples of this magnitude the average standard errors in amplitude are likely to be of the order of $\pm 22\%$ and $\pm 10\%$ respectively. Assuming an average value of $-\log_e \rho$ of 4 nepers such errors in amplitude give rise to errors of about $\pm 0{\cdot}1$ to $\pm 0{\cdot}2$ nepers in estimates of the absolute ionospheric absorption. The analysis of Section 2.2 thus indicates that, on the average, sampling errors alone may give rise to differences of $\pm 0{\cdot}3$ nepers between the daily measurements of $-\log_e \rho$ at Slough and Swansea. It should be remembered that these represent average estimates and in individual cases much larger differences may occur. On the other hand in monthly mean values the inaccuracy due to this cause may be expected to be much reduced.

From Table 1 it may be seen that over the year the mean values of $-\log_e \rho$ at Swansea and Slough differ only by 0·14 neper (approximately 3 per cent). The small magnitude of this difference is fortuitous, since it is indeed much less than might be expected from errors in absolute calibration of the measuring equipments. However, a study of the individual monthly mean values shows some quite large differences particularly in the winter months. For example, in November, December and January the differences between monthly mean values are 0·69, 0·55, and 0·39 neper respectively—an average difference of 14%. In the summer months May, June and July the differences between monthly mean values are $-0{\cdot}04$, $-0{\cdot}04$, and $-0{\cdot}22$ neper—an average difference of only 2%. In considering the apparent large differences in the mean winter values, consideration must be given to the mean standard deviations shown in Table 1. For the three winter months the standard deviation averages about 1·2 nepers (28%) whereas in summer it is approximately 0·6 neper (14%). This very marked seasonal difference in the day-to-day variability of ionospheric absorption at any one station is almost certainly related to the corresponding seasonal variation in the differences between monthly mean values. A study of the differences in the measured absorption at the two stations on individual days shows that occasionally a large divergence coincides with magnetically disturbed conditions but there are many occasions in which no such explanation is possible. We have tried to detect a general correlation with magnetic activity, using as an index the sum of the Kp values for the periods 0–12 and 12–15 G.M.T. (Kp is the planetary three hour range index defined by Bartels, 1949.) In Fig. 6 the average magnitude of the difference between $-\log_e \rho$ at Swansea and Slough for wide ranges of ΣKp is plotted. It will be seen that there is a wide scatter of the points with no evidence of correlation. Fig. 7 shows the effect of separating the data for the winter (November, December, January) and the summer months (May, June, July). This shows that in the summer months there is again no correlation at all between magnetic

VOL. 5 1954

activity and the magnitude of the observed differences in absorption, but that in the winter period there may be slightly larger differences on days of high activity. It must be stressed that we are here using only a very limited sample of data and

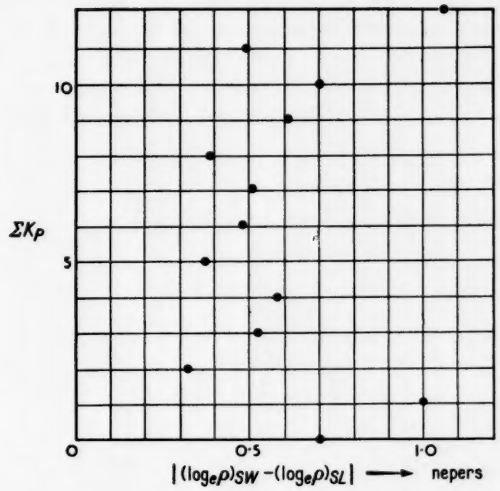

Fig. 6. Magnitude of average daily difference in $-\log_e \rho$ at Swansea and Slough and magnetic activity.

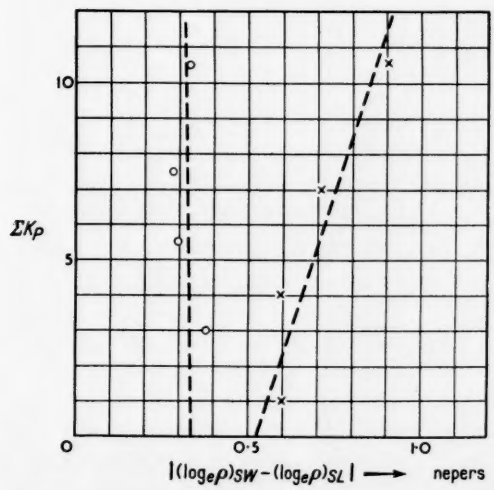

Fig. 7. Magnitude of average daily difference in $-\log_e \rho$ at Swansea and Slough for summer and winter months.
o ——— o Summer × – – – × Winter

the suggestion of correlation with magnetic activity during the winter may not be statistically significant. In any case Fig. 7 shows that for zero magnetic disturbance for both summer and winter there is still a residual difference of about 0·3 neper in summer and about 0·5 neper in winter which must be ascribed to some other cause.

It is now well known that on many days during the winter the observed ionospheric absorption is exceptionally high. This winter absorption phenomenon has recently been discussed by DIEMINGER (1952) and is also considered in another communication by the present authors. It is of interest to study the magnitude of the difference in absorption at Swansea and Slough on these days of abnormally high absorption. In each month the four or five days of highest absorption have been selected and the *magnitude* of the mean difference in absorption between Slough and Swansea has been examined. This difference is plotted in Fig. 8 and it

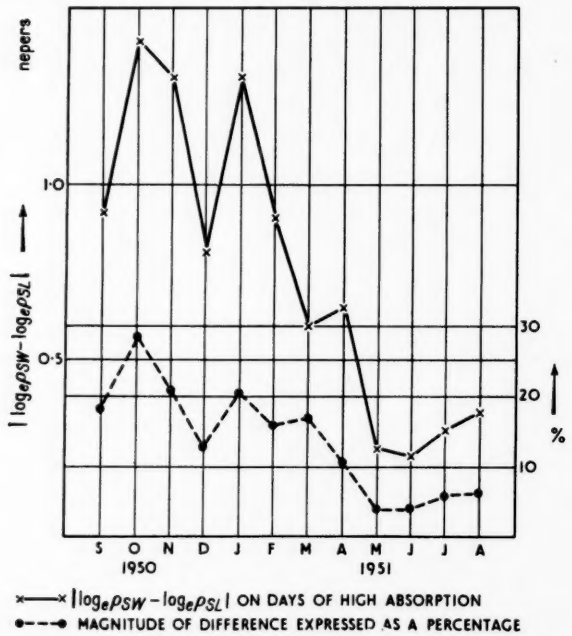

Fig. 8. Magnitude of average daily difference in $-\log_e \rho$ on days of high absorption.
×——× • ····· • Magnitude of difference expressed as a percentage.

will be noted that its magnitude (irrespective of sign) is always appreciably larger in the winter than in the summer. Differences expressed as percentages of the measured absorption are also shown in Fig. 8 and it will be seen that this curve shows the same seasonal tendency as is found for the absolute magnitudes. It would thus appear that the high absorption observed on certain winter days shows considerable spatial irregularity over this distance of 230 km and that the low layer responsible for such absorption is probably sporadic in character.

5.2. *Correlation coefficients*

5.2.1. *Vertical incidence measurements.* RAWER (1951) has compared various absorption parameters for noon conditions at Slough and Freiburg (400 km apart). For the case of the 2·0 Mc/s observations RAWER gives his results in terms of a correlation number—an index which is more easily calculated than the usual

VOL. 5 1954

correlation coefficient. He considers that the significance of this correlation number is comparable with that of the correlation coefficient, and in the following discussion we shall assume that this is the case. Over a 26 month period, RAWER finds that the monthly correlation numbers vary from $-0{\cdot}34$ to $+0{\cdot}99$ with an average value of 0·40 and a median value of 0·50. In six cases (four of them in the summer months) the monthly correlation numbers were negative. In the present Swansea-Slough comparison for the period September 1950 to August 1951, no negative correlation coefficients are found and the magnitudes of the coefficients range from 0·53 to 0·89 with an average value of 0·74. If we group the data into winter and summer periods, then for the Swansea-Slough results we find that the

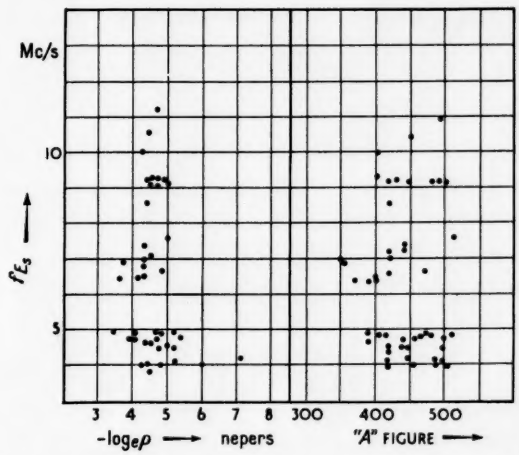

Fig. 9. $(-\log_e \rho)_{2\ \mathrm{Mc/s}}$ and absorption "A" figure (Slough) and fE_s.

average correlation coefficient for the three winter months November, December and January is 0·85 and that for the three summer months May, June and July is 0·81.

It will be noted that in the present results and those of RAWER there is evidence of a reduced correlation in the summer months. In the present case the seasonal change is comparatively small and may not be statistically significant, but in RAWER's case the summer correlation numbers are very much lower than the winter ones and indeed, as stated above, are often negative. RAWER queries whether this may be due to the influence of sporadic E ionization. In the case of measurements on 2 Mc/s it seems unlikely that any irregular incidence of sporadic E ionization would seriously affect the absorption measurements, since such ionization is generally produced at a higher level than the level of reflection of the 2 Mc/s signal. This supposition is confirmed from a study of many months data in which no significant difference in the absorption on 2 Mc/s (or in the Slough "A" figures) can be detected on days of high or low fE_s. Thus in Fig. 9 we have plotted $-\log_e \rho$ for 2 Mc/s and the Slough "A" figure for the five days of maximum and five days of minimum fE_s for the summer months of 1950. It is clear that the values of $-\log_e \rho$ (and of A) are substantially the same over a very wide range of values of fE_s. The reduction in the degree of correlation from winter to summer

noted by Rawer for both the A figures and the 2 Mc/s absorption values thus seems to be unrelated to the incidence of sporadic E ionization. In the case of the Swansea-Slough results the average value of the magnetic disturbance index Kp (over the period 0900—1500 G.M.T.) is slightly larger for the summer months but we have no evidence that this is related to the slight reduction in correlation.

It should be remembered that both sets of measurements are subject to sampling errors of the type discussed in Section 2.2. These sampling errors necessarily place an upper limit on the calculated correlation coefficients and might also give rise to an apparent seasonal change in the degree of correlation.

5.2.2. *C.W. relative field-strength observations.* It is reasonable to suppose that the degree of correlation between oblique and vertical incidence signal intensities will decrease with increasing distance between the sender and receiver. This fact

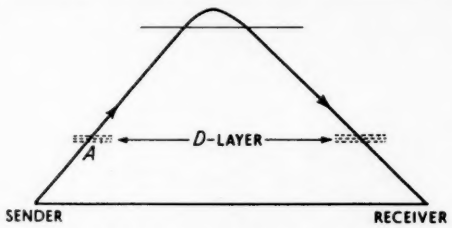

Fig. 10. Location of absorption points in oblique incidence path.

VOL. 5 1954

is already indicated in the Slough-Swansea and Slough-Freiburg results discussed above. It is of interest to investigate whether the relative field-strength c.w. measurements described in Sections 4.1 and 4.2 are at all consistent with the vertical incidence pulse observations.

In discussing the c.w. measurements it is to be noted that the Allouis results show conclusively that in these experiments the absorption occurred in the D-layer and also that the major part of the received signal was contributed by the $1F$ reflection. In the case of the Skelton signals there were occasions when the equivalent frequency approached the vertical incidence frequency giving rise to appreciable absorption at the top of the trajectory but it is clear that in general the predominant absorption again occurred in the D-layer (cf. the S curve of Fig. 4 with the 2 Mc/s (E) curve of Fig. 5). In the case of both sets of field strength measurements the upper limit to the degree of correlation with vertical incidence observations at Swansea will be set by conditions at the controlling point in the absorbing D-layer most remote from Swansea. In the case of the Skelton signals this means that the coefficients will refer to the correlation between conditions overhead at Swansea and those at a point A about 330 km from Swansea (Fig. 10). For the Allouis signals the corresponding point will be about 540 km from Swansea.

Table 2 summarizes the mean values of the correlation coefficients (or numbers) for the four sets of data discussed above. The figures given in Table 2 are only completely consistent for the winter period in showing the steady decline in correlation with increasing distance, but when we consider the different approaches to the problem which are involved in the four sets of results, the degree of agreement is satisfactory. It will be noted that the figures suggest that the correlation

Table 2

Stations	*Distance between points correlated (km)*	*Period of observations*	*Correlation coefficients**		
			Whole period	*Winter period Nov., Dec., Jan.*	*Summer period May, June, July*
Swansea—Slough	230	Sept. 1950—Aug. 1951	0·74	0·85	0·81
Swansea—Skelton	330	Oct. 1950—Jan. 1952	0·68	0·76	0·43
Slough—Freiburg	400	Nov. 1948—Dec. 1950	0·40	0·67	0·15
Swansea—Allouis	540	Feb. 1951—Dec. 1951	0·40	0·65†	0·30

* In the case of Slough-Freiburg, RAWER's Correlation Numbers are given.
† Average coefficient for November, December, and February.

coefficient falls off more rapidly during the summer months. In the case of the oblique c.w. signals a possible explanation would appear to be the irregular incidence of sporadic *E* ionization, but this explanation would not apply to the vertical incidence absorption data. In the case of the latter, the effect of sampling errors on the magnitude of the correlation coefficients will need further study.

6. The Estimation of Ionospheric Absorption from C.W. Data

One of the great advantages of the pulse technique for radio investigations of the ionosphere is the fact that multiple reflections are clearly separated one from the other. However, there are a number of practical difficulties attached to the existing pulse method of measuring vertical incidence absorption. Thus the procedure is tedious and requires a competent observer and suitable pulse equipment. On the other hand the recording of the relative field strength of the signal received from a short wave broadcast sender is a comparatively simple matter, requiring no special equipment or very skilled attention. Of course, in the case of the reception of c.w. signals the contributions of the various order reflections are not readily ascertained and care must be exercised in interpreting the results obtained. However, a simple analysis of the problem shows that for short distance transmissions, even under conditions of small ionospheric absorption, the major contribution to the received

signal intensity comes from the first order reflection. Under conditions of appreciable ionospheric absorption, theory indicates that for short distance transmission the received signal intensity will be almost entirely due to the contribution of the first order reflection. Such conditions might be expected to occur during the daytime especially for some hours around noon.

It is of interest to examine the possibilities of using simple field strength recording of c.w. signals as a quantitative index of the day-to-day changes in ionospheric absorption. For this purpose we now briefly consider again the results described in Section 4.1 above.

Table 3. *Ionospheric absorption* (6·0 *Mc/s*)

Month	*Deduced from c.w. observations (nepers)*	*Measured at vertical incidence (nepers)*
November 1950	0·64	1·07
December	0·65	1·21
January 1951	0·96	1·04
February	1·53	1·20
March–April	1·24	1·16
May	2·52	1·51
June–July	1·94	1·57
August	1·95	1·97
October	0·86	0·93
November	0·66	0·68
December	0·76	1·00
January 1952	1·22	1·59

Table 3 gives the monthly mean ionospheric absorption estimated from the field strength data for Skelton and the vertical incidence absorption measured at Swansea on the equivalent frequency (near 6·0 Mc/s). In this particular set of values the differences between estimated and observed absorption range from $-0{\cdot}56$ to $+1{\cdot}01$ nepers, the average being $\pm 0{\cdot}30$ neper. It should be emphasized that here we have been concerned with reflections from region F_2 and that the accuracy of estimating the overall absorption is probably considerably less than could be achieved in the case of c.w. recording on a lower frequency such that the signals would be reflected by region E and the equivalent vertical incidence frequency always appreciably less than fE.

Acknowledgments

This work was carried out as part of the programme of the Radio Research Board and this paper is published by permission of the Director of Radio Research of the Department of Scientific and Industrial Research.

The authors are indebted to Professor F. Llewellyn Jones for facilities in the Department of Physics, University College of Swansea.

VOL. 5 1954

References

Bartels, J.	1949	J. Geophys. Res. **54,** 296
Chapman, S., and Bartels, J.	1940	Geomagnetism, p. 482
Dieminger, W.	1952	Über die Ursache der exzessiven Absorption in der Ionosphëre an Wintertagen. J. Atmosph. Terr. Phys. **2,** 309
Piggott, W. R.	1953	The reflection and absorption of radio waves in the ionosphere. Proc. Inst. Elect. Engrs. **100,** III, 61
Rawer, K.	1951	Comparison des résultats de mesures de l' absorption ionosphérique effectuées. J. Atmosph. Terr. Phys. **2,** 38
Ratcliffe, J. A.	1948	Diffraction from the ionosphere and the fading of radio waves. Nature **162,** 9

DL.
954

Journal of Atmospheric and Terrestrial Physics, 1954, Vol. 5, pp. 290 to 297. Pergamon Press Ltd., London

F_2-layer regularities at Ibadan

N. J. Skinner and R. W. Wright
Physics Dept., University College, Ibadan, Nigeria.

(*Received* 2 *April* 1954)

ABSTRACT

The mean daily variation throughout the year of n (the total electron content in a column of unit cross-section below the height of maximum ionization (h_m) in the F_2-layer), and N_m (the maximum electron density of the F_2-layer), show clearly that n behaves in a more regular manner than N_m. It is shown that in calculating n, it is important to use values of the equivalent layer semi-thickness deduced assuming non-parabolic electron distributions where necessary. The Appleton-Beynon (1947) method for "parabolic" layers is not, therefore, completely adequate in tropical regions. Inclusion of the contribution by the F_1-layer to the total electron content has no appreciable effect upon the regularity of the diurnal variation of n.

A new method is described and used for deducing the coefficient of recombination (α), and the rate of ion production per cc (q), from the daily variation of n.

The pronounced sunset minimum in the virtual height of F_2, as reported by some observers, is discussed and considered to be largely spurious.

An h_m and y_m histogram is plotted and is found to be dissimilar to that at Huancayo, and similar to that at College, Alaska.

1. Introduction

Appleton (1950) has identified the ionospheric equator in the F_2-layer from a consideration of the annual variation of noon $h'F_2$, and by his criteria Ibadan is a typical equatorial station, since noon $h'F_2$ varies very nearly sinusoidally with time, with a period of six months. Accordingly, there is normally a midday minimum in the variation of the critical frequency of the F_2-layer with time of day, and in a previous communication we have discussed some implications of this, especially with reference to the formation of ridges. Ratcliffe (1951a) has developed a quick method of analyzing $(h' - f)$ records so as to obtain the total number (n) of electrons below the level of maximum electron density (h_m) in a column of unit cross-section in the F_2-region. He found that at Huancayo, considering magnetically quiet days only, the anomalies present in diurnal distribution of N_m (the maximum electron density) were removed when the quantity n was studied instead. A similar analysis has been made by Osborne (1952) for Singapore and it was found that whereas n showed a greater similarity to a $\cos\chi$ variation than N_m, several anomalies were still evident. Chatterjee (1953) has claimed that if the contribution of the F_1-layer is added to n for the F_2-layer the regularity becomes more pronounced.

In this paper, we describe the results obtained from a complete reduction of n for all days in the period December 1951–January 1953, for which we have records. A method has been developed whereby values of q, the rate of ionization, and α, the coefficient of recombination, can be obtained from the mean diurnal variation of n.

2. Electron Concentration (N_m) and Total Electron Content n

Using Ratcliffe's (1951a) technique applied to parabolic, linear, and second power distributions of electron density with height, values of $T_{eq.}$, the equivalent semi-thickness of the F_2-layer, were calculated. Corresponding values of n were

VOL. 5 1954

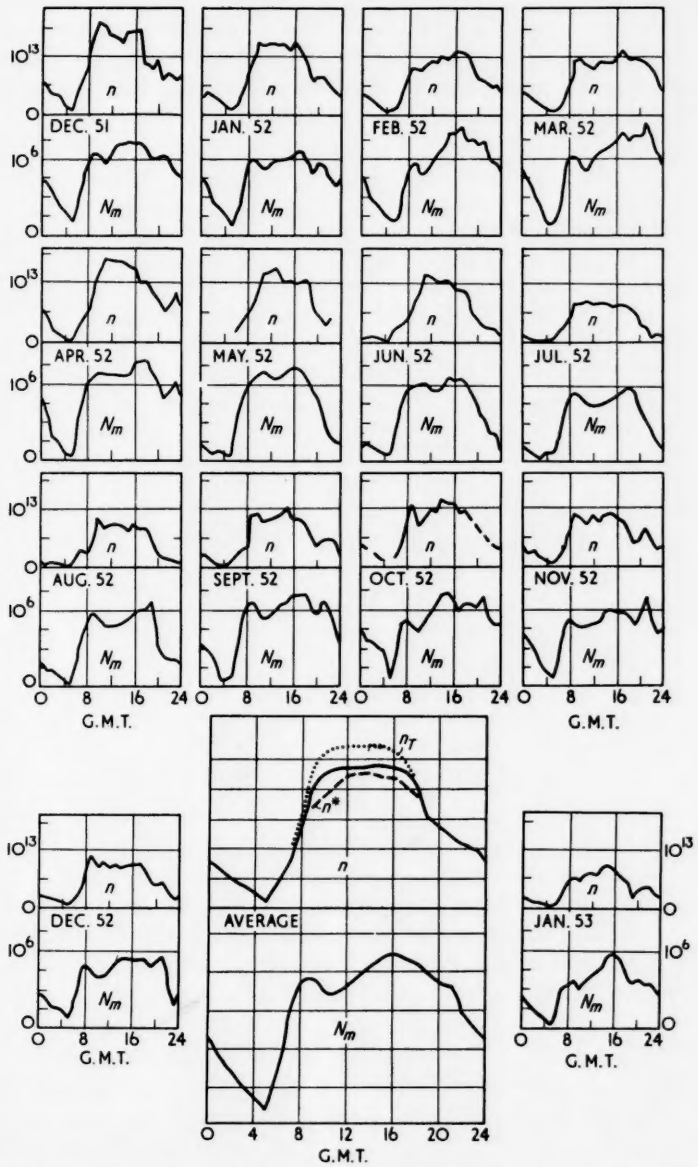

Fig. 1. Monthly mean values of the maximum concentration of ionization (N_m) and the total electron content per unit column below the maximum in the F_2-layer (n). The annual means of N_m and n are also shown with the mean annual values of n^* and n_T (see text).

then deduced from the relationship $n = 2/3\ T_{\text{eq.}} N_m$. It was found to be especially important to consider $T_{\text{eq.}}$ rather than values of y_m obtained by APPLETON and BEYNON's method, since at Ibadan thick layer phenomenon (i.e., nonparabolic F_2-layers) occurs daily. Values of n calculated from y_m's only, are denoted by n^* and

Fig. 1 shows the monthly means of n and N_m and also the annual means of N_m, n, and n^*. It is evident that CHATTERJEE's (1953) analysis of Singapore data must, therefore, necessarily be incorrect for the daylight hours when ridges are often present, since he used values of y_m (reduced by APPLETON and BEYNON's method) published by the Radio Research Station, Slough.

The behaviour of the F_1-layer at Ibadan is very constant throughout the year and the effect of adding in its contribution to n is seen in the annual mean curve of Fig. 1, where n_T, half the total electron content in a column of unit cross-section in the F-layer, is plotted on the same axes as n and n^*. A constant value of 80 km

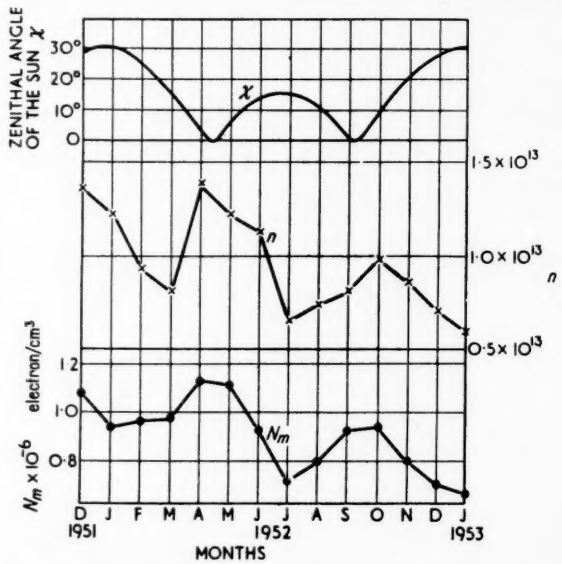

Fig. 2. Seasonal variation of noon values of χ, N_m, and n.

has been assumed for the semi-thickness of the F_1-layer, which fits many of the records analyzed. It is seen that the shape of the curve is not effectively altered by considering n_T instead of n. From the monthly mean curves it is seen that, in general, the variation of n shows negligible "bite-out" and is usually a fairly flat topped curve.

It should be pointed out, however, that the above picture is further complicated if one accepts the modern view that the F_1- and F_2-layers are manifestations of a single Chapman region with bifurcation due to rapidly decreasing α with height. Neither layer will resemble a single Chapman layer (which assumes constant α and temperature with height), with regard either to maximum electron concentration or total electron content. The seasonal variations of n, N_m, and χ at noon are shown in Fig. 2. It will be seen that N_m and n acquire maximum values when χ is zero. The progressive overall decrease of n and N_m is attributed to the advancement of the sun-spot cycle. This would also explain the considerable difference in the average noon value of n at Ibadan in 1952 ($1{\cdot}0 \cdot 10^{13}$ electrons), and n at Singapore in 1949 ($1{\cdot}9 \cdot 10^{13}$ electrons).

VOL. 5 1954

3. Rate of Ionization and Coefficient of Recombination

Values of the rate of ionization q_m and the coefficient of recombination α_m have in the past been deduced from the daily variation of N_m by assuming the equation

$$dN_m/dt = q_m - \alpha_m N_m^2 \tag{1}$$

and that α_m and q_m are the same at times equidistant from noon. If this is applied to equatorial values of N_m where a pronounced midday minimum is normally present, then negative values of q_m are obtained, indicating, as would be expected, that some removal of ionization occurs. At Ibadan negative values of α_m are also obtained which are impossible to interpret. Following Ratcliffe's suggestion that the noon minimum is removed when n is considered, we have endeavoured to modify equation (1) to apply to the curve of n, and thus take into account the decrease of N_m, due to a thickening of the layer. In order to do this the whole of the unit column below h_m must be considered, and then

$$dn/dt = \bar{q} y_m - \bar{\alpha}(n/y_m)^2 y_m \tag{2}$$

where $\bar{q}$ is the mean rate of ionization from the bottom of the layer to the height of maximum ionization defined by

$$q y_m = \int_{h=h_o}^{h=h_m} q\, dh \tag{3}$$

and α is the mean coefficient of recombination defined by

$$\alpha(n/y_m)^2 y_m = \int_{h=h_o}^{h=h_m} \alpha N^2\, dh \tag{4}$$

It should be noted that equation (2) contains no term in dy_m/dt. If such a term is included then equation (2) becomes identical with equation (1). It is this difference which removes the effect of changes in layer thickners (such as will be produced by vertical motions of the ions) from the values of q obtained. If the layer is considered to be approximately parabolic, as is often the case, then it can be shown that

$$\bar{q} = q_m/3 \tag{5}$$

and

$$\bar{\alpha} = 3/4\ \alpha_m \tag{6}$$

It should be noted that equation (5) has been derived assuming dn/dt to be zero and it is thus an approximation, true only near noon. Equation (2) has been applied to the annual means of n^* and n, and Fig. 3 shows the variations of $\bar{q}$ with time of day. Graph 1 shows the values of $\bar{q}$ obtained from the n curve. Graph 2 shows the values of $\bar{q}$ obtained from the n^* curve, whilst Graph 3 shows the values of q_m obtained from equation (2). Table 1 gives the values obtained for q_m and α_m throughout the day, derived from $\bar{q}$ and $\bar{\alpha}$ by equations (5) and (6).

It must, of course, be fully realized that the method has gross over-simplifications associated with it. It assumes that α and q vary symmetrically about noon and that the proportion of ionization below the maximum is constant. This latter condition is unlikely to be satisfied in view of the vertical drifts of ions produced by tidal forces. However, the values obtained for α_m are in fair agreement with those of other workers, it being remembered that this is the average value throughout the bottom half of F_2. Mitra (1952) has quoted α at 8×10^{-11} cm^3/sec during the day, rising to 30×10^{-11} during the night, and higher values still in the

F_1-region. In general, equation (2) does seem to realize interpretable results when equation (1) does not. There is still, however, some further factor to be taken into consideration, since $\bar{q}$ and q_m should have a single maximum at noon.

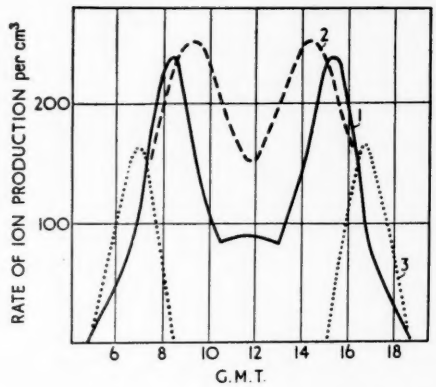

Fig. 3.
Graph I. Values of $\bar{q}$ obtained from the mean curve of n.
Graph II. Values of $\bar{q}$ obtained from the mean curve of n^*.
Graph III. Values of q_m obtained from the mean curve of N_m.

Values of q_m and α_m obtained from $\bar{q}$ and $\bar{\alpha}$ at times appreciably removed from noon are in error because only at noon does the simple Chapman theory give an approximately parabolic distribution of ionization. However, since RATCLIFFE

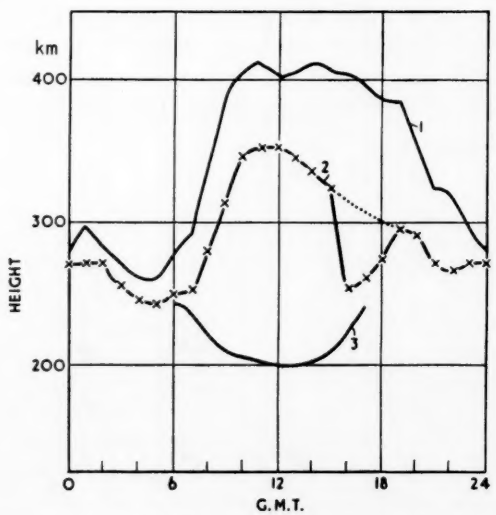

Fig. 4. Annual mean values for the diurnal variation of (1) h_m, (2) $h'F_2$, and (3) $h'F_1$.

(1951b) has observed that after sunset the F_2-layer rapidly assumes a parabolic shape, this criticism is possibly not very important. It also means that equation (2) may be applied during the night hours, putting $\bar{q} = 0$.

VOL. 5 1954

4. The Sunset Minimum of $h'F_2$

This phenomenon has been discussed by Osborne (1951) for Singapore and is associated with a slight increase of ionization around the same time. This occurs soon after the afternoon ridge, and could be a phenomenon linked with it. We feel, however, that the observed maximum and minimum at 1900 hrs and 1600 hrs respectively have no real existence, and that the evidence for them is spurious. We consider that it arises from slight errors in the standard reduction of the records. Fig. 4 shows the annual mean values of h_m (Curve 1), and $h'F_2$ (Curve 2), and $h'F_1$

Table 1

Time G.M.T	*From n*		*From n**	
	q_m	α_m	q_m	α_m
	$(3\bar{q})$	$(4/3\bar{\alpha})$	$(3\bar{q})$	$(4/3\bar{\alpha})$
0600 1800	96	$22 \cdot 10^{-11}$	168	$24 \cdot 10^{-11}$
0700 1700	248	$26 \cdot 10^{-11}$	224	$24 \cdot 10^{-11}$
0800 1600	576	$48 \cdot 10^{-11}$	480	$43 \cdot 10^{-11}$
0900 1500	672	$58 \cdot 10^{-11}$	694	$64 \cdot 10^{-11}$
1000 1400	424	$58 \cdot 10^{-11}$	808	$88 \cdot 10^{-11}$
1100 1300	264	$30 \cdot 10^{-11}$	704	$80 \cdot 10^{-11}$
1200	288	$34 \cdot 10^{-11}$	480	$56 \cdot 10^{-11}$

(Curve 3). Around 1600 hrs the F_1-layer has lost its well defined maximum of ionization and becomes an added bulge to the F_2-layer. In such cases the virtual height of the bottom of the F_2-layer, $h'F_2$, cannot be measured, and according to the international convention L should be recorded in the reduction sheets. Thus from about 1600 hrs to 1900 hrs when F_1 has completely disappeared there should be no numerical values for $h'F_2$. On some occasions F_1 and F_2 may merge together during these hours and will appear as F_2 only. The bottom of the layer is then taken as $h'F_2$, when in reality it is $h'F_1$. Thus the monthly mean values of $h'F_2$ during the hours 1600, 1700, and 1800 will in general become far too small and will approach the values of $h'F_1$. In our records during some months so few values of $h'F_2$ at 1600 hrs and 1700 hrs could be obtained that no monthly means could be

given for these hours. This does seem to explain the graphs in Fig. 4 and the hypothesis is borne out by the fact that the curve for h_m, unlike $h'F_2$, does not show any minimum at sunset.

5. CORRELATION OF h_m AND y_m

We have constructed a histogram of h_m and y_m, and it will be seen by reference to Fig. 5, which includes about 3000 values, that the relationship between h_m and y_m is not linear. For large values of y_m, h_m remains roughly constant. These figures have been obtained from the $h'f$ records by the use of APPLETON and BEYNON's methods, which assumes a parabolic layer. It has been seen that the very thick layers do not in general approximate to parabolic layers, and this fact may explain the shape of Fig. 5. There also appears to be a tendency for a few layers with small y_m to occur at large heights h_m, but it is felt that these are due to the presence of ridges in F_2,

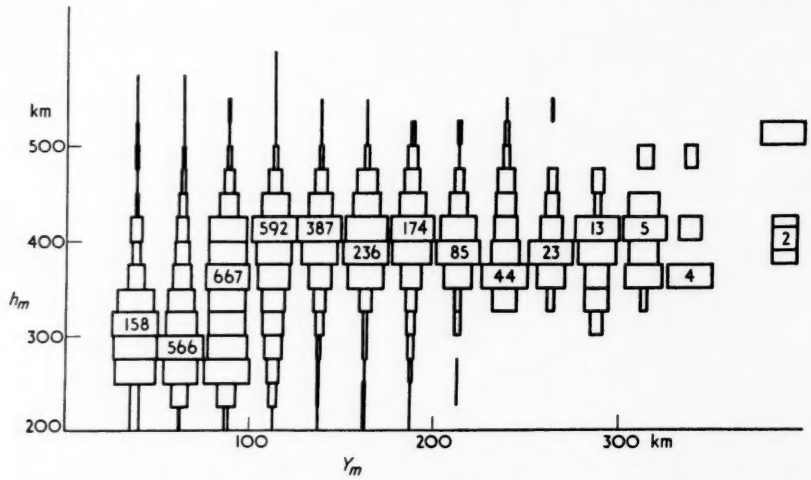

Fig. 5. A histogram showing how the value of h_m affects y_m. (This incorporates about 3000 values taken during 1952.)

when measurement of the top layer leads to a value of h_m which is misleading. If the histogram's axes were reversed it would be seen more clearly that a very large proportion of the few layers with great y_m do give a slight indication that h_m begins to decrease as y_m increases. If this effect is real it may easily be due to the fact that with very thick layers, readings are not often taken, as usually the layer will not be parabolic, but if such $h'f$ curves are treated by APPLETON and BEYNON's method then they may give rise to low values of h_m.

However, Fig. 5 does establish the fact that y_m is not a linear function of h_m. RATCLIFFE (1951b) has shown that for two stations y_m is roughly proportional to h_m but that for the station at College, Alaska, the relationship he obtained is very similar to that shown in Fig. 5. This may be due to the fact that we have considered all days, whereas RATCLIFFE only considered magnetically quiet days, and at College, Alaska, even "quiet" days will be relatively disturbed.

VOL. 5 1954

Acknowledgments—The authors are indebted to the Radio Research Station, Slough, for the loan of equipment, and particularly to Mr. W. R. PIGGOTT for stimulating discussion.

REFERENCES

APPLETON, E. V.	1950	J. Atmosph. Terr. Phys. **1,** 106
APPLETON, E. V., and BEYNON, W. G. J.	1947	Proc. Phys. Soc. **59,** 58
CHATTERJEE, B.	1953	J. Geophys. Res. **58,** 353
MITRA, S. K.	1952	The Upper Atmosphere (Asiatic Society, Calcutta)
Monthly Bulletins of Ionospheric Characteristics		Published by D.S.I.R. Radio Research Station, Slough
OSBORNE, B. W.	1951	J. Atmosph. Terr. Phys. **2,** 56
OSBORNE, B. W.	1952	J. Atmosph. Terr. Phys. **3,** 58
RATCLIFFE, J. A.	1951a	J. Geophys. Res. **56,** 463
RATCLIFFE, J. A.	1951b	J. Geophys. Res. **56,** 487
SKINNER, N. J., BROWN, R. A., and WRIGHT, R. W.	1954	J. Atmosph. Terr. Phys. **5,** 92

DL.
5
954

Journal of Atmospheric and Terrestrial Physics, 1954, Vol. 5, pp. 298 to 315. Pergamon Press Ltd., London

Ionospheric thermal radiation at radio frequencies

II. Further observations

F. F. GARDNER
Division of Radiophysics, Commonwealth Scientific and Industrial Research Organization, Australia

(*Received* 5 *April* 1954)

CONTENTS

	PAGE
1. Introduction	298
2. Experimental Procedure	299
2.1. Site and aerials	299
2.2. Measurement of equivalent aerial temperature	300
2.3. Aerial efficiency, α	301
2.4. Determination of ionospheric temperature	302
3. Observations	303
3.1. General	303
3.2. Observed temperatures	305
3.3. Effect of sudden ionospheric disturbances (SID's)	308
3.4. Polarization results	309
3.5. Noise of tropospheric origin	309
4. Discussion	312
5. Conclusions	314

VOL. 5 1954

ABSTRACT

The results of a series of observations of 2 Mc/s radio noise over a period of about a year at a very quiet site are described. The noise received during the midday hours is thought to have been due almost entirely to ionospheric thermal radiation. The derived ionospheric temperatures ranged between about 200° and 250° Kelvin, varied appreciably from day to day and were lower and less variable in winter.

During SID's the ionospheric temperature increased by up to 40°K. This increase is probably due to a height change of the 2 Mc/s absorbing region.

Polarization measurements showed that in September 1951 the intensity of the extraordinary component, absorbed at the lower ionospheric level, corresponded to a temperature about 20°K higher than the ordinary. This established that the absorbing regions were then located at a level where the temperature decreased with height.

Information on the location of the absorbing regions was obtained from an auxiliary set of pulse reflection measurements. The experimental observations can be explained reasonably in terms of a fixed temperature-height model, similar to that determined by rocket measurements, but having a minimum of 217°K at 80 km.

1. INTRODUCTION

It was shown in a previous communication by PAWSEY, MCCREADY, and the author (1951), to be referred to as Paper I, that radio noise at medium frequencies contains a component due to thermal radiation from the ionosphere. This component is very small, but can be measured during the midday hours at places remote from electrical machinery.

The observations of noise in Paper I were not systematic, were made at locations where interference was generally still appreciable, and lacked experimental information on the region of its origin. To remedy the first two defects the series of observations to be described in this paper was made at frequencies near 2 Mc/s over a period of about a year at a site as remote as practicable from sources of

man-made noise. To remedy the third, an auxiliary set of *D*-region observations, using pulses on an adjacent frequency, were made by PAWSEY and the author (GARDNER and PAWSEY, 1953), and these showed that the absorbing structure of the lower ionosphere could be determined. These measurements, although not made simultaneously with the noise recordings, have enabled us to interpret results in terms of an average temperature-height distribution.

2. EXPERIMENTAL PROCEDURE

2.1. *Site and aerials*

Fig. 1 shows the recording site at Urisino (30° S, 144° E) in relation to the location of electrical transmission systems in the eastern Australian states. The site was chosen to minimize man-made noise, a large proportion of which is radiated

Fig. 1. Recording site at Urisino, shown in relation to electricity distribution systems, shown ——, and contours ---- showing the average number of days per year when thunder was audible. Sites of previous observations at Rankins Springs and Burragorang Valley are also shown.

from power lines. Figure 1 also shows the thunderstorm frequency distribution compiled from 10 years' meteorological observations. From an examination of the contours one would expect that the level of atmospherics would be about the same at Urisino and at Burragorang near Sydney (where the original observations of Paper I were made), as the thunderstorm frequency and the distance from the centre of activity in south-east Queensland are about the same for both places.

The aerial normally used was a single horizontal resonant dipole, directed north–south, and suspended from two 80-foot poles, 235 feet apart. It was connected to the recording equipment in a vehicle stationed below the dipole centre

by about 75 feet of fabricated 70-ohm twin feeder. The horizontal top wires plus the downleads connected together at the bottom served as a vertical aerial when this was required.

For the last recording period in September 1951, a supplementary east–west dipole (centres of both dipoles coincident) was added for the reception of circularly-polarized waves. In this case the outputs of the two dipoles, which had identical downleads, were combined using an extra quarter-wave line in the conventional manner. The impedance of each dipole matched the feeder to within 5 per cent. The finite attenuation of the quarter-wave section caused the suppression of the component with the opposite sense of rotation to be slightly imperfect. Its effect was allowed for in the deductions of Section 4.

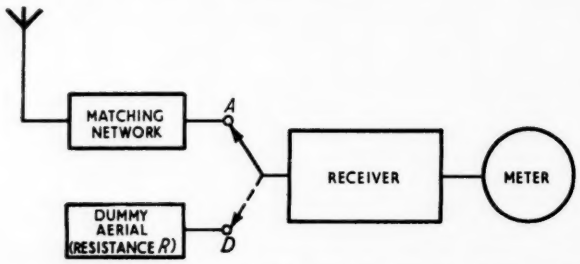

Fig. 2. Arrangement of equipment. The matching network is adjusted to make the impedence at A identical to that of the dummy aerial at D.

VOL. 5 1954

2.2. *Measurement of equivalent aerial temperature*

The measurement of the equivalent aerial temperature T_a was discussed in Paper I, and the method is illustrated in Fig. 2. The impedance at A is adjusted to equal that of a resistor R used as a dummy aerial. The aerial temperature is measured with respect to the temperature of this comparison resistor. The calibration of the temperature scale at values above room temperature is made with a high-impedance noise diode shunted across the resistance R. The scale below room temperature is determined by extrapolation. The bandwidth, which was that of the receiver alone, was the same for both recording and calibration. Experimentally, it was checked that the system was free from regeneration of an amount which could cause the gain during recording to differ from the gain during calibration.

If the impedance at A differs from R, then the measured aerial temperature will be in error. To a first order approximation, for small errors in matching, only the difference in the resistive components is important, and if the resistive component of the impedance at A is $R + \Delta R$, then the true temperature T_a can be found from the measured value $T_a + \Delta T_a$ using the relation

$$\frac{\Delta T_a}{T_a} = \frac{\Delta R}{R}.$$

The reading error under good observing conditions, when dummy aerial readings were taken frequently, as in Fig. 4(a), can be seen to be 2 or 3°K. To keep errors due to the matching down to the same order of magnitude, the aerial was matched within 1 per cent under normal weather conditions. With

strong winds, however, errors of up to about 3 per cent could occur with the horizontal aerials and even greater errors with the vertical or circularly-polarized aerials.

Errors in the temperature of the comparison resistor were less than $\frac{1}{2}$°K, and did not contribute appreciably to the overall error in T_a.

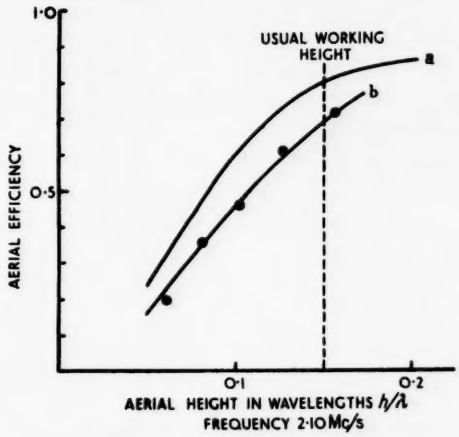

Fig. 3. Aerial efficiency as a function of height: (a) calculated for average ground constants $\epsilon/\epsilon_0 \approx 25$, $\sigma = 1{\cdot}3 \times 10^{-2}$ mho/metres, and (b) determined from impedance measurements in September 1951.

2.3. *Aerial efficiency*, α

The derivation of the ionospheric temperature from the observed aerial temperature requires a knowledge of α, the aerial efficiency. In Paper I α was obtained in two ways:

(a) from the direct measurement of the aerial gain in a vertical direction using a balloon-borne oscillator, and

(b) from the results of a theoretical analysis by SOMMERFELD and RENNER (1942)* using estimated values for the ground constants. The former was found to be inaccurate and was not employed further. For the numerical evaluation using the latter method the ground constants were measured at the receiving site for the periods in November 1950 and in April and September 1951 by the "wave tilt" method (see NORTON, 1937). At 2 Mc/s the characteristics of the ground are largely controlled by the conductivity, and this was found to be high (σ never below 10^{-2} mho/metre), and substantially the same at different periods. Fig. 3 shows the aerial efficiency calculated as a function of height for the average ground constants ($\varepsilon/\varepsilon_0 \approx 25$, $\sigma = 1{\cdot}3 \times 10^{-2}$ mho/metre).

The efficiency can be determined more directly from a measurement of the dipole input impedance if the current distribution is known. From the current distribution and the ground properties, the total power radiated above ground,

*This analysis is for an infinitesimal horizontal radiator. General but not exact agreement would be expected with a half-wave radiator.

$R_R'I^2$, is calculated,* while the power fed to the dipole is given by $R_{in}I^2$, where R_{in} is the resistive component of its input resistance. Then

$$\alpha = \frac{R_R'}{R_{in}}.$$

We note that over most of the height range of interest $\alpha \approx \frac{R_R}{R_{in}}$, where R_R is the radiation resistance in the presence of a perfectly conducting earth.

Assuming a sinusoidal current distribution and with an approximate knowledge of the ground constants, R_R' and therefore α can be determined as a function of height. This was done for April and September 1951, when aerial impedances over a range of heights were measured. The final result for September is compared with the theoretical curve (a) in Fig. 3. There is reasonable agreement between the two and the mean value $0{\cdot}75 \pm 0{\cdot}05$ was adopted as the efficiency with the aerial at its usual height.

2.4. *Determination of ionospheric temperature*

In Paper I, it was seen that the equivalent aerial temperature T_a was a weighted mean of the temperatures of the ionosphere T_i and of the ground T_g

$$T_a = \alpha \,.\, T_i + (1 - \alpha)T_g$$

where α is the efficiency of the aerial (ohmic losses in the aerial are negligible). This result can be extended to include transmission losses, at a different temperature T_t, occurring between the aerials terminal and the receiver input, and then becomes

$$T_a = [\alpha \,.\, \eta_T] \,.\, T_i + [(1 - \alpha) \,.\, \eta_T] \,.\, T_g + [1 - \eta_T] \,.\, T_t$$

where η_T is the efficiency of the matching unit and transmission line when terminated with the dipole impedance.

Under typical conditions this becomes

$$T_a = 0{\cdot}65\ T_i + 0{\cdot}20\ T_g + 0{\cdot}15\ T_t. \qquad (1)$$

The measurement of T_a was covered in Section 2.2.

The ground temperature required, T_g, is a weighted mean to a considerable depth below the surface. (The skin depth is approximately 10 feet.) An experimental check on the temperature 9 inches below the surface showed that the daily mean temperature there was the same as that above the ground, but the range of variation through the day was approximately halved. It seems reasonable therefore to consider T_g as constant and equal to the mean above-ground temperature for the period concerned. From observations at Urisino and figures published by the Commonwealth Weather Bureau, the mean above-ground temperature was estimated to within a few °K.

*In making this computation the field at any point is determined by combining the free-space wave with a wave reflected from the ground with the appropriate plane wave reflection coefficient, taking account of phase and path differences. This procedure, known to be correct for large values of h/λ, can be justified from the expressions given by NORTON (1937) for horizontal dipole field intensities.

VOL. 5 1954

The temperature T_t of the transmission system was principally that of the fabricated twin line, which was nearly vertical and freely exposed to the atmosphere over its entire length. With the sun obscured by cloud, T_t should equal shade temperature, but with the sun shining a reasonable estimate of its maximum increase is about 8°K. In taking its mean temperature as that inside the recording vehicle, the error should not exceed 5°K.

From equation (1) with reasonable estimates of the quantities involved, it was concluded that the probable systematic error in deduced ionospheric temperature was about 5°K. In addition, the probable random error of a single observation over 3 minutes was also about 5°K under normal weather conditions. The random error in the mean of a series of independently matched readings should be reduced to less than half this amount.

3. Observations

3.1. *General*

Six series of observations each of about 10 days' duration were made at intervals of about two months. The details of the recording periods are given in Table 1. In the absence of severe atmospherics, measurements were normally made from about 0800 to 1700 hours. A frequency near 2 Mc/s was usually employed. Its actual value was changed over a small range to avoid interference.

Table 1.

Period	*Year*	*Interval*	*Polarization*	*Auxiliary measurements*
I	1950	11 July–21 July	Linear	—
II	1950	21 Sept.–2 Oct.	Linear	—
III	1950	20 Nov.–1 Dec.	Linear	Ground constants
IV	1951	19 Feb.–27 Feb.	Linear	—
V	1951	14 April–27 April	Linear	Ground constants—aerial impedance
VI	1951	20 Sept.–5 Oct.	Linear and circular	Ground constants—aerial impedance

The typical diurnal variation of noise received with a horizontal dipole, at Burragorang, near Sydney, was described in Paper I. There the level at night was always high (above 10^6 °K) and very variable, but gradually settled down through the day to a low, fairly steady value near noon (order 1000°K). At Urisino, the more remote site, the level during the day was much more constant, while at night the background level measured between individual atmospherics crashes, was considerably lower than at Burragorang. Interference from radio stations (generally from harmonics) was, however, found to be relatively more troublesome. This might be expected, as transmitting stations are distributed more randomly than the emitters of man-made noise (large cities). The sensitivity to such interference is illustrated by the fact that an increase in aerial temperature of 10°K

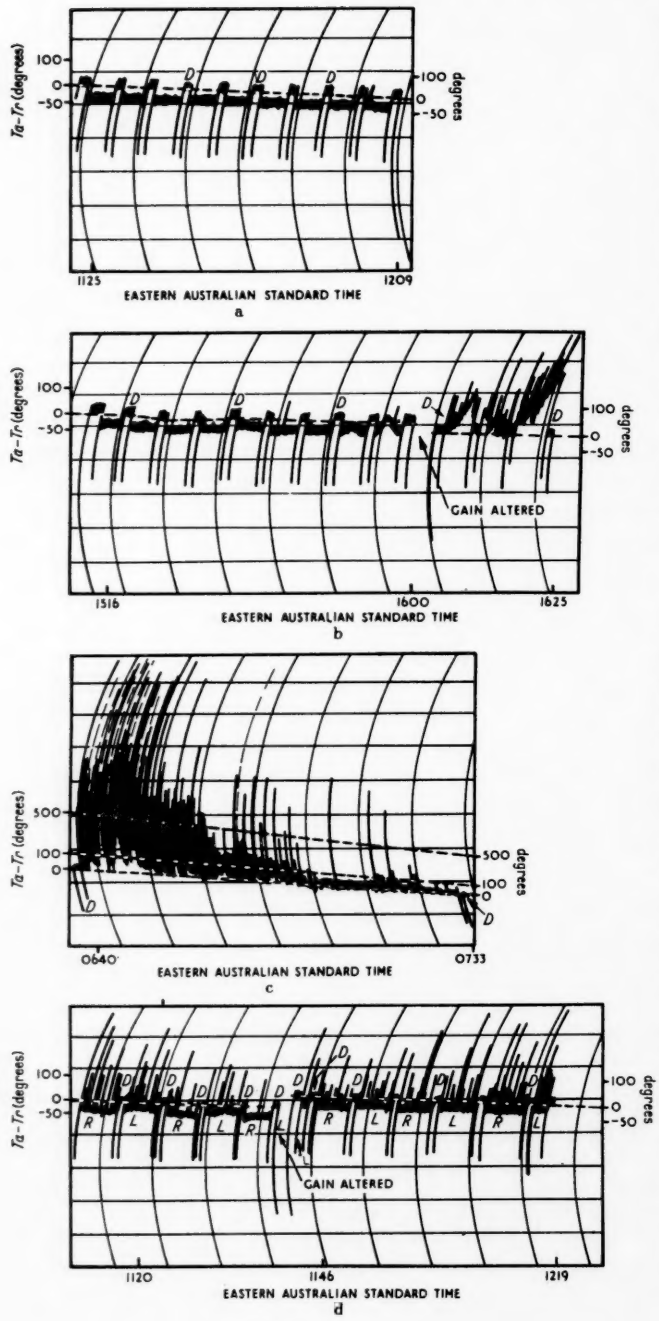

Fig. 4. (a) Midday record when interference and atmospherics negligible. $T_a - T_R$ is the aerial temperature relative to ambient, 290°K. *D* indicates connection to dummy aerial. Note that only one atmospheric occurred through the period shown. (Urisino, 2·1 Mc/s, horizontal polarization, 23 April 1951, 1125–1209 E.A.S.T.). (b) Record showing interference increasing in the late afternoon (same frequency, polarization and date as in (a), 1516–1625 E.A.S.T.). (c) Typical morning record near midsummer. Only a slight change in base level accompanies a large reduction in the atmospherics (Urisino, 1·6 Mc/s, horizontal polarization, 1 December 1950, 0640–0733 E.A.S.T.). (d) Typical record with circularly polarized receiving aerials. The left-handed and right-handed aerials are matched separately to equality with the dummy aerial (Urisino, 2·07 Mc/s, 29 September 1951, 1120–1219 E.A.S.T.).

VOL. 5 1954

with the received bandwidth of 5 kc/s would be produced by a wave arriving from near the zenith with a field strength of $1{\cdot}5 \times 10^{-10}$ volts/metre. Practically all interference at Urisino is thought to have involved ionospheric transmission.

Fig. 4(a) shows a midday record when interference and atmospherics were negligible. In Fig. 4(b), variations in the base level which increase as evening approaches are apparent from about 1530 hours, and by 1600 hours fluctuating interference and atmospherics increasing in amplitude and frequency of occurrence are clearly visible. Fig. 4(c) illustrates typical behaviour during the reverse transition on a summer morning. Only a slight change in base level occurs while the atmospherics are reduced by more than 10 to 1 in amplitude. The gradual change in gain is due to batteries running down. Its effect has been allowed for in the intensity scale on the figure.

The aerial temperature observed with vertical polarization was usually around 270°K near noon, compared with 240–250°K with horizontal polarization. However, distant atmospherics and fluctuating interference when present were usually stronger with vertical polarization (3–4 times in amplitude).

3.2. *Observed temperatures*

Histograms showing the noise intensities observed between 0900 and 1500 hours and 1000 and 1400 hours separately are shown in Fig. 5 for the different recording periods. In this figure all noise intensities have been converted to equivalent ionospheric temperatures. For the first four periods, the histograms were compiled from readings of the minimum base level (to the nearest 5°K in T_a) in each 3-minute period. This procedure was adopted to reduce the effect of fluctuating interference from atmospherics and radio stations. During the last two periods the atmospherics were not troublesome and station interference was reduced by more careful monitoring. The overall measuring accuracy was increased and reading variations were principally due to random effects. To reduce these, the median of six $\frac{1}{2}$-minute readings of T_a, to the nearest °K, was taken from the 3-minute reading used in the histogram. An experimental check was made of the average difference between the temperatures measured in the two ways under conditions free from interference. It was found that the minimum corresponded to an ionospheric temperature about 3°K lower than the median.

In Fig. 5 it can be seen that the median temperature was lowest for the periods near mid-winter, July 1950 and April 1951. For both these periods the occasional high readings, above 250°K, were largely confined to times between 0900 and 1000 and between 1400 and 1500 hours. The high readings, up to about 300°K, in September and November 1950 show no such diurnal behaviour, and it is thought that they contain a component resembling random noise, which originates in the lower atmosphere, but not at a great distance (see Section 3.5). For the period in April 1951, 85 per cent of the readings are concentrated between 210 and 230°K. In September 1951, when experimental errors and interference were certainly not greater than in April, the spread has increased appreciably and the distribution has become skewed towards the higher temperatures.

Measurements were made on occasions through the frequency range 1·6 to 2·6 Mc/s. It appeared that the ionospheric temperature increased with decreasing

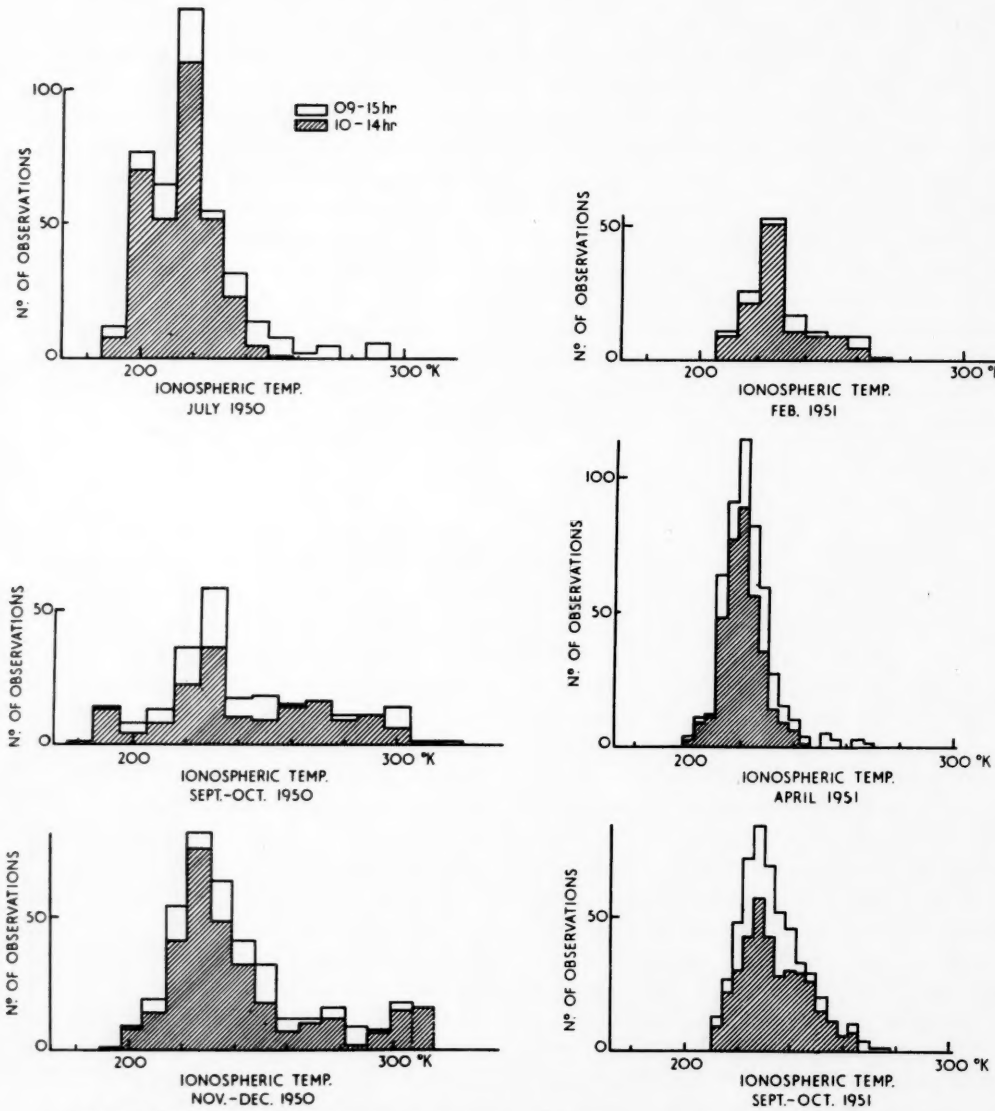

Fig. 5. Midday noise levels, observed with horizontal polarization, expressed as ionospheric temperatures for the different observing periods. Readings between 0900 and 1500 hours are shown unshaded and between 1000 and 1400 hours shaded. Minimum intensities observed in each 3-minute interval are employed for the first four periods; for the last two, medians of six ½-minute readings are used. All readings above 300°K are included in range 307–315°K, shown dotted.

VOL. 5 1954

frequency. The accuracy involved was not high, since the losses increase rapidly as the dipole impedance becomes largely reactive. Most records were taken near the dipole resonant frequency.

The diurnal variation of the base level of the received noise at Rankins Springs (see Fig. 1) for May–June 1950 was studied in Paper I by plotting the mean and the range of the minimum hourly levels. The smoothed curve, reproduced in Fig. 6(a), shows a significant diurnal variation. Below it, the results at Urisino for June–July

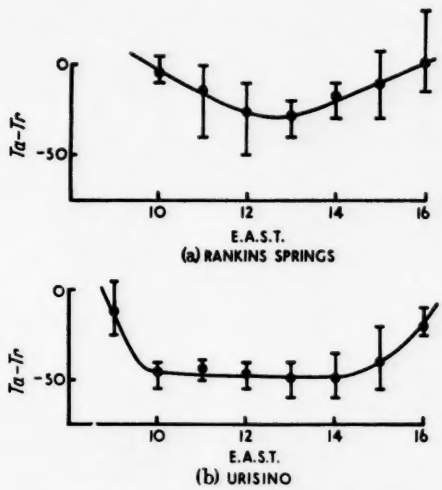

Fig. 6. Means and extreme ranges of minimum aerial temperatures relative to ambient recorded in each hour (a) at Rankins Springs, 31 May to 8 June 1950, and (b) at Urisino, 11 to 21 July 1950.

1950, also near mid-winter, are plotted in the same way. Between 1000 and 1400 hours the mean level is now constant. The higher levels before 1000 and after 1400 hours are presumably due to increases in ionospherically-propagated interference, and it appears that a small residue of such interference continued throughout the day at Rankins Springs.

The results from the other periods at Urisino, when examined in this way, were all reasonably constant near midday. The period of constancy, however, extended from before 0900 to beyond 1500 hours.

Examination of the midday variations in more detail failed to reveal any real diurnal variation. Fig. 7 shows a typical result obtained by superposing seven daily curves taken with a single horizontal aerial in September 1951. Any real diurnal trend is masked by a larger randomly-occurring variations. These changes throughout the day and from day to day can only be partly due to experimental error and external interference, and it is thought that the largest increases, at least, are associated with increases in ionospheric absorption probably caused by variations in the sun's ionizing radiation. The two days on which high temperatures were most prominent were 21 April and 21 September 1951 (21 September is shown in Fig. 7). On both these days f_{min} (the minimum frequency) on which ionospheric echoes are observed on a P'-f recorder) at Canberra was for quite long

periods appreciably higher than usual, but no definite sudden ionospheric disturbances were indicated on short-wave absorption measurements made near Sydney. A solar noise storm of considerable intensity occurred on 21 April.

3.3. *Effect of sudden ionospheric disturbances (SID's)*

In assessing the effect on 2 Mc/s noise of a sudden ionospheric disturbance (SID), it was found convenient to use as a measure of its intensity the decrease in cosmic noise level observed at 18·3 Mc/s.* Taking the larger SID's (1 db attenuation or above at 18 Mc/s at vertical incidence) and restricting attention to the midday hours

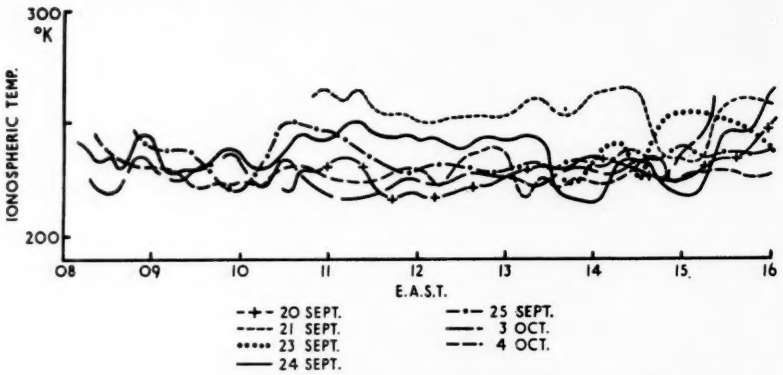

Fig. 7. Diurnal variation of ionospheric temperature for seven days in September–October 1951 (frequency 2·1 Mc/s, horizontal polarization).

1000 to 1400, the observed temperatures during 40 minutes from the start of an SID were compared with the average temperature readings for the recording period in April 1951 from Fig. 5.† The two distributions are compared in Fig. 8(a), which includes four SID's. It is apparent that the ionospheric temperature was *significantly higher during an SID.*

To examine the detailed time structure, $\frac{1}{2}$-minute temperature readings through all SID's greater than 1 db in April (six in all) were combined in a superposed epoch plot with the 18 Mc/s SID commencement at zero time. Fig. 8(b) shows the median curve (i) obtained by this method, and also the largest observed SID (ii) (7 db on 18 Mc/s at vertical incidence).

We see then that a very definite rise in ionospheric temperature of up to about 40°K occurs during an SID. The time of start and the average duration of about an hour are, within experimental uncertainties, the same as those for the short-wave absorption increase. There is, however, an indication of lack of proportionality between the temperature increase and the short-wave absorption, and that, with the largest SID, the temperature has reached a "saturation" level.

Apart from the occurrences discussed for April, only two other SID's of appreciable size were observed. These two occurred in September 1951, and again produced definite temperature increases.

* This investigation, carried out at the Radiophysics Laboratory, has been described by SHAIN and MITRA (1954). The information for our analysis was kindly provided by Mr. SHAIN.

† Fig. 5 does not contain readings obtained during these SID's.

VOL. 5 1954

3.4. *Polarization results*

The results of the polarization measurements made near noon over a period of three days in September–October 1951 are shown in histogram form in Fig. 9. It is apparent that the temperature is greater for the L.H. or extraordinary component, the medians for the two distributions differing by about 17°K. The histograms

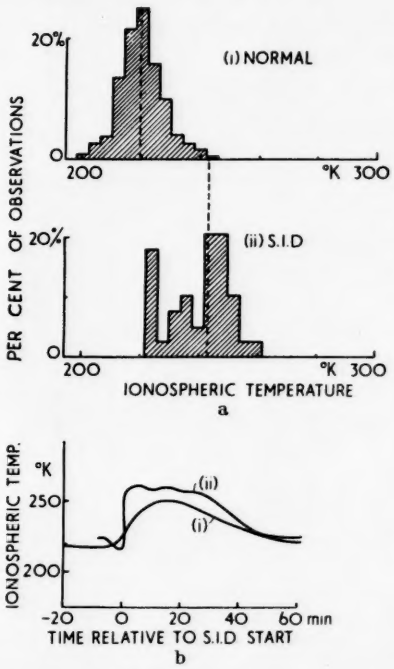

Fig. 8. (a) Histograms showing ionospheric temperatures (3-minute readings) observed between 1000 and 1400 hours in April 1951, (ii) during 40 minutes from the commencement of large SID's, and (i) during the remainder of the period. The medians of the two distributions are indicated.
(b) Superposed epoch plot for April 1951 of ionospheric temperature relative to SID starting time. (i) is the median curve for 6 SID's and (ii) is the curve for the largest SID.

establish the general result, but it was further observed that on changing from R.H. to L.H. polarization, the temperature usually increased, but at no time was it ever observed to decrease. Fig. 4(d) shows a sample polarization record.

Remembering that the extraordinary component suffers the greater absorption, it is of interest to note that both the observed polarization and SID effects are opposite to those expected if an appreciable amount of ionospherically-propagated noise were present, and the effects were due to changes in this component.

3.5. *Noise of tropospheric origin*

During the course of the observations, certain types of noise increases occurred which did not appear to be due to increases either in ionospheric emission or in man-made noise. (Largely on account of their association with particular weather conditions, their source is thought to be in the lower atmosphere.) They are listed

in Table 2 in order of decreasing size. Of these, only the well-known atmospherics crashes (A) would cause serious interference to communication. Their effect on our noise recordings was discussed in Paper I. This further series at Urisino has reinforced the conclusion of the previous paper that at 2 Mc/s atmospherics propagated over a distance produce no measurable component resembling random noise. Individual crashes are always evident. While the cause of both types (B) and (E) was recognized, it is not profitable, with our limited information, to investigate

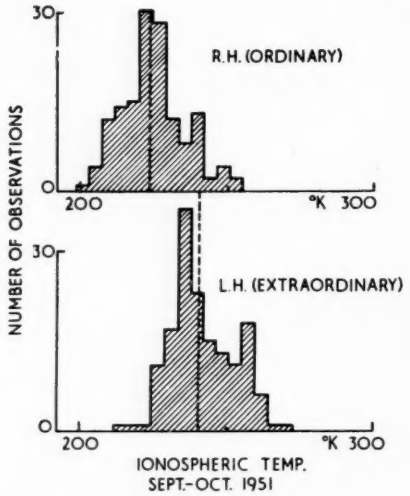

Fig. 9. Histograms showing ionospheric temperatures ($\frac{1}{2}$-minute readings) observed with circularly-polarized receiving aerials in September 1951. The medians of the two distributions are indicated.

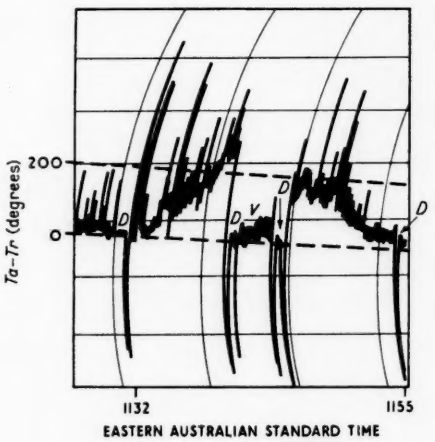

Fig. 10. A record showing an increase in level approximately symmetrical in form lasting about 20 minutes (type C). Near the maximum a brief change from the horizontal to a vertical aerial with about the same sensitivity takes place. The portion recorded with the vertical aerial is marked V (Urisino, 1·97 Mc/s, 29 November 1950, 1132–1155 E.A.S.T.).

mechanisms for their generation. The origin of increases (C) and (D) is not known. Noise increases of types (B), (C), and (D) were associated with unsettled weather, and on such days, thunder clouds or nearby atmospherics were usually observed at some subsequent time.

Rain static (B) has been recognized by other observers (see HUCKE, 1939), and its identification presents no difficulty. Aurally, it resembled the usual description of precipitation static encountered by aircraft given by HUCKE, although the two phenomena are obviously different. Its magnitude was such that it would be observable at any site where the noise level did not much exceed 1 microvolt/metre. It occurred very infrequently and was only observed during the one period (November–December 1950). Usually, no change in the recorded level accompanied rain.

An increase of type (C) is shown in Fig. 10. On changing to vertical polarization near its peak, an appreciable decrease in level occurred, indicating that the noise

VOL. 5 1954

was arriving roughly from overhead. Because of the comparatively short duration and infrequent occurrence (only in November–December period), such increases were easily recognized, and were not included in the ionospheric temperature readings. This was not possible, however, with the slow increases of type (D), which

Table 2. Noise of tropospheric origin

Observed variation in noise intensity	*Associated atmospheric disturbance*	*Audio characteristics*	*Remarks*
A. Large increases of order of 1 second duration, atmospherics	Cloud discharges	Familar crashes, "grinders," etc	Usually no measurable increase in level between distinct crashes even when local electrostatic field high.
B. Large increases of order of 10 minutes duration, rain static	Rain—probably caused by stopping of charged drops near aerial	High-pitched "crying" sound	Due to an exceptional type of rain. T_a increase of up to 10^9 degrees. Maximum increase when rain hardest. Increase may start before rain reaches aerial.
C. Approximately symmetrical increase and decrease lasting about 10 minutes	Possibly charging processes in clouds	Random, pulsating sound	Maximum increase about 1000 degrees in T_a. Increase often larger with horizontal than with vertical aerial. Possibly correlated with small clouds passing overhead.
D. Slow change in level over period of about 1 hour	Unknown	Similar to random noise	T_a increase of up to 100 degrees. Noise level rather steady.
E. Small increases of order of 1 second duration repeated at frequent intervals	Strong winds	Numerous clicks	Order of 30 degrees increase in T_a. Probably not due to impedance changes as changes in level are predominantly increases.
			Note. Values of T_a refer to reasonably efficient aerials.

provided the only serious interference to the measurement of ionospheric temperature. Their inclusion in the histograms of Fig. 5 for the periods September and November 1950, when they were observed, caused the extension of the observed temperatures to above 300°K.

The short "clicks" (E), often associated with strong winds, were observed at some time in each period, and in their presence the reading accuracy was reduced slightly.

4. DISCUSSION

Contributions to the measured ionospheric temperature T_i originate through an appreciable volume of the ionosphere. If the temperature varies with height in this region, then T_i will represent an average temperature. For a model ionosphere in which the temperature, T, electron density, N, and collisional frequency, ν, are known functions of height, the effective aerial temperature along any ray direction* can be determined for each magneto-ionic component (in general the two differ) and to obtain T_i these temperatures must be weighted in accordance with the angular and polarization characteristics of the receiving aerial.

From a consideration of the average sensitivity of the horizontal dipole aerials per unit cone angle (measured from the vertical), it can be shown that the largest contributions to the received power originate at zenith angles of 30 to 35°, and the corresponding ray temperature should be within a few °K of T_i if the temperature and electron density vary smoothly with height.

The ionospheric temperatures recorded with the circularly-polarized aerials do not correspond precisely to the temperatures for the two magneto-ionic components since the polarized aerials only function correctly for a single wave direction. Assuming the energent polarizations for each individual ray direction to equal approximately the magneto-ionic polarizations with collisional frequency $\nu = 0$, it can be shown that about 10 per cent of the power received by the right-handed (R.H.) aerial, set for the reception of the ordinary component, corresponds to the extraordinary. A similar amount of unwanted ordinary component is received by the left-handed (L.H.) aerial. The observed difference between the temperatures recorded with R.H. and L.H. aerials will then be about 20 per cent lower than the true difference between the two components. The temperature with a single horizontal aerial is very nearly the mean of the temperatures of the ordinary and extraordinary components.

To derive information on the temperature-height distribution in the ionosphere it is necessary to know N and ν at the relevant heights. It was shown in GARDNER and PAWSEY (1953) that these quantities could be determined from pulse observations of the lower ionosphere, and consequently we can fix two heights (more precisely two narrow height ranges) at the lower of which the temperature is that of the extraordinary component and at the upper that of the ordinary. With a linear aerial the mean temperature at these two heights is measured. The observations in GARDNER and PAWSEY (1953) were not made simultaneously with the noise recordings and therefore it is not possible to assess directly the relative importance of changes in the absorbing and in the temperature structures of the ionosphere in producing the aerial temperature variations observed. Our results can be interpreted reasonably in terms of a model having a fixed temperature-height scale similar to that obtained from the pooled results of a number of different investigations and published by the Rocket Panel (1952). The fact that no change occurs throughout the year in the temperature-height distribution from rocket measurements, supports this interpretation. The particulars of our scale are

*In Paper I the method for determining the ray temperature was outlined. In our case there is negligible deviation of the rays through the absorbing region.

VOL. 5 1954

obtained from the temperatures for April 1951 combined with the ionospheric structure determined at the same time of year.

From the midday ionospheric structure determined in GARDNER and PAWSEY (1953) for a normal day, 6 May 1952, we fix the two absorption levels 72–75 km and 80–84 km as appropriate for the extraordinary and ordinary components respectively. A lateral shift of 12°K of the Rocket Panel curve is required to give

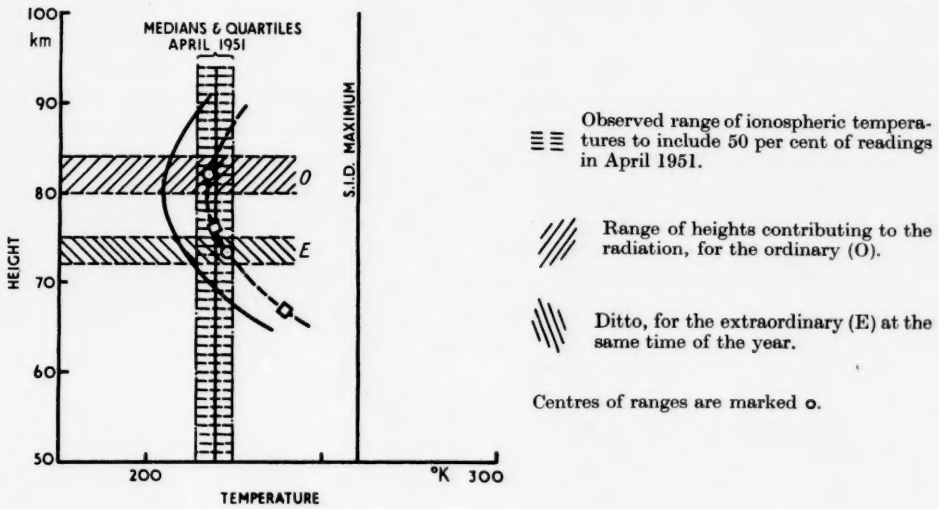

Fig. 11. Temperature-height relation given by the Rocket Panel for White Sands, U.S.A., is shown as full line ———, and is shown dashed ------ when shifted laterally to fit observed results for April 1951. Possible heights of centres of contributing regions for September-October 1951 are shown □. Maximum temperature observed during an SID is shown.

a mean temperature equal to the value 219°K observed for 14–27 April. The shift required is about twice our probable systematic error, estimated in Section 2.4. The two curves are given in Fig. 11, which also shows the observed range of temperatures in April to include half the readings.

Fig. 5 showed that temperatures in summer are higher than in winter. In terms of our fixed temperature-height model this would require that absorption levels in summer should be lower than in winter. Such a change is indicated from very long wave results (BRACEWELL *et al.*, 1951).

During the September-October period in 1951, the temperature of the extraordinary component was found to be about 22°K (corrected value) higher than the ordinary, while their mean was 230°K. This establishes that the absorbing regions were then located where the temperature is increasing with decreasing height (the mesosphere in CHAPMAN'S notation). Possible absorption levels, shown in Fig. 11, are well below the minimum in the temperature-height curve, whereas those for April were almost at the minimum. This interpretation is supported by the greater spread and skewness of the September readings in Fig. 5.

We should expect that the short-lived and day-to-day variations in observed

temperature would be due to changes in ionization rather than in the temperature-height distribution*. This view is supported by the increase in noise intensity found on days of abnormal absorption (see Section 3.2).

During a sudden ionospheric disturbance, the observed temperature was found to increase by an amount of up to 40°K in a matter of minutes. This increase is no more than might reasonably be expected from a downward movement of the absorbing regions of an amount indicated by very long wave measurements (BRACEWELL *et al.*, 1951). A consideration of the rate at which an electron loses the excess energy at its liberation in subsequent collisions indicates that differences between electron and molecular temperatures should be negligible. In view of the smallness of the molecular temperature increase, thought to take place over the complete period of daylight (see previous footnote), an increase of 40°K in a matter of minutes would be remarkable. There is an indication of lack of proportionality between the absorption increase at 18 Mc/s and the observed SID temperature increase, and with the largest SID, T_i appears to increase to a saturation level. This might be expected if the absorbing regions (perhaps only that of the extraordinary component) moved down to a level where the temperature changed slowly with height. This question can only be settled when the effect of an SID on the structure of the *D*-region has been determined.

5. CONCLUSIONS

It has been found possible to measure the ionospheric temperature near the 80 km level with considerable accuracy. The temperatures ranged from about 200° to 250°K, and were lowest near mid-winter. The measured electron temperatures, which should not depart appreciably from the molecular temperatures, can be explained reasonably in terms of a fixed temperature-height scale with a minimum of 217°K at 80 km, the observed temperature variations being due to changes in the heights of origin of the thermal radiation. It is possible, however, that changes in the temperature scale do occur.

Using polarized receiving aerials, it has been shown that the absorbing region in September 1951 was located at a level where the temperature is decreasing with increasing height.

During an SID, temperature increases of up to 40°K have been observed. It is thought that the increase is due primarily to a descent of the region of absorption.

In the absence of man-made noise, background noise intensities near 2 Mc/s (with horizontal or vertical dipoles) have not been observed to exceed 1000°K (0·003 microvolt/metre r.m.s. in a 5 kc/s band) except for short periods. Atmospherics have always appeared as distinct crashes. It is therefore suggested that, in any world-wide surveys of atmospheric noise, attention should be given to the character of the measured noise, as only the atmospherics portion (readily distinguished aurally, at least below 5 Mc/s) would be expected to show a reasonably continuous world distribution. Anomalies found in such surveys (see THOMAS, 1950, p. 343) might then disappear.

*Results obtained by JOHNSON (1953), indicate that the temperature at 70-km altitude responds very slowly to changes in the normal solar radiation. The diurnal range of temperatures should not exceed 1°K.

VOL. 5 1954

Acknowledgments—The author is indebted to Dr. J. L. PAWSEY for his advice and guidance throughout this investigation, to Mr. J. P. GRAY for assistance with the observations, and to Mr. J. W. HUGHES for his co-operation and hospitality at Urisino.

REFERENCES

BRACEWELL, R. N., BUDDEN, K. G., RATCLIFFE, J. A., STRAKER, T. W., and WEEKES, K.	1951	Proc. Inst. Elec. Eng. III **98,** 221
HUCKE, H. M.	1939	Proc. Inst. Radio Engrs. **27,** 301
GARDNER, F. F., and PAWSEY, J. L.	1953	J. Atmosph. Terr. Phys. **3,** 321
JOHNSON, F. S.	1953	Bull. Amer. Met. Soc. **34,** 106
NORTON, K. A.	1937	Proc. Inst. Radio Engrs. **25,** 1203
PAWSEY, J. L., MCCREADY, L. L., and GARDNER, F. F.	1951	J. Atmosph. Terr. Phys. **1,** 261
SHAIN, C. A., and MITRA, A. P.	1954	J. Atmosph. Terr. Phys.; to be published
SOMMERFELD, A., and RENNER, F.	1942	Wireless Eng. **19,** 357–359, 409–414 and 457–462
The Rocket Panel	1952	Phys. Rev. **88,** 1027
THOMAS, H. A.	1950	Proc. Inst. Elec. Engr. III **97,** 335

OL.
5
954

Journal of Atmospheric and Terrestrial Physics, 1954, Vol. 5, pp. 316 to 328. Pergamon Press Ltd., London

Effects of solar flares on the absorption of 18·3 Mc/s cosmic noise

C. A. SHAIN* and A. P. MITRA†

(*Received 5 April* 1954)

ABSTRACT

Two effects of solar flares on the received intensity of 18·3 Mc/s cosmic noise are discussed.

It is shown that observations of the variations in 18·3 Mc/s cosmic noise intensity provide a very sensitive method of detecting sudden ionospheric disturbances (SIDs). The characteristics of the increases in absorption observed during SIDs are discussed and comparisons made with other SID observations, particularly very long wave sudden phase anomalies. It is shown that an increase of 1 db in the absorption of 18·3 Mc/s radiation passing once through the ionosphere is probably associated with a sudden phase anomaly of size about 200 degrees at 16 kc/s. Such a relationship is incompatible with a *D*-region of the simple Chapman type or one of the "exhaustion region" type.

About 30 hours after certain solar flares of Class 3 the absorption of cosmic noise increased, the increase lasting for periods of the order of 10 hours. Magnetic storms did not follow until some time later and at the time of the abnormally high attenuation there were no outstanding peculiarities in magnetic records. It is uncertain whether the excess attenuation occurs within the ionosphere or well away from the earth.

1. INTRODUCTION

In a previous paper (MITRA and SHAIN, in press) it was shown how observations of 18·3 Mc/s cosmic noise could be used to measure the attenuation suffered by radiation passing completely through the ionosphere. Although the amount of attenuation was small, it could be measured with considerable accuracy. The equipment used was simple, comprising an aerial array (beamwidth 17° overall to half-power) directed overhead and connected to a communications receiver. The output of the receiver was recorded and the scale was calibrated using a diode noise generator. The paper discussed the variation of absorption with season and time of day under normal conditions. Since, however, the record of absorption is virtually continuous, it is possible to study in detail the variation of absorption under abnormal ionospheric conditions, and in particular short term variations, such as those observed during sudden ionospheric disturbances, are readily detected.

This second paper presents observations of abnormal ionospheric absorption which were made, using the same technique, during the period July 1950 to June 1951. Most of the cases of unusually high absorption appear to be connected with solar flares, although there were occasional abnormal increases associated with ionospheric storms, lasting for periods of the order of one hour. The latter increases in absorption will not be considered in this paper.

The most striking effects of solar flares are the sudden ionospheric disturbances (SIDs) which occur at the time of the flare; the observation of the characteristic ionospheric effects of these disturbances is a good indication that a solar flare has occurred. BRACEWELL and STRAKER (1949) have shown that the study of the variations in the phase of very long waves reflected from the ionosphere can give detailed information concerning the development of the flare. They also showed

* Division of Radiophysics, Commonwealth Scientific, and Industrial Research Organization, Australia.

† On leave from the Institute of Radiophysics and Electronics, University of Calcutta, and the Council of Scientific and Industrial Research, Government of India.

VOL. 5 1954

that observations of these "sudden phase anomalies" (SPAs) provided much more sensitive indications of SIDs than the better-known fadeouts of short waves. If an attempt is made to record these fadeouts by measuring the field of a short wave transmitter, it is difficult to detect small changes in absorption because of the considerable fading always present on field strength records. Furthermore, during intense SIDs, the field strength may be reduced below the limit of sensitivity of the recording equipment so that no information is obtained concerning the progress of the disturbance near its maximum, which may be a most interesting phase.

Radio waves from outside the earth also suffer additional absorption during an SID as was shown first by JANSKY (1937) and later by HEY, PARSONS, and PHILLIPS (1947). Since the records of cosmic noise are very smooth, apart from occasional periods of interference from atmospherics or radio stations, small changes in absorption can be detected and even during a very intense SID the intensity of cosmic noise at frequencies near 20 Mc/s is well above the limit of sensitivity, so that a continuous record is available of the progress of the disturbance. On some occasions, however, several minutes of the record may be lost during intense bursts of solar noise accompanying the flare. The sudden increase in cosmic noise absorption during an SID will be referred to as an SCA ("sudden cosmic-noise absorption") and Section 2 discusses the observations of SCAs.

Besides the direct effect of solar flares, it became apparent during the course of the work that for some flares, absorption increased about 30 hours after the flare occurred, and three particular cases will be discussed in Section 3.

2. SUDDEN INCREASES IN COSMIC NOISE ABSORPTION

Fig. 1 shows the record of cosmic noise made at Hornsby, N.S.W. (latitude 34° S, longitude 151° E) during a severe SID, together with a simultaneous record of the field strength of station VLQ3 (9·6 Mc/s, distance 650 km). The decrease in

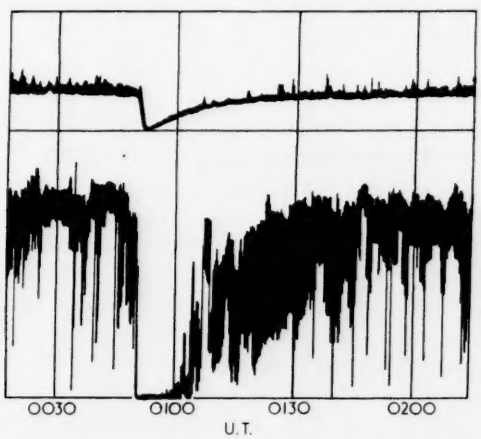

Fig. 1. Records of the received cosmic noise power (above) and of the field strength of VLQ3 (9·6 Mc/s, distance 650 km) (below) at the time of the very severe sudden ionospheric disturbance on April 20, 1951.

the received intensity of cosmic noise accompanying the increase in absorption is clearly seen. Several other typical examples of the variation in cosmic noise intensity during SIDs are shown in Fig. 2 and these illustrate the utility of this technique in observing SIDs. In Fig. 2 the full lines represent records during SCAs and the dashed lines the variations to be expected if the SCAs had not occurred (obtained for example from records at the same sidereal time on neighbouring days).

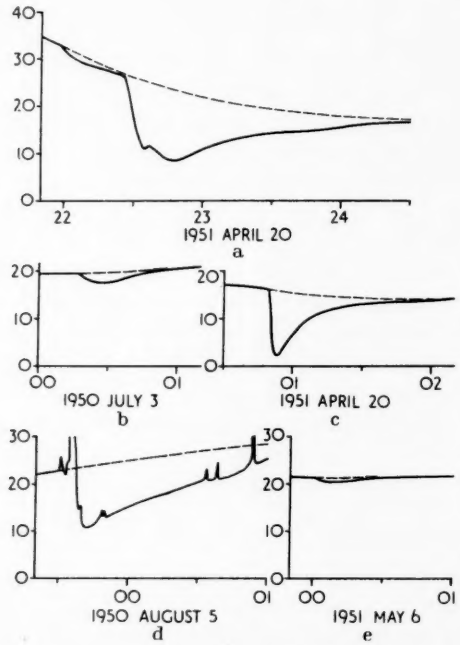

Fig. 2. Typical variations of observed cosmic noise intensity during sudden ionospheric disturbances. Abscissae: hours (U.T.) on the dates shown; ordinates: relative received power. The full line shows the variation on the day of the disturbance and the dashed line the variation to be expected if there had been no disturbance.

Figure 2(a) illustrates the advantage of having a continuous and accurate record of absorption. A small SCA commenced at 2159. Before recovery was complete, a second and larger SCA commenced at 2226. The appearance of the record during this SCA, with two absorption maxima (corresponding to the two minima in received power at 2234 and 2248) suggests that it was, in fact, due to two overlapping flares, the second commencing at 2237. With a cruder form of recording it is probable that the compound nature of the last SCA would not have been noticed.

Of the other cases illustrated all are simple SCAs. Figure 2(b) shows a fairly small SCA and Fig. 2(e) one of the smallest detectable. Figure 2(d) shows the reception of an intense burst of solar noise just after the start of the SCA with smaller bursts at other times.

Figure 2(c) is taken from the record shown in Fig. 1 and shows the most intense

VOL. 5 1954

SCA recorded during more than two years' operation. It corresponded to an increase in absorption of over 7 decibels at 18·3 Mc/s during a single passage through the ionosphere at vertical incidence. It was recorded as a complete fadeout on communications circuits and also by the Canberra ionosphere recorder; the cosmic noise record is the only one that gives a continuous record of the absorption variations.

It is of interest first to compare the data concerning the occurrence of solar flares and of SCAs; later the statistics of the SCAs themselves will be considered and comparisons made with other methods of observing SIDs.

2.1. *SCAs and solar flares*

During the year July 1950 to June 1951 inclusive, 176 SCAs were recorded and for the same period the *Quarterly Bulletin on Solar Activity* reported 171 flares during daylight hours at Hornsby. The observations of flares and SCAs are summarized in Table 1. In considering Table 1 it should be remembered that the

Table 1. *Observations of solar flares and SCAs*

Of 171 flares observed during the period,
- 49 coincided with SCAs,
- 42 occurred at times for which there were no cosmic noise records,
- 43 occurred during the presence of interference (31 occasions) or of strong solar noise (12 occasions),
- 37 were not accompanied by SCAs, although there was little or no interference.

Of 176 SCAs observed during the period,
- 49 coincided with solar flares,
- 89 occurred at times when there were no solar observations,
- 38 occurred when the sun was under observation but no flares were reported.

equipment was not used primarily for observing SCAs, so that many may not have been detected while the equipment was being used for special purposes. For example on 12 occasions when flares were observed, the aerial was directed towards the sun during severe solar noise storms. The received noise intensity was fluctuating violently and only a very large SCA would have been detected. Also no great precautions were taken to avoid interference from radio stations or atmospherics. Large SCAs can still be detected even during fairly heavy interference. If equipment to suppress interference, such as suggested by LAFFINEUR and KOURGANOFF (1950), had been used, the 31 occasions on which flares but no SCAs were observed due to interference would, no doubt, have been much reduced in number. Even with the simple observing technique used, station interference and atmospherics were responsible for reducing the sensitivity on less than one quarter of the occasions on which flares were observed; on the other hand the sun was not watched, according to the diagrams in the *Quarterly Bulletins*, on one half the occasions on which SCAs were recorded.

On all of the 37 occasions on which a flare was reported but no SCA, conditions being generally favourable, the flare was of Class 1 and of comparatively short duration. Some of these occurred within an hour of sunrise or of sunset and also on some occasions slight interference may have masked a small SCA which would

otherwise have been observed. On the other hand some of the 38 SCAs recorded when no flare was reported, although the sun was listed as being under visual observation, were very large and in fact included the second largest recorded. As suggested by BRACEWELL and STRAKER (1949) it is probable that on at least some of these occasions the solar observations were intermittent, or confined to one portion of the sun's disk.

The relation between the importance of a flare and the maximum absorption during the associated SCA on the occasions when both were recorded is indicated in Fig. 3. In this figure each strip represents one of 44 SCAs, arranged in order of maximum absorption, the importance of the solar flare being indicated by

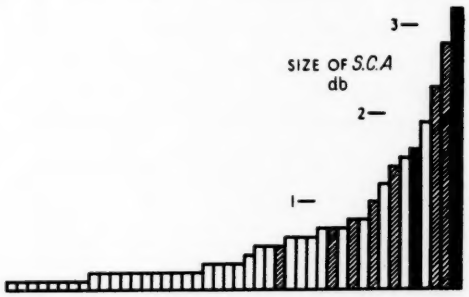

Fig. 3. Illustrating the relation between the size of SCAs and the importance of the associated solar flare. Vertical strips represent SCAs arranged in order of size. If the associated flare was of Class 1 the strip has been left white. For flares of Classes 2 and 3 the strips are shaded and black respectively.

shading. It is seen that the flares classed 2 or 3 are clearly associated with the larger SCAs. Examination of Fig. 3 shows that if the classification of the flares had been carried out on the basis of the maximum absorption during the associated SCA, taking the boundaries between classes at 0·6 db and 2 db, then 80 per cent, 60 per cent, and 50 per cent of the flares classed 1, 2, or 3 respectively on the basis of optical observations would have been placed in the same class.

It has been reported by MCINTOSH (1951) and by ELLISON (1950) that communications fadeouts commence on the average some five minutes after the start of the associated flare, whereas observations of SPAs indicate that a flare has an effect on the ionosphere almost as soon as it becomes visible in the spectrohelioscope. In the course of the present work, times of start were recorded with an accuracy of about ± 2 minutes for practically all SCAs. However, of the 49 occasions on which an associated flare was reported, on only 18 of these were definite times of start given. From these 18 occurrences the delay between the times of start of the flare and of the SCA was found to be 1 ± 1 minute, which for the small number of occurrences is not significantly different from zero. Presumably the higher values of this delay previously reported for communications fadeouts are due to the fact that under those operating conditions ionospheric absorption must increase considerably at the start of an SID before its effect is noted, whereas with the present technique very small changes can be detected.

VOL. 5 1954

2.2. *Characteristics of SCAs*

For each SCA the following data were recorded: time of start; time of maximum absorption; the size, being the maximum absorption in decibels; and the time at which the cosmic noise intensity had apparently returned to normal. The times of start and of maximum absorption could be estimated to within one or two minutes, but the accuracy of the times of ending was much less, since towards the end of an SCA the rate of change of absorption is very slow so that the end of

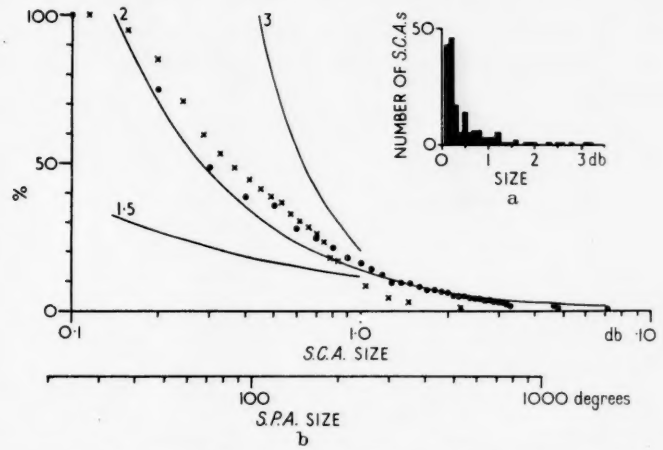

Fig. 4. (a) (Inset) The frequency distribution of SCAs of different sizes. (b) The cumulative frequency distribution for SCAs and SPAs. Each full circle represents the percentage of the total number of SCAs observed which had the appropriate size or greater. The crosses give similar figures for SPAs. The curves are possible empirical distributions as explained in the text.

an SCA is ill-defined. The time of finish was defined as the time at which the absorption had fallen to 10 per cent of its maximum value. This time was generally estimated directly from the appearance of the record; a more accurate estimate could be obtained by detailed comparison of the record on which the SCA occurred with records on neighbouring days. Maximum absorption was calculated by taking the ratio in decibels of the received power at the time of maximum absorption to the power that would have been received in the absence of the SCA. It may be remarked that the absorption as measured corresponds to a single passage of the radiation through the absorbing region, and that the absorption at other frequencies not too close to the gyro-frequency should be inversely proportional to the square of the frequency. In some cases the aerial was not directed to the zenith and the observed absorption was multiplied by the cosine of the zenith angle of the direction of maximum sensitivity of the aerial beam to obtain an estimate of the absorption that would have been observed at vertical incidence. The zenith angle of the aerial beam was generally less than 20° although occasionally it was 40°, so the correction applied was never large.

Figure 4(a) shows a histogram of the frequency of occurrence of SCAs of various sizes and Fig. 4(b) shows (full circles) the cumulative frequency distribution—the percentage of the total number of SCAs having a given size or greater.

The mode of the distribution in Fig. 4(a) is at 0·2 db, SCAs of size 0·1 db being less frequent. This suggests that 0·2 db was the size of the smallest SCA which could be readily detected under average conditions, smaller SCAs being detected only under more favourable circumstances.

The curves drawn in Fig. 4(b) represent the cumulative frequency distribution to be expected if the number, $n\,dS$, of SCAs in a small range, ds, of sizes were related to the size, S, by a relation of the form

$$n\,dS = kS^{-p}\,dS$$

k being a constant and the numbers on the curves corresponding to different values of p. It is seen that the experimental points are fitted well for a value of p close to 2. That is

$$n\,dS \doteqdot kS^{-2}\,dS.$$

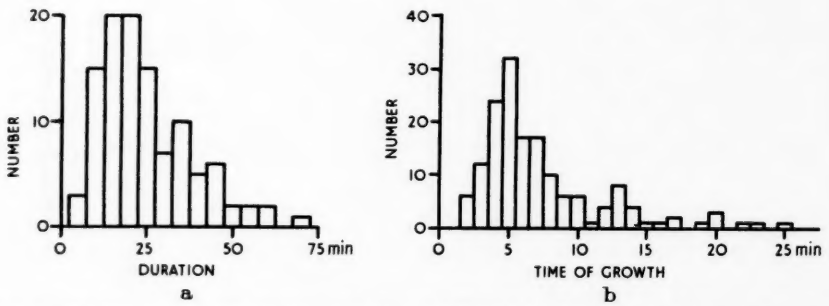

Fig. 5. The frequency distribution of SCAs of different (a) durations, (b) times of growth.

Figure 5 shows histograms of (a) duration and (b) time of growth. These have been compared with similar histograms given by BRACEWELL and STRAKER for SPAs. In each case the general form of the histograms is the same; the median and quartiles for each of the two cases are given in Table 2. It is seen that both

Table 2

		Median	*Quartiles*
Time of growth	SCA	5 min.	4, 9 min.
	SPA	7½	5½, 10½
Duration	SCA	21	15, 34
	SPA	33	26, 48

for duration and for time of growth the relative spread of the values, as indicated by the range of the quartiles, is nearly the same. The times for SCAs are in each case shorter than the times for SPAs but the differences are not great. Part, at least, of the difference in duration of SCAs and SPAs may be due to a possible underestimate of the durations of some SCAs, although this should not affect

VOL. 5 1954

the time of growth. Figure 6 is a scatter diagram of duration against the size of the SCAs. As might be expected, the larger SCAs tend to have longer durations; there are few large SCAs of short duration.

It has been reported previously (McIntosh, 1951) that communications fadeouts occur more frequently in the morning than in the afternoon. A similar result was found for the present observations of SCAs. This, however, is almost certainly an instrumental effect, due to atmospheric interference. The ratio of the number of SCAs in the morning to the number in the afternoon was greatest in summer, when atmospherics were often strong during the later hours of the day, and reduced to unity in winter. It is probable that the excess of morning

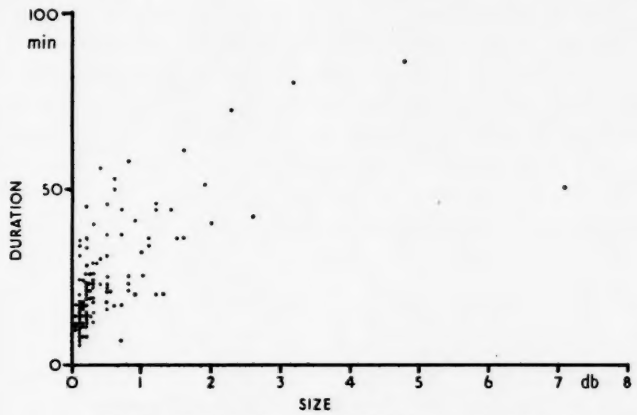

Fig. 6. Scatter diagram of SCA duration against size.

over afternoon communications fadeouts is similarly affected by the observational conditions (for example, the variation of maximum usable frequencies during the day) and it is considered that at present there is no certain evidence for a real forenoon bias in the occurrence of SIDs.

2.3. *Relationship between the sizes of SCAs and SPAs*

There are difficulties in observing SPAs in Australia and a detailed comparison of individual SCAs and SPAs was not possible. However some idea of the relationship between the sizes of SCAs and SPAs may be obtained by comparing the observations of SCAs (made in Australia during 1950–51) with Bracewell and Straker's observations of SPAs (made in England during 1947–48). Even such a rough comparison should be of value in connection with theoretical studies of the *D*-region.

Figure 4 includes (crosses) the cumulative frequency distribution of sizes of SPAs. The (logarithmic) scale of SPA sizes has been shifted so that the distributions of the sizes of SCAs and SPAs fit as closely as possible. It is seen that the distributions fit well over a wide range of sizes with a linear relationship between sizes of SPAs and SCAs, an SCA of size 1 db corresponding to an SPA of size 240 degrees. This relationship may not hold for the larger disturbances.

A relationship between SCA and SPA sizes was also obtained by finding the median sizes corresponding to small ranges of duration of the two phenomena (from Fig. 6 and a similar figure in BRACEWELL and STRAKER'S paper). This suggested that an SCA of size 1 db corresponded to an SPA of size 130 degrees.

Although these estimates must be only rough, it would appear that at present a reasonably good approximation is that an SCA of size 1 db would be associated with an SPA of size 200 degrees.

2.4. *Discussion—(i) Sensitivity of the present technique*

BRACEWELL and STRAKER (1949) have shown that communications fadeouts are not reported unless the corresponding SPA has reached a size of 150 to 200 degrees. Taking a 1 db SCA as corresponding to a 200-degree SPA, this implies that communications fadeouts cannot be recognized unless the ionospheric absorption has increased to such an extent as to produce an SCA of size 0·75 db to 1 db. The threshold for SPAs is much smaller, 40 degrees, corresponding to an SCA of 0·2 db. Since the threshold for the detection of SCAs with the Hornsby equipment is also 0·2 db it appears that the present method of detecting SIDs is as sensitive as the observation of very long wave phase anomalies. It has the great advantage over the latter method of not requiring nearby high-powered very long wave transmitters which are few and far between.

VOL. 5 1954

(*ii*) *The relationship between the sizes of SCAs and SPAs*

It has been shown (BERKNER and WELLS, 1937) that during an SID the *E*- and *F*-regions of the ionosphere are practically unaffected by the additional ionizing radiation, but a great change occurs in the *D*-region. Although the cosmic noise radiation passes completely through the ionosphere and normally suffers attenuation in both the *D*- and *F*-regions (MITRA and SHAIN, 1953), it is reasonable to assume that the extra absorption revealed as an SCA also occurs in the *D*-region. It is of interest to see how the present information concerning the relative sizes of SCAs and SPAs agrees with certain theories of the formation of the *D*-region.

BRACEWELL (1952) has shown that for a simple Chapman region, a large SPA, involving a fall of the 16 kc/s reflecting level by two scale heights from a height initially two scale heights below the level of maximum ionization, could be explained only if the intensity of the incident solar radiation increased by a factor of the order 10^{20}. This would lead to an increase in the maximum ionization density and in the absorption of radiation passing through the region by a factor of the order 10^{10}. To obviate the need for such prohibitively large increases in ionization density, and hence absorption, BRACEWELL abandoned the assumption, implicit in the Chapman theory, that the number of electrons is a small fraction of the number of ionizable particles, and he considered the case of "exhaustion regions," the limiting case being that in which all the ionizable particles are ionized down to a certain level, below which there is practically no ionization. He found that an SPA of the size considered above could be produced by only moderate increases (about 15 times) in the intensity of the solar ionizing radiation. However, it may be shown from Section 2.3 of BRACEWELL'S paper that in these circumstances the increase in absorption during the SCA corresponding to an SPA

is too small to account for the relationship between the sizes of SCAs and SPAs found above unless the maximum electron density of the region was very high (of the order of 10^9 per cc for only a moderately large SID) in the undisturbed condition before the SPA commenced. That is, although BRACEWELL found that SPAs could be produced in a simple Chapman region only with very great difficulty, in his "exhaustion region" SPAs can be produced too easily.

Further theoretical work concerning the formation of the region causing SIDs is necessary, but it is apparent that the detailed comparison, during particular SIDs, of the variations in apparent height of reflection of long waves and the variations in total absorption, by observation of the accompanying SCAs, should be of great value in checking possible theories.

3. Increased Absorption after Certain Solar Flares

In the course of the analysis of the cosmic noise records, it became apparent that at certain times ionospheric absorption was considerably higher than the average values for the same periods on neighbouring days. Absorption depends markedly on the critical frequency of the F_2 region, f_0F_2, which varies considerably from day to day, but on these occasions f_0F_2 was not exceptionally high, nor was there evidence of increased absorption due to SCAs. It was thought that these periods of increased absorption might be delayed effects of solar flares. An attempt was made to study this effect statistically by the superposed epoch method taking as the zero time the times of start of Class 2 flares (there was none of Class 3) which occurred in the months for which the records had previously been analyzed for absorption, namely July, September, November, and December 1950. However, owing to gaps in the records and the comparatively large number of flares no clear evidence for a delayed absorption effect could be found, although there was some indication of such an effect. It was therefore decided to study in detail the absorption after those major flares (Class 3) for which records were available on several days before and after the days on which the flares occurred. Three cases were available for study and the particulars of the flares are given in Table 3.

Table 3

Time of start of flare (U.T.)	*Distance from central meridian*	*Class*	*Observatory*
1950 August 4 2254	3° W	3	Mt. Wilson
1951 February 19 1401	79° E	3	Edinburgh
March 24 1135	18° W	3	Edinburgh

In each case absorption was calculated for each hour on several days on either side of the day on which the flare occurred and the average values were found for each hour of the day. Then the variation from the mean was found for each hour from 10 hours before to more than 50 hours after the start of the flare. The values were slightly smoothed by taking three-hourly running means and

the results are shown in Fig. 7 where deviation of absorption from the mean is plotted against time from the start of the flare. Underneath each time scale is indicated the corresponding 150° E time. In the case of the August flare, the flare was accompanied by a large SCA which shows up as the high absorption near hour zero. The other two flares occurred during darkness at Hornsby so that no direct effects are to be expected.

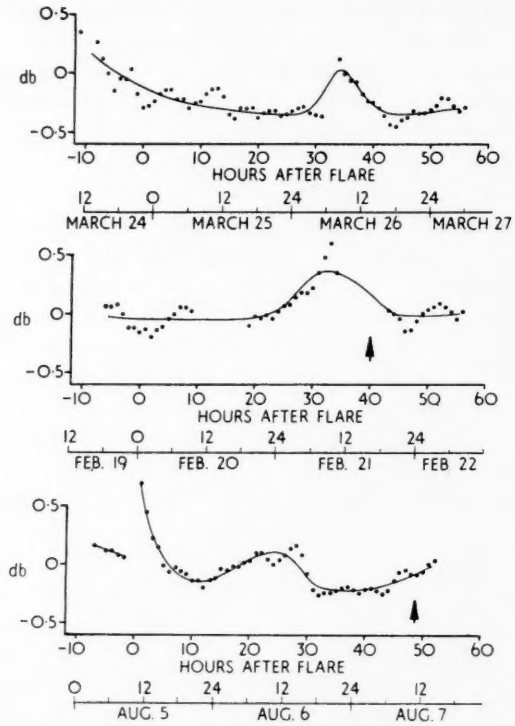

Fig. 7. Three-hourly running means of the deviations of absorption from the average hourly values, plotted against time after a solar flare. Underneath each time scale is given the appropriate 150° E time. In the case of the August and February flares, arrows indicate the earliest time of beginning of magnetic storms after the flare. For the March flare the earliest magnetic storm began 63 hours after the flare.

It will be seen that for each flare there is a pronounced increase in absorption with a maximum between 24 and 36 hours after the flare began. The increase is large, corresponding to nearly one quarter of the normal average maximum absorption at noon. In each case the maximum excess absorption occurs near 0900 150° E time and the increase begins before sunrise.

It was at first thought that the increased absorption might be associated with magnetic storms, which often appear a day or so after important solar flares. However, from the list of storms given in the appropriate issues of the *Journal of Geophysical Research*, it was found that magnetic storms did not begin until some further time had elapsed after the maximum of the absorption increase. The arrows in Fig. 7 under the curves for the August and the February flares

VOL. 5 1954

indicate the earliest report of the beginning of magnetic storms. March 1951 was a generally disturbed month; the earliest storm reported began 63 hours after the flare. In each case the storm began with a "sudden commencement." Examination of the lists of the magnetic K-indices showed that the increased absorption occurred during periods which were relatively quiet compared with neighbouring days. In a further search for any magnetic effect, the hourly values of the magnetic elements H, D, and Z as recorded at Toolangi (latitude 38° S, longitude 146° E) and Watheroo (latitude 30° S, longitude 116° E) were treated in a similar fashion to the absorption measurements. Departures from the means of the hourly values over 7 days were found for the period 10 hours before to over 50 hours after the times of the flares. There was no definite evidence of any characteristic magnetic variation during the absorption increase but the curves suggested that there may have been small (about 10 gammas or less) decreases in H and increases in Z compared with the average values. It is clear that more data are required before any conclusion can be reached concerning possible associated magnetic effects, but it is suggested that in future when storm time variations of the magnetic elements are being examined in detail, the work might well be extended to include data for a day or so *before* as well as *after* the commencement of the magnetic storms.

The origin of the increased absorption is obscure. Detailed examination of the values of f_0F_2 during the periods of interest showed that at least the normal variation of absorption with f_0F_2 discussed by MITRA and SHAIN (1953) could not account for the abnormally high absorption measured. The other parameters of the F-region did not have exceptional values during these times and it is unlikely that the origin of the excess absorption lies in the F-region. A brief examination of the Slough data on D-region absorption at noon, as depicted by LANGE-HESSE (1953) for the period April 1947 to March 1952, suggests that the measured values of the absorption index are not exceptionally high on days following Class 3 flares, at least during summer. During the winter months, the wide variations from day to day would mask an effect of the type under discussion. The fact that the excess absorption is apparent before sunrise suggests that any D-region effect should be readily observed in appropriate pulse reflection experiments.

A further possibility exists, namely that the absorption may be due to attenuation in a cloud of ionized particles outside the earth. Such a cloud, if sufficiently dense, could either cause divergence of the ray paths to the aerial or possibly change by refraction the direction from which the aerial was receiving radiation, so that the aerial might observe a less "noisy" part of the sky than expected. Such refraction would cause an apparent increase in absorption but it is most unlikely to be serious since the increased absorption occurs for periods greater than 12 hours and it would be expected that for some times of the day refraction would increase rather than decrease the aerial noise power. If the hypothetical cloud of corpuscles is coming from the sun and is later responsible for the magnetic storms observed, it is difficult to account for any effect, either by divergence or refraction, before sunrise.

We conclude that present data are insufficient to give any clear indication of

the origin of the excess absorption. The next steps would appear to be the study of more cases both by the cosmic noise and pulse techniques. The combination of the two methods should indicate whether the origin is in the ionosphere or not.

4. CONCLUSION

The results presented in Section 2 show clearly that observations of the changes in the intensity of cosmic noise provide a very sensitive method of detecting and of obtaining detailed information concerning the progress of sudden ionospheric disturbances, and hence of solar flares. Of considerable practical importance is the fact that this method, while one of the most sensitive, is very simple. The operation of several stations well distributed in longitude, which was not readily possible with the very long wave, sudden phase anomaly technique, is quite feasible and would give valuable information both for forecasting magnetic and ionospheric conditions and also for the study of the solar flares themselves. In addition it has been shown that the cosmic noise observations in conjunction with other observations of SIDs should help in the study of the physical conditions in the ionosphere during such disturbances.

The result that increased absorption follows at least some solar flares after an interval of the order of one day, even though the earth's magnetic field is not greatly disturbed, is worth following up since it may throw further light on the magnetic and ionospheric disturbances associated with flares.

VOL.
5
1954

Acknowledgments—The authors are indebted to Mr. C. S. HIGGINS, of the Radiophysics Laboratory, for assistance in making the observations on which this paper is based. They also wish to thank the Chief Geophysicist, Bureau of Mineral Resources, for supplying magnetic data from the Toolangi and Watheroo Magnetic Observatories. During this investigation, A. P. MITRA was the holder of a Fellowship awarded by the Australian Government under the Colombo Plan.

REFERENCES

BERKNER, L. V., and WELLS, H. W.	1937	Terr. Mag. **42,** 301–309
BRACEWELL, R. N.	1952	J. Atmosph. Terr. Phys. **2,** 226–235
BRACEWELL, R. N., and STRAKER, T. W.	1949	Mon. Not. Roy. Astr. Soc. **109,** 28–45
ELLISON, M. A.	1950	Publications of the Royal Observatory, Edinburgh **1,** 53–72
HEY, J. S., PARSONS, S. J., and PHILLIPS, J. W.	1947	Nature **160,** 371
JANSKY, K. G.	1937	Proc. Inst. Radio Engrs. **25,** 1517–1530
LAFFINEUR, M., and KOURGANOFF, V.	1950	Proc. Gen. Assy. U.R.S.I. Zurich, Part 2, 261–265
LANGE-HESSE, G.	1953	J. Atmosph. Terr. Phys. **3,** 153–162
MCINTOSH, D. H.	1951	J. Atmosph. Terr. Phys. **1,** 315–342
MITRA, A. P., and SHAIN, C. A.	1953	J. Atmosph. Terr. Phys. **4,** 204–218

Journal of Atmospheric and Terrestrial Physics, 1954, Vol. 5, pp. 329 to 344. Pergamon Press Ltd., London

Theoretical considerations regarding the dayglow

D. R. Bates and A. Dalgarno
Department of Applied Mathematics, Queen's University of Belfast

(*Received* 30 *May* 1954)

ABSTRACT
The measurements on the dayglow made with rocket borne instruments are discussed critically. It is contended that the reported great altitude and great luminosity of the emissive source cannot be reconciled with the natural supposition that the phenomenon is due to direct photo-action by the incident solar radiation. An attempt is made to predict the main features of the airglow likely to result from resonant and fluorescent scattering, photo-dissociation, photo-ionization, and recombination in the ionized layers.

1. Introduction

Numerous studies have been made of the nocturnal emission from the Earth's upper atmosphere, that is of the *nightglow*, but similar studies of the analogous *dayglow* have until recently been impracticable because of the dominance of Rayleigh scattered light near ground level. The development of the rocket as a research tool has changed the situation, for, though the technical difficulties are formidable, observations can now be made from levels above which Rayleigh scattering is inappreciable. An account of the results obtained so far has just been published by Miley, Cullington, and Bedinger (1953). After considering the problem of interpreting these we shall make an attempt at predicting the general features of the dayglow.

2. Discussion of Observational Data

2.1. Miley *et al.* (1953) report that the intensity of the light recorded by photometers mounted on rockets falls off with altitude until the 30 km level is passed but that between the 40 km level and the 135 km level (which is the highest attained) it remains essentially *constant*. They attribute the initial decrease to the diminution of the contribution from Rayleigh scattering and deduce that the measurements made at altitudes above 40 km refer to the true dayglow, the source of which they place at an altitude of more than 135 km to explain the observed constancy. Perhaps the most remarkable conclusion reached is that concerning the absolute intensity. The spectral region from λ 6360 to λ 4260 was surveyed by means of eight interference filters. No great variation with wave length was found and according to Miley *et al.* the energy flux in the various 20 Å bands sampled is of order 0·5 microwatts/cm^2. If this is correct it would appear that the *total* energy flux exceeds 50 microwatts/cm^2 or 3×10^{14} eV/cm^2 sec, and that the photon intensity of the dayglow is more than 10^{14}/cm^2 sec.

2.2. Consider now the incident solar radiation. Table 1 gives information on the photon intensities in some wave length ranges of interest. The first five entries are based on the work of Pettit (1940), the next four and the last four are based on the rocket measurements described in the reviews by Newell (1953) and Tousey (1953); the remaining entries (in brackets) are based on the assumption

Table 1. *Incident solar radiation*

Wave length range (Å)	*Photon intensity* (/cm² sec)	
7000–6000	6×10^{16}	
6000–5000	6×10^{16}	
5000–4000	4×10^{16}	
4000–3500	1×10^{16}	
3500–3000	6×10^{15}	
3000–2800	2×10^{15}	
2800–2600	6×10^{14}	
2600–2400	2×10^{14}	
2400–2200	1×10^{14}	
	$\theta = 5000°K$	$\theta = 4500°K$
2200–2000	(5×10^{13})	(1×10^{13})
2000–1800	(2×10^{13})	(3×10^{12})
1800–1600	(5×10^{12})	(8×10^{11})
1650–1425	2×10^{11}	
1340–1230	1×10^{10}	
1230–1040*	2×10^{10}	
1050– 910	10^{11} to 10^{12}	

* Includes Ly(α), λ 1216.

Table 2. *Properties of some molecular electronic transitions*

Molecule	*Transition* (→ allowed, ↛ forbidden)		*Wavelength at absorption threshold* (Å)	*Spectral region of main emission*
O_2	$X\ ^3\Sigma_g^- \nrightarrow a\ ^1\Delta_g$	infra-red atmospheric	12690	infra-red
	$\nrightarrow b\ ^1\Sigma_g^+$	red atmospheric	7620	visible and infra-red
	$\nrightarrow A\ ^3\Delta_u$	*	~3000	visible and ultra-violet
	$\nrightarrow A\ ^3\Sigma_u^+$	HERZBERG	2860	visible and ultra-violet
	$\nrightarrow c\ ^1\Sigma_u^-$	*	2760	visible and ultra-violet
	$\rightarrow B\ ^3\Sigma_u$	SCHUMANN-RUNGE	2030	visible and ultra-violet
N_2	$X\ ^1\Sigma_g^+ \nrightarrow A\ ^3\Sigma_u^+$	VEGARD-KAPLAN	2010	visible and ultra-violet
NO	$X\ ^2\Pi \rightarrow A\ ^2\Sigma^+$	γ	2260	ultra-violet
	$\rightarrow B\ ^2\Pi$	β	2200	visible and ultra-violet
	$\rightarrow C\ ^2\Sigma^+$	δ	1910	ultra-violet
	$\rightarrow D\ ^2\Sigma^+$	ε	1880	ultra-violet
CO	$X\ ^1\Sigma^+ \nrightarrow a\ ^3\Pi$	CAMERON	2060	ultra-violet
OH	$X\ ^2\Pi \rightarrow A\ ^2\Sigma^+$	resonance	3090	ultra-violet
O_2^+	$X\ ^2\Pi_g \rightarrow A\ ^2\Pi_u$	2nd negative	2620	ultra-violet
N_2^+	$X\ ^2\Sigma_g^+ \rightarrow A\ ^2\Pi_u$	MEINEL	11130	infra-red
	$\rightarrow B\ ^2\Sigma_u^+$	1st negative	3910	visible

* The $^3\Delta_u$ and $^1\Sigma_u^-$ terms are those discussed theoretically by MOFFETT (1951) and studied experimentally by HERZBERG (1953).

VOL. 5 1954

that the effective temperature of the Sun between λ 2200 and λ 1600 is either 5000°K or 4500°K* (cf. NICOLET, 1945; GREENSTEIN, 1949).

Even allowing for improbably large errors in the values cited it is apparent that if the photon intensity of the dayglow is indeed in excess of 10^{14}/cm^2 sec then the solar radiation responsible would have to be either that in the unexplored region to the short wave length side of λ 910 or that in the region to the long wave length side of λ 1800. For convenience we shall designate these regions as A and B respectively. It may be remarked that the photon energies in the first are more than 13·6 eV and those in the second are less than 6·9 eV.

Though the photon intensity in region A has not been determined directly some information on it is available from the radio studies of the *E*- and *F*-layers. The value even at the maximum of the sunspot cycle is usually given to be only 10^{10}/cm^2 sec. This may be an underestimate (BATES, 1951) but there is little doubt that the true value is also quite insufficient: thus confining our attention to the wave length ranges in which the radiation suffers considerable attenuation before the 135 km level is reached, we readily see that the photon intensity in these cannot be as much as 10^{12}/cm^2 sec, for if it were the rate of production of O^+ ions at the level where the number intensity $n(O)$ is 10^9/cm^3 would be at least some 10^3/cm^3 sec, which is an unacceptably high rate for such a slowly recombining species.

Region B requires closer scrutiny but is also most unpromising, it being difficult to see how a strong emission, mainly from above an altitude of 135 km, could arise since the atmosphere is extremely transparent to the radiation concerned, most of which actually penetrates to below the 50 km level (cf. VASSY and VASSY, 1942; HOPFIELD, 1946; TOUSEY, WATANABE, and PURCELL, 1951).

Chemical processes cannot be the source sought since even if sufficient energy could be absorbed in photo-dissociation continua (and this does not seem possible), its liberation would require the association of *major* constituents through two-body radiative collisions or through three-body collisions leading to excitation, both of which proceed so slowly that any emission originating from the high altitude region under discussion would persist long after sunset.

Resonant or fluorescent scattering might appear a rather more attractive possibility. Except in the case of a constituent forming a suitably localized layer it is open to the objection that owing to absorption in the wings the emission would in general continue to occur deep in the atmosphere so that the luminosity observed from the 40 km level would be greater than that observed from the 135 km level. However, it might be argued that the unwanted part of the emission is suppressed by deactivating collisions; and though this argument is most implausible (as may be seen by following it through in detail) we judge it best not to regard the objection mentioned as final and shall examine other aspects of resonance and fluorescence.

To make the position clear we have listed in Table 2 the electronic transitions of the normal diatomic molecules† present which in absorption have a threshold to

* These are the effective temperatures just beyond the long and short wave length limits of the region. Within the region 5000°K is therefore likely to be an overestimate and 4500°K an underestimate.

† Polyatomic molecules may be neglected since apart from other considerations they are concentrated at relatively low altitudes (cf. BATES and WITHERSPOON, 1952). Free atoms may easily be shown to provide much too feeble a source in the atmospheric region above the 135 km level. The total contribution from them is discussed in the next section.

the long wave length side of λ 1800 and have indicated the significant characteristics of each. A striking feature is that the ensuing emissions are mainly outside the spectral range λ 6360–4260 studied by Miley *et al.*, some being in the infra-red but most in the ultra-violet. Moreover, the majority of the transitions which result in emissions in the visible are forbidden and therefore utterly unimportant in the present connection. As an illustration of this let us consider the red atmospheric system of O_2 which is favoured compared with the others by having a very low excitation energy. Though the (0, 0) band lies at λ 7596 we will treat it as it is the strongest member. Noting that the associated Einstein coefficient, $\mathscr{A}$ ((0), $b\,{}^1\Sigma_g^+ - (0), X\,{}^3\Sigma_g^-$; O_2), is about 0·16/sec (Childs and Mecke, 1931; Van de Hulst, 1945) and neglecting the effect of Fraunhofer lines we find from the standard resonance scattering formula (see appendix) that the photon emission rate per illuminated molecule

$$\pi((0), b\,{}^1\Sigma_g^+ - (0), X\,{}^3\Sigma_g^-;\ O_2) \leqslant 1{\cdot}4 \times 10^{-8}/\text{sec}. \qquad (1)^*$$

As an upper limit the number of O_2 molecules above the 135 km level, $\mathscr{N}(O_2 \mid 135$ km), may be taken to be $10^{16}/\text{cm}^2$ column† (cf. Nicolet and Mange, 1954). We hence have that the photon intensity coming from above this level

$$\Pi((0), b\,{}^1\Sigma_g^+ - (0), X\,{}^3\Sigma_g^-;\ O_2 \mid 135\text{ km}) \leqslant \sim 10^8/\text{cm}^2\text{ sec}. \qquad (2)$$

It is manifest without detailed calculations that the other forbidden systems cannot be invoked to explain the observations of Miley *et al.*; thus the oxygen systems extract only a minute fraction of the incident radiation even in equivalent air path of some 10^4 atoms-cm. (Herzberg, 1952, 1953); and the nitrogen system has never yet been detected in absorption.

Two of the allowed systems which fluoresce in the visible, the β system of NO and the first negative system of N_2^+, belong to rare constituents and can also be dismissed with assurance.

Migeotte and Nevin (1952) have shown that the abundance of nitric oxide molecules in the atmosphere does not exceed $5 \times 10^{17}/\text{cm}^2$ column, and there is no doubt that $\mathscr{N}$(NO | 135 km) is many orders of magnitude smaller (cf. Bates, 1952a). From the absorption coefficients given by Watanabe, Zelikoff, and Inn (1953) and the formulae in the appendix we hence obtain that the photon intensity

$$\Pi(B\,{}^2\Pi - X\,{}^2\Pi;\ \text{NO} \mid 135\text{ km}) \ll 10^{11}/\text{cm}^2\text{ sec}. \qquad (3)$$

At the time of the airglow observations the number of ions of all types in the F-layers cannot have been more than about $10^{13}/\text{cm}^2$ column. Of these probably only a small fraction can have been N_2^+ ions, for according to the laboratory measurements of Biondi and Brown (1949) and of Faire, Fundingsland; and Aden (1954) the rate coefficient of the dissociative recombination process

$$N_2^+ + e \rightarrow N' + N'' \qquad (4)$$

is far greater than the effective recombination coefficient found in the layers by

* Here and throughout the paper the insertion of the $\leqslant$ sign without comment signifies that deactivation has been ignored but may be appreciable.

† Allowance is made here for departure from local photo-chemical equilibrium.

VOL. 5 1954

the radio workers. Accepting this and revising some earlier calculations on scattering in the first negative system (BATES, 1949) by replacing the original estimate of the Einstein coefficient by the later value given by SHULL (1951) we find

$$\Pi(B\,^2\Sigma_u^+ - X\,^2\Sigma_g^+;\ N_2^+ \mid 135\text{ km}) \ll 10^{13}/\text{cm}^2\text{ sec.} \qquad (5)$$

It may be remarked incidentally that there are few other scattering processes involving visible radiation which might be very much more effective during the day than during the twilight period.

The only other allowed system which need be discussed is that of SCHUMANN-RUNGE. In spite of the fact that it belongs to a major atmospheric constituent it also provides too feeble a source in the region above the 135 km level, the reasons being that the excitation energy is high and that the relevant Franck-Condon factors are very small. Taking $\mathcal{N}(O_2 \mid 135\text{ km})$ to be at most about $10^{16}/\text{cm}^2$ column, as before, and using the measured absorption coefficients (WATANABE *et al.*, 1953) we obtain

$$\Pi(B\,^3\Sigma_u^- - X\,^3\Sigma_g^-;\ O_2 \mid 135\text{ km}) < \sim 10^8/\text{cm}^2\text{ sec.} \qquad (6)$$

which is extremely low.

In our discussion of resonant and fluorescent scattering we have so far confined our attention to *normal* molecules. It might, however, be suggested that scattering by *excited* molecules produces the main luminosity.

Against electronic excitation being important in this connection it may be urged that if the terms concerned were populated by direct photo-action or by collisions with fast photo-electrons* the mechanism would be a *double* one; and hence the *square* of the solar dilution factor, that is of the very small number $5{\cdot}44 \times 10^{-6}$, would appear in the external factor of the formula for the intensity. The conclusion indicated by this potent general argument is strongly supported by investigations which were carried out on what seem the more favourable cases. Details of these need not be presented.

In many instances vibrational excitation would lead to a marked increase of the scattering owing to the entry of very much larger Franck-Condon factors. However, it seems improbable that the effect can account for the intensity reported. The SCHUMANN-RUNGE system is the one likely to be most enhanced but it would still be too weak even if 10% of the oxygen molecules above the 135 km level had vibrational energy of as much as 2 eV. Little plausibility can be attached to such a high degree of excitation.

The survey we have made clearly suggests that the tenuous air at altitudes greater than 135 km cannot extract enough energy from the incoming solar radiation to supply a source having a photon intensity of some $10^{14}/\text{cm}^2$ sec. There is, moreover, evidence that it does not do so, for reference to Table 1 shows that if it did many strong telluric lines would be formed, whereas the solar spectrum is in fact remarkably free from such lines; thus CLEARMAN (1953) and BABCOCK, MOORE, and COFFEEN (1948) find none in the ranges λ 2285–3000 and λ 2935–3060 respectively; and in their standard compilation ST. JOHN *et al.* (1928) list none

* Chemical processes cannot be invoked without difficulties arising in connection with the nightglow.

until λ 5400 is reached* (when members of the O_2, $X\,^3\Sigma_g^- - b\,^1\Sigma_g^+$ system naturally begin to appear due to absorption *low* in the atmosphere).

3. THEORY

As we have seen there are cogent reasons for believing that the results of MILEY *et al.* cannot be understood in terms of direct photo action.† The anomalies revealed are indeed sufficiently grave to justify a repetition of the rocket measurements. Though it is conceivable that the dayglow is a manifestation of some quite unexpected phenomenon (such as that the electron temperature in the F-layers is very high) we do not think that an exploration of purely speculative hypotheses would be justified at the present stage. Instead of pursuing such an exploration we shall discuss the emission to be expected from processes known to be operative‡ supposing the solar emission is as indicated in Table 2 and (unless otherwise stated) that Fraunhofer lines are absent. We shall use the adjective *feeble* to describe any spectral feature having a photon intensity of less than $10^9/\text{cm}^2$ sec.

3.1. *Atomic emissions.*

For convenience we shall consider the various atmospheric constituents separately.

3.1.1. *Oxygen.* The excitation of the forbidden red and green lines§ through

$$O\,(^3P) + h\nu \rightarrow O\,(^1D) \tag{7}$$

and

$$O\,(^3P) + h\nu \rightarrow O\,(^1S) \tag{8}$$

respectively has been considered by many authors in connection with the twilight flash. Cascading effects are of course unimportant. Taking the distribution amongst the levels of the ground term‖ to be that corresponding to a temperature of about 200°K and adopting the $\mathscr{A}$'s given by GARSTANG (1951) we find that the photon emission rates per illuminated atom are

$$\pi(^1D - {}^3P;\ \text{OI} \mid 90\ \text{km}) \leqslant 7{\cdot}4 \times 10^{-10}/\text{sec} \tag{9}$$

and

$$\pi(^1S - {}^1D;\ \text{OI} \mid 90\ \text{km}) \leqslant 3{\cdot}5 \times 10^{-12}/\text{sec} \tag{10}$$

where, as always, the $\leqslant$ sign indicates that account has not been taken of possible deactivation. Since $\mathscr{N}(\text{OI} \mid 90\ \text{km})$ is of order $5 \times 10^{18}/\text{cm}^2$ column¶ the total yields due to resonance and fluorescence are thus

$$\Pi(^1D - {}^3P;\ \text{OI} \mid 90\ \text{km}) \leqslant 4 \times 10^9/\text{cm}^2\ \text{sec}. \tag{11}$$

$$\Pi(^1S - {}^1D;\ \text{OI} \mid 90\ \text{km}) \leqslant 2 \times 10^7/\text{cm}^2\ \text{sec}. \tag{12}$$

* Admittedly this does not mean that there are no weak telluric lines; ST. JOHN *et al.*, for example, do not list the lines of the HUGGINS system of ozone (cf. PETTIT, 1940). It should perhaps be mentioned that BABCOCK (1945) has proposed that certain spectral features should be attributed to the O_2, $X\,^3\Sigma_g^- - A\,^3\Sigma_g^+$ and O_2, $X\,^3\Sigma_g^- - B\,^3\Sigma_u^-$ systems. However, he states that they are of solar origin; and in any event they are very faint.

† [*Note added in proof*] In harmony with our conclusions, Dr. BEDINGER informs us that it now seems possible that the observations refer, not to the true dayglow, but to an extra-terrestrial luminosity, the zodiacal light.

‡ We shall not discuss processes which also contribute to the nightglow.

§ The forbidden ultra-violet line does not require separate treatment since its photon intensity is necessarily about a tenth that of the green line.

‖ The usual procedure is to regard the triplet as degenerate. This introduces slight errors, the derived intensities of the red and green lines being 0·8 and 2·0 times the true intensities.

¶ The abundance of atomic oxygen below the 90 km level is comparatively small.

VOL. 5 1954

As may readily be verified from figures given by BATES and MASSEY (1946), both are greater than the corresponding yields from

$$O^-(^2P) + h\nu \rightarrow O(^1D \text{ or } ^1S) + e. \tag{13}$$

Production of $O(^1D)$ results from the photo-dissociation of molecular oxygen in the SCHUMANN-RUNGE continuum

$$O_2(X\ ^3\Sigma_g^-) + h\nu \rightarrow O(^1D) + O(^3P) \tag{14}$$

which causes the solar radiation in the range λ 1300–1760 to be almost completely absorbed shortly after entering the region where the $n(O_2)/n(O)$ ratio is high. Taking θ, the effective temperature of the Sun, to be 5000°K we obtain

$$\Pi(^1D - {}^3P;\ \text{OI} \mid 90\text{ km}) \leqslant 4 \times 10^{12}/\text{cm}^2\,\text{sec} \tag{15}$$

and taking it to be 4500°K, which is perhaps more realistic, we obtain

$$\Pi(^1D - {}^3P;\ \text{OI} \mid 90\text{ km}) \leqslant 6 \times 10^{11}/\text{cm}^2\,\text{sec}. \tag{16}$$

A further source of $O(^1D)$ is the photo-dissociation of ozone in the HARTLEY continuum

$$O_3 + h\nu \rightarrow O(^1D) + O_2(X\ ^3\Sigma_g^-). \tag{17}$$

Some calculations carried out in another connection (BATES and WITHERSPOON, 1952), but not published in full, indicate the respective total production rates above the 75, 65, 55, and 40 km levels are of order 10^{12}, 10^{13}, 10^{14}, and 10^{15}/cm^2 sec.

Other processes may also give rise to $O(^1D)$ atoms and so may certain recombination processes, but the probable yields are not such as to make it necessary to raise the limits already given.

Consideration must be given to the possible effects of deactivation of $O(^1D)$, the radiative lifetime of which is about 110 sec (GARSTANG, 1951). From the quantal calculations of SEATON (1953a) it may be shown at once that

$$O(^1D) + e \rightarrow O(^3P) + e \tag{18}$$

is of little importance. However, collisions with neutral particles probably cause serious destruction. In particular

$$O(^1D) + O_2(X\ ^3\Sigma_g^-, v = 0) \rightarrow O(^3P_2) + O_2(b\ ^1\Sigma_g^+, v = 2) \tag{19}$$

is in essentially exact energy resonance and may be quite efficient. Even if the associated rate coefficient were but 10^{-15} cm^3/sec there would be a great suppression of the red line: for example, though the emission from near the 90 km level would be reduced by a factor of only about 0·3 the corresponding factors for the emission from near the 75, 65, 55, and 40 km levels would be 5×10^{-2}, 8×10^{-3}, 3×10^{-3}, and 7×10^{-4} respectively (which would nevertheless still leave the line very strong). The coefficient may of course be larger, but bearing in mind that the reverse process

$$O(^3P_2) + O_2(b\ ^1\Sigma_g^+, v = 2) \rightarrow O(^1D) + O_2(X\ ^3\Sigma_g^-, v = 0) \tag{20}$$

also occurs it would seem unlikely that the suppression is very severe in the upper part of the excitation zone. We tentatively suggest then that $\Pi(^1D - {}^3P, \text{OI} \mid z)$,

the photon intensity of the red line viewed from an altitude z, is at least of order $10^{11}/\text{cm}^2$ sec when z is 90 km; that it is considerably lower when z greatly exceeds this; and that it may be about the same or may be much higher when z is less depending on whether the deactivation coefficient is large or is small.

Though the suppression of the red line at moderate altitudes may well be almost complete the excitation energy of the $O(^1D)$ atoms is not necessarily lost to the dayglow, it may merely be transferred* to other constituents which may themselves radiate—process (19), for example, leads to the formation of $O_2(b\,^1\Sigma_g^+, v = 2)$ molecules. In view of the extremely large number of photons absorbed in the Hartley continuum this transference may be of great importance.

Lack of basic laboratory data prevents any reliable estimate of the contribution to the green line from processes other than fluorescent scattering. However, it is worth drawing attention to what is perhaps the most promising source. The absorption spectrum of molecular oxygen shows a number of diffuse features in the region λ 1150–1350 (cf. Watanabe, Zelikoff, and Inn, 1953). Some of these may be true photo-dissociation continua and the remainder are probably bands broadened by pre-dissociation (Price and Collins, 1935). Tanaka (1952) has suggested that $O(^1S)$ atoms are one of the major dissociation products. Should this be the case the green line might appear quite strongly in the dayglow, a photon intensity of the order of $10^{10}/\text{cm}^2$ sec being not impossible (cf. Table 1). Molecular oxygen naturally also absorbs at shorter wave lengths (cf. Weissler and Lee, 1952) and in particular does so in the region near the Lyman limit where the incident solar flux is thought to be high. An even greater photon intensity cannot therefore be excluded. Whichever spectral region is the ultimate source of the energy it is to be expected that the main emission occurs at altitudes not far from 100 km.

VOL. 5 1954

Examination of the processes likely to be operative suggests that the observable allowed lines of atomic oxygen can scarcely be other than feeble (in the sense defined at the beginning of this section). Amongst the factors which militate against their appearance are their high excitation energies and the depopulation of the upper levels concerned by the lines in the vacuum ultra-violet.

Excited ions may be formed through

$$O(^3P) + h\nu(> 16{\cdot}9\text{ eV}) \rightarrow O^+(^2D) + e \qquad (21)$$

and

$$O(^3P) + h\nu(> 18{\cdot}6\text{ eV}) \rightarrow O^+(^2P) + e. \qquad (22)$$

Since $O^+(^2D)$ has an extremely long natural lifetime (Ufford and Gilmour, 1950) and is rapidly deactivated by electron collisions (Seaton, 1953b) emission from it is inappreciable. Suppression of the emission from $O^+(^2P)$ is far from being so effective but in view of the high threshold of (22), and of the fact that there are other much stronger continua in the same spectral region, it is probable that λ 7330, ^2P–^2D, and certain that λ 2470, ^2P–^4S, is feeble.

3.1.2. *Nitrogen.* Dufay (1951) has observed that the forbidden line λ 5199 is emitted during twilight and the early part of the night, its photon intensity decaying slowly from an initial value of the order $10^6/\text{cm}^2$ sec. Since the radiative life in the ^2D term is some 20 hours (Garstang, 1951) and the work of Dufay

* Conversion of electronic into translational energy is not readily accomplished (cf. Massey and Burhop, 1952).

shows that deactivation is not very pronounced it follows that the line is also extremely feeble in the dayglow; and it follows too that so are the other forbidden lines, λ 3466 and λ 10,400, for emission from the ^2P term populates the upper term of λ 5199 with an efficiency of almost unity. These conclusions are consistent with (but much more definite than) those indicated by an examination of the individual processes.

The observable allowed lines are likely to be even weaker than the similar lines of atomic oxygen.

3.1.3. *Sodium and other elements.* Reasonance scattering by free sodium atoms in a layer located in the 70–90 km region (BARBIER, 1948; HUNTEN and SHEPHERD, 1954) causes the *D*-lines to be a prominent feature of the spectrum of the twilight sky, their photon intensity being about 10^{10}/cm^2 sec* (BRICARD and KASTLER, 1944; BARBIER, 1948). This scattering must also occur during the day. It is possible too that the effect might be increased† by the liberation of some of the combined sodium by photo action.

Doubtless the atmosphere contains traces of other elements having low lying levels which can be reached through allowed transitions. Such elements might conceivably contribute to the dayglow in spite of the fact that twilight observations give no indication of their presence. It would, however, be necessary for most of the free atoms concerned to be removed by chemical processes immediately after sunset. Sufficiently rapid removal is scarcely possible except at altitudes below perhaps the 80 km level.

3.2. *Molecular emissions.*

Detailed calculations are scarcely possible at present and we shall confine ourselves to making some general comments. An instructive approach is to consider the fate of the solar radiation in the various spectral regions. Figure 1 shows the penetration-wave length curve deduced by TOUSEY, WATANABE, and PURCELL (1951) and indicates the more important absorption processes. The estimated or measured incident photon intensities have already been given but are also included for ease of reference.

Radiation to the short wave-length side of λ 910 is mainly absorbed well above the 100 km level owing to the great opacity both of atomic oxygen (BATES and SEATON, 1949) and of molecular nitrogen (WEISSLER, LEE, and MOHR, 1952). Most of the absorption is undoubtedly due to the photo-ionization continua. The subsequent recombination probably leads mainly to line emission. However, band emission would ensue if one or more of the primary processes result in the formation of excited ions. In particular

$$N_2(X\,^1\Sigma_g^+) + h\nu\,(> 16{\cdot}7\text{ eV}) \rightarrow N_2^+(A\,^2\Pi_u) + e \qquad (23)$$

and

$$N_2(X\,^1\Sigma_g^+) + h\nu\,(> 18.7\text{ eV}) \rightarrow N_2^+(B\,^2\Sigma_u^+) + e \qquad (24)$$

* It may be mentioned that an elementary calculation shows that the *D*-lines must be at least about a hundred times stronger than any of the other sodium lines.

† With a Fraunhofer central intensity of about 0·05 (SHANE, 1941) the photon yield per sodium atom is approximately 1/sec in the case of an optically thin layer; but if the number of sodium atoms is increased much beyond 10^{11}/cm^2 column the yield falls off owing to reabsorption (BRICARD and KASTLER, 1944) so that the possible day intensification of the *D*-lines is limited.

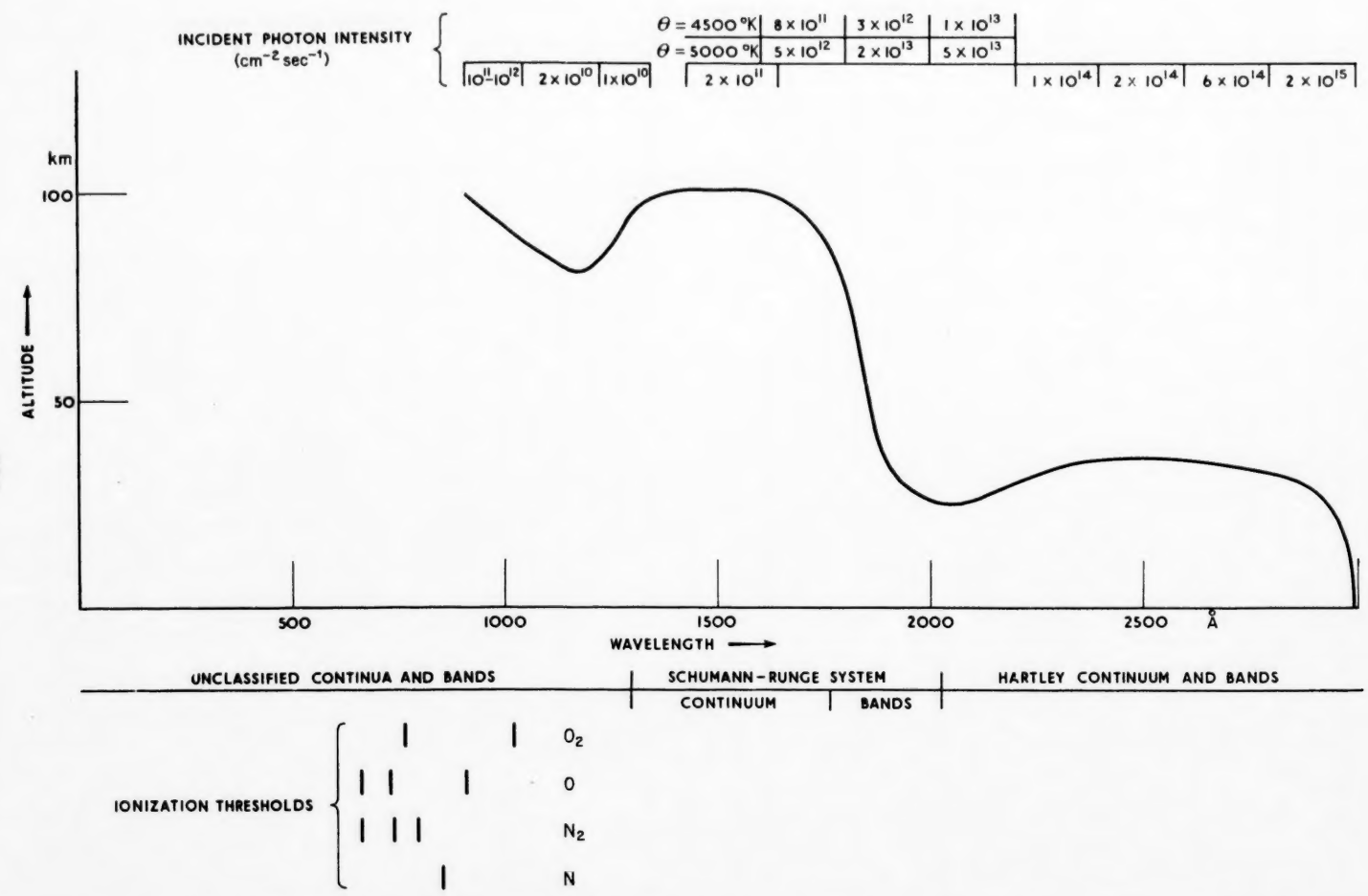

Fig. 1. Altitude for one per cent transmission of the solar radiation plotted against wavelength. The incident photon intensities in various spectral ranges and the main absorption processes are indicated.

are potential sources of the MEINEL and first negative systems respectively.* Unfortunately the solar flux beyond the rather high thresholds involved is unknown so that little can be said about the photon intensities except that they can scarcely, exceed some 10^{10}/cm² sec and may well be much less. Another possibility is that the photo-ionization processes eject electrons with sufficient energy to excite the VEGARD-KAPLAN system by inelastic collisions with nitrogen molecules

$$N_2(X\,^1\Sigma_g^+) + e \rightarrow N_2(A\,^3\Sigma_u^+) + e \qquad (25)$$

but it is unlikely that this gives an appreciable contribution.

Between λ 910 and λ 1300 the atmosphere is comparatively transparent so that the incident radiation penetrates quite deeply. The various transitions concerned in the absorption are as yet far from being fully classified (cf. WEISSLER, LEE, and MOHR, 1952; WEISSLER and LEE, 1952; TANAKA, 1952; WATANABE, ZELIKOFF, and INN, 1953). Some lead merely to ionization or dissociation. Others may lead to fluorescence, but as far as can be judged from the Grotrian diagrams degradation into the visible is unlikely to be important, most of the emission should instead be in the ultra-violet.

The region from λ 1300 to λ 1760 is dominated by the SCHUMANN-RUNGE continuum which has already been discussed in connection with the forbidden red line of atomic oxygen. Beyond this, and extending to about λ 2000, lie the SCHUMANN-RUNGE bands. Near the short wave length limit the solar radiation penetrates to about the 90 km level and near the long wave length limit to about the 40 km level.† As the incident photon intensity in the spectral range concerned is probably at least some 3×10^{12}/cm² sec SCHUMANN-RUNGE fluorescence, which is mainly in the ultra-violet but partly in the visible, must make a significant contribution to the airglow. The magnitude and character of the contribution naturally depends on the observing altitude. Above the 90 km level the emission must be principally in the higher v'-bands and may be influenced by Fraunhofer lines due to molecular oxygen; with decreasing altitude these bands should grow more intense and broader (due to absorption in the wings) and the lower v'-bands should enter to an increasing extent; and from the 40 km level the emission may appear as a continuum.

The major absorption process to the long wave length side of λ 2000 is the photo-dissociation of ozone in the HARTLEY continuum. In addition there are, however, several discrete systems which may give rise to appreciable resonant or fluorescent emission.

Using the measured oscillator strengths associated with the individual bands of O_2, $X\,^3\Sigma_g^- - b\,^1\Sigma_g^+$ (CHILDS and MECKE, 1931; VAN DE HULST, 1945) we find that in the region above 90 km the total rates of entry into the $v' = 0$, 1, 2, and 3 vibrational levels of the upper term are of order 2×10^{11}, 6×10^9, 1×10^8, and 4×10^6/cm² sec respectively; that the corresponding values in the region above 70 km are 4×10^{12}, 2×10^{11}, 3×10^9, and 1×10^8/cm² sec; and that those in the

* As an indication of the intensity distributions in the two systems it may be mentioned that application of the general tables of BATES (1952b) gives the Franck-Condon factors connecting the $v'' = 0$ level of $N_2(X\,^1\Sigma_g^+)$ to the $v' = 0$, 1, 2, 3 levels of N_2^+ $(A\,^2\Pi_u)$ and N_2^+ $(B\,^2\Sigma_u^+)$ to be 0·18, 0·27, 0·25, 0·18, and 0·90, 0·10, 0·00, 0·00 respectively.

† The penetration-wave length curve is of course very irregular; that shown in Fig. 1 has been smoothed.

region above the 50 km level are (5×10^{13}), 2×10^{12}, 4×10^{10}, and 1×10^{9}/cm² sec.* As mentioned earlier, collision process (19) may also contribute to the excitation. The intensity of the red atmospheric system should therefore be very considerable.

Owing to lack of basic data the extent of the scattering in O_2, $X\,^3\Sigma_g^- - A\,^3\Sigma_u^+$ (that is in the HERZBERG system) cannot be estimated. However, it should be noted that though the transition is strongly forbidden its contribution to the airglow is not necessarily negligible. For example, if the oscillator strengths of the stronger absorption bands were even 10^{-10} the total excitation rate above the 50 km level would be about 10^{10}/cm² sec. A considerable fraction of the emission would of course be in the ultra-violet (PILLOW, 1953).

It is known that N_2^+ scatters strongly in the first negative system, $\pi(B\,^2\Sigma_u^+ - X\,^2\Sigma_g^+;\ N_2^+)$, the photon yield per illuminated ion, being as much as 0·4/sec (BATES, 1949; SHULL, 1951); and $\pi(A\,^2\Pi_u - X\,^2\Sigma_g^+;\ N_2^+)$, the corresponding yield for the MEINEL system, may be comparable in magnitude. The total abundance of N_2^+ in the F-layers is uncertain (cf. § 2.2) but may be sufficient to give a photon intensity of some 10^{10}/cm² sec. or even more in either system.

Scattering in OH, $X\,^2\Pi - A\,^2\Sigma^+$ is another possibility. From the oscillator strength measured by DWYER and OLDENBERG (1944) we find that $\pi(X\,^2\Pi - A\,^2\Sigma^+, \mathrm{OH})$ is about 3×10^{-4}/sec, allowance being made for the Fraunhofer lines. According to BATES and NICOLET (1950) hydroxyl is quite abundant near the 65 km level; indeed they tentatively suggest that $\mathcal{N}(\mathrm{OH} \mid 60\ \mathrm{km})$ is of order 10^{14}/cm². If this is correct we see that the photon intensity would be some 3×10^{10}/cm² sec; but of course the uncertainty is considerable. The stronger bands are in the λ 3000–2800 region.

Several other systems, such as NO, $X\,^2\Pi - B\,^2\Pi$ may also contribute. However, their main emission lies in the crowded ultra-violet and they are unlikely to be sufficiently intense to be prominent features.

VOL. 5 1954

Appendix: basic formulae

1. GENERAL REMARKS

Resonant and fluorescent scattering by the Earth's atmosphere are very complicated phenomena but there are two comparatively simple limiting cases of special importance. In one case the absorption process does not cause significant attenuation of the incoming solar radiation because the transition is feeble or the constituent concerned is rare; in the other case, the absorption processes cause almost complete attenuation well into the wings. We shall refer to these as the *small* $\mathcal{N}f$ and *large* $\mathcal{N}f$ cases respectively, $\mathcal{N}$ denoting the number of active atoms or molecules per cm² column and f the oscillator strength associated with the initial transition.

On the linear part of the curve of growth the equivalent width $\Delta\lambda_E$ of an absorption line of wave length λ is given by

$$\Delta\lambda_E = \frac{\pi e^2 \lambda^2 \mathcal{N} f}{mc^2} \tag{1}$$

where e, m, and c are the standard symbols for the fundamental constants (cf. ALLER, 1953).

* Saturation effects (which have been neglected) may cause the bracketed value to be an overestimate.

The Doppler half-intensity width $\Delta\lambda_D$ is given by

$$\Delta\lambda_D = \frac{2\lambda}{c}\left\{\frac{2kT\ln 2}{M}\right\}^{\frac{1}{2}} \tag{2}$$

where k is BOLTZMANN'S constant, T is the temperature, and M is the mass of the atom or molecule (cf. MITCHELL and ZEMANSKY, 1934). Thus $\mathcal{N}f$ can be regarded as small or large according as the parameter

$$q = \left\{\frac{\pi e^2}{2mc(2kT\ln 2)^{\frac{1}{2}}}\right\}\lambda(M/T)^{\frac{1}{2}}\mathcal{N}f \tag{3}$$

is much less or much greater than unity. If λ is measured in Ångstroms, T in degrees Kelvin, and M on the ordinary chemical scale, then

$$q = 1{\cdot}2 \times 10^{-14}\lambda(M/T)^{\frac{1}{2}}\mathcal{N}f \tag{4}$$

This formula is applicable to a single *line* and it is in general necessary to take account of both fine and rotational structure.

2. SMALL $\mathcal{N}f$ CASE

When $\mathcal{N}f$ is small the rate of population of any excited level j may readily be found from considerations of quasi-thermodynamic equilibrium. Denoting the number density of A, the constituent concerned, by $N(A)$, it may be seen that the contribution from direct absorption from lower levels i is $N(A)R(\sum i - j)$ with

$$R(\textstyle\sum i - j) = \left\{\omega_j\Omega Z^{-1}\exp\left(\frac{-\varepsilon_j}{k\theta}\right)\sum_i F_{ij}r_i\mathscr{A}_{ji}\right\} \tag{5}$$

and that from cascading from higher levels k is $N(A)R(\sum k - j)$ with

$$R(\textstyle\sum k - j) = \left\{\sum_k \omega_k Z^{-1}\exp\left(\frac{-\varepsilon_k}{k\theta}\right) r_k\mathscr{A}_{ki}\right\} \tag{6}$$

where the ω's, ε's, and $\mathscr{A}$'s are statistical weights, excitation energies, and Einstein spontaneous emission coefficients, the subscripts designating the levels involved; θ is the effective temperature of the solar radiation, Ω is its dilution, and F_{ij} is the fraction by which its intensity at photon energy $(\varepsilon_j - \varepsilon_i)$ is reduced by the presence of a Fraunhofer line; r is the ratio of the actual value of the population to the value it would have if T were equal to θ; and

$$Z = \sum_{\text{all levels}} \omega\exp\left(\frac{-\varepsilon}{k\theta}\right) \tag{7}$$

The rates of loss due to spontaneous transitions to other levels (including radiationless transitions to an adjacent continuum C) and collisional deactivation are $N_j(A)S(j - \sum i)$ and $N_j(A)s(j - \sum i)$ respectively where $N_j(A)$ is the number density of atoms or molecules in the excited level j and

$$S(j - \textstyle\sum i) = \sum_i \mathscr{A}_{ji} \tag{8}$$

$$s(j - \textstyle\sum i) = \beta_j N(X) \tag{9}$$

β_j being a mean deactivation coefficient and $N(X)$ the total number density of atoms and molecules. In the absence of other excitation processes,

$$N_j(A) = N(A)\left[\frac{R(\sum i - j) + R(\sum k - j)}{S(j - \sum i) + s(j - \sum i)}\right] \tag{10}*$$

* The effects of loss from level j due to absorption, and entry into level j due to deactivation of higher levels, are not included as in general they may be ignored in the atmospheric regions with which we are concerned.

and the N_i's and N_k's (which also appear in (10) through the r's) are determined by similar equations. The set may be solved by standard methods and so the photon emission rate per illuminated atom or molecule at any given altitude

$$\pi(j - i) = N_j(A)\, \mathscr{A}_{ji}/N(A) \tag{11}$$

can in principle be obtained. If $N_j(A)/N(A)$ is constant, the photo emission rate per cm^2 column is then

$$\Pi(j - i) = \mathscr{N}(A)\pi(j - i). \tag{12}$$

The general formula is rather cumbersome but it may often be simplified without introducing any significant error. Usually only the ground term need be taken into account in the $R(\sum i - j)$ summation,* unless there exists a metastable level from which the excited level concerned can be reached through an allowed low energy transition. Cascading can generally be ignored at least when the solar flux is a rapidly decreasing function of the photon energy, though again there are exceptions when the transition probability to the upper of the two levels is much greater than that to the lower level. Deactivation may be neglected except in the case of metastable levels, for which it may cause a considerable reduction in intensity especially in regions where the gas density is high. Very little information is available on the rate coefficients, β, of most interest (cf. MASSEY and BURHOP, 1952) and it is in general necessary to omit $s(j - \sum i)$ from (10) and therefore obtain but an upper limit to the intensity.

The $S(j - \sum i)$ summation introduces no complication into the numerical work. For resonance transitions it consists of but a single member. If there are a number of levels lying below level j, or if there is an adjacent continuum, $S(j - \sum i)$ may be much greater than the dominant $\mathscr{A}_{ji}$ appearing in the numerator of (10) and the intensity may be considerably reduced. This is of particular importance in connection with the excitation of band systems. For the sake of clarity, suppose that the only terms of the band system involved are I the ground term, and J an excited term, that rotational and fine structure may be ignored and that the Einstein coefficient $\mathscr{A}_{ji}$ connecting the vibrational level v_j of J with the vibrational level v_i of I may be taken as $\mathscr{A}_{JI}p(v_j, v_i)$ where $\mathscr{A}_{JI}$ is the coefficient associated with the whole system and $p(v_j, v_i)$ is the Franck-Condon factor† of the band which is of course such that

$$\sum_i p(v_j, v_i) = \sum_j p(v_j, v_i) = 1. \tag{13}$$

Suppose further that all upward transitions originate on the zeroth vibrational level of the ground term and that Fraunhofer lines are absent. In these circumstances the general formula for the photon emission rate in the $(j - i)$ band reduces to

$$\pi(j - i) = N(A)\, \frac{\omega_J}{\omega_I}\, \Omega \exp\left(\frac{\varepsilon_j - \varepsilon_i}{k\theta}\right) \frac{\mathscr{A}^2_{JI}\, p(v_j, 0)\, p(v_j, v_i)}{\mathscr{A}_{JI} + s(j - \sum_i)} \tag{14}$$

If the equilibrium nuclear separations of the two terms differ greatly, $p(v_j, 0)$ is extremely small for the lower v_j values.

Absorption followed by emission tends to disturb the thermal distribution of the population amongst the levels of the ground term. This may be important in high sunlit aurorae (BATES, 1949) but collisions are probably sufficent to maintain a thermal distribution at least at altitudes below about 100 km.

* It should be noted that if this term is a multiplet, its levels must be treated separately. Their relative population may not be simply proportional to their statistical weights at the low temperatures prevailing and the transition probabilities to an upper level may be widely different.

† This factor is the square of the so-called nuclear overlap integral.

VOL. 5 1954

3. Large $\mathcal{N}f$ Case

The absorption cross section at the central wave length λ_0 of a Doppler broadened atomic or molecular line of oscillator strength f_{ij} (cf. Mitchell and Zemansky, 1934) is given by

$$\kappa_{\lambda_0} = \{\pi e^2/mc(2k\pi)^{\frac{1}{2}}\}(M/T)^{\frac{1}{2}}\,\lambda_0 f_{ij} \tag{15}$$

$$= 1{\cdot}2 \times 10^{-14}(M/T)^{\frac{1}{2}}\,\lambda_0 f_{ij}\ \mathrm{cm}^2 \tag{16}$$

the customary units being used. From formula (2), the Doppler half-intensity width is

$$\Delta\lambda_D = \{7{\cdot}2 \times 10^{-7}(T/M)^{\frac{1}{2}}\,\lambda_0\}\,\text{Å} \tag{17}$$

If only natural damping is important the absorption cross section at wave length λ such that

$$|\,\lambda - \lambda_0\,| \gg \Delta\lambda_D \tag{18}$$

is

$$\kappa_\lambda = \kappa_{\lambda_0}\{8\pi c(\pi \ln 2)^{\frac{1}{2}}\}^{-1}\,\frac{\lambda_0{}^2\Delta_D}{(\lambda - \lambda_0)^2}\,S(j - \textstyle\sum i) \tag{19}$$

$$= \{7{\cdot}5 \times 10^{-41}\,\lambda_0{}^4 f_{ij} S(j - \textstyle\sum i)/(\lambda - \lambda_0)^2\}\ \mathrm{cm}^2 \tag{20}$$

This formula is useful in estimating the wave length range over which a line absorbs appreciably in the presence of a competing continuum. In practice account must be taken of rotational and fine structure which increase the effective wave length range. For an isolated line the equivalent width is simply

$$\Delta\lambda_E = \left\{\frac{e^2}{mc^3}\,\mathcal{N}_i f_{ij}\,S(j - \textstyle\sum i)\right\}^{\frac{1}{2}}\,\lambda_0{}^2 \tag{21}$$

$$= \{3{\cdot}1 \times 10^{-20}(\mathcal{N}_i f_{ij} S(j - \textstyle\sum i))^{\frac{1}{2}}\,\lambda_0{}^2\}\,\text{Å} \tag{22}$$

collision broadening being again neglected (cf. Mitchell and Zemansky, 1934). The rate of absorption of photons can thus readily be estimated. In this connection it may be noted that if the Sun is taken as a black body at temperature θ then in the absence of a Fraunhofer line the incident photon flux between λ and $\lambda + d\lambda$ is given by

$$P_\lambda d\lambda = \{4{\cdot}1 \times 10^{30}\,\lambda^{-4} \exp(-x) d\lambda\}\ \mathrm{cm}^{-2}\,\mathrm{sec}^{-1} \tag{23}$$

$$= \{1{\cdot}7 \times 10^{14}\,\varepsilon^4 \exp(-x) d\lambda\}\ \mathrm{cm}^{-2}\,\mathrm{sec}^{-1} \tag{24}$$

where

$$x = 1{\cdot}438 \times 10^8/\lambda\theta = 1{\cdot}161 \times 10^4\,\varepsilon/\theta \tag{25}$$

and ε is the photon energy measured in electron volts.

References

Aller, L. H.	1953	Astrophysics (Ronald, New York)
Babcock, H. D.	1945	Astrophys. J. **102**, 154
Babcock, H. D., Moore, Charlotte E., and Coffeen, Mary F.	1948	Astrophys. J. **107**, 287
Barbier, D.	1948	Ann. de. Geophys. **4**, 193
Bates, D. R.	1949	Proc. Roy. Soc. A. **196**, 562
Bates, D. R.	1951	Proc. Phys. Soc. B. **64**, 805
Bates, D. R.	1952a	Ann. de Geophys. **8**, 194
Bates, D. R.	1952b	Mon. Not. Roy. Astr. Soc. **112**, 614
Bates, D. R., and Massey, H. S. W.	1946	Proc. Roy. Soc. A. **187**, 261
Bates, D. R., and Nicolet, M.	1950	J. Geophys. Res. **55**, 301

Bates, D. R., and Seaton, M. J.	1949	Mon. Not. Roy. Astr. Soc. **109,** 698
Bates, D. R., and Witherspoon, Agnes E.	1952	Mon. Not. Roy. Astr. Soc. **112,** 101
Biondi, M. A., and Brown, S. C.	1949	Phys. Rev. **76,** 1697
Bricard, J., and Kastler, A.	1944	Ann. de Geophys. **1,** 53
Childs, W. H. J., and Mecke, R.	1931	Z. Physik, **68,** 344
Clearman, H. E.	1953	Astrophys. J. **117,** 29
Dufay, M.	1951	Comptes Rendus (Paris) **233,** 419
Dwyer, R. J., and Oldenberg, O.	1944	J. Chem. Phys. **12,** 351
Faire, A. C., Fundingsland, O. T., and Aden, A. L.	1954	Phys. Rev. **93,** 650
Garstang, R. H.	1951	Mon. Not. Roy. Astr. Soc. **111,** 115
Greenstein, J. L.	1949	The Atmospheres of the Earth and Planets (Ed. G. P. Kuiper) (Chicago, University Press)
Herzberg, G.	1952	Canad. J. Phys. **30,** 185
Herzberg, G.	1953	Canad. J. Phys. **31,** 657
Hopfield, J. J.	1946	Astrophys. J. **104,** 208
Hunten, D. M., and Shepherd, G. G.	1954	J. Atmosph. and Terr. Phys. **5,** 57
Massey, H. S. W., and Burhop, E. H. S.	1952	Electronic and Ionic Impact Phenomena (Oxford, Clarendon Press)
Migeotte, M., and Nevin, L.	1952	Mémoires de la Societe Royale des Sciences de Liège, **12,** 165
Miley, H. A., Cullington, E. H., and Bedinger, J. F.	1953	Trans. American Geophys. Union **34,** 680
Mitchell, A. C. G., and Zemansky, M. W.	1934	Resonance Radiation and Excited Atoms (Cambridge, University Press)
Moffitt, W.	1951	Proc. Roy. Soc. A. **210,** 224
Newell, H. E.	1953	High Altitude Rocket Research (New York, Academic Press)
Nicolet, M.	1945	Inst. R. Met. Belgique, Misc. No. 18
Nicolet, M., and Mange, P.	1954	J. Geophys. Res. **59,** 15
Pettit, E.	1940	Astrophys. J. **91,** 159
Pillow, M. E.	1953	Proc. Phys. Soc. A. **66,** 1064
Price, W. C., and Collins, G.	1935	Phys. Rev. **48,** 714
Seaton, M. J.	1953a	Phil. Trans. Roy. Soc. A. **245,** 269
Seaton, M. J.	1953b	Proc. Roy. Soc. A. **218,** 400
Shane, C. D.	1941	Lick Observatory Bulletin **19,** 119
Shull, H.	1951	Astrophys. J. **114,** 546
St. John, C. E., Moore, Charlotte E., Ware, Louise M., Adams, E. F., and Babcock, H. D.	1928	Revision of Rowland's Preliminary Table of Solar Wavelength (Washington, Carnegie Institution)
Tanaka, Y.	1952	J. Chem. Phys. **20,** 1728
Tousey, R.	1953	The Sun (Ed. G. P. Kuiper) (Chicago, University Press)
Tousey, R., Watanabe, K., and Purcell, J. D.	1951	Phys. Rev. **83,** 792
Weissler, G. L., and Lee, Po	1952	J. Opt. Soc. Amer. **42,** 200
Weissler, G. L., Lee, Po, and Mohr, E. I.	1952	J. Opt. Soc. Amer. **42,** 84
Ufford, C. W., and Gilmour, R. M.	1950	Astrophys. J. **111,** 580
Van de Hulst, H. C.	1945	Ann. d'Astrophys. **8,** 12
Vassy, A. and Vassy, É.	1942	Cahiers de Physique **9,** 28

VOL. 5 1954

RESEARCH NOTES

The disappearance of condensation nuclei in a sealed room: Remarks on a paper by Smith and Schilling

(*Received* 29 *July* 1954)

L. G. SMITH and G. F. SCHILLING (1954) examined the variation of the electrical conductivity of the air in a sealed room. They interpreted their results by postulating for the disappearance of the nuclei the relation

$$dZ/dt = -\psi Z^{3/2} \tag{1}$$

We propose to show that over the concentration range involved, the equation

$$dZ/dt = -\gamma Z^2 - \lambda Z \tag{2}$$

gives virtually the same variation of nucleus concentration with time. In equation (2) the γZ^2 term represents loss by coagulation and the λZ term represents loss by diffusion and sedimentation. Equation (1), however, has no physical basis and even if it represents measurements fairly well over a limited range, should be used only with caution.

SMITH and SCHILLING calculated the nucleus concentration from the equilibrium equation $q = \alpha n^2 + bnZ$, using the value $b = 2 \times 10^{-6}$. (SCHWEIDLER'S equation is $q = \alpha n^2 + \beta n$.) Adopting the same value, we calculate from the figures given by SMITH and SCHILLING that $Z = 32{,}000$ initially and that $Z = 350$ after one hundred hours. The concentrations at intervening times, calculated by means of the 3/2 power decay law, are shown in column Z of Table 1. It can be shown that these calculated values fit equation (2) moderately well.

If we integrate equation (2) we obtain

$$\log_e (Z + \lambda/\gamma) - \log_e Z = \lambda t + C \tag{3}$$

If we assume a value of λ/γ we can test relation (3) graphically. By trial the value of λ/γ which gives the closest approach to a linear relation may be found. Table 1 gives the figures for this test with $\lambda/\gamma = 2000$. If the differences of the logs shown in column Δ are plotted against t, the points lie close to a straight line. The slope of this line gives $\lambda = 5{\cdot}12 \times 10^{-6}$ sec^{-1}. Thus $\gamma = \lambda/2000 = 2{\cdot}56 \times 10^{-9}$ cm^3 sec^{-1}.

No great accuracy can be claimed for this method. For example, a test with $\lambda/\gamma = 1800$, giving quite as good agreement with the linear relation, yields $\lambda = 4{\cdot}96 \times 10^{-6}$ and $\gamma = 2{\cdot}76 \times 10^{-9}$.

The value of b assumed (2×10^{-6}) corresponds to nuclei of radius about 3×10^{-6} cm. The value of γ calculated for this radius by applying the STOKES-MILLIKAN and the SMOLUCHOWSKI formulae is $1{\cdot}24 \times 10^{-9}$ (NOLAN and KENNAN, 1949). The large disagreement between the two values of γ can be removed by postulating that the radius is about 2×10^{-6}. The corresponding value of b is $1{\cdot}25 \times 10^{-6}$. If this smaller value of b is applied, the values of Z are increased in the ratio 2/1·25. If λ/γ is increased in the same ratio, the values of Δ are unchanged and we obtain the same value for λ. The value of γ now becomes $1{\cdot}60 \times 10^{-9}$ in rough agreement with the STOKES-MILLIKAN-SMOLUCHOWSKI value $1{\cdot}75 \times 10^{-9}$ for radius 2×10^{-6}.

Table 1

Time hour	Z	$Z + 2000$	$\log_e (Z + 2000)$	$\log_e Z$	Δ
0	32,000	34,000	10·433	10·373	0·060
20	4,350	6,350	8·756	8·378	0·378
40	1,635	3,635	8·198	7·399	0·799
60	850	2,850	7·955	6·745	1·210
80	519	2,519	7·832	6·252	1·580
100	350	2,350	7·762	5·858	1·904

We thus obtain good agreement between the theoretical formulae and the results of SMITH and SCHILLING. In Dublin, room nuclei normally have a radius about 3×10^{-6}, smaller nuclei of radius 2×10^{-6} being observed only in summer. It is possible that in California with a lower relative humidity the nuclei may be smaller than in Dublin (NOLAN and TEDDE, 1950). It is worthy of note that our emendation entails an initial concentration of 51,000.

The value of λ obtained in this way is independent of the value of b selected. The value obtained for a room is unexpectedly large in view of the fact that we have found a value of the same order for a gasometer.

Another method of exhibiting the correspondence between equations (1) and (2) is to calculate from equation (2) the values of Z at various times, using the values $\lambda = 5{\cdot}12 \times 10^{-6}$, $\gamma = 2{\cdot}56 \times 10^{-9}$, and initial concentration 32,000.

Table 2

Hour	*Equation* (1)	*Equation* (2)
0	32,000	32,000
20	4,350	3,730
40	1,635	1,638
60	850	903
80	519	549
100	350	350

A large discrepancy occurs only at 20 hours.

In this discussion we have assumed that the size of the nuclei remains constant during the decay. Undoubtedly growth by coagulation will occur. This involves a variation in b, which is of importance only in the initial stages of the decay when Z is large.

PATRICK J. NOLAN

University College, Dublin

REFERENCES

NOLAN, P. J., and KENNAN, E. L. (1949) *Proc. Roy. Irish Acad.* **52,** 171
NOLAN, P. J., and TEDDE, P. G. (1950) *Arch. Met. Geoph. Biokl.* A2, 374
SMITH, L. G., and SCHILLING, G. F. (1954) *J. Atmosph. Terr. Phys.* **4,** 314

VOL. 5 1954

Note on the seasonal variation of sodium *D*-line emission in twilight

(*Received* 29 *July* 1954)

A pronounced annual variation of the atmospheric sodium *D*-line radiation from the night sky was first demonstrated by the spectrographic observations (1940-44) of DUFAY and TCHENG MAO-LIN (1946, 1947), and more recently confirmed by the photo-electric records obtained during 1948-51 by ROACH, BARBIER, and PETTIT (1950, 1951). In the northern hemisphere it is characterized by a minimum intensity in June–July, and a maximum in November–December with a three- to five-fold increase of intensity.

In the southern hemisphere BRICARD and KASTLER (1944, 1950) find a similar variation of the twilight radiation, maximum emission occurring in the winter months with a minimum in summer. The same investigators find from observations in the south of France that the enhanced twilight emission has a seasonal fluctuation in phase with that of the nocturnal *D*-line radiation.

Some photoelectric measurements of unpolarized sodium *D*-emission from zenithal twilight made here with a polarization photometer on twenty evenings during the three years, 1949-51, in quiet solar and geomagnetic conditions, suggest that the seasonal variation of the twilight emission originating in the altitude range 70–110 km may not correspond exactly with its counterpart in the night sky at 200–250 km. The *D*-line radiation was isolated by filters transmitting an effective band-width of 170 Å; and a type-H "Polaroid" filter, rotated above the photocell aperture, served as analyzer.

In the table below appear three-monthly group mean values of the unpolarized radiation at 5893 Å observed in twilight within an effective height-range of 30 to 65 km (solar

Observed seasonal mean values of unpolarized D-line radiation in band 170 Å *wide at* 5893 Å

Effective height		30	35	40	45	50	55	60	65 km
Solar depression		3·8	4·4	5·0	5·5	5·9	6·3	6·7	7·0 deg.
Season	*Evenings*	*Band intensity in millilux*							
Spring Mar.–May	7	−60	−32	−15	−2	−1	±0	+1*	+1*
Summer June–Aug.	5	−32	−13	±0	+4	+7	+11	+10*	+6*
Autumn Sept.–Nov.	4	−10	+2	−4	−10	−11	−12	−12*	−13*
Winter Dec.–Feb.	4	−3	+7	+18	+20	+19	+18	+20*	+19*

Note—Negative values indicate that the observed intensity of the band was lower than that of an equal band of sky continuum, i.e., the band was observed in absorption. Marked thus * are extrapolated values.

depressions, 3·8 to 7·0 degrees). The number of observations associated with each seasonal group is given in the second column of the table. Not more than half-weight should be assigned to intensity values entered in the last two columns and marked with an asterisk, since these have been extrapolated from the experimental data.

The Sidmouth results confirm the very marked uncertainty of appearance of the *D*-lines in emission at twilight noted by other observers: they suggest also that the enhanced radiation is frequently either absent, or very weak in spring and autumn; moderately strong in summer; and very strong in winter, the primary maximum occurring in December with a secondary maximum in July. After correcting for the effects of the overlying ozone and water-vapour absorptions,* the mean zenithal intensity ratio (winter/summer) of emission observed at solar Z.D. 95°–96° is 3·7, in good agreement with the most recent value found for the nocturnal emission (ROACH and PETTIT, 1951). However, the secondary maximum found here in summer and the much lower values in spring and autumn suggest a seasonal fluctuation which differs markedly from that obtained by BRICARD and KASTLER at the Pic du Midi in 1942-43. The cause of this discrepancy must remain obscure pending the accumulation of fresh experimental data covering a much longer period than that on which the provisional results presented here are based.

D. R. BARBER.

Norman Lockyer Observatory
of the University College of the South West,
Sidmouth, Devon.

REFERENCES

BARBIER, D., and ROACH, F. E.	1950	*Trans. Amer. Geophysical Union* **31,** 13
BRICARD, J., and KASTLER, A.	1944	*Ann. de Geophys.* **1,** 53
	1950	*ibid.* **6,** 298
DUFAY, J., and TCHENG MAO-LIN	1946	*Ann de Geophys.* **2,** 189
	1947	*ibid.* **3,** 153
ROACH, F. E., and PETTIT, H. B.	1951	*Ann. d'Astrophys.* **14,** 392

VOL. 5 1954

The anomalous equatorial belt in the F_2-layer

Anomalous behaviour in the F_2-layer was first detected in seasonal studies of noon values of fF_2 at Slough. These indicated that the F_2-layer *maximum* electron density, N_m, was less in summer than in winter. APPLETON and NAISMITH (1935), who described this effect, considered that the lower summer value of N_m was the result of "the total ionization being spread out over a greater vertical thickness." Indications that such abnormally low summer noon values of N_m are, in fact, due to the general electronic inflation of the F_2-layer were first confirmed qualitatively in the course of ionospheric forecasting by the "parabolic"-layer method of APPLETON and BEYNON (1940; 1947). The height of the level of N_m (i.e., h_m), and also the semi-thickness of the F_2-layer, y_0, were both found to be greater, at Slough, in summer than in winter. The same result is indicated by determinations of the transmission factor (M3000)F_2 by the method of NEWBERN SMITH (1937; 1938), the inverse

* The combined effect of ozone and water-vapour normally present in the atmosphere will be to reduce the intensity of *D*-line emission observed in summer relative to its winter value by about 8 per cent, a quantity just significant in relation to the probable error of computation, and to the observed seasonal fluctuation.

of which quantity is a quite reliable indication of variations in the height of N_m. The magnitude of this factor is lower in summer than in winter, indicating the reverse relationship in h_m. Greater quantitative precision has been given to these notions by RATCLIFFE (1951) and by CHATTERJEE (1953), who have estimated the total layer electron content (per unit cross-section), $\Sigma N \,.\, dh$, and found that this quantity exhibits the normal seasonal relation.

When geomagnetic control of the F_2-layer was identified (APPLETON, 1946) with the "trough" of low values of noon N_m centred on the magnetic equator, it was pointed out that such low values were associated with general ionospheric characteristics reminiscent of summer conditions at Slough. In other words, it was indicated that, at noon, there was abnormal elevation and upward distension of the F_2-layer over a belt centred on the magnetic equator. This is confirmed by the fact that equinox noon h_m, as indicated by transmission factors, is abnormally high over the equatorial region characterized by the "trough" in N_m. Still more convincing evidence has recently been advanced by RATCLIFFE (1951) and by CHATTERJEE (1954), who have found that when an estimate is made of the total layer electron content (per unit cross-section), $\Sigma N \,.\, dh$, no equatorial "trough," such as is observed in N_m, is indicated. Since, however, the maximum of the quantity $\Sigma N \,.\, dh$ is found on the magnetic equator, rather than on the geographical equator, the phenomenon of the geomagnetic control of F_2-layer morphology remains.

By examining the relation between N_m and geomagnetic latitude for hours of the equinox day other than noon, a new result has recently been obtained. It is found that, whereas there is a "trough" of abnormally low values of N_m centred on the magnetic equator at noon, this "trough" tends to disappear during the afternoon until, during the late evening period 1800 h. to 0000 h., it is replaced by a "crest" of abnormally high values of N_m over an equatorial belt of comparable extent. After midnight the equatorial "crest" in N_m falls rapidly, and, by 0300 h., the anomaly has largely disappeared. As noon approaches the equatorial "trough" in N_m values again develops. This diurnal variation of the equatorial geomagnetic anomaly is illustrated in Figs. 1, 2, and 3, in which values of fF_2 for March 1951 are plotted with geomagnetic latitude for both hemispheres for the local times of 1200 h., 2100 h., and 0900 h., respectively.

This late evening maintenance of abnormally high values of N_m on the equatorial belt cannot be ascribed, as was once suggested (APPLETON, 1946), to the influence of a low recombination coefficient after sunset, which occurs at 1800 h., because of the striking difference in N_m behaviour exhibited during the two halves of the night-time period. The high values of N_m during the first half of the night appear to be due to a *contraction* of the vertical extent of the layer, which may be compared with the *expansion* of the same quantity which causes the noon minimum. It may be mentioned that the equivalent height of the F_2-layer, $h'F_2$, which is a fair index of layer expansion and contraction, reaches its daily *minimum* on the magnetic equator at midnight; while h_m, as indicated by the transmission factor, having been high in the day-time, falls steadily at the same site during the period 1900 h. to 2400 h. at the equinoxes. If such F_2-layer expansion and contraction are due to vertical drift (MARTYN, 1947 a,b; 1948 a.b; MITRA, 1952; WEISS, 1953; MAEDA, 1953), it is clear that there is a belt centred on the magnetic equator in which such drift is markedly, and preferentially, developed.

It should be emphasized that the evening events in the equatorial belt, identified above, are anomalous in that the difference between high- and low-latitude phenomena is not due to some diurnal influence of uniform phase whose amplitude varies smoothly—increasing, for example as the geomagnetic latitude falls. It will be noticed that in Fig. 2, which refers to the local time of 2100 h., the value of fF_2 is shown to be less on the magnetic equator than it is at slightly higher latitudes within the anomalous belt. Drawing the

continuous curve in this way can be amply justified from the consideration of more extended data.

Studies of the response of N_m to increasing solar activity also confirm the existence of the anomalous equatorial belt, in that the ratio of the values of N_m at sunspot maximum

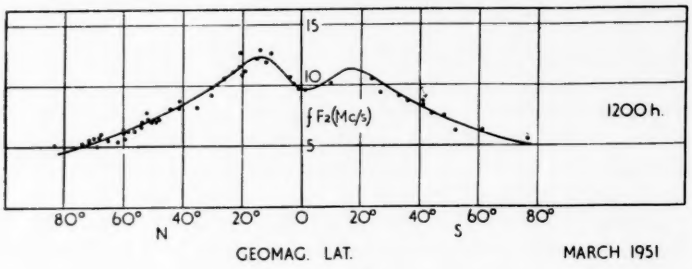

Fig. 1

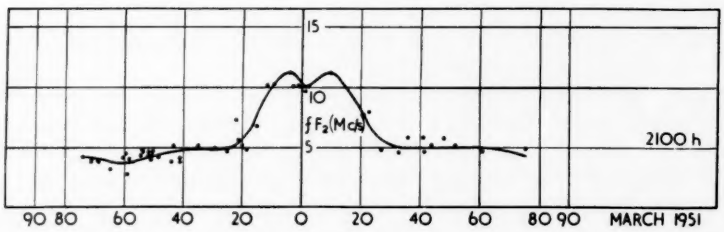

Fig. 2

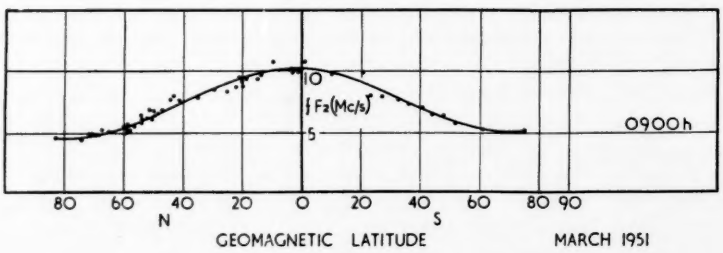

Fig. 3

and at sunspot minimum changes fairly abruptly, at certain hours of the day, when the equatorial belt is reached with decreasing geomagnetic latitude. For example, at 2100 h., local time, this ratio is a maximum at the outer boundary of the belt in either hemisphere and falls to its lowest world value on the magnetic equator.

It will readily be seen that the anomalous equatorial belt in the F_2-layer is about 4000 km wide.

Acknowledgments—The work described above was carried out as part of the programme of the Radio Research Board of the Department of Scientific and Industrial Research. I am much indebted to Mrs. A. G. Pritchard for assistance in its prosecution.

The University,
Edinburgh

Edward V. Appleton

VOL. 5 1954

REFERENCES

APPLETON, E. V.	1946	*Nature* **157,** 691
APPLETON, E. V., and NAISMITH, R.	1935	*Proc. Roy. Soc.* **A150,** 685
APPLETON, E. V., and BEYNON, W. J. G.	1940	*Proc. Phys. Soc.* **52,** 518
	1947	*Proc. Phys. Soc.* **59,** 58
CHATTERJEE, B.	1953	*J. Geophys. Res.* **58,** 353
	1954	*Nature* **173,** 263
MAEDA, K.	1953	*Rep. Ion. Res. Jap.* **7,** 81
MARTYN, D. F.	1947a	*Proc. Roy. Soc.* **A189,** 241
	1947b	*ibid.* **190,** 273
	1948a	*ibid.* **194,** 429
	1948b	*ibid.* **194,** 445
MITRA, A. P.	1952	*Ind. J. Phys.* **26,** 79
RATCLIFFE, J. A.	1951	*J. Geophys. Res.* **56,** 463
SMITH, NEWBERN	1937	*J. Res. Nat. Bur. Stand* **19,** 89
	1938	*ibid.* **20,** 683
WEISS, A. A.	1953	*J. Atmosph. Terr. Phys.*. **3,** 30

DL.
5
954

Determination of electron densities in the ionosphere from experimental (h', f_s) curves

I am indebted to Professor J. M. KELSO (1954) for drawing attention to an error in the argument I used (1951) as the basis of the paper with the above title. This invalidates the method as described. However, since the use of the reference curves in Fig. 4 does lead to electron density distributions which are physically acceptable (whereas the use of the "no-field" curve does not) in the case of (h', f) curves for Region E containing cusps and "tails" (Fig. 2) it is possible that a rigorous argument can be given for the use of similar curves.

I have not been able to derive such an argument and it seems that the mathematical difficulties involved are very great.

H. A. WHALE

Seagrove Rudio Research Station,
Auckland, N.Z.

REFERENCES

KELSO, J. M.	(1954)	*J. Atmosph. Terr. Phys.* **5,** 11
WHALE, H. A.	(1951)	*J. Atmosph. Terr. Phys.* **1,** 244

Journal of Atmospheric and Terrestrial Physics, 1954, Vol. 5. pp. 352 and 353. Pergamon Press Ltd., London

Indices of geomagnetic activity

of the Observatories ABINGER (*Ab*), ESKDALEMUIR (*Es*), and LERWICK (*Le*)

July and August 1954

The figures given on pages 352 and 353 represent the K-indices for three-hour intervals, beginning with 00–03 hrs for the first and ending with 21–24 hrs for the eighth figure.

July 1954

Day	*Ab* Range for $K = 9 : 500\gamma$			*Es* Range for $K = 9 : 750\gamma$			*Le* Range for $K = 9 : 1000\gamma$			*Day*
	K-Indices		*Sum*	*K-Indices*		*Sum*	*K-Indices*		*Sum*	
1	4332	3221	20	3332	3221	19	3332	2110	15	1
2	1212	3222	15	0100	2222	9	0110	2122	9	2
3	1222	2212	14	1221	2211	12	0111	2111	8	3
4	1221	3121	13	1012	2010	7	0110	2111	7	4
5	0123	2322	15	0122	1331	13	0111	2321	11	5
6	2232	3332	20	2121	2332	16	2222	2232	17	6
7	3113	2221	15	3113	2211	14	3212	2111	13	7
8	1122	2331	15	1002	2221	10	1111	2221	11	8
9	2122	2222	15	2000	1111	6	1111	1111	8	9
10	1122	2212	13	1111	2212	11	1111	1112	9	10
11	2222	2222	16	2222	1111	12	1212	1111	10	11
12	3322	3434	24	2212	3423	19	2112	3424	19	12
13	2112	1222	13	2012	2222	13	3111	2112	12	13
14	3332	3322	21	3322	3312	19	2331	3311	17	14
15	1133	4321	18	0123	3211	13	1123	3211	14	15
16	1122	3342	18	1112	2331	14	1011	1232	11	16
17	2332	2224	20	1221	1114	13	1331	1113	14	17
18	5322	3322	22	4321	2222	18	4321	1212	16	18
19	2222	3342	20	2102	2342	16	2101	2231	12	19
20	3222	2311	16	3221	2201	13	2222	2211	14	20
21	1232	2432	19	0221	2322	14	1111	2322	13	21
22	1122	2221	13	1011	2110	7	1111	2110	8	22
23	0223	2221	14	0102	1221	9	0112	1211	9	23
24	3322	3222	19	3321	2220	15	3321	2110	13	24
25	3333	3323	23	2333	3222	20	2333	3212	19	25
26	2223	3321	18	2122	3311	15	2121	2211	12	26
27	3323	3333	23	2323	3323	21	3312	2223	18	27
28	2423	4433	25	2323	4422	22	3322	3333	22	28
29	3323	3321	20	3322	2321	18	3222	2221	16	29
30	3113	3312	17	3112	2312	15	3112	2212	14	30
31	2232	3223	19	2122	3223	17	1122	2223	15	31

VOL. 5 1954

August 1954

Day	*Ab* Range for $K = 9 : 500\gamma$			*Es* Range for $K = 9 : 750\gamma$			*Le* Range for $K = 9 : 1000\gamma$			*Day*
	K-Indices		*Sum*	*K-Indices*		*Sum*	*K-Indices*		*Sum*	
1	2223	3331	19	1113	3321	15	2113	3221	15	1
2	2322	2321	17	2322	2221	16	2312	1222	15	2
3	1222	2232	16	1113	2222	14	1112	1122	11	3
4	1232	2231	16	1221	2231	14	1121	2120	10	4
5	2222	2323	18	1211	2223	14	1111	1223	12	5
6	2332	3354	25	2232	3254	23	2322	3244	22	6
7	3223	3432	22	3013	3432	19	3112	3331	17	7
8	2232	3312	18	2112	2211	12	2111	2211	11	8
9	2222	4433	22	2121	4323	18	1121	4323	17	9
10	3132	2322	18	2122	1322	15	3211	1322	15	10
11	3222	2321	17	2222	1321	15	3211	2221	14	11
12	3223	3222	19	3223	2211	16	3212	2211	14	12
13	0223	3321	16	0213	3321	15	1121	2321	13	13
14	3223	2223	19	3122	2223	17	3111	1223	14	14
15	3123	2243	20	3011	2233	15	3111	1243	16	15
16	1233	4322	20	1222	4322	18	3122	4222	18	16
17	2233	3222	19	2133	3221	17	1123	2221	14	17
18	2223	3332	20	2223	3232	19	2222	3232	18	18
19	4232	2333	22	4212	2323	19	3212	1223	16	19
20	3222	2322	18	3222	2310	15	3220	2211	13	20
21	2334	3222	21	1234	3221	18	1233	2121	15	21
22	4432	2223	22	4432	2213	21	5441	2213	22	22
23	3212	2243	19	3102	2233	16	3211	1232	15	23
24	3333	5444	29	2233	5344	26	3232	4343	24	24
25	4223	3222	20	3212	2222	16	3212	2211	14	25
26	2443	3333	25	1443	3333	24	1442	3233	22	26
27	5223	2233	22	5123	2233	21	5323	2233	23	27
28	3322	3324	22	3322	3324	22	3321	2224	19	28
29	3334	3233	24	3323	3232	21	3323	2223	20	29
30	2222	3332	19	2122	3332	18	2211	3332	17	30
31	2222	2343	20	2111	2333	16	2110	1333	14	31

OL.
5
954

Book reviews

LEWIS, I. A. D., and F. H. WELLS; **Millimicrosecond Pulse Techniques** (Pergamon Science Series: Electronics and Waves. Editor: D. W. Fry, Harwell). Pergamon Press Ltd., London, and McGraw-Hill Co., New York. xiv + 310 pp. 161 figures. 40s. net or $7.50.

This book is one of a series of monographs entitled "Electronics and Waves." It is the aim of the series to report on research carried out on electronics and applied physics in a condensed form and to make the information readily and quickly available. This volume succeeds admirably in this aim, and it will be of great help to those who have to design and use millimicrosecond circuitry.

In addition to a very brief chapter on circuit theory, in which the Laplace transform method is introduced, there are five chapters on circuit theory, viz., transmission lines, transformers, pulse generators, amplifiers, and cathode ray oscilloscopes. The first two of these chapters include a simple Laplace treatment of transmission lines and a good theoretical account of impedance matching by means of tapered lines. There is also a brief mention of lumped transformers, delay lines consisting of filter sections, as well as a practical account of transmission-line pulse invertors. Among the topics of particular interest in the chapters on pulse generators, amplifiers, and oscilloscopes are secondary emission valves used in amplifiers and trigger circuits, distributed amplifiers, and travelling wave deflection systems in high-speed oscilloscopes. The book concludes with two chapters on the applications of the techniques described with a strong bias towards nuclear physics. In these chapters there are sections on scintillation counters, pulse amplitude discriminators, fast scalers, and coincidence circuitry, etc.

The book is written in a style suited to the practical approach adopted. Each topic is discussed in a manner which shows the limiting factors, and future trends are often indicated. Much practical information is included, and the performance of each of the many circuits reproduced is clearly stated. The collecting together of these circuits alone ensures the usefulness of the book. There is an excellent bibliography and a comprehensive list of references.

The only serious criticism which may be made concerns the disproportionate treatment of lumped pulse transformers and transmission lines used as pulse transformers. As there is at least an equal interest in the two techniques, it is unfortunate that the authors have not found it possible to give a more complete treatment of lumped transformers.

B. COLLINGE

VOL.
5
1954

A Textbook of Radar, by the Staff of the Radiophysics Laboratory, Council for Scientific and Industrial Research, Australia. Edited by E. G. BOWEN—Second Edition. Pp. 617 + xiii. Plates XLI. Cambridge University Press, 1954. Price 45s. net.

The first edition of this work was published in Australia in 1947, and in England a year later. It comprised twenty chapters by as many different authors, including an introduction by the present editor. In the second edition, now under review, the first sixteen chapters have been reproduced by the photo-offset process after all errors had been corrected and various minor details, such as the types of valves in some of the circuit diagrams, had been brought up to date. In thus reproducing the first 512 pages, an important disadvantage of the first edition has been corrected, in that most, but not all, of the references to unpublished reports produced during the war in Great Britain, America, and Australia have now been replaced by the corresponding references to the papers which have been published in the standard scientific and technical journals and which are therefore available in the libraries of the world.

The range of subjects dealt with in this reproduced material is very wide; it includes chapters on the essential components of the technique of radar, such as magnetrons and klystrons, triode-power oscillators and modulator technique, microwave transmission lines, cavity resonators and waveguides, and radar systems, with display and automatic ranging circuits. Few details of actual equipments are given and they are included only when necessary to illustrate principles and practice.

The last four chapters of the first edition have been replaced by three which have been completely rewritten in order to take account of the different perspective in which military radar now stands in relation to civil developments and to the extensive applications of radar technique to the physical sciences which have taken place in the past seven years or so. The first of the new chapters on "Military Radar Systems" covers the whole field of ground-based, naval, airborne, and secondary radar systems. This is admittedly a compressed account, but it is justified by the fairly extensive literature now available, a selected bibliography to which is given at the end of the chapter. A comparable space is devoted in the succeeding chapter to the development of radar as an aid to civil air and marine navigation and to surveying. In the final chapter a concise summary is given of the "Applications of Radar Systems to Physical Science." This naturally treats of the development of the new science of radio astronomy, in which the editor and his colleagues in the Australian C.S.I.R.O. have played such a conspicuous part. A concluding section on the velocity of electromagnetic waves illustrates the manner in which, under pressure from a successful application, the precision of measurement of a pure physical quantity has been considerably enhanced.

The book concludes with three useful appendices, containing charts of the hyperbolic tangent and tables of constants and conversion factors applicable to the MKS units which are used throughout.

The whole work reflects great credit on the contributors and the excellent co-ordination achieved by the editor; and it may unhesitatingly be recommended to graduate and research students of universities, and to engineers engaged in research and development in the radio and electronics industry.

R. L. SMITH-ROSE

OL.
5
954

WOODWARD, P. M.; **Probability and Information Theory, with Applications to Radar.** London: Pergamon Press Ltd. Pp. x + 128. 1953. 21s.

The object of this monograph is to explain by relatively easy stages how the theory of probability is applied to some communication problems and particularly to the statistical problem of the reception and analysis of radar information.

The first two chapters present an introduction to probability theory and its application to waveform analysis and noise. As the author states in the preface, these are concerned with established mathematical techniques and they describe the code in which so much of the mathematical theory of radar is nowadays expressed. The third chapter is a summary of SHANNON'S original work on information theory and describes the basic ideas of the rate of communication of information and the manner in which the information capacity of a communication channel is limited or destroyed by the incidence of random noise. This subject is elaborated in the fourth chapter on "The Statistical Problem of Reception."

The remaining three chapters deal with the special problems of the detection and analysis of radar signals; they are based on the results of the author's own research in this field, and summarize and extend material which has already been published in scientific and technical journals. As a result of this work, a great deal of advance has been made in recent years in the analysis of radar information; but it is stated in the concluding paragraph on the last page of the book "that the basic question of what to transmit remains substantially unanswered."

It is thus clear that there is room for much more research in this whole field; and particularly in that part which is concerned with the application of the theoretical concepts of the transmission of information to the practical problem of improving the efficiency of communication and radar systems. The book under review should provide a useful introduction to the subject for the engineer and scientist, of modern mathematical ability, working in this field.

R. L. SMITH-ROSE

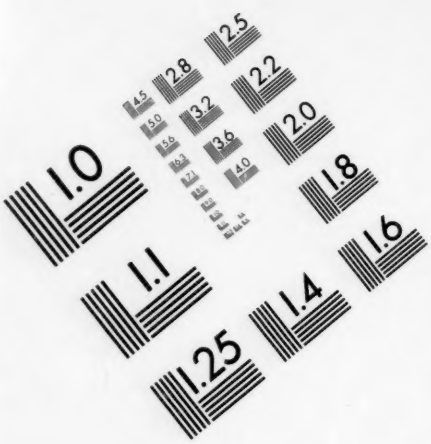

NATIONAL MICROGRAPHICS ASSOCIATION

MS303-1980

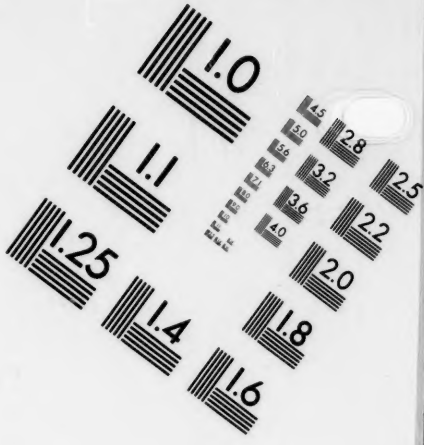

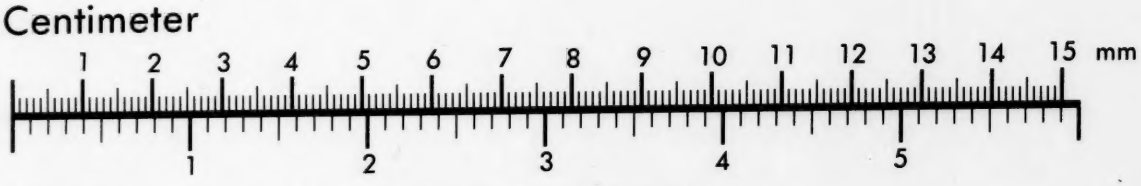

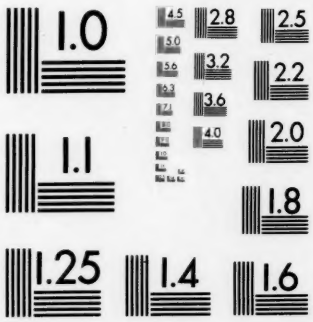

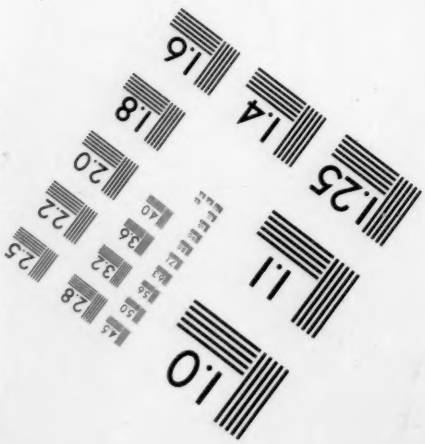

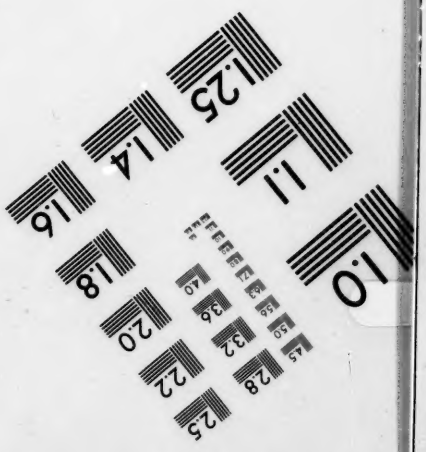

PERGAMON PRESS INC.

MICROFORMS INTERNATIONAL
MARKETING CORPORATION
FAIRVIEW PARK, ELMSFORD, NEW YORK 10523

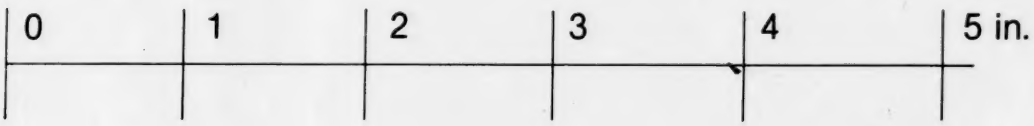

PRODUCED AT

**MIMC MICROFORMS LABORATORY
ELMSFORD, NEW YORK**